Field Trip Guide

for the 69th Annual Meeting of the New York State Geological Association

Hamilton College
Clinton, New York
September 26-28, 1997

Field Trip Guide for the 69th Annual Meeting of the New York State Geological Association

Edited by:

Todd W. Rayne
David G. Bailey
Barbara J. Tewksbury

September 26-28, 1997
Hamilton College
Clinton, NY

This guidebook was published by the New York State Geological Association. Additional copies may be obtained from the Executive Secretary of the NYSGA:

Dr. William Kelly
Executive Secretary, NYSGA
Rm. 3140, Cultural Education Center
New York State Geological Survey
Albany, NY 12230

ISSN: 1061-8724

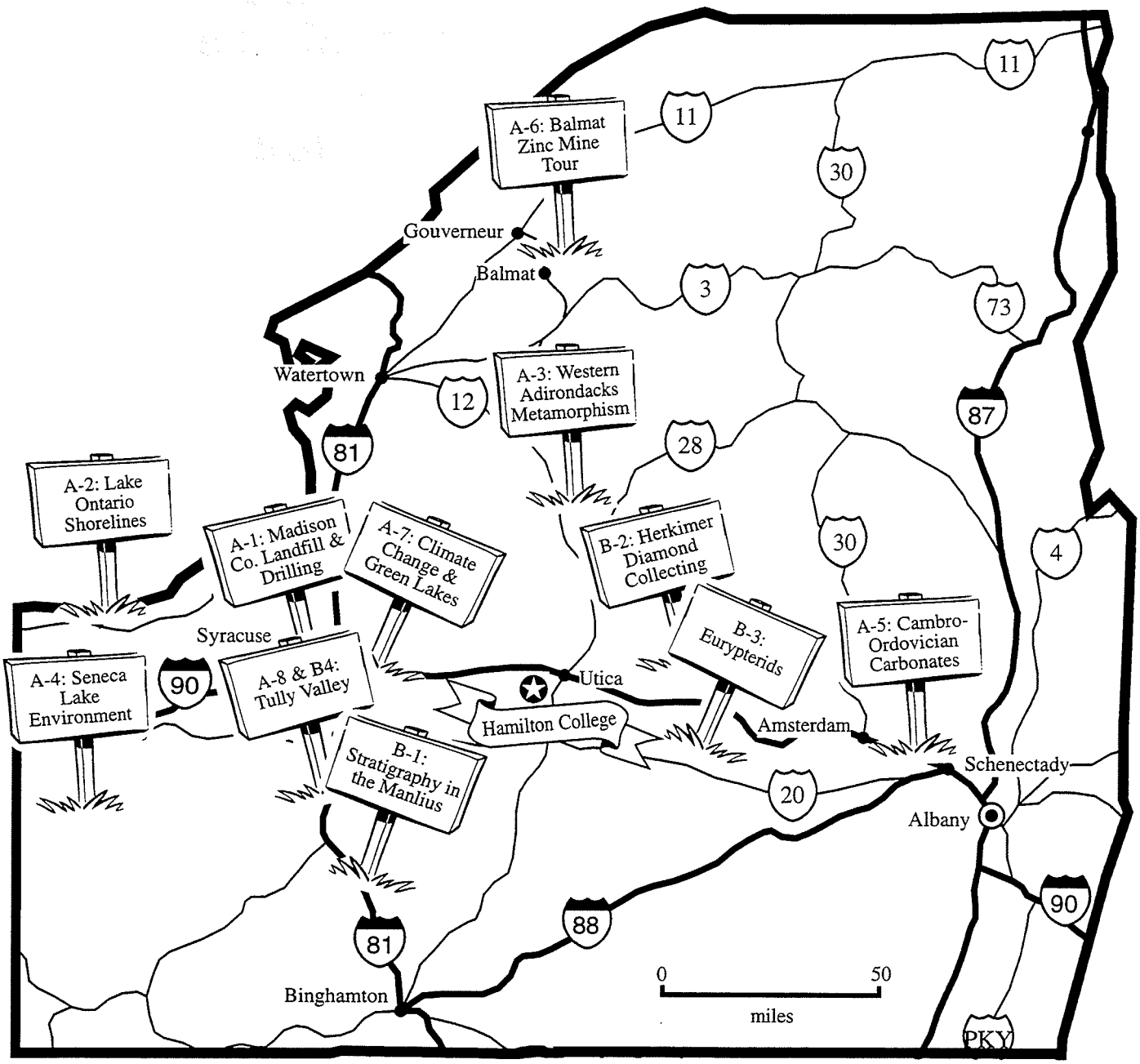

General Locations of Field Trips for the 69th Annual Meeting of the NYSGA

Table of Contents

Table of Contents (cont.)

Madison County Department of Solid Waste Landfill Facilities

Paul W. Miller
Assistant Director
Madison County Department of Solid Waste
P.O. Box 27, Wampsville, NY 13163

General

Madison County runs a comprehensive solid waste and recycling program at its facilities located astride Buyea Road in the Town of Lincoln, Madison County, New York. Madison County is home to about 72,000 souls with numerous small villages and only one city, Oneida, with about 10,000 residents. Madison County contains the geographic center of New York State and is genuinely proud of its rural nature.

Two large abandoned marginal farmland properties have been used for landfilling activities since early 1973. Over time the changing regulatory requirements for solid waste management have necessitated numerous changes in construction standards for landfill facilities and environmental monitoring. Ideal geologic conditions have allowed operations to keep pace with changing requirements with reasonable economic investment. All expenses at the Solid Waste Department facilities are paid by user fees. No general tax revenue is used to support Department operations. In Madison County waste-pays-for-waste now but the changing world of solid waste management is creating economic pressures and challenges necessitating creative management.

Landfilling Activities

Four landfill areas on the landfill properties are evidence of changing regulatory requirements. Landfilling on-site has been conducted in the following areas:

1) A sixteen acre, unlined facility operated from about 1978 to 1985 and closed with a soil cap in 1986.
2) An eight-acre unlined facility operated from about 1973 to 1978 and closed in 1990 with a PVC membrane cap and passive venting of landfill gas.
3) A 16 acre facility with constructed in 1986 with a clay liner and a rudimentary leachate collection system. This facility is undergoing final closure with a recovery system even though the facility is below the regulatory threshold for mandatory active landfill gas management measures.
4) A seven and one half acre state-of-the-art double composite lined facility constructed under the latest 6NYCRR Part 360 requirements. This landfill, which meets Subtitle D requirements, opened in 1996 and will have landfill gas recovery features built in as landfilling progresses. Nearly all natural materials for the liner system were available on-site or nearby.

Environmental Monitoring

Just as construction standards have changed over time, so have environmental monitoring standards. All facilities are surrounded with up-gradient, down-gradient, and cross-gradient monitoring wells for assessing potential impacts on water quality. Most well sites have clusters of two or three wells to sample water quality at different levels in the water table and geologic strata. New standards for monitoring are expensive and testing requirements are extensive.

Site Geology

Understanding of the local geology has proven this site to be an excellent choice for landfill activities. Located atop the Helderberg escarpment, which runs east to west across the state, the landfill site sits on a thick bed of glacial till deposited during the last glaciation. This till, which made farming difficult, has proven suitable for liner construction with little constructive effort. The till varies in depth from ten to fifty feet across the 480 acre site.

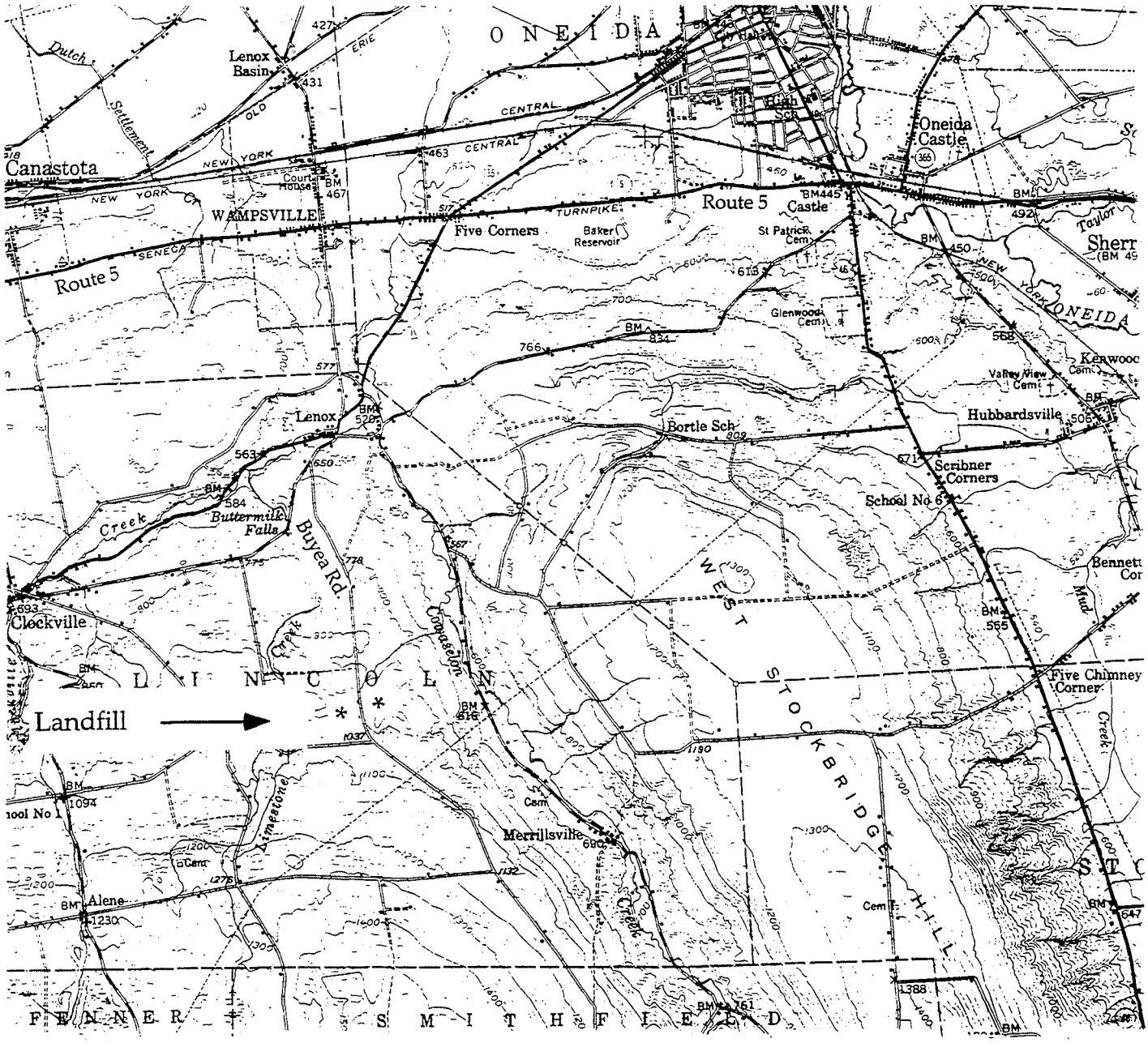

Location of the Madison County Landfill (*) on Buyea Road. Map is part of the Oneida (NY) 15-min. series. Village of Oneida and NY Route 5 are shown for reference

Environmental and Geotechnical Drilling

Mr. William Morrow, P.G. and Mr. Stephen Crook, P.G.
Parratt-Wolff, Inc.
5879 Fisher Road
East Syracuse, New York 13057

Environmental and Geotechnical drilling projects provide subsurface data critical in the evaluation of a site. Whether the purpose of the investigation is to assess for the presence of soil or ground water contamination or for the design and construction of structures, proper subsurface investigations must be performed. Drilling provides one of the most fundamental ways in which subsurface information is obtained for evaluation by a geologist or engineer. In the text that follows, a brief overview of environmental and geotechnical drilling is provided. Also included are typical methods for describing soil and rock samples.

Drilling Methods

Prior to choosing a particular drilling method, consideration should be given to a number of variables including:

- Type of formation to be drilled (unconsolidated or consolidated material),
- Borehole depth,
- Borehole diameter,
- Quality of samples desired,
- Cross Contamination potential, and
- Whether a well will be installed in the borehole.

Once these variables have been considered one of the following four drilling methods are commonly used to make the boring.

Cable Tool Method

In the cable tool method, the borehole is advanced by lifting and dropping a heavy string of drilling tools (Figure 1). The tools are suspended on a steel cable and terminate in a chisel shaped bit. The impact of the bit breaks up the formation, which must then be removed from the borehole. Typically, the soil or rock cuttings suspended in water and are removed with a large bailer. In unconsolidated formations, temporary casing is advanced during drilling to keep the borehole from collapsing. The temporary casing also minimizes potential cross-contamination between materials in environmental investigations. Formation samples can either be collected from the bailer or with a variety of different soil samplers (see Section 2.1).

Fluid Rotary Method

Fluid rotary drilling involves rotation of a drill rod and bit. The most common type of bit is a tri-cone roller bit, designed to cut through soil and rock. A drilling fluid is circulated through the drill rod and bit and up the annular space between the rod and borehole (see Figure 2). The drilling fluid is used to lubricate the bit, carry cuttings to the surface and maintain hole stability. Additives, such as bentonite, are often mixed with water to increase the weight and viscosity of drilling fluid. Bentonite fluid drilling is often referred to as "mud rotary". Fluid rotary is a rapid way of advancing a large diameter borehole. However, soil samples recovered from the drilling fluid are marginal for accuracy due to loss of fine-grained materials. In addition, fluid remaining in the formation after drilling may lower borehole permeability and potentially alter ground-water chemistry.

Air Rotary Method

Air rotary drilling is similar to fluid rotary except that air compressed is used to cool the bit and carry cuttings to the surface. Air rotary drilling is generally limited to consolidated formations because air alone will not maintain an open hole in unconsolidated material. Air rotary is a very effective rock drilling methods. When combined with a downhole hammer drill bit, boreholes can be drilled very rapidly in bedrock. Another advantage of air rotary drilling is that water produced from the rock is carried to the surface allowing evaluation of the relative productivity of various strata. However, soil or rock sampling is limited to evaluating the drill cuttings as they are conveyed out of the borehole by the air.

Hollow Stem Auger Method

Hollow stem auger drilling is the most commonly used method in both environmental and geotechnical investigations. Figure 3 provides an illustration of the typical components in a hollow stem auger. This method is fast, relatively inexpensive and provides excellent sampling capabilities. With hollow stem augers, the hole is advanced by rotating and pressing the auger into the soil. As the auger is advanced into the soil, cuttings are conveyed upwards on the auger flights. This method is limited to unconsolidated materials and to depths generally less than 100 feet. The hollow stem auger method allows the collection of representative soil samples ahead of the lead auger. The hollow stem augers also permit the installation of monitoring wells.

Monitoring Well Installation

Monitoring wells are installed for a variety of purposes but generally to allow discrete sampling of ground water. These purposes must be defined prior to installation so that a well can be properly designed and constructed from the right materials. The objectives for installing monitoring wells may include:

- Determining ground-water elevations, flow directions and velocities,
- Sampling and monitoring for the presence of contaminants, and
- Assessing aquifer characteristics (e.g., hydraulic conductivity).

Most monitoring wells are completed in the first permeable, water-bearing zone encountered. Care must be taken to assure that the well is completed at a depth sufficient to allow for seasonal water-table fluctuations. Monitoring well construction materials include: riser pipe and screen materials, annular materials and protective covers. The selection of well construction materials depends on the method of drilling, type of contamination expected, and the natural water quality.

Riser pipe and screen materials are specified by diameter, type of material and thickness of pipe. Well screens require an additional specification of slot size. Riser pipe and screen materials are commonly constructed from polyvinyl chloride (PVC); although Teflon, carbon steel, stainless steel, and galvanized steel are also available. The annular space between the borehole and the screen is usually backfilled with sand to an elevation 2 to 3 feet above the top of the screen. Bentonite is then placed on top of the sand pack and expands by absorbing water. This provides a seal between the screened interval and the rest of the annular space and formation. Cement grout is placed on top of the bentonite to ground the surface. The grout stabilizes the well and limits the potential of surface runoff reaching the screened interval. Grout, as applied to environmental or engineering projects, is typically a mixture of cement, bentonite and water.

A steel protective casing is often placed around the monitoring well. The protective casing has a locking cover and is set into a concrete pad. Small-diameter manholes are also available for situations requiring ground surface completions (i.e. wells located in roadways or parking lots). The purpose of the protective cover or manhole is to prevent vandalism that may result in groundwater contamination. An example of a monitoring well completion diagram is included as Figure 4. ASTM Standard Practice Design and Installation of Groundwater Monitoring Well in Aquifers (D5092-90) provides additional detailed information on the installation of monitoring wells.

Soil and Rock Sampling Methods

Although preliminary sample information can be obtained from soil or rock cuttings, far more accurate soil and rock samples can be obtained by collecting discrete soil samples or rock coring.

Soil Sampling

Discrete soil sampling consists of pressing or driving a sampler into the soil. The samplers can collect either disturbed or undisturbed soil samples. An example of a disturbed sample is one that is driven into place (i.e. split spoon sample, Geoprobe® sample, etc.). An undisturbed sample is one recovered in such a way that the physical structure and soil properties are relatively unchanged during sampling. These samples are typically obtained by pressing a thin-walled tube (such as a Shelby tube) through the desired interval. These galvanized steel tubes are typically 3 inches outside diameter with a sample length of about 30 inches. The retrieved tube is then sealed for shipment to a physical-testing laboratory. Detailed information about undisturbed sampling may be found in the ASTM Standard Practice for Thin-Walled Tube Sampling of Soils (D1587-83).

A disturbed sample is collected by driving the sampler into the soil with either a free-falling hammer or hydraulic hammer. These samples are usually either a split spoon sampler or a tube sampler. The split spoon sampler is driven through the desired interval by dropping a 140-pound hammer 30 inches. The number of blows required to drive the sampler for 6-inch increments are recorded and used to compare the penetration resistance between samples. The split spoon sampler normally measures 2 inches or 3 inches outside diameter with a minimum sample length of 18 inches. At the surface, the sampler is opened, allowing for soil classification and containerization for subsequent evaluation. Tube samplers, such as those made by Geoprobe®, are lined with plastic sleeves and driven into the soil with a hydraulic percussion hammer. After removal from the borehole, the sleeve is removed and the sample classified and contained. Additional information about split spoon sampling may be found in the ASTM Method for Penetration Test and Split Barrel Sampling of Soils (D1586-84).

Rock Coring

Rock coring is used to collect discrete rock samples. The rock is cored with a tubular diamond-studded bit attached to a core barrel. As the diamond bit cuts the rock, a cylindrical-shaped rock sample is pushed into an inner barrel. Removal of the rock core from the subsurface is normally accomplished by lowering a wireline with a coupling into the drill rods, latching onto and pulling out the inner barrel. The recovered rock core is then removed from the inner barrel for examination or testing. The inner barrel is reinserted and the diamond bit advanced to the end of the next sampling interval. Water is constantly pumped down the rods during sampling to cool the core bit and flush cuttings to the ground surface. Diamond core barrels come in a variety of diameters and lengths. In environmental and geotechnical drilling, typically 2.0" or 2.5" diameter rock cores are collected (NX or HX size respectively) in 5.0-foot penetration runs.

Sample Description

Soil penetration tests and rock coring provide the geologist or engineer samples that can be used to make a variety of interpretations. The first step, however, is to describe and classify the recovered soil or rock sample.

Soil Description

Soils may be described and classified using a variety of methods. The most common method is the Unified Soil Classification System (USCS). This method identifies soil types on the basis of grain size and liquid limits. The soil is then categorized using a series of descriptive terms, followed by a two-letter symbol. In the USCS system, all soils are broken down into two broad categories - fine-grained soils (silt and clay) and coarse-grained soils (sand and gravel). The order of description for fine-grained soils is:

- Consistency (determined from blow counts)
- Moisture Content
- Color
- Modifying Soil
- Major Soil
- Other soil components
- Observations

An example of a fine-grained soil described according to the USCS classification system is "Moist red-brown silty CLAY, trace rounded quartz gravel (CL)". The order of description for coarse-grained soils is:

- Moisture
- Color
- Modifying soil
- Angularity
- Gradation
- Major Soil
- Other soil components
- Observations

An example of a coarse-grained soil is "Dry brown clayey fine to coarse SAND, little subangular fine gravel (SW-SC)". ASTM Practice for Description and Identification of Soils (visual-manual procedure) (D2488) is an excellent reference for describing and classifying soils.

Rock Description

The components typically used to describe a rock core are color, thickness of bedding, rock type, weathering state, hardness, and joint or fracture spacing. Additional components, such as texture, are used to further describe the rock as needed. An example of a rock description could be "Brown, thin bedded, fine-grained SANDSTONE, highly weathered, soft, close fractured". The definition of each of the components is given in Figure 5. Another important component worth noting in a core run is its structural integrity. This component can be approximated by calculating the rock quality designation (RQD). The RQD is determined by adding the total lengths of all pieces exceeding 4 inches and dividing by the total length of the coring run, to obtain a percentage (see Figure 6). The percentages between different core runs can be compared to quickly assess the rock quality between samples.

Well Log Preparation

Well logs provide documentation of drilling activities conducted during environmental and geotechnical investigations. The importance of properly completed well logs can not be overemphasized. The information well logs contain is used by the geologist or engineer to make decisions which are critical to the successful completion of a project. It is the responsibility of the individual overseeing the drilling activities to prepare well logs that are accurate, consistent and legible. Most well logs include the following information:

- Project name and location,
- Boring/Well number,
- Date(s) drilling started and finished,
- Boring location and elevation,
- Page number and total number of pages for each boring,
- Depth of each sample taken,
- Depth at which obstacles were encountered while advancing the borehole (boulders, etc.),
- Length of drive for soil samples and length of sample recovered,
- Number of blows required to drive sampler when standard penetration test is used,
- Length of each run for rock core and footage of core recovered,
- RQD values for each run,
- Changes in drilling rate and fluid loss when coring rock,
- Full description of soil and/or rock samples, as discussed in Section 3.0,
- Reason for boring abandonment when specified depth is not reached,
- Unusual conditions encountered in advancing the boring and in sampling,
- Complete description of well materials used and depths (if applicable), and
- Depth to water while drilling, prior to removal of any casing and 24 hours after all down-hole tools have been removed.

An example of a boring log used by Parratt-Wolff, Inc. is shown in Figure 7.

Conclusion

The methods and procedures described provide a general overview of environmental and geotechnical drilling and sampling. These methods and procedures are used to provide critical subsurface data on many projects. The references that follow are just a partial list of the many publications currently available about Environmental and Geotechnical drilling.

References

Aller, L. et al. 1989. Handbook of suggested practices for the design and installation of groundwater monitoring wells; National Water Well Association, Dubin, Ohio, 398 p.

American Society for Testing Materials (ASTM), 1993. Proceedings from Groundwater Monitoring and Sampling Technology Short Course: Design, Installation, Development and Sampling of Groundwater Monitoring Wells; American Society for Testing Materials, Philadelphia, Pennsylvania, 244 p.

American Society for Testing Materials (ASTM), 1995. Practices for design and installation of groundwater monitoring well in aquifers: D5092; 1997 Annual Book of American Society for Testing Materials Standards, Philadelphia, Pennsylvania, Vol. 04.09 pp. 77-87.

American Society for Testing Materials (ASTM), 1994. Practice for thin-walled tube sampling of soils: D1587; 1997 Annual Book of American Society for Testing Materials standards, Philadelphia, Pennsylvania, Vol. 04.08 pp. 142-144.

American Society for Testing Materials (ASTM), 1992. Test method for penetration test and split barrel sampling of soils: D1586; 1997 Annual Book of American Society for Testing Materials standards, Philadelphia, Pennsylvania, Vol. 04.08 pp. 137-141.

American Society for Testing Materials (ASTM), 1993. Practice for description and identification of soils (visual/manual procedure: D2488; 1997 Annual Book of American Society for Testing Materials standards, Philadelphia, Pennsylvania, Vol. 04.08 pp. 228-238.

Driscoll, F.G., 1986. Ground water and wells, 2nd edition; Johnson Division, St. Paul, Minnesota, 1089 pp.

Company Profile

Parratt-Wolff, Inc. (PWI) was founded in 1969 to provide soil and rock drilling to the Northeast. Since then, PWI has grown to a company of two offices, 45 employees and 29 major pieces of field equipment. Our service area includes all states from New Hampshire to Florida. Each year, PWI makes thousands of borings in both soil and rock. We keep a test boring log on nearly every hole drilled, giving us a comprehensive geologic data base. If you are in the Syracuse area and would like to tour PWI's facility or would like to discuss subsurface conditions in your project area, give us a call.

William H. Morrow, P.G. or Steve Crook, P.G.
Parratt-Wolff, Inc.
5876 Fisher Road
East Syracuse, NY 13057
(315) 437-1429

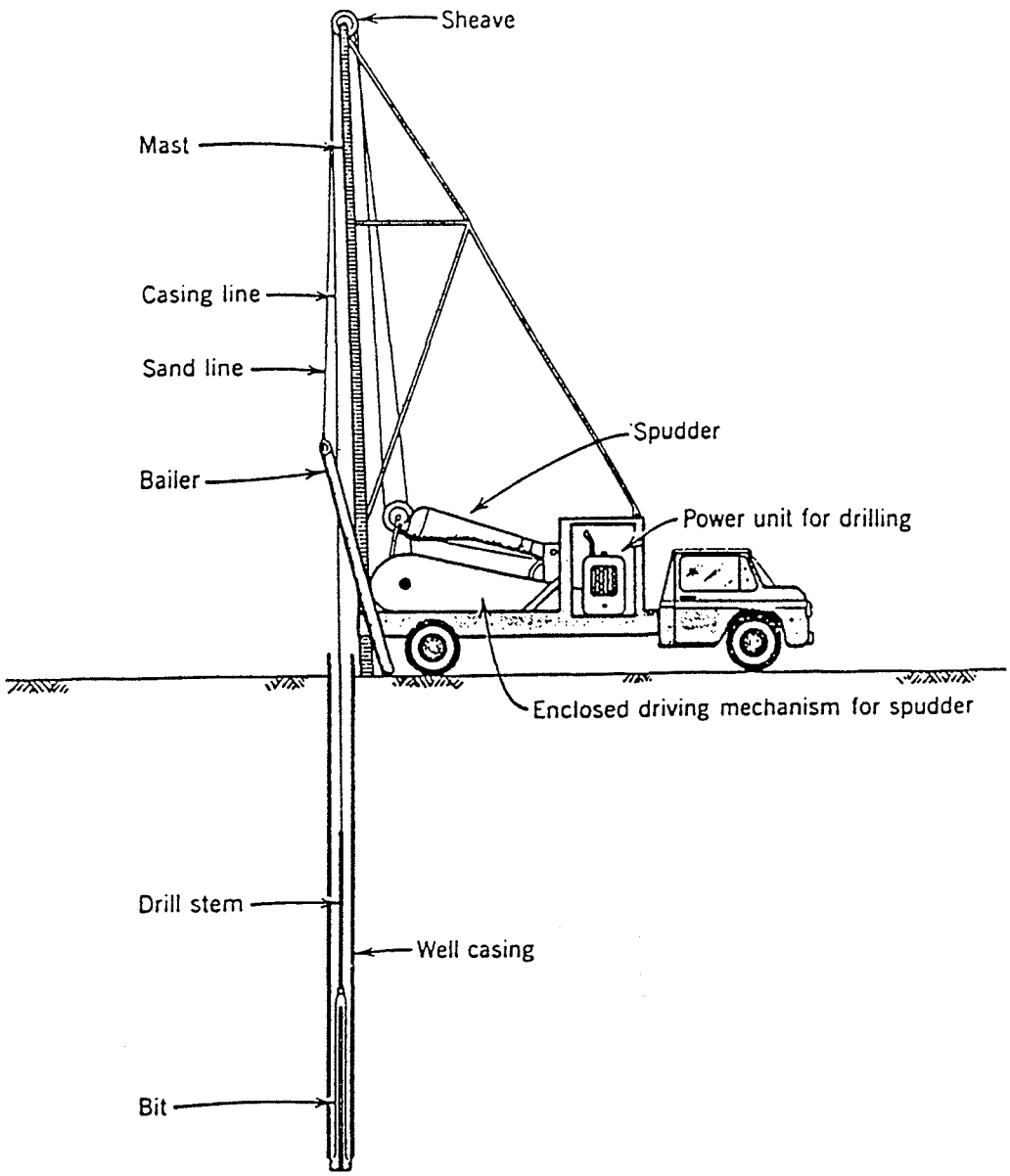

Figure 1. Cable tool method for making boreholes. The casing is advanced as the borehole is drilled in unconsolidated formations (Aller et al, 1989).

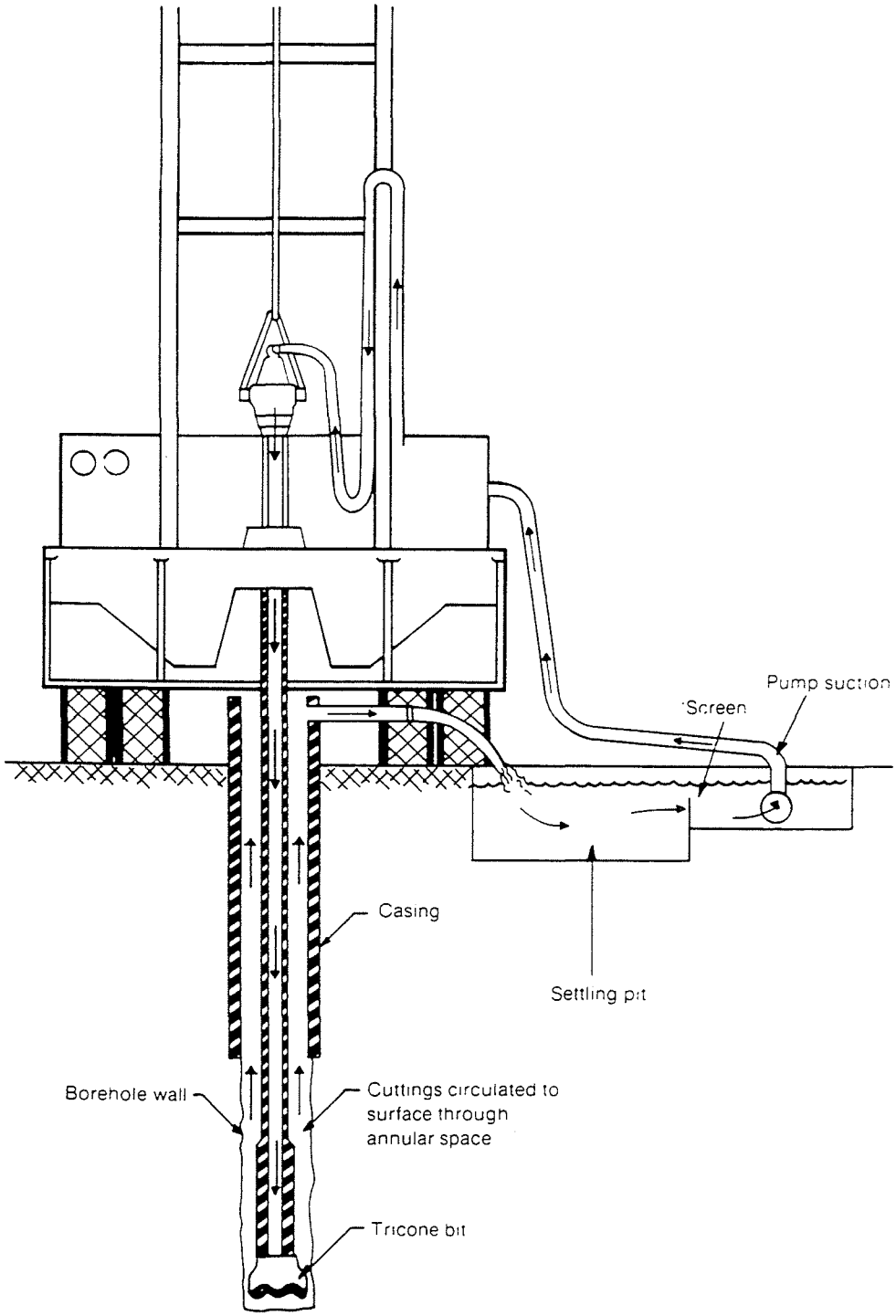

Figure 2. Diagram of direct fluid rotary circulation system (From Aller et al, 1989).

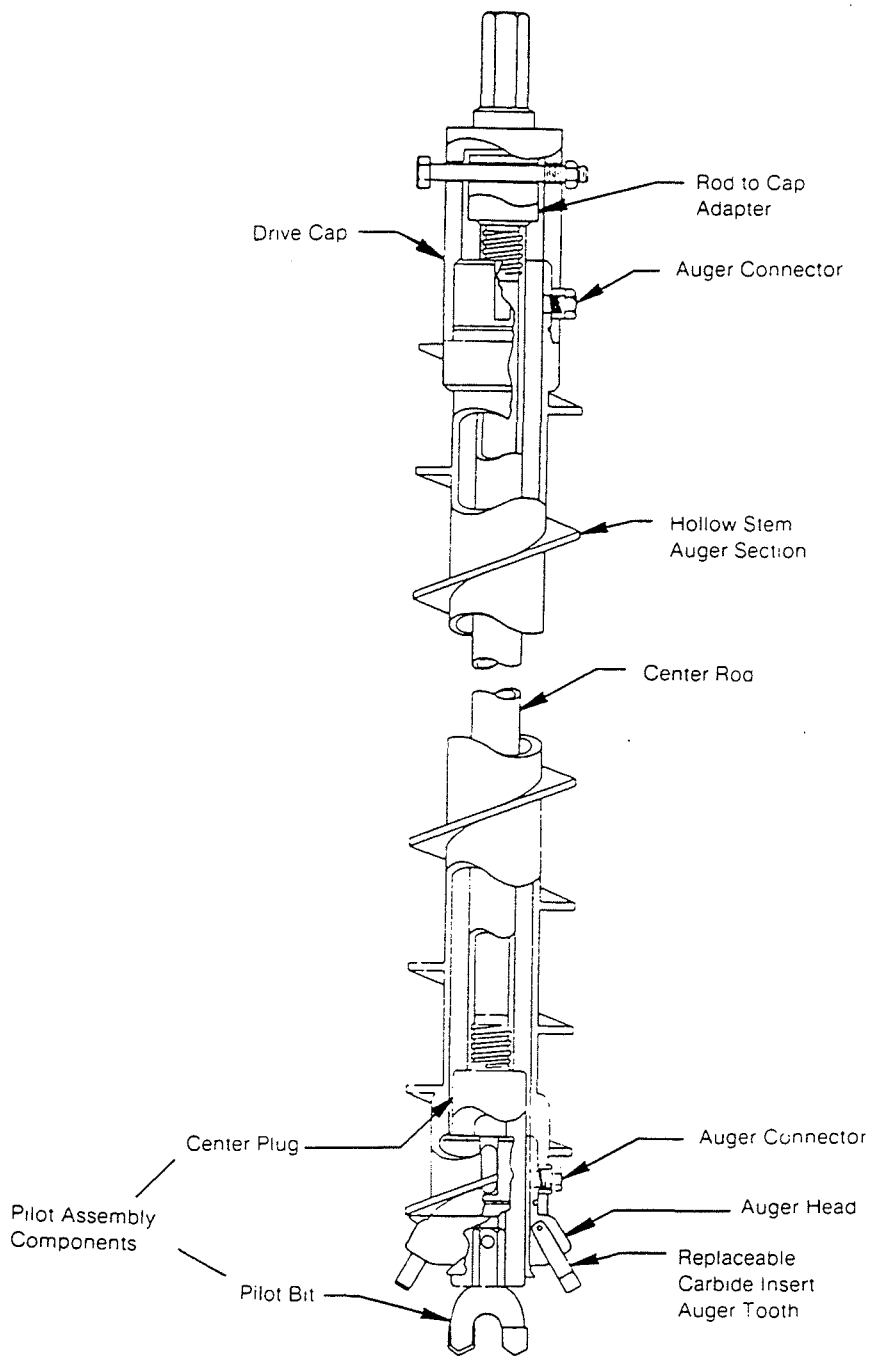

Figure 3. Typical components of the down-hole tools used with the hollow-stem auger drilling method (Aller et al, 1989).

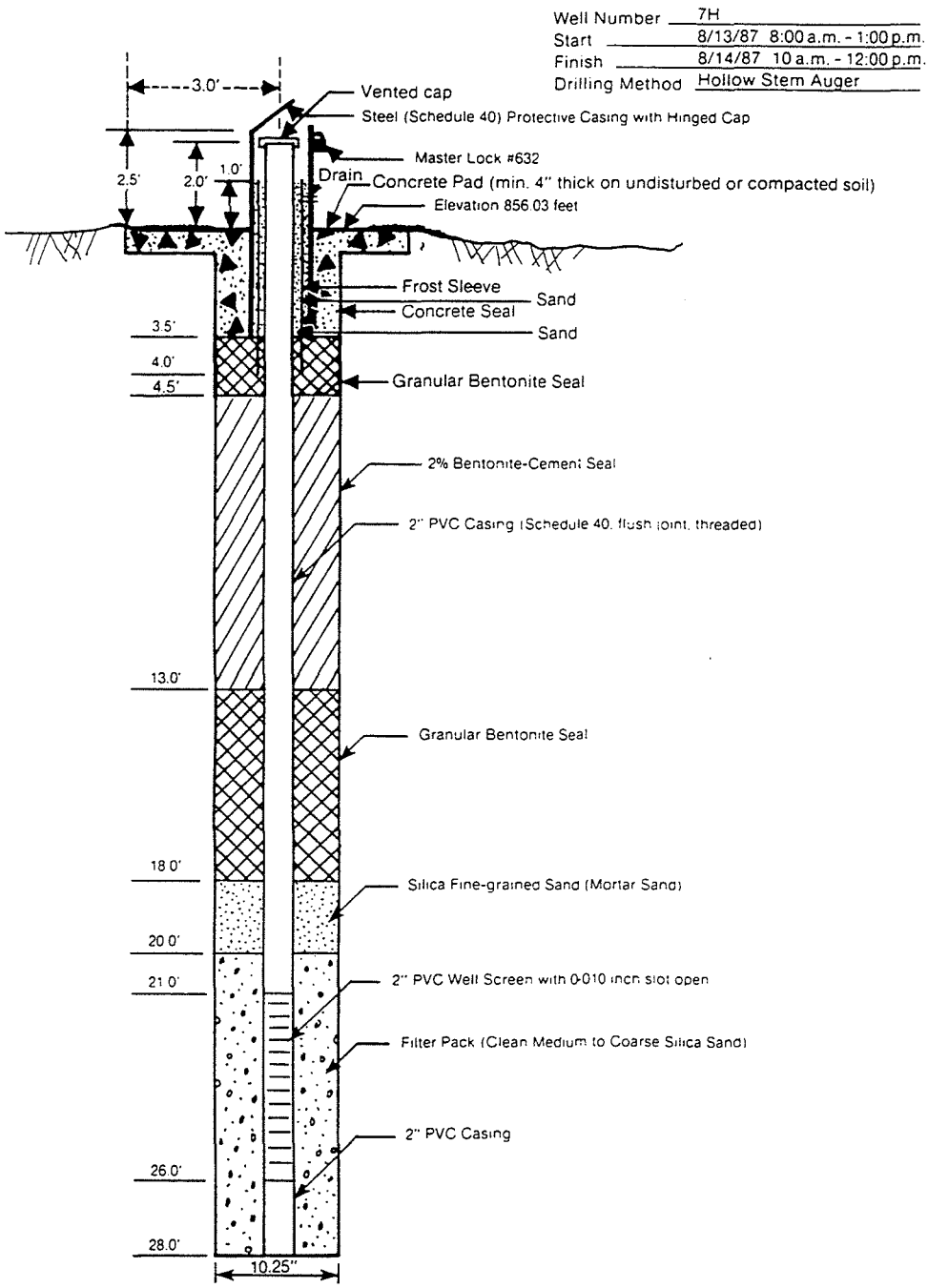

Figure 4. Typical monitoring well completion diagram showing the materials and dimensions of each component (Aller et al, 1989).

ROCK CORE DESCRIPTION

parratt wolff inc

The following components are commonly used by our drillers to describe collected rock cores:

depth of core run;
run number (R-1, R-2, etc.);
recovery (in feet);
rate of penetration - recorded as "minutes per foot" of penetration (ex: MPF = 6); and
generalized rock description (i.e. Red/brown sandstone).

If the rock is logged by a Parratt-Wolff, Inc. geologist, the rock core descriptions will also commonly include:

recovery (in percent);
rock quality designation (RQD); and
detailed rock description.

The RQD or "Rock Quality Designation" is the combined length of all core pieces whose individual lengths are greater than four inches, divided by the length of the core run. RQD is typically only used when describing NX cores or larger.

EXAMPLE OF DETAILED ROCK DESCRIPTION:

"Brown, thin bedded, fine-grained sandstone, highly weathered, soft, close fractured".

The components used to describe the rock core in detail are color, thickness of bedding, rock type, weathering state, hardness, and joint or fracture spacing. Additional components, such as texture, are used to further describe the rock as needed. The following tables include the definitions of these different rock descriptive terms.

Component	Term	Defining Characteristic
Bedding Thickness	Laminated	< 0.1 in.
	Very Thin Bedded	0.1 - 1.0 in.
	Thin Bedded	1.0 - 4.0 in.
	Medium Bedded	4.0 - 12.0 in.
	Thick Bedded	12.0 - 36.0 in.
	Massive	> 36 in.
Hardness	Soft	Scratched with fingernail
	Medium Hard	Scratched with a knife
	Hard	Difficult to scratch with a knife
	Very Hard	Can not be scratched with a knife
Joint or Fracture Spacing	Very Close	< 1.0 in.
	Close	1.0 - 2.0 in.
	Moderately Close	2.0 - 12.0 in.
	Wide	12.0 - 36.0 in.
	Very Wide	> 36.0 in.
Weathering State	Fresh	No visible sign of decomposition or discoloration
	Slightly Weathered	Slight discoloration inward from open fractures
	Moderately Weathered	Discoloration throughout fracture. Weaker minerals such as feldspar are decomposed.
	Highly Weathered	Most minerals are somewhat decomposed. Specimens can be crumbled by hand with effort and easily scraped by a knife.
	Extremely Weathered	Rock is decomposed to extent that it looks like soil, but original fabric or structure are preserved.

Figure 5 Components & Definitions Used to Describe Rock Core Samples

Calculations:

Core recovery = total length of all recovered pieces.

RQD = the sum of all pieces greater than 4" in length, divided by the length of the run.

Example:

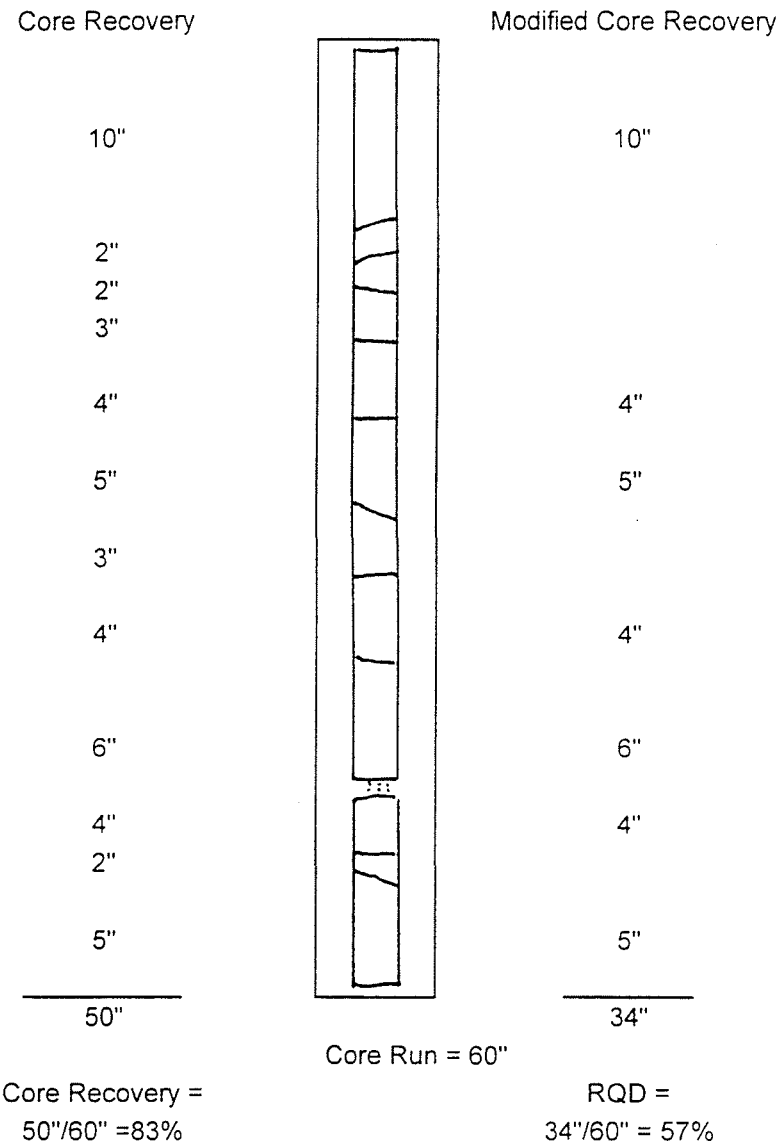

Figure 6 Method for calculating RQD - Rock Quality Designation.

TEST BORING LOG

parratt wolff inc

PROJECT XYZ Facility

HOLE NO. B-1

LOCATION Syracuse, New York

JOB NUMBER: 9700

GROUNDWATER DEPTH
WHILE DRILLING 12.0'

DATE STARTED 8/10/97
DATE COMPLETED 8/10/97

BEFORE CASING
REMOVED 22.0'

N - NO. OF BLOWS TO DRIVE SAMPLER 12" W/140# HAMMER FALLING 30" - ASTM D-1586 STANDARD PENETRATION TEST

AFTER CASING
REMOVED 19.0'

C - NO. OF BLOWS TO DRIVE CASING 12" W/ # HAMMER FALLING "/ OR PERCENT CORE RECOVERY

CASING TYPE HOLLOW STEM AUGER, NQ WIRELINE

SHEET 1 OF 1

Subsurface Elevation: 100.0'

DEPTH	SAMPLE DEPTH	SAMPLE NO.	C	SAMPLE DRIVE RECORD PER 6"		N	DESCRIPTION OF MATERIAL	STRATA CHANGE DEPTH
	0.0'-	1		11	15		Dry brown clayey fine to coarse SAND with	
	2.0'			17	5	32	little fine gravel (SW-SC)	
5.0								7.0'
	7.0'-	2		1	2		Firm moist red-brown silty CLAY with trace	
	9.0'			4	6	6	gravel (CL)	
10.0								
15.0								15.0'
	15.0'-	3		10	25		Hard moist brown silty SAND with some fine	
	17.0'			30	30	55	subrounded gravel (SM)	
20.0							Top of Weathered Rock	20.0'
	20.0'-	R-1	Rec	NX CORE			Brown thin bedded fine grained SANDSTONE,	
	25.0'		5.0'				highly weathered, soft, close fractured	
			100%					
			RQD=68%					
25.0								
	25.0'-	R-2	Rec				Gray thick bedded CRYSTALINE LIMESTONE,	
	30.0'		4.0'				slightly weathered, medium hard, wide	
			80%				fractured	
			RQD=90%					
30.0							Bottom of Boring	30.0'

Figure 7
Typical Test Boring Log

☐ P.O. Box 56, 5879 Fisher Road, East Syracuse, NY 13057 Telephone 315-437-1429 or 800-782-7260 FAX 315-437-1770
☐ P.O. Box 1029, 501 Millstone Drive, Hillsborough, NC 27278 Telephone 919-644-2814 or 800-627-7920 FAX 919-644-2817

Drumlin-Bluff And Baymouth-Barrier Erosion Along the Southeastern Shore of Lake Ontario, New York

Paul R. Pinet
Charles E. McClennen
Department of Geology
Colgate University
Hamilton, NY 13346
email: ppinet@center.colgate.edu
email: cmcclennen@center.colgate.edu

Introduction

The coastline of Lake Ontario has a long, complicated history of rapid morphologic development. The purpose of the trip is to examine the principal landform elements of this lakeshore sector -- drumlin bluffs and baymouth barriers (Fig. 1) -- in order to understand the shoreline's primary evolutionary history. Our focus will be on the coastal geomorphic changes that have occurred since the beginning of this century. The specific goals are 1) to assess our proposed model of coastal bluff evolution, 2) to examine the sedimentological interconnections between bluffs and baymouth barriers, and 3) to appraise the long-term impact (50-100 years) of engineered shore-stabilization structures.

A Synopsis of the Pleistocene-Holocene History of Southeastern Lake Ontario

The present-day shoreline processes of Lake Ontario are best understood against the backdrop of 1) glaciation/deglaciation that occurred between 35,000 and 10,000 years ago and 2) the post-glacial events of the Holocene. The relevant geologic events of these two time periods are summarized below.

Late Pleistocene Events

Pleistocene glaciation which began about 2 million years ago has had a profound effect on the land morphology and surficial deposits of Upstate New York. Repeated advancements and retreats by thick continental ice sheets originating in Canada have carved the bedrock, laid down glacial tills, and produced a variety of glacial landforms. The most recent advancement of the Laurentide Ice Sheet reached its maximum southerly extent some 35,000 to 25,0000 years ago, at which time it covered virtually all of New York State. The topography immediately south of Lake Ontario is dominated by an extensive drumlin field, which reflects the former presence of thick continental ice sheets in central and northern New York. Drumlins are elongated hills of glacial till that in Upstate New York range in height between 15 and 50 m and that are oriented north-south parallel to the inferred regional flow direction of the the Ontario Lobe of the Laurentide Ice Sheet. The specific origin of these drumlins is controversial. Although the consensus among glacial geologists is that the drumlins were formed and sculpted by the flow of ice (Dremains and Goldthwaite, 1973), others have recently proposed that meltwater at the base of the ice sheet during deglaciation is an unappreciated agent of drumlin construction (Shaw, 1983; Shaw and Gilbert, 1990). Regardless of their exact genesis, drumlins eroded by waves serve as the foremost point sources of sediment currently supplying the southern Ontario lakeshore. The drumlins are closely spaced to one another, and the low areas between them along the coast appear as bays, wetland swamps, harbors, and agricultural fields.

Holocene Events

With the waning of the Pleistocene, the various ice lobes of the Laurentide Ice Sheet retreated and released copious quantities of meltwater that produced numerous small and a few large glacial lakes. Some of this meltwater filled in topographic depressions, and some of it was ponded against the southern terminus of the receding ice sheet. An example of the latter in Upstate New York is Glacial Lake Iroquois, which was created about 11,0000 years ago

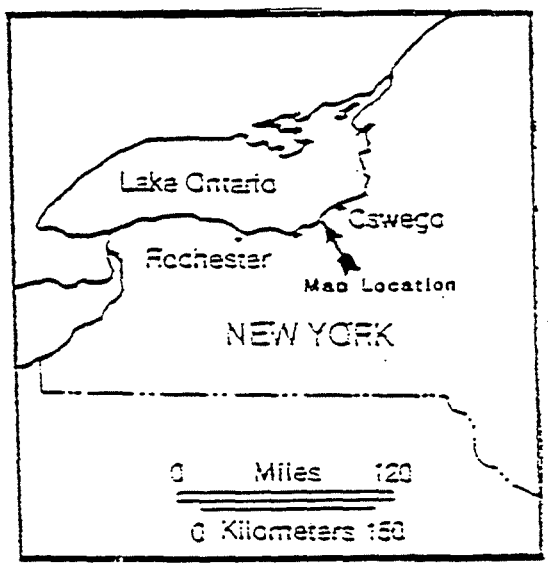

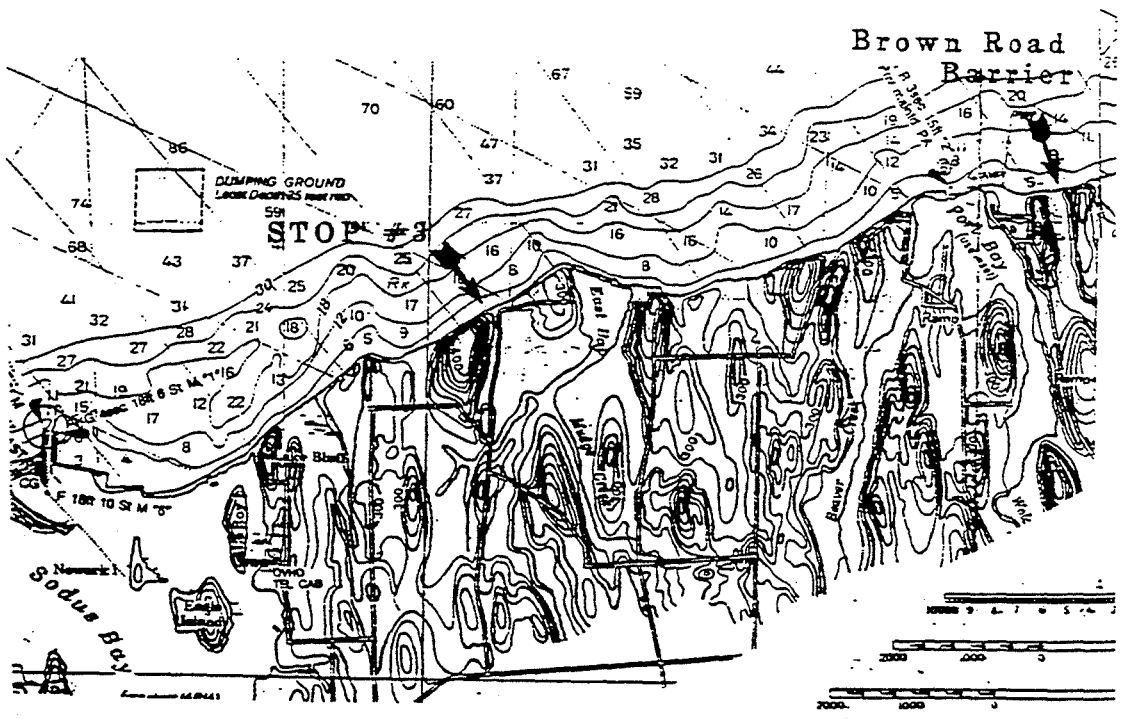

Figure 1. Coastal chart of a stretch of the southeastern shore of Lake Ontario that shows location of three main field stops.

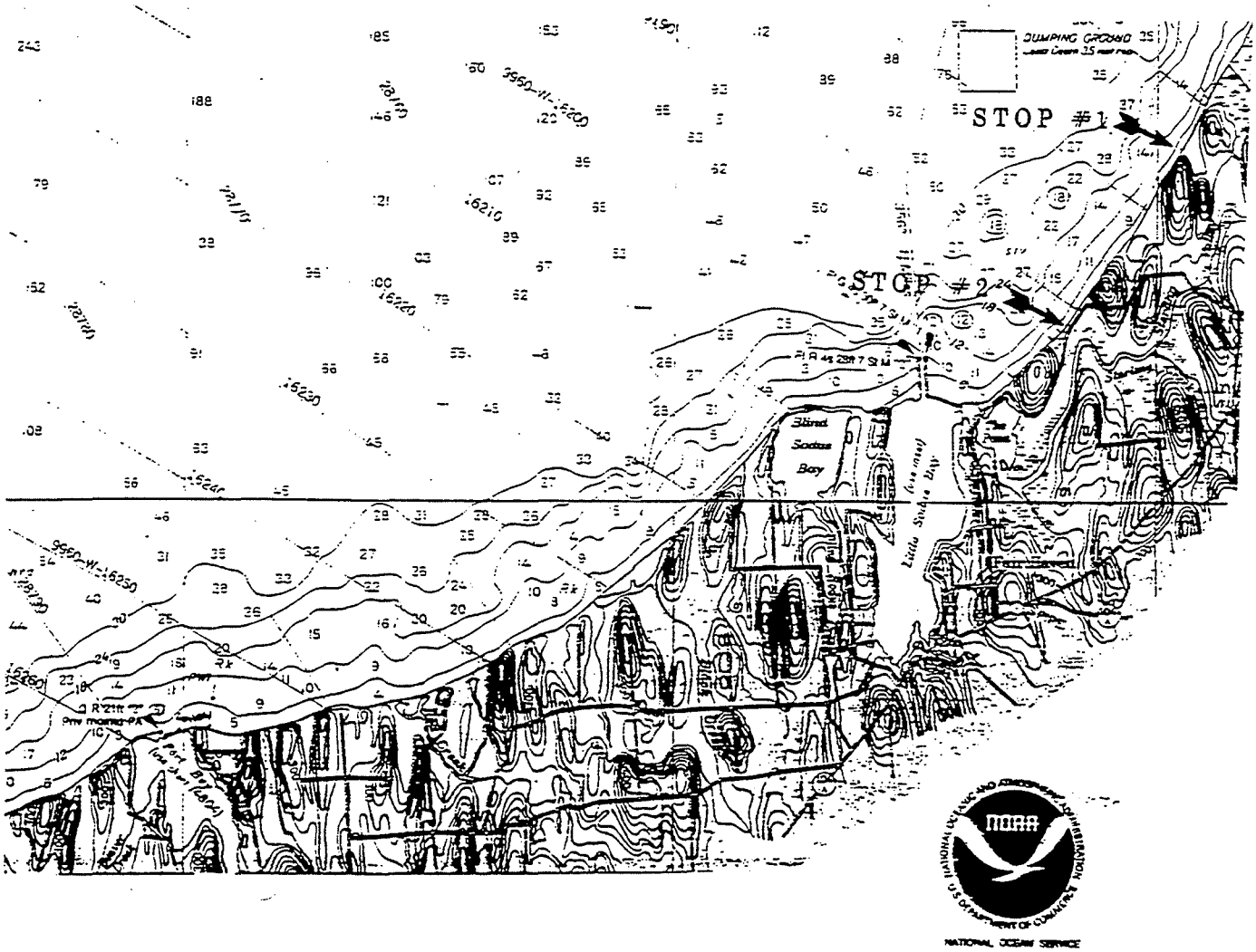

Polyconic Projection
Scale 1:80,000
North American Datum of 1983
(World Geodetic System 1984)
SOUNDINGS IN FEET

UNITED STATES — GREAT LAKES

LAKE ONTARIO - NEW YORK

FEET

YARDS

METERS

(Karrow and others, 1961; Calkin, 1970). Lake Ontario is a remnant of this much deeper and more extensive body of water. About 55 km of the Lake Iroquois shoreline between Rochester and Sodus Bay can be followed by tracing a series of truncated drumlins, downdrift baymouth barriers, wave-cut terraces, and flat lake plains on topographic maps (Muller and Cadwell, 1986; McKinney, 1997). Lake Iroquois was almost 50 m deeper than Lake Ontario is today, implying that present-day coastal drumlins were covered by water; this explains the truncation of and the presence of water-worked deposits on the crests of some of the taller drumlins, such as Chimney Bluffs. Field studies indicate that the main outlet of Lake Iroquois was to the east near Rome, New York with the lakewater discharging into the Mohawk Valley and Hudson River watershed. As the glacial ice dam to the north of Lake Iroquois melted, the lake's level dropped markedly as water discharge was established through the lowlands of the St. Lawrence River, as it remains today for Lake Ontario.

Once Lake Iroquois drained, a new strandline was established somewhere to the north (lakeward) of the current Lake Ontario shore. Drumlins that earlier had been submerged beneath Lake Iroquois water were subaerially exposed as the lake drained. The southern lakeshore then entered a stage of erosional transgression as the basin was tilted southward by differential isostatic uplift. Because the ice sheet was thicker and retreated later in Canada than in New York, glacial rebound was and continues to be greater along the northern than the southern margin of Lake Ontario. Drumlins in Upstate New York were systematically eroded away by breaking waves as the shoreline advanced southward to its current position. The former presence of offshore drumlins is indicated by boulder pavements that occupy about 40 % of the lake bottom to a distance of 4 km offshore (Fig. 2). Based on their distribution and shape, the boulder fields are interpreted as lag deposits of the largest materials (boulders and large cobbles) in the drumlin till that could not be carried away by wave activity and longshore currents (Mutch and McClennen, 1996).

At present, the southeastern shoreline of Lake Ontario consists of a series of alternating drumlin bluffs and baymouth barriers (Fig. 1). Wave notching, slumping, and gullying of the drumlin bluffs provide sediment to the nearshore and offshore zones. The mud component is suspended and fluxed offshore (Sutton and others, 1974; Thomas and others, 1972; McKnight and McClennen, 1997), whereas the coarse fraction -- sand and gravel -- is dispersed to the east by the prevailing longshore drift and is accreted to baymouth barriers that separate bays, ponds, and marshes from the lake proper (Brennan and Calkin, 1984; Christensen and others, 1990). Our studies suggest that the Ontario strandline can be subdivided into coastal compartments, each consisting of a drumlin bluff-baymouth barrier couplet (Fig. 3); the bluff serves as a point source of sand and gravel in the compartment which are fluxed eastward to a downdrift baymouth barrier (Pinet and others, 1992; Pinet and others, 1993). Although these compartments appear to be closed over the short term (years to decades), it is unclear whether or not they "leak" sediment into adjoining compartments over the long term. During the course of this trip, we will examine several of these coastal couplets, and offer an argument for their closure at least over the short term (~50 yrs).

Model of Bluff Evolution

A cursory examination of Lake Ontario bluffs reveals that their morphological character depends on the relative interplay of wave notching, slumping, and gullying. The extent of gullying is directly correlated to the height of the bluff (Fig. 4). The taller the bluff, the more deeply incised and larger the gullies tend to be. Bluffs that are no higher than about 15 m are ungullied and display steep, planar surfaces created by slumping activity (Covello and others, 1993; Pinet and others, 1997).

Our field studies indicate that the individual coastal bluffs of Ontario undergo distinct phases of morphological development, progressing systematically through young, mature, old, and terminal stages (Pinet and others, 1997). As the drumlin is eroded back by the transgressing lakeshore, its bluff height changes systematically, at first increasing until it attains a maximum height above the lake level that depends on the elevation of the drumlin's crest and thereafter decreasing until the last vestige of the drumlin is destroyed by wave erosion (Fig. 5). Below we describe the features and processes that characterize each of the four morphological bluff stages.

Young Bluff Stage

When lake waves first bite into the northern end of the drumlin, they create a low bluff. Wave notching directed at the bluff's base destabilizes the slope and causes slumping (Fig. 6). The slumped debris that collects at the foot of

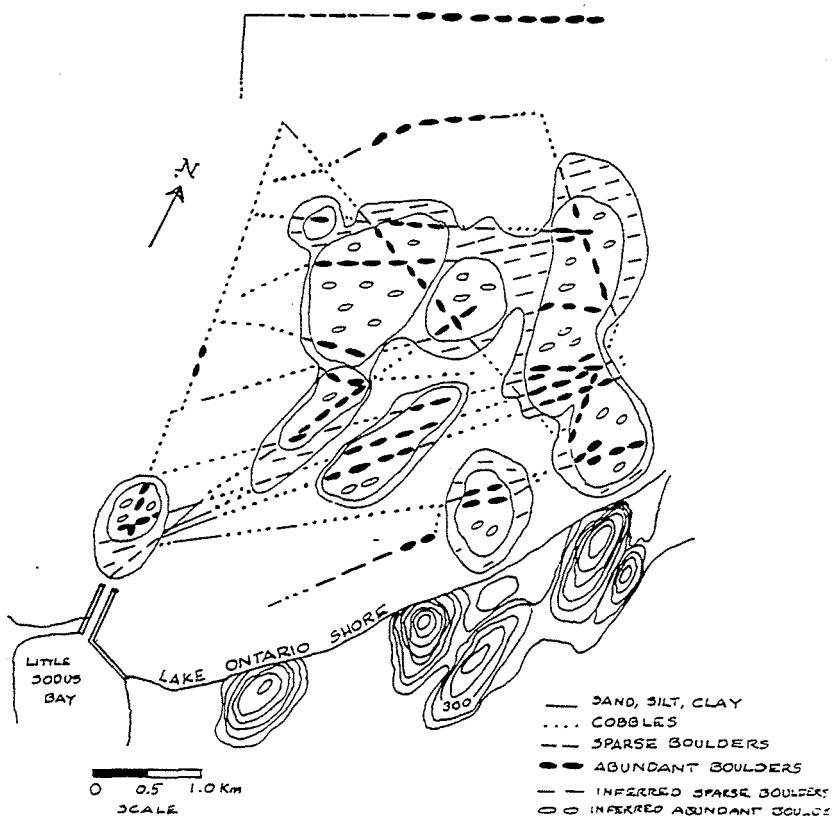

Figure 2. Interpretive map of side-scan data showing locations of boulder fields that are interpreted as lag deposits of formerly-existing drumlins.

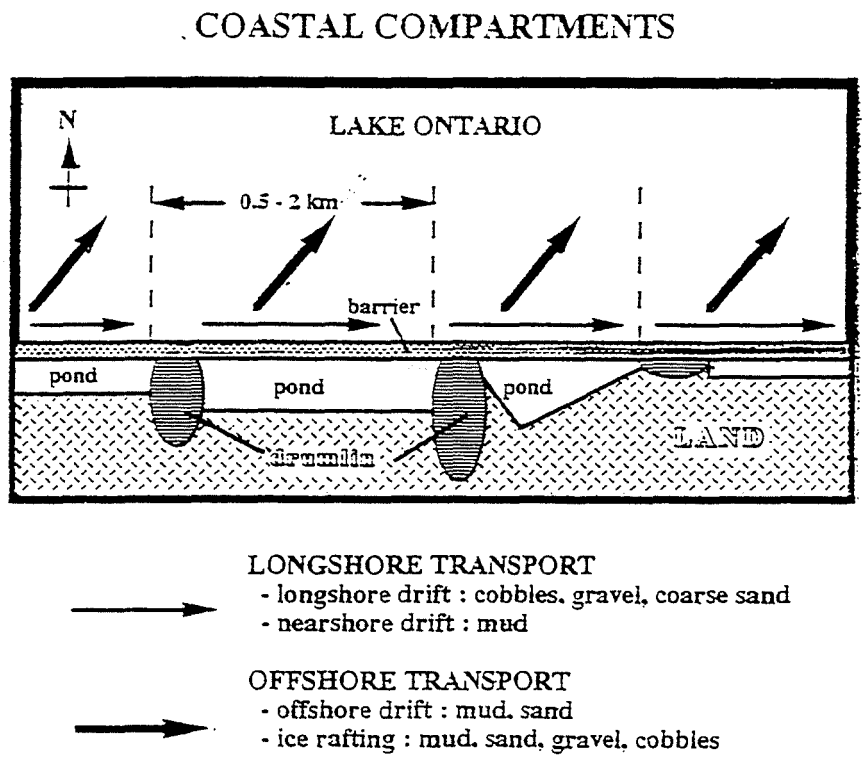

Figure 3. The southeastern Ontario lakeshore can be divided into coastal compartments, each consisting of a drumlin bluff - baymouth barrier couplet. The coastal compartments seem to function as closed systems over the short (< 50 yrs) term.

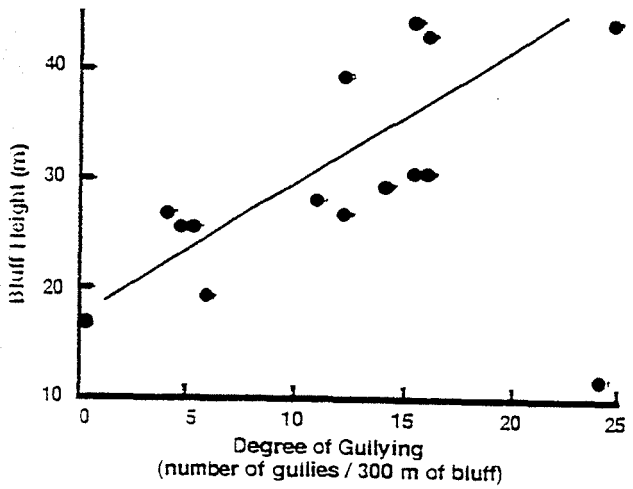

Figure 4. There is a strong correlation between the topographic height of a bluff and the degree of gullying.

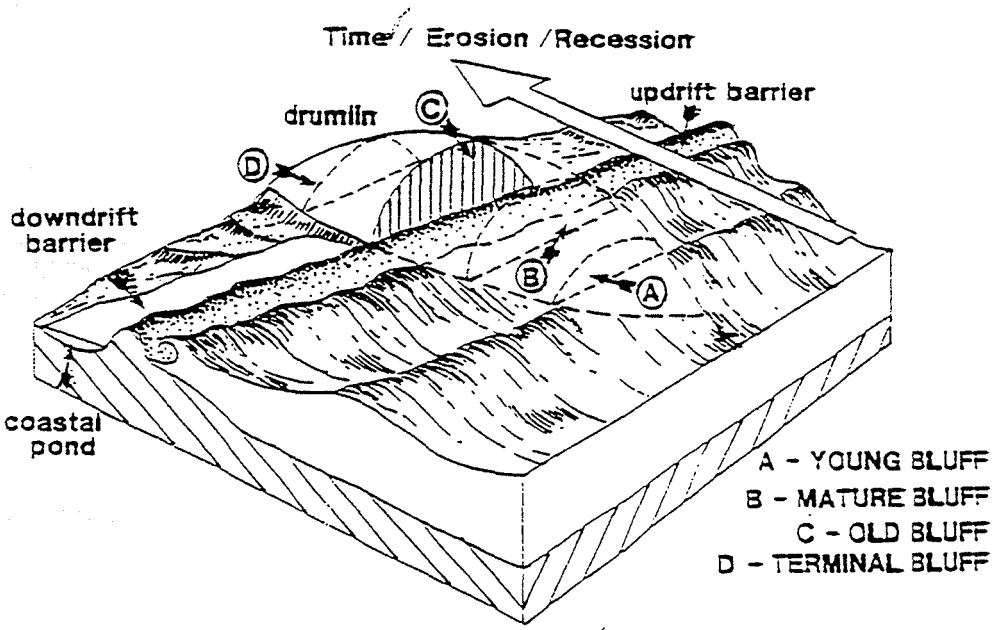

Figure 5. As a drumlin is eroded by a transgressing shoreline, the breadth and height of the resultant bluff change systematically. We have identified four distinct developmental stages -- young, mature, old, and terminal -- that are related to these morphologic changes.

the drumlin is sparse because of the low height of the bluff. In short order, breakers sort out the material in the slump masses that collects at the base, moving the suspended mud offshore and dispersing the sand and gravel to the east promoting the development of a downdrift baymouth barrier. As the drumlin is eroded back, the bluff increases in height due to the parabolic shape of the drumlin's longitudinal axis; this results in increasingly greater amounts of debris that is supplied to the adjoining beach, which as a result grows in height and width. Groundwater seepage and surface runoff (Fig. 7) carve rills and channels into the steep slump face. However, the channels do not evolve into large gullies because of the frequency of gravity slides that result from the persistent destabilization of the cliff by wave notching. This condition reflects the meager quantities of sediment that are supplied to the beach by the still relatively low-lying bluff. The domination of gravity sliding maintains a steep (> 45 degrees), planar bluff face, and the base and top of the bluff retreat landward at similar rates (Fig. 6).

Mature Bluff Stage

Recent field measurements (Montesi and Pinet, 1997) suggest that when bluffs attain a height of about 22 m above the lake level, the system crosses a geomorphic threshold and the dominant processes that denude the drumlin change dramatically. This changeover reflects the increasing quantities of sediment supplied to the beach by the collapsing bluff face which grows in height as more of the drumlin is excavated by the transgressing shoreline. Because the sediment input by gravity sliding to the beach exceeds the rate at which the debris effectively can be removed by waves and longshore currents, the base of the bluff becomes increasingly more protected from wave notching except under extreme storm conditions and/or under unusually high lake levels. This armoring effect reduces the frequency of slumping events because the bluff face is now rarely undercut and, hence, destabilized by wave attack.

The steep, stable face of a mature bluff is subjected to extensive groundwater seepage and surface runoff (Fig. 7) that in some cases are controlled by joint systems in the semi-indurated glacial till. As a consequence, channels become enlarged, as they are deepened by downcutting, and widened and lenghtened by lateral and headward erosion respectively. Eventually an extensive gully network is incised into the bluff face. The gullies when fully formed have a characteristic shape that includes a steep headwall that surrounds a bowl-shaped head region (this reflects control by groundwater stoping which promotes slumping), near vertical sidewalls that converge down gully into a narrow throat, moderate (< 45 degrees) longitudinal gradients to the gully bottom, and the presence of a colluvial fan composed of mud flow deposits that build outward onto the beach. Colluvial fans at adjoining gully mouths can coalesce to form an extensive colluvial terrace on the upper beach.

The sedimentological system of a mature bluff differs markedly from that of a young bluff. As described above, young bluffs are affected largely by lake conditions, whereby waves cut away at the bluff's base and induce frequent slumping. By contrast, mature bluff systems are controlled by the terrestrial environment, as groundwater seepage and surface runoff incise gullies into the bluff face. Headward erosion causes the gully system to lengthen and to cut deeply and irregularly into the drumlin (Fig. 6). Under heavy, persistent rain, slumped material that accumulates at the base of the gully's headwall is liquefied, producing mud flows that work there way downcanyon, eventually passing through the topographic constriction at the gully's throat and spilling onto the beach to form a colluvial fan. These fans effectively protect the bluff's base from direct wave attack which serves to stabilize the lower bluff. Hence, the top of a mature bluff erodes landward rapidly and is irregular in plan view, whereas the cliff's base is stabilized by the deposition of ample quantities of colluvium that spills out of the active gully mouths onto the beach deposits (Fig. 6). The colluvium protects the cliff base from direct wave attack, and reduces its recessional rate.

Old Bluff Stage

Groundwater and surface water drainage change appreciably with the onset of the old stage of bluff evolution. After about half of the drumlin is eroded, little groundwater and surface runoff drain lakeward; most of it flows landward away from the bluff face (Fig. 7). As such, the well developed network of gulleys becomes relatively dry and inactive. This reduces the supply of sediment to the beach, allowing waves to erode the beach back and eventually to undercut the bluff, causing slumping and reestablishment of a steep slump face that is superimposed on the gulley-floor profile (Fig. 6). As noted earlier, during the mature phase of bluff development, the top of the cliff retreats

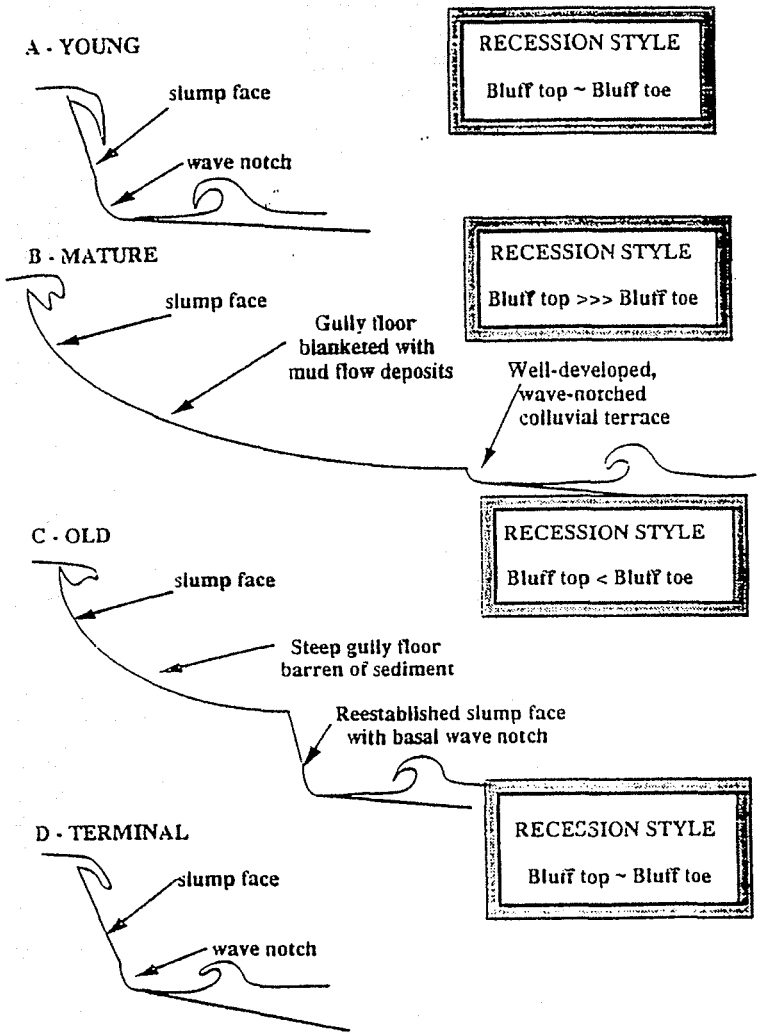

Figure 6. As described in the text, the height and morphological character of the bluff depends directly on its stage of development. Also, the recessional rate of both the top and base of the bluff vary widely depending on the bluff's evolutionary stage.

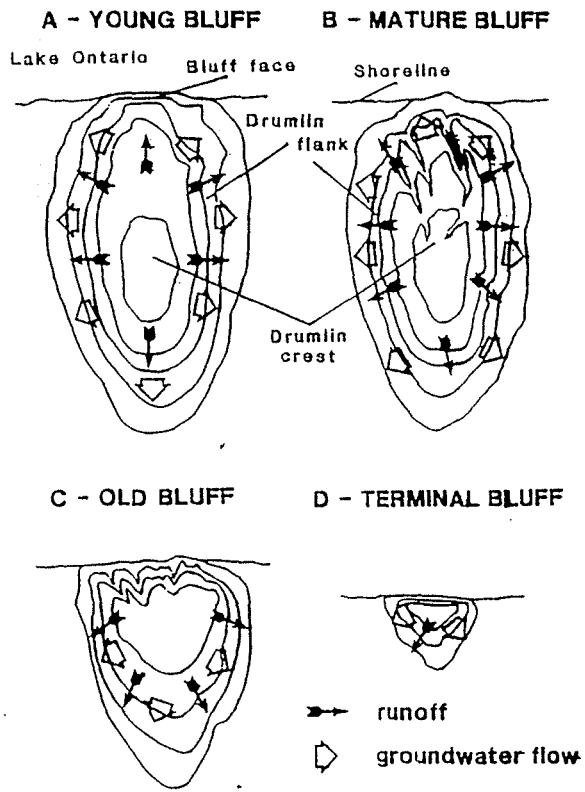

Figure 7. Young and mature bluffs are significantly affected by groundwater and surface water drainage. In contrast, old and terminal bluffs are not, drainage being directed landward away from the bluff face.

rapidly by headward erosion, whereas the cliff's toe remains more-or-less fixed because of the protection from wave activity afforded by an ample sediment supply to the beach. Once the mature bluff reaches the old stage of development, erosion of the cliff's base is reactivated and the cliff's top becomes relatively stable due to a reduction in the rate of headward erosion. With time, the steep slump face grows in height as it retreats, until the gully profile is eradicated entirely, at which point recession of the top and bottom of the cliff occurs at a uniform rate. As the drumlin is eroded further, the bluff height decreases causing a systematic diminution of the sediment supply to the cliff's base.

Terminal Bluff Stage

The final phase, the terminal stage, is a topographically low, steep bluff that results from the domination of wave notching and slump collapse of the cliff (Fig. 6). The bluff contributes increasingly less sediment to the beach as the last vestige of the drumlin is obliterated by the advancing shoreline. The only surviving evidence for the former existence of a drumlin is a boulder field (a lag deposit) in the nearshore zone that approximates the shape of the original drumlin (Fig. 2).

The Drumlin Bluff - Baymouth Barrier Couplet

Sand and gravel that are fractionated from the drumlin till and mud flow deposits of the colluvial fans are transported to the east by the prevailing longshore currents where they are shaped by waves into a baymouth barrier (Fig. 3). Clearly, any change in the rate of bluff erosion is going to affect the supply of sediment to the downdrift barrier. Rapid retreat of the bluff assures an ample longshore drift of sand and gravel, which results in a broad (> 20 m), high (~ 2 m) baymouth barrier. Conversely, the slow recession of a drumlin cliff depletes the sediment supply to the adjoining barrier which will then be low-lying and narrow. This sediment-starved barrier will be susceptible to wave overwash and, as such, will migrate landward by "rollover" processes, as sand and gravel on the lake side of the barrier are transported by overwah over the low crest to the backside of the barrier. This very process has occurred at the Brown Road barrier (Fig. 1) as waves associated with a severe storm overtopped the crest of the lowlying barrier causing it to shift landward by several meters (Fig. 8A). The same storm had no effect on the tall Juniper Pond barrier which lies downdrift of Sitts Bluff, the drumlin located to the west of McIntyres Bluff (Fig. 8B).

According to our model , the supply of sediment to the cliff base and by extrapolation to the downdrift barrier depends directly on the bluff's stage of development. The quantity of sediment that is fluxed to the downdrift barrier is greatest for the mature bluff stage when large colluvial fans at the mouth of the gulleys are growing onto the beach and even into the lake. Storm waves erode these deposits and longshore currents transport the material downdrift. Coversely, the amount of sediment eroded from the drumlin cliffs is least during the early young and late terminal bluff stages, times when the bluff height and hence sediment supply to the beach and baymouth barrier are low. In essence, the sustained and rapid erosion of a bluff results in a robust baymouth barrier, whereas a protected or stabilized bluff produces a narrow, landward-migrating baymouth barrier. As we shall see, protecting the base of drumlin cliffs with shore-stabilization structures accelerates the erosion and landward migration of the coastal compartment's downdrift barrier.

The Long-Term Impact of Shore Stabilization Measures at Little Sodus Bay

Little Sodus Bay (Figs. 1 and 9), located in Cayuga County about 25 km to the west of Oswego, New York, has been a center for trade and commerce dating back to the late 17th Century. Because of shifting shoals that interfered with shipping, jetties were constructed to stabilize the bay's inlet and to provide harbor protection. Construction on the west jetty began in 1854 and was completed by 1885; construction of the east jetty, initiated in 1872, was finished by 1906. Hence, the harbor mouth has been stabilized for about a century, offering an opportunity to assess the long-term consequences of these shore-protection structures.

Other artificial structures were built in the region in order to mitigate coastal erosion. For example, jetties stabilizing the inlet to The Pond (Fig. 9) are evident in aerial photos from 1938 to 1963, are not apparent in 1974 photos, but are visible on 1978 photos. Also, two groins were emplaced about 0.8 and 1.2 km to the east of Little Sodus Bay sometime before 1938; only the easternmost one survives today. Two additional groins (piers) were built

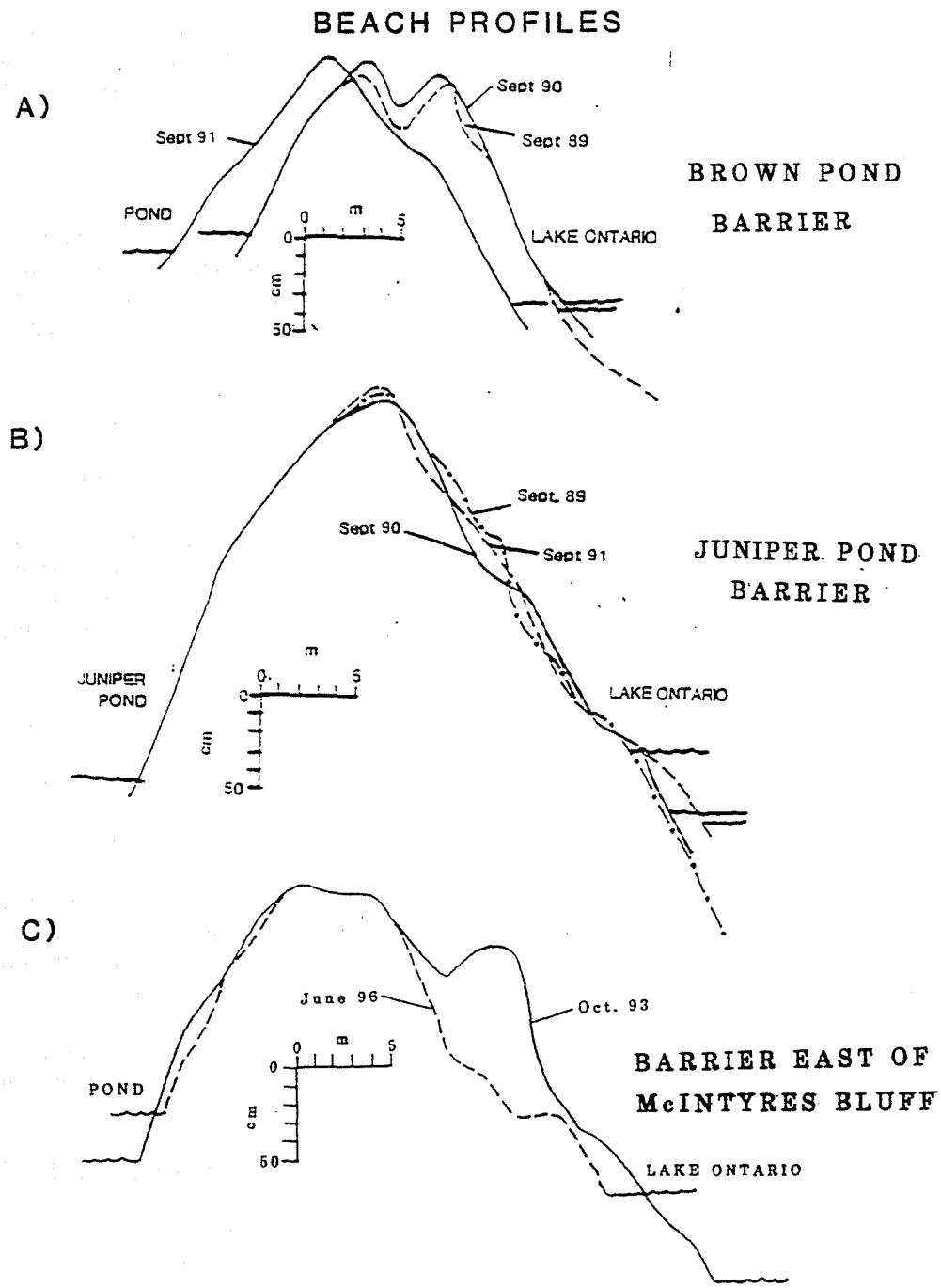

Figure 8. Beach profiles measured at selected shore sites. There exact locations are shown in Figures 1 and 12. All the profiles are drawn with a vertical exaggeration of 10X.

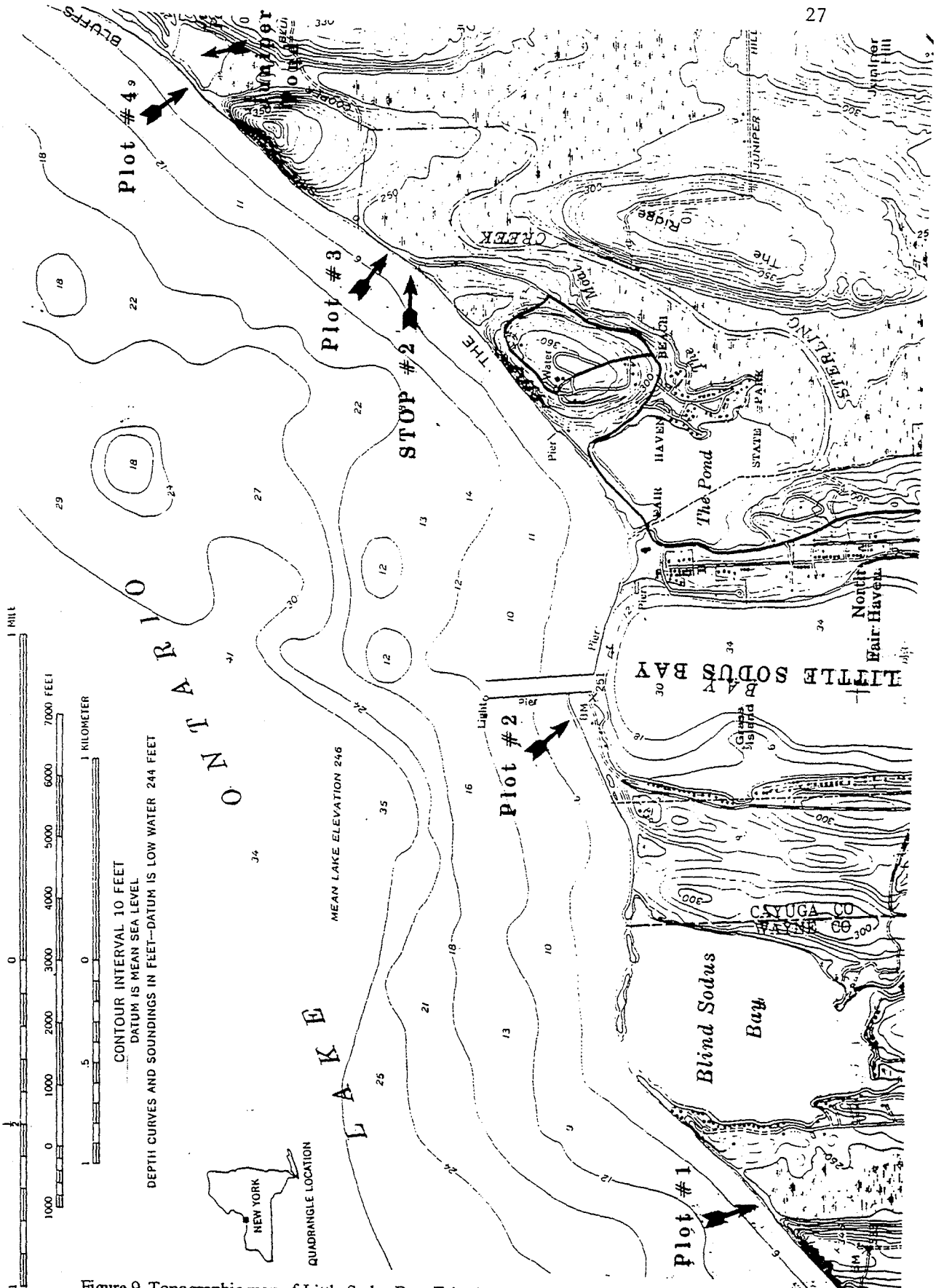

Figure 9. Topographic map of Little Sodus Bay, Fair Haven, showing the location of Stop #2 and of four sites (Plots 1 -4) where recessional rates were estimated from a comparison of aerial photos; the latter are reproduced in Figure 10.

sometime between 1954 and 1960 about 2.2 and 2.4 km to the east of the harbor mouth. In addition, the entire shoreline extending from the east jetty of Little Sodus Bay to the the eastern edge of the drumlin bluff that is part of Fair Haven Beach State Park -- almost 2 km of lakeshore -- has been armored with an array of seawalls, revetments, and riprap.

A careful comparison of a series of aerial photos and in the case of the harbor mouth old survey charts reveals the 50- to 100-year long history of coastal change for four specific sites (Figs. 9 and 10). Our studies indicate that the net longshore drift is to the east, with short-term reversals of the prevailing drift during Nor'easters. We assume that the shore system consists of a series of coastal compartments consisting of a drumlin bluff-baymouth barrier couplet, the latter receiving the bulk of its sediment supply from erosion of the former. Our general conclusions are as follows:

1. The trend over time for the barrier located on the west side of Blind Sodus Bay has been net erosion, amounting to about 40 m of retreat since 1954; this translates to an average recessional rate of a bit more than 1m/yr. Note the marked shoreline progradation that occurred in the 1960s (Fig. 10). The limited amount of sediment supplied to the barrier presumably is derived from erosion of the drumlin bluff located updrift of the baymouth barrier (Fig. 9).

2. Since 1880, the beach adjacent to the west jetty of Little Sodus Bay has prograded by more than 140 m, due to entrapment of longshore drift (Fig. 10). This amounts to an average accretional rate of about 1.25 m/yr. However, note that the build-up was completed by the 1950s, and that there have been significant erosional periods during the 1970's. A dynamic "steady state" may have been reached since the 1950s. The lakeshore immediately downdrift of the east jetty has no sediment whatsoever (Fig. 9); an artificial breakwater separates the water of Little Sodus Bay from Lake Ontario.

3. The drumlin located immediately to the east of The Pond lies within the Fair Haven Beach State Park (Fig. 9); it is extensively armored with riprap and older sections of steel revetments. Also, the bluff is vegetated; this has stabilized its slope and reduced channeling and gullying of its face. These engineering measures have successfully reduced erosion of the bluff; however, this has interfered with the natural supply of sand and gravel to the small downdrift baymouth barrier of the compartment. This sediment-starved barrier is narrow and low, and has been and continues to be subjected to regular overwash which has resulted in rapid landward migration of the barrier into the backshore marsh. Our measurements indicate that the barrier has retreated landward by about 100 m since 1938, which amounts to a mean recessional rate of almost 2 m/yr (Fig. 10), a magnitude that is one of the highest that we have observed along the southeasten lakeshore of Ontario.

4. The Juniper Pond baymouth barrier (Fig. 9) appears to be in a quasi-equilibrium state since 1954, after having retreated by about 35 m between 1938 and 1954 (Fig. 10). Sitts Bluff, located updrift of the Juniper Pond barrier, is the supplier of sand and gravel for this coastal compartment. It is a mature bluff, judging from its morphology, and it is supplying sufficient sediment such that the barrier is relatively tall and broad, and, hence, stable (Fig. 8B).

References

Brennan, S. F., and Calkin, P. E., 1984, Analysis of bluff erosion along the southern coastline of Lake Ontario, New York: New York Sea Grant Institute, Albany, New York, 74 p.

Calkin, P. E., 1970, Strand lines and chronology of the glacial Great Lakes in northwestern New York: The Ohio Journal of Science, v. 70, n. 2, p. 78-96.

Christensen, S., McClennen, C. E., and Pinet, P. R., 1990, Coastal erosion: Southeastern Lake Ontario shore: Geological Society of America Abstracts with Programs, v. 22, p. 7.

Covello, , D. M., Knotts, K. A., Pinet, P. R., and McClennen, C. E., 1993, Erosional dynamics and morphological analysis along the southeastern Lake Ontario shoreline: Geological Society of America Abstracts with Programs, v. 25, p. 10.

Dreimanis, P. E., and Goldthwaite, R. P., 1973, Wisconsin Glaciation in the Huron, Erie, and Ontario Lobes: Geological Society of America Memoir 36, p. 71-106.

Karrow, P. F., Clark, J. R., Terasmae, J., 1961, The age of Lake Iroquois, Lake Ontario: Journal of Geology, v. 69, p. 659-667.

McClennen, C. E., and Pinet, P. R., 1993, Contrasts of lake and ocean beach sediments explained by Lake Ontario field

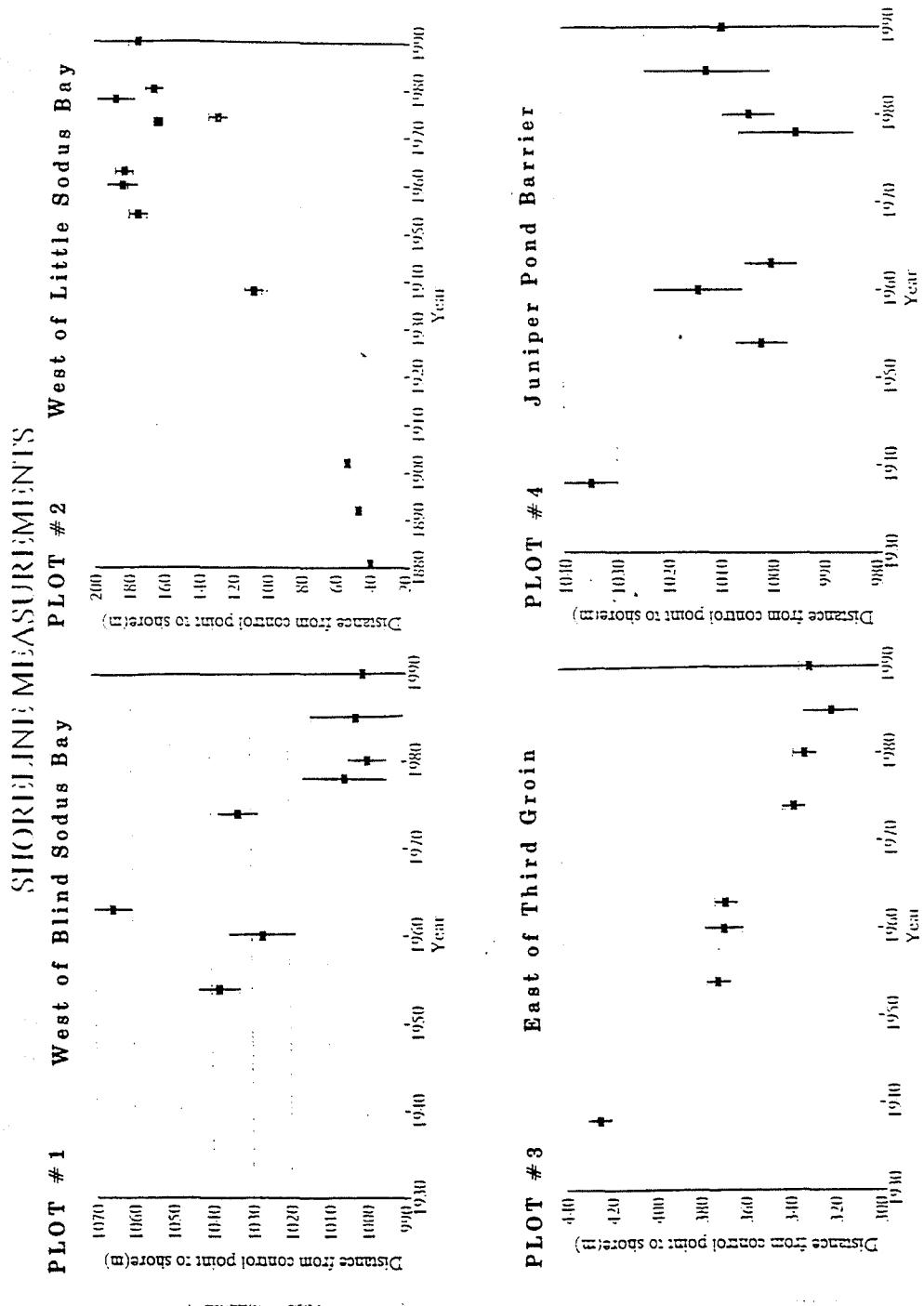

Figure 10. Each graph represents the position of the shore relative to a fixed, identifiable point on land as a function of time. The smaller the distance between the shore and the fixed control point on land, the greater the degree of erosion. The location of the plots are shown in Figure 9. Plot #1 and #3 show net erosion over time, plot #2 net deposition over time, and plot #4 little net change since 1954.

observations: Geological Society of America Abstracts and Programs, v. 25, p. A368.
McKinney, D. B., 1997, Glacial geology and badlands topography of Chimney Bluffs State Park, Wayne County, New York: The National Association of Geoscience Teachers Field Trip Guidebook, p. 1.1-1.13.
McKnight, A., and McClennen, C. E., 1997, Exploratory use of Chirp technology sub-bottom profiler in research of sediments and stratigraphy in southeastern Lake Ontario: Geological Society of America, v. 29, p. A65-A66.
Montesi, J. P., and Pinet, P. R., 1997, Assessment of geomorphic thresholds for coastal bluffs along the southeastern shore of Lake Ontario: Geological Society of America Abstracts and Programs, v. 29, p. A68.
Muller E. H., and Cadwell, D. H., 1986, Surficial geologic map of New York, Finger Lakes Sheet: New York State Museum -- Geologic Survey, Map and Chart Series #40.
Mutch, A., and McClennen, C. E., 1996, Side-scan sonar images of contemporary sediment transport and lage deposits on a coastal erosion terrace along the southeastern shore of Lake Ontario: Geological Society of America Abstracts and Programs, v. 28, p. 86.
Pinet, P. R., McClennen, C. E., and Moore, L. J., 1997, Resolving environmental complexity: A geologic appraisal of process-response elements and scale as controls of shoreline erosion along southeastern Lake Ontario, New York, *in* Welby, C. W., and Gowan, M. E., eds., A Paradox of Power: Voices of Warning and Reason in the Geosciences: Geological Society of America, in press.
Pinet, P. R., McClennen, C. E., and Moore, L. J., 1993, Coastal compartments of the southeastern shoreline of Lake Ontario: Geological Society of America Abstracts with Programs, v. 25, p. A368.
Pinet, P. R., McClennen, C. E., and Frederick, B. C., 1992, Sedimentation-erosion patterns along the southeastern shoreline of Lake Ontario: *in* April, R. H., ed., New York State Geological Association Guidebook, 64th Annual Meeting, p. 155-169.
Shaw, J., 1983, Drumlin formation related to inverted melt-water erosional marks: Journal of Glaciology, v. 29, p. 461-478.
Shaw, J., and Gilbert, R., 1990, Evidence of large-scale subglacial meltwater flood events in southern Ontario and northern New York State: Geology, v. 18, p. 1169-1172.
Sutton, R. G., Lewis, T. L., and Woodrow, D. L., 1974, Sand dispersal in eastern and southern Lake Ontario: Journal of Sedimentary Petrology, v. 44, p. 705-715.
Thomas, R. L., Kemp, A. L. W., and Lewis, C. F. M., 1972, Distribution, composition, and characterisitcs of the surficial sediments of Lake Ontario: Journal of Sedimentary Petrology, v. 42, p. 66-84.

Road Log

Cumulative Mileage	Miles From Last Point	Route Description
0	0	Start at Campus Road, Hamilton College, Clinton, NY. Head east on College Hill Road.
0.5	0.5	Turn left (north) onto Rt. 233 at bottom of hill. Drive past Rt. 5 crossing and through Westmoreland.
5.5	5.0	Turn right for Rt. 90.
5.7	0.2	Turn left to Rt. 90 tollgate and proceed onto 90 West.
38.7	33.0	Exit onto Rt. 481 North to Oswego. Interstate 481N becomes NY State 481N after about 6 miles.
63.2	24.5	Enter Fulton, staying on 481N.
64.3	1.1	Turn left onto Rt. 3 West (third traffic light at a Wendys). Continue through Hannibal on Rt. 3W.
75.8	11.5	At stop sign at the end of Rt. 3, turn right onto Rt. 104A North towards Oswego.
77.0	1.2	Just outside of Sterling Valley before a narow bridge, turn left (120 degree turn!) onto MacNeil Road.
77.1	0.1	Make a quick right (the first possible one) and continue on MacNeil Road.
77.7	0.6	Continue straight through stop sign.
78.2	0.5	Take the second right after last stop sign onto McIntyre Road (MacNeal curves to the left).
79.6	1.4	Continue onto unpaved extension ("seasonal use") of McIntyre Road.
79.7	0.1	Just before descending the hill to Lake Ontario, park between the trees on the right side of the road.

STOP #1. McIntyres Bluff and Environ

We will walk out to the edge of McIntyres Bluff in order to get an overview of this coastal compartment. BE VERY CAREFUL, BECAUSE THE EDGES OF THE BLUFF TOP ARE SUSCEPTIBLE TO COLLAPSE. Also, because the western end of McIntyres Bluff is private property with a home owner who values his privacy, we will confine our field inspection to the eastern half of the drumlin. Please comply with this request.

McIntyres Bluff is a north-south-trending drumlin. Note (Fig. 11) that the drumlin's axis lies oblique to the shoreline which east of Little Sodus Bay runs norhteast-southwest. Gravel and sand eroded from the drumlin till are transported by longshore currents to the northeast and nourish a low-lying baymouth barrier. Notice how narrow the gravel and cobble beach is at the base of the bluff. This is due to two factors: 1) the lake level this past spring has been unusually high which has resulted in more beach erosion than usual, and 2) the gullies are not supplying much debris to the beach, as indicated by the dearth of mud flows that typically fill the V-shaped gully floors as well as by the absence of colluvial fans at the gully mouths. Nine years ago when we began our field studies of the southeast Lake Ontario shore, a well-developed colluvial terrace occupied the upper beach which at that time was much broader than at present due to the availability of sediment.

Features that are important to note as we inspect the gully network include:
i. the bowl-shaped head region of the gully system and its control by jointing;
ii. wet spots on the headwall that identify zones of groundwater seepage;
iii. the ubiquity of fresh slump masses at the base of the headwall;
iv. the steep-flanked ridges and narrow throat of the gullies;
v. the presence of mud flow deposits in the stretch of gully below the headwall, and of cobble and boulder lag deposits in narrow channels that are cut into the gully fill;
vi. the angularity of the large clasts in the till and mud flow deposits and the subrounded to rounded shapes of cobbles and gravel on the beach proper;
vii. the presence of a wave notch at the bluff's base and the development of a slump scarp running the full extent of the bluff.

Given the above morphological characteristics, what stage of bluff development does McIntyres Bluff represent?

Now we will hike along the beach to the east, in order to examine the morphology and sediment character of the downdrift baymouth barrier (Fig. 11). Note that the surface of the beach that runs the length of McIntyres Bluff is dominated by boulders, cobbles, and gravel, despite the large quantities of sand in the glacial till of the drumlin. Clearly, these coarse sediments are lag and storm deposits, the sand having been eroded and transported offshore by high-energy waves. Unlike ocean beach systems, there is no long-period swell in Lake Ontario, and fair-weather waves are incapable of transporting the nearshore storm-deposited sands back onto the beach (McClennen and Pinet, 1993). As such, the beach deposits are out of equilibrium with the fair-weather conditions that prevail along the lakeshore.

Note the numerous trees that have been uprooted and fallen as a consequence of the rapidly transgressing shoreline. During the past four years, this baymouth barrier has been relatively stable as indicated by our profiling surveys (Fig. 8C). This past spring, the barrier has been overtopped by storm waves forming overwash deposits. The onset of overwash along this barrier seems related to the unsually high lake levels during the past spring, in conjunction with a significant reduction in tha amount of longshore drift due to the recent inactive nature of the gullies that are incised into McIntyres Bluff. Although McIntyres Bluff is in a mature morphological state, it is temporarily behaving as a bluff in old "age," because of the inactive nature of its gully system as indicated by 1) the lack of mud flow deposits and colluvial fans, and 2) the narrowness of the beach at the bluff's base. Presumably, the temporary reduction of sediment influx eroded from the bluff that supplies the coastal compartment is related to diminished groundwater seepage and surface runoff.

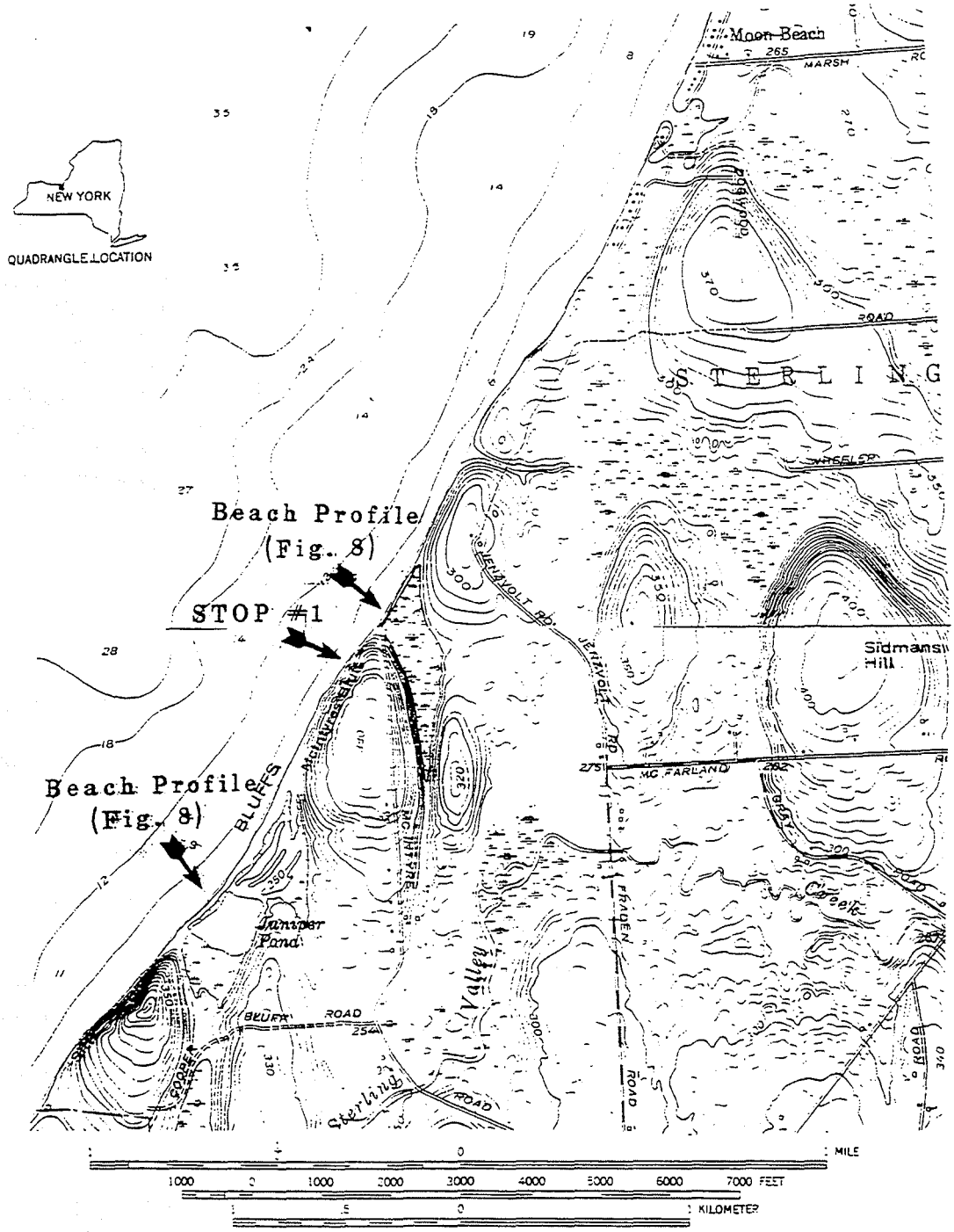

Figure 11. A topographic map of McIntyres Bluff and environs, the area to be visited at Stop #1. The beach profiles are reproduced in Figure 8.

About 0.5 km from the eastern edge of McIntyres Bluff (Fig. 11), we encounter a small bluff with a steep face and a wave notch. This small drumlin has just begun to be eroded by storm waves, and is a classic example of a bluff in a young stage of morphological development. Note the numerous fresh slumps at the bluff's base, the steep face (> 45 degrees), and the presence of rills and a few channels etched into the bluff's surface. Given that the crest of this small drumlin does not rise more than 20 m above the lake level, which is slightly below the geomorphic threshold that we believe separates young from mature bluffs (Montesi and Pinet, 1997), we expect that it will not undergo extensive gully development as the drumlin is cut back by the advancing shoreline; rather it will remain a young bluff and eventually pass directly (i.e., bypass the mature and old stages) into the final terminal stage of morphological development. However, if the gullies of McIntyres Bluff are reactivated and supply copious sediment to this downdrift barrier such that the beach widens substantially, then its possible that this small bluff will be protected from frequent wave attack, allowing the onset of gullying despite its small topographic stature.

Road Log (cont.)

Cumulative Mileage	Miles From Last Point	Route Description
79.7	0	Turn around and head away from lake Ontario.
81.2	1.5	Turn right (southwest) at yield sign onto Sterling Center Road.
81.9	0.7	Turn right (west) at stop sign onto Old State Road. You will be driving over a series of prominent drumlin hills.
84.2	2.3	Bear right onto 104A at yield sign, continuing west toward Fair Haven.
84.6	0.4	Just outside of Fair Haven, turn right onto road leading to Fair Haven Beach State Park.
85.9	1.3	At Park toll gate, continue straight on the road, proceeding past a series of parking lots and picnic grounds that are scattered along a barrier beach.
86.9	1.0	Bear right. Do not go left, uphill to a "Camping and Bluff Picnic Area."
87.3	0.4	Continue straight onto a gravel road and follow to the end.
87.7	0.4	Park by quarried limestone blocks right at the Lake Ontario shore.

STOP #2. Beach at Base of Drumlin Immediately to the West of Sitts Bluff

The lakeshore from this point westward to Little Sodus Bay (Fig. 9) has undergone extensive engineering in order to stabilize the shore of North Fair Haven and Fair Haven Beach State Park. The 1.5-km-long strand has been armored with jetties, seawalls, revetments, riprap, and groins. All of these structures are accessible by walking along the beach to the west. If we look to the northeast, we can see Sitts Bluff with its towering, unvegetated cliffs (Fig. 9). To the southwest, we can see a large drumlin that lies within the State Park. Note that it is vegetated and is stabilized by a revetment along the shore.

After examining a groin (pier) that has been reattached to the shore with riprap, we will proceed to the northeast in order to examine a baymouth barrier that is retreating at a rapid rate, at almost 2 m/yr (Figs. 9 and 10). This is not surprising, given that the net longshore drift is to the east and the barrier lies downdrift of jetties and groins, and that the base of the two bluffs between The Pond and the baymouth barrier are protected by seawalls, riprap, and revetments. This section of the lakeshore is sediment starved. Therefore, the baymouth barrier is retreating landward rapidly as storm waves overtop the beach ridge causing extensive overwash. Note the well-rounded character of the beach material.

One reason why we believe that at least segments of the southeastern Lake Ontario shoreline consist of discrete coastal comparments is that sediment starvation here is confined to the drumlin bluff-baymouth barrier couplet. Downdrift of us lies Sitts Bluff, an unprotected drumlin in a late mature stage of morphological development that is supplying coarse sediment to its dowdrift baymouth barrier. Our beach-profiling studies (Fig. 8) indicate clearly that the barrier to the east of Sitts Bluuff has been in a quasi-equilibrium state since 1950, and has not retreated appreciably in contrast to the barrier that we are currently examining. In other words, the past 50 years of severe sediment starvation that characterizes the segment of the lakeshore that we are now examining has not affected the

adjoining downdrift compartment, suggesting that bluff-barrier couplets are self-contained entities to a large degree.

Road Log (cont.)

Cumulative Mileage	Miles From Last Point	Route Description
87.7	0	Depart Stop 2 parking area and head out of park the same way you entered it.
89.5	1.8	Pass through Park toll gate.
90.8	1.3	Turn right (west) at stop sign onto Rt. 104A ("Seaway Trail") and proceed through Fair Haven.
96.4	5.6	Rt. 104A turns to the right in the town of Red Creek; continue on Rt. 104A.
97.6	1.2	Rt. 104A ends at traffic light; turn right (west) onto Rt. 104 West.
100.2	2.6	Turn right (north) onto Ridge Road, following the "Seaway Trail" to Wolcott and to "Rt. 89" and passing through Wolcott Falls.
101.8	1.6	In Wolcott, turn right onto Main Street, still following the "Seaway Trail."
102.8	1.0	After State Police Station, turn right onto Loomisville Road.
106.8	3.8	Turn right onto East Bay Road (Caution - the road sign reads E Bay Road).
108.7	2.1	Turn right (north), continuing on East Bay Road just after wetlands and stream.
109.6	0.9	Park in the lots at the end of East Bay Road at the Ontario lakeshore.

STOP #3. Chimney Bluffs

Chimney Bluffs (Fig. 12), an undeveloped State Park, is located about 22 km to the west of Stop #2 (Fig. 1), and about 3 km to the east of Sodus Bay. This excursion adds a considerable amount of time (1-2 hrs) to the trip. Chimney Bluffs is a high, broad drumlin with enormous, deeply-incised gullies that are unusually long for the Ontario lakeshore. According to our classification, it looks to be in a very late mature stage of morphological development, as judged from its appearnace on topo maps (almost half of the drumlin has been eroded) and clear signs of old "age" in the field. As we walk along the beach to the west, note how the steep, planar, low sides of the bluff which are controlled by gravity slides are replaced by small and then large gullies as the bluff height increases toward the drumlin's center. Also, note that the gully floors are devoid of thick accumulations of mud flow deposits. However, there are remnants of colluvial fans at the gully mouths that have been eroded back by waves to the bluff face; observe how difficult it is to distinguish glacial till from mud flow deposits which grade into one another at the gully mouths. Wave notching and a slump scarp at the bluff's base are clear evidence of a lack of sediment supply to the adjoining beach. If our interpretation that Chimney Bluffs is in the old stage of morphological evolution is correct, we expect that the rate of retreat of the top surface of the bluff will diminish with time, whereas recession of the base of the bluff will likely accelerate as the sediment supply to the beach is reduced, allowing storm waves to undermine the bluff and cause increasingly more slumping with time.

As we approach the west flank of the drumlin, we will encounter varved lake sediments deposited in glacial Lake Iroquois. Typically the varves are millimeters thick, and alternate between clay-rich and silty sand-rich laminations, the former representing low energy winter conditions when the lake surface was frozen, the latter higher-energy conditions associated with spring melting. Ice-rafted dropstones are common. Some of the varve sequences are distorted, crumpled into tight folds, that represent either soft-sediment deformation, iceberg keel groundings, or minor glacial ice readvancements during the retreat of the Ontario Lobe of the Laurentide Ice Sheet.

We can return to our vehicles by climbing up the bluff along a crestal trail which provides a superb panorama of the gullies, embayments, fans, and beach and nearshore features. BEWARE OF TREACHEROUS FOOTING AND UNSTABLE CLIFF EDGES. If you prefer, you may return to our starting point by retracing your steps along the beach. For those of us hiking the ridge line, note the appearance of the gullies from above and the nature of the shoulders of adjoining gullies. Also, the map view of Chimney Bluffs shows a flat top to the drumlin, a feature that is attibuted to wave planation when the drumlin was immersed beneath Lake Iroquois. Support for this interpretation is provided by irregular lag deposits of gravel that are visible at the very top of some of the gully headwalls. Presumably, the glacial gravel was sorted and the pebbles were rounded by shallow-water wave activity

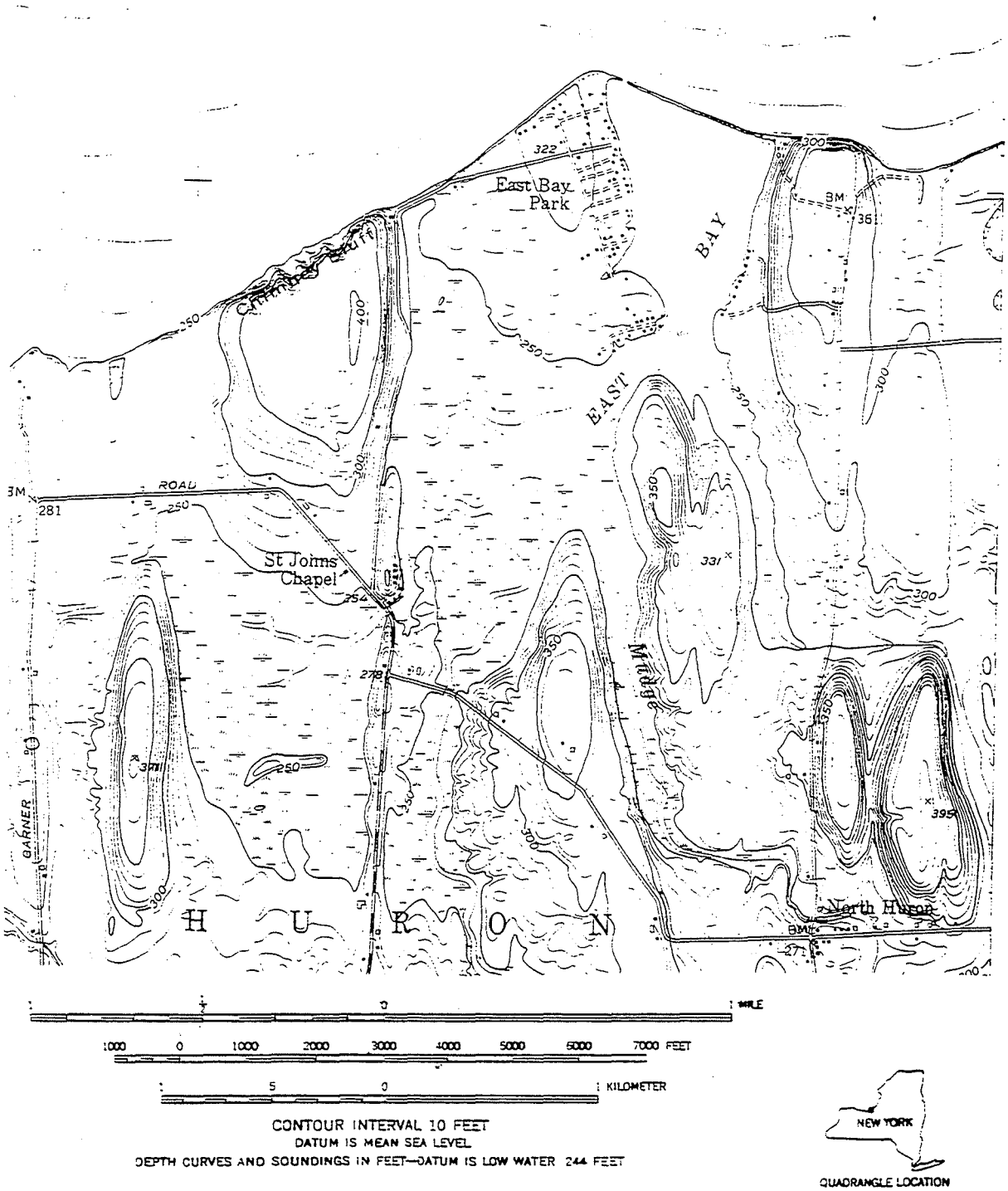

Figure 12. A topographic map of Stop #3, Chimney Bluff.

on this former shoal which at that time was located several kilometers offshore of the southern Lake Iroquois shore.

Road Log (Return to Clinton)

Cumulative Mileage	Miles From Last Point	Route Description
109.6	0	Head south from parking lot along East Bay Road.
110.5	0.9	At stop sign, turn left and continue on East bay Road.
112.6	2.1	Turn left at stop sign onto Loomisville Road.
116.4	3.8	Turn left (east) at stop sign onto West Main Street, heading into Wolcott.
117.4	1.0	In Wolcott, bear left after traffic light onto Oswego Street which becomes Ridge Road. Follow signs "to 104 East."
120.1	2.7	Continue across Rt. 104, staying on Ridge Road.
122.2	2.1	Bear right onto Rt. 370, and pass through Victory, Cato, Meridian, and Baldwinsville.
143.5	21.3	In Baldwinsville, turn left onto Rt. 690 South.
148.9	5.4	Take exit for Thruway Rt. 90 East.
195.4	46.5	Take Exit 32 for Westmoreland-Rome and Rt. 233.
195.6	0.2	Turn left heading south on Rt. 233.
200.6	5.0	Turn right onto College Hill Road at blinker.
201.1	0.5	Turn right onto Campus Road of Hamilton College.

Timing of Intrusion, Anatexis, and Metamorphism in the Port Leyden Area of the Western Adirondacks

Frank P. Florence
Science Division, Jefferson Community College
Watertown, NY 13601
frank_florence@ccmgate.sunyjefferson.edu

Robert S. Darling
Dept. of Geology, SUNY College at Cortland
P.O. Box 2000, Cortland, NY 13045
darlingr@snycorva.cortland.edu

Introduction

The purpose of this field trip is to examine evidence of the igneous, metamorphic, and tectonic history of the western Adirondack Highlands preserved in rocks in the vicinity of Port Leyden, NY. We will visit and discuss rocks and structures at six sites that include interlayered metasedimentary and metaigneous lithologies and a distinctive nelsonite (apatite-magnetite-ilmenite) dike. Rocks at these sites display structural fabrics and cross-cutting relationships formed through a sequence of metamorphic, hydrothermal, and melting events. Recent geochronological studies confirm that this area has undergone a complex tectonothermal history.

In particular, this trip will focus on uncertainties concerning the anatectic or intrusive origin of leucogranitic gneisses and melt veins in the gneiss surrounding the nelsonite dike. By clarifying structural and field relationships, we hope to discriminate between interpretations of igneous activity and metamorphism in these gneisses. Potentially, this may establish useful constraints on regional interpretations of orogenic sequence.

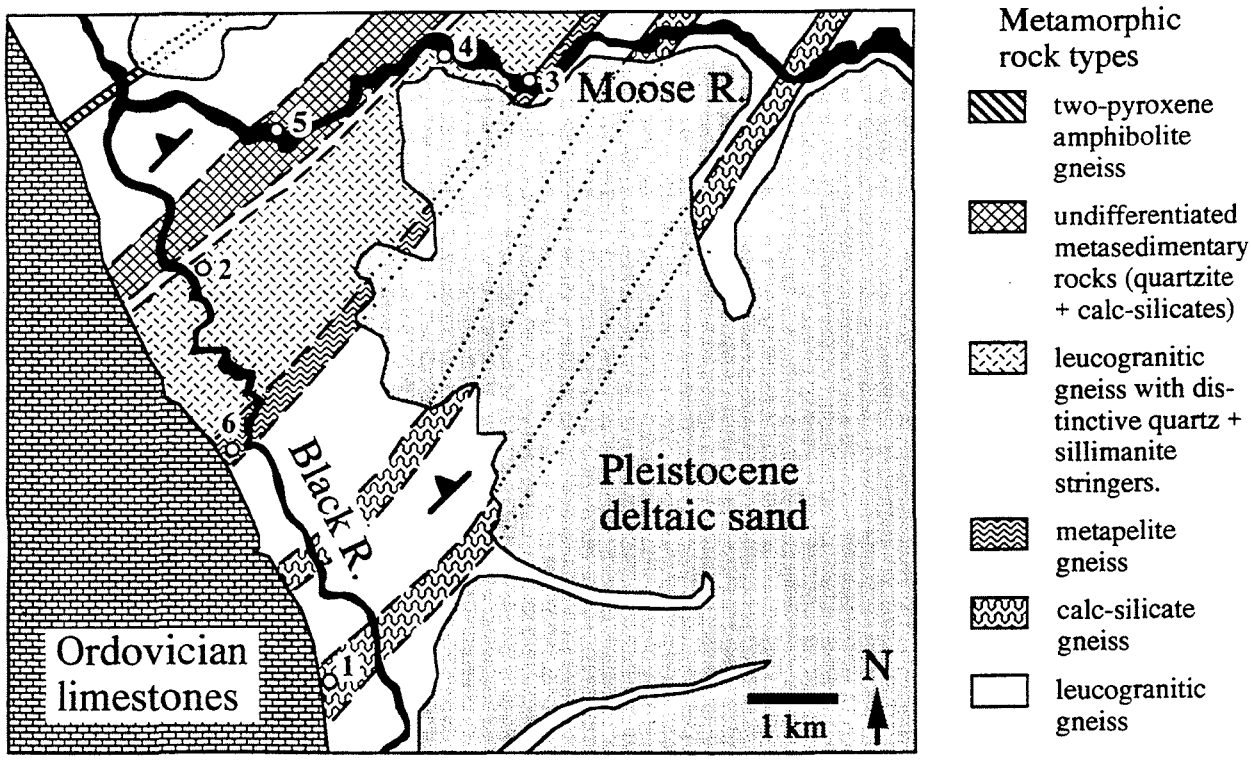

Fig. 1. Geologic Map of the northern portion of the Port Leyden 7 1/2' quadrangle. Field trip stops are indicated.

Geologic Setting

The Port Leyden area lies in the western Adirondack Highlands (Fig. 2), a region composed of Proterozoic orthogneiss and paragneiss of the Grenville Province that preserve mineral assemblages formed under granulite facies conditions. A package of interlayered metasedimentary gneisses, amphibolites, and leucocratic quartzofeldspathic gneisses are well exposed between the towns of Port Leyden and Lyons Falls, close to the confluence of the Moose and Black Rivers and immediately east of the unconformity with Ordovician carbonates (Fig. 1). They occur as uniformly northeast trending, northwest dipping compositional layers. Thick deposits of Quaternary alluvium prevent tracing these units far east of the Moose River, but lithologically similar units occur approximately 10 km along strike in the McKeever and Number Four quadrangles (Whitney et al., 1997).

The Adirondack Highlands have experienced a common igneous and metamorphic history since at least 1150 Ma. Intrusion of anorthosite massifs and associated mangerites, charnockites and leucocratic granitic rocks (the AMCG suite) occurred in the central and eastern Adirondacks between 1125 and 1157 Ma (McLelland et al., 1988; Chiarenzelli and McLelland, 1991). Whitney (1992) correlated geochemically similar charnockites, hornblende granitic gneisses, and leucocratic gneisses in the western Adirondacks with the AMCG suite. No mangerites are recognized in the western Adirondacks and only a few, small bodies of anorthositic rocks are present (Fig. 2), none of which outcrops within 25 km of Port Leyden. The AMCG suite intruded a supracrustal package of rocks that now include marbles, calc-silicate rocks, quartzites, and pelitic gneisses. Intrusion of AMCG rocks in the eastern Adirondacks probably occurred at relatively shallow crustal depths (Valley and O'Neil, 1982). Whitney (1992) has inferred similar depths of emplacement for charnockites and granitic rocks in the western Adirondacks.

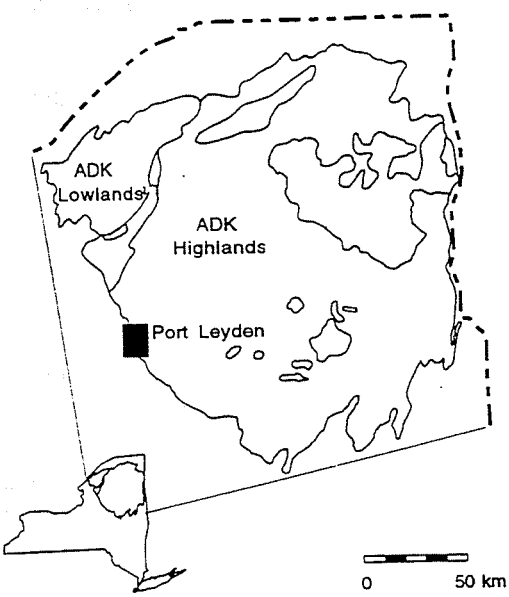

Fig. 2.. Location of the Port Leyden 7 1/2 " quadrangle. Also shown are the locations of exposed anorthosite rock in the Adirondack Highlands.

Younger episodes of intrusive activity occurred subsequent to emplacement of the AMCG suite during approximate intervals of 1090-1100 Ma and 1060-1080 Ma (Chiarenzelli and McLelland, 1991). Metamorphic mineral ages date granulite facies metamorphism throughout the Adirondack Highlands at approximately 1000-1050 Ma (Mezger et al., 1991; Chiarenzelli and McLelland, 1993; Florence et al., 1995), corresponding to the Ottawan phase of the Grenville Orogeny. 996-1026 Ma zircon ages from oxide rich rocks in the central Highlands may be the result of protracted cooling from temperatures greater than 750 ° (Mezger et al., 1991).

Recent studies of crystalline rocks in the Port Leyden area have raised questions about their origin and the relative ages of textural features in them. Darling and Florence (1995) proposed that anorthosite magmatism extended into the western Adirondacks based on the recognition of a distinctive igneous dike in Port Leyden composed of apatite-magnetite-ilmenite with minor sulfide. This rock type, named nelsonite, separates as an immisible melt from a parent ferrodiorite magma during fractional crystallization of anorthosite (Philpotts, 1967, 1981; Kolker, 1982; Epler, 1987). The nelsonite dike is hosted by metapelitic gneiss that experienced partial melting, which Florence et al. (1995) suggested was in response to contact heating from anorthosite intrusion. The metapelitic host rock is interlayered with leucocratic granitic gneisses, and both rocks contain nodular lenses and stringers containing quartz and sillimanite. These quartz-sillimanite features have recently been interpreted to result from high temperature hydrothermal alteration due to late-stage magmatic fluids in a deforming, crystallizing magmatic environment (Cunningham and Willis; 1996; Olson and Brackett, 1997). Orrell and McLelland (1995) obtained a 1031±8 Ma age from zircon in the leucogranitic gneiss. They correlated the gneiss with lithologically similar, late

leucogranitic rocks in the northern and eastern Adirondack Highlands and interpreted the quartz-sillimanite features as textures produced in a deforming crystal-melt system. This interpretation brings into question the emplacement age of the nelsonite dike and the timing of partial melting in the surrounding gneiss.

Rock Descriptions

Metasedimentary rocks exposed in the field trip area include calc-silicate rocks, scattered, discontinuous marble layers, quartzites, and metapelitic gneisses (kinzigites). This association suggests that protoliths likely were deposited in a shallow marine, possibly shelf, environment. Rocks of likely igneous parentage include the nelsonite dike and amphibolite. Granitic gneisses, with variable amounts of biotite, garnet, and sillimanite may represent intrusions that have assimilated surrounding material or metavolcanics with some detrital component.

Metasedimentary rocks

Calc-silicate Rocks

Two bands of calc-silicate rocks striking approximately N50E are exposed SE of Port Leyden. These appear in outcrop as gray-green units or, occasionally, xenoliths, with a pronounced gneissic foliation. Mineralogy consists of green diopside, quartz, microcline, minor garnet, titanite, and pyrite, and scattered grains of scapolite and wollastonite. Contacts with other lithologies can be diffuse and calc-silicates rocks sometimes grade to more aluminous bulk compositions. East of Lyonsdale, along the Moose River, coarse calcite marble crops out near the contact of a 0.3 km wide band of calc-silicates with felsic gneiss.

Quartzite

Rocks largely composed of or nearly all quartz are collectively referred to as quartzites, although the nature of their protoliths is unclear. There are a number of well exposed outcrops of these rocks along the Moose River near Kosterville and Goulds Mill. In addition to quartz, these rocks contain abundant sillimanite, a few percent magnetite, as well as scattered garnet. Some acicular sillimanite is aligned with the foliation. In other places, clusters of bladed sillimanite appear as sprays. Locally, the rock appears to contain quartz nodules that may be relict pebbles. Weathered outcrop surfaces commonly are colored by hematite staining.

Metapelitic Gneiss (kinzigite)

A garnet-sillimanite-biotite metapelitic gneiss occurs throughout a zone a few hundred meters wide from the south end of the town of Port Leyden to the Moose River immediately upstream of the dam at Lyonsdale. It is a gray to pink rock with granoblastic texture made up of coarse grains of microperthite and quartz. For the most part, foliation is defined by abundant, aligned biotite and quartz-feldspar veins and leucosomes. Along the Moose River, the gneiss contains distinctly biotite-rich layers. Cm size nodular segregations of quartz and coarse sillimanite commonly occur and are elongate in the plane of foliation. Small amounts of magnetite and hercynite spinel occur in these features. Garnet is abundant in these rocks and occurs throughout.

Meta-igneous rocks

Nelsonite

The Port Leyden nelsonite is a dark, equigranular, and fine grained rock composed of approximately 40% each of magnetite and apatite, 8 to 15 % ilmenite, and up to 5 % pyrite or pyrrhotite. Scattered grains of siderite and zircon are distributed through the rock and a few percent of garnet, monazite, and chlorite are present near dike margins. Reaction zones up to 5 cm wide commonly are present at the contact between nelsonite and gneiss and contain very coarse, fluorine-rich, titaniferous biotite and unstrained, equigranular labradorite to andesine plagioclase. Similar reaction features are found surrounding xenoliths entrained in the dike.

Amphibolite

A narrow band of amphibolite crops out in the village of Lyons Falls and to the northeast. The dominant mineralogy is orthopyroxene, clinopyroxene, hornblende and plagioclase, with minor amounts of biotite, magnetite, and ilmenite. Near its southeastern margin, close to the contact with quartzofeldspathic gneiss, the amphibolite contains thin, segregated layers of microcline-quartz or sodic plagioclase-quartz.

Leucogranitic gneisses

These light pink to gray rocks are composed of abundant perthitic feldspar or microcline and quartz. Plagioclase is absent or occurs as scattered grains in perthitic varieties. Foliation in these gneisses is defined primarily by aligned quartzofeldspathic segregations and nodular lenses and elongate stringers of quartz and sillimanite with subordinate amounts of magnetite. There are intermixed layers in which biotite and plagioclase are more common but generally not abundant. Garnet is often present in the gneiss, usually as small, disseminated grains, but it may be abundant or present as large grain with irregular margins. In some layers with biotite, garnets are surrounded by cm wide biotite-free halos.

Leucogranitic rocks southeast of the town of Port Leyden are homogeneous in composition and texture. These rocks are readily distinguished in the field from granitic gneiss that occurs in a 1.5 km wide band extending northeastward from Port Leyden. In this band, virtually all outcrops contain quartz-sillimanite nodules and stringers aligned with foliation. Nodules range from a few cm to nearly 1 m length and may have originated as veins that were rotated and separated along shear planes. The volume of rock composed of these nodules and segregations ranges from a few percent to nearly 50%. Whitney et al. (1996) describes similar nodular rocks about 20 km along strike to the northeast in the area of Otter Creek.

Pegmatites

Abundant pegmatites and quartz veins are present in all lithologies other than the nelsonite. They exist as conformable layers and as cross-cutting features that are folded, boudinaged, or undeformed. Many pegmatites have granitic compositions with subequal amounts of albite and microcline. Others have only one feldspar present. Compositional zonation is recognized in some pegmatites mainly on the basis of albite-rich margins. Magnetite is a common accessory mineral and sillimanite is sometimes present. Hercynite spinel has been recognized in at least one undeformed pegmatite at Lyonsdale (Olson, pers. comm.)

Metamorphism

Throughout much of the Adirondack Highlands granulite facies metamorphism, accompanied by variable amounts of strain, resulted in extensive recrystallization and compositional modification in mineral assemblages. Preserved mineral compositions appear to represent equilibration among silicates and oxides at about the time of granulite metamorphism, followed by modification during an extended period of slow cooling (Bohlen et al., 1985; Mezger et al., 1991). In the eastern and central Adirondacks, preserved mineral compositions indicate that pressures of metamorphism were 7 to 8 kbar (Bohlen et al., 1985, Spear and Markussen, 1997). The independent geobarometry calibrations used to obtain these estimates include garnet-sillimanite-plagioclase-quartz, garnet-anorthite-ferrosilite-quartz, garnet-anorthite-fayalite, and garnet-rutile-sillimanite-ilmenite-quartz. High pressure granulite facies metamorphism is supported by the presence of akermanite close to the Marcy massif (Valley and Essene, 1980a). Temperatures of metamorphism in the eastern and central Adirondacks have been estimated at between about 675 °C and greater than 775 °C (Bohlen et al., 1985).

Although there are few geothermometry estimates of regional temperatures of metamorphism in the western Adirondacks, high temperatures caused partial melting in a variety of rock types. Granitic rocks and amphibolite locally contain leucosomes of quartz and feldspar. Felsic and metapelitic gneisses display migmatitic textures at outcrop scale and melt textures in thin section. Garnet, sillimanite, and hercynite spinel are common in metapelites and probably formed during anatectic melting.

In contrast to high pressure metamorphism elsewhere in the Adirondacks, rocks in the vicinity of Port Leyden record lower pressures of between 4 and 6.4 kbar (Florence et al., 1995). They based their pressure estimates on compositions from minerals associated with melt textures and veins. Notably, hercynite spinel was found in contact with quartz and associated with garnet neoblasts and plagioclase-rich veins. Geobarometry estimates obtained from garnet-sillimanite-plagioclase-quartz and garnet-sillimanite-spinel-quartz equilibria coincide over the temperature range 700-770 °C (Fig. 3). Partial melting involving biotite dehydration has produced resorbed biotite rimmed by plagioclase-rich veins. Experimental work by Clemens and Wall (1981) and LeBreton and Thompson (1988) locate the vapor-absent solidus for this reaction in the range 700-750 °C at pressures coincident with the mineral equilibria. It therefore seems clear that the discrepancy in calculated pressures between the Port Leyden area and the eastern and central Adirondacks can not be satisfactorily explained as an artifact of comparing results from different geobarometers.

Effects of retrograde metamorphism include the exchange of Fe-Mg between biotite, garnet, and oxides, producing garnet compositional profiles with Fe/(Fe+Mg) increasing toward the rim. In a layer of sillimanite-rich, felsic gneiss 1 km east of Goulds Mill, garnet rims are replaced by prismatic sillimanite and biotite. Biotite surrounds some garnet rims in the leucogranitic gneiss. Similar reactions have not been recognized in metapelitic gneisses.

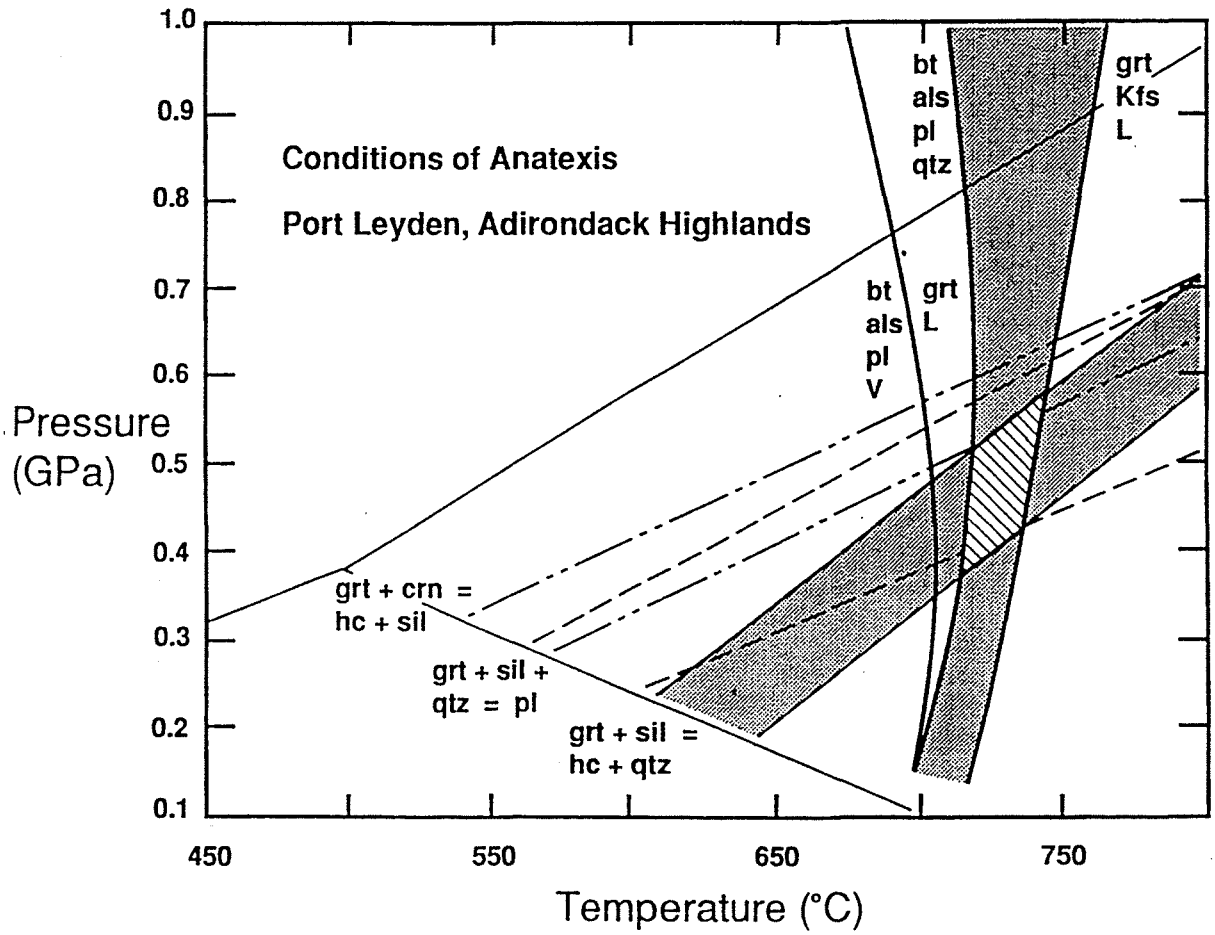

Fig. 3. P-T conditions estimated from phases associated with melt textures in metapelitic gneiss (Florence et al., 1995). Estimated P and T are defined by the intersection of the biotite dehydration melting region and garnet-sillimanite-hercynite-quartz equilibria. Dot-dash pattern shows range of garnet-corundum-hercynite-sillimanite equilibria. Dashed lines show range of garnet-sillimanite-quartz-plagioclase equilibria.

Geochronology from Port Leyden Rocks

Recent geochronologic studies in the Port Leyden area reveal complex U/Pb systematics that indicate either inheritance or isotopic resetting comparable to the disturbed U/Pb geochronology demonstrated by Chiarenzelli and McLelland (1993) in the central Highlands. Zircons from a variety of rocks record inheritance from >1100 Ma and recrystallization or profound radiogenic Pb loss at 1030-1040 Ma (Florence et al., 1995, Orrell and McLelland, 1996). In a U/Pb study of zircons from the nelsonite dike, Florence et al. (1995) obtained a discordant, non-linear array of fractions that included nine single grain measurements. A single grain analysis yielded a minimum Pb/Pb age of 1105 Ma. Three other single grain analyses were close to concordant with Pb/Pb ages between 1024 and 1035 Ma. Florence et al. (1995) attributed the non-linear array to recrystallization and lead loss dating from a profound disturbance related to granulite facies metamorphism. Zircons from the hosting pelitic gneiss were dated and 7 fractions and single grain analyses produced a linear array with an upper intercept at 1166±53 Ma. The 1105 and 1165 Ma age were interpreted by Florence et al. (1995) as minimum and maximum age constraints on the timing of anorthosite intrusion and associated contact metamorphism and melting. Orrell and McLelland (1996) obtained a concordant single grain zircon age of 1031±8 Ma from the leucogranitic rock and interpreted this as the age of granite intrusion. Other zircons from this rock form a non-linear array which were interpreted as inherited. The oldest discordant grain has a minimum Pb/Pb age of 1119 Ma.

The time of granulite facies metamorphism is dated by a monazite U/Pb age of 1041±9 Ma from the pelitic gneiss (Florence et al., 1995). Undeformed pegmatite with zircon dated at 1027±8 Ma cross-cuts regional foliation (Orrell and McLelland, 1996) and fixes the lower age of tectonism in the region.

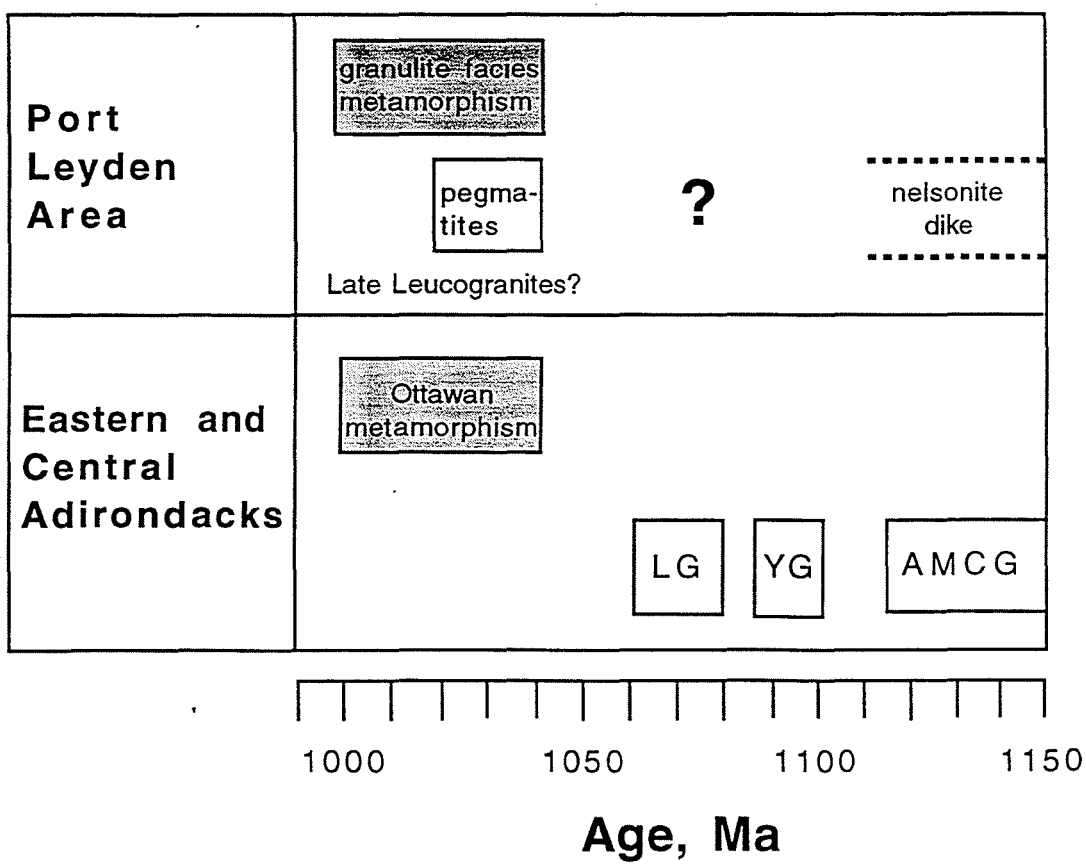

Fig. 4. Generalized geochronology from Port Leyden and from elsewhere in the Adirondack Highlands. Lg = late leucogranites. YG = younger granites. AMCG = anorthosite-mangerite-charnockite-granite suite rocks.

Trip Objectives

This trip highlights some of the controversial structural and chronological relationships among rock units. When visiting the stops on this trip, you are encouraged to consider these questions:

1. What was the timing of penetrative deformation and to what extent, if any, can mineral assemblages and textures formed during the intrusion of the AMCG suite be recognized in the Port Leyden area rocks?
2. Unstrained phases that crystallized from melts occur in veins, reaction zones, and in equigranular granitic rocks. Is granitic intrusion implied by these features? Which features might be anatectic? Can anatexis explain the 1032 Ma zircon age date from granitic gneiss?
3. Are the quartz-sillimanite nodules and stringers (or their protoliths) relatively early features that were present in the surrounding gneiss prior to penetrative deformation or did they form relatively late due to hydrothermal activity in a crystallizing magma?
4. Did pegmatites originate from late-magmatic fluids at the time of granite intrusion or are they a result of fluids evolved from *in situ* rocks at the time of the peak of metamorphism?
5. What tectonic significance can be placed on the moderate (vs. high) pressure estimates obtained from this region of the Adirondack Highlands?

Acknowledgments

Our thanks to Phil Whitney for his valued input during our research and for making available preliminary mapping in the western Adirondacks. Thanks to Jim McLelland, Bill Kelly, Bruce Selleck, and John Valley for comments, insights, and constructive debate during various portions of our work. We are especially indebted to Sue Orrell for her unflagging efforts to obtain meaningful geochronologic data from these rocks.

Road Log

The trip log begins on Route 12, approximately 2 miles north of Boonville. Set trip odometer to 0.0 at the Lewis County boundary sign. Proceed north on Route 12.

Cumulative Mileage	Miles From Last Point	Route Description
0.0	0.0	Lewis County line.
0.5	0.5	Low roadcuts of Ordovician Black River Group limestone.
0.7	0.2	Barrett quarry.
1.5	0.8	Highway parking area. View of historic Black River canal quadruple locks.
3.0	1.5	STOP 1. Pull off right side of road adjacent to outcrop. Park.

STOP #1. Rt. 12. Calc-silicate and Aluminous Metasedimentary Rocks

These rocks comprise one of two narrow but mappable bands of calc-silicate gneiss that extend northeastward, under the Pleistocene deltaic sands, and reappear along the Moose River (Fig. 1). Foliation in both calc-silicate bands strikes northeast and dips moderately northwest.

A variety of bulk compositions can be observed in this exposure, but the dominant minerals are clinopyroxene, biotite, K-feldspar, and quartz. Other minerals include grandite garnet, titanite, wollastonite, calcite, and scapolite. Compositional data are limited, but EDXF spectra from the garnet show mostly grossular with a small

andradite component. The scapolite is mostly meionitic. In thin section, the margins of wollastonite grains contain thin rims of retrograde garnet identical to that described by Valley et al. (1983) from drill cores just 3.0 kilometers NE of this location. This garnet is unusual because it contains stoichiometric fluorine (up to 0.76 wt.%; Valley et al., 1983). Wollastonite occurs in apparent textural equilibrium with calcite and quartz.

As noted in some other Adirondack marbles, the occurrence of regional metamorphic wollastonite suggests an H_2O-rich fluid composition (Valley and Essene, 1977; 1980b). We interpret these rocks similarly. Specifically, at the PT conditions in this region (700-750 °C and 4-6 kbar), a fluid composition of $XH_2O \approx 0.80$-0.90 is necessary to stabilize these minerals (Jacobs and Kerrick, 1981). The margins of some quartz ± pink K-feldspar veins are characterized by an assemblage of epidote + specular hematite, suggesting a higher O_2 fugacity compared to that in the country rocks.

At the northernmost part of the roadcut there is a small exposure of leucocratic K-feldspar + quartz + sillimanite gneiss. Minor amounts of biotite, magnetite and almandine garnet occur locally. The presence of matrix sillimanite in these exposures, coupled with the bulk composition of the calc-silicate gneisses, strongly argue in favor of a sedimentary origin for both rock types.

		Continue north on Route 12.
4.8	1.8	Village of Port Leyden traffic light. Continue north.
5.1	0.3	Turn right. Stop at sign. Turn left (north) onto Kelpytown Road.
5.5	0.4	Intersection with Davis Bridge Road. Bear right.
5.7	0.2	Intersection with Davis Bridge Exit. Turn right (east).
5.9	0.2	One lane bridge across Black River. Proceed with care. Bear left after bridge. Continue on Davis Bridge Road.
6.2	0.3	STOP 2. Park on sandy shoulder on right side of road. Outcrop on left (west) side of road is visible through trees.

STOP #2. Davis Bridge Road. Leucogranitic Gneiss with Quartz-Sillimanite Stringers

Outcrops in the woods on both sides of the road consist of relatively homogeneous, granitic gneiss. Abundant, cm-wide stringers of quartz and sillimanite, with minor oxides, biotite, and garnet, are distributed throughout these rocks. Orientation of these stringers parallels the gneissic foliation defined by biotite and oxides, which locally varies between N20E and N50E. These exposures lie within a 1.5 km wide band of leucogranitic gneiss that can be traced N40E from the Black River to exposures along the Moose River at Lyonsdale (Fig. 1).

Immediately west of the road, and about 5 m uphill, are a few exposed knobs that also contain quartz-rich layers (leucosomes?) parallel to foliation. Biotite and magnetite occur in mm thick margins on these layers. Note that tight to isoclinal folds deform the quartz layers and are parallel to foliation and the quartz-sillimanite stringers.

Walk across to the east side of the road, enter the woods, and continue walking to the northeast for about 100 m to where a large dome of pink, granitic gneiss is exposed. On the southwest side of the outcrop there is a boudinaged quartz pegmatite layer. Sheared layers of leucogneiss parallel the margins of the boudin and flow inward around the necks. Coarse K-feldspar, possibly precipitated as a melt or hydrothermal phase, extends from margins through the pegmatite. Boudin margins contain bladed sillimanite, biotite, and magnetite. Additional folded and disrupted quartz veins are displayed around the right side of the outcrop.

Quartz-sillimanite stringers are distributed throughout the rock. Their orientation relative to penetrative deformation is well displayed across the top of the dome, where these features can be seen to form parallel to the plane of foliation. NE trending isoclinal folds deform some quartz-sillimanite segregations.

		Return to cars and continue north on Davis Bridge Road
6.4	0.2	Outcrop of leucogranitic gneiss.
6.8	0.4	Stop Sign. Turn right (southeast) onto River Road.
7.0	0.2	Turn left (east) onto Burnt Shanty Road (gravel).
8.3	1.3	Stop sign. Turn left (northeast) onto Marmon Road.
9.6	1.3	Intersection with Lowdale Road. Lyonsdale cogeneration facility on left. Turn right (northeast). Cross one lane bridge. CAUTION! Be prepared to yield right-of-way to oncoming traffic.
9.8	0.2	STOP 3. Park on sandy shoulder on right side of road by "Recreational Trail - Canoe Launch " sign.

STOP #3. Lyonsdale. Metapelitic Gneiss, Leucogranitic Gneiss, Sillimanite Nodules, and Undeformed Pegmatites

Walk down to Moose River. Follow trail upstream approximately 250 m to northward bend in river. Continue around bend, then walk down to the river's edge to metapelitic gneiss.

The river's orientation through this scenic section is parallel to lithologic layering. A low angle wall of homogenous quartzofeldspathic gneiss is exposed across the river. Garnet-rich metapelitic rock (kinzigite) is exposed for over 200 m along strike on this side, close to the water's edge. There is a sharp compositional boundary between the metapelitic gneiss and adjacent leucocratic gneiss about 5-15 m away from the river. From this contact back to the bridge, the gneiss contains less biotite and garnet.

A meter scale isoclinal fold is exposed in the metapelite layer on the southern end of the outcrop, with fold layers made up of gray, biotite-rich and pinker, perthite-rich layers. Garnet is ubiquitous; some layers contain coarse garnets > 1 cm. Elsewhere, pods of abundant small garnets form in quartz veins. Sillimanite is distributed throughout some layers and absent in others. Florence et al. (1995) found undeformed melt veins along grain boundaries locally in the metapelite. Small (0.1 mm) inclusion-free, euhedral garnet neoblasts occur with plagioclase and K-feldspar-quartz segregations surrounding embayed biotite. These textures indicate partial melting according to the biotite-dehydration reaction: Bt + Sill = Grt + Kspar + melt.

Walk back towards the parking area along the trail. Notice the pink leucogranitic rock at the canoe launch by the bridge. This gneiss clearly displays nodules of quartz and sillimanite. Two orientations can be observed, and a deformed pegmatite is seen to truncate and cross-cut the quartz-sillimanite veins.

Return to the road, cross it to a dirt road, and walk along the road in the downstream direction. After about 100 m, walk left through the woods and out onto a broad exposure of orange-pink, perthitic, leucogranitic rock with many quartz-sillimanite stringers, veins, and lenses. At least two orientations of quartz-sillimanite veins are displayed here: N50E veins are cross-cut by N20E veins (Cunningham and Willis, 1996). En echelon gash veins indicate extension and rotation within a shear zone and some small-scale granite melt veins truncate quartz-sillimanite veins. Deformed pegmatite and quartz layers are common. Large (0.5 m width), undeformed pegmatites dated at 1027 Ma cross-cut all other features.

Scattered calc-silicate inclusions are present in the gneiss throughout the outcrop area. 250 m below the bridge, biotite-rich and garnetiferous horizons become common. These layers contain sodic plagioclase, as well as microcline. Quartz-sillimanite nodules are absent in these layers, although sillimanite is present in the rock. Notice that quartz-sillimanite nodules reappear in pink, leucogranitic layers.

Postel (1952) and Whitney and Olmsted (1988) have described rocks in the northeastern Highlands that are similar to the leucogranitic gneiss. Whitney and Olmsted (1988) referred to these rocks as the Lyon Mountain Gneiss and interpreted them to be metamorphosed products of altered volcanic rocks and interlayered basin sediments. Chiarenzelli and McLelland (1990) suggest the alternative hypothesis that the interlayered lithologies may have

been the result of "emplacement of sheet-like intrusions combined with high strain to yield tectonic layering." If the leucogranitic gneiss at Lyonsdale is properly correlated with Lyon Mountain Gneiss, then correctly establishing its origin is has regional consequence.

Undeformed pegmatites cross-cut all lithologies in this area. These demonstrate fluid flow at and immediately after the peak of granulite facies metamorphism and anatexis, or during late crystallization of granite intrusives. If the PT estimates of Florence et al. (1995) represent conditions of granulite facies metamorphism, then these dikes likely formed under thermal and stress conditions that permitted fractures at between 4 and 6 kbar pressure.

		Turn around. Recross one lane bridge.
10.0	0.2	Turn right (west) onto Lyonsdale Road.
10.4	0.4	Agers Falls recreation site entrance. Proceed through gate, bear left, follow signs to Agers Falls. Park within site of Moose River. STOP 4.

STOP #4. Agers Falls. Leucogranitic Gneiss

Extensive outcrops of leucogranitic gneiss are exposed along the Moose River in this vicinity. This is the same leucogranitic gneiss seen upriver at Lyonsdale, although here it appears more homogeneous. The rock is composed largely of quartz and perthitic feldspar, with minor amounts of iron oxide, biotite, sillimanite, and garnet. Through much of the outcrop the rock has an equigranular texture and is largely lacking a gneissic fabric. Numerous pegmatites and coarse, irregular granite veins transect the gneiss.

Scattered grains or cm long veins of sodic plagioclase are recognizable in thin sections from this exposure. Plagioclase is sometimes myrmekitic and commonly exhibits erose grain margins, suggestive of resorption. Locally, oxide grains surround plagioclase margins. Garnets are almandine-rich and show irregular grain margins. Some garnets are surrounded by small biotite grains. This texture suggests the retrograde reaction: $Kfs + Grt + H_2O = Bt + Sill$.

Elongate and nodular quartz-sillimanite segregations are abundant throughout the outcrop. Two sets of nodules are recognizable: one is aligned with the NE trending regional structure and a second, cross-cutting set is oriented at about N20E. Discontinuous layering defined by these features sometimes exhibits swirl patterns. Hercynite spinel is commonly present in the quartz-sillimanite segregations.

The single zircon grain dated at 1031±8 by Orrell and McLelland (1996) was collected at this outcrop. They describe the sample grain as clear and prismatic and the determined age is concordant. They consider the leucogranitic gneiss to be a late- to post-tectonic intrusion emplaced into relatively shallow crust. Essentially all vein features are viewed as having formed during a single hydrothermal event that accompanied and ultimately outlasted magmatic intrusion. In this interpretation, the quartz-sillimanite features must have formed at about the time of emplacement or closely afterwards, when the intrusion was still partly molten or at a temperature sufficiently high to permit ductile deformation.

Our alternative interpretation suggests that anatexis of *in situ* lithologies has produced the many magmatic features observable in the Port Leyden region and that the zircon age reported by Orrell and McLelland (1996) dates the formation of granite veins in this rock. The quartz-sillimanite±spinel veins and nodules are considered to be relict features that have been rotated into their current configuration. The zircon age obtained at this outcrop and mineral ages from nearby sites define the time of a widespread thermal event that coincided with the development of the pervasive fabric and compositional layering seen at the regional scale. It needs to be emphasized that other zircon grains from here and at Lyonsdale demonstrate that cores and overgrowths do not record the same ages. Abraded cores yielded ages up to 1119 Ma that Orrell and McLelland (1995) view as inherited from older granitic rock present in the magma source region. We consider it more likely that these older zircon ages reflect crystallization within this crustal horizon in response to an earlier episode of igneous or metamorphic activity.

		Return to Lyonsdale Road.
10.8	0.4	Lyonsdale Road. Turn right (west).
11.4	0.6	Low outcrop of foliated, pink and gray felsic gneiss.
11.7	0.3	Moose River hydroelectric power facility.
11.8	0.1	Low outcrops of pink and gray felsic gneiss.
12.3	0.5	Outcrop of foliated, leucogranitic gneiss with deformed pegmatites.
12.4	0.1	Shibley Road. Turn right (northeast).
12.6	0.2	Continue across bridge over Moose River.
12.7	0.1	STOP 5. Park along sandy shoulder.

STOP #5. Goulds Mill, Shibley Road. Quartz-rich Gneiss

Walk along a dirt road parallel to the river for approximately 50 m, then cut down through trees to broad exposures along the river banks. A quartz-rich unit is exposed beginning under the bridge immediately below the dam and continuing downstream for over 50 m. Locally, the rock appears to be conglomeritic. In other places, it gives the appearance of being composed of many parallel quartz veins. The rock displays a red to yellowish coloration indicating presence of hematite and iron hydroxides. Portions of the rock are tinted green, probably due to formation of chlorite. Weathering of sillimanite and/or feldspar has produced a white wispy streaking throughout the rock.

Downstream from the bridge sillimanite needles occur in a quartz-rich matrix. Individual grains are often aligned with the dominant fabric in the rock. Some coarse sillimanite also forms fan-shaped sprays. Some pegmatites and potassium feldspar-rich veins are aligned with the rock fabric. Also present are relatively undeformed pegmatite veins that cross-cut lithologic layering. These veins contain commonly potassium feldspar and sillimanite associated with quartz.

The protolith for this quartz-rich gneiss is uncertain. Possibilities include arkosic sandstone, hydrothermally altered felsic volcanics, or a hydrothermally altered felsic intrusion.

Possible brittle deformation features crop out on the right (northern) side downstream of the bridge. A continuous 1 to 5 m thick, apparently horizontal rock layer displays a crackled texture, in contrast to the massive character of the rock on either side. This layer cross-cuts the steeply NW dipping foliation. Cm scale patches of dark colored, cryptocrystalline material is present on outcrop surfaces and along small scale joints or shear planes. Currently, studies are underway to determine the composition of this material.

		Return to cars. Turn around and recross bridge.
13.0	0.3	Intersection with Lyonsdale Road. Continue straight.
13.1	0.1	Intersection with Seymour Road. Continue straight.
13.3	0.2	River Road. Turn left (southeast).
14.4	1.1	Intersection with Murphy Road. Continue straight.
14.5	0.1	Marmom Road. Turn right (south) towards Port Leyden.
15.3	0.8	Turn right (west) at "T".
15.6	0.3	Cross Black River in Village of Port Leyden.
15.7	0.1	Turn right (north) onto Lincoln Street.
15.9	0.2	Turn right onto North Street (dirt). Continue for approximately 100 m. Park on left side near Cataldo Electric garage. STOP 6.
		This concludes the field trip road log. Proceed back to Lincoln Street to return to Route 12.

STOP #6. Port Leyden. Nelsonite Dike and Metapelitic Gneiss

This is the only described occurrence of titanium-rich nelsonite that does not occur within or in close proximity to large volumes of anorthositic rocks. Because of the strong field and experimental evidence supporting the formation of nelsonite by magmatic immiscibility during evolution of anorthosite suite rocks, we infer that anorthosite must have once been present in the western Adirondacks.

From the parking spot, cross to the south side of the road, walk over a rounded outcrop with quartz-sillimanite nodules and stringers, and down to the left. Continue walking for approximately 40 m to the southeast. Notice the low outcrops of foliated , light pink pelitic gneiss along the way. Abrupt transition to dark rocks delineates the contact with the nelsonite. Look at your compass to see the effect of standing over a body of rock that is about 40% magnetite! Good specimens of nelsonite material may be obtained from the waste pile on the south side of the mine shaft.

The nelsonite occurs as an elongate, nearly parallel sided body. Width is between 3 and 4 m and the dike is 30 m along strike at the surface. Contacts with the surrounding metapelitic gneiss are generally sharp, and locally parallel to foliation. At the northern end of the dike, the contacts truncate regional foliation defined by quartzofeldspathic layering. Detailed mapping and geophysical studies indicate that the nelsonite strikes north-south and has a near-vertical dip (LaForce et al., 1994). This attitude cross-cuts the N30E to N50E foliation in surrounding outcrops of gneiss.

The rock is equigranular and homogenous except towards the margins, where the relative abundance of pyrite increases shows a weak foliation. Garnet crystallizes interstitially to magnetite and apatite at the expense of ilmenite in this zone. A silicate-rich, 5 cm wide outer portion of the contact zone contains abundant plagioclase and is essentially sillimanite-free. A variety of textures indicate that plagioclase crystallized from a melt, including myrmekitic and symplectic plagioclase, and intergranular veins of plagioclase with associated magnetite. Anorthite content in plagioclase decreases with distance away from the dike margin. This suggests plagioclase grew in response to apatite breakdown and Ca flux outward from the dike. A model whole rock reaction for the contact zone is

Mag + Ap + Ilm + perthitic Kfs + Qtz + Sill = Grt + Mnz + titaniferous fluoro-Bt + Pl-rich melt.

Florence (1997) proposed that halogen release associated with apatite breakdown lowered the solidus temperature, leading to partial melting. Did this melting event occur at the time of nelsonite intrusion or during later granulite facies metamorphism?

References

Bohlen, S. R., Valley, J. W , Essene, E. J., 1985, Metamorphism in the Adirondacks, I. Petrology, pressure, and temperature: Journal of Petrology, v.26, p.971-992.

Chiarenzelli, J. R. and McLelland, J. M., 1991, Age and regional relationships of granitoid rocks of the Adirondack highlands: Journal of Geology, v.99, p.571-590.

Chiarenzelli, J. R. and McLelland, J. M., 1993, Granulite facies metamorphism, paleo-isotherms and disturbance of the U-Pb systematics of zircon in anorogenic plutonic rocks from the Adirondack Highlands; Journal of Metamorphic Petrology, v.11, p.59-70.

Clemens, J. D. and Wall, V. J., 1981, Origin and crystallization of some peraluminous (S-type) granitic magmas: Canadian Mineralogist, v.19, p.111-131.

Cunningham, B., and Willis, W. 1996, The evolution of Lyon Mt. gneiss, associated quartz-sillimanite nodules, and fluid inclusions at Lyonsdale, NY: Geological Society of America Abstracts with Programs, v.28, p.46.

Darling, R. S. and Florence, F. P., 1995, Apatite light rare earth element chemistry of the Port Leyden nelsonite, Adirondack Highlands, New York: Implications for the origin of nelsonite in anorthosite suite rocks: Economic Geology, v.90, p.964-968.

Epler, N. A., 1987, Experimental study of Fe-Ti oxide ores from the Sybille Pit in the Laramie anorthosite, Wyoming [Master's thesis]: State University of New York at Stony Brook.

Florence, F. P., 1997, Melt-forming reactions at the Port Leyden nelsonite-pelitic gneiss contact: a disequilibrium record of tectonic history: Geological Society of America Abstracts with Programs, v.29, p.45.

Florence, F. P., Darling, R. S., and Orrell, S. E., 1995 Moderate pressure metamorphism and anatexis due to anorthosite intrusion, western Adirondack Highlands, New York: v.121, p.424-436.

Jacobs, G. K., and Kerrick, D. M., 1981, Devolitization equilibria in H_2O-CO_2 and H_2O-CO_2-NaCl fluids: An experimental and thermodynamic evaluation at elevated temperatures and pressures: American Mineralogist, v.66, p.1135-1153.

Kolker, A., 1982, Mineralogy and geochemistry of Fe-Ti oxide and apatite (nelsonite) deposits and evaluation of the liquid immiscibility hypothesis: Economic Geology, v.77, p.1146-1158.

LaForce, M. J., Darling, R. S., and Hay, R. E., 1994, Geophysical investigation of the Port Leyden nelsonite: Geological Society of America Abstracts with Programs, v.26, p.30.

LeBreton, N. C. and Thompson, A. B., 1988, Fluid-absent (dehydration) melting of biotite in metapelites in the early stages of crustal anatexis: Contributions to Mineralogy and Petrology, v.99, p.226-237.

McLelland, J. M., Chiarenzelli, J., Whitney, P., and Isachsen, Y., 1988, U-Pb geochronology of the Adirondack Mountains and implications for their geologic evolution: Geology, v.16, p.920-924.

Mezger, K., Rawnsley, C. M., Bohlen, S. R., and Hanson, G. N., 1991, U-Pb garnet, sphene, monazite, and rutile ages: implications for the duration of high-grade metamorphism and cooling histories, Adirondack Mts., New York: Journal of Geology, v.99, p.415-428.

Olson, C., and Brackett, C., 1997, High temperature hydrothermal alteration and the origin of quartz-sillimanite nodular granite near Port Leyden, Adirondack Highlands, New York: Geological Society of America Abstracts with Programs, v.29, p.70.

Orrell, S. E., and McLelland, J., 1996, New single grain zircon and monazite U-Pb ages for Lyon Mt. gneiss, western Adirondacks and the end of the Ottawan orogeny: Geological Society of America Abstracts with Programs, v.28, p.#.

Philpotts, A. R., 1967, Origin of certain iron-titanium oxide and apatite rocks: Economic Geology, v.62, p.303-315.

Philpotts, A., R., 1981, A model for the generation of massif-type anorthosites: Canadian Mineralogist, v.19, p.233-253.

Spear, F. S., and Markussen, J. C., 1997, Journal of Petrology, in press.

Valley, J. W. and Essene, E.J., 1977, Regional metamorphic wollastonite in the Adirondacks: Geological Society of America Abstracts with Programs, v.9, p.326-327.

Valley, J. W., and Essene, E. J., 1980a, Akermanite in the Cascade Slide xenolith and its significance for metamorphism in the Adirondacks: Contributions to Mineralogy and Petrology, v.74, p. 143-152.

Valley, J. W. and Essene, E. J., 1980b, Calc-silicate reactions in Adirondack marbles: the role of fluids and solid solutions: Parts I and II: Geological Society of America Bulletin, v.91, p.114-117, 720-815.

Valley, J. W. and O'Neil, J. R., 1982, Oxygen isotope evidence for shallow emplacement of Adirondack anorthosite: Nature, v.300, p.497-50.

Valley, J. W., Essene, E. J., and Peacor, D. R., 1983, Fluorine-bearing garnets in Adirondack calc-silicates: American Mineralogist, v.68, p.444-448.

Whitney, P. R., 1991, Stratiform mafic gneisses of the anorthosite suite, west-central Adirondack Highlands: Geological Society of America Abstracts with Programs, v.23, p.49.

Whitney, P. R., 1992, Charnockites and granites of the western Adirondacks, New York, USA: a differentiated A-type suite: Precambrian research, v.57, p.1-19.

Whitney, P. R., 1996, Fakundiny, R. H., and Nyahay, R. M., West-central Adirondack Highlands field trip guide, Friends of the Grenville, 24 p.

Whitney, P., R. Isachsen, Y. W., Fakundiny, R. H., and Nyahay, R. M., 1997, Geologic map of the west-central Adirondack Highlands, Geological Society of America Abstracts with Programs, v.29, n.1, p.89.

Stratigraphy, Sedimentology, and Geochemistry of Seneca Lake, New York

John D. Halfman
Department of Geoscience
Hobart and William Smith Colleges
Geneva, NY 14456, halfman@hws.edu

Donald L. Woodrow
Department of Geoscience
Hobart and William Smith Colleges
Geneva, NY 14456, woodrow@hws.edu

Introduction

The purpose of this field trip is to look at the stratigraphy, sedimentology and Chloride geochemistry of Seneca Lake, and how they relate to deglaciation of the area. Our field trip (cruise), aboard the H-WS Explorer, will focus on representative sediments that have accumulated in the northern part of the lake since deglaciation which are typical of what is found in the other Finger Lakes. We will also highlight our ongoing efforts to collect and interpret high-resolution (2 - 12 kHz) seismic reflection profiles that image down to the glacial drift, and highlight Mike Wing's and Bill Ahrnbrak's recent understanding of the high chloride concentrations in Seneca Lake in comparison to the other Finger Lakes.

The Finger Lakes of central New York State consist of 11 elongated, north-south trending basins just south of Lake Ontario (Fig. 1). The basins are glacially scoured into the northern edge of the Appalachian Plateau (Coates, 1968, 1974). At Seneca Lake, the bedrock is primarily Devonian shales (Hamilton Group in the northern end of the lake), and lesser amounts of sandstones and carbonates that gently dip to the south-southwest. Silurian carbonates, shales and most importantly evaporites (mostly halite) are found below the Devonian section.

Seneca Lake is the largest (by volume) and deepest of the Finger Lakes (Fig. 1, Table 1). Only Cayuga Lake immediately to the east of Seneca is longer (61 km) and almost as deep (132 m). The other basins are smaller, ranging in length from 5 to 32 km and maximum water depth from 9 to 84 m. The present day lake is drained to the north-northeast through the Seneca River (New York State Cayuga-Seneca Barge Canal).

Table 1. Seneca Lake Statistics (Bloomfield, 1978)

Length	57 km
Maximum Width	5.2 km
Surface Elevation	136 m above mean sea level
Water Volume	15.54 km^3
Surface Area	175 km^2
Maximum Water Depth	186 m
Water Residence Time	18-20 years

Deglaciation of the Finger Lakes Region

Deglaciation of the Laurentide Ice Sheet, as recorded by recessional moraines and kame deposits, is linked to the present day erosional and depositional geomorphology of the Finger Lakes Region (Fig. 2, Muller and Cadwell, 1986), and specifically, the excavation and subsequent filling of the Finger Lake Basins. The best developed moraines are the East-West trending moraines near Geneva (north of Geneva near the Freeway and south of Geneva intersecting the lake near Glass Factory Bay), and the kame moraines immediately to the south of each Finger Lake.

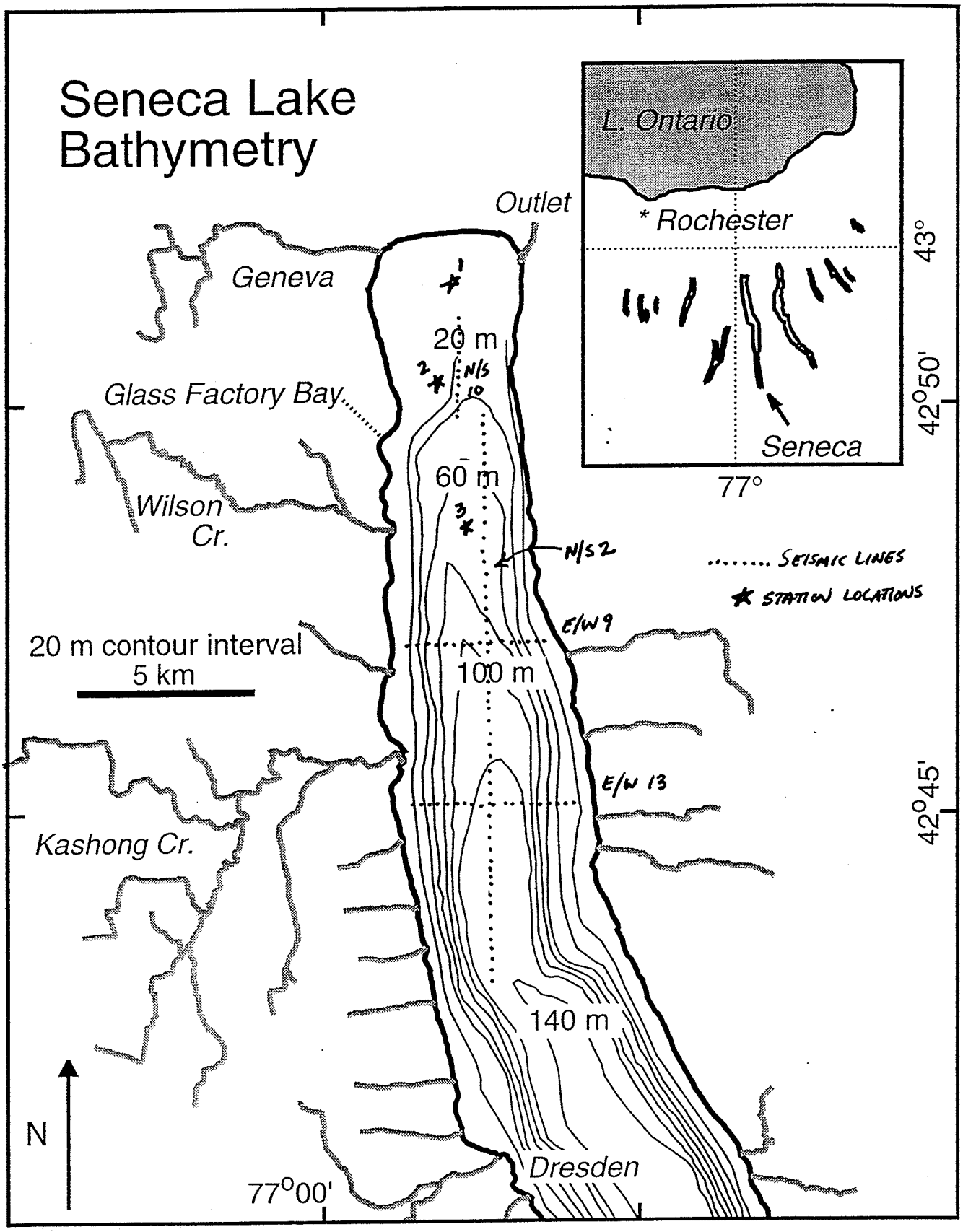

(*)

Figure 1. Bathymetric map of northern Seneca Lake with station locations for this field trip. The insert shows the location of Seneca Lake in relation to the other large lakes in the area.

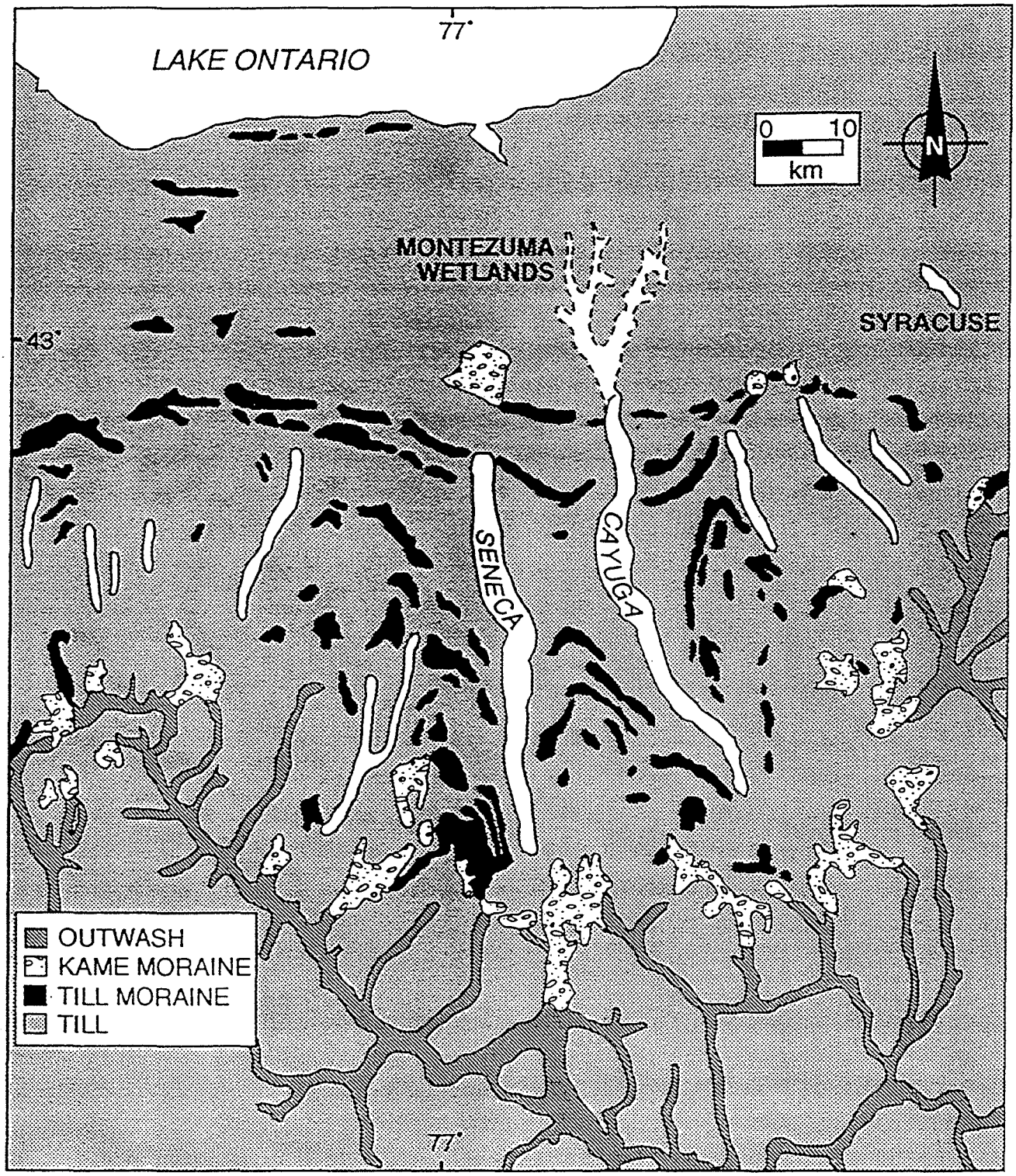

Figure 2. Generalized geomorphology of the Finger Lakes region (redrawn from Muller and Cadwell, 1986 by Mullins et al., 1996).

The kame moraines are collectively known as the Valley Heads Moraine that dam each lake at their southern margins, are restricted to the valleys and reveal evidence for deposition by moving water. It suggests that glacial erosion aided by large volumes of glacial meltwater during the occupation of the Valley Heads Moraine were the erosional agents for the Finger Lake Basins (Coates, 1968) and is consistent with Mullins' interpretations of recent Uniboom seismic reflection profiles of the basins.

In Seneca Lake, Uniboom seismic reflection profiles reveal a deep V-shaped notch cut into the bedrock with up to 270 m of sediment fill onlapping onto the erosional bedrock surface (Mullins and Hinchey, 1989; Mullins et al., 1996). It is deep enough to erode into the Silurian evaporites, which is important to the Chloride geochemical story presented below. Mullins proposed that pressurized meltwaters flowing under the ice excavated the basin when the ice occupied the Valley Heads moraine. Mullins links the majority of the sediment fill to deglaciation of the region as well. The seismostratigraphy of the sediment fill is interpreted as late glacial sediments with a thin cover of postglacial sediments based on acoustic character and correlation to short piston cores and on-land drilling. Mullins and coworkers differentiated 3 lower seismic sequences of ice-contact and water-lain sands and gravels fining upward to ice-proximal lacustrine muds that are related to the retreat of the Laurentian Ice Sheet from the Valley Heads moraine at the southern margin of the lake to the Geneva Moraine at the northern extent of the lake. The upper sequences are relatively thin and are interpreted to correspond to the proglacial rythmites, locally known as pink clays, which were deposited during a proglacial, high, lake-level phase of Seneca Lake when the ice front blocked the present day outlet to the north, massive brown muds, which are related to the rapid lowering of lake level when the lower, modern-day outlet opened to the north, and profundal postglacial, black to gray, stratified muds, which have accumulated in the lake since deglaciation. Timing of these events is not well constrained. Limited number of radiocarbon dates suggest that the Valley Heads moraine was occupied about 14.4 ka, and the brown mud - postglacial transition was 13.9 ka and suggests that the retreat of the ice sheet and deposition of the ice-related sediments occurred in a rapid period of time (Mullins et al., 1996).

The basin bathymetry is similar to a steep-sided (bedrock cut), flat-floored trough (sediment fill). The lake floor gradually deepens from north to south before shoaling at the southern end of the lake near Watkins Glen. East/West profiles gently deepen to the central portion of the lake, north of Glass Factory Bay. Farther south, the lake bottom gently deepens in nearshore locations, then quickly descends to a flat lying basin in the central part of the lake. A grade of 10% or more is not uncommon on the steepest slopes south of Wilson Creek. Farther to the south, the nearshore areas are narrower and the steep slopes are steeper.

Stratigraphy - Ice-Contact, Ice-Proximal and Postglacial Sediments (after Woodrow et al., 1969 & Woodrow, 1978)

Short cores and surface grab samples reveal a number of sediment types within the basin (Woodrow et al., 1969; Woodrow, 1978; Mullins et al., 1996; Halfman and Herrick, submitted). Glacial drift (ice-contact and ice-proximal) fine sands and silts underlie proglacial rythmites (pink clays). Both outcrop in the northern and other shallow water margins of the lake. Lacustrine marls, muds with photosynthetically-induced microcrystalline carbonate with fossil mollusk layers and macroscopic plant fragments are also sporadically observed in water depths shallower than 20 m. The deep profundal zone contains olive-gray to black, laminated, fossil poor, organic rich muds. Massive brown muds are found between the younger postglacial muds and older pink clays. Halfman and Herrick (submitted) recently detected evidence for basin-scale mass movements of the pink clays during the waning stages of pink clay deposition (see below).

Sedimentology - High-Resolution Seismic Reflection Profiles (after Halfman and Herrick, submitted)

Over 100 km of high-resolution (2 - 12 kHz) seismic reflection profiles, collected from the northern end of the lake delineate the upper stratigraphy and investigate the depositional and erosional processes in the basin (Halfman and Herrick, submitted). The seismic system images up to 30 meters of section. Four major acoustic sequences encompassing the upper part of the glacial drift to the postglacial sediments were identified based on acoustic character and correlation with short (1 to 3 m) piston cores and surface grab samples (Fig. 3, Table 2).

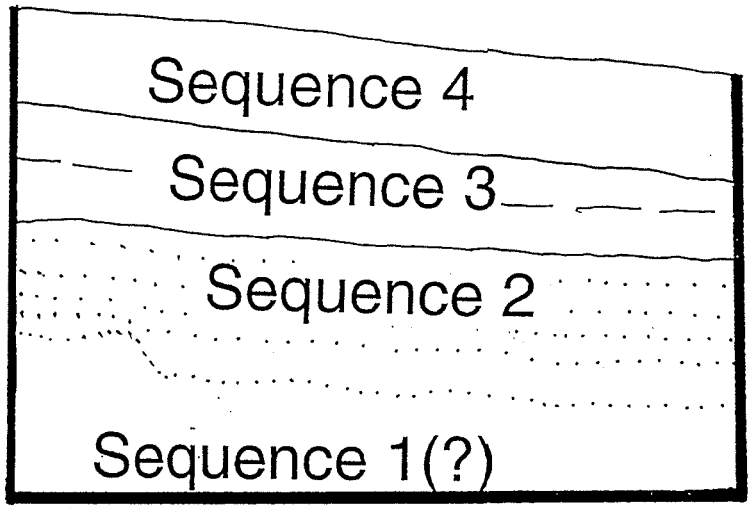

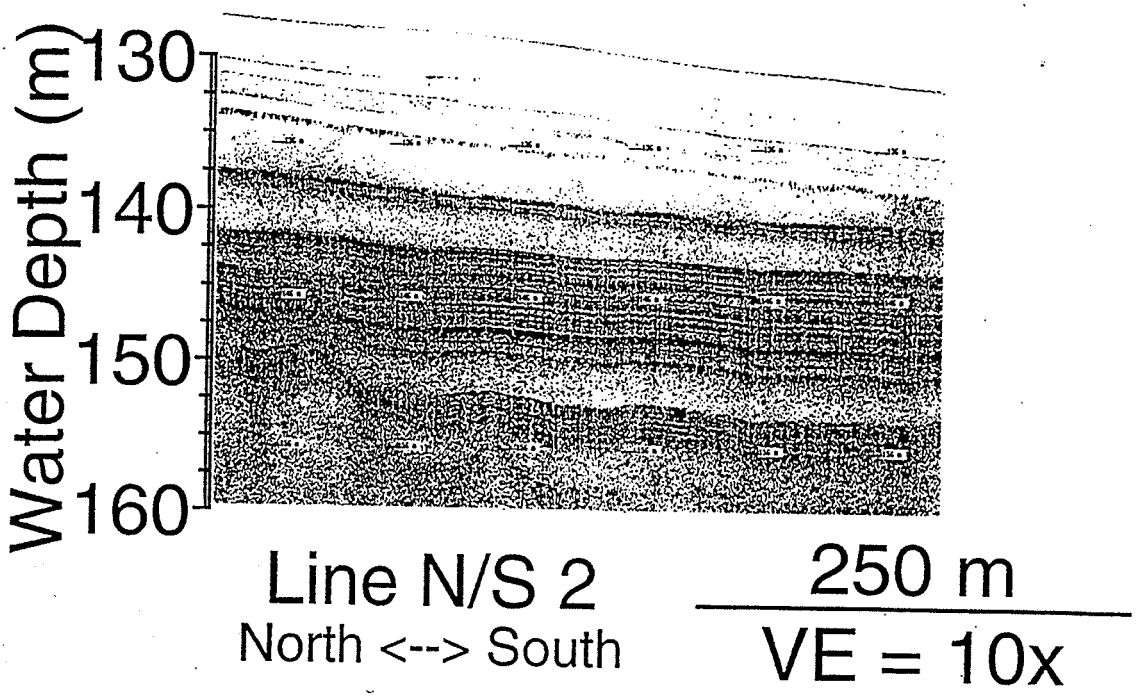

Figure 3. An example of the acoustic stratigraphy of the upper 30m of sediment in the deeper portion of Seneca Lake (from Halfman and Herrick, submitted). The line drawing outlines the major sequences identified in the text (Table 2).

Table 1. High-Resolution Seismostratigraphic Sequences (from Halfman and Herrick, submitted)

Sequence	Acoustic Character and Interpretation
4	Low amplitude surface and internal reflectors that onlap onto older sequences. Postglacial laminated muds & underlying brown muds
3	Two and locally more transparent units with surface reflectors similar to sequence 2. Mass movement deposits of pink clays
2	High-amplitude surface and parallel to subparallel internal reflectors on decimeter scale. Proglacial rythmites (pink clays)
1	High-amplitude surface and occasional internal point reflectors. Glacial drift
Others	Transparent section, the seismic signal is typically attenuated by gas (biogenic methane?). Lacustrine early-Holocene marls (detected in isolated nearshore areas, water depths < 20 m)

The high-resolution seismic reflection profiles portion of the field guide focuses on evidence for: (1) mass movement of the pink clays, and (2) sediment reworking to water depths of 60 m by wind-driven surface waves and currents, wind-driven internal waves and currents associated with seiche activity along the thermocline, and a possible 20 m lowstand of the lake during the Holocene.

Mass Movement of the Pink Clays

Sequence 3 is a previously unidentified seismostratigraphic unit, and is interpreted as two main and locally more mass movement deposits of the pink clays. A number of observations support our hypothesis. The sequence is found abruptly between and above the pink clays, filling the bathymetric lows in the lake (Fig. 4). The sequence thins to the south, and slowly gains additional high-amplitude internal reflectors that are characteristic of the older pink clays. Isolated "pods" of pink clays are laterally encased in a package of sequence 3 and suggests that the pods are parent material caught in a flow of proglacial rythmites (Fig. 5). Woodrow and coworkers (1969) described folded and faulted pink clays recovered from the margins of the deep basin. They hypothesized that the deformed strata were the product of down slope movement of pink clays from the neighboring steep sides of the basin. We hypothesize that sequence 3 is a subaqueous, down slope movement of upper portions of pink clays. Movement was towards the center of the basin and towards the south along the long axis of the lake. We infer that the movement was intense enough to disturb the internal stratigraphy of the pink clays but the intensity of disturbance decreased to the south. Timing of the two main flows is stratigraphically restricted to the waning stages of pink clay deposition in the basin about 14 ka. The triggering mechanisms could be pulses of meltwater or meltwater sediments, rapid drawdown of the lake as a lower outlet was opened to the north, melting of stagnant ice within the glacial drift along the central portion of the basin, and/or earthquake activity.

Sediment Reworking and Possible Lower Lake Levels

The postglacial muds are 5 to 8 meters thick and blanket the profundal portions of the basin. The thickness of postglacial sediments decreases rapidly on the steep slopes, where normal faults, slumping, accurate glide planes, and other evidence for episodic down slope movement of sediments is evident. The postglacial muds only form a thin veneer of material that unconformibly covers pink clays and glacial drift in shallow water areas, down to water depths of 60 m in the northern part of the lake. Surface waves and associated currents rework shallow-water sediments. Theoretical calculations for Seneca Lake suggest that surface waves from sustained 50 kph winds can erode fine sands at water depths up to 20 meters in the lake (Johnson, 1980). This 20 meter depth is a maximum estimate because parameters like effective fetch were deliberately overestimated in the calculations.

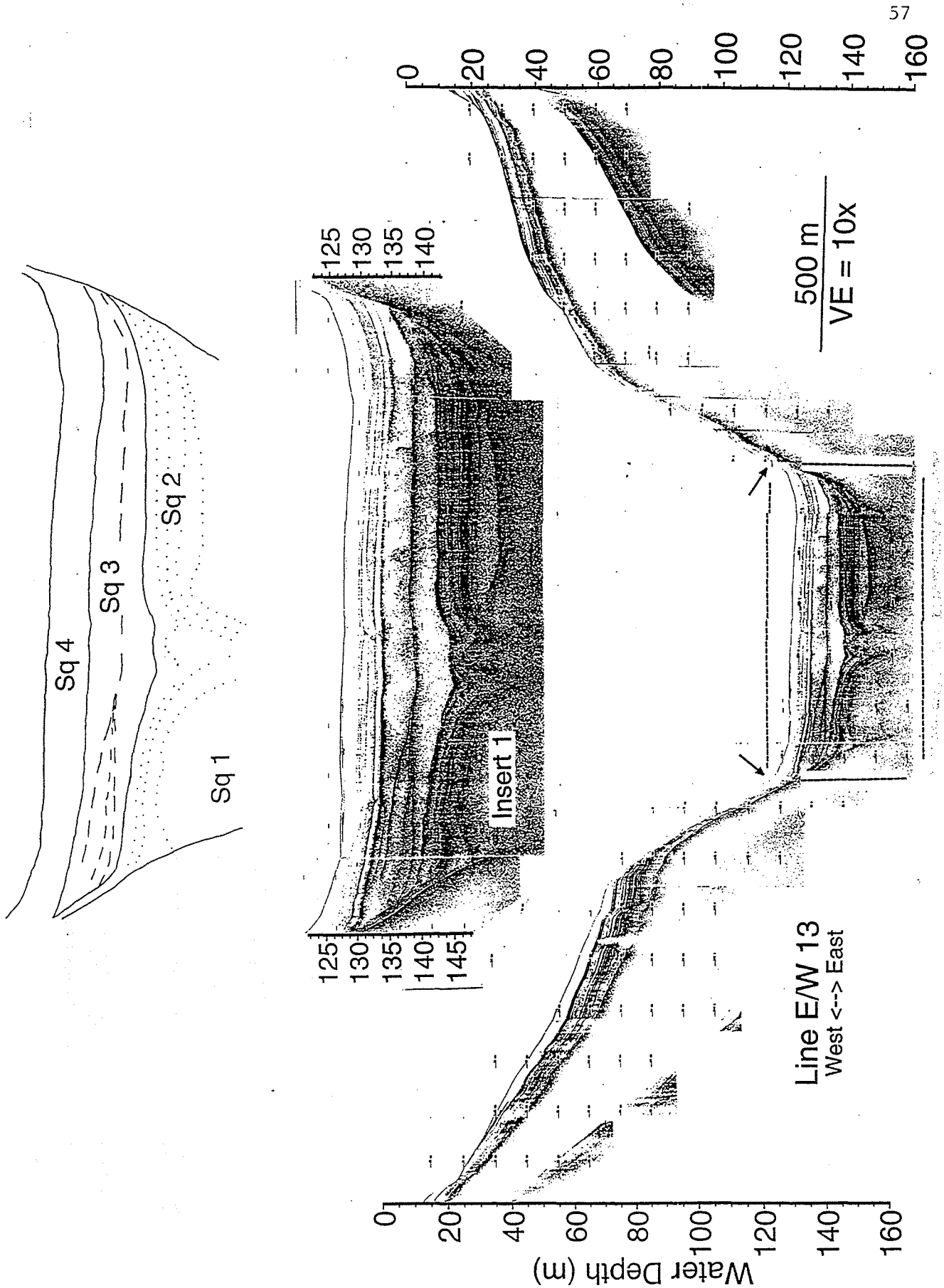

Figure 4. East/West seismic profiles from the lake with sequence 3 found between and above the pink clays (after Halfman and Herrick, submitted).

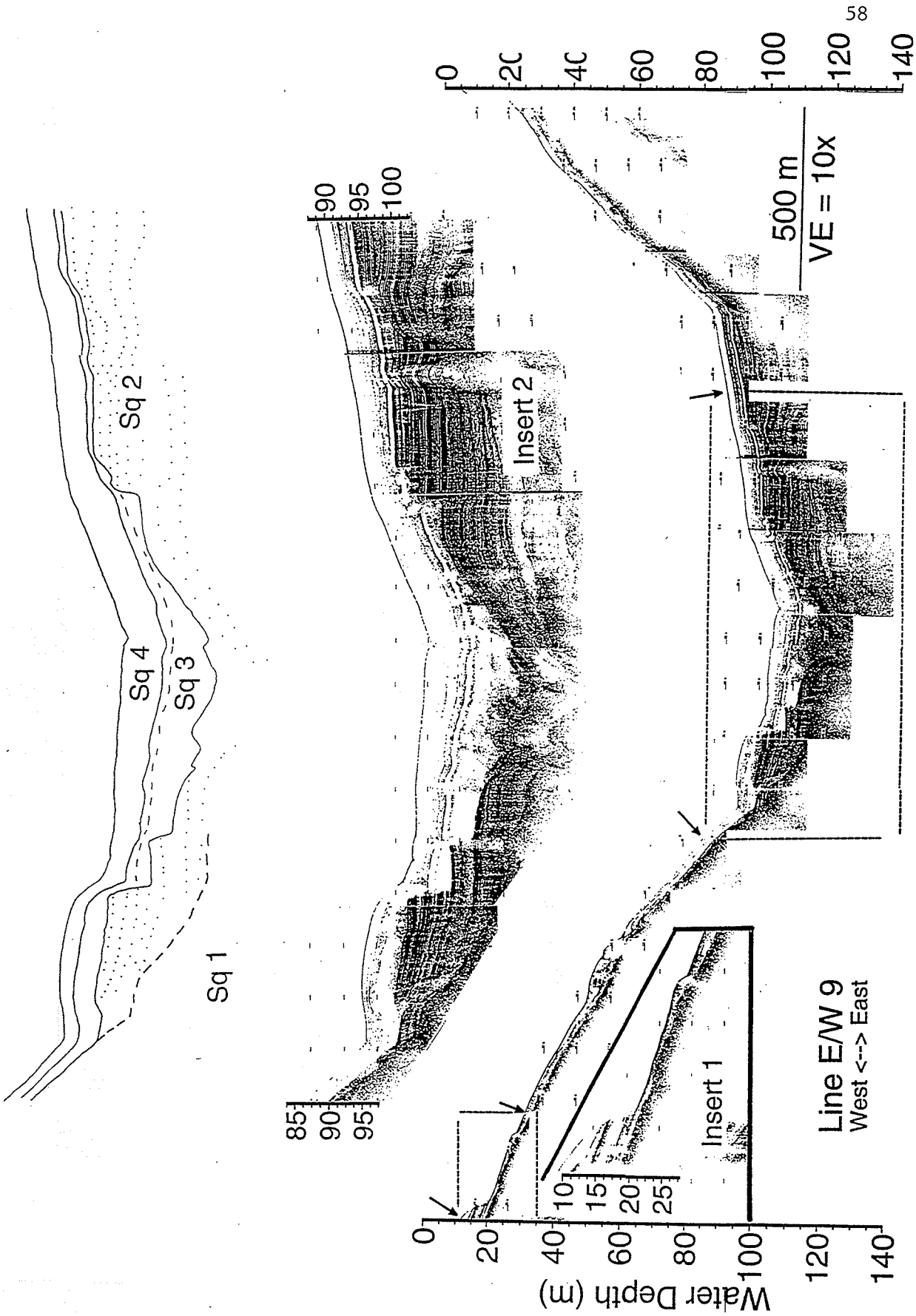

Figure 4. East/West seismic profiles from the lake with sequence 3 found between and above the pink clays (after Halfman and Herrick, submitted).

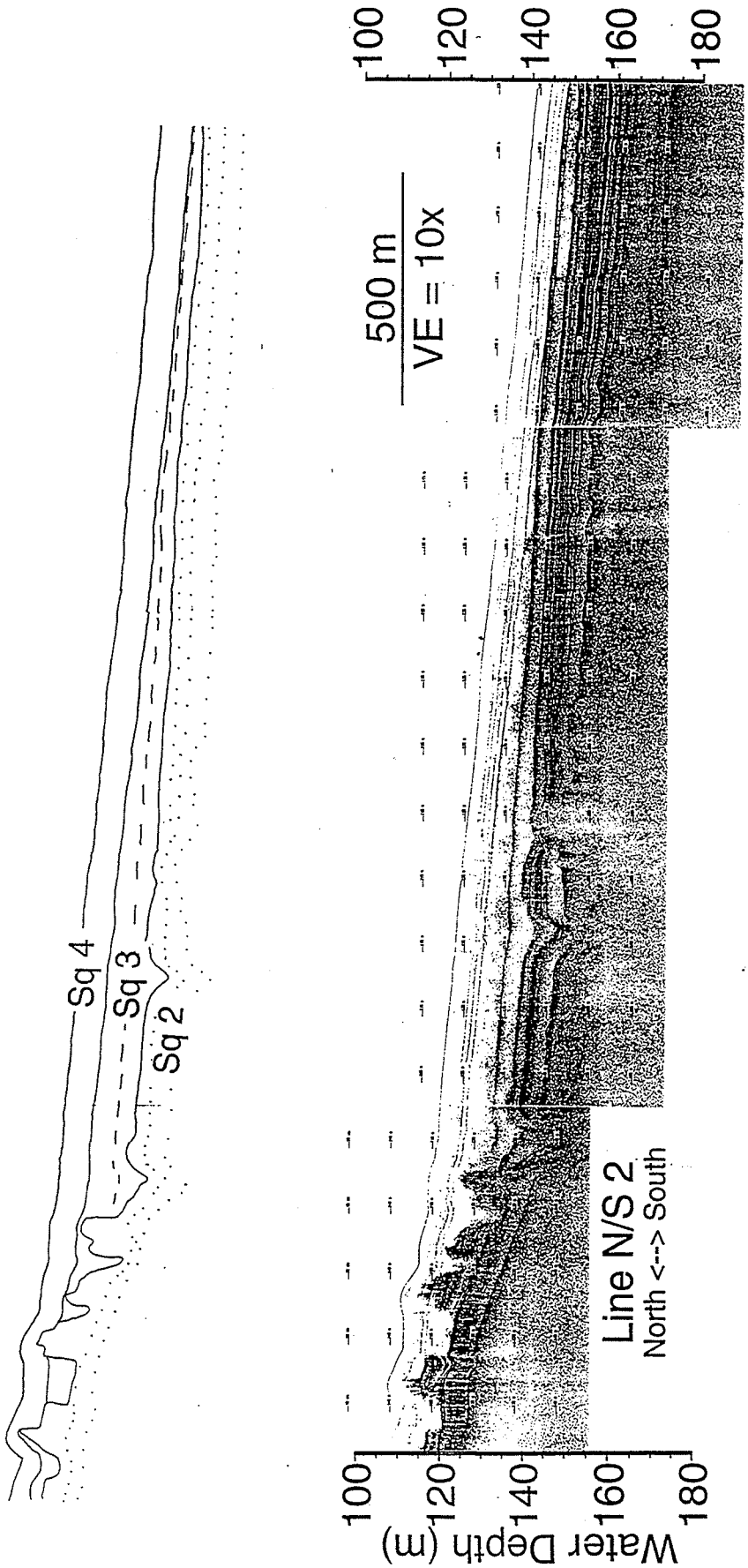

Figure 5. Pods of pink clay encased in a package of sequence 3. It suggests that sequence 3 is a mass movement of pink clays during the waning stages of deglaciation in the basin (after Halfman and Herrick, submitted).

Twenty years of current meter data collected by Bill Ahrnsbrak (Hobart and William Smith Colleges) indicate that currents and internal waves associated with seiche activity are significant in Seneca Lake (e.g., Ahrnsbrak, 1974; Ahrnsbrak et al., 1996). For example, current velocities of 30 cm/s have been recorded 1 meter above the lake floor at a water depth of 66 m this past Fall (1996) but only immediately after strong southerly wind events associated with the passage of a front. These currents must impact sedimentation in the lake at water depths deeper than 20 m, apparently down to 60 m. The strong seiche activity is probably enhanced by the elongated nature of the basin.

A lake-floor scarp, where the lake bottom quickly descends from approximately 15 to 20 meters, is observed in Seneca Lake (Fig. 6). We are presently investigating the following hypotheses for its origin (1) The scarp may be the result subaqueous sediment redistribution and deposition by the reworking processes mentioned above, and the reworked sediments have prograded lakeward with time. (2) The scarp could be the lakeward extent of marl deposition. (3) The scarp may be a wave-cut feature, i.e. the result of sediment truncation by surface, wind-driven waves during a lowstand of the lake sometime after the deposition of the early-Holocene marls. The preliminary data favor the later hypothesis but additional data are required to confirm our tentative hypothesis.

Geochemistry - Seneca Lake Chloride Concentration (after Wing et al., 1995)

Seneca Lake is the water supply for many of the inhabitants within its drainage basin. Thus, water quality of the lake is a concern to many. Chloride concentrations are 8 to 10 times higher in Seneca Lake (approximately 150 ppm) than they are in the other Finger Lakes (5 to 20 ppm, and 80 ppm in Cayuga Lake), high enough to pose a long-term health hazard for individuals prone to heart disease who use Seneca Lake water for drinking. The higher concentration is not the result of landuse or mining practices in the basin, because the annual chloride loading to Seneca Lake by streams and local mines is similar to those found at the other Finger Lakes, and more importantly, is deficient by an estimated 170×10^6 kg of salt. The deficiency suggests an interesting hypothesis. Seneca Lake is the only Finger Lake (with the partial exception for Cayuga Lake) deep enough to intersect the Silurian evaporites. Thus, its great depth provides a conduit to an extra source of Chloride, which is not available to the other shallower Finger Lakes. Cayuga Lake is the exception to this rule. Wing and coworkers (1995) propose that it's second deepest status is consistent with its second highest chloride concentrations among the Finger Lakes.

Field data collected in 1991 and 1992 support this hypothesis. Chloride concentrations were observed to increase in the hypolimnion, the water mass below the thermocline, during the summer of 1991 and 1992. The saltier water was mixed into the rest of the lake in early winter when the lake became isothermal (isopycnal). Sediment pore waters reveal large regions of higher salinity water several meters below the sediment-water interface, where chloride concentrations as high as 30 ppt have been found. Analysis of pore waters from piston cores reveal increasing Chloride concentrations with increasing burial depth.

H-WS Explorer

H-WS Explorer is a steel hulled, single screw, diesel powered vessel built in 1954 for the United States Navy. Hobart and William Smith Colleges acquired the vessel in 1976 after it had also been used in, e.g., the lobster and fishing industries. The vessel is documented "Oceanographic" by the United States Coast Guard and meets all of the standards applicable to such a vessel. In 1989, major renovations resulted in the construction of a 20 by 10 ft laboratory on the main deck to compliment the growing list of standard oceanographic/limnologic equipment including 2 Sea Bird CTD's (Conductivity, Temperature, Dissolved Oxygen, pH, Turbidity and Depth sensors), TSK Micro BT temperature profiler, EdgeTech (EG&G) X-Star high-resolution seismic reflection system, EdgeTech sidescan sonar, computers, flume hood, weather station and other equipment. The pilot house has a full compliment of safety, navigation and communication equipment including up-to-date radar, satellite navigation, marine radio-telephone, cellular phone and other equipment. Most importantly, the vessel is operated by a licensed captain and mate. It provides a safe, well-equipped platform useful under most weather conditions experienced on Seneca Lake.

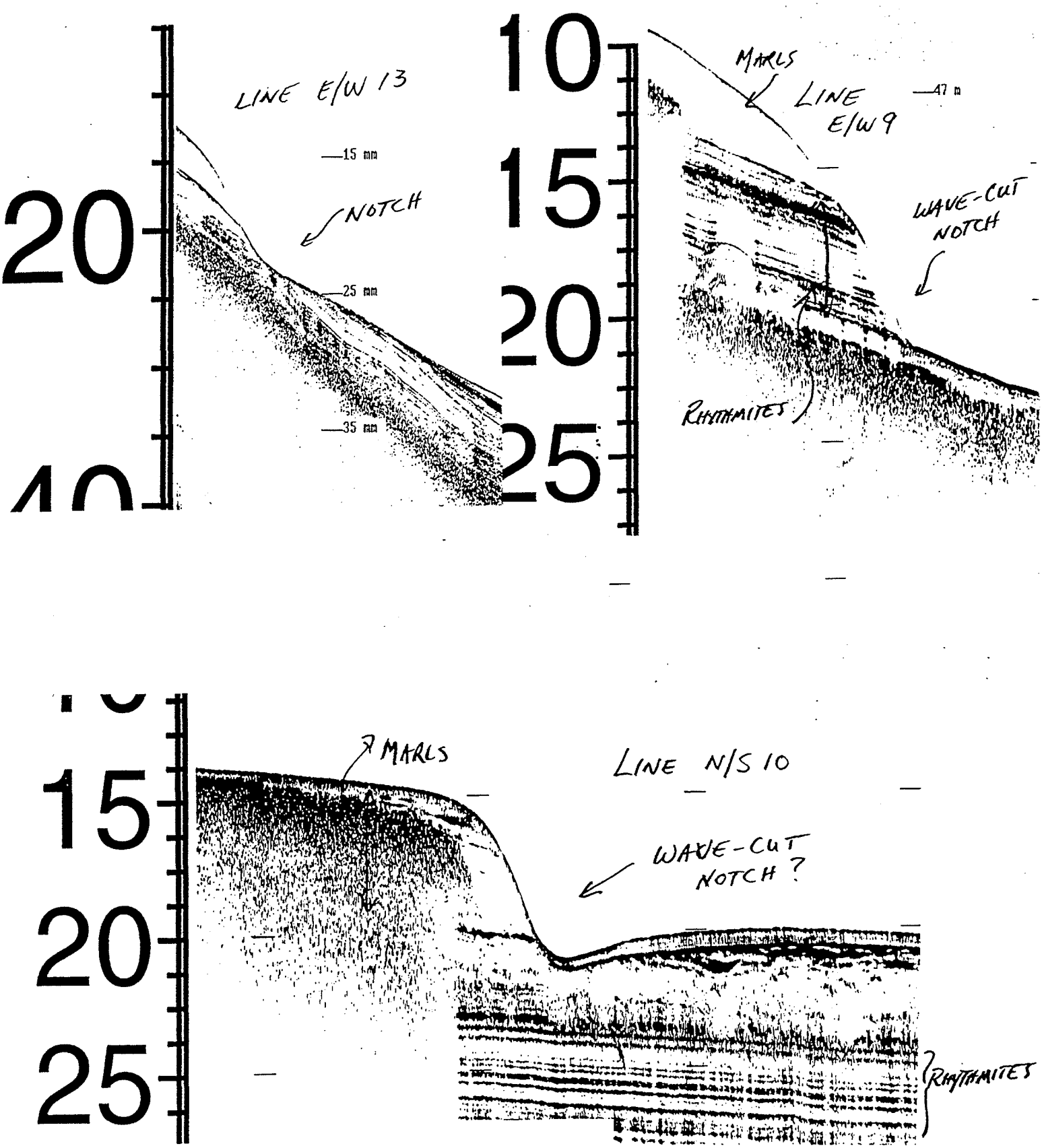

Figure 6. A scarp at 15 to 20 meters of water is found through out the basin. Its origin is currently being investigated.

References

Ahrnsbrak, W. F., 1974, Some additional light shed on surges: Journal of Geophysical Research, v. 79, p. 3482-3483.

Ahrnsbrak, W. F., Valengavich, A. and Konkle, A., 1996, Near-shore circulation features in (Longitudinal) mid-Seneca Lake, NY, and their relationships to internal wave activity and synoptic-scale wind changes: Geological Society of America Abstracts with Programs, v. 28.

Bloomfield, J. A., 1978, Lakes of New York state, Vol. 1, Ecology of the Finger Lakes: New York, Academy Press, 499 p.

Coates, D. R., 1968, Finger Lakes, Fairbridge, R. W., ed., Encyclopedia of geomorphology: New York, Reinhold Corporation, p. 351-357.

Coates, D. R., 1974, Reappraisal of the glaciated Appalachian Plateau, in Coates, D. R., ed., Glacial geomorphology: Binghamton, New York, State University of New York Publications, p. 205-243.

Halfman, J. D., and Herrick, D. T., submitted, Reworking of late glacial and postglacial sediments by waves, seiche activity and a possible mid-Holocene lowstand in Northern Seneca Lake, New York. Bulletin, Geological Society of America.

Johnson, T. C., 1980, Sediment redistribution by waves in lakes, reservoir and embayments, in Proceedings of the Symposium on Surface Water Impoundments, American Society of Civil Engineers: Minneapolis, American Society of Civil Engineers, p. 1307 - 1317.

Muller, E. H., and Cadwell, D. H., 1986, Surficial geologic map of New York - Finger Lakes sheet: Albany, New York State Museum, Geological Survey Map and Chart Series no. 40, 1 sheet, scale 1:250,000.

Mullins, H. T., and Hinchey, E. J., 1989, Erosion and infill of New York Finger Lakes: Implications for Laurentide ice sheet deglaciation: Geology, v. 17, p. 622-625.

Mullins, H. T., and others, 1996, Seismic stratigraphy of the Finger Lakes: A continental record of Heinrich event H-1 and Laurentide ice sheet instability, in Mullins, H. T., and Eyles, N., eds., Subsurface geologic investigations of New York Finger Lakes: Implications for Late Quaternary deglaciation and Environmental change: Boulder Colorado, Geological Society of America Special Paper 331, p. 1-35.

Wing, M. R., Preston, A., Acquisto, N., and Ahrnsbrak, W.F., 1995, Intrusion of saline groundwater into Seneca and Cayuga Lakes, New York: Limnology and Oceanography, v. 40, p. 791-810.

Woodrow, D. L., 1978, Surface and near-surface sediments in the northern part of Seneca Lake, NY: New York State Geological Association Field Trip Guidebook 50, p. 250-255.

Woodrow, D. L., Blackburn, T. R., and Monahan, E. C., 1969, Geological, chemical and physical attributes of sediments in Seneca Lake, New York, in Proceedings, Twelfth Conference on Great Lakes Research, p. 380-396.

Cruise Log

This field trip starts and stops aboard the H-WS Explorer, and investigates the sediment character and water chemistry at selected locations (Fig. 1). We will look at the X-Star seismic stratigraphy of the sediments while underway between stations. Surface grab samples will be collected at the first two stops, and a short piston core at the third stop. We will also deploy the CTD and collect water samples to analyze at the third station as well. We will not concern ourselves with the lacustrine marls because they compose a small fraction of the sediments in the lake.

STATION #1. Shallow-Water Sandy Silts - Northern end of Seneca Lake

The lake floor is covered by sandy silts, with the coarsest sediments in the northwest margin of the lake. Shell and plant debris and the occasional ice-raft pebble make up the other minor components. We believe that these sediments must be derived from the reworking of and erosion of glacial drift. Subbottom images suggests that the sand forms a thin wedge of sediment above the pink clays and/or glacial drift. In many places the seismic images are attenuated by gas (biogenic methane?).

Suitable substrate (coarse materials) is covered by zebra mussels. Zebra mussels are an exotic species that has been recently (1991?) introduced in the lake. They are prolific filter feeders, filtering, on average, a few liters of water each day, extracting the plankton from the water column. One possible measure of their impact is historical Secchi disk data. Secchi disk are used to measure water clarity. To a first approximation, deeper Secchi disk depths correspond to less turbid water (e.g., smaller plankton concentrations). Historical Secchi disk data have shown increasing Secchi depths over the past decade from a few meters to over 5 meters deep during the productive early summer months. This change is consistent with a decrease in chlorophyll concentrations. The exact reasons for the increase in water clarity (and decrease in chlorophyll) are not completely understood but the Secchi disk data suggests two hypotheses: that the burgeoning population of zebra mussels has become large enough to significantly reduce the standing crop of plankton, and/or an increase in the quality of sewage treatment by lake-shore residents has reduced the anthropogenic "nutrient loading" to the lake.

STATION #2. Proglacial Rythmites - Offshore of Belhurst Castle - Geneva Country Club

To the south of station 1, pink clays may be found below a thin veneer of postglacial material. The pink clays are well stratified, very cohesive and exhibit light red to pink colors. Single pebble to granule sized grains and ostracode shells are found widely scattered in the sequence. Well defined, parallel to subparallel reflectors characterize these clays in the subbottom profiles. The reflectors commonly outcrop onto the lake floor in shallow water. We interpret these clays as proglacial rythmites, typical of many proglacial lakes. It is unclear whether the couplet are annual events (varves). In the northern part of the lake, the pink clays are folded. The subbottom profiles suggest that the pink clays collapsed into ice-block holes in the underlying drift and/or the ice front experienced small re-advances.

STATION #3. Postglacial Muds & Lake Geochemistry - Offshore of Clarks Point

Moving south across exposures of glacial drift, the lake floor descends to a flatter floor typical of the deeper parts of the lake. At this location the sediments are very fine grained, black to gray, stratified and rich in organics. These sediments blanket the older materials with thicknesses up to 8 meters in the subbottom profiles. The sequence thins rapidly in water depths shallower than 60 meters and on the steep slopes on either side of the basin. They contain no shell material, a few coarse grains of silt and sulfide minerals. These muds are interpreted as the postglacial sediments deposited since deglaciation. The source is the suspension of fine material carried into the lake by streams and/or erosion of older, shallow-water bottom sediments by surface and internal waves.

We will also deploy the CTD and analyze the surface water for its chloride concentration to discuss the source of the "extra" Chloride to Seneca Lake.

CAMBRO-ORDOVICIAN AND MODERN CARBONATE FACIES OF THE MOHAWK-HUDSON VALLEYS, NEW YORK

Gerald M. Friedman
Department of Geology, Brooklyn College and Graduate School of the City University of New York, Brooklyn, NY 11210, and Northeastern Science Foundation affiliated with Brooklyn College, Rensselaer Center of Applied Geology, 15 Third Street, P.O. Box 746, Troy, NY 12181-0746, gmfriedman@juno.com

Introduction

A shallow epeiric sea covered most of the North American continent. The shallow water limestones and dolostones that accumulated on this platform make up the Upper Cambrian, Hoyt and Galway formations and the Lower Ordovician Tribes Hill Formation that we will examine during this field trip. These carbonates were deposited in a roughly east-west belt at 20° S latitude. Quartz sand and dolomite were deposited in varying intermixed quantities (Galway Formation) with localized algal reefs (Hoyt Limestone) fringing the southern Adirondack shore. The limestones and dolostones of the Tribes Hill Formation were laid down along the eastern edge of the craton about 35 miles west of the shelf edge. As they were deposited close to the shelf edge they were affected by the tidal fluctuations of the adjacent waters of the deep ocean. To the east of the platform, deep-water shales and carbonate clast conglomerates accumulated on the continental slope and rise.

The end of Early Ordovician time is marked in the rock record by the Knox unconformity which exposed the broad continental shelf. In Middle Ordovician, the Taconic Orogeny was initiated followed by the Acadian Orogeny in the Devonian and the Alleghanian Orogeny in the Late Carboniferous with intervening periods of quiescence and carbonate deposition. The eastern edge of the craton was subjected to deformation during the Appalachian orogenies but in the region of the Mohawk Valley and Saratoga Springs of the present field trip, the Cambro-Ordovician

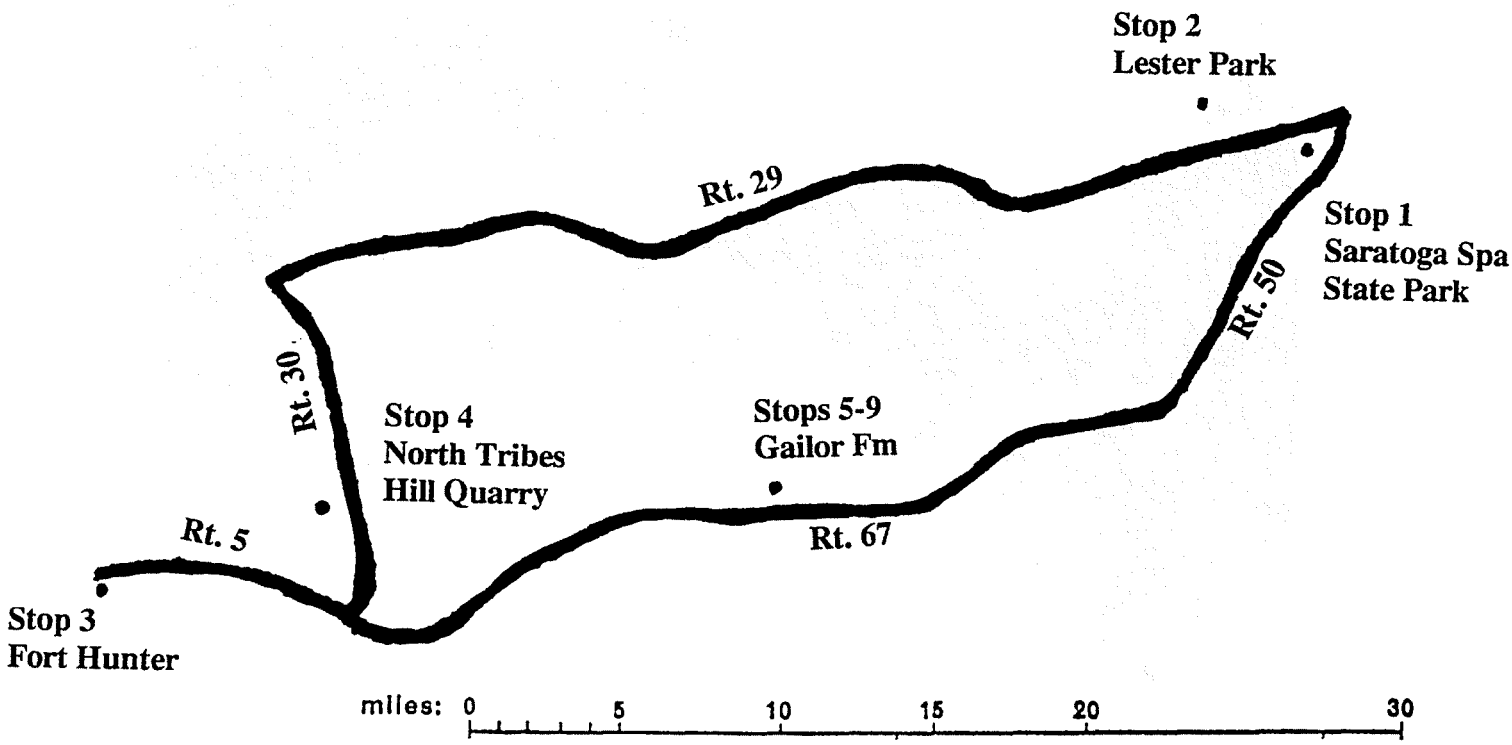

Figure 1. Field-trip log.

platform strata are relatively undeformed. Figure 1 is a map showing the field-trip route marked with the location of the stops.

Road Log

From Saratoga drive to NY50 East Parking Lot of the Saratoga Performing Arts Center (necessitating a left turn). Park near box office of Arts Center.

STOP #1. Saratoga Spa State Park: Modern Nonmarine Limestones (Travertine)

This stop can also be reached through the Main Gate of the State Park on Route 9.

Route of Walk

Walk downhill into a small wood with picnic tables towards a stone building. Bicarbonate- charged, saline waters issue from a faucet at the side of the building and pass through a pipe below dirt road, re-emerging on the bank of Geyser Brook. Calcite precipitates on the steep slope of this bank, forming a terrace of travertine. The water is known as Orenda Spring and the terrace as Orenda Terrace; we will get a better view of this terrace later from below. A walk of a few hundred feet along dirt road leads to the Hayes Well Spring at bridge across Geyser Brook. A taste of this water is "rewarding" for its initial effect. Prolonged drinking is not recommended. From Hayes Well Spring you see the Island Spouter "Geyser" a few hundred feet upstream. The water of this fascinating "geyser" is from a well; the water spouts from a small orifice to a height of about 30 feet. This well was drilled about 80 years ago and the large cone of travertine has formed since.

Follow the path along Geyser Brook upstream. In the bank on the left is an exposure of Middle Ordovician Canajoharie Shale, an outer shelf to slope facies. On occasion, graptolites can be found in this shale. Continue to Orenda terrace to study travertine (Fig.2). Note the rippled surface of the travertine and the brown iron-oxide

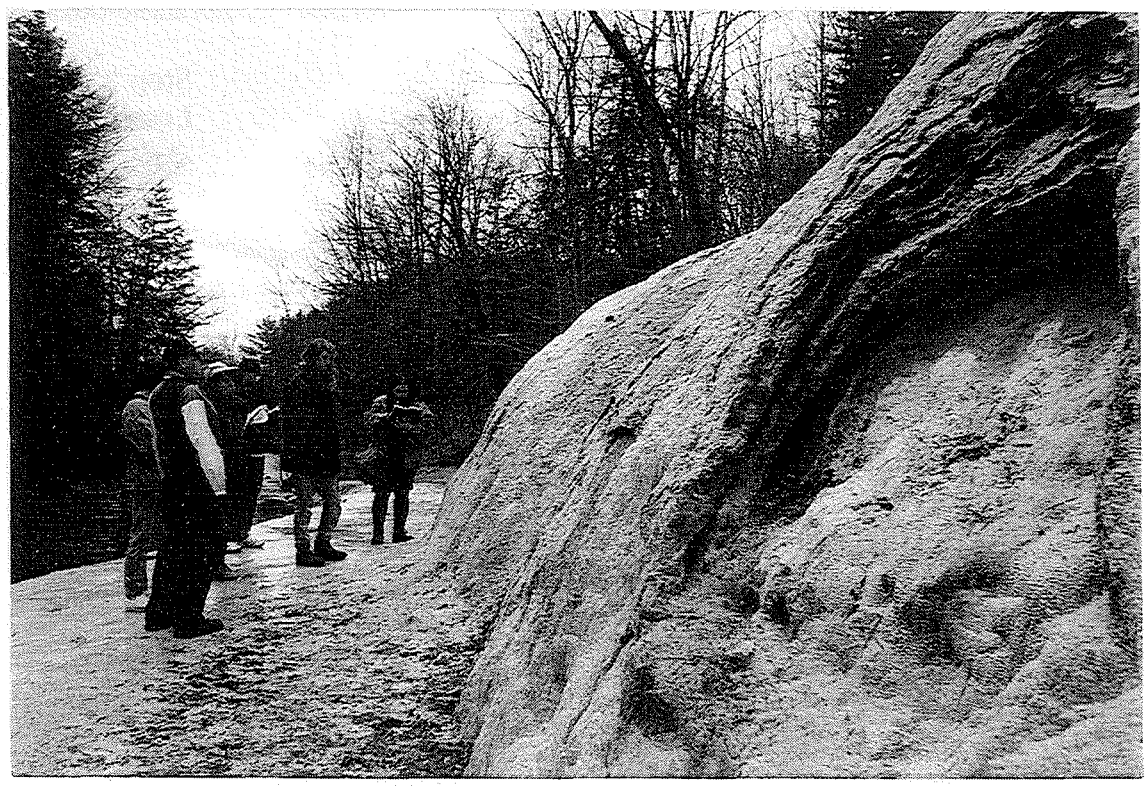

Figure 2. Orenda Terrace. Cone of travertine exposed at bank of Geyser Brook.

coloration that occurs in streaks. Up to approximately 4 cm of calcite may precipitate annually at the foot of the terrace. Note "caves" and dripstone at far end of terrace and search for calcite-coated twigs and leaves or impressions of leaves in the travertine. Pisolites occur in abundance on the walkway between travertine cone and bank of brook. Spheroids and ooliths are likewise present (Schreiber et al. 1981).

Discussion

Although in the classical studies on limestones, including the authoritative work of Pia (1933), nonmarine limestones are accorded some measure of importance, the literature on modern carbonates neglects nonmarine carbonates. At this stop you'll see an excellent example of travertine, a rock which, like reef-rock, crystallizes in an initially stony condition.

The term travertine is derived from the Italian word, travertino, a corruption of tiburtino, "the stone of Tibur", which is a former name of the locality now called Tivoli (see Sanders and Friedman, 1967, p. 176), The type locality at Tivoli has been classically described by Lyell (1830, p. 207-210) and Cohn (1864). Some authors make a sharp distinction between the terms travertine, tufa and sinter: others use these terms synonymously (Pia, 1933; Gwinner, 1959, Sanders and Friedman, 1967, p. 176).

Travertine in Saratoga Spa Park gathers around the orifice of wells, on terraces from which water descends, or as a cone around a "geyser". Waters enriched in calcium bicarbonate issue from the subsurface, lose their carbon dioxide and insoluble calcite precipitates:

$$2HCO_3^- + Ca^{++} \rightleftharpoons 2CaCO_3 + H_2O + CO_2 .$$

Twigs and leaves of beech, maple, and oak are preserved as they become coated with calcite or leaves form impressions in the travertine. The calcium bicarbonate-enriched waters originate nearly 1,000 feet below the surface in the underlying Cambrian-Ordovician limestones and dolostones, especially in the Gailor Dolomite. The waters are confined as in an artesian well beneath a thick cover of impervious Canajoharie Shale from which drilling recovers them. In the early years, the springs issued from natural crevices in the rocks, particularly from the prominent MacGregor fault. Later, pits were dug; the present wells flow through pipes set in bore holes.

The composition of the Saratoga mineral waters is unique among waters that precipitate travertine (Back et al. 1995; New York State Department of Health 1959; Young and Putnam 1979). Most waters that make travertine, especially those of the classical areas in Europe, drain areas of karst, and are of low salinity. By contrast, analyses of Saratoga waters give salinities that geologists classify as "brackish" (approximately 11 %). Inspection of tables of analyses (e.g. Kemp, 1912) indicates the closeness of the composition of these waters to that of formation waters. This is especially true of the high concentration of NaCl. As the waters in the subsurface apparently dissolve limestones and dolostones, the concentration of the calcium, magnesium, and bicarbonate is higher than that of many formation waters. As in most formation waters, the sulfate content is low. Although the origin of the mineral waters is controversial (Hewitt, McClennan, and Nilsson, 1965), this controversy parallels that of the origin of formation waters. The mineral waters are probably formation waters whose salinity has been lowered as a result of mixing with meteoric water.

Newly precipitated calcite from the Orenda Springs gives a strontium isotopic value of 0.716429 (10) $^{87}Sr/^{86}Sr$ (+/- 2S.D)*, a continental crust signature (Fig. 3). If the waters were derived Upper Cambrian formation water, an Upper Cambrian seawater signature would have been obtained (see Fig. 3).

According to Siegel (1996) carbon isotopic analyses likewise hint that the carbon may be expelled from the mantle

---

* The Sr analyses are normalized to $^{86}Sr/^{88}Sr = 0.11940$.
Analyses of NBS 987 averaged 0.710241 (09) (n = 39) during the period of these analyses.
Errors on $^{87}Sr/^{86}Sr$ are given as 2 sigma (95%) in the last two digits.

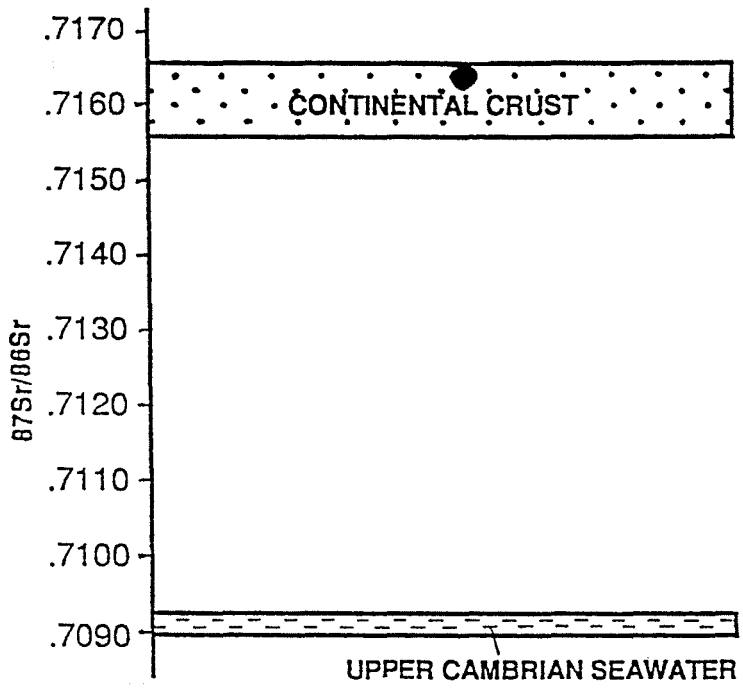

Figure 3. Strontium isotopic composition of carbonate travertine of Orenda Spring (see large dot).

many kilometers below the fault zone.

The aquifer containing the mineralized water is under carbon-dioxide pore pressures which are estimated to be as high as five atmospheres that spew mineral water and gas several meters high (Siegel 1996). The acidity of the mineral waters depends on how much carbonic acid they contain; pH typically ranges from 5.5 to 6.5. The mineral springs discharge cold water (Sneeringer and Dunn, 1981).

The distribution of the wells, a total of about 200, is controlled by the MacGregor Fault and its subsidiary faults. The mineral waters always occur on the eastern (downthrown side) of the fault.

Puzzling is the observation that the precipitate is calcite rather than aragonite. Travertine in other places is usually calcite, but the composition of the responsible mineral waters shows depletion in magnesium. By contrast the mineral waters of Saratoga are enriched in magnesium and because the magnesium ion inhibits the formation of calcite, aragonite should result, but apparently does not. This question deserves study.

Leave parking lot of Performing Arts Center and turn north on NY 50.

Cumulative Mileage	Miles From Last Point	Route Description
0.6	0.6	Bear left following sign to NY 29.
1.8	1.2	Drive to traffic light and turn left (west) on NY 29.
3.9	2.1	Turn right (north) on Petrified Sea Gardens Road. Drive past "Petrified Gardens" to Lester Park.
5.1	1.2	Alight at Lester Park.

STOP #2. Lester Park: Domed Cyanobacterial Cabbage Heads: (Stromatolites).

This locality is the site of one of the finest domed microbial mats to be seen anywhere preserved in ancient rocks. On the east side of the road in Lester Park a glaciated surface exposes horizontal sections of the cabbage-shaped heads

composed of vertically stacked, hemispherical algal layers (Fig. 4). These structures, known as Cryptozoons, have been classically described by James Hall (1847, 1883), Cushing and Ruedemann (1914), and Goldring (1938); an even earlier study drew attention to the presence of ooids as the first reported ooid occurrence in North America (Steele, 1825). Interest in these rocks has been revived as they are useful environmental indicators (Logan, 1961; Fisher, 1965, Halley, 1971). The heads are composed of discrete club-shaped or columnar structures built of hemispheroidal microbial mats expanding upward from a base, although continued expansion may result in the fusion of neighboring colonies into a Collenia-type structure (Logan, Rezak and Ginsburg, 1964). The stromatolites are part of the Hoyt Limestone of Late Cambrian (Trempealeauan) age. Their intertidal origin has been inferred by (1) observations in the rocks, and (2) by analogy with similar modern microbial heads.

Figure 4. Top view of stromatolites showing domed structures known as cabbage-head structures, Hoyt Limestone (Upper Cambrian), Lester Park, New York.

The evidence for deposition under tidal conditions for the Hoyt Limestone at Lester Park includes: (1) mud cracks, (2) flat-pebble conglomerate, (3) small channels, (4) cross-beds, (5) bird's eye structures, (6) syngenetic dolomite, and (7) stromatolites (for criteria on recognition of tidal limestones, see Friedman, et al 1993). The analogy with modern environments relates to the occurrence of cabbage-shaped microbial heads in the intertidal zone of Shark Bay, western Australia, in which the height of the domes is controlled by the degree of turbulence (Logan, Rezak and Ginsburg, 1964; Hoffman, Logan and Gebelein, 1969). With increasing wave and current energy the height of the domes increases; the relief of the domes decreases landward towards quieter water conditions.

At Lester Park the heads which are circular in horizontal section range in diameter from one inch to three feet; many are compound heads. The size of the larger heads suggests that they formed in highly turbulent waters.

The line of depositional strike along which the domed microbial mats occur was probably where the waves were breaking as they came across the deeper ocean from the east and impinged on the shallow shelf.

Several petrographic observations in these rocks permit an analogy with modern microbial mats in hypersaline pools of the Red Sea Coast (Friedman and others, 1972; Friedman and others, 1985). Mat-forming cyanobacteria secrete

radial ooids, oncolites, and grapestones which occur in these rocks; interlaminated calcite and dolomite which in part compose the stromatolites of the Hoyt Limestone correspond to alternating aragonite and high-magnesian calcite laminites which modern blue-green cyanobacteria secrete. In modern microbial mats the high-magnesian calcite laminites contain abundant organic matter in which magnesium has been concentrated to form a magnesium-organic complex. Between the magnesium concentration of the high-magnesian calcite and that of the organic matter sufficient magnesium exists in modern microbial laminites to form dolomite. Hence the observation in ancient stromatolites, such as observed in the Hoyt Limestone, that calcite and dolomite are interlaminated, with calcite probably forming at the expense of aragonite and dolomite forming from high-magnesian calcite.

Note ooids, skeletal fragments, and coarse quartz particles dispersed between the microbial heads.

The dominant microbial process active in the deposition of the Hoyt Formation appears to have been binding, as microbial boundstones comprise most of the beds observed in the outcrop. There is, however, an abundance of forms in the Hoyt Formation. Logan (1961) and Logan et al. (1964) have shown that morphologic variations in microbial mats are largely related to the amount of energy or turbulence of the depositional environment. The Hoyt lithologies indicate a wide range of energy conditions.

The Hoyt Formation shows only minor evidence of the destruction (or bioturbation) of microbial mats by organisms. Evidence of both microbial binding and precipitation of calcium carbonate is present in the Hoyt Formation, with binding the dominant process during deposition.

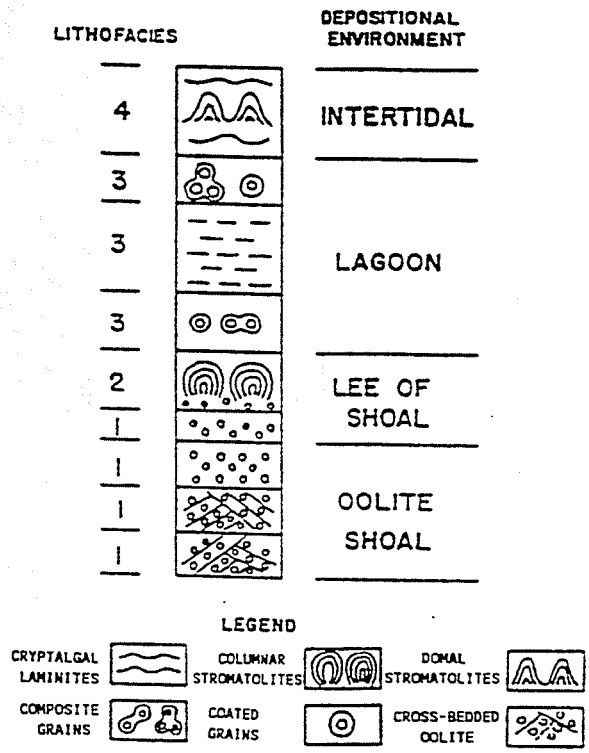

Figure 5. Vertical sequence, lower Lester Park section. This section reflects a vertically continuous progradational sequence. The upward increase in lithofacies number suggests progressively shoreward deposition (Owen and Friedman, 1984; Friedman 1988).

The lower part of the Lester Park section on the west side of the road provides the most complete sequence observed in the Hoyt Formation. A vertical sequence from Lithofacies 1 to Lithofacies 4 (Fig. 5) is represented. Depositional environments ranging from the lee of an oolite shoal upward to the lower intertidal zone are shown in the lower Lester Park section. The sequence seen here may have resulted from the lowering of sea level (regression) or from the depositional buildup of carbonates (progradation).

The ooids at Lester Park were the first to have been described from North America (Steele, 1825).

Figure 6 presents a cross-section of the hypothesized Hoyt depositional model. The following observations support the model: 1) the presence of well-developed ooids in the Hoyt lithologies suggests that the offshore energy barrier was an oolite shoal perhaps similar to that of the western Bahama Bank (Ball, 1967) or to that of Abu Dhabi on the Trucial coast (Kendall and Skipwith, 1969; Friedman 1995); 2) the presence in the Hoyt of reef-like development of high-relief columnar stromatolites immediately overlying cross- bedded oolite, and the dependence of stromatolite morphology on energy (Logan et al., 1964), suggest that the large microbial heads were restricted to high-energy areas surrounding tidal washover deltas; 3) the presence of coarse calcarenite infilling the heads. Storm surges may account for mixing of carbonate grains in the different lithofacies.

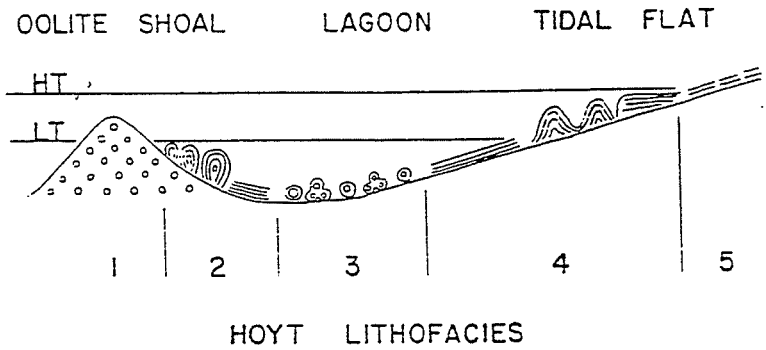

Figure 6. Hypothesized depositional model, plan view. The lagoon and intertidal zone are greatly shortened. Total width of Hoyt deposition was probably on the order of 10 to 20 miles (Owen and Friedman, 1984; Friedman 1988).

Figure 7 shows facies relations of the Hoyt Limestone.

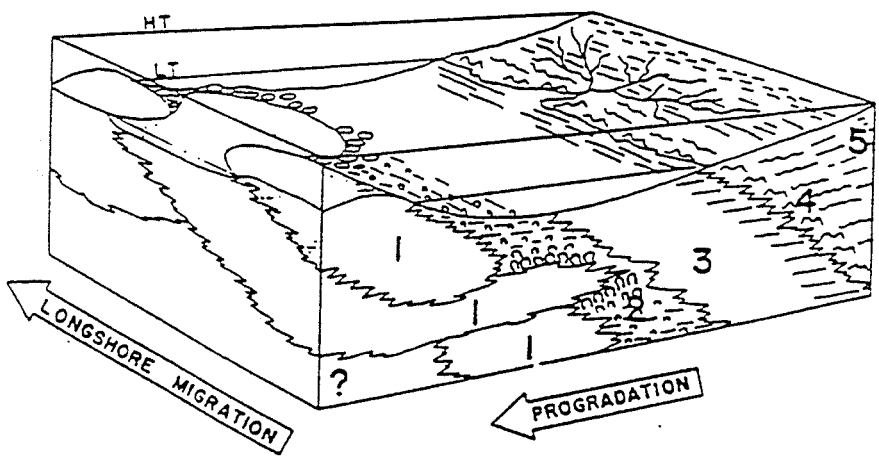

Figure 7. Facies relations resulting from longshore migration of oolite shoals and progradation of carbonate build-up. Block diagram shows generalized facies relations interpreted for dynamic Hoyt depositional model (Owen and Friedman, 1984; Friedman 1988).

Students should prepare a map of the planed, glaciated surface beneath which the domed microbial mats are exposed. An ecologic zonation may be observed based on the density of microbial heads. This distribution should be shown on the map. Sketches should be prepared of the different kinds of heads: single and compound heads, large heads vs. small heads. Is it possible from this map to determine the depositional strike of the original geologic setting? Note the kinds of particles occurring between the heads. Lie flat on your belly and use a handlens to advantage. Note the coarse quartz particles scattered among the carbonate particles.

The vertical section on the west side of the road reveals a ledge of ooids. Examine but do not destroy this ledge. Remember, as this article points out, you are treading on hallowed ground. These oolites were the first to have been described from North America, back in 1825.

Cumulative Mileage	Miles From Last Point	Route Description
		Turn around and drive back (south)to NY 29.
6.3	1.2	Turn right (west) on NY 29. Pass basal Paleozoic quartz-cobble conglomerate (a possible talus deposit) on weathered Pre-Cambrian gneiss 1/2 mi. east of Cymbal's Corners (NY 147).
25.4	19.1	Turn left (south) on NY 30.
31.7	6.3	City limits of Amsterdam
33.1	1.4	Cross bridge over Mohawk River.
33.3	0.2	Drive straight on Bridge Street (leaving NY 30).
33.4	0.1	Traffic light below Amsterdam Armory; Turn right on Florida Avenue and go west;
33.9	0.5	Turn right on Broadway;
34.7	0.8	Turn right (west) on NY 5;
37.1	2.4	Fort Hunter, turn right (north) on Main Street;
37.3	0.2	Turn right (east) to Queen Ann Street.
38.2	0.9	STOP 3. Fort Hunter Quarry.

STOP #3. Fort Hunter Quarry

Alight at slight bend in road and walk to Fort Hunter Quarry which is across a former railroad track (now a bicycle pass) close to Mohawk River. (Fort Hunter Quarry cannot be seen from road; another small quarry visible from road is approximately 0.1 mile farther east, but will not be visited on this trip).

Products of Tidal Environment: Stromatolites

Stromatolites in the Fort Hunter quarry consist almost entirely of dolomite in the form of irregularly bedded, finely-laminated, undulating structures. The rocks in this quarry are part of the Tribes Hill Formation of earliest Ordovician (Fisher, 1954). The lithofacies of the Tribes Hill Formation have been studied in detail by Braun and Friedman (1969) within the stratigraphic framework established by Fisher (1954). Figure 8 is a columnar section showing the relationship of ten lithofacies to four members of the Tribes Hill Formation. At Fort Hunter we will study the lowermost two lithofacies of the Fort Johnson Member (see column at right (east) end of section, in fig. 8 .

Two lithofacies are observed: (1) lithofacies 1, mottled feldspathic dolomite, and (2) lithofacies 2, laminated feldspathic dolomite. Lithofacies 1 is at the bottom of the quarry, and lithofacies 2 is approximately half way up.

Lithofacies 1

This facies occurs as thin dolostone beds, 2 cm to 25 cm but locally more than 50 cm thick, with a few thin interbeds of black argillaceous dolostone which are up to 5 cm thick. In the field, the dolomite shows gray-black mottling and in places bird's eye structures. In one sample, the infilling of the bird's eyes shows a black bituminous rim which may be anthraxolite. In the field, trace fossils are abundant, but fossils were not noted. Authigenic alkali feldspar (microcline) is ubiquitous throughout this lithofacies. The insoluble residue makes up 22 to 54% by weight of the sediment in samples studied with most of the residue composed of authigenic feldspar.

Lithofacies 2

This lithofacies is mineralogically identical to the previous facies but differs from it texturally and structurally in being irregularly bedded and in containing abundant undulating stromatolitic structures ("pseudo-ripples") (fig. 9)

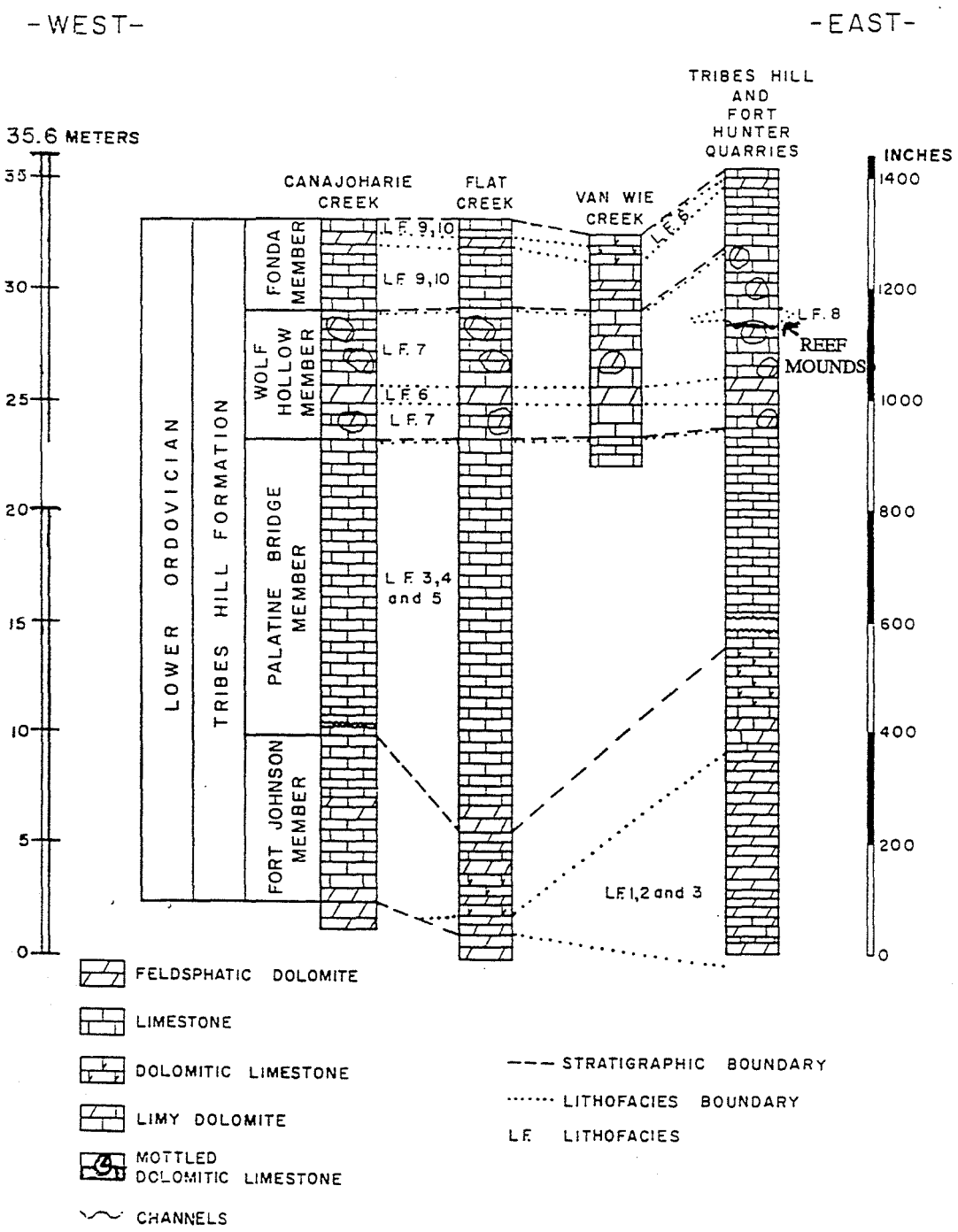

Figure 8. Columnar section showing the relationship of ten lithofacies to four members in Tribes Hill Formation (Lower Ordovician) (after Braun and Friedman, 1969).

as well as disturbed and discontinuous laminae. In places there are a few thin interbeds of black argillaceous dolostone. The thickness of the laminites of this facies ranges from 1/2 mm to 2 or 3 mm; on freshly broken surfaces the color of the thinner laminae is black and that of the thicker ones is gray. The insoluble residue, for the most part composed of authigenic feldspar, constitutes between 35% and 67% by weight in samples studied.

These two lithofacies which form the basal unit of the Ordovician, were formed on a broad shallow shelf.

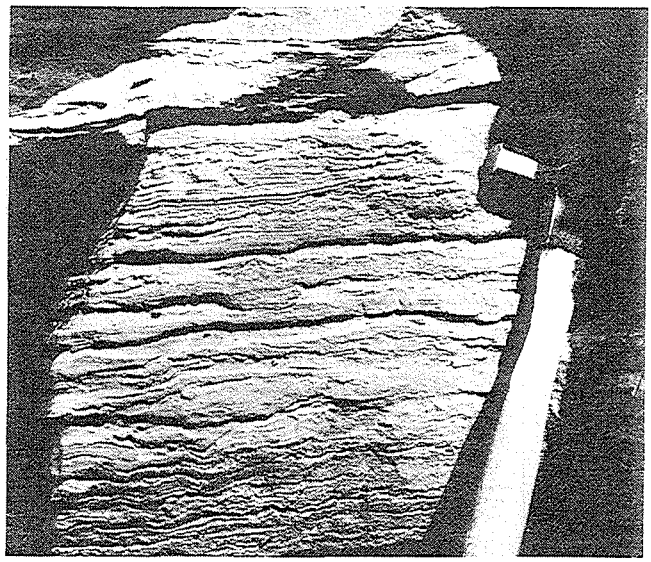

Figure 9. Stromatolite in dolostone rock of lithofacies 2 (laminated feldspathic dolomite), Tribes Hill Formation (Lower Ordovician), Fort Hunter quarry. (M. Braun and G.M. Friedman, 1969, fig. 3, p. 117; G.M. Friedman, 1972a, fig. 5, p. 21; Friedman et al. 1992, fig. 7-41).

Stromatolites, bird's eye structures, scarcity of fossils, bituminous material, syngenetic dolomite, and mottling suggest that these rocks were deposited in a peritidal environment (Friedman, et al 1992). Based on analogy with the carbonate sediments in the modern Bahamas, Braun and Friedman (1969) concluded that these two lithofacies formed under supratidal conditions. However in the Persian Gulf flat microbial mats prefer the uppermost intertidal environment, and along the Red Sea coast they flourish where entirely immersed in seawater, provided hypersaline conditions keep away burrowers and grazers (Friedman and others, 1973). Hence on this field trip we may conclude that the stromatolites indicate peritidal conditions without distinguishing between intertidal and supratidal. For more details on these lithofacies refer to Braun and Friedman (1969).

Data obtained from the analyses of fluid inclusions in calcite-healed fractures of these Lower Ordovician carbonate strata, in which microcline crystals are so prominent, indicate higher paleotemperatures and greater depth of burial than have previously been inferred for the rocks of this region (Urschel and Friedman 1984; Friedman 1987a,b). Average fluid- homogenization temperatures range from 96° C to 159° C . These high paleotemperatures are supported by oxygen-isotope and conodont-alteration data (Harris et al. 1978). A former depth of burial > 7 km is implied when a geothermal gradient of 26° C/km (Friedman and Sanders 1982; 1983) is used.

The study of the authigenic alkali feldspar from this quarry yielded an age of uplift of approximately 320 Ma (Friedman 1990), Carboniferous in age. The observation that authigenic feldspar in Cambro-Ordovician carbonates occurs along the proto-Atlantic shelf from the Appalachian Basin to Newfoundland, Scotland, and Greenland paralleling the Taconic belt suggests active crustal epeirogeny in Pennsylvanian-Permian time.

Thus, following subsidence to great depth, Pennsylvanian to Permian epeirogeny uplifted the strata, resulting in deep erosion. This leads to the surprising conclusion that isostatic unroofing following uplift has stripped off thick sections of strata whose presence was previously unsuspected.

Cumulative Mileage	**Miles From Last Point**	**Route Description**
		Turn around and drive back to Main Street, Fort Hunter.
39.1	0.9	Turn right (north) into Main Street, Fort Hunter
39.2	0.1	Cross original Erie Canal, built in 1822. Amos Eaton surveyed this route at the request of Stephen Van Rensselaer (1764-1839); after this survey Amos Eaton (1776-1842) and Van Rensselaer decided to found a school for surveying,

Cumulative Mileage	Miles From Last Point	Route Description
		geological and agricultural training which became Rensselaer Polytechnic Institute.
		Follow Main Street through Fort Hunter.
39.8	0.6	Cross Mohawk River.
40.3	0.5	Turn right (east) on Mohawk Drive (town of Tribes Hill).
40.7	0.4	Turn left (north) on Stoner Trail.
40.9	0.2	Cross Route 5 and continue on Stoner Trail.
43.6	2.7	Turn right on NY 67 (east).
45.1	1.5	Fulton-Montgomery Community College; continue on NY 67.
46.7	1.6	STOP 4. North Tribes Hill Quarry (on left).

STOP #4. North Tribes Hill Quarry

Route of Walk

Take the trail towards old abandoned crusher, but instead of heading towards the quarry move uphill to the first rock exposures. The rocks to be examined are near the edge of steep cliff.

Description and Discussion

At this stop microbial reef mounds are exposed (Friedman, 1996). Ordovician domal thrombolites, termed here microbial reef mounds, occupied the basal part of meter-scale shallowing-upward cycles (Fig. 10). They are part of a high-energy facies that a sharp transgressive surface separates from an underlying low-energy peritidal setting. This erosional surface served as the surface on which one of the reef mounds established itself during initial transgression before further deepening. The others overlie a floor of skeletal grainstone reflecting a high-stand sea-level facies tract. Skeletal grainstone composes the fill between the mounds. A channel and several aggrading hummocks occupy inter-reef mound areas resulting from storm events in a subtidal setting.

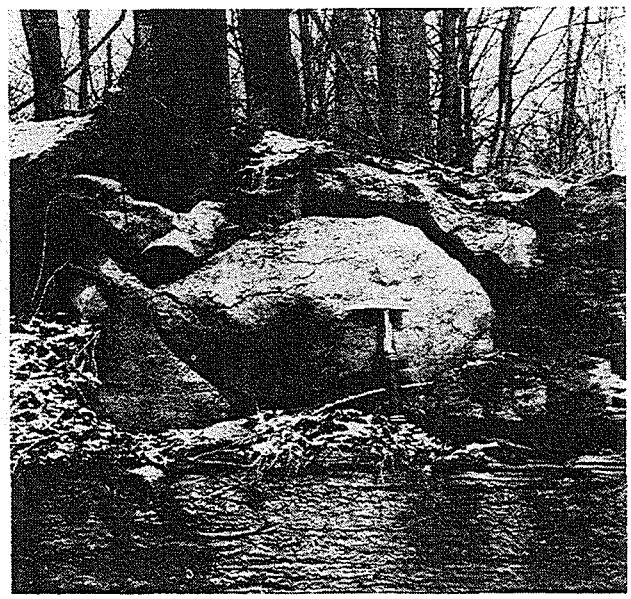

Figure 10. Microbial reef mound developed on underlying grainstone (which vegetation obscures). Bench below grainstone is a transgressive marine flooding surface which terminated an underlying shallowing-upward cycle (Friedman 1996).

Reef mounds formed at or near the base of upward-shallowing parasequences. They are part of a high-energy facies which a parasequence surface of emergence or near emergence separates from an underlying parasequence which terminated a low-energy peritidal setting. This erosional surface between the two parasequences is interpreted as a partly lithified hard ground. As elsewhere in the Cambro-Ordovician of North America, microbial reef mounds commonly occur near the bases of upward-shallowing cycles and most rest directly on underlying cycle caps (Osleger and Montañez 1996).

Mound-Foundation Facies

Braun and Friedman (1969) designated the facies underlying the reef mounds as Lithofacies 7: Mottled Dolomitic Micrite and Biomicrite of the Wolf Hollow member (Fig. 8). This lithofacies is made up of a well-bedded, mottled limestone in which the mottles are composed of irregular patches of dolomite. On weathered surfaces, the limestone is whitish and the dolomite buff, but on freshly broken surfaces both limestone and dolomite are very light gray with the limestone somewhat darker and the dolomite of granular appearance. The outlines of large gastropods and cephalopods stand out, in places, on weathered bedding planes. A list of fossils found in this lithofacies was given by Fisher (1954, p. 88-89). Bird's eye structures are present in some beds as are pyrite patches. The limestone contains abundant dolomite-filled burrows, most of which are horizontal (or sub-horizontal) to the bedding plane, but some burrows have oblique to perpendicular orientations with respect to bedding. Many gastropods, especially Ophileta and Ecculiomphalous are found with the dolomite-filled burrows suggesting that these burrows may have been made by gastropods rather than by worms. However, the morphology of the shells suggests that these gastropods were not burrowers. Hence, worms or other soft-bodied organisms must have been abundant and produced the burrows.

This facies which is part of the Wolf Hollow Member (see Fig. 8), represents a low-energy deposit of micrite of a shallowing-upward cycle terminating in a sharp, planar erosion surface. This erosional parasequence surface is a marine flooding surface and represents a transgressive event for the next high-energy cycle in which the reef mounds formed. Below one of the reef mounds the underlying micrite of mound-foundation facies compacted (Fig. 11).

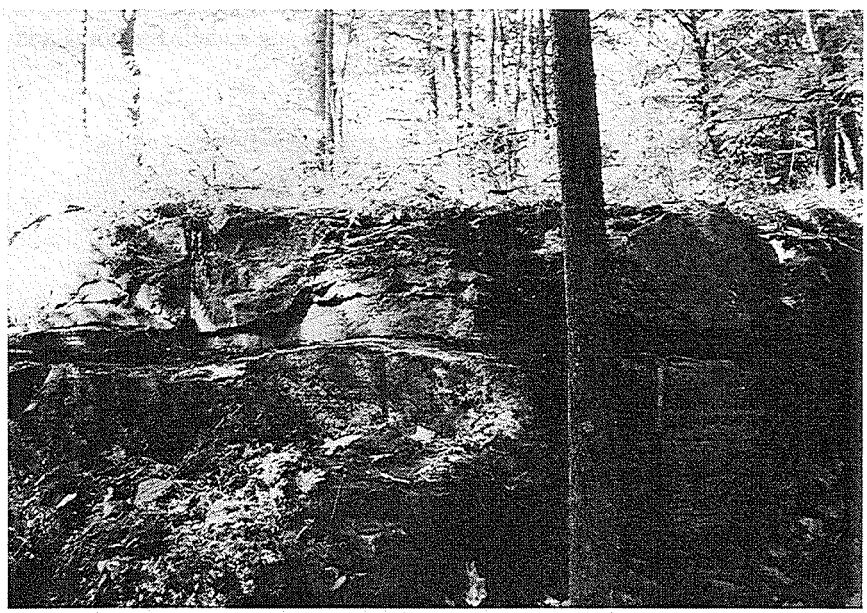

Figure 11. Undulating bench (on which pick hangs) is the transgressive surface separating the underlying micrite of low-stand sea-level facies tract (Lithofacies 7) from overlying high-stand sea-level facies tract consisting of skeletal grainstone (biosparite) and reef mounds. Note mound to right of tree; a second mound is on left edge of photograph on the same level. To left of tree note aggrading hummocks of grainstone (above the trace of drill). Below reef mound on left edge of photograph note grainstone bed which can be traced to lowermost hummock to the right (still left of tree). Below this mound and grainstone bed the underlying micrite of mound- foundation facies compacted resulting in the undulating bench (Friedman 1996, fig. 6, p. 231).

Differential compaction of this former lime mud, as the solid reef grew, suggests that the lime mud had not yet fully lithified (Friedman 1996). This observation differs somewhat from that of reef mounds in Virginia and Argentina where a solid hard ground served as foundation for the reef mounds (Read and Grover 1977; Cañas and Carrera 1993). However, the original lime mud of the mound-foundation facies of the Tribes Hill mounds was sufficiently lithified to support the growing mounds (Friedman 1996).

Microbial Reef-Mound Facies

Reef mounds are prominent in the Wolf Hollow Member of the Tribes Hill Formation (Figs. 10, 11). They occur as isolated mounds (Friedman 1996). These mounds are approximately one meter m length (measurements vary from 95 cm to 135 cm) and 60 to 70cm in thickness. These measurements are approximate dimensions because the mounds do not stand out freely, and disappear in the enveloping facies. Moreover in the exposure, it is difficult to differentiate between short and long axes of the mounds.

The reef mounds are composed of clotted and peloidal microcrystalline matrix which was microbially precipitated, comparable to that in modern reefs (Friedman et al. 1974). In modern reef settings, peloids display the pattern of calcified coccoid cells which cyanobacteria or chemoorganotrophic bacteria degrading the cyanobacterial organic matter precipitate (Friedman et al. 1985; Krumbein 1983). These textural features are products precipitated by the micro- environment of cyanobacteria (Nadson 1903; Kalkowsky 1908; Pia 1927; Johnson 1954; Endo 1961; Friedman et al. 1973). Peloids have been described as calcified algal filaments (Friedman et al. 1974); such calcification may be the result of precipitation of calcium carbonate on cyano-bacterial filaments in the presence of live bacteria (Chafetz and Buczynski 1992).

Because they are composed of microcrystalline carbonate matrix, the microbial reef mounds have a texture similar to that of the mound-foundation facies lithofacies 7 (see Fig. 8), a micrite. The term matrix has been commonly misapplied as a synonym of micrite, but the mounds are not composed of micrite. Mechanically deposited lime mud, following lithification, is known as micrite (Folk 1959). Identifying even modern reef rock is an experience in frustration: submarine microcrystalline or cryptocrystalline matrix that is biologically precipitated within millimeters to centimeters of the surfaces of reef rock is identical in appearance to micrite of mechanical origin. Case histories abound in which unwary geologists have misidentified the reef rock for low-energy facies composed of micrite (Friedman 1985, 1994). Since micrite of low-energy origin and microcrystalline or cryptocrystalline matrix of reefs are indistinguishable it is easy to confuse high-energy reef facies for low-energy lime- mud facies (Friedman 1985, 1994). This textural similarity led initially to an interpretation that mounds may be blocks of lithofacies 7 (micrite and biomicrite) that foundered and became lodged in channels (Braun and Friedman 1969). These reef mounds resemble blocks of micrite in tidal channels of the Bahamas that are derived by undercutting of the banks of the channels (Braun and Friedman 1969).

The reef mounds were included with lithofacies 8 of Braun and Friedman (1969) designated intrasparite and biosparite; the lithology is for the most part a skeletal grainstone. This lithofacies was referred to as channel fill, comparable to the Lower Ordovician reef mounds of western Argentina, of which Cañas and Carrera (1993, p. 169) noted "the reef mounds are dissected by conspicuous channels filled with coarse crinoidal grainstone and lithoclastic rudstone" (Fig. 11). This same observation applies in part to the setting of the Tribes Hill Formation. As in western Argentina, the reef mounds of the Tribes Hill Formation formed in part on a previously lithified or partly lithified sediment surface (Cañas and Carrera 1993, p. 169); and as in other places in North America, they occur near the base of an upward-shallowing cycle. The surface on which one of the mounds developed is a sharp transgressive parasequence surface separating the underlying peritidal lithofacies 7 (micrite and biomicrite) from the overlying subtidal reef-mound facies. The other reef mounds nucleated near the transgressive parasequence surface, but on top of underlying skeletal grainstone, during the initial transgression before rapid deepening occurred, a setting which is similar to that of comparable facies in the Great Basin, U.S.A. (Osleger and Montañez 1996).

Inter-Reef Mound Facies

Skeletal grainstone composes the fill between the reef mounds. One channel and several hummocks occupy the inter-reef mound areas (Fig. 12). The top of one of the hummocks rolls into the channel fill. The grainstones form

lenses that build on top of one another. The channel displays the typical asymmetric profile of a tidal channel with a

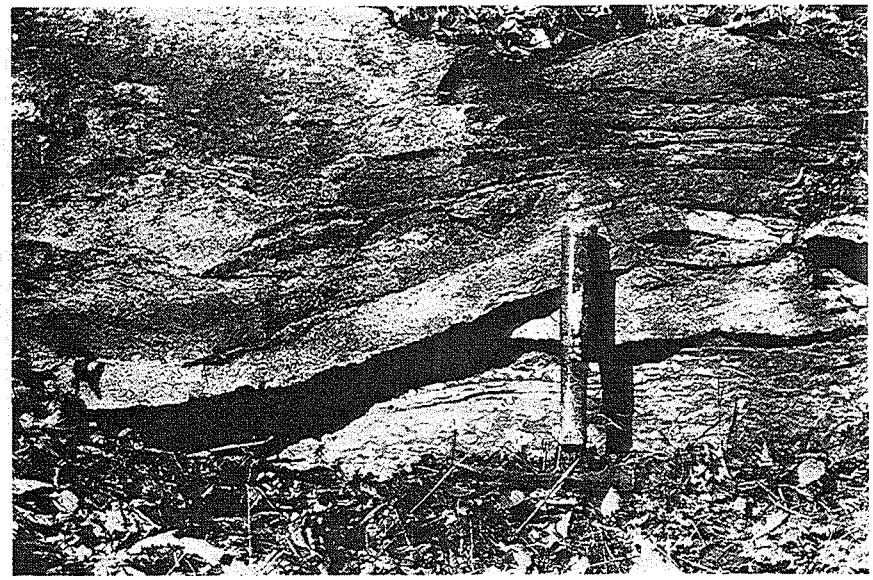

Figure 12. Truncation at base of slip-off-slope side of storm tidal channel. Hummock of grainstone underlies truncation surface to right of hammer. Channel is made up of high-energy grainstone of lithofacies 8 (intrasparite and biosparite) and cuts into lithofacies 8 grainstone. Below flat base of the hammer is lithofacies 7 (mottled dolomitic micrite and biomicrite). Lithofacies 7 represents low-energy peritidal flats (Friedman 1996, fig. 17, p. 236).

steep cut-bank and a low-angle slip-off slope (Fig. 12). However, the channel is entirely within grainstone, hence it is not a normal tidal channel which would be fine-grained on the steep side and coarse-grained on the opposing side. In normal tidal channels, as the channel shifts it leaves behind a layer of coarse debris at the bottom of the channel (Friedman, et al. 1992). No such channel-floor lag layer is present in the inter-reef mound facies. Hence the channel must be related to storm deposition of the grainstone since filling is not the result of the shifting of the channel. Truncation by the channel and aggradation of the hummocks occurred at the same time. The channel and hummocks formed as a result of storm events in a subtidal setting. Following transgression, storm tides and currents generated this channel between which reef mounds and inter-reef mound facies accumulated. This channel, which was incised down to 30 cm into the underlying grainstone, is conspicuous and displays sharp margins (Fig. 12).

Of the various reef mounds one rests directly on the mound-foundation surface; grainstone of inter-reef mound facies makes up the floor of all the others.

The reef mounds formed in shallow-subtidal to possibly low intertidal settings in an agitated environment devoid of lime mud.

Going east on Route 67, after the intersection with Route 147, five roadcuts on either side of Route 67 expose outcrops of the Lower Ordovician Gailor Formation.

STOP #5: Exposures of Gailor Formation

On the north and south sides of the road are exposed a massive dolostone unit overlain by a bedded dolostone unit. Roughly 10' of section are exposed here. The massive unit is dark gray in color while the upper bedded unit is lighter gray and coarser as well. Large clasts in a variety of shapes and sizes, composed of micrite and medium-textured dolostones are scattered all over the outcrop and concentrated in the basal massive unit. Pods and lenses of chert colored black and white are profuse. Calcite mineralization is also a common feature, occurring in patches and veins in orange, white and black. Stromatolites are observed in the section on the north side of the road.

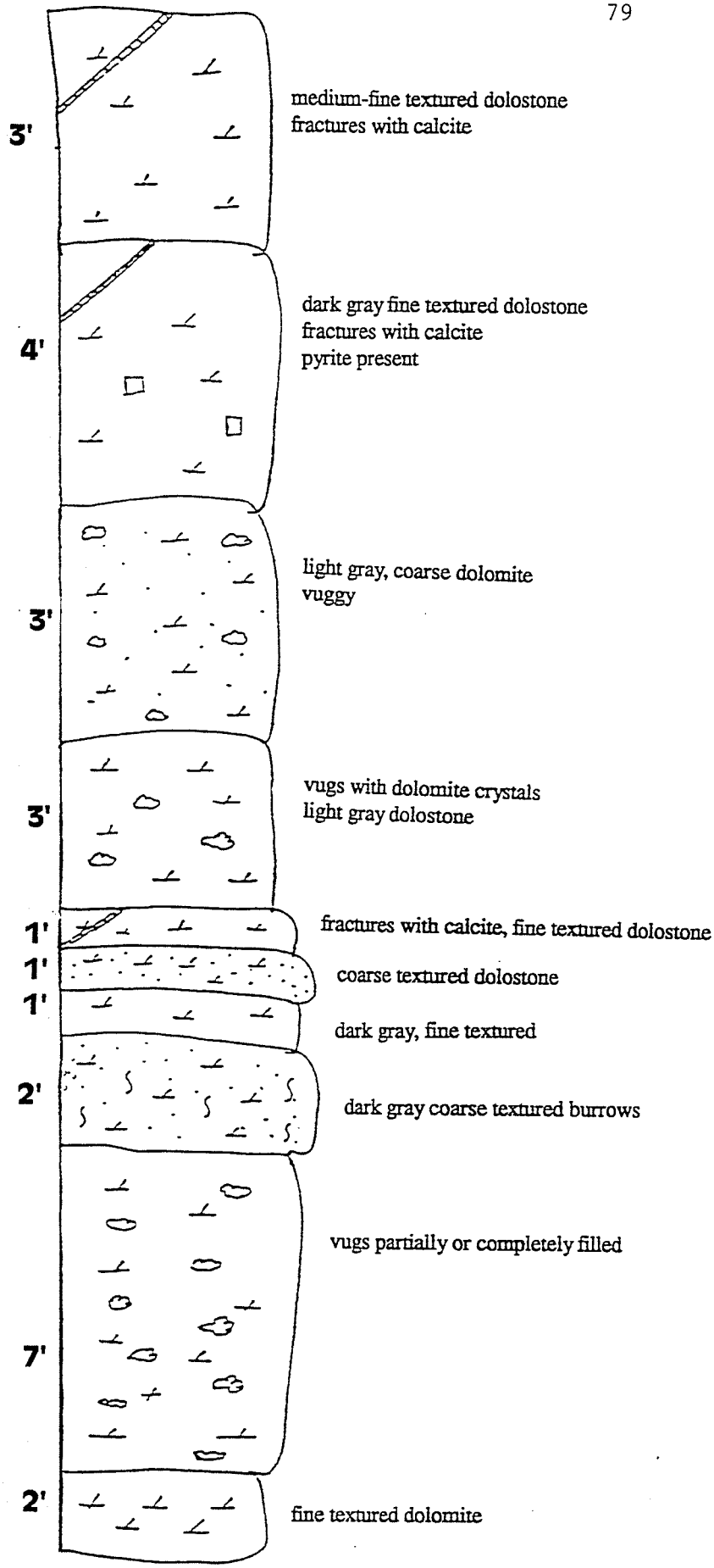

Figure 13. Section on Route 67.

The breccia observed in the section perhaps represents dissolution collapse. The massive unit in the lower part of the section may be a microbial build up. The stromatolites suggest a peritidal origin for these dolostones.

STOP #6.

Farther east on the north and south side of 67 are exposed roughly 27' of section. The following features are observed:

-wavy beds,
-massive units alternating with bedded dolostone units,
-the massive units appear to have a lenticular mound-like form, perhaps representing former microbial build-ups,
-the beds overlying the mounds display dips on flanks of the mounds perhaps indication fore-reef slopes,
-pervasive dolomitization seems to have obliterated original depositional features,
-alternatively the wavy bedding may represent tidal channels or hummocky cross stratification,
-other features observed in these units are fine laminae in the dolostones, burrow mottling, stylolites, presence of pyrite and white calcite mineralization in vugs and fractures.

Figure 13 is a sketch of the section exposed at this stop.

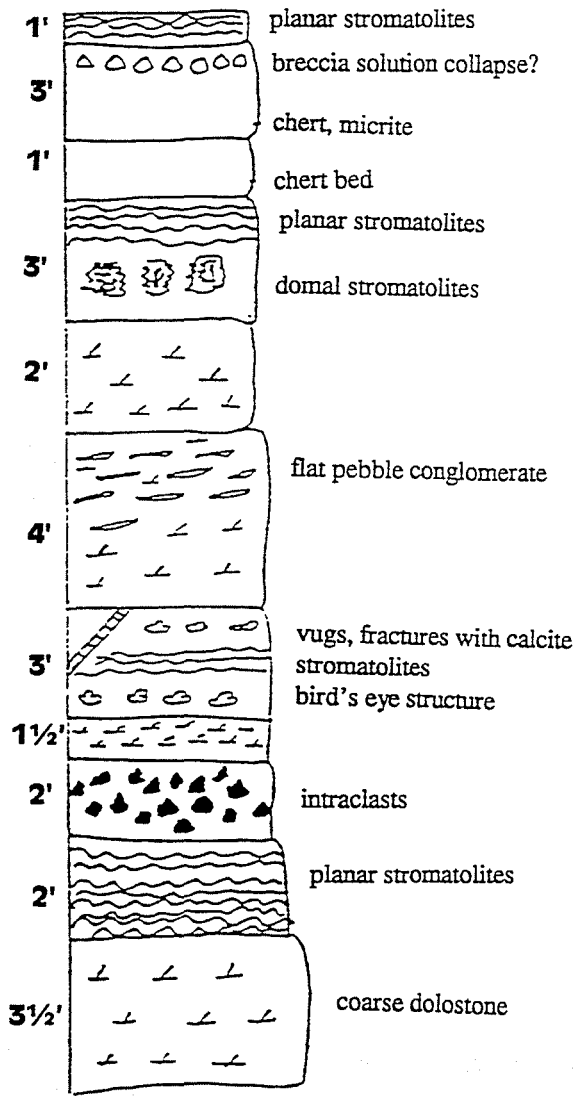

Figure 14. Section exposed at Manny Corners.

STOP #7.

Farther east are exposed roughly 15' of bedded dolostones displaying planar stromatolites, intraclasts, and bird's eye structures indicating peritidal environments of deposition.

STOP #8.

This is a small section on the north side of 67 near Waite Road. The section displays intraclasts and stromatolites.

STOP #9.

Farther east on Route 67 near Manny Corners is a section exposing roughly 26' of bedded dolostones. The following features are observed here:

- planar and domal stromatolites,
- intraclasts ranging in size from 1 to 2 inches,
- vugs and fractures partially or completely filled with black and white calcite,
- bird's eye structures,
-bedded and nodular chert,
-breccia representing dissolution collapse?

The above mentioned features displayed in these fine- to medium-textured dolostones point to a peritidal environment of deposition.

Figure 14 is a sketch of the section exposed at this stop.

References

Back, W., Landa, E. R., and Meeks, L., 1995, Bottled water spas, and early years of water chemistry: Ground Water, v.33, p.605-614.

Ball, M. M., 1967, Carbonate sand bodies of Florida and the Bahamas: Journal of Sedimentary Petrology, v.37, p.556-591.

Braun, Moshe, and Friedman, G.M., 1969, Carbonate lithofacies and environments of the Tribes Hill Formation (Lower Ordovician) of the Mohawk Valley, New York: Journal of Sedimentary Petrology, v.39, p.113-135.

Cañas, Fernando, and Carrera, Marcelo, 1993, Early Ordovician Microbial-Sponge-Receptaculitid Bioherms of the Precordillera, Western Argentina: Facies, v.29, p.169-178.

Chafetz, H.S., and Buczynski, Chris, 1992, Bacterially Induced Lithification of Microbial Mats: Palaios, v.7, p.277-293.

Cushing, H.P., and Ruedemann, Rudolf, 1914, Geology of Saratoga Springs and vicinity: New York State Museum Bulletin, v.169, 177p.

Endo, R., 1961, Phylogenetic Relationships Among the Calcareous Algae: Saitama University Science Report Ser. B Endo Commem., p.1-48.

Fisher, D.W., 1954, Lower Ordovician stratigraphy of the Mohawk Valley, N.Y.: Geological Society of America Bulletin, v.65, p.71-96.

Fisher, D.W., 1965, Mohawk Valley Strata and structure, Saratoga to Canajoharie: Guidebook - Field Trips in the Schenectady Area, New York State Geological Association, 37th Annual Meeting, p.A1-A58.

Folk, R.L., 1959, Practical Petrographic Classification of Limestones: American Association of Petroleum Geologists Bulletin, v.43, p.1-38.

Friedman, G.M., 1985, Cambro-Ordovician shoaling and tidal deposits marginal to Iapetus Ocean and Middle to Upper Devonian peritidal deposits of the Catskill fan-deltaic complex: *in* R.H. Lindeman ed., New York State Geological Association, 57th annual meeting: Field Trip Guidebook, p.5-28.

Friedman, G.M., 1987a, Vertical movements of the crust: case histories from the northern Appalachian Basin: Geology, v. 15, p.1130-1133.

Friedman, G.M., 1987b, Deep-burial diagenesis: its implications for vertical movements of the crust, uplift of the lithosphere and isostatic unroofing: a review: Sedimentary Geology, v.50, p.67-94.

Friedman, G.M., 1988a, Cambro-Orrovician Shoaling and Tidal Deposits Marginal to Iapetus Ocean and Middle to Upper Devonian Peritidal Deposits of the Catskill Fan-Deltaic Complex: Field Trip Guidebook, New York State Geological Association, 57th Annual Meeting, September 27-29, 1985, Department of Geology, Skidmore College, p.5-28.

Friedman, G.M., 1988b, Spectacular Domed Microbial Mats (Cabbage Heads) and Oolitic Limestone at Lester Park near Saratoga, New York: Northeastern Geology, v.10, no.1, p.8-12.

Friedman, G.M., 1990, Anthracite and concentrations of alkaline feldspar (microcline) in flat-lying undeformed Paleozoic strata; a key to large- scale vertical crustal uplift *in* Sediments and environmental geochemistry: selected aspects and case historie; D. Heling, et al., eds., Springer Verlag, p.16-28.

Friedman, G.M., 1994, Recognition of Reefs in the Subsurface Rock Record: An Experience in Frustration. John T. Galey Memorial Address: Virginia Division of Mineral Resources, v.132, p.116-118.

Friedman, G.M., 1995, The Arid Peritidal Complex of Abu Dhabi: A Historical Perspective: Carbonates and Evaporites, v.10, no.1, p.2-7.

Friedman, G.M., 1996, Early Ordovician Microbial Reef Mounds of the Tribes Hill Formation, Mohawk Valley, New York: Carbonates and Evaporites, v.11, no.2, p.226-240.

Friedman, G.M., and Sanders, J.E., 1982, Time-temperature-burial significance of Devonian anthracite implies former great (~6.5 km) depth of burial of Catskill Mountains, New York: Geology, v.10, p.93-96.

Friedman, G.M., and Sanders, J.E., 1983, Reply on: Time-temperature-burial significance of Devonian anthracite implies former great (~6.5 km) depth of burial of Catskill Mountains, New York: Geology, v.11, p.123-124.

Friedman, G.M., Amiel, A.J., Braun, Moshe, and Miller, D.S., 1972, Algal mats, carbonate laminites, oöids, oncolites, pellets, and cements in hypersaline, sea-marginal pool, Gulf of Aqaba, Red Sea: American Association of Petroleum Geologists Bulletin, v.56, p.618.

Friedman, G.M., Amiel, A.J., Braun, M. and Miller, D.S., 1973, Generation of Carbonate Particles and Laminites in Algal Mats: Example From Sea-Marginal Hypersaline Pool, Gulf of Aqaba, Red Sea: American Association of Petroleum Geologists Bulletin, v.57, p.541-557.

Friedman, G.M., Amiel, A.J., and Schneidermann, N., 1974, Submarine Cementation in Reefs: Example From the Red Sea: Journal of Sedimentary Petrology, v.44, p.816-825.

Friedman, G.M., Sanders, J.E., and Kopaska-merkel, D.C., 1992, Principles of Sedimentary Deposits: Stratigraphy and Sedimentology. Macmillan Publishing Co., New York, 717p.

Friedman, G.M., Sneh, A., and Owen, R.W., 1985, The Ras Muhammad Pool: implications for the Gavish Sabkha, p.218-237 *in*

Friedman, G.M. and Krumbein, W.E., eds., 1985, Hypersaline ecosystems. The Gavish Sabkha. Ecological Studies 53, Berlin, Springer-Verlag, 484p.

Goldring, Winifred, 1938, Algal barrier reefs in the Lower Ordovician of New York (with a chapter on the importance of coralline algae as reef builders through the ages): New York State Museum Bulletin, no.315, p.1-75.

Gwinner, M., 1959, Die Geologie des Blattes Urach (Nr. 7522) 1:25000 (Schwäbische Alb): Arb. a. d. Geol. Palaont. Inst. d. T.H. Stutgart, v.24, Stutgart, no pagination.

Hall, James, 1847, Natural history of New York. Organic remains of the Lower Division of the New York System: Paleontology, v.1, p.1-338.

Halley, R.B., 1971, Paleo-environmental interpretations of the Upper Cambrian cryptalgal limestones of New York State: unpubl. M.S. Thesis, Brown University, 93p.

Harris, A.G., Harris, L.D., and Epstein, J.B., 1978, Oil and gas data from Paleozoic rocks in the Appalachian basin: Maps for assessing hydrocarbon potential and thermal maturity (conodont color alteration isograds and overburden isopachs): U.S. Geological Survey Miscellaneous Investigations Map I-917-E, scale 1:2,500,000, 4 sheets.

Hewitt, P.C., Mcclennan, W.E., Jr., and Nilsson, Harold, 1965, Geologic phenomena in the Schenectady area: Guidebook - Field Trips in Schenectady Area, New York State Geological Association, 37th Annual Meeting, p.D1-D13.

Hoffman, Paul, Logan, B.W., and Gebelein, C.D., 1969, Biological versus environmental factors governing the morphology and internal structure of Recent algal stromatolites in Shark Bay, Western Australia: Abstracts with Programs for 1969, Part I, Northeastern Section Geological Society of America, p.28-29.

Johnson, J.H., 1954, An Introduction to the Study of Rock-building Algae and Algal Limestones: Colorado School of Mines, v.Q49, 117p.

Kalkowsky, E., 1908, Oolith und Stromatolith im Norddeutschen Buntsandstein: Zeitschrift der Deutschen Geologischen Gesellschaft, v.60, p.68-125.

Kemp, J.F., 1912, The mineral springs of Saratoga: New York State Museum Bulletin, v.159, 79p.

Kendall, C.G.St.C. and Skipwith, Sir P.A.d'E., 1969, Holocene and shallow-water carbonate (sic) and evaporite sediments of Khor al Bazam, Abu Dhabi, southwest Persian Gulf: American Assoication of Petroleum Geologists Bulletin, v.53, p.841-869.

Krumbein, W.E., 1983, Stromatolites-challenge of Term Through Space and Time: Precambrian Res., v.20, p.493-531.

Logan, B.W., 1961, Cryptozoon and associated stromatolites from the Recent, Shark Bay, Western Australia: Journal of Geology, v.69, p.517-533.

Logan, B.W., Rezak, R., and Ginsburg, R.N., 1964, Classification and environmental significance of algal stromatolites: Journal of Geology, v.72, p.68-83.

Nadson, G., 1903, Die Mikroorganismen als Geologische Faktoren. Petersburger Arb. Komm. Erf. Min Seen, Slavjansk, Petersburg.

New York State Department of Health, 1959, Analysis of springs at Saratoga Springs Spa: Div. Laboratory and Research Environmental Health Center, Report.

Osleger, D.A., and Montañez, I.P., 1996, Cross-platform Architecture of a Sequence Boundary in Mixed Siliciclastic-Carbonate Lithofacies, Middle Cambrian, Southern Great Basin, USA: Sedimentology, v.43, p.197-217.

Pia, J., 1927, Thallophyta. *In*: Hirmer M. (ed.) Handbuch der Palaeobotanik, Hirmer, Leipzig, v.1, p.1-136.

Pia, J., 1933, Die Rezenten Kalksteine. Akademie Verlag, Leipzig, 420p.

Read, J.F., and Grover, G.A., 1977, Scalloped and Planar Erosion Surfaces, Middle Ordovician Limestones, Virginia; Analogues of Holocene Exposed Karst or Tidal Rock Platforms: Journal of Sedimentary Petrology, v.47, p.956-972.

Sanders, J.E., and Friedman, G.M., 1967, Origin and occurrence of limestones, p.169-265, *in* Chilingar, G.V., Bissell, H.J., and Fairbridge, R.W., eds., Carbonate Rocks, Developments in Sedimentology 9A. Elsevier Publ. Co., Amsterdam, 471p.

Schreiber, B.C., Smith, Denys, and Screiber, Edward, 1981, Spring Peas from New York State: Nucleation and Growth of Fresh Water Hollow Ooliths and Pisoliths: Journal of Sedimentary Petrology, v.51, no.4, p.1341-1346.

Siegel, D.I., 1996, Natural Bubbling Brew: The Carbonated: Geotimes, v.41, no.5, p.20-23.

Sneeringer, M.R., and Dunn, J.R., 1981, Exploration for Geothermal Resources in the Capital District of New York: Final Report, prepared for New York State Energy Research and Development Authority, Project Manager Dr. Burton Krakow and United States Department of Energy, Grant Number DE-FG05-79, Prepared by DUNN GEOSCIENCE CORPORATION, Latham NY, ERDA Report 81-11.

Steele, J.H., 1825, A description of the Oolite Formation lately discovered in the country of Saratoga and in the State of New York: American Journal of Science, v.9, p.16-19.

Urschel, S.F., and Friedman, G.M., 1984, Paleodepth of burial of Lower Ordovician Beekmantown Group carbonates in New York State: Compass of Sigma Gamma Epsilon, v.61, p.205-215.

Young, J.R., and Putnam, G.W., 1985, Stratigraphy, structure, and the mineral waters of Saratoga Springs---Implications for Neogene rifting, p.272-291 *in* Friedman, G.M., editor, New York State Geological Association 51st Annual Meeting and New England Intercollegiate Geology Conference 71st Annual Meeting, 457p.

Geologic Field Guide to the Balmat Zinc Mine, St. Lawrence County, New York

W.F. deLorraine and J. Johnson
Mining Division, Zinc Corporation of America Mines, Inc.
Balmat, NY 13609

Introduction and Geologic Setting

Orebodies of the Balmat-Edwards-Pierrepont Zinc mining district in the Northwest Adirondacks of New York State rank as world-class deposits with over 45 million tons of past production plus total reserves. Orebodies occur in "clean" Proterozoic siliceous dolomitic marble that was metamorphosed and polydeformed during the Grenvillian Orogeny about 1.1 billion years ago. The NW Adirondack Lowlands are underlain by metasedimentary rocks, predominantly marble, calc-silicate and subordinate paragneiss and metavolcanic rocks. The Adirondack Highlands to the east are predominantly underlain by anorthosite-mangerite-charnockite-granite suite (AMCG) rocks metamorphosed to granulite facies. The two provinces are separated by the Carthage-Colton line or "Highlands-Lowlands" boundary, a narrow northeasterly-trending, northwest-dipping zone of mylonitization separating the upper amphibolite- facies Lowlands from the granulite- facies Highlands to the east. Flat-lying lower Paleozoic rocks surround and unconformably overlie the crystalline rocks of the Adirondack dome.

Regional Stratigraphy

Several lineaments or fault zones divide the NW Adirondack Lowlands into NE-trending fault panels, each of which has a characteristic metasedimentary package and structural style. Differences between adjacent fault panels have led to speculation that individual panels have their own unique structural and stratigraphic histories (Grant and Yang 1992). There are, however, stratigraphic threads across and common to all fault pannels, beginning with the structurally lowermost rock unit, the Hyde School Gneiss. A regional column can be reconstructed by piecing together metasedimentary sections overlying the Hyde School Gneiss in individual fault panels and comparing these with adjacent fault panels. In places thrust faults or tectonic slides can be inferred where significant portions of the stratigraphic column are absent and where there are structural discontinuities across opposite sides of the inferred fault trace. Nevertheless, several key, distinctive marker units spanning the 40-km-wide Lowlands are present within each fault panel, thus permitting reconstruction of the section. There are apparent structural discontinuities between some of the four formations underlying the Lowlands so that in part the column may reflect a lithotectonic stacking sequence.

Leucogranitic gneiss ranging from alaskitic to granitic to trondhijemitic composition lies at the base of the section in the NW Lowlands (Fig. 8) (Editor's note: figures in this paper start with figure 8). Leucogneiss is characterized by relatively high content of disseminated magnetite and presence of thin conformable amphibolite layers. The leucogranitic gnisses is referred to as Hyde School Gneiss and its origin is controversial. Although long regarded as a basal metavolcanic complex, because of conformity of amphibolite layers, unique structural/stratigraphic position underlying the basal member of the Lower Marble formation, lack of sills, apophyses, dykes, or xenoliths of surrounding rocks, the Hyde School Gneiss has recently been interpreted as intrusive in orign. Sillimanite-garnet-corundum-spinel assemblages in surrounding garnet-sillimanite gneiss suggest temperatures of 850°C, much higher than reported regional metamorphic temperatures (McLelland et al . 1992). Hudson (1994) reported 830°-860° for the same garnet gneiss. Accordingly, these assemblages were interpreted as contact metamorphic phenomena associated with intrusion of Hyde School Gneiss. Amphibolite layers were interpreted as highly tectonized dykes resulting in completely transposed "straight" gneiss.

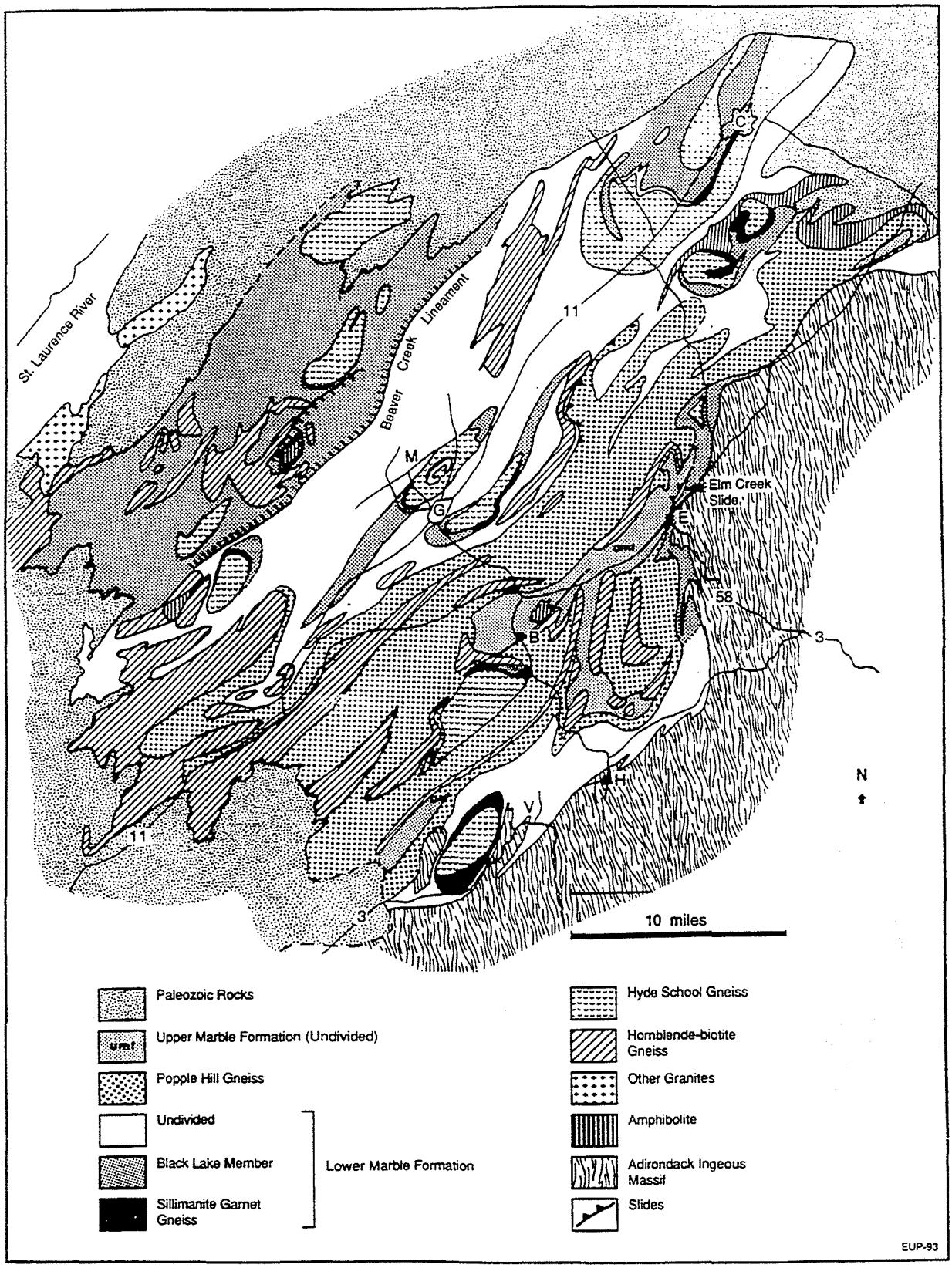

Figure 8. Generalized geologic map of the Northwest Adirondack Lowlands. G = Gouverneur; B = Balmat; E = Edwards. Modified from Isachsen and Fisher (1970).

intrusion of Hyde School Gneiss. Amphibolite layers were interpreted as highly tectonized dykes resulting in completely transposed "straight" gneiss.

Overlying the Hyde School Gneiss is the Lower Marble formation (Fig.8), a diverse assemblage of predominantly calcitic marble with intercalated calc-silicate units, biotite gneiss, quartzite, tourmalinite and pelitic gneiss. Calcitic marble is banded gray and white and characterized by the presence of abundant disseminated granular diopside, graphite, phlogopite, and disseminated brown to black tourmaline. This rock type is common and appears in numerous localities across the Adirondack Highlands and to the northwest in Canada. Migmatitic gneiss of overall dacitic composition referred to as Popple Hill gneiss overlies the Lower Marble formation (Fig 8.) The contact may be tectonic, based on the recognition of structural discontinuities below (Foose 1974), presence of mylonites (Hudson 1994; Hudson and Grant 1989), and excision of several members of Lower Marble formation below (deLorraine, personal mapping observation). Dolomitic and siliceous dolomitic marble of the Upper Marble formation lie at the top of the regional stratigraphic column. Exposures of this unit are limited to narrow fold belts relatively close to the Highlands-Lowlands boundary between Balmat-Edwards and Pierrepont, New York (Fig 8). The Upper and Lower Marble formations are in structural contact at Edwards where the entire section of Popple Hill gneiss has been excised along the Elm Creek slide (Fig. 8). The slide is manifested by the presence of mylonitized slivers of Hyde School and Popple Hill gneiss in addition to the juxtaposition of major stratigraphic units. This major discontinuity was recognized earlier by Gilluly (1934).

Regional Structure and Metamorphism

Metasediments of the northwest Adirondacks have undergone upper amphibolite facies metamorphism and polyphase deformation during the Grenvillian orogeny dated at about 1130-1170 Ma (Grant et al. 1986; McLelland et al.1988; Mezger et al. 1991). The regional structure is complex, the product of at least four phases of deformation. Large-scale recumbent folds, nappe structures, and tectonic slides are believed to have developed during the early phases of deformation (deLorraine 1979; Foose 1980; Wiener et al.1984; Brown 1989; McLelland et al.1993). First-phase deformation at high metamorphic grade produced axial planar foliations which define the regional foliation. Tewksbury (1991), and Tweksbury and Kirby (1992), have shown that what was described as the "main regional foliation" in many places has the characteristics of a ductile shear fabric. Furthermore, these authors propose that the early deformation leading to the main regional foliation occurred in a deep-seated ductile shear regime in a continental collision plate-tectonic setting. In general, grain size in gneiss is fine to medium and at certain levels, such as the base and top of Popple Hill gneiss, mylonite is present. Migmatite also developed during early phase deformation. Recognition of map-scale first-phase folds is uncertain and minor folds are rare as well. Where present, early phase folds are rootless isoclines or intra-folial isoclinal folds with well-developed axial planar foliation. The second-phase of deformation has been subdivided into phases 2A and 2B. Phase 2A minor folds are interpreted to have developed coevally with major second-phase isoclines, and phase 2B folds are interpreted as shear folds associated with southeast overturning of those major isoclines, such as the Sylvia Lake syncline. Phase 2A isoclinal folds refold early isoclines, their axial-planar foliations, and early mylonite. In the Lowlands, axial surfaces of phase 2A folds strike northeast, defining the prominent NE-SW regional grain. Axial surfaces dip moderately to the northwest. Fold axes are curvilinear within second-phase axial surfaces and can be described as "porpoising" within them (Fig.9).The doubly plunging Sylvia Lake syncline between Balmat and Edwards hosts the zinc orebodies of the district and is an example of a major phase 2A isoclinal fold. The North Gouverneur nappe of Brown (1989) is interpreted herein as a second-phase fold, as is the Great Somerville anticline and Sherman Lake syncline of Buddington (1934). Tectonic slides, axial planar shears and thrust faults are common elements of major phase-two isoclines. In contrast to Tewksbury, we do not interpret domes of Hyde School Gneiss as products of progressive regional ductile shear in which irregularities within the shear zone amplified into sheath folds. Rather, domes of Hyde School Gneiss are seen herein as doubly-plunging cores of regional, NE-SW trending accordion-style phase 2A folds superimposed on phase-one shear fabrics and lithotectonic stacking sequences, as the orogen experienced further contraction (deLorraine, internal ZCA documents). Phase 2B isoclinal folds are

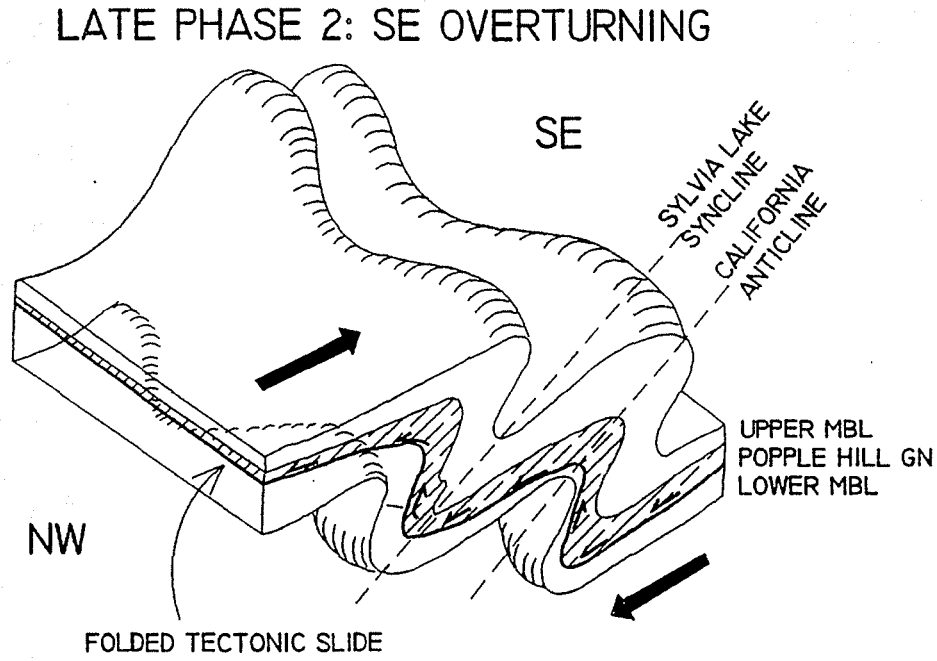

Figure 9. Generalized 3-D, NW-SE section across the Lowlands showing phase 2A isoclines overturned to the southeast during late phase 2 deformation (phase 2B). Note curvilinear hinges of major folds. The basal unit, Hyde School gneiss, is not shown but occupies the cores of doubly-plunging anticlines.

recognized in the mines where they refold straight marble tectonite which developed along phase 2A shear zones and thrust faults. Rotation senses are uniformly clockwise and commonly the short limbs are sheared out in contrast to phase 2A structures which have counter-clockwise asymetrics on the upper limb of the Sylvia Lake syncline and clockwise asymetries on the lower. In the mines, the prinicipal manifestation of phase 2A folds is the re-activation and refolding of phase 2A straight marble fabrics paralleling shear zones and slides. Third-phase folds of "S" asymmetric sense and more or less coaxial with local second-phase folds also trend to the NE. Interplay of phase 2A and third-phase folds locally produced hook and crescent-shaped interference patterns. A fourth weakly developed northwest-trending phase of folding was thought to have produced the apparent modified dome and basin pattern in the northwest Adirondacks by interference with earlier northeast-trending folds (Foose 1974, 1980; deLorraine1979; Wiener et al.1984). The preferred interpretation here, based in part on large-scale reconstructions of the Sylvia Lake syncline at the Balmat No. 4 mine, is that the pattern results from curvilinear or "porpoising," doubly-plunging, phase 2A sheath fold hinges. Thus apparent domical structures cored by Hyde School Gneiss are seen as apical projections of tongue or sheath-like folds protruding through the erosional surface (Fig.9). This view of phase 2A fold geometry derived from mine district observations supports, in part, the interpretations of Tewksbury (1993), who also views domes of Hyde School Gneiss as sheath fold hinges. Many of the "domes" are overturned to the southeast so that interference of southeast- overturned second-phase isoclines with NW-trending folds, if it occurred, should have produced "heart-and-anchor" interference patterns, rather than the observed ovoid patterns.

Metamorphic grade increases gradually from upper amphibolite facies in the Lowlands to granulite facies eastwardly toward the Adirondack Highlands. Reported temperatures of metamorphism were 640°-700° C near Gouverneur increasing to 750° C in the southwestern Highlands; pressure increased from about 7.2 kb to 7.6 kb (Seal 1986). At Balmat, temperatures of at least 625° C are inferred from calcite/dolomite geothermometry and sulphur isotopic fractions between co-existing anhydrite-pyrite pairs (Whelan 1979). Other mineral assemblages including end-member forsterite suggest that temperatures could have been ~725° C at > 0.7 XCO2 (Petch 1992).

Balmat Lithology And Depositional Environment

The "Balmat" or Upper Marble Formation stratigraphic column is presented in Figure 10. The section is characterized by an alternation of nearly pure dolomitic marble and silicated dolomitic marble units. Distributed throughout this 16 unit sequence are distinct "marker units" and periodic occurrences of anhydrite.

Units 1, 3, 5, 7, 9, and 12 are medium-to coarse-grained, gray to white dolomitic marble with very minor quartz, diopside and serpentine. Serpentine occurs as replacements of both diopside and forsterite. Silicated marble units 4, 6, 8, and 11 consist of interlayered glassy quartzite, gray to white diopside and white to gray dolomitic marble beds with minor buff calcitic marble layers. Much of the quartz-diopside rock is thinly banded to laminated and much of the finely laminated rock may be biogenic in origin. Units 4 and 11 are now recognized as stromatolitic (Isachsen and Landing 1983) thus providing the only unequivocal sense of tops in the Adirondack region to date. Each silicated unit has its own set of distinctive marker sub-strata, textures, and proportions of quartz-diopside relative to dolomite allowing recognition as individual stratigraphic units and not as a single unit repeated by isoclinal folding as had been suggested by Wiener et al. 1984. The same subunits of Unit 6 at Balmat can be recognized in drill cores at the Hyatt Mine some six miles along strike to the northeast. Were it not for the presence of "marker" beds or units intercalated within the Upper Marble section, the structural geology of the Balmat district would be much harder to decipher.

Persistent marker horizons of distinctive mineralogy, texture, or colour include a graphitic pyritic schist, Unit 2, separating dolomitic marble units 1 and 3. The "7 Bed", a medium-grained, dark gray, fetid, dolomitic marble contrasts with other dolomitic units which are white to light gray. The "10 Bed" is a fine-

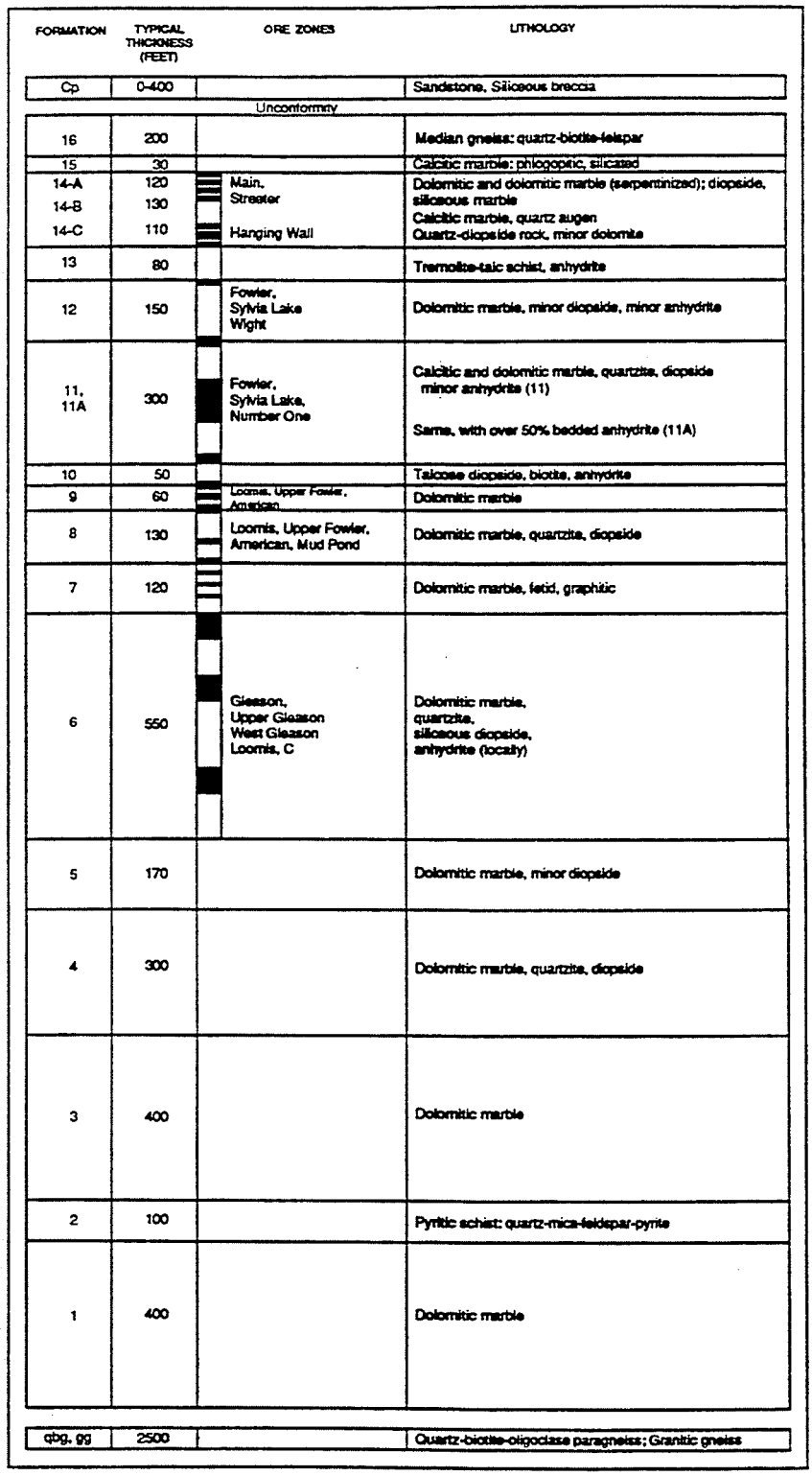

Figure 10. Stratigraphic column for Upper Marble formation at Balmat. The term "quartzite" refers to metamorphosed chert. The relative stratigraphic positions of orebodies are plotted as black bars.

grained, milky pea green, serpentinous calc-silicate rock with anhydrite and a local biotite schist substratum. Unit 13 is perhaps the most useful marker unit consisting of distinctive cream-coloured talc-tremolite-anthophyllite schist, hexagonite schist, and braunite-hexagonite schist.

Lavendar to pink bedded anhydrite occurs in Units 6 and 10 through 14. Anhydrite is most prominent within the upper half of the section, particularly in units 11A and 13. It is believed to be of evaporitic origin on isotopic evidence (Whelan 1974; Whelan et al. 1990), conformity with surrounding units (some of which are stromatolitic), and its internally bedded character. The most significant accumulation of anhydrite is in the 11A unit, particularly notable where it is greatly thickened within the axial region of the Sylvia Lake syncline. (Fig. 11). These Proterozoic anhydrite rocks are thought to represent some of the oldest evaporites in the geologic record of any volumetric significance.

The range of ore-bearing horizons has an estimated stratigraphic thickness of about 1800 feet (550 m). Orebodies are restricted to units 6 through 14 (Fig. 10). Occurrences of anhydrite are limited to the same interval but association with sulphides is indirect in that the two are never in mutual contact except along ductile faults and shears where the contact is structurally imposed.

Protoliths conjectured for some of the Balmat metasedimentary rocks are dolomitic limestone for the pure marble, cherty dolomite for the interlayered quartz-diopside and dolomitic marble units (Hauer 1995), chert for "quartzite" and impure evaporite for the anhydrite-rich units. Protoliths for the pyritic schist (unit 2) might be sulphidic black shale, evaporitic rocks of uncertain composition for unit 10, and siliceous magnesite-bearing and anhydrite-rich evaporite for the tremolite-talc unit 13.

Depositional environment, as conjectured from these assumed protoliths and from stromatolitic evidence, appears to have occurred in a marine, shallow-water continental shelf setting with very minor detrital material derived from the adjacent shield (Whelan et al. 1990; Hauer 1995). Deposition of the Upper Marble formation began after the accumulation of volcaniclastic and pelitic rocks, represented by the Popple Hill gneiss. Deposition was punctuated by periodic episodes of restricted circulation leading to the accumulation of evaporite. Occurrence of stromatolites and some graphite in the marble suggests organic activity, perhaps an abundant supply of algae or cyanobacterial organisms. Chert first appears about a third of the way up the column, also marking the first appearance of stromatolites. Midway in the sequence (unit 6), and thereafter, marine waters became periodically isolated from the ocean, so that under an arid environment evaporite accumulated, locally attaining significant thickness. Evaporite precipitation reached its peak in a long shallow-water period now represented by Unit 11A. Evaporite deposition continued until not long before the sequence was capped by calcareous graywacke or marl (Unit 16), again in somewhat deeper marine water. Unit 13 may record extreme evaporite deposition and perhaps required magnesite and anhydrite as well as silica in the protolith (Petersen et al. 1993).

Balmat Structure

Host rocks of the Balmat mine area have undergone at least four phases of deformation resulting in complex geometry. During first-phase deformation, a prominent axial planar foliation formed in talc-tremolite-anthophyllite schist of Unit 13 and also in Units 2 and 15. Early-phase intrafolial folds deform bedding and compositional layering but not foliation, hence they are the oldest structures recognized in the area. Compositional layering is interpreted as bedding wherein layers of varying thickness, colour, texture, and composition are concordant with each other and with contacts between major lithologic units. Where finely-laminated quartz-diopside rocks persist laterally away from stromatolites, and where the laminations are parallel to compositional layering, this is regarded as relict bedding. Major first-phase folds have not been identified and it is possible that foliation and minor structures formed in a regional ductile shear regime (Tewksbury 1993), with the direction of tectonic transport northwest toward the Grenville Front.

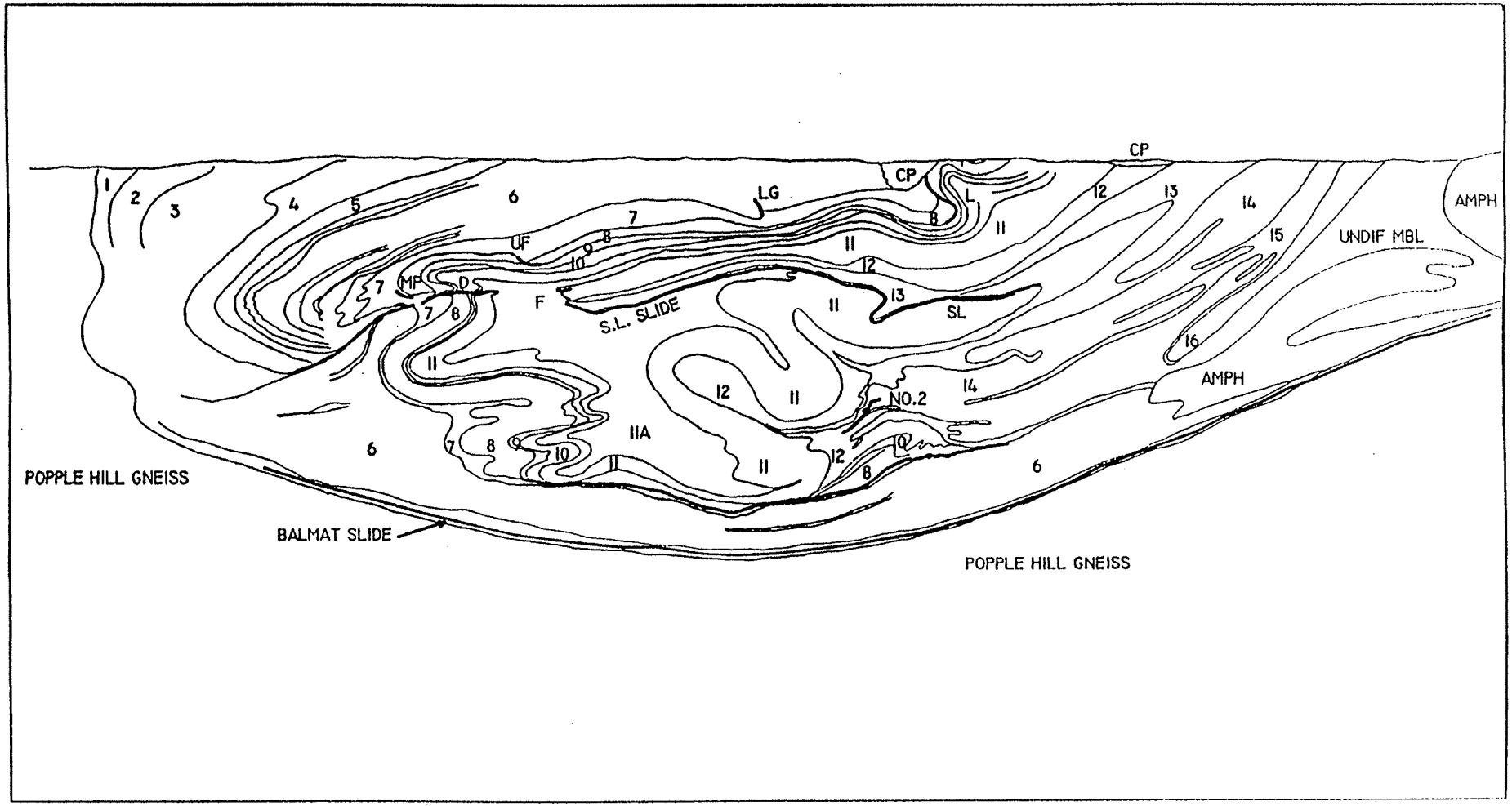

Figure 11. Generalized W–E cross-section through the Sylvia Lake syncline at Balmat. Orebodies represented by black lines as follows: MP = Mud Pond; D = Davis; F = Fowler; UF = Upper Fowler; LG = Lower Gleason; L = Loomis; SL = Sylvia Lake. The Sylvia Lake syncline is a compound fold with its core at "No. 2" and another, the Fowler Lake syncline, lying above, with its upper limb above and its lower limb below the Sylvia Lake slide.

Phase 2A folds isoclinally refold early isoclines and associated axial planar schistositiy. Their axial surface traces strike northeasterly, but vary in strike locally where they are refolded by third-phase folds. The Sylvia Lake syncline is a major, doubly- plunging Phase 2A fold which dominates the structure of the district. It is interpreted as a regional sheath fold, shaped like a "pita pocket" because hinges of the major and associated minor folds are curvilinear, plunging NNW in the southern end of the Balmat district and then swinging to the NE at the northern end. At Edwards the major fold plunges NW back towards Balmat. (Fig. 12).

Similarly, drilling and mining at Pierrepont has shown that structure to be a smaller, doubly-plunging isocline with sheath fold-like geometry (Fig.12). There is no evidence at mine scale or regional scale that later, NW-trending fourth-phase folds interfered with earlier NE-trending folds to produce apparent sheath fold geometry *unless* the movement line of third-phase folds was contained strictly within axial surfaces of the second-phase isoclines. The Sylvia Lake syncline is currently interpreted as a recumbent, compound fold. The Fowler syncline at No. 4 mine shaft, the American anticline, and the syncline at No. 2 mine shaft (Fig. 11), are all Phase 2A minor isoclines located in the core of the fold. The short limb of the Fowler syncline is faulted out, sheared and attenuated along a thrust fault referred to as the Sylvia Lake slide (Fig 11). Apparent net displacement along the slide is on the order of 4000 feet. Outside of the immediate vicinities of the Fowler and the Sylvia Lake orebodies where discordant relationships are obvious, there is scant field evidence to suggest major tectonic discontinuity because in most places compositional layering and major unit contacts are layer-parallel to the slide. The Davis and Mud Pond orebodies occur in stratigraphically lower units farther west along the trace of the Sylvia Lake slide. Mineralization in both is transgressive across Units 7, 8, 9, 10, and 11. Strain within unit 11A anhydrite between the Fowler and Davis orebodies may have been accommodated by ductile flow of anhydrite rather than by shearing along a discrete shear surface. "Straight marble" is common where mineralization transgresses major stratigraphic units, with the foliation defining the layering in the ductile marble parallel to shears cross-cutting less ductile, layered, calc-silicate marble units. Such "straight" marble layering is present in the Fowler, Upper Fowler, Sylvia Lake, Davis and Mud Pond orebodies and where observed is regarded largely as a second-phase ductile shear deformational fabric. Major offset is observed between Fowler/Sylvia Lake orebodies with the Fowler thrust faulted > 4000 feet, N55° W, *relative* to the Sylvia Lake (see Fig.11). Relative offset of the Davis and Mud Pond orebodies, though of similar sense, is of much lesser magnitude, and that of Upper Fowler is of the opposite sense.

Phase 2B folds isoclinally refold straight marble foliation in the Davis, Fowler, Upper Fowler and Sylvia Lake orebodies. Phase 2B folds are isoclinal in style and often take the form of elongate, sheared-out, tabular folds with pointed hinges. Rotation senses are clockwise on both limbs of the Sylvia Lake syncline which suggests a major shear couple was superimposed on the entire fold or alternatively, that the Sylvia Lake syncline was itself of the limb of a much larger regional fold. Clockwise asymmetric sense of phase 2B folds is compatible with southeast overturning of the Sylvia Lake syncline in the later stages of phase 2 folding, hence the term " phase 2B" (Fig. 9). Implications of this are important because on the upper limb of the Sylvia Lake syncline, clockwise phase 2B overprinting of counter-clockwise phase 2A structures had a net subtractive effect. Accordingly, phase 2A rotation or offset along ductile faults was reversed by phase 2B strain of opposite asymmetric sense, partitioned along these reactivated faults. For example, the Loomis, Mud Pond, and Fowler (relative to Sylvia Lake) orebodies show phase 2A counter-clockwise net rotation senses while the Upper Fowler shows clockwise, phase 2B net offset along the Upper Fowler fault. Although all the orebodies on the upper limb experienced phase 2B clockwise rotations, it was only in the Upper Fowler orebody that phase 2B strain was of sufficient magnitude to reverse or negate the effects of Phase 2A. A simpler situation exists on the lower limb of the Sylvia Lake syncline where the effects of phase 2A clockwise, and phase 2B clockwise rotations, were additive. Effects of Phase 2B folding in the Fowler orebody include rotation of Units 12 and 13 from the core of the Fowler syncline into a position axial planar to the Fowler syncline and x-cutting Unit 11 (Figs. 13,14) and clockwise isoclinal refolding of the Davis shear zone and associated straight marble fabrics.

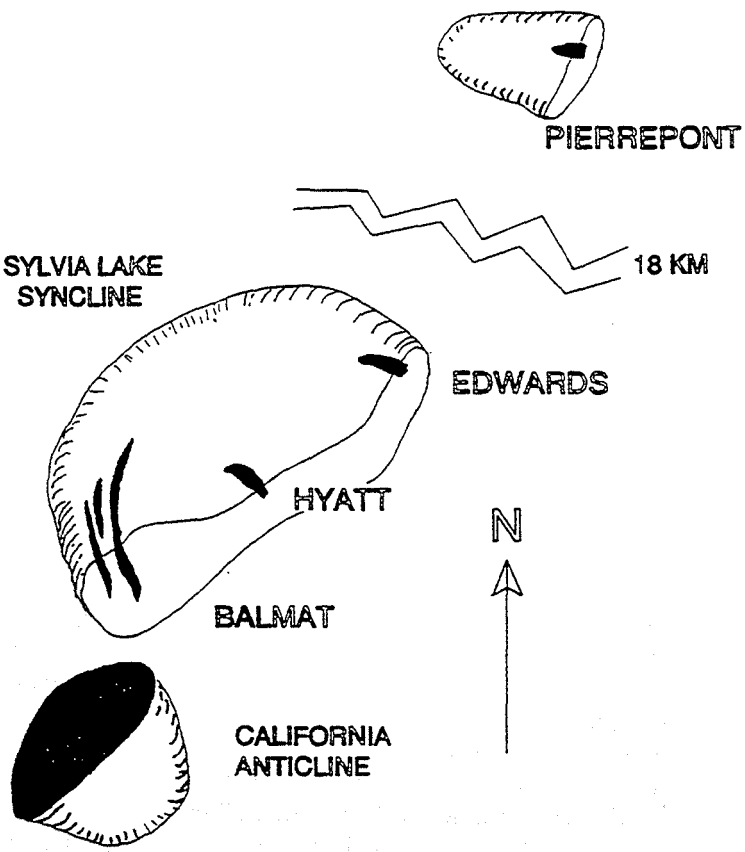

Figure 12. Composite map view and 3D representation of the Sylvia Lake syncline and the Pierrepont fold showing "pita pocket", doubly plunging geometry. The California anticline is sheath fold complementary to the Sylvia Lake syncline.

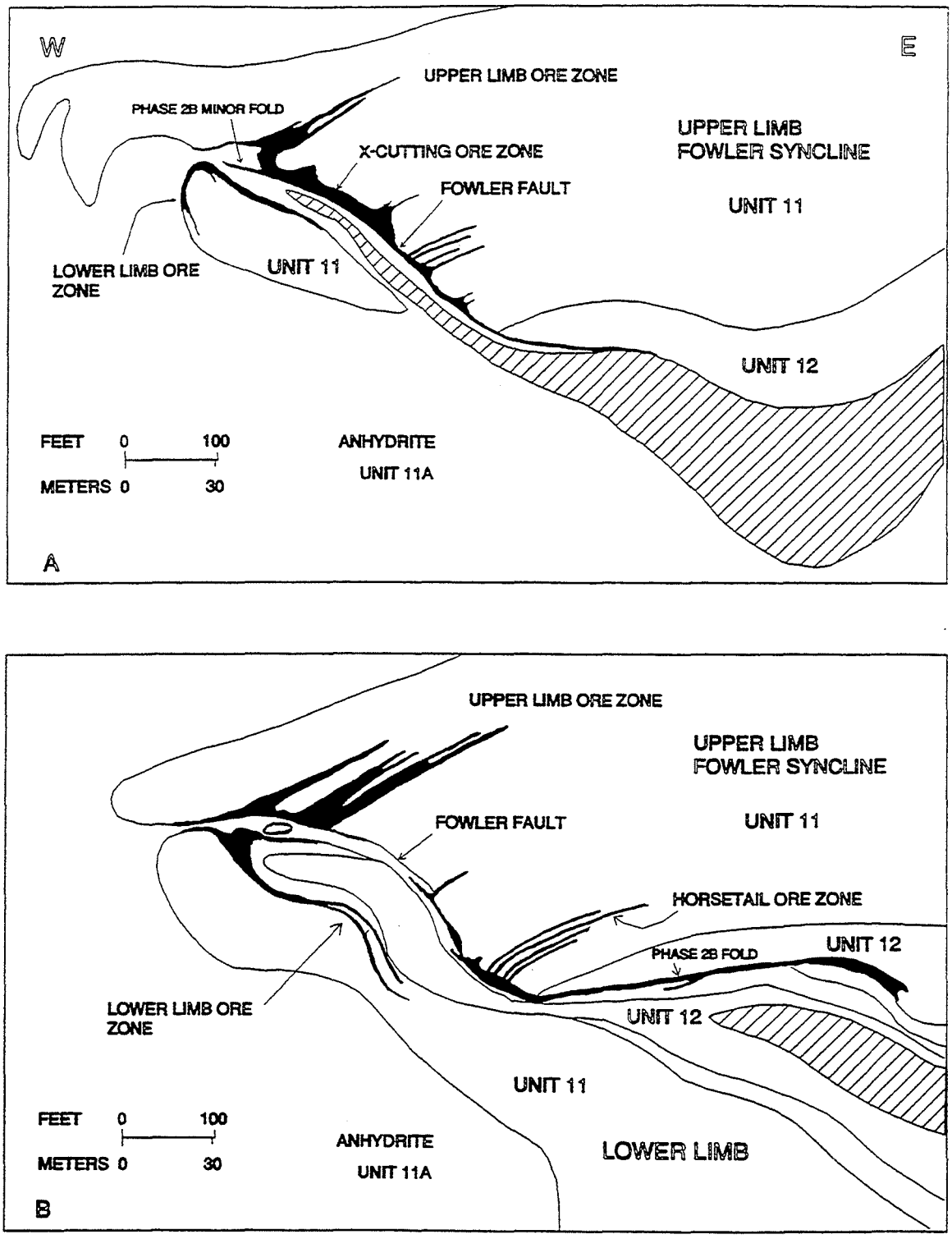

Figure 13. W-E sections through the Fowler orebody showing ore zones and structure. Hatched pattern = unit 13; ore = black; 13A is a section up plunge, 13B several hundred feet farther down plunge to north.

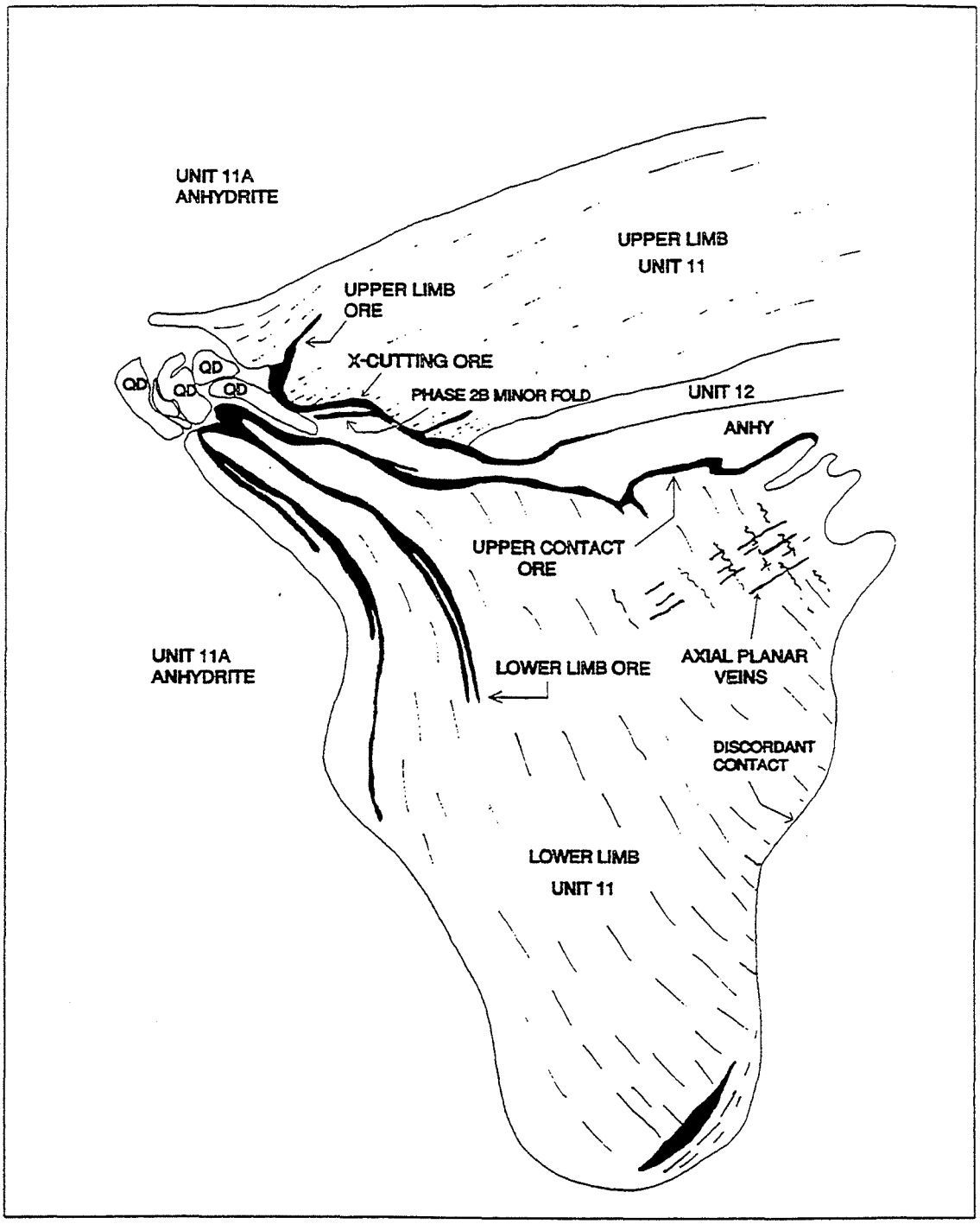

Figure 14. W-E cross section through the Fowler orebody showing large lower limb "tectonic mullion". The wedge-shaped mass is fault-bounded at its eastern contact with unit 11A anhydrite and at its contact with the Upper Contact ore zone. Interpreted as the wedge-shaped core mass of the fold depicted in Figure 18. Axial planar ore veins cross-out bedding in unit 11.

Third-phase minor folds refold Phase 2A and 2B axial surfaces about steeply-dipping, NNE-striking axial surfaces. Plunges of third-phase folds are NNE, roughly co-axial with the local second-phase folds. Manifestations of third-phase folds are observed in Fowler and Upper Fowler orebodies where the latest folding is defined by "top-side-west" or counter-clockwise refolds of Phase 2A straight marble fabrics paralleling ductile faults and Phase 2B sheared-out isoclines.

Fourth-phase folds have NW-striking, steeply dipping axial surfaces and are open in style. They have been observed only locally in the Fowler orebody. Where fourth-phase folds are prominent, as on the 2100 level of the Fowler, they interfere with earlier NE-trending folds to form modified dome-and-basin patterns (deLorraine 1979). Below 2100 level, the plunge of the Fowler orebody steepens to 45°. Fourth-phase folds are not seen in Figure 11 because their axial surfaces parallel the plane of the section.

One might question whether it is really possible to identify stratigraphic successions (which define folds), given the complexity of polyphase deformation and tectonic sliding, especially in view of the high metamorphic grade and extreme strain implied by sheath folding. Might we be looking entirely at shear fabrics or transposition of layering? Part of the answer lies in the mode of preservation of stromatolites now represented by domes of finely-laminated quartz-diopside rock. The senior author believes that bedding, including stromatolites and cryptalgal lamination, was diagenically enhanced or replaced by silica. Reaction of chert and dolomite layers under high-grade metamorphic conditions produced diopside layers which mimic or enhance original bedding — hence the term relict bedding. Quartz-diopside rocks behaved as structural buttresses where as marble units were extremely ductile, having accommodated large strains by plastic flow leaving stromatolites and relict bedding largely intact. Second, overall doubly-plunging aspect of major folds approaches "pita pocket" geometry more so than true sheath fold geometry. Strain was accommodated by plastic flow, tectonic sliding and ductile faulting such that despite attenuation of and breaks between major stratigraphic units, it is still possible to define lithic successions that are predictable from place to place across the northwest Adirondacks. Overall strain was not as extreme as that which would be expected from true sheath fold geometry.

The Orebodies

General

The presently known zinc orebodies of the Balmat mine lie within one mile of the central No. 4 shaft, in an area of approximately two square miles. A majority of the ore shoots are arranged in clusters customarily known as the Balmat No. 2, 3, and 4 mines, after the shafts which service them. In this guide, the ore clusters will be described as belonging to No. 2, 3, and 4 mines, although these are more properly interconnected mining units now centralized around No. 4 shaft, from which Balmat ore is hoisted to the adjacent mill (Fig. 15).

There is much diversity in characteristics of the orebodies, but it is possible to make some generalizations. Sulphides are intimately associated with fold hinges and may be defined as massive stratabound and stratiform. In detail, however, sulphides are locally found along transgressive shear zones and faults associated with major second-phase folds. Ore occurs as tabular, podiform or lenticular bodies of moderate cross-sectional areas (2 to 50 feet thickness by 50 to 800 feet on strike), but characteristically have a large, often extremely large dimension (6000') in the plunge direction of Phase 2 A fold hinges, with which they are initially associated (Figure 15). Thickening of sulphides occurs locally in second-phase fold hinges, with thinning occurring along the attenuated and sheared limbs. Sulphides tend to be localized along boundaries of dissimilar lithologies, such as contacts between dolomite and diopside layers. Contacts of sulphides with bordering rock are generally sharp, with disseminations extending into wall rock being the exception rather than the rule. Wallrock alteration is limited to local envelopes of silicification paralleling shear zones. Cross-cutting veinlets of quartz-sphalerite-pyrite locally mineralize crackle breccia in silicated dolomitic

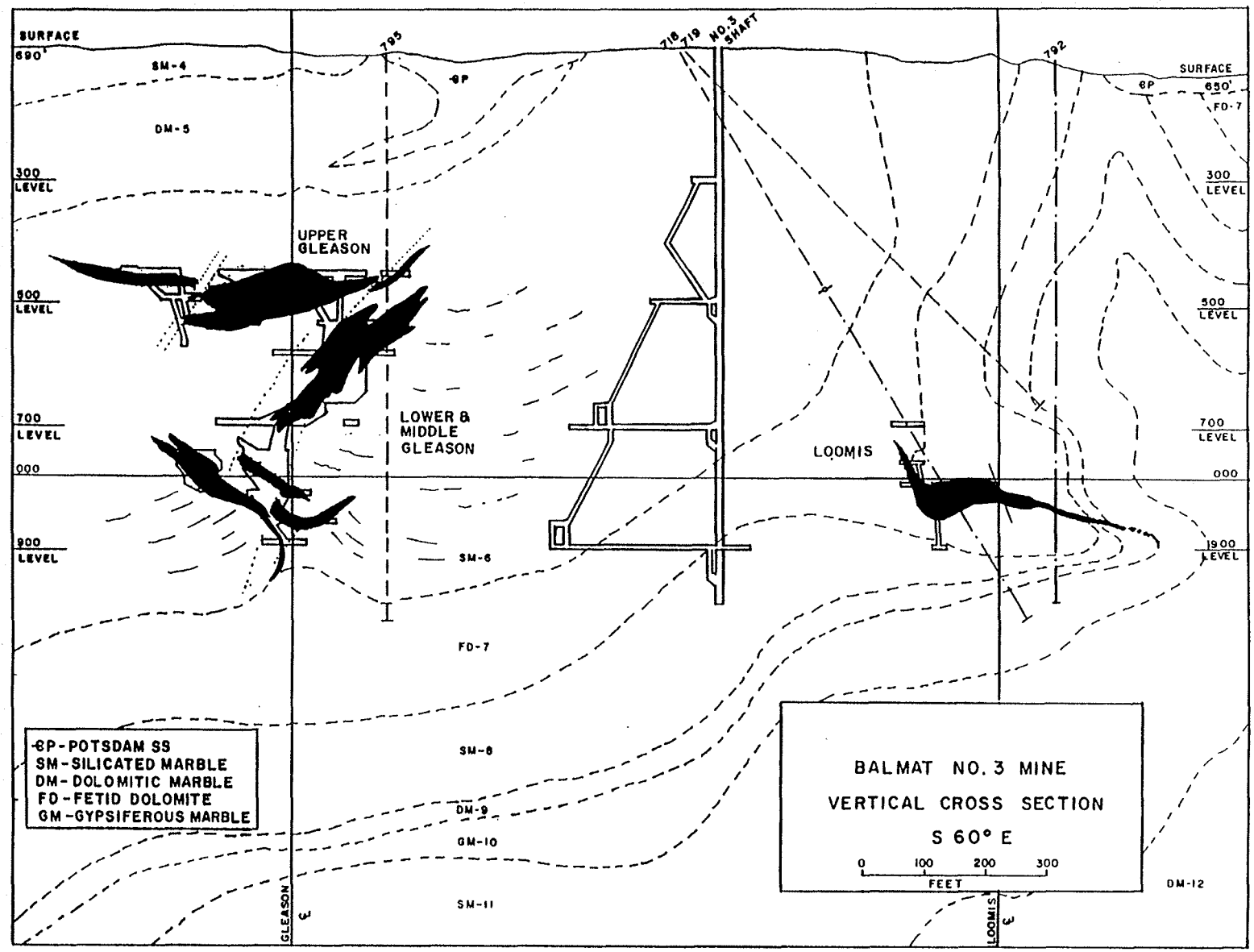

Figure 17. Cross-section through No. 3 mine. Upper Gleason ore is massive high-grade; Middle and Lower Gleason cross-cut stratigraphy and are lower grade.

quartz gangue. "Supergene" hematite derived from oxidation of iron in sphalerite or pyrite occurs locally along fractures.

The **Lower Gleason** orebody occurs in Unit 6 near and at the contact with Unit 7, along a high-angle reverse fault referred to as the Gleason fault (Fig. 17). The Gleason fault is associated with a Phase 2A minor fold plunging sub-horizontally N35° E. Rotation sense of the fold is "S", consistent with its location on the upper limb of the Sylvia Lake syncline. Cross-cutting mineralization dies out rapidly away from the Gleason fault; contacts of the stringers and veinlets with wall rocks are sharp. Much ore is also present as medium-to-fine grained, highly deformed streaks and layers in well-foliated marble tectonite lying parallel to the fault. Later, steeply dipping, WNW-trending faults of dominantly strike-slip character segment the orebody into panels within which hematization of the ore zone and talcose alteration of diopside are locally extensive. Offset between panels is minor. The Lower Gleason orebody attains its greatest grade and tonnage where it passes under and crosses the trend of the Upper Gleason (Fig.17). The reason for this is unclear, but there is a nebulous mineralized zone which crosses stratigraphy and seems to connect the two orebodies at the cross-over point. This raises the possibility that the Upper Gleason orebody may have served as the source reservoir supplying the Lower Gleason orebody.

The **Loomis** orebody occurs in the hinge and along the sheared short limb of a Phase 2A fold referred to as the Loomis "S" Fold, so named for its sense of asymmetry (Fig. 17). The Loomis "S" Fold plunges gently N35°-40° E., but undergoes localized reversals in plunge within the mine area. This may be a consequence of gentle re-folding or natural variations in fold profile and geometry in the down-plunge dimension. Full plunge dimensions are presently uncertain, but mining extended down-plunge over 3500 feet. Ore occurs as coarse-grained masses and veins within Unit 8 at the 7/8 contact, as banded marble-sphalerite tectonite within Unit 9 along a cross-cutting shear zone in the short limb of the "S" fold, and within Unit 10 along the 9/10 contact (Fig. 17). Sphalerite is the dominant ore mineral, while pyrite is very minor in amount and galena present only as traces. Late faults transect and segment the orebody as in the Gleason orebodies; hematite and willemite replacement of sulphides along late faults is locally extensive and in some places complete. Secondary willemite is locally abundant and is restricted to hematitized zones within the orebody. Interestingly, clastic dykes of Potsdam sandstone in places extend downward nearly 750 feet below the present surface.

The undeveloped **West Gleason** mineralized zone lies down-dip a few hundred feet west of the Lower Gleason (Fig. 15). Its structural setting, in Unit 6 near its contact with Unit 7, appears to resemble that of the Lower Gleason but on a smaller scale. The narrow and relatively low-grade ore shoot extends down the plunge for at least 3000 feet. Its remarkably straight course suggests fault control associated with folding in diopside-rich host rocks.

The **Loomis C,** also undeveloped, is a small satellite orebody directly overlying the Loomis. It is confined to a minor structure in Unit 6 near the 6/7 contact and extends for about 1000 feet along the plunge.

Orebodies at No. 4 Mine

In addition to being the main hoisting shaft for most of the orebodies of the Balmat Mine, the No. 4 shaft specifically serves the Fowler, Upper Fowler, Davis and Mud Pond orebodies, which are located 1500 to 3500 feet northwest of the shaft (Fig. 15).

The **Fowler** orebody is localized within the axial region of the Fowler syncline (Fig. 11), which plunges N5-15^0 E at 15-45^0. The mineable portion of the Fowler orebody has a down-plunge longitudinal extent of nearly 5000 feet, from 1200 feet below surface to more than 3000 feet below surface.

The Fowler syncline is interpreted as a Phase 2A recumbent fold whose limbs were dissected by synmetamorphic faults, of which the Fowler fault (Fig. 13) and Upper Contact fault (Fig. 14) are the most

prominent. Anhydrite, large slices of Units 12 and 13, and tectonic melange comprised of anhydrite, blocks of Unit 11, and slivers of Units 12 and 13 occur between the Fowler upper and lower limbs (Figs. 13B,14).

The "Lower Limb" (Fig. 14) is a large wedge-shaped body of Unit 11 that is surrounded by 11A anhydrite. Bedding is truncated along the Upper Contact fault and at the footwall of the structure. (Fig. 14) shows that the lower limb is an immense rod-like tectonic block or tectonic mullion. The Lower Limb pinches out down-plunge with a concomitant increase in size of the Upper Limb. Silicified tectonic breccia zones and occurrences of white "bull" quartz are present locally along the Fowler and Upper Contact faults.

Five ore zones have been recognized as subdivisions of the Fowler orebody because they occupy particular structural domains within the axial region of the Fowler syncline. The Upper Limb and Horsetail ore zones each consist of conformable layers which extend updip along bedding into the upper limb where they lense out. (Fig. 13). Sulphide layering is common in both ore zones. The Cross-cutting ore zone is so named because it lies along the Fowler fault. It extends from the beginning of the Upper Limb ore zone down dip to the east across the Horsetail ore zone and thence along the Unit 12/13 fault contact (Fig. 13B). Conformable ore extending away from the Upper Contact fault down dip into the lower limb constitute the Lower Limb ore zone. Lower Limb ore is truncated by the Upper Contact ore zone, which lies along the Upper Contact fault. The Upper Contact and Fowler faults probably represent opposing faces or sides of a single fault separating the Upper and Lower fold limbs, and in any case the Fowler fault is actually a segment of the Sylvia Lake slide, recognized where it transgresses Unit 11 at a high angle.

Ore mineralogy is relatively simple and uniform. Medium to coarse-grained sphalerite, varied proportions of pyrite, gray quartz and local occurrences of galena characterize Upper and Lower Limb ores. Unlike these ore zones, Horsetail ore is essentially monomineralic: massive coarse-grained sphalerite generally with very minor pyrite and quartz. The most interesting concentrations of galena in the Fowler orebody occur at the up-dip ends of some of the Horsetail horizons and in gash fractures between individual Horsetail layers. Sulphides in the Cross-cutting and Upper Contact ore zones are quite varied but normally consist of massive medium- to coarse-grained sphalerite and pyrite with quartz. Segregation layering, defined by alternate sphalerite and pyrite-rich layers, is locally prominent in massive sulphides parallel to the two major faults. In places, inclusions of ribbon-like anhydrite, rounded quartz, diopside, dolomite and tremolite are abundant. There is a tendency toward finer grain size, increasing numbers of inclusions, and greater development of Durchbewegung textures along the Fowler fault in a direction down dip away from the Upper Limb ore zone and thence out along the Unit 12/13 contact. Mineralization in both the Cross-cutting and Upper Contact ore zones truncates bedding at high angles. In places along both faults there are silicified zones consisting of masses and pods of white "bull" quartz+calcite+disseminated pyrite and sphalerite+breccia fragments of diopsidic wallrocks. Silicified zones can be difficult to identify but are inferred where anastomosing veins of diopside form trellis-like patterns in dolomite. Figure 18 shows in diagrammatic form the interpreted "proto" Fowler syncline fold hinge and associated ore zones within it during early stage 2A dismemberment. The Fowler fault is interpreted to have formed as a radial extensional fracture approximately axial planar to the Fowler syncline. Sulphide ore filling it became the cross-cutting ore zone. Another such fracture is located at the base of the Lower Limb. As the Fowler and Sylvia Lake synclines evolved and competed for space, the Upper Limb of the Fowler syncline detached from the Sylvia Lake limb and was transported westerly *relative* to the Sylvia Lake limb along the Sylvia Lake slide. Points of detachment are thought to be in Unit 11 at the Fowler and Sylvia Lake orebodies representing nearly 5000 feet of displacement. Apparent net displacement is 4200' following phase 2B strain of opposite rotation sense. (Fig. 11). The Lower Limb is seen as an immense tectonic mullion that broke out between radial extensional fractures in the hinge of the Fowler syncline. It is now thought that significant differences in mechanical response to folding existed between the Upper Limb of the Sylvia Lake syncline (structurally above Unit 13) and the anhydrite-rich core such that it is possible that much, or most, tectonic transport may have been the Sylvia Lake limb transported to the SE (counter-clockwise rotation).

Evolution of the Fowler Orebody

Just prior to the breakup of the Fowler syncline, conformable ore now represented by the Upper and Lower Limb ore zones is interpreted to have migrated by plastic flow and metamorphic fluid phases into the Crosscutting/Upper contact extensional fracture (Fig. 18). This was accompanied by local silicification as silica was mobilized with sulphides into the extensional (dilatent) zone. There was also considerable migration of calcite and some lead into the extensional zone. With complete segmentation and dismemberment of the Fowler syncline, anhydrite enveloped the Lower Limb rock mass (Fig.14). At this time, anhydrite-sulphide tectonite developed along the Fowler and Upper contact faults and the Fowler and Sylvia Lake orebodies were separated by 5000 feet along the Sylvia Lake slide. Phase 2B deformation of the opposite, or clockwise, rotation sense, subsequently rotated elements of the core of the fold, Units 12 and 13 specifically, into positions cross-cutting Unit 11 and axial planar to the upper limb, (Fig. 13). This was facilitated by phase 2B ductile reactivation of the Sylvia Lake slide.

The **Upper Fowler** orebody structurally overlies the Fowler (Fig. 11) (underlies stratigraphically). It is an elongate, tabular orebody plunging N20°E at 1°-20°; longitudinal dimensions exceed 6000 feet. Width along strike increases down-plunge from 100 feet to over 400 feet. Thicknesses vary from 1 to 10 feet; contacts with footwall and hangingwall are sharp. Upper Fowler ore is localized along a low angle fault referred to as the Upper Fowler fault. As a result, Upper Fowler mineralization is not stratiform, but occurs in contact with Units 7, 8, 9, and 10 (Fig. 19).

Ore consists of fine-to medium-grained, light chocolate brown sphalerite with very minor fine-grained pyrite in a fine-grained calcitic marble matrix. Rounded dolomitic marble or diopside inclusions are abundant yielding Durchbewegung textures. Minor coarser-grained sphalerite occurs in thin layers, extensional fractures, and irregular veins in both the hangingwall and footwall of the fault. Locally, in competent silicated units, ore extends for short distances away from the fault along two sets of fractures, one set paralleling the bedding, the other in a shear orientation parallel to the fault. Upper Fowler ore is unique in that no concordant "source" bed can be identified for any of the host rock units, though the 7/8 contact is suspected.

The **Mud Pond** orebody is the most westerly in the Balmat Mine (Fig.15). It is located in Units 6,7, and 8 in a refolded ductile fault within a minor fold in the hinge of the Sylvia Lake syncline. The orebody extends at least 2000 feet downplunge, trends N25°E and plunges gently at 10° - 15°. A sister orebody, the Davis, occurs along the eastern extension of the same ductile fault that hosts the Mud Pond orebody. It appears at this early point of development of both orebodies that Mud Pond mineralization is transgressive along the base of Unit 8 hangingwall to the ductile fault which crosses it and that Davis ore is transgressive across the top of Unit 8 footwall to the fault some 400-500 feet farther east..

Unassigned Orebodies

The **Sylvia Lake orebody** is located on the northwest limb of the American anticline (Fig. 11). From surface to 900 feet ore may occur as a comformable band in Unit 11 and also along a transverse shear plane extending from the conformable band across Unit 12. Below 1,100 feet the ore is localized along a major ductile fault at the contact of Units 11 and 12. The body is tabular, with thicknesses of 2 to 10 feet and strike lengths of 200 to 300 feet. Characterized by fine to medium grain size and numerous inclusions of wall rock, "Durchbewegung" textures are common. It is now known to represent detached remnants of ore in the Sylvia Lake limb of the Fowler syncline. As such, the Fowler and Sylvia Lake orebodies were initially one contiguous mass before detachment along the Syliva Lake slide.

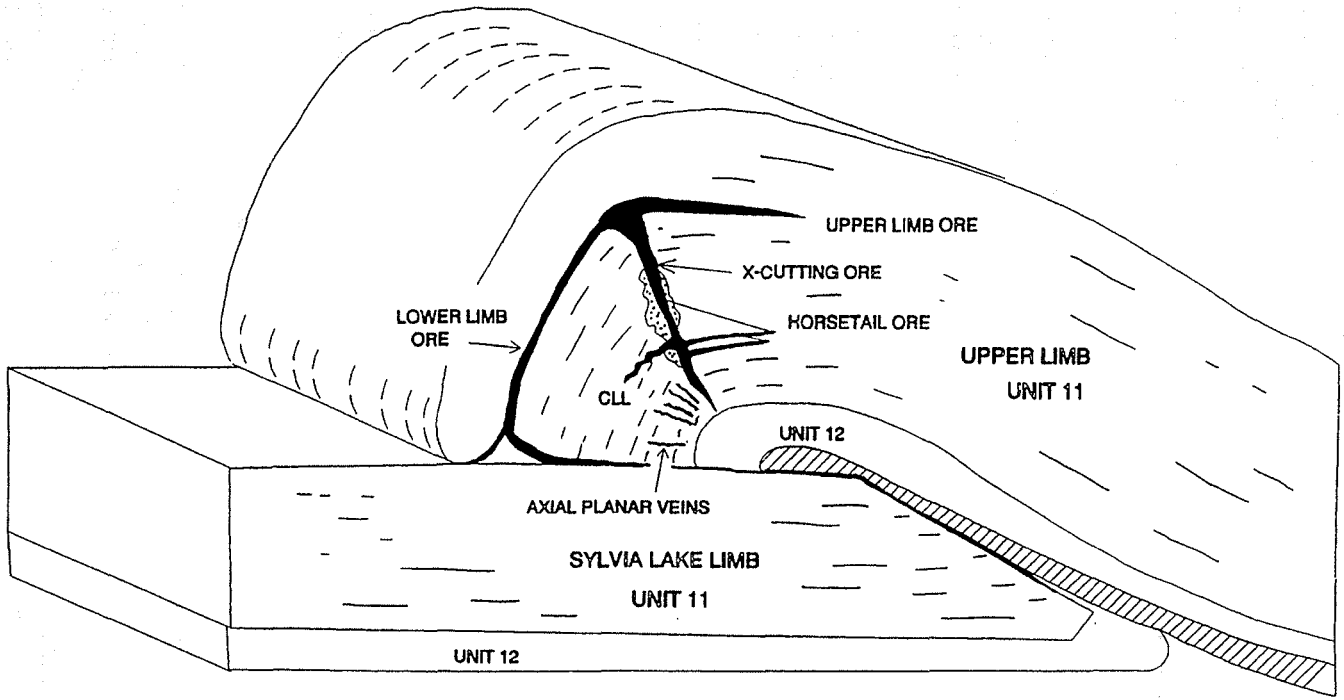

Figure 18. Three-dimensional section through the Fowler/Sylvia Lake orebodies during initial stages of Phase 2A fold dismemberment. Net displacement is N55°W, 4200 feet.

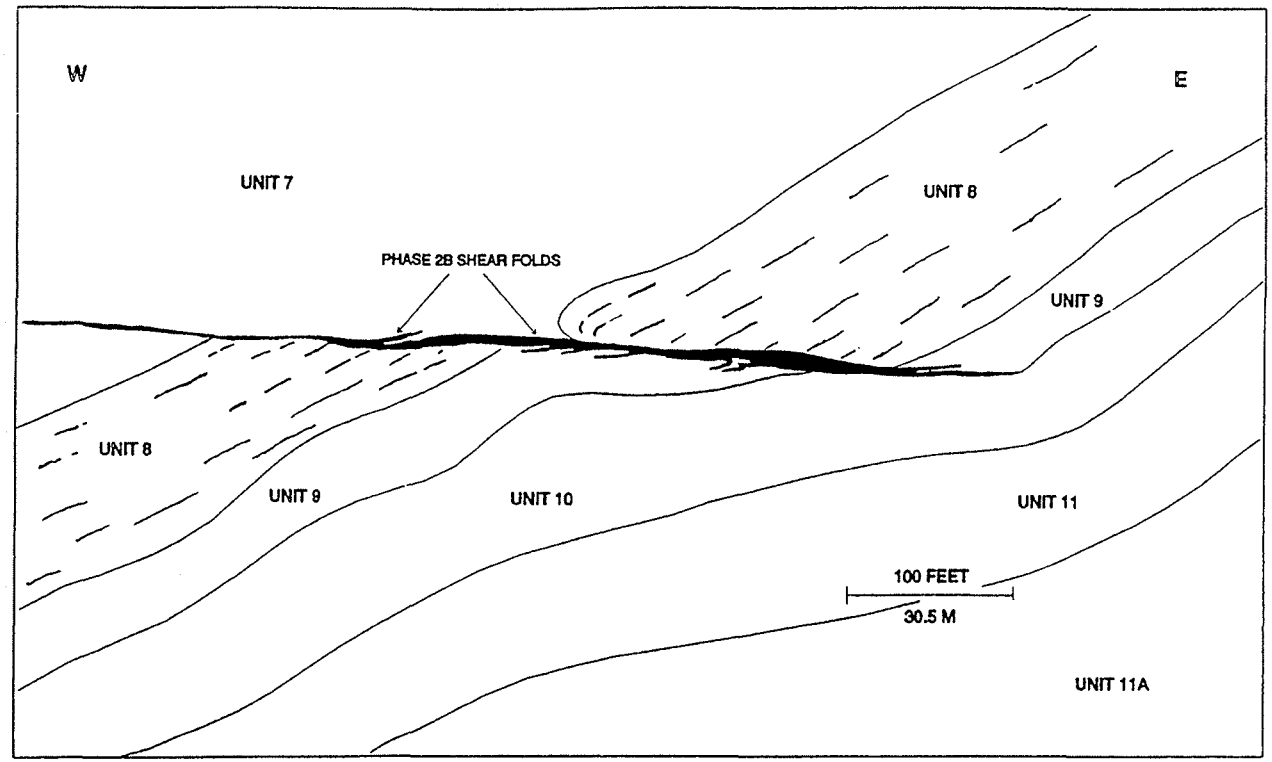

Figure 19. W-E section through the Upper Fowler orebody. Durchbewegung ore cross-cuts units 7–10. Phase 2B shear folds display clockwise rotation senses which oppose those incurred during phase 2A. Hangingwall unit 8 was originally emplaced farther west than footwall unit 8 at the end of phase 2A.

The **Wight** orebody (Fig.15), is a minor occurrence in the immediate hangingwall of the Wight talc mine workings. The ore shoot is lenticular and limited to a thin diopside-quartz member of Unit 12 at the contact with Unit 13. Thickness of the lens is from 2 to 14 feet, strike length a maximum of 600 feet, and down-dip it is restricted to a vertical range of 150 to 400 feet below the surface.

Distribution of Metals in the Ores

Investigation of the distribution of minor and trace metals in the sphalerite, both laterally and stratigraphically, has been done by analysis of flotation concentrates made from drill core composites of orebodies (Swanson 1979). Lateral variations of Fe, Hg, Cu and other minor and trace elements in sphalerite do not appear to fit into well-defined zonal patterns within any of the orebodies. Between orebodies, however, some consistent stratigraphic controls are evident. Most strikingly, the Hg content in sphalerite gradually decreases stratigraphically upward culminating in an abrupt drop to an almost background level in the Main and Streeter orebodies, highest in the column. Content of Fe and FeS in sphalerite consistently increases upward in the column, with the exception of Fe in the stratigraphically intermediate American and Number One sphalerites which is as high as in the uppermost Main and Streeter orebodies. Differences in cobalt and nickel concentrations in orebody pyrite VS. disseminated pyrite in host rock marble led Doe (1962A) to the conclusion that orebody pyrite is not related genetically to that in the surrounding metasedimentary strata, and that the carbonates are not the primary source of the ore metals. Arsenic has been noted in the form of trace to minor occurrences of jordanite, orpiment and realgar, and arsenopyrite in the Main and Fowler orebodies.

Lead Isotopes

Results of early isotopic studies (Doe 1962B) showed that lead isotopic compositions lie close to the normal growth curve for conformable ore deposits (Stanton and Russell 1959). Before that time, sulphide ores were interpreted to be of igneous, hydrothermal replacement origin (Doe 1960). Later, Doe concluded (1962B) that ore lead could have been extracted from nearby granite only if radiogenic lead had been added to the feldspar in the granite after the formation of the ores. While not completely negating this possibility, it was thought that hydrothermal replacement was a less promising candidate for formation of the orebodies. Reynolds and Russell (1968) showed that small but distinct differences exist between orebody lead and rock lead at Balmat. It is apparent from existing analyses that ore lead compositions differ substantially from many Mississippi Valley type deposits (Brown and Kulp 1959; Fletcher et al. 1978) which are characterized by radiogenic, or J-type, lead (Heyl et al. 1974).

Sulphur Isotopes

Isotopic compositions have now been determined for most of the known anhydrite horizons in the Balmat stratigraphic column, demonstrating large changes in composition from isotopically light sulphate sulphur in Unit 6 (average $\delta^{34}S$ = 9‰) to heavy sulphate sulphur in Unit 11A ($\delta^{34}S$ = 30‰ maximum), followed by a decrease to lighter sulphate in Units 13 and 14 ($\delta^{34}S$ = 17 to 20‰; Figure 11; Whelan et al. 1984). Such fluctuations have also been recognized in Phanerozoic evaporite but over longer time spans. Early work by Solomon (1963) led to the suggestion that sulphide sulphur was not magmatic in origin but probably marine.

Close-spaced sampling of two major anhydrite sub-units has shown sulphur isotope variations which further detail cyclical events in the deposition of Balmat evaporite. The lower (Unit 6A) anhydrite and upper (Unit 11A) anhydrite give $\delta^{34}S$ values from 7.6 to 10.2‰ and 24.1 to 30.1‰ respectively, a substantial difference in isotopic composition considering the intervening stratigraphic interval of only about 1000 feet. Further, the values within each anhydrite bed increase systematically from bottom to top stratigraphically.

These variations are believed to be premetamorphic in origin and are attributed to simultaneous evaporitic sulphate deposition and bacterial sulphate reduction within a restricted basin (Whelan et al. 1984; Whelan et al. 1990).

Sulphide $\delta^{34}S$ values also show interesting variations. Two groups were analyzed, one of the same suite of orebody sphalerite composites used in the metal distribution study, the other a collection of various sulphide-sulphate combinations within the Fowler orebody.

Small variations of $\delta^{34}S$ in sphalerite are established in the analysis of orebody composites. Total range of values is 13 to 15‰, considerably less pronounced than the range of 8 to 30‰ for anhydrite (Fig. 20). Sphalerite in Units 6 through 9 has isotopically lighter sulphur, that in Unit 11 the heaviest (up to 15.38‰) and that in Units 12 through 14 again have relatively light sulphur. Curves drawn from $\delta^{34}S$ variability VS. stratigraphic position are dissimilar for both anhydrite and sphalerite (Fig. 20). The two do not vary sympathetically, suggesting that the orebody sulphur was not extracted directly from coeval seawater sulphate (Whelan et al. 1984).

It is evident that large-scale, pre-metamorphic sulphur isotope distributions have been preserved during metamorphism. Preliminary data from the Fowler orebody sulphides, however, indicate that metamorphic changes in sulphur isotope systematics have been superimposed on the original isotope distributions. Specifically, sulphide $\delta^{34}S$ values are lightest in the axial region of the Fowler syncline and increase gradually away from it. Preferential migration of isotopically lighter sulphur to the hinge region of the early fold is consistent with the data. Orebody sulphide $\delta^{34}S$ compositions are distinctively different from those of pyrite from surrounding metasedimentary rocks as reported by Buddington et al. (1969), Brown (1973) and Whelan et al. (1984). Pyrite from meta-sedimentary strata is isotopically light, averaging -10‰ $\delta^{34}S$ (Buddington et al. 1969). Pyrite disseminated in the host marble but removed from massive sulphide is also isotopically light and therefore distinct from orebody sulphide (Whelan et al. 1984).

Ore Genesis

One of the most interesting and greatest challenges of Balmat geology is concerned with the genesis of the ores. It is clear that the ores are pre-metamorphic in origin and have been extensively reworked, remobilized and recrystallized during metamorphism. Genetic clues have been largely erased save for bulk geochemical trends, massive nature of the mineralization, and stratigraphically equivalent disseminated traces of mineralization persistent distal to some orebodies. Accordingly, several genetic models have been proposed. These include: Mississippi Valley type; volcanogenic exhalative; and sedimentary exhalative.

Metamophosed Mississippi Valley Type: Probably because the ores are hosted by carbonate rocks the MVT model is attractive to many. The basic tenet of this model is that upon high-grade metamorphism epigenetic sulphides initially disseminated in the stratigraphic pile were drawn to low pressure sites or dilatant zones in fold hinges where they presumably accumulated as massive sulphides. This would require wholesale evacuation of metal to hinge zones, leaving no traces or depletion haloes behind. Difficulties with this model are that orebody pyrite and host rock pyrite compositions are dissimilar, Pb isotopic compositions between ore and host rocks are different, and there are no geochemical haloes or depleted auras around fold hinges. There are also many unmineralized fold hinges which should host at least minimal mineralization if premetamorphic mineralization was disseminated over broad areas. In the case of Pb isotopic values, the approach to single stage evolution of the lead isotopes requires the metals to have been leached from large volumes of heterogeneous source rocks as suggested by Doe and Stacy (1974). Differences between ore and rock lead, however, preclude the carbonate and granitic rocks in the area as primary sources of the lead.

Volcanogenic Exhalative: This genetic model was proposed by some investigators primarily because of the massive nature of the ores and approach of Pb isotope systematics to single-stage growth compositions

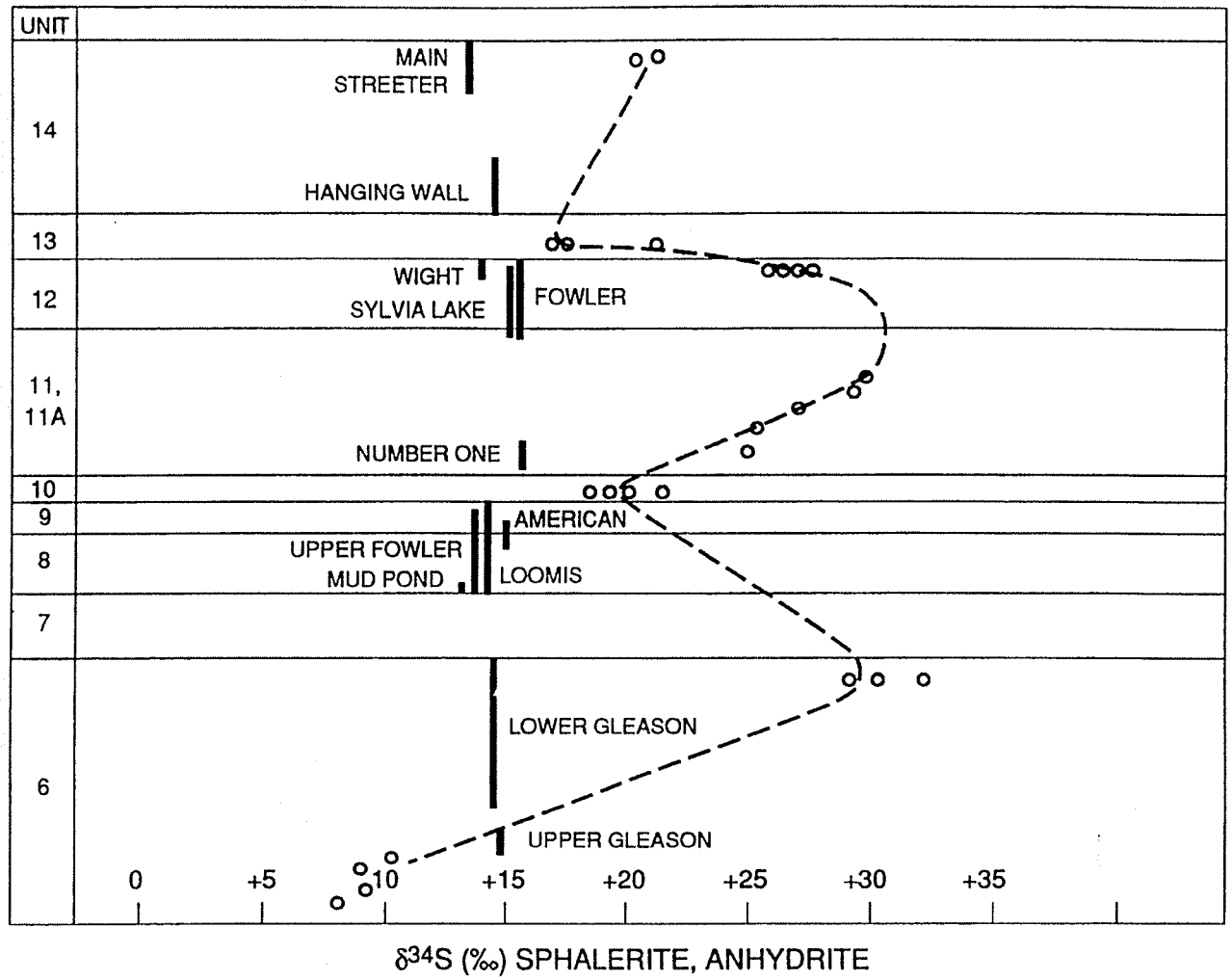

Figure 20. Sulphur isotope variations in orebody sulphur and anhydrite sulphate plotted against stratigraphic position.

similar to many know volcanogenic deposits. A requirement of this model is that vent sites would bear a distal relationship to the site of deposition. Inasmuch as there are essentially no intercalated volcaniclastics rocks in the Balmat stratigraphic section, this genetic model appears inadequate to explain available data. As well, there are no pipe-like "stringer ore" zones developed in altered or silicified volcanics in the stratigraphic footwall of any of the massive sulphide lenses.

Sedimentary Exhalative: Certain aspects of the orebodies lend themselves well to a "SED-EX" model (Swanson 1979; deLorraine and Dill 1982). These are principally the massive nature of the ores, apparent minor element compositional dependence upon stratigraphic position, localization within clean carbonate strata and laterally equivalent . disseminated traces of sulphide. Basic features of this model involve large volumes of chloride-rich fluids leaching metals as they migrated through the sedimentary/volcanic pile. Evolved basin brines, perhaps chemically similar to those having produced Mississippi Valley type deposits (Whelan et al., 1984), would constitute ideal ore fluids. Fluid migration could have been initiated by sudden collapse of the sedimentary pile as it reached a critical thickness, leading to basin dewatering (Cathles and Smith 1983). Migration could also have been the result of seismic pumping, or have been driven by convective circulation driven by plutonism. In any case, metalliferous brines ultimately would be channelled through conduits, such as faults, to discharge sites on the sea floor. The process would have operated repeatedly to produce the observed stratigraphic spread of the mineralization. Deposition would necessarily be rapid, leading to accumulation of massive sulphide sheets and lenses. Metals, ultimately derived from sediments/volcanic rocks and leached from them by large volumes of chloride-rich brines, would be carried in solution in complexed form. Hg would be depleted earliest from source strata correlative with higher values in stratigraphically lower orebodies (Swanson 1979). Sulphur may have been derived from evaporite beds in the sedimentary pile and complexed in the same fluids. Such large-scale fluid movement might be expected to mix and homogenize sulphur isotopes derived from heterogeneous source beds and might have the same effect on lead isotopes as well. Thus, the requirements for essentially uniform sulphur isotopic composition and approach to single-stage Pb isotope systematics of the ores would be satisfied. A "SED-EX" model accounts for the stratiform/stratabound nature of the ores and compositional dependence on stratigraphic position as well. General presence of gray quartz and local conspicuous amounts associated with concordant sulphides may represent silica exhalite. Less obvious is the conduit or discharge vent site(s) for the metalliferous fluids. A purely speculative candidate might be the Balmat Fault. A long, protracted history, perhaps extending back to deposition of host rocks, is suggested by 1) lithic differences in Upper Marble formation on either side of the fault trace, and 2) presence of the Balmat amphibolite body on the fault trace. Foliation in the amphibolite is folded by second-phase isoclines, indicating that it was intruded either pre-or syn-early-phase folding. These two scanty lines of evidence suggest that the Balmat fault is relict of an old structure tapping a deep source for the metagabbro, but are inconclusive as to whether it was an active structure during sedimentation, let alone whether it may have served as conduit to the sea floor. But to speculate further, it might be reasonable to postulate a mild intracratonic rifted environment accompanied by evaporite deposition in foundered crustal blocks. Minor mafic plutonism may have played a role in driving convective cells which leached metals in their paths.

Summary

Orebodies of the Balmat-Edwards-Pierrepont district are believed to have been of the massive stratiform sulphide class of sedimentary exhalative association.

Minor element distribution and sulphur isotope variations suggest that the pre-metamorphic sulphides had a close stratigraphic affinity with the host rocks, whose lithology and sedimentary environment are fairly well understood. Orebody compositions depend on stratigraphic position. Accordingly, the sulphides appear to have been deposited syngenetically on the Grenville continental shelf or shallow intracratonic (rifted?) basin in shallow marine waters of restricted circulation and dimension. Deposition was characterized by cyclical sedimentation of siliceous dolostone and evaporitic anhydrite. Deposition of sulphide ores recurred over a stratigraphic interval of 1800 feet. The Balmat fault may have been active during sedimentation and may be

a manifestation of mild intracratonic rifting. Lithic differences across the fault trace suggest the possibility that it exerted some control on sedimentation, perhaps even to the extent that it or others like it caused restricted circulation leading to evaporite deposition.

There is no obvious source of the metals. No evidence exists for sea floor springs nor for association with volcanism. It is tentatively proposed that the sulphides were sedimentary exhalative with perhaps a distal relationship to the vent site. Metals may have been leached from sediments or volcanic rocks lower in the stratigraphic pile and carried as complexes in solution VIA permeable pathways and along faults into restricted basis or lagoons, where they debouched on the sea floor as sulphide sediments. Sulphide sulphur may have also been leached from evaporitic sediments in the pile, homogenized, and complexed into the same ore fluids as the metals. Ore fluids may have been evolved basin brines, chemically similar to MVT-type fluids, or may have been highly-charged chloride brines in convective circulation cells driven by plutonic "heat engines". The exhalative process was repeated numerous times through the stratigraphic sequence.

REFERENCES

Appleyard, E.G., and Stott, G.M. 1975. Grenville gneisses in the Madawaska Highlands, eastern Ontario. Geological Association of Canada, Field Trip 2, Guidebook, pp. 26–61.

Bernier, L., Pouliot, G., and MacLean, W.C. 1987. Geology and metamorphism of the Montauban north gold zone: a metamorphosed polymetallic exhalative deposit, Grenville Province, Quebec. Economic Geology, **82**: 2076–2090.

Bishop, C., and Jourdain, C. 1987. Grenville polymetallics, the Montauban and New Calumet deposits. The Northern Miner Magazine, **2**: 15–17.

Bohlen, S.R., Valley, J.W., and Whitney. P.R. 1989. The Adirondack Mountains – a section of deep Proterozoic crust. Field Trip Guidebook T164, Montreal, Canada to Albany, New York, June 30–July 8, 1989.

Bohlen, S.R., and Essene, E.J. 1977. Feldspar and oxide thermometry of granulites in the Adirondack Highlands. Contributions Mineralogy Petrology, **62**: 153–169.

Bohlen, S.R., Essene, E.J., and Hoffman, K.S. 1980*b*. Feldspar and oxide thermometry in the Adirondacks; an update. Geological Society America Bulletin, **91**: 110–113.

Bohlen, S.R., Peacor, D.R., and Essene, E.J. 1980*a*. Crystal chemistry of a metamorphic biotite and its significance in water barometry. American Mineralogist, **65**: 55–62.

Bohlen, S.R., Valley, J.W., and Essene, E.J. 1985. Metamorphism in the Adirondacks. I. Pressure and temperature. Journal Petrology, **26** (4): 971–992.

Brown, C.E. 1989. Geologic map of the Beaver Creek area in the Grenville Lowlands, St. Lawrence County, New York. United States Geological Survey, Miscellaneous Investigation Series Map I-1725.

Brown, J.S. 1973. Sulfur isotopes of Precambrian sulfates and sulfides in the Grenville of New York and Ontario. Economic Geology, **68**: 362–370.

Brown, J.S., and Engel, A.E.J. 1956. Revision of Grenville stratigraphy and structure in the Balmat-Edwards district, northwest Adirondacks, N.Y. Geological Society America Bulletin, **67**: 1599–1622.

Brown, J.S., and Kulp, J.L. 1959. Lead isotopes from the Balmat area, New York. Economic Geology, **54**: 137–138.

Brown, P.E., Essene, E.J., and Kelly, W.C. 1978. Sphalerite geobarometry in the Balmat–Edwards district, New York. American Mineralogist, **63**: 250–257.

Buddington, A.F. 1934. Geology and Mineral Resources of the Hammond, Antwerp, and Lowville Quadrangles. New York State Museum Bulletin No. 296.

Buddington, A.F., Jensen, M.L., and Mauger, R.L. 1969. Sulfur isotopes and origin of northwest Adirondack sulfide deposits. Geological Society of America, Memoir 115, pp. 423–451.

Carl, J.D. 1981. Alkali metasomatism in the Major gneiss, northwest Adirondacks, New York: open system or closed? Geochimica Cosmochimica Acta, **45**: 1603–1607.

Carl, J.D. 1988. Popple Hill gneiss as dacite volcanics: a geochemical study of mesosome and leucosome, northwest Adirondacks, New York. Geological Society America Bulletin, **100**: 841–849.

Carl, J.D., and Van Diver, B. 1971. Some aspects of Grenville geology and the Precambrian/Paleozoic unconformity, northwest Adirondacks, New York. New York State Geological Association, 43rd Annual Meeting, Potsdam, Guidebook, pp. A1–A39.

Carl, J.D., and Van Diver, B. 1975. Precambrian Grenville alaskite bodies as ash-flow tuffs, northwest Adirondacks, New York. Geological Society America Bulletin, **86**: 1691–1707.

Carter, T.R. 1984. Metallogeny of the Grenville Province, southeastern Ontario. Ontario Geological Survey, Open File Report 5515.

Carter, T.R., Colvine, A.C., and Meyn, H.D. 1980. Geology of base metal, precious metal, iron and molybdenum deposits in the Pembroke-Renfrew area. Ontario Geological Survey, Mineral Deposits Circular 20.

Cathles, L.M., and Smith, A.T. 1983. Thermal constraints on the formation of Mississippi Valley-type lead-zinc deposits and their implications for episodic basin dewatering and deposit genesis. Economic Geology, **68**: 332–352.

deLorraine, W.F. 1979. Geology of the Fowler orebody, Balmat No. 4 mine, northwest Adirondacks, New York. M.Sc. thesis, University of Massachusetts, Amherst, Massachusetts.

deLorraine, W.F., and Dill, D.B. 1982. Structure, stratigraphic controls and genesis of the Balmat zinc deposits, NW Adirondacks, New York. *In* Precambrian sulphide deposits. *Edited by* R.W. Hutchinson, C.D. Spence, and J.M. Franklin. Geological Association of Canada, Special Paper 25, pp. 571–596.

Doe, B.R. 1960. The distribution and composition of sulfide minerals at Balmat, New York. Ph.D. thesis, California Institute of Technology.

Doe, B.R. 1962*a*, Distribution and composition of sulfide minerals at Balmat, New York. Geological Society of America Bulletin, 73: 833–854.

Doe, B.R. 1962*b*. Relationships of lead isotopes among granites, pegmatites, and sulfide ores near Balmat, New York. Journal Geophysical Research, 67: 2895–2906.

Doe, B.R., and Stacey, J.S. 1974. The application of lead isotopes to the problems of ore genesis and ore prospect evaluation: a review. Economic Geology, 69: 757–776.

Edwards, L., and Essene, E.J. 1988. Pressure, temperature and C-O-H fluid fugacities across the amphibolite-granulite transition, northwest Adirondack Mountains, New York. Journal Petrology, 29: 39–72.

Energy Mines and Resources Canada. 1989. Canadian mineral deposits not being mined in 1989. Mineral Policy Sector MR223.

Engel, A.E.J., and Engel, C.G. 1958. Progressive metamorphism and granitization of the major paragneiss, northwest Adirondack Mountains, New York, part 1: total-rock: Geological Society America Bulletin, 69: 1369–1413.

Fletcher, I.R. 1979. A lead isotopic study of lead-zinc mineralization associated with the Central Metasedimentary Belt of the Grenville Province. Ph.D. thesis, University of Toronto, Toronto, Ontario.

Fletcher, I.R., and Farquhar, R.M. 1982. Lead isotopic compositions of Balmat ores and their genetic implications. Economic Geology, 77: 664–673.

Fletcher, I.R., Farquhar, R.M., and Kuybida, P.R. 1978. Lead isotope evidence for the existence and possible origin of some Mississippi Valley type deposits in southeastern Ontario. *In* Short Papers of the Fourth International Conference Geochronology, Cosmochronology, Isotope Geology. *Edited by* R.E. Zartman. United States Geological Survey, Open File Report 78-701, pp. 117–119.

Foose, M.P. 1974. The structure, stratigraphy and metamorphic history of the Bigelow area, northwest Adirondacks, New York. PhD. thesis, Princeton University, Princeton, New Jersey.

Foose, M.P. 1980. A reinterpretation of the structural and stratigraphic setting of the Balmat–Edwards zinc deposits, northwest Adirondack Lowlands, New York. Economic Geology, 75: 130–133.

Gauthier, M., and Brown, A.C. 1986. Zinc and iron metallogeny in the Maniwaki-Gracefield district, southwestern Quebec. Economic Geology, 81: 89–112.

Gauthier, M., Brown, A.C., and Morin, G. 1987. Small iron formations as a guide to base- and precious-metal deposits in the Grenville Province of southern Quebec. *In* Precambrian Iron Formations. *Edited by* P.W. Appel and G.L. LaBerge. Theophrastus, Athens, pp. 297–327.

Gilluly, I. 1934. Geology of the Gouverneur talc district, New York. New York State Museum, W.P.A.-U.S.G.S. Project (unpublished manuscript).

Grant, N.K., and Yang, Y. 1992. The importance of tectonic discontinuities in Adirondack geology. American Geophysical Union, Spring Meeting, Montreal, Canada, Abstracts, p. 340.

Grant, N., Lepak, R., Maher, T., Hudson, M., and Carl, J. 1986. Geochronological framework of the Grenville Province of the Adirondack Mountains. Geological Society America, Abstracts with Programs, 18: 620.

Hauer, K.L. 1995. Protoliths, diagenesis, and depositional history of the Upper Marble, Adirondack Lowlands, New York. Ph.D. thesis, Miami University, Oxford, Ohio.

Heyl, A.V., Landis, G.P., and Zartman, R.E. 1974. Isotopic evidence for the origin of Mississippi Valley type mineral deposits: a review. Economic Geology, 69: 992–1006.

Hudson, M.R. 1994. P-T-X-t constraints on ductile deformation zones within the Adirondack Lowlands. Ph.D. thesis, Miami University, Oxford, Ohio.

Hudson M., and Grant, N. 1989. Garnet-sillimanite tectonites in the northwest Adirondack Mountains, New York. Geological Society America, Abstracts with Programs, **21**: A237.

Isachsen, Y.W., and Fisher, D.W. 1970. Geologic map of New York State, Adirondack sheet. New York State Museum, Map and Chart Series 16.

Isachsen, Y., and Landing, E. 1983. First Proterozoic stromatolites from the Adirondack Massif: stratigraphic, structural and depositional implications. Geological Society America, Abstracts with Programs, **15**: 601.

Jourdain, V., Gauthier, M., and Guja, J. 1990. Métallogénie de l'or dans le sud-ouest de la province de Grenville. Geological Survey of Canada, Open File 2287.

King, H.F. 1956. Notes on ore occurrence in highly metamorphosed Precambrian rocks. *In* F.L. Stillwell Anniversary Volume. Australasian Institute of Mining and Metallurgy, pp. 143–161.

Lea, E.R., and Dill, D.B. 1968. Zinc deposits of the Balmat–Edwards district, New York. *In* Ore Deposits of the United States 1933-1967 (Graton-Sales Volume). *Edited by* J.D. Ridge. American Institute Mining, Metallurgy and Petroleum Engineers, New York, Vol. 1, pp. 26–48.

McLelland, J., Chiarenzelli, J., Whitney, P, and Isachsen, Y. 1988. U-Pb zircon geochronology of the Adirondack Mountains and implications for their geologic evolution. Geology, **16**: 920–924.

McLelland, J.M., Chiarenzell, J., and Perham, A. 1992. Age, field, and petrologic relationships of the Hyde School gneiss, Adirondack Lowlands, New York. Journal of Geology, **100**: 69–90.

McLelland, J.M., Daly, S., and Chiarenzelli, J. 1993. Sm-Nd and U-Pb isotopic evidence for juvenile crust in the Adirondack Lowlands and implications for the evolution of the Adirondack Mts. Journal Geology, **101**: 97–105.

Mezger, K., Rawnsley, C.M., Bohlen, S.R., and Hanson, G.N. 1990. U-Pb garnet, sphene, monazite, and rutile ages: implications for the duration of high-grade metamorphism and cooling histories, Adirondack Mts., New York. Journal of Geology, **99**: 415–428.

Morin, G. 1987. Deposits of the Montauban region. Ministère de l'Énergie et des Ressources du Québec, MM 86-02

Nadeau, L., and van Breemen, O. 1991. Do the 1.45–1.39 Ga Montauban Group and the La Bostonnais complex constitute a Grenvillian accreted terrane? Geological Association of Canada, Program with Abstracts, **19**: A81.

Petch, C. 1992. Temperature and $X(CO_2)$ conditions in the Balmat District, N.W. Adirondacks. B.Sc. thesis, McGill University, Montreal, Quebec.

Petersen, E.V., Totten, F., and Guida, M. 1993. Tremolite talc occurrences in the Balmat-Edwards District *In* Selected Mineral Deposits of Vermont and the Adirondack Mountains, New York. *Edited by* E.V. Petersen. Social Economic Geology, Guidebook Series Vol. 17, pp. 54–63.

Reynolds, P.H., and Russell, R.D. 1968. Isotopic compositions of lead from Balmat, New York. Canadian Journal of Earth Sciences, 5: 1239–1245.

Rivers, T., Martingole, J., Gower, C.F., and Davidson, A. 1989. New tectonic divisions of the Grenville Province, southeast Canadian Shield. Tectonics, 8: 63–84.

Sangster, A.L. 1967. Metamorphism of the New Calumet sulphide deposit, Quebec. M.Sc. thesis, Carleton University, Ottawa, Ontario.

Sangster, A.L. 1970. Metallogeny of base metal, gold and iron deposits of the Grenville Province of southwestern Quebec. Ph.D. thesis, Queen's University, Kingston, Ontario.

Sangster, A.L. 1991. Geology and geochemistry of marble-hosted Zn occurrences, Central Metasedimentary Belt (CMB), Grenville Province, Ontario and Quebec. Geological Association of Canada, Program with Abstracts, **16**: A110.

Sangster, A.L,. and Bourne, J. 1982. Geology of the Grenville Province and regional metallogeny of the Grenville Supergroup. *In* Precambrian sulphide deposits. *Edited by* R.W. Hutchinson, C.D. Spence, and J.M. Franklin. Geological Association of Canada., Special Paper 25, pp. 91–126.

Seal, T.L. 1986. Pre-Grenville dehydration metamorphism in the Adirondack Mountains, New York. M.Sc. thesis, State University of New York, Stony Brook, New York.

Smith, J.R. 1956. Montauban-les-Mines area. Quebec Department of Mines, Geological Report 65.

Soever, A., and Meusy, G. 1986. Cadieux (Renprior) zinc deposit. *In* Mineral deposits of the Central Metasedimentary Belt, Grenville Province, Ontario and Quebec. *Edited by* R.M. Easton, T.R. Carter, and J.S. Springer. Geological Association of Canada, Field Trip 3, Guidebook, pp. 43–45.

Solomon, P.J. 1963. Sulphur isotopic and textural studies of the ores at Balmat, New York, and Mount Isa, Queensalnd. Ph.D. thesis, Harvard University, Cambridge, Massachusetts.

Stanton, R.L., and Russell, R.D. 1959. Anomalous leads and the emplacement of lead sulfide ores. Economic Geology, 54: 588–607.

Swanson, M.T. 1979. Geochemistry of sphalerite concentrates from the Balmat–Edwards zinc ores, St. Lawrence County, N.Y. M.Sc. thesis, Lehigh University, Lehigh, Pennsylvania.

Tewksbury, B.J. 1993. Re-thinking Grenville-age deformation—ductile shear in granitie gneiss of the Lowlands. Friends of the Grenville, 1993 Field Trip, Guidebook (unpublished).

Tewksbury, B.J., and Kirby, G. 1992. Shear fabric development in leucogranitic gneisses of the Payne Lake and Dodds Creek bodies, Muskellunge Lake Quadrangle, N.Y. Geologic Society of America. Abstracts with Programs, 24.

Whelan, J.F. 1974. Trace element and sulfur isotope comparison of anhydrites from Balmat-Edwards, N.Y., with sedimentary and hydrothermal anhydrite. M.Sc. thesis, Pennsylvania State University.

Whelan, J.F., Rye, R.O., and deLorraine, W. 1984. The Balmat-Edwards zinc-lead deposits – synsedimentary ore from Mississippi Valley-type fluids. Economic Geology, 79: 239–265.

Whelan, J.F., Rye, R.O., deLorraine, W.F., and Ohmoto, H. 1990. Isotopic geochemistry of a Mid-Proterozoic evaporite basin: Balmat, New York. American Journal of Science, 290: 396–424.

Wiener, R., McLelland, J.M., Isachsen, Y.W., and Hall, L. 1984. Stratigraphy and structural geology of the Adirondack Mountains, New York: review and synthesis. *In* The Grenville Event in the Appalachians and Related Topics. *Edited by* M.J. Bartholemew, E.R. Force, A.K. Sinha, and J. Herz. Geological Society of America, Special Paper 1941, pp. 1–55.

Williams, P.J. 1989. Gold deposits at Calumet, Quebec (Grenville Province): an example of the problem of metamorphic versus metamorphosed ore. XXVIII International Geological Congress, Abstracts, 3: 362–363.

Wolff, J.M. 1982*a*. The Long Lake zinc deposit, description and classification. Economic Geology, 77: 488–496.

Wolff, J.M. 1982*b*. Geology of the Long Lake area. Ontario Geological Survey, Report 216.

Volkes, F.M. 1969. A review of the metamorphism of sulfide deposits. Earth Science Reviews, 5: 99–143.

Zartman, R.E., and Doe, B.R. 1981. Plumbotectonics – the model. Tectonophysics, 75: 135–162.

Holocene Paleoenvironmental Records from the Western Hemisphere: A Workshop

Henry T. Mullins, Geoffrey O. Seltzer, William P. Paterson
Dept. of Earth Sciences, Syracuse University, Syracuse NY 13244

Eugene W. Domack
Dept. of Geology, Hamilton College, Clinton, NY 13323

Amy R. Leventer
Dept. of Geology, Colgate University, Hamilton, NY 13346

The purpose of the workshop is to bring together a diversity of paleo-proxy records from the southern high latitudes, equatorial South America, and central to northeastern United States. We will compare these records to standard Holocene reference sections, such as the GISP2 ice core from Greenland. In so doing we encourage discussion and exchange of ideas regarding forcing mechanisms, and linkages among the ocean, atmosphere, and cryosphere. We also will discuss the variation in resolution of the different records and what temporal restrictions have to contribute to the large picture of decadal to millennial scale changes.

We will convene at 9:00 AM at the boat house at Green Lakes State Park, Fayetteville, New York (map next page). If the weather is inclement we will relocate to a sheltered location. Participants are encouraged to bring poster-sized examples of their paleoclimate records and be prepared to explain the limitations and advantages of their particular data sets. Easels will be available for poster presentations. At the start, the organizers will present a short 15-20 minute synopsis of their work. We will try to wrap up the morning session by 12:00 PM, in time for lunch (bring your own bag lunch). Participants can then reconvene at 1:00 PM for the Green Lakes portion of the excursion.

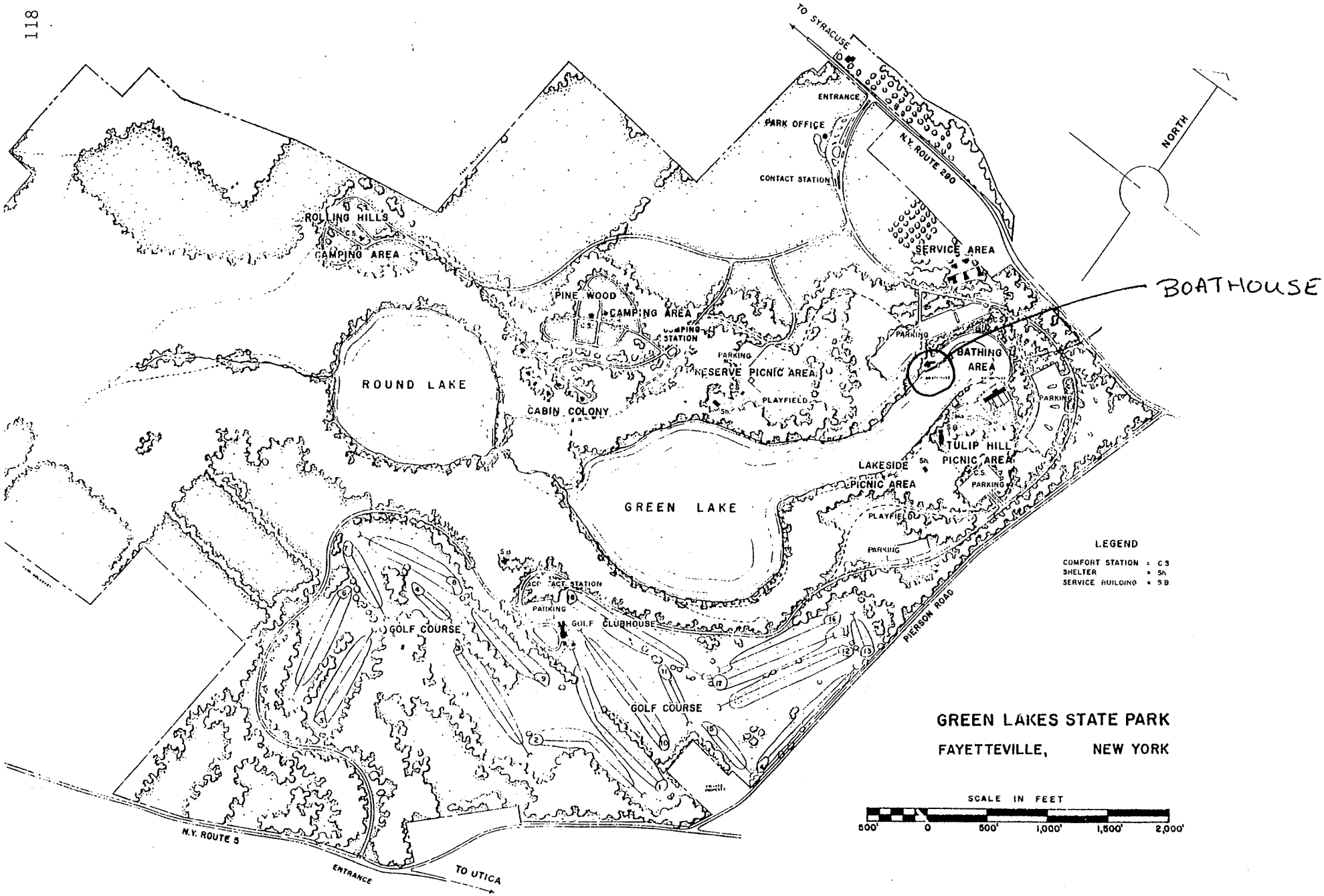
TO SYRACUSE
ENTRANCE
PARK OFFICE
CONTACT STATION
N.Y. ROUTE 290
NORTH
ROLLING HILLS
CAMPING AREA
SERVICE AREA
BOATHOUSE
PINE WOOD
CAMPING AREA
CAMPING STATION
PARKING
BATHING AREA
ROUND LAKE
RESERVE PICNIC AREA
PLAYFIELD
CABIN COLONY
TULIP HILL
PICNIC AREA
LAKESIDE
PICNIC AREA
GREEN LAKE
LEGEND
COMFORT STATION = C.S
SHELTER = Sh
SERVICE BUILDING = S.B
CONTACT STATION
PARKING
GOLF CLUBHOUSE
GOLF COURSE
GOLF COURSE
PIERSON ROAD
GREEN LAKES STATE PARK
FAYETTEVILLE, NEW YORK
SCALE IN FEET
500' 0 500' 1,000' 1,500' 2,000'
N.Y. ROUTE 5
ENTRANCE
TO UTICA

HOLOCENE PALEOENVIRONMENTAL RECORDS FROM ANTARCTIC GLACIAL MARINE SEDIMENTS

Eugene W. Domack,
Hamilton College, Department of Geology, Clinton, New York 13323 USA,
email: edomack@hamilton.edu

Our NSF funded work at Hamilton College has focused upon the Holocene time frame in order to resolve such issues as the role of sea ice, outlet glacier fluctuation, and productivity in determining sedimentation patterns across the Antarctic continental shelf. We have tried to resolve events in terms of varying resolution from fjords (high resolution) to the inner shelf basins (low to very high resolution). Areas we have worked in include the fjords and inner shelf of the western Antarctic Peninsula, Ross Sea, and East Antarctic margin. We have recognised that the Holocene does indeed contain a variable record of changing paleoenvironments, but one which needs a multiparameter approach to resolve. Chronologic constraints are based upon detailed AMS radiocarbon dating and 210Pb analyses. Records of magnetic susceptibility, grain size, ice rafted detritus, diatom floras, foraminifera, and organic geochemistry have allowed us to recognise both a middle Holocene climatic optimum and a late Holocene cooling or Neoglacial. These long term trends contain within them higher frequency oscillations including a 200-300 year cycle that is most prevalent along the western side of the Antarctic Peninsula. The Little Ice Age is the most severe of the Late Holocene events and is marked by growth of ice shelves within the fjords of the Antarctic Peninsula. Subsequent 20th Century warming has reduced the extent of these ice shelves as documented by other authors.

Our paleoenvironmental records correlate well with lacustrine sequences from the Antarctic Peninsula and in some cases with ice cores (particularly the late Holocene cooling event). The 200-300 years cycles have yet to be fully defined in terms of absolute time but preliminary comparisons with northern hemisphere ice cores (GISP2) and tree ring proxies for solar variability are promising (Leventer et al., 1996; Domack and Mayweski, in preparation).

Collaborating investigators include: Amy Leventer (Colgate University), Scott Ishman (USGS), Patricia Manley (Middlebury College), Charles McClennen (Colgate University), Stefanie Brachfeld (University of Minnesota), Wendy Cunningham (University of Colorado), Stephanie Shipp and John Anderson (Rice University).

Recent publications include:

Shevenell, A. E., Domack, E. W., and Kernan, G., 1996. Record of Holocene Paleoclimatic Change Along the Antarctic Peninsula: Evidence from Glacial Marine Sediments, Lallemand Fjord, In, Banks, M. R., and Brown, M. J. (eds.), Climate Succession and Glacial History Over the Past Five Million Years, Royal Society of Tasmania, Papers and Proceedings, v. 130, p. 55-64.

Leventer, A. R., Domack, E. W., Ishman, S. E., Brachfeld, S., McClennen, C. E., and Manley, P. 1996. Productivity cycles of 200-300 years in the Antarctic Peninsula region: understanding linkages among the sun, atmosphere, oceans, sea ice, and biota. Geological Society America Bulletin, v. 108 p. 1626-1644.

Domack, E. W., and McClennen, C. E., 1996. Accumulation of glacial marine sediments in fjords of the Antarctic Peninsula and their use as late Holocene paleoenvironmental indicators. In, R. Ross, E. Hoffman, and L. Quetin (eds.) Foundations for Ecosystem Research West of the Antarctic Peninsula, Antarctic Research Series, American Geophysical Union, Washington D.C.. p. 135-154.

Domack, E. W., Ishman, S. E., Stein, A. B., McClennen, C. E., and Jull, A.J. T., 1995, Late Holocene advance of the Muller Ice Shelf, Antarctic Peninsula: sedimentologic, geochemical, and paleontological evidence. Antarctic Science, 7, 159-170.

Domack, E. W., Mashiotta, T. A., Burkley, L. A., and Ishman, S. E., 1993. 300 year cyclicity in organic matter preservation in Antarctic fjord sediments. In: Kennett J. P. and Warnke D. A. (Eds.) The Antarctic Paleoenvironment: A Perspective on Global Change (Part 2) Antarctic Research Series, v. 60, American Geophysical Union, Washington D. C., p.265-272.

Domack, E. W., Jull, A. J. T., and Nakao, S., 1991. Advance of East Antarctic outlet glaciers during the Hypsithermal: implications for the volume state of the Antarctic ice sheet under global warming. Geology, v. 19, p. 1059-

CLIMATIC SUCCESSION AND GLACIAL HISTORY OF THE SOUTHERN HEMISPHERE OVER THE LAST FIVE MILLION YEARS

The Tasmanian Division of the Australian and New Zealand Association for the Advancement of Science organised a symposium late in 1995 on the topic noted above. One of the aims of the symposium was to document changes in climate in the region before human activities could have had any influence — to provide a benchmark against which possible Greenhouse effects could be measured.

Arising from the symposium 31 authors prepared 13 papers on the Antarctic, sub-Antarctic, New Zealand and Tasmanian climatic and glacial records and, for comparison, present climates in the region. One paper includes reference to possible contemporaneity of Northern and Southern Hemisphere events. The papers were refereed internationally and are now published by the Royal Society of Tasmania as *Papers and Proceedings*, Volume 130, Pt 2. A synopsis of the contents follows:

Quilty — Pliocene environment of Antarctica.
Hill & Jordan — Macrofossils as climatic indicators, Plio-Pleistocene of Tasmania and Antarctica.
Chinn — Glacial record, Antarctica & New Zealand.
Adamson et al. — Palaeoenvironments, Macquarie Island - palaeobeaches and sedimentary deposits.
Colhoun et al. — Late Wisconsin glaciation, Tasmania.
Harris et al. — Late Quaternary history, Mac. Robertson Shelf, East Antarctica.
Shevenell et al. — Holocene climatic changes, Antarctic Peninsula.
Cook et al. — Increases in Tasmanian Huon pine ring widths ... greenhouse warming?
Gibson & Burton — Meromictic Antarctic lakes as recorders of climatic change.
O'Brien & Harris — Past behaviour of Lambert Glacier, Antarctica.
Rao et al. — Skeletal carbonate mineralogy and isotopic composition, Antarctica and Tasmania.
Simmonds — Relationship of sea ice and extra-tropical cyclones.
Salinger & Jones — Modern Southern Hemisphere climates.

This volume is available from the Royal Society for Aus$30 (includes the cost of handling and postage). An order form is appended. Enquiries may be directed to Professor P.G. Quilty, fax number 61-03-62-323351 or email pat_qui@antdiv.gov.au

.....

CLIMATIC SUCCESSION AND GLACIAL HISTORY OF THE SOUTHERN HEMISPHERE OVER THE PAST FIVE MILLION YEARS

ORDER FORM

To: ROYAL SOCIETY OF TASMANIA,
GPO Box 1166M,
Hobart,
Tasmania 7001,
Australia

Please supply ..... copy(ies) of the publication "Climatic succession and glacial history of the Southern Hemisphere over the past five million years."

I enclose a cheque/bank draft for Aus$.....

Name .....

Address .....

.....

Signed ..... Date .....

Geoffrey O. Seltzer

My approach to paleoclimatic and paleoenvironmental reconstruction involves the analysis and interpretation of glacial landforms and lake sediments in the tropical Andes of South America. High mountains (>5000 m) in the Andes support small, cirque glaciers that expanded well beyond their modern limits to deposit moraines downvalley during the late Pleistocene and Holocene. The climatic interpretation of a past phase of glaciation is a difficult problem because of the mutlitude of factors that can lead to glacial advances. Changes in the mass and energy balances of a glacier include changes in precipitation, temperature, receipt of solar radiation, humidity and wind speed. Thus the recognition of a moraine on the landscape in itself can be interpreted many different ways in terms of possible climate change and it is necessary to have other lines of evidence that can be used to limit the possible range of paleoclimatic interpretations.

An advantage of using the glacial geologic evidence in paleoclimatic reconstructions, if it is possible to determine that the moraines were not deposited by surging glaciers and that the glaciers were not calving into a large body of water, is that it is clear that some climatic change perturbed the energy and mass balance of the glaciers in the past. Furthermore, given the elevations of terminal moraines and/or their extent of weathering and slope modification it may be possible to correlate over broad distances a climatic change associated with a past glaciation. On the other hand glacial moraines record only relative glacial maxima. Moraines deposited during glacial retreat or during periods when glaciers were not as extensive as subsequent glaciations are not preserved on the landscape. Thus what is left is a discontinuous record of glaciation or climatic change. It is also very difficult to uniquely interpret glaciation in terms of a specific climatic change.

The use of records from cores of lake sediments in paleoclimatic analysis helps to circumvent with some of the limitations posed by working with glacial moraines. the approach I use to working with lake sediments includes methods that are common to most limnological and oceanographic studies: seismic reflection work to determine the nature and structure of sediments in the bottom of the lakes; basic physical properties such as magnetic susceptibility, bulk density, organic and inorganic carbon content, color and visual descriptions; detailed analysis of pollen and diatoms to determine past limnic and terrestrial vegetation; and geochemical analysis of the carbonates and organic matter to determine changes in the hydrology of the basin. It is also possible to develop continuous records of change based on radiocarbon chronologies of the lake cores. In many ways the multi-proxy approach of working with lake sediments can yield significant information about paleoclimates, but in conjunction with direct evidence from the surrounding landscape this approach is even more powerful.

Finally, you might ask, "why the tropical Andes?". Work in this region over the last several years has been motivated by two factors: 1) the early work by the CLIMAP group on sea-surface temperatures, which suggested that on glacial-to-interglacial time scales the tropics were relatively complacent from a climatological point of view, and the need to test this hypothesis; and 2) the desire to obtain more information from regions that lack paleclimatic data to look for possible "teleconnections" with higher latitude regions. Establishing whether or not events such as the last glacial maximum, last glacial-to-interglacial transition, the Younger Dryas, and the Little Ice Age were global in extent or not has implications for understanding the mechanisms that produce such changes.

RECENT PUBLICATIONS ON THE GLACIAL GEOLOGY AND PALECLIMATOLOGY OF THE TROPICAL ANDES

Abbott, M., Seltzer, G., Kelts, K., and Southton, J. (1997). *Holocene Climate Variability of the Northern Bolivian Andes*. Quaternary Research, 47:70-80.

Osborn, G., Clapperton, C., Davis, P.T., Reasoner, M., Rodbell, D.T., Seltzer, G.O., Zielinski, G. (1996). *Potential glacial evidence for the Younger Dryas event in the cordillera of North and South America.* Quaternary Science Reviews, 14, 823-832.

Seltzer, G.O., Rodbell, D.T., and Abbott, M. (1995). *Andean Glacial Lakes and Climate Variability Since the Last Glacial Maximum.* Bulletin de l'Institut Francais d'Estudes Andines, vol. 24, 539-550.

Seltzer, G.O. (1994). *Climatic interpretation of alpine snowline variations on millennial time scales*. Quaternary Research, 41, 154-159.

Seltzer, G.O. (1994). *A lacustrine record of late-Pleistocene climatic change in the subtropical Andes*. Boreas, 23, 105-111.

Seltzer, G.O. (1994). *Andean snowline evidence for cooler subtropics at the last glacial maximum.* Proceedings of the NATO Advanced Study Institute, Long Term Climatic Variations - Data and Modeling, pp. 371-378.

Hansen, B. S., Seltzer, G. O., and Wright, H. E. (1994). *Late-Quaternary vegetation change in the central Peruvian Andes*. Palaeogeography, Palaeoclimatology, Palaeoecology, 109, 263-285.

Wright, H.E., Jr. and Seltzer, G.O.(in press) *Late-Pleistocene climatic history of the central Andes*, in: Ice Age Peoples of South America, Oregon State University Press.

Seltzer, G.O. (1993). *Late Quaternary glaciation as a proxy for climate change in the central Andes.* Proceedings of the congress, "Mountain Geoecology of the Southern Andes: Resource Management and Sustainable Development", Santiago de Chile Oct-Nov 1991. Mountain Research and Development, 13, 129-138.

Seltzer, G.O. (1992). *Late Quaternary glaciation of the Cordillera Real, Bolivia.* Journal of Quaternary Science, 7, 87-98.

Seltzer, G.O., and Wright, H.E., Jr. (1991). *Deglaciation in Peru and Bolivia since the late Pleistocene* (in Spanish with an English summary). Boletín de la Sociedad Geológica Boliviana, 26, 13-32.

Seltzer, G.O. (1990). *Recent glacial history and paleoclimate of the Peruvian-Bolivian Andes*. Quaternary Science Reviews, 9:137-152.

Seltzer, G.O., and Hastorf, C.A. (1990). *Climatic change and its effect on prehispanic agriculture in the central Peruvian Andes*. Journal of Field Archaeology, 17, 397-414.

Wright, H.E., Jr., Seltzer, G.O., and Hansen, B.C.S. (1989). *Glacial and climatic history of the central Peruvian Andes*. National Geographic Research, 5, 439-446.

PALEOCLIMATOLOGY OF THE FINGER LAKES REGION

Henry T. Mullins
Department of Earth Sciences, Syracuse University, Syracuse, New York 13244

ABSTRACT

We have recently discovered that the Finger Lakes region central New York State contains a truly exceptional record of climate change over the past 14,000 ^{14}C years. Sediments within the Finger Lake basins are characterized by high accumulation rates (>1m/1000 years) and an abundance of calcium carbonate which make them ideal for paleoclimatic studies. During the past five years we have employed a variety of approaches to our study of AMS radiocarbon dated sediment cores from these lakes in order to unravel both regional and global environmental change throughout the Holocene.

Wetland Stratigraphy- The lithostratigraphy of wetlands in the Finger Lake basins has proven to be an extremely valuable proxy for relative lake-level change, and thus climate (precipitation) change. Fossiliferous lacustrine marls (with up to 90% $CaCO_3$) sandwiched between wetland peat deposits document relative changes in lake level. Wellner and Dwyer (1996) first recognized the regional utility of such sequences, and Dwyer *et al.* (1996) used this approach in their discovery that the Holocene Hypsithermal (~9-4 ka ^{14}C) was a warm-wet interval in the northeastern United States, contrary to the commonly held view of widespread drought. Wetland deposits both north and south of Cayuga Lake have further revealed five cycles of Holocene relative lake-level change with a recurrence interval of ~2000 years (Mullins, in prep.). Abundant fossils in the marls have also been used to identify numerous small-scale relative lake-level fluctuations which may have been driven by solar variability.

Stable Isotopes- The abundance of lacustrine calcite coupled with the relatively short water residence times of the Finger Lakes also makes them ideal for stable isotope studies. $\delta^{18}O$ values are used as a proxy for temperature and/or atmospheric moisture source changes over time, whereas $\delta^{13}C$ values record changes in lake productivity. Isotopic data from deep water cores in Seneca Lake have documented a previously unknown cold/dry interval between ~10-8 ka 14C which followed the well known Younger Dryas period (Anderson *et al.*, 1997); whereas, a littoral zone core from south of Seneca Lake has been used to isotopically define significant century- to millenial-scale climate instability during the Holocene Hypsithermal which may have been driven by latitudinal shifts in the mean position of the polar jet stream (Anderson *et al.*, in prep.)

Calcite Content- Today, calcite precipitates from open waters of many of the Finger Lakes during "whiting events", as it has throughout much of the Holocene. Because this calcite precipitation is mediated by the photosynthetic activity of phytoplankton, simple calcite contents can be used as a proxy for gross photosynthesis over time. Cores received from Cayuga Lake have shown that there is a remarkable correlation between calcite content and Greenland ice core $\delta^{18}O$ values (i.e. temperature) throughout the Holocene (r=0.93), as well as between calcite content and the anthropogenic rise of atmospheric carbon dioxide over the past 200 years (r=0.96). These results strongly suggest that calcite precipitation has been controlled by global change, both natural and anthropogenic over the past 10,000 years. The recent rise of calcite content in Cayuga sediments could be due to global warming and/or CO_2 fertilization, but appears to be evidence that anthropogenically linked global change has already begun to affect temperate lacustrine ecosystems (Mullins, submitted).

REFERENCES CITED

Anderson, W.T., Mullins, H.T., and Ito, E., 1997, Stable isotope record from Seneca Lake, New York: Evidence for a cold paleoclimate following the Younger Dryas: Geology, v. 25, p. 135-138.

Anderson, W.T., Mullins, H.T., Ito, E., and Good, S.C., in prep., Stable isotope and paleoecological evidence for climate instability during the Holocene Hypsithermal: Geology.

Dwyer, T.R., Mullins, H.T., and Good, S.C., 1996, Paleoclimate implications of Holocene lake-level fluctuations, Owasco Lake, New York: Geology, v. 24, p. 519-522.

Mullins, H.T., submitted, Global change and lacustrine carbonate: Cayuga Lake, New York: Geology.

Mullins, H.T., in prep., Lacustrine marls of the Cayuga Lake basin, New York: A stratigraphic record of century- to millenial-scale climate change during the past 11,000 years: Journal of Sedimentary Research.

Wellner, R.W., and Dwyer, T.R., 1996, Late Pleistocene-Holocene lake-level fluctuations and paleoclimate at Canandaigua Lake, New York, in- Mullins, H.T., and Eyles, N., eds., Subsurface Geologic Investigations of New York Finger Lakes: Implications for Late Quaternary Deglaciation and Environmental Change: Geologic Society of America Special Paper 311, p. 65-76.

NORTH AMERICAN CONTINENTAL SEASONALITY DURING THE LAST MILLENNIUM: HIGH-RESOLUTION ANALYSIS OF SAGITTAL OTOLITHS

William P. Patterson
Syracuse University, Department of Earth Sciences, Heroy Geology Laboratory, Syracuse NY 13244 USA

Abstract

$\delta^{18}O_{(CaCO3)}$ values of late Holocene sagittal fish otoliths from Lake Erie provide a record of seasonal temperature variation for mid-western North America. Freshwater drum (*Aplodinotus grunniens*) sagittal otoliths obtained from PaleoIndian middens, ranging in age from ≈AD 985 to AD 1530 as well as a recent specimen, were sampled at a resolution representing time-averaging of as little as 3-5 days to estimate seasonal climatic variation over the last thousand years.

Regional differences in climate, as well as asynchronous variation inferred by comparison with historical records of Europe, Greenland and Iceland, suggest that the climate trends of eastern North America may not always correspond to those of Europe or even the North Atlantic. Results suggest that summer temperatures of the Laurentian Great Lakes region at the beginning of the millennium were 2-6°C warmer, while winter temperatures may have been nearly 2°C cooler than the 20th-century average. By the late 1200's, summer temperatures decreased to nearly modern values. In the 1400's and through the 1500's, summer maxima exhibited enhanced intra-annual variation as well as temperatures which were as much as 8°C cooler, while winter temperatures were 0.4-2.7°C warmer than 20th-century values.

An additional outcome of this research is the estimation of lake water $d^{18}O$ values for several time periods throughout the Holocene. Mean annual temperatures inferred from $\delta^{18}O_{(H_2O)}$ values display a decrease from AD 985 through at least AD 1530, concomitant with summer temperature trends. The long residence time of these large lakes suggests that secular trends in $\delta^{18}O$ values must represent long-term variation in climate which can be used in concert with the short-term, high-resolution temperature record for a comprehensive estimation of climatic trends. Temperature variation and paleohydrology of the Great Lakes region is discussed in terms of variation in storm tracks and source region with time. $d^{18}O$ values of lake water coupled with paleotemperature data suggest that changing climate is the result of secular variation in the position, shape, and strength of the circumpolar vortex.

Key words: Otoliths, paleoclimatology, precipitation, seasonality, stable isotopes

PUBLISHED ARTICLES

Patterson, W.P. 1992. Syndepositional dissolution and recrystallization of shallow marine carbonates: evidence from isotopic and elemental data, MS thesis, University of Michigan, Ann Arbor, MI 48105-1063, 56p.

Patterson, W. P., Smith, G. R., and Lohmann, K. C. 1993. Continental paleothermometry and seasonality using the isotopic composition of aragonitic otoliths of freshwater fishes, *in* P. Swart, K.C Lohmann, J. McKenzie and S. Savin (eds.) *Amer. Geophys. Union Monogr. Continental Climate Change from Isotopic Indicators*, p. 191-202.

Walter, L. M., Bischof, S. A., Patterson, W. P., and Lyons, T. W. 1993. Dissolution and recrystallization in modern shelf carbonates: evidence from pore water and solid phase chemistry: *Philosophical Transactions of the Royal Society of London*, v. 344, p. 27-36.

Smith, G.R., and Patterson, W.P. 1994. Mio-Pliocene seasonality on the Snake River Plain: Comparison of faunal and oxygen isotopic evidence, *in Paleogeography, Paleoclimatology, Paleoecology, Special Publication, Geochemistry of Vertebrates: Evidence for Diet and Climate, v. 107, p. 291-302.*

Patterson, W. P., and Walter, L. M. 1994. Syndepositional diagensis of modern platform carbonates: evidence from isotopic and minor element data, *Geology,* v. 22, p. 127-130.

Patterson, W. P., and Walter, L. M. 1994. Depletion of $\delta^{13}C$ in seawater $\sum CO_2$ on modern carbonate platforms: significance for the carbon isotopic record of carbonates: Geology, v. 22, p. 885-888.

Drummond, C. N., Patterson, W. P., and Walker, J.C.G., 1995. Climate forcing of carbon-oxygen isotopic covariance in temperate region marl lakes. Geology, v. 23, p. 1031-1034.

Patterson, W.P. 1997. North American Continental Seasonality During the Last Millennium: High-Resolution Analysis of Sagittae (*Palaeogeography, Palaeoclimatology, Palaeoecology-reviewed, awaiting final acceptance*).

Smith, G.R., Patterson, W.P., and Todd, T. 1997. Ecologic factors of intralucustrine speciation: life history of *Coregonus hoyi* from isotopic evidence, (in prep.).

Patterson, W.P. 1997. Thermal and salinity characteristics of Jurassic seawater: evidence from Bathonian-aged otoliths (in prep.).

Walter, L.M. and Patterson, W.P. 1997. Mechanisms for variation in $\delta^{13}C$ values of shallow marine water, (in prep).

Coburn, J.C., Patterson, W.P., and Smith, G.R. 1997. Regional climate variation of the Mio-Pliocene western North American interior: stable oxygen isotope evidence from fish-bone phosphate (in prep.).

Walter, L. M., Patterson, W. P., and Muehlenbachs, K. 1997. Carbon isotopic equilibration of recent platform carbonate sediment with pore fluids: implications for secular variations in ocean chemistry, (in prep.).

Walter, L. M., Patterson, W. P., Lyons, T. W. 1997. Syndepositional diagenesis of shallow marine carbonates: evidence from pore fluid chemistry (in prep.).

Geology, Limnology and Paleoclimatology of Green Lakes State Park, New York

Martin F. Hilfinger IV and Henry T. Mullins

Department of Earth Sciences
Heroy Geology Laboratory
Syracuse University
Syracuse, New York 13244

Introduction

Green Lakes State Park, located ~15 km east of Syracuse, New York near the village of Fayetteville, is a stunning geologic and limnologic wonderland (Fig. 1). Located along the axis of a narrow glacial meltwater channel, the Park consists of two small, moderately deep (maximum water depth of ~53 m) lake basins (Green Lake and Round Lake), protected along their flanks by steep walls of Silurian bedrock and separated from each other by a small modern wetland (Figs. 2 and 3).

These lakes are unusual, not only for their geologic setting, but also their water characteristics which have attracted the attention of limnologists for decades. In fact, limnologically, Green Lake is one of the best studied lakes in the world (Torgersen et al., 1981; Thompson et al., 1990). There are two aspects of the limnology of Green Lake which make it so interesting. Foremost is the fact that it is a meromictic lake (as is Round Lake) which means that when the water column turns over seasonally, it does so only above a strong chemically-controlled density boundary or chemocline at a water depth of ~18 m (Fig. 4).[1] Because of this, bottom waters >18 m deep are permanently stratified and devoid of oxygen (anoxic). The second unusual limnologic feature of these lakes is that they annually precipitate large amounts of calcium carbonate (calcite), both from the open, wind-mixed surface waters of the lake (epilimnion) and along their shallow, near shore (littoral zone) margins in the form of "reefs" or bioherms.

The annual precipitation of calcite from the epilimnion coupled with the fact that deep bottom waters are anoxic, results in the deposition and preservation (no bioturbation) of annual sediment laminations or true varves. Because of this, Green Lake and Round Lakes have enormous potential from unraveling decadal to annual scale climate change (paleoclimatology) for at least the entire Holocene (past 10,000 years). With our current interest and concerns about possible global warming, the meromictic lakes of Green Lakes State Park may well provide a long-term, high-resolution template of natural climatic variability in which to view future environmental change.

The purpose of this fieldtrip is to acquaint you with the basic geology, limnology, and preliminary paleoclimatology of Green Lakes State Park. We will draw upon an extensive published literature to discuss: (1) the geologic origin of the lakes; (2) their fundamental limnology; (3) the annual, open water precipitation of calcium carbonate which will explain why "Green Lake is green"; and, (4) the origin of their "fringing reefs"; we will then draw upon new, unpublished data that will: (5) document the natural history of relative lake level fluctuations, and thus climate change, throughout the Holocene; and finally, (6) examine in high resolution, the natural and anthropogenic environmental changes which have occurred over the past 2,500 years.

This fieldtrip will be a leisurely half-day walking tour around both Green and Round Lakes. Scientific information will be provided via a series of large, colorful posters supplemented by on site examination of sediment cores. There will be ample time for discussion, and if the weather cooperates, we will be treated to a spectacular feast of fall foliage against the backdrop of aqua lakes; so, bring an open mind and your cameras!

---

[1] That part of the water column which mixes during turnover is referred to as the mixolimnion whereas that which does not mix is the monimolimnion.

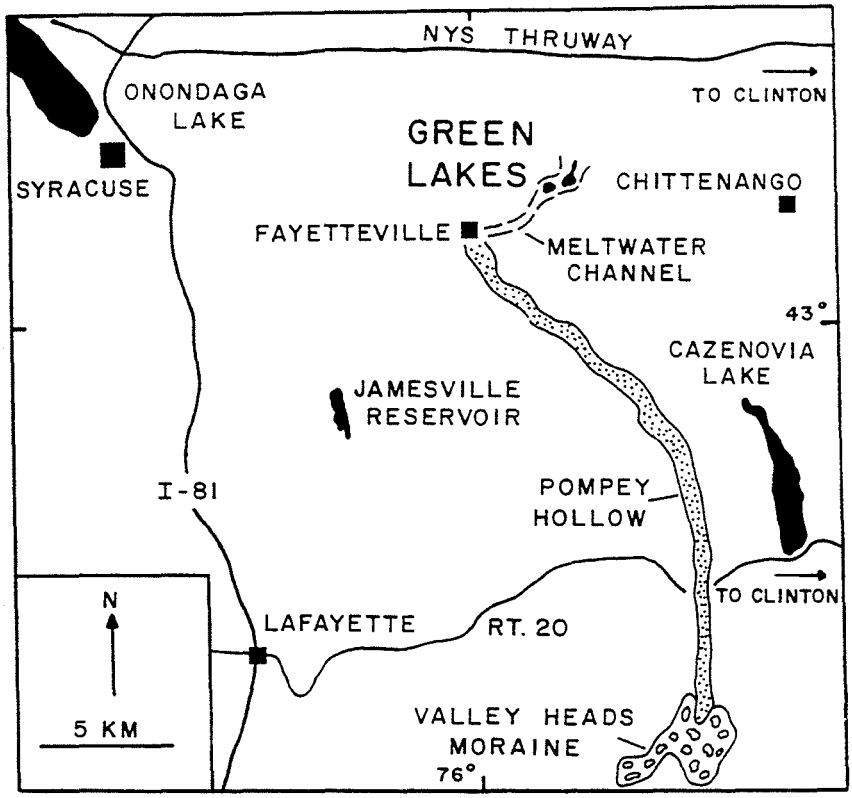

Fig. 1: General index map of Green Lakes State Park region of central New York, illustrating location of Green Lakes relative to Pompey Hollow (glacial trough) and Valley Heads Moraine (~14.4 ka). Major highways also shown. To reach the Park from Hamilton College in Clinton, go north and take the N.Y.S. Thruway west to exit 34. From Canastota take Rt. 13 to Chittenango and then Rt. 5 to Green Lakes State Park. Alternatively, head south from Clinton and take Rt. 20 west to Cazenovia and then Rt. 92 to Manlius. Follow signs to Fayetteville and then signs to the Park. We will meet at the boathouse on the northwest corner of Green Lake.

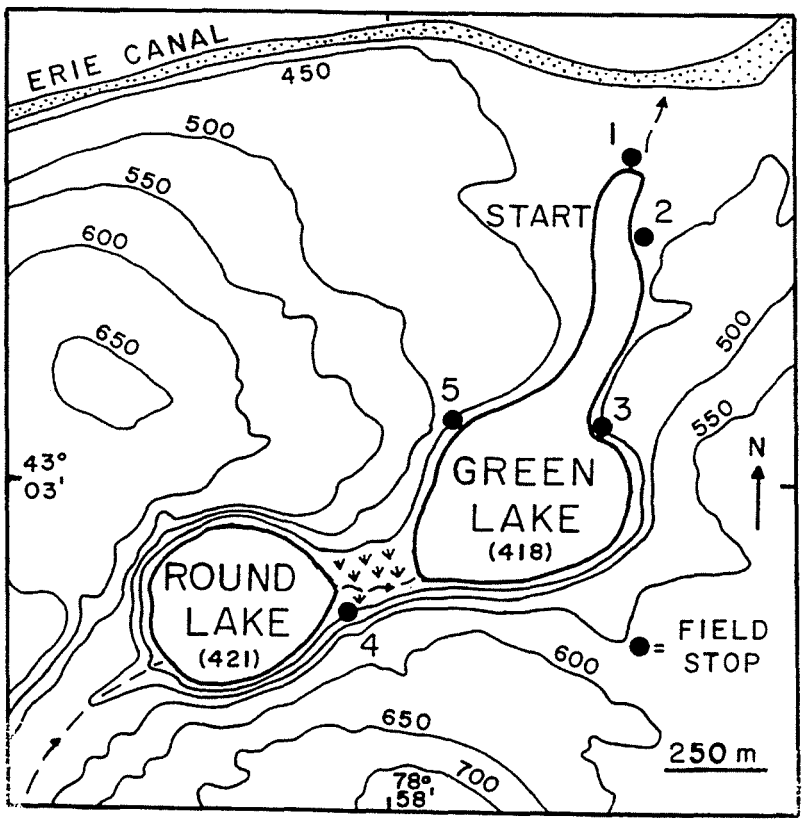

Fig. 2: Location map for Green Lake State Park illustrating local topography. Note that both Green and Round Lake are located in a SW-NE trending "cross channel". Numbered circles correspond to field trip stops. Elevations in feet above sea level (100'= 30.5 m).

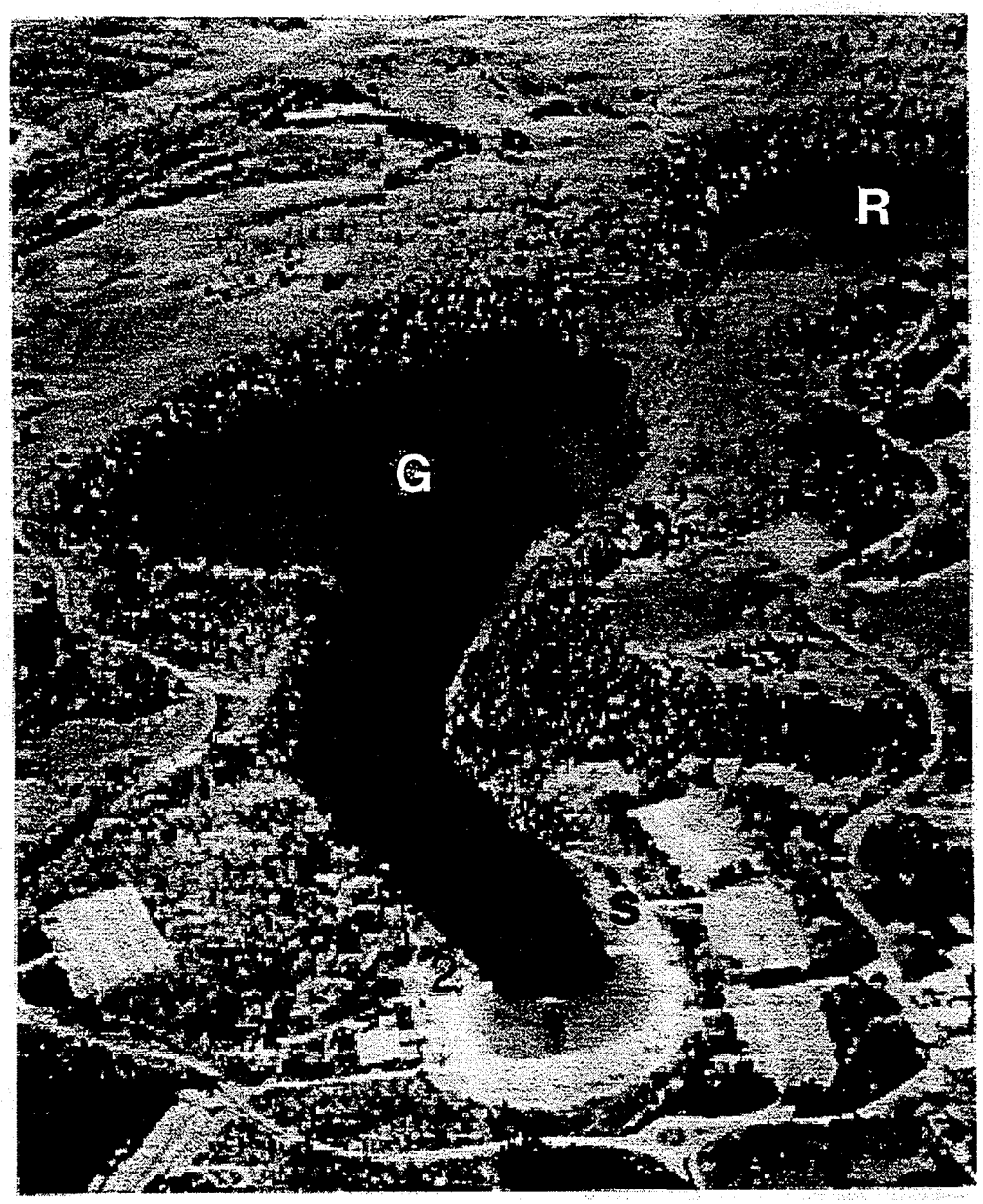

Fig. 3: Aerial photograph (looking south) of Green Lakes State Park illustrating main basins of Green (G) and Round (R) Lake and the "neck" of Green Lake, as well as the wetland (W) between the two lakes. Field trip stops highlighted by numbers; S= start.

Field Trip Stops

This field trip will begin at the boathouse near the northwest corner of Green Lake. We will then proceed clockwise around both Green Lake and Round Lake before returning to the boathouse. There will be a total of five stops to discuss the geology, limnology and paleoclimatology of Green Lakes State Park and to observe the scenic beauty of this local treasure.

Stop #1: Geologic Setting and Origin of the Lakes

Our discussion of the geology of Green Lakes State Park will take place on the swimming beach at the north end of Green Lake. From here we will have an unobstructed view to the south along the axis of the glacial meltwater channel in which Green and Round Lakes reside.

As we look to the south, steep bedrock walls can be seen rising from the surface of Green Lake at an elevation of 418 ft. (127 m) to at least 550 ft. (168 m) above sea level, although the highest summit (South Hill) adjacent to the park extends to an elevation of 788 ft. (240 m) (Fig. 2)(Muller, 1967). Total bedrock relief in the area, as measured from the top of South Hill to the bottom of Green Lake is 543 ft. (166 m). However this value should be considered a minimum because the thickness of sediments beneath the floor of Green Lake is not known, although Muller (1967) reported that drilling "just north" of Green Lake penetrated 138 ft. (42 m) of unconsolidated sediment without reaching bedrock.

The rocks that make up the walls of the meltwater channel in Green Lakes State Park are part of the Salina Group of Silurian (~440 to 410 million years ago) age (Muller, 1967). The oldest stratigraphic unit in the Park is the Vernon Shale which consists largely of easily eroded red and green shale as well as gypsum ($CaSO_4 \cdot H_2O$). The top of the Vernon Shale extends upward to within ~40 ft. (12 m) of the surface of Green Lake (Fig. 4; Muller, 1967). Overlying the Vernon Shale is more shale and argillaceous dolostone of the Syracuse Formation which contains evidence ("hopper casts") of evaporite minerals such as halite (NaCl) and gypsum. This middle unit extends upward to about the present day surface elevation of Green Lake (Fig. 4). The remainder of Silurian stratigraphy here consists of a relatively resistant dolostone member of the Syracuse Formation (Fig. 4) and the overlying Camillus Shale capped by a dolostone of the Bertie Formation which forms the summits of surrounding hills (Muller, 1967). The lake basins, however, rest within shales and evaporites of the Syracuse Formation and underlying Vernon Shale (Fig. 4).

Both Green Lake and Round Lake are located in an east-northeast "cross channel" (Fairchild, 1909; Sissons, 1960) which cuts obliquely across the Onondaga Escarpment at the northern edge of the Appalachian Plateau (Fig. 1 and 2). Today, this cross channel is drained by a "markedly underfit stream" (Muller, 1967) and near its southwestern end there is an abrupt topographic drop of ~100 ft. (30.5 m) from a dolostone member of the Syracuse Formation to the surface of Round Lake (Fig. 2).

As noted by Muller (1967), Green Lake (which was originally known as Lake Sodom) was first depth sounded by Vanuxem (1839) and subsequently by Miner (1933), who also sounded (via lead-line) Round Lake. Both lakes consist of steep-sided, flat-floored, semi-circular basins with maximum water depths slightly >50 m. However, Green Lake also contains an elongated "neck" or "handle" which shoals to the north (Fig. 2). As also noted by Muller (1967), the surface elevations of Green Lake (418 ft; 127 m) and Round Lake (421 ft.; 128 m) are significantly (~6 m) below the highest stand of pro-glacial Lake Iroquois which existed from ~12.5 to 11.4 ka ^{14}C (Muller and Prest, 1985; Anderson and Lewis, 1985). The surface of Green Lake is also ~6 ft. (2 m) lower in elevation then the water surface of the nearby Erie Canal (Fig. 2).

Green Lakes State Park is located north of the Valley Heads Moraine which was deposited ~14.4 ka ^{14}C (Muller and Calkin, 1993) during a brief phase of Laurentide ice sheet instability coincident with Heinrich event H-1 (Mullins et al., 1996). Thus, modern Green Lake and Round Lake must be less than 14,400 ^{14}C years in age (Fig. 5). The meltwater channel in which both lakes reside connects in the village of Fayetteville with Pompey Hollow, a large glacial trough whose origin is likely linked with the nearby Finger Lakes (Mullins et al., 1996). The Green Lakes meltwater channel is but one of many east-west orientated glacial drainages in the Syracuse-Oneida region (Sissons, 1960).

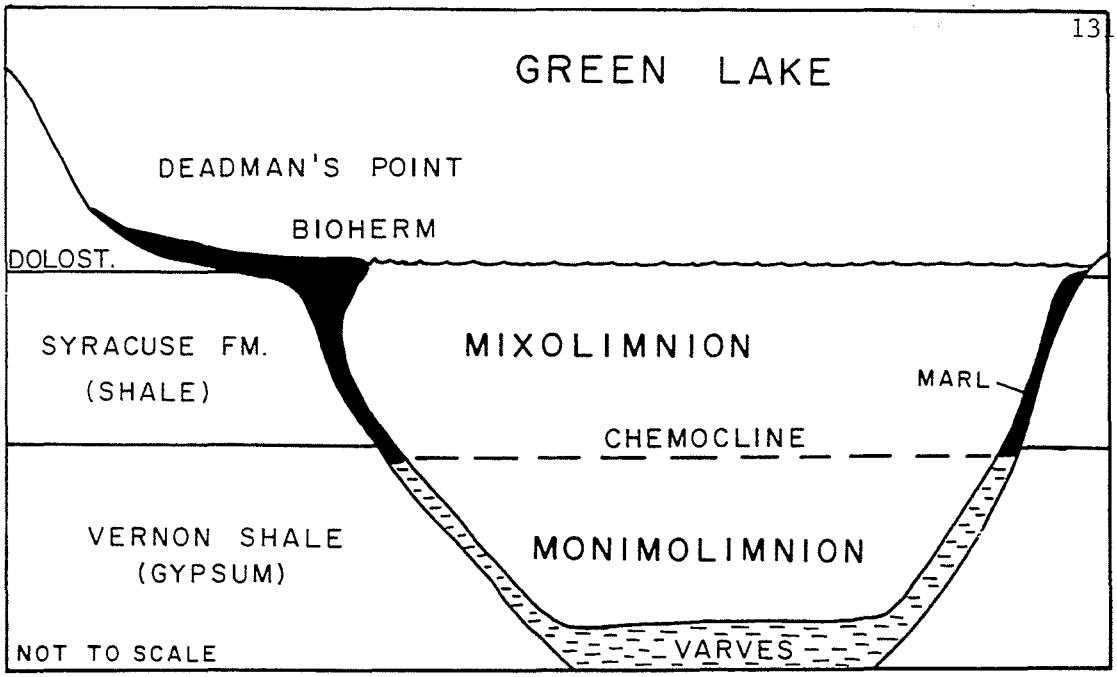

Fig. 4: Stratigraphic cross-section across main basin of Green Lake illustrating bedrock lithology, water depth and position of chemocline, which divides lake into an upper mixolimnion and a lower monimolimnion. Based on Dean and Fouch (1983).

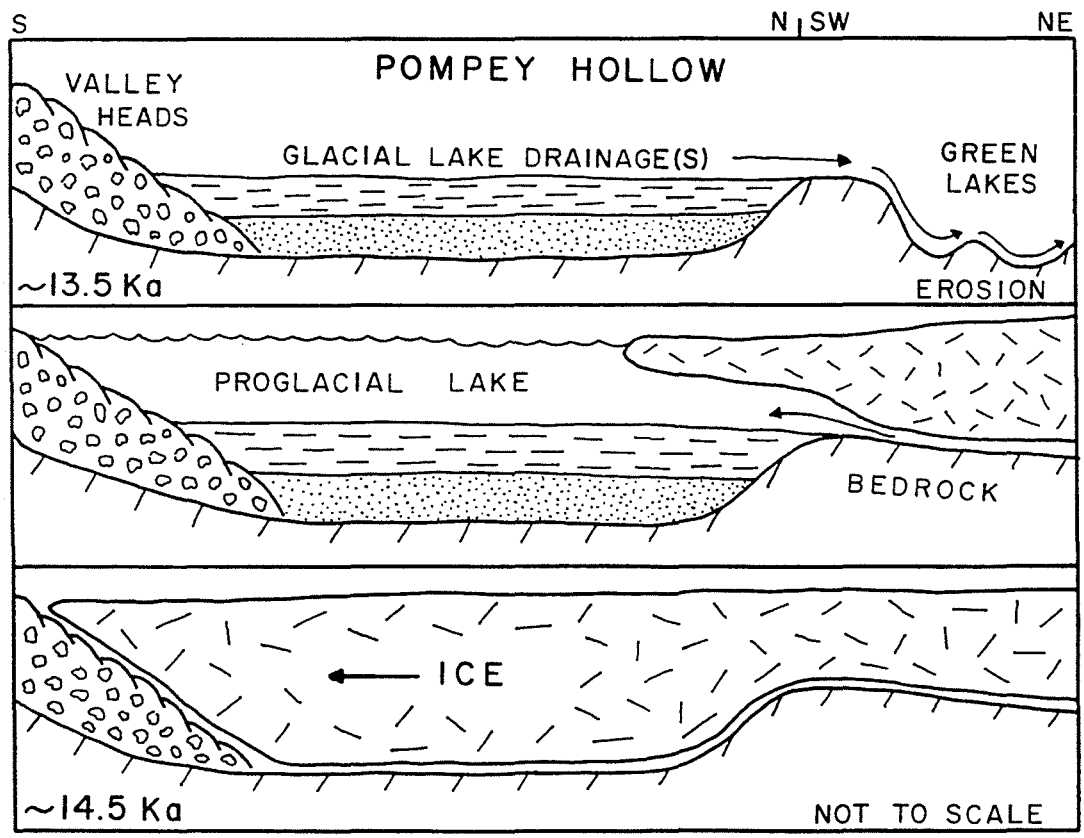

Fig. 5: Schematic cartoon illustrating possible source of meltwater for the Green Lakes plunge-pools. Panels are sequential from bottom (~14.5 ka) to top (~13.5 ka ^{14}C). Lowest panel illustrates surge of ice through Pompey Hollow and deposition of Valley Heads Moraine. Middle panel depicts retreating ice margin and the development of a proglacial lake with bottom sediment. In upper panel, ice withdraws to expose lower elevation outlet along Green Lakes meltwater channel and catastrophic outflow to erode plunge-pool basins. Note change in direction of panels from S-N to SW-NE. Glacial trough relationships based on Mullins et al. (1996).

The origin of the Green Lake and Round Lake basins is still uncertain although a number of hypotheses have been proposed (Muller, 1967), including: (1) plunge-pools; (2) solution sinkholes; and, (3) subglacial meltwater "potholes". Native American legend of "Kayahao" originally suggested that the lakes were volcanic in origin although there is no evidence to support it. This legend speaks of a Native American woman who infuriated the spirit of the lake which then "...spit forth fire and flame, (and) caused a great commotion of the waters..." (Gibson, 1925, p. 21).

The most widely accepted hypothesis is that these lake basins were scoured out at the base of large, late-glacial waterfalls. Based on stratigraphic relationships and morphology, Miner (1933) developed the hypothesis that the lakes are glacial plunge-pool basins (Fig. 6) which followed Vanuxem's (1839) earlier suggestion that they were eroded by a "whirlpool of great magnitude". However, problems with this hypothesis have centered around the source of water for the waterfalls plus the fact that there are two ("twin") lake basins.

Fairchild (1899) suggested that water impounded in highstanding proglacial lakes to the south of the Park may have cut the Green Lakes meltwater channel, whereas Sissons (1960) argued that water flowed from the Great Lakes in a complex system of marginal, subglacial and englacial conduits. If Fairchild's (1899) view of a proglacial source of water is correct, then Pompey Hollow, which connects with the Green Lakes meltwater channel at an elevation of ~530 ft. (162 m), is a likely source. Pompey Hollow, a 1 km wide, flat-floored (~780 ft., 238 m) trough, with as much as 520 ft. (159 m) of relief, extends south of the Park for ~20 km (Fig. 1). As ice receded from the Valley Heads Moraine at Delphi Falls shortly after 14.4 ka ^{14}C proglacial lake waters would likely have been impounded in Pompey Hollow, dammed by the Valley Heads Moraine to the south and the Laurentide ice sheet to the north (Fig. 5). In the nearby Finger Lakes, high-standing proglacial lakes existed until ~13.9 ka ^{14}C when the ice sheet retreated north of the Onondaga Escarpment opening up lower elevation outlets to the east which resulted in catastrophic drops of proglacial lake levels, cutting of gorges (glens), and a drainage reversal (Mullins et al., 1996). Muller (1967) has argued that the Green Lakes Channel originated as a pre-late Wisconsin feature. If correct, then as the northward retreating Laurentide Ice Sheet uncovered the precursor Green Lakes Channel impounded proglacial lake waters in Pompey Hollow (hundreds of feet higher in elevation) may have catastrophically poured through the Green Lakes meltwater channel (Fig. 5). Today, unlike the Finger Lakes, Pompey Hollow is a dry, flat-floored lake valley.

Such a scenario may have been similar to that documented for the Syracuse meltwater channels which experienced catastrophic floods with waterfalls the size of Niagra Falls when a 600 ft. (183 m) deep proglacial lake in the Onondaga-Tully trough drained to the east (Hand and Muller, 1972; Hand, 1978) creating a plunge-pool basin at Clark Reservation. Hand (1978) estimated that such catastrophic floods may have had water discharge as high as 7,000,000 $ft.^3/sec.$ (~$2.1x10^6$ $m^3/sec.$) and flow velocities exceeding 50 ft./sec. (~15 m/sec.)! Similar catastrophic floods from Pompey Hollow, flowing over relatively resistant dolostone caprock as a waterfall in Green Lakes Channel may have eroded underlying shales to produce plunge pool basins which today we know as Green and Round Lakes.

The second problem which must be overcome for the plunge pool hypothesis to be viable, is the origin of "twin basins" which has previously been discussed by Muller (1967). Because simple headward erosion of a waterfall should result in a single gorge, Fairchild (1909) proposed a simple solution; that the Green and Round Lake basins do occupy a single bedrock trough but have been isolated by post-glacial sediment accumulation (Fig. 6). If correct, then the depth to bedrock beneath the wetland between Green and Round Lakes should be similar to that beneath the basins (i.e. >50 m). However, we have collected sediment cores only up to 11 m in length from this wetland (see Stop #4) which represent ~9,100 ^{14}C years. Also, one of our cores from the center of the wetland penetrated only 4.8 m and appeared to bottom on bedrock. Thus, there may be a bedrock high or sill separating Green and Round Lakes. A land-based seismic reflection/refraction profile along the axis of this wetland would likely resolve the question of whether or not the lakes are separated by a bedrock sill.

A second possibility is that the lake basins formed sequentially, with Green Lake having formed first. This would necessitate a phase of rapid waterfall retreat to form the elongated "neck" of Green Lake followed by a pause in the rate of retreat to form the main basin of Green Lake. A second phase of rapid waterfall retreat would then be required followed by a second pause to excavate the Round Lake basin. Such a scenario could be reconciled if the outpouring of proglacial lake waters from Pompey Hollow occurred in the two discrete phases, perhaps as a result of glacial oscillation (Muller, 1967).

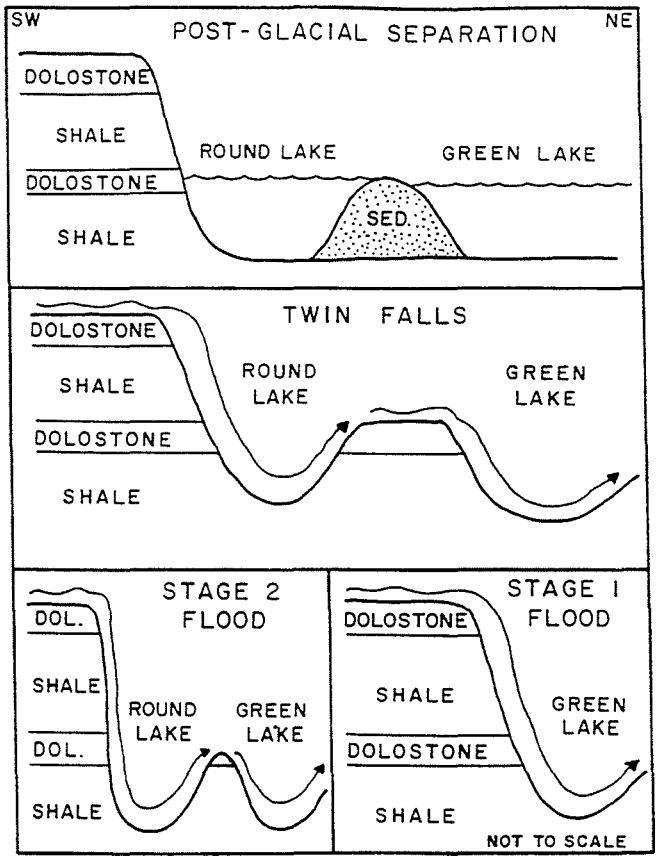

Fig. 6: Schematic cartoons illustrating possible explanations for "twin" plunge-pool basins at Green Lakes State Park. (Top) Post-glacial separation caused by sediment accumulation (Fairchild, 1909). (Middle) Twin falls flowing over two dolostone caprocks (Muller, 1967). (Bottom) Two stage outflow of proglacial lake waters impounded in Pompey Hollow.

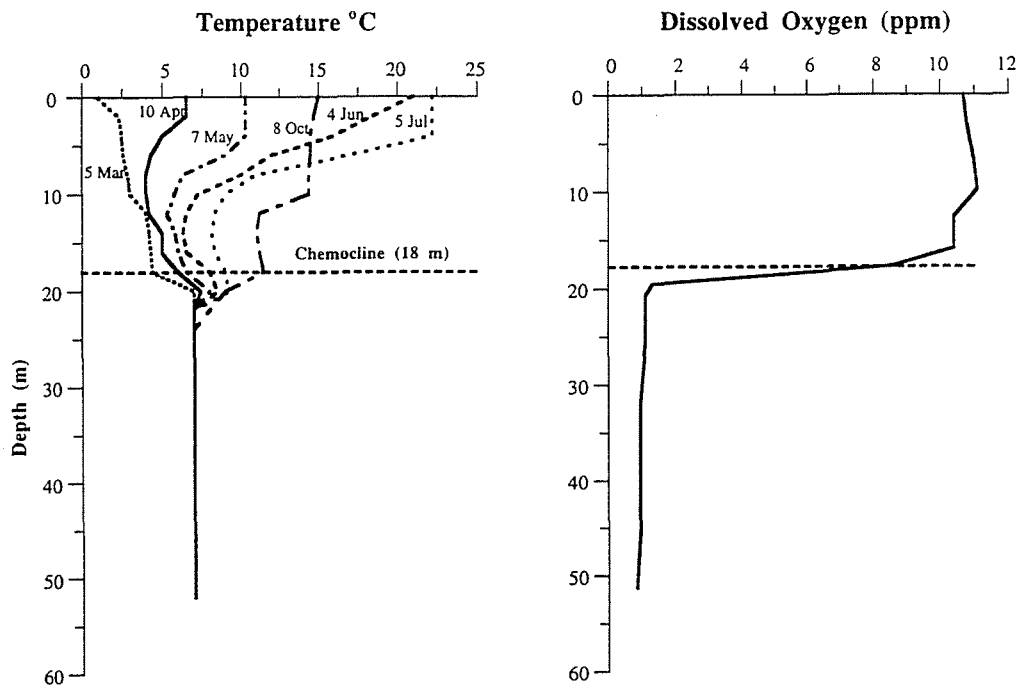

Fig. 7: Vertical distribution of temperature (left) and oxygen (right) versus water depth in Green Lake. Temperature data are seasonal, but note that water below chemocline is a constant 7 °C (from Culver and Brunskill, 1969). Note "anoxic" nature of water below the chemocline versus oxygenated water above (from Turano and Rand, 1967).

A third hypothesis, advocated by Muller, 1967), is that there were twin waterfalls which migrated headward simultaneously. For this mechanism to work there must have been some stratigraphic (or structural) control to initiate twin falls during a single meltwater episode. Muller (1967) suggests that both basins were controlled by water falling over dolostone caprocks; Green Lake basin by the "Middle Dolomite" of the Syracuse Formation and Round Lake basin by the "Upper Dolomite". The fact that there is no headwall scarp at the southwest end of Green Lake (as there is at Round Lake) would have to be explained by either incision and erosion of the lower caprock or by "burial" of the scarp by subsequent impounding of waters in Green Lake (Muller, 1967).

It is apparent from the above discussion that the origin of Green and Round Lakes continues to be uncertain. However, morphologically, they do appear to be plunge-pool basins but satisfactory explanations for the source of the water and why there are "twin basins" must be acceptable. Most useful would be the acquisition of subsurface data, both geophysical and drill core.

Stop #2: Limnologic Setting of Green Lake

From our vantage point at Stop #1 we will progress clockwise and walk a few hundred meters along the lake path to an open area just south of the diving platform. Here we will continue to have an open view of Green Lake and have an opportunity to present and discuss it's basic limnology (characteristics of the water column). Limnologically Green Lake is probably the best studied meromictic lakes in the world (Thompson et al., 1990); thus, there are considerable data from which to draw upon.

According to Thompson et al. (1990), Clark (1849) was the first to report (quoting L.C. Beck) that there was something unusual about the limnology of Green Lake: "Water drawn from a depth of one hundred and sixty-eight feet (51 m) was found to be strongly charged with sulphurated hydrogen... (which) blackened silver powerfully, and gave copious precipitates...". In 1931 Eggleton also noted the "foul odor of deeper mud deposits" and speculated that Green Lake might be stagnate, characterized by "incomplete spring and fall overturns" and perhaps a complete lack of whole-lake circulation. Eggleton's (1931) account of Green Lake is believed to be the first of a meromictic lake anywhere in North America (Thompson et al., 1990). Following his early assessment, Eggleton (1956) also reported results of a 25-year study of Green Lake concluding that "for all practical purposes, there is no significant amount of dissolved oxygen in the water below 19-20 m at any time of the year" (Thompson et al., 1990).

More recent studies have confirmed Eggleton's pioneering work on Green Lake, while enhancing our understanding of why Green Lake is meromictic. Of particular importance are publications by Deevey et al. (1963), Turano and Rand (1967), Takahashi et al. (1968), Brunskill and Ludlam (1969) and Torgensen et al. (1981). Based on a study of sulfur and carbon isotopes in Green Lake, Deevey et al. (1963) noted unusual quantities of sulphate which they suggested were derived from nearby outcrops of Silurian gypsum entering the lake as surface waters and perhaps "gypsiferous springs". Deevey et al. (1963) concluded that geochemically, Green Lake is more akin to Gulf Coast salt dome systems than to most temperate lakes.

In 1965, Turano and Rand (1967) conducted a series of measurements on the temperature and water chemistry of Green Lake from late winter (February 25) to early spring (April 18). They found that waters of the mixolimnion are colder (3-5 °C) than waters below the chemocline (~7 °C). However, surface water temperature of Green Lake varies greatly (3-22 °C) as a function of season whereas the monimolimnion maintains a relatively constant temperature of ~7 °C (Fig. 7; Brunskill and Ludlam, 1969).

Turano and Rand (1967) also found that dissolved oxygen concentrations are highest in the mixolimnion ($\geq$ 10 ppm) of the lake, decrease abruptly between 16 and 19 m and then remain relatively stable to the bottom of the lake (Fig. 7), consistent with previous results. However, unlike Eggleton (1956) who reported that the monimolimnion of Green Lake was completely devoid of oxygen, Turano and Rand (1967) did detect very low levels of oxygen (~1 ppm). Based on these data they concluded that the monimolimnion of Green Lake is not completely stagnant but rather must have some exchange with other waters, perhaps groundwater. However, Turano and Rand (1967) are the only investigations who have reported some oxygen below the chemocline.

Turano and Rand (1967) also found that both sulfate (oxidized) and suphide (reduced) increase below the chemocline (Fig. 8) but that only sulphate is present above the chemocline. In the monimolimnion, sulphide concentrations are high (up to 50 ppm) representing a "very considerable quantity" of H_2S (Turano and Rand, 1967). Maximum concentrations of sulphide occur near the bottom of the lake suggesting a source via the degradation of organic matter in the sediment primarily by sulfur reducing bacteria (Turano and Rand, 1967). However, sulphide is also oxidized by purple, photosynthetic bacteria that inhabit the chemocline in Green Lake (Culver and Brunskill, 1969). The abundance of sulphide in the monimolimnion and absence in the mixolimnion, of Green Lake, though, is directly related to oxygen concentrations.

Carbon dioxide and pH values in Green Lake are mirror images of each other (Fig. 9): CO_2 concentrations are relatively low in the mixolimnion and high in the monimolimnion whereas just the opposite is true for pH (Turano and Rand, 1967). CO_2 concentrations are controlled largely by photosynthesis above the chemocline and decomposition of organic matter below the chemocline. pH (a negative measure of hydrogen ion concentration) is inversely controlled by CO_2 concentrations. However, pH values are neutral or above (~7.2-8.0) throughout the entire water column of Green Lake (Fig. 9).

Turano and Rand (1967) also used data on water hardness (Ca, Mg concentrations), alkalinity, pH and temperature to calculate the saturation state of Green Lake with respect to calcium carbonate, both above and below the chemocline. They found that both water layers of the lake are "considerably supersaturated" with respect to calcium carbonate which should promote the precipitation of large quantities of marl.

In 1968 Takahashi et al. published their geochemical study of Green Lake. Although Green Lake had traditionally been believed to be meromictic because of "its great depth... and small area..." (Deevey et al., 1963), Takahashi et al. (1968) concluded that Green Lake's meromixis is a result of two different water types entering the lake. Below ~18 m groundwater entering the basin must be nearly twice as saline as surface waters, regardless of temperature (Takahashi et al., 1968). They found that surface waters are $4x10^{-4}$ g/cm^3 less dense than deep water. Thus, the permanent stratification of Green Lakes can be fully explained by salinity differences, which is contrary to most lakes which stratify due to temperature-controlled differences in density. This is verified by conductivity (a gross measure of salinity) measurements in Green Lake which display an abrupt increase at ~18 m water depth (Fig. 10; Brunskill and Ludlam, 1969). Thus, the meromixis of Green Lake is the consequence of a chemically-controlled density boundary or chemocline. However, the salinity of Green Lake is controlled not by Na and Cl as in the oceans, but rather by Ca and SO^4 derived from gypsum in surrounding bedrock (Takahashi et al., 1968).

That the chemocline in Green Lake is the result of the inflow of saline groundwater is further supported by chemical studies of interstitial waters recovered from bottom sediments. Brunskill and Harriss (1969) found that interstitial waters in a core from the deep (>50 m) central basin of Green Lake show continuous increases of Na, Mg, Sr, Ca, Cl and Br with depth indicating the mixing of monimolimnetic waters with more saline groundwater diffusing upwards into the bottom sediment.

Takahashi et al. (1968) also estimated the residence time (the amount of time a water molecule resides in the lake before being removed) of waters in Green Lake. It had previously been known that the surface outflow of Green Lake exceeds the surface inflow by about an order of magnitude (Turano and Rand, 1967); thus, there must be appreciable inflow of groundwaters. Because of this, plus the meromictic nature of the lake, considerable differences in residence times might be expected. Takahashi et al. (1968) indicated a residence time on the order of only 2 years for surface waters whereas deep waters are replaced no less than once every 35 years. Brunskill and Ludlam (1969) concurred with the short surface water residence times estimated by Takahashi et al. (1968), and further argued that surface inflow supplies <50% of water flow into Green Lake. Based on ^3H-^3He water mass ages in Green Lake, Torgensen et al. (1981) have confirmed the short residence times of the mixolimnion. However, they concluded that the residence time of water in the monimolimnion is considerably less than previously reported, ranging up to only ~7 years. Torgensen et al. (1981) also present evidence for a secondary chemocline at ~33m where there is a significant increase in the concentration of S, CH_4, CO_2, Na, and Cl. They explain both the short residence time of the monimolimnion and the secondary chemocline as a consequence of diffuse groundwater input.

Stop # 3: Precipitation of Calcium Carbonate

From Stop #2, near the dive platform of Green Lake, we will continue our clockwise walk around the lake to Deadman's Point, located at the eastern junction of the "neck" and main basin of Green Lake. Here we will first

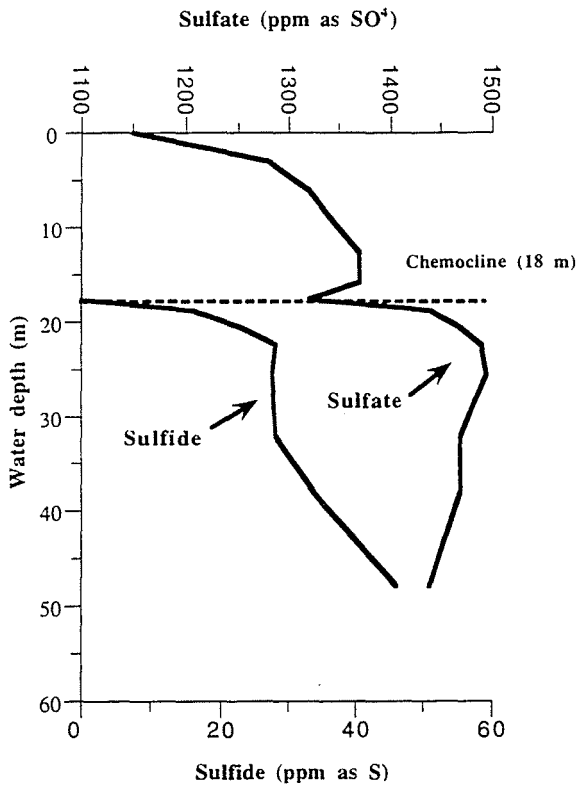

Fig. 8: Distribution of sulphate (oxidized) and sulphide (reduced) versus water depth in Green Lake. Note that sulphate is present both above and below chemocline whereas sulphide occurs only below ~18 m water depth. Decrease in sulphate concentration along chemocline is due to presence of purple sulphate reducing bacteria (from Turano and Rand, 1967).

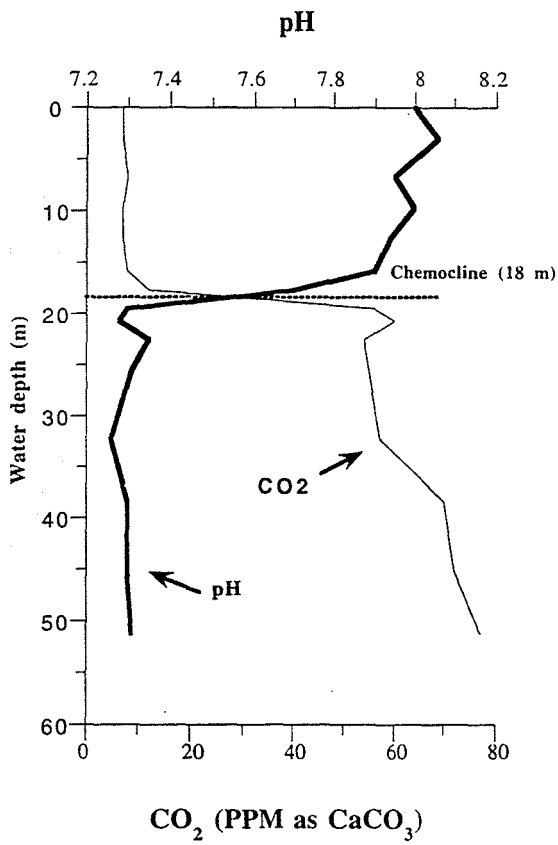

Fig. 9: Vertical distribution of carbon dioxide and pH versus water depth in Green Lake. Note abundance of CO_2 below chemocline and a concomitant decrease in pH. However, all pH values in Green Lake are above neutral (i.e.->7; from Turano and Rand, 1967).

discuss the seasonal, open water precipitation of calcium carbonate ("whitings") from Green Lake, followed by a discussion of littoral zone precipitation and the formation of the prominent "reef" or bioherm that we will see at Deadman's Point.

Whiting Events

One of the most commonly asked questions about Green Lake is "why is it green"? Well, the truth is that the lake is not always green. During winter (when not frozen) and early spring months, open waters of the lake tend to be blue, whereas they become green from late spring through fall, when most people visit the Park.

The color of water in a lake varies largely as a function of the amount and type of particulate matter in the water column. Oligotrophic (low nutrient) lakes with little particulate matter, like Skaneateles Lake, tend to display a blue color, whereas those lakes with high concentrations of particulate matter from primary biological productivity, like Oneida Lake, tend to be green, especially during the summer. The reason for this is that clear water scatters light predominantly from the blue portion of the electromagnectic spectrum, whereas when the amount of particulate matter increases in the water column longer wavelength radiation is preferentially scattered, and the lake appears green (Wetzel, 1975).

Green Lake is an oligotropic lake (Thompson et al., 1997) with annual primary productivity estimated at ~290 g C/m^2 (Culver and Brunskill, 1969). However, ~83% of this annual primary production in Green Lake occurs within the primary chemocline (~18 m water depth) due to the photosynthetic activity of purple sulfide oxidizing bacteria. Obviously, an alternative explanation for the seasonal green color of Green Lake is required. A hint comes from Wetzel's (1975) statement that lake sediments rich in light-colored calcium carbonate (marl) reflect more light than non-marl sediments, and that lakes with large amounts of suspended calcium carbonate backscatter energy from the green spectrum of visible light.

The abundance of calcium carbonate deposits in Green Lake has long been known (Clark, 1849; Bradley, 1929, 1963; Howe, 1932; Eggleton, 1956; Brunskill, 1969). Takahashi et al. (1968) as well as Brunskill (1969) documented that the entire water column of Green Lake is supersaturated with respect to calcium carbonate. However, based on $\delta^{13}C$ data, Takahashi et al. (1968) concluded that calcite precipitates only from the surface waters of Green Lake. They showed (via data from Deevey et al., 1963) that calcite crystals from the sediment of Green Lake have a $\delta^{13}C$ (a measure of the ratio of $^{13}C/^{12}C$) value of -4 ‰, which is much more similar to that of surface waters (-7 ‰) than to waters below the chemocline (-18 ‰). By independent means Brunskill (1969) also showed that a 3-4 fold increase in calcite supersaturation occurs in the mixolimnion of Green Lake from May through August, which is the time of massive precipitation of calcite at rates as high as 2 g/m^2/day. From sediment trap studies, Brunskill (1969) found calcite crystal loads in the water column of 35 g/m^2 in June and July of 1967 (Fig. 11). He argued that the precipitation of calcite in Green Lake is an inorganic process controlled largely by seasonal temperature change- "...temperature is the direct causal factor in the initiation of calcite precipitation... with photosynthesis playing only a secondary, and probably minor, role" (Brunskill, 1969, p. 844).

However, this concept of a purely inorganic origin for calcite precipitation in Green Lake has recently been challenged by Thompson and Ferris (1990) and Thompson et al. (1997). Based on experimental and transmission electron microscopy results of waters collected from Green Lake, Thompson and Ferris (1990) concluded that calcite precipitation is the direct result of the photosynthetic activity of the cyanobacterial picoplankton (0.2-2.0 μm) *Synechococcus* which occurs at concentrations of ~10^5 cells/ml of water in the mixolimnion of Green Lake. They convincingly demonstrated that calcite (as well as a gypsum and perhaps magnesite) precipitates epicelluarly around *Synechococcus* cells (Fig. 12). The reason for this is that the photosynthetic metabolism of *Synechococcus* directly results in the alkalinization (increase pH) of the microenvironment immediately surrounding the cell because of its ability to use bicarbonate (HCO_3^-) as a carbon source which results in the production of hydroxyl (OH^-) ions (Thompson and Ferris, 1990). Calcium (Ca^{2+}) ions which concentrate on the surface of *Synechococcus* cells serve as nucleation sites for the precipitation of calcite and gypsum (Fig. 13).

This new view of Green Lake "whiting events" (direct precipitation of fine-grained calcite from the open water column) was further tested by direct monthly field measurements from May 1989 to April 1990 (Thompson et al., 1997). Secchi disk data (Fig. 14) clearly document the onset of the annual Green Lake whiting in May, when water clarity diminishes dramatically (Secchi disk readings decrease from 18 to 8 m). Minimum water clarity (Secchi disk readings of 4.5 m) occurred during July and August and then gradually improved through fall, winter and early spring

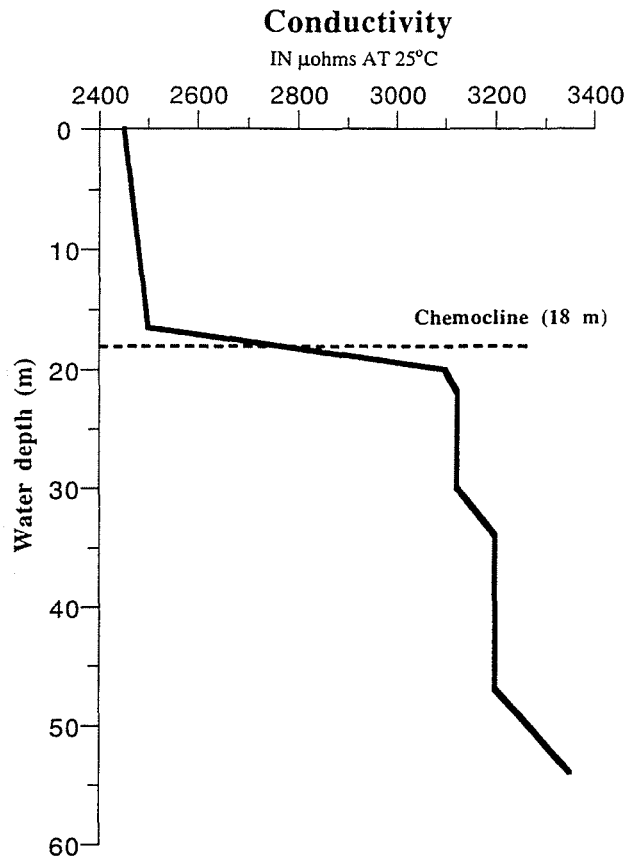

Fig. 10: Vertical distribution of conductivity versus water depth in Green Lake. Conductivity is rough measure of salinity. Note abrupt increase along chemocline at ~18 m (from Brunskill and Ludlam, 1969).

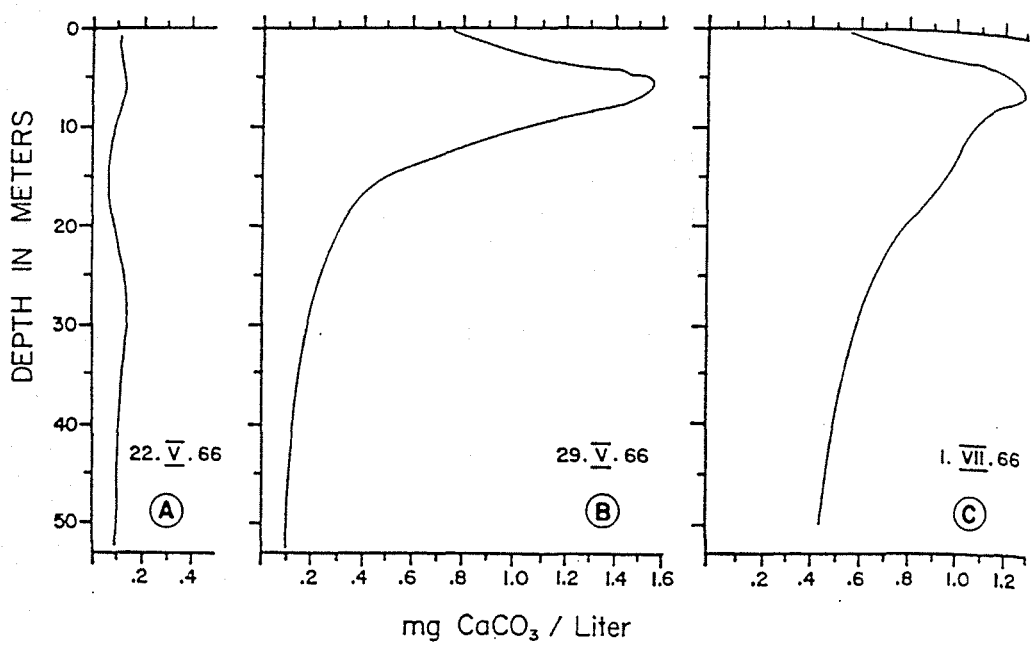

Fig. 11: Distribution of suspended calcite crystals versus water depth in Green Lake on May 22, 1966 (left), May 29, 1966 (center), and July 1, 1966 (right). Note peak abundance (~1.6 mg $CaCO_3$/l) at ~5 m water depth on May 29, 1966 due to spring whiting event (from Brunskill, 1969).

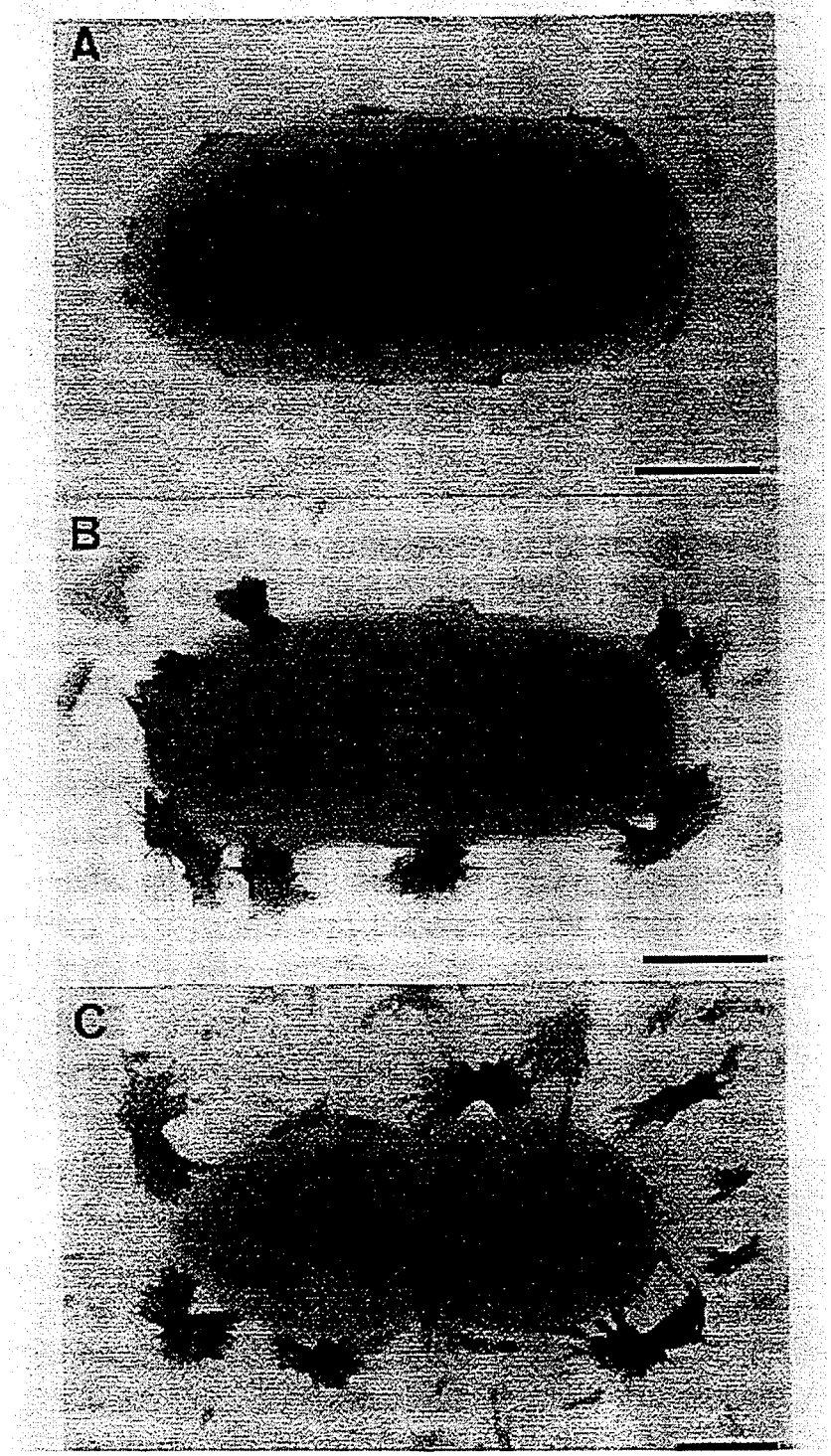

Fig. 12: Transmission electron microscope (TEM) photographs illustrating progressive (A to C) mineral deposition on surface of *Synechococcus* cell. Cell beginning to divide in C; bar scale =500 nm (from Thompson and Ferris, 1990).

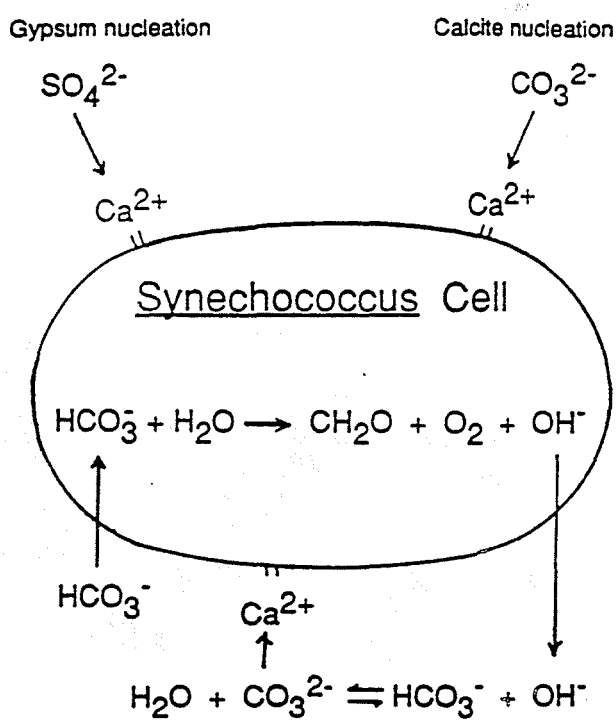

Fig. 13: Schematic cartoon illustrating basic biogeochemical reactions both on and within idealized *Synechococcus* cell during mineral precipitation (from Thompson and Ferris, 1990).

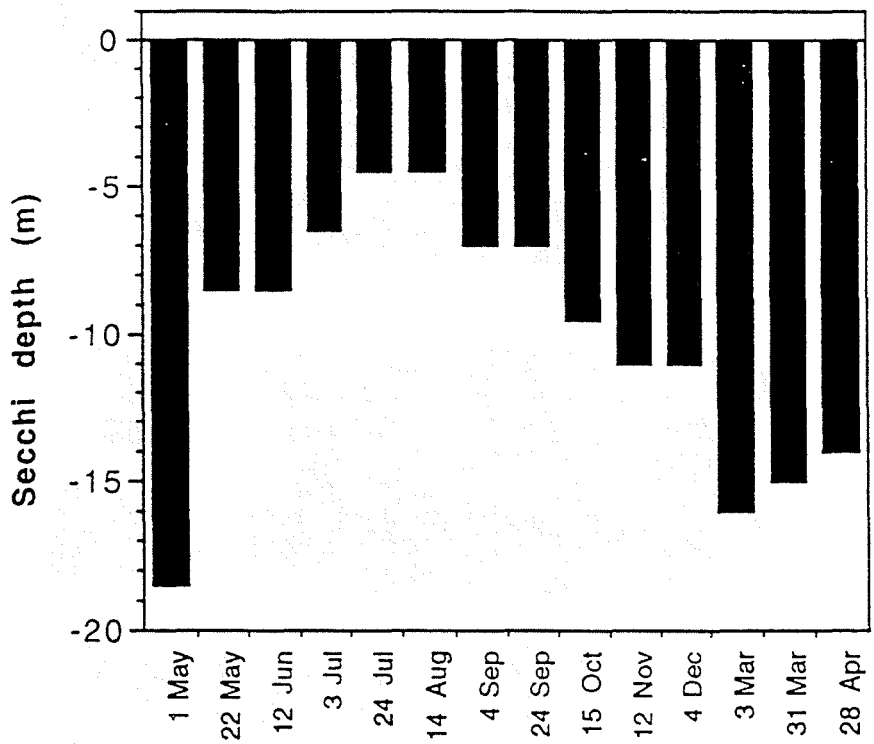

Fig. 14: Seasonal (1989) Secchi Disk data for Green Lake documenting low visibility (i.e.- low water clarity) during late spring/summer months due to suspended calcite crystals precipitated during whiting event (from Thompson et al., 1997).

(Thompson et al., 1997). During this whiting event the color of Green Lake changed from bluish-green to greenish-white (Thompson et al., 1997).

The onset of this whiting event was directly related to the spring bloom of *Synechococcus* triggered by increasing temperatures and light intensities (Fig. 15; Thompson et al., 1997). That *Synechococcus* is directly responsible for the precipitation of calcite is supported by $\delta^{13}C$ data which reveal that whiting calcite (as well as sediment calcite) in Green Lake is enriched by ~3-5 ‰ relative to the $\delta^{13}C$ of dissolved inorganic carbon (DIC) of summer surface waters (Thompson et al., 1997). The reason for this isotopic enrichment is the preferential uptake of relatively light ^{12}C by the photosynthetic picoplankton (Fig. 16). According to Thompson et al. (1997) individual cells of *Synechococcus* can precipitate calcite crystals a number of times per season because they periodically shed their outer "S-layer" once it is mineralized.

To summarize, the reason that Green Lake is green (particularly during spring and summer) is because of the widespread precipitation of calcium carbonate. Calcite crystals precipitated around picoplankton result in an increase of particulate matter in the water column which preferentially scatters back green light. In addition, the accumulation of calcium carbonate in littoral zone waters of Green Lake provides a permanent surface of reflection for wavelengths within the green spectrum of visible light.

Bioherms

Here at Stop #3 we can literally stand on a massive, *in situ* accumulation of calcium carbonate or bioherm. Although the best developed bioherms in Green Lake are here at Deadman's Point, they are also found across the lake along the south-facing shoreline (Fig. 17). These unusual littoral zone accumulations of massive carbonate in Green Lake have been known for many decades (Walcott, 1914; Bradley, 1929; Howe, 1932; Eggleton, 1956).

The bioherms of Green Lake have traditionally been viewed as algal in origin, a concept most recently advocated by Dean and Eggleston (1975), Eggleston and Dean (1976), Dean (1981), and Dean and Fouch (1983). In fact, Dean and Eggleston (1975) compared these freshwater bioherms of Green Lake to marine algal "cup" reefs of Bermuda.

However, Thompson et al. (1990) have reinterpreted the "algal bioherms" of Green Lake as thrombolitic microbialites which simply means a massive carbonate accumulation precipitated by microbes (rather than algae). SCUBA observations here at Deadman's Point revealed that the microbialites have grown up and out from dolostone beds within the Syracuse Formation. They are lobate features that protrude as overhangs into Green Lake and are as much as 10 m thick (Fig. 18). The undersides of the overhangs are colonized by aquatic mosses as well as sponges, and have laminated stromatolitic caps (Thompson et al., 1990). The internal structure of these features is characterized by a non-laminar, clotted texture. The active, outer growing portion of these bioherms is heavily colonized by a benthic variety of *Synechococcus* (Thompson et al., 1990). They believe that this benthic species of cyanobacteria, rather than algae, is responsible for the *in situ* development of the bioherms in Green Lake. *Synechococcus* is specifically adapted for life in oligotrophic, hardwater lakes like Green Lake because of its ability to directly use bicarbonate (HCO_3^-) as a carbon source and its very low nutrient requirements (Thompson et al., 1990).

Benthic forms of *Synechococcus* colonize most any hard surface in the lake as evidenced by the accumulation of calcite on human artifacts such as bottles and cans (Fig. 19; Dean and Fouch, 1983). It is also common to see a white calcite coating on trees that have fallen into the lake. However, if one assumes that the bioherms at Deadman's Point originated shortly after Green Lake formed (~11-12 ka) their growth rate would only be ~1 mm/year (Thompson et al., 1990).

Before leaving Deadman's Point for our next stop, please take a few minutes to examine the marl deposit which extends to ~1 m above present day lake level. This calcite-rich deposit contains an abundance of lacustrine, littoral zone gastropods, thus providing clear evidence for a previous highstand of Green Lake (Eggleton, 1956). Harmon (1970) assumed that the level of Green Lake dropped when the Erie Canal (which is located just north of Green Lake; Fig. 1) was built in the early 1800's. However, as we will see at our next stop, there is a well preserved record of natural lake level fluctuations beneath the wetland which connects Green and Round Lakes.

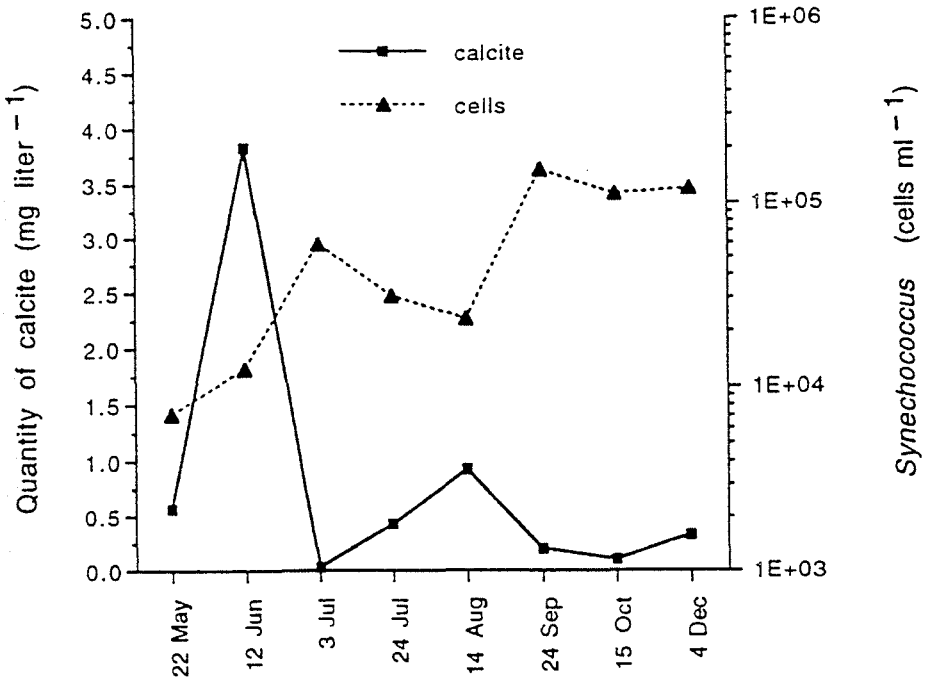

Fig. 15: Seasonal (1989) abundance of suspended calcite crystals and *Synechococcus* cells in Green Lake. Note late spring peak (~4 mg/l) of calcite crystals at 4 m water depth is coincident with the seasonal rise in the abundance of cyanobacterial picoplankton (from Thompson et al., 1997).

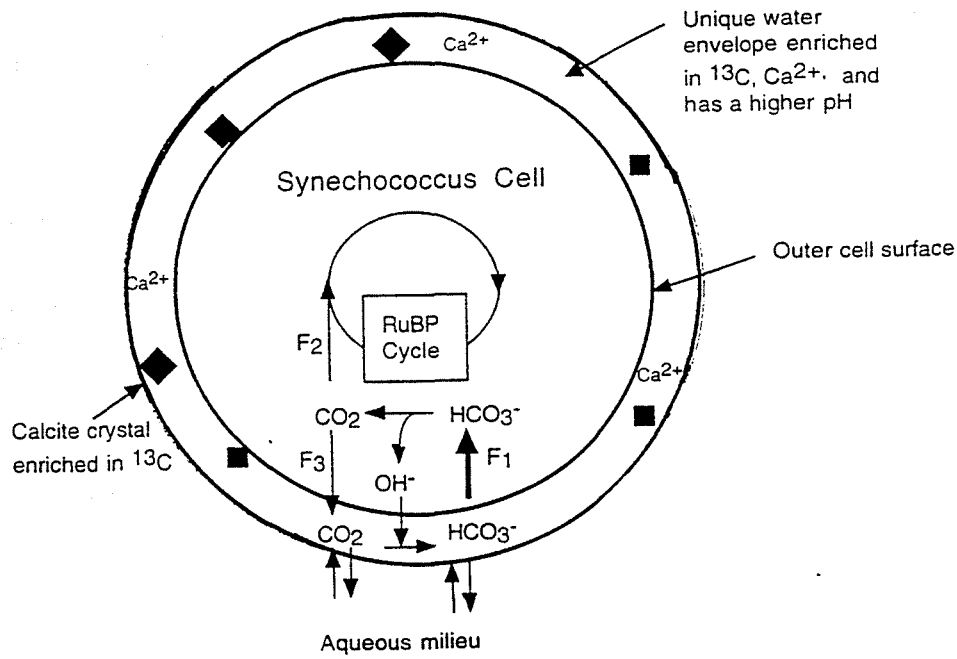

Fig. 16: Schematic cartoon illustrating *Synechococcus* metabolism reactions and epicelluar precipitation of calcite crystals in surrounding microenvironment. $\delta^{13}C$ enrichment of calcite due to preferential uptake of ^{12}C by the picoplankton (from Thompson et al., 1997).

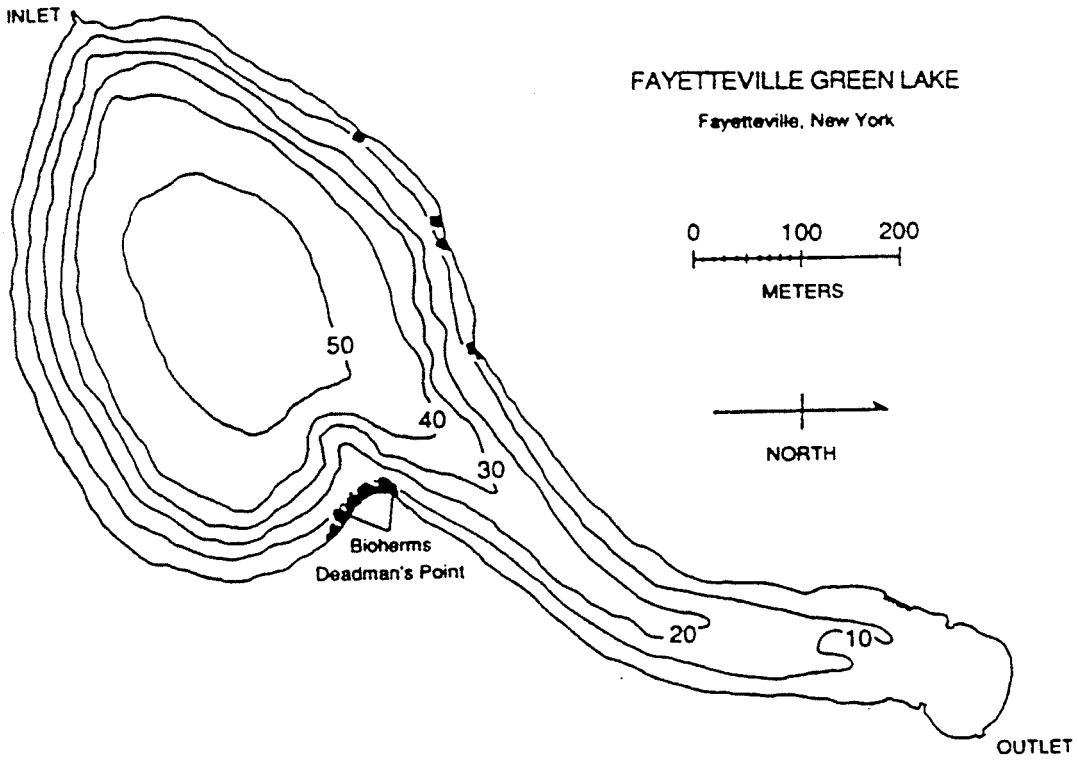

Fig. 17: Distribution of bioherms along the shore of Green Lake. Note major development at Deadman's Point (Stop #3) as well as lesser development along south-facing littoral zone (from Thompson et al., 1990). Contours are in meters.

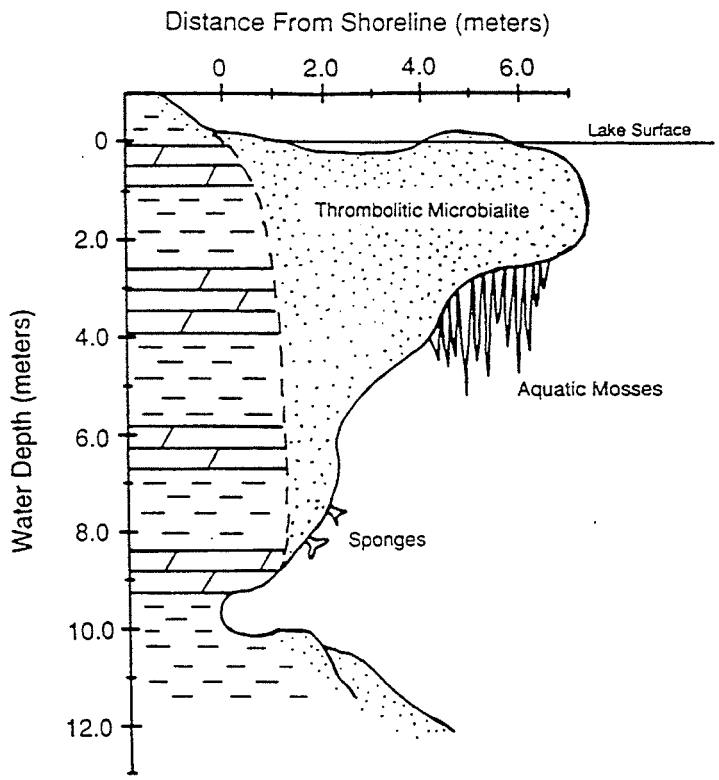

Fig. 18: Vertical cross-section of "bioherm" (thrombolitic microbialite) at Deadman's Point (from Thompson et al., 1990).

Stop #4: Wetland Stratigraphy and Natural Lake Level Fluctuations

From Deadman's Point we will continue our clockwise journey to the southern end of Green Lake. Here the path will divide and we will bear to the left. This will take us along the intervening wetland between the two lake basins (Figs. 2 and 3). We will stop at the next juncture of the path at the east end of Round Lake to present the subsurface stratigraphy of the wetland and discuss its implications for natural lake level fluctuations as well as regional paleoclimate change over the past ~8,000 years. Sediment cores previously recovered from the wetland will be available for viewing and discussion at this stop.

During the summer of 1996 we collected sediment cores, up to 11.2 m long, from three sites in the wetland between Green and Round Lakes (Fig. 20). There is at least 11 m of sediment beneath both the eastern and western ends of the wetland (Fig. 20). However, at the middle site only ~5 m of sediment was recovered before terminating on what appeared to be bedrock. If correct, there is a very shallow bedrock sill separating the Green and Round Lake basins.

Most of the sediment recovered at all three sites is fossiliferous marl consisting of 60-90% calcium carbonate (Figs. 21 and 22). The abundance of lacustrine fossils indicates deposition in relatively shallow, oxic waters (i.e.-littoral zone). However, a number of organic-rich (up to 90%) peat layers, representing various wetland environments, were also recovered and radiocarbon dated (Fig. 21). Based on radiocarbon data, the cores extend back to ~9.1 ka ^{14}C. Average sediment accumulation rates for the long cores are on the order of ~1.2 m/1000 years, although intervals of marl have accumulated at rates of up to 2.6 m/1000 years (Fig. 23).

Of particular interest is the series of marl-peat cycles (N=4) recovered at core site GLWL-3 nearest to Green Lake (Fig. 22). The four peat layers have been radiocarbon dated (University of Texas Radiocarbon Lab #'s TX-9191, TX-9136 through TX-9133), from bottom to top, at 7,570±70 years, 5,620±70 years, 4,545±65 years, and 2,169±50 years. Calculation of an average period for these cycles yields an average of ~1800 years (range 1075 to 2385).

The marls obviously represent open lacustrine connections between Green and Round Lakes whereas the peats represent wetland environments similar to those that exist today. The modern surface peat has developed during the past ~2,000 years. Thus, it seems highly unlikely that the marl outcrop that we saw ~1 m above modern lake level at Deadman's Point was stranded by an anthropogenic lowering of lake level less than 200 years ago during construction of the Erie Canal. This is supported by tree-ring counts from the wetland which indicate that living trees predate the construction of the Erie Canal (Brunskill and Ludlam, 1967).

The marl-peat cycles most likely record natural fluctuations of relative lake level approximately every 2,000 years over the past 8,000 ^{14}C years. If we interpret such natural lake level fluctuations (Fig. 24) as products of regional changes in precipitation minus evaporation, the data further imply relatively dry climatic conditions at ~ 8 ka, 6 ka, 4 ka, and 2 ka with relatively wet climates inbetween. This is consistent with results from a recent series of cores collected from the Montezuma wetlands (north end of Cayuga Lake) which also revealed relatively dry events at ~8 ka, 6 ka, and 4 ka (Mullins, in prep.). Thus, the relative lake level fluctuations recorded from the wetland in Green Lakes State Park are likely a response to regional climate changes rather than local drainage basin effects.

The ~ 8 ka ^{14}C relative lake lowstand at Green Lakes coincides with the end of a cool, dry period (10.1-8.2 ka ^{14}C) defined by stable isotope data from Seneca Lake (Anderson et al., 1997). This event followed the well-known Younger Dryas cold interval (~10.8-10.3 ka ^{14}C), and was correlative with a rapid phase of melting of the Laurentide ice sheet which poured large volumes of cold, isotopically light meltwater into the Great Lakes (Anderson et al., 1997). It also occurred quite close (~7.5 ka ^{14}C) to a recently discovered North Atlantic cool/dry event defined in Greenland ice cores (Alley et al., 1997).

The ~6 ka ^{14}C relative lake lowering defined at Green Lakes may also be a reflection of broader scale climate changes. In her review of natural lake levels throughout eastern North America, Harrison (1989) discovered that lakes here in general reached their lowest levels ~6 ka ^{14}C, implying widespread drought for at least a short interval of time. Cores from Montezuma wetlands also display a marked drop in the percentage of calcium carbonate at this time, implying relatively dry and/or cool conditions (Mullins, in prep).

The ~4 ka ^{14}C relative lake drop at Green Lakes coincides with widespread regional peat development, which effectively ceased marl deposition in the Finger Lakes region (Mullins, in prep.) Approximately 4 ka also marks the

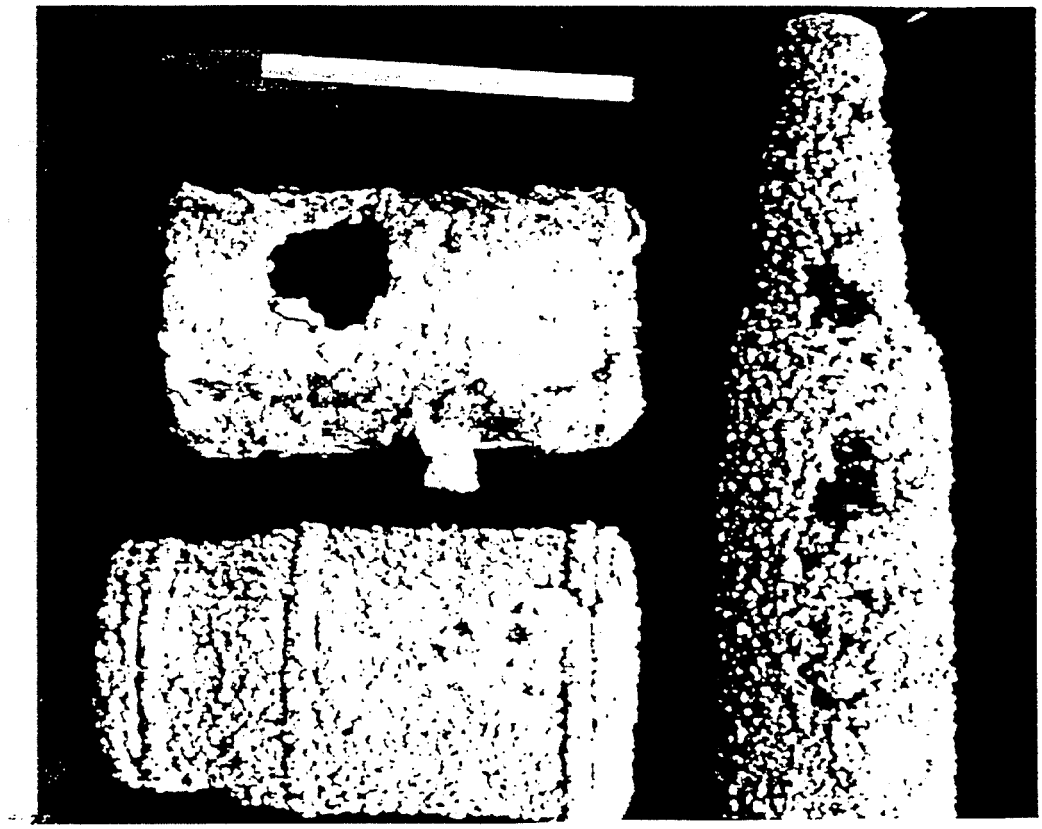

Fig. 19: Photograph of bottle and cans recovered from Green Lake with a thick coating of calcium carbonate documenting rapid rate of precipitation (from Dean and Fouch, 1983).

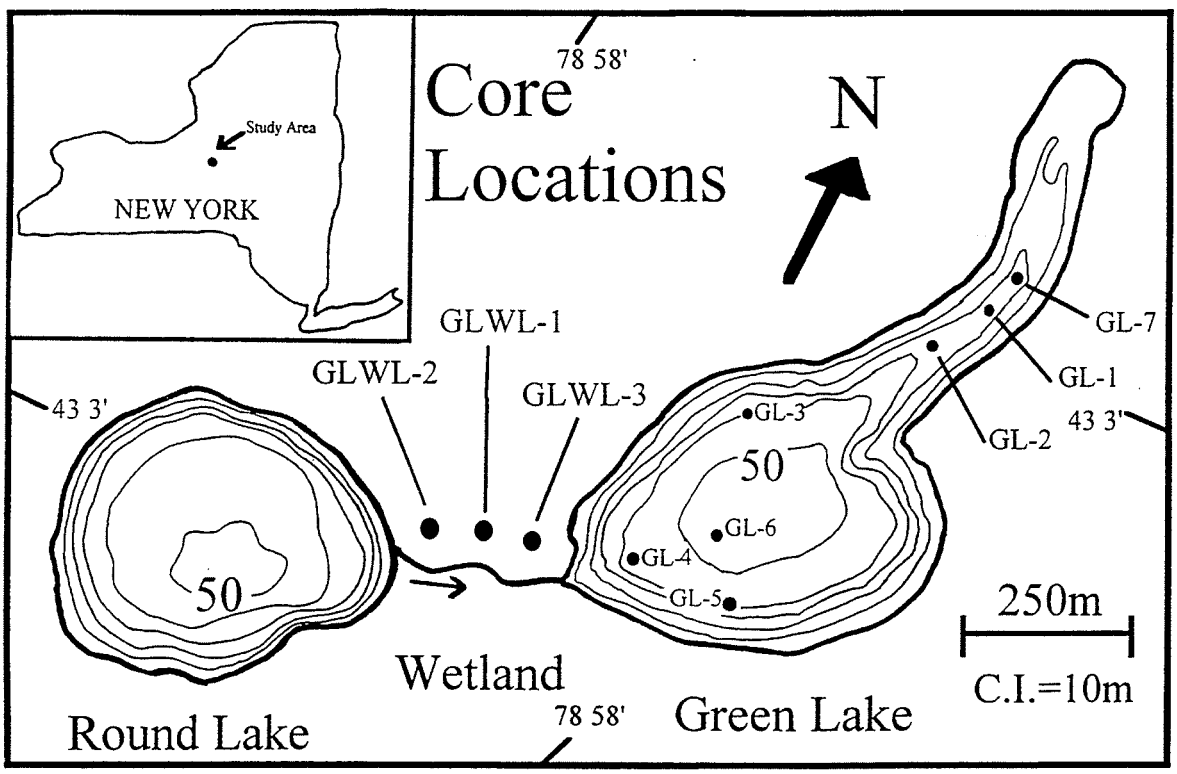

Fig. 20: Bathymetry of Green and Round Lakes including location of Green Lake (GL) sediment cores as well as cores recovered from the Green Lake wetland (GLWL) that will be discussed at stops #4 and 5.

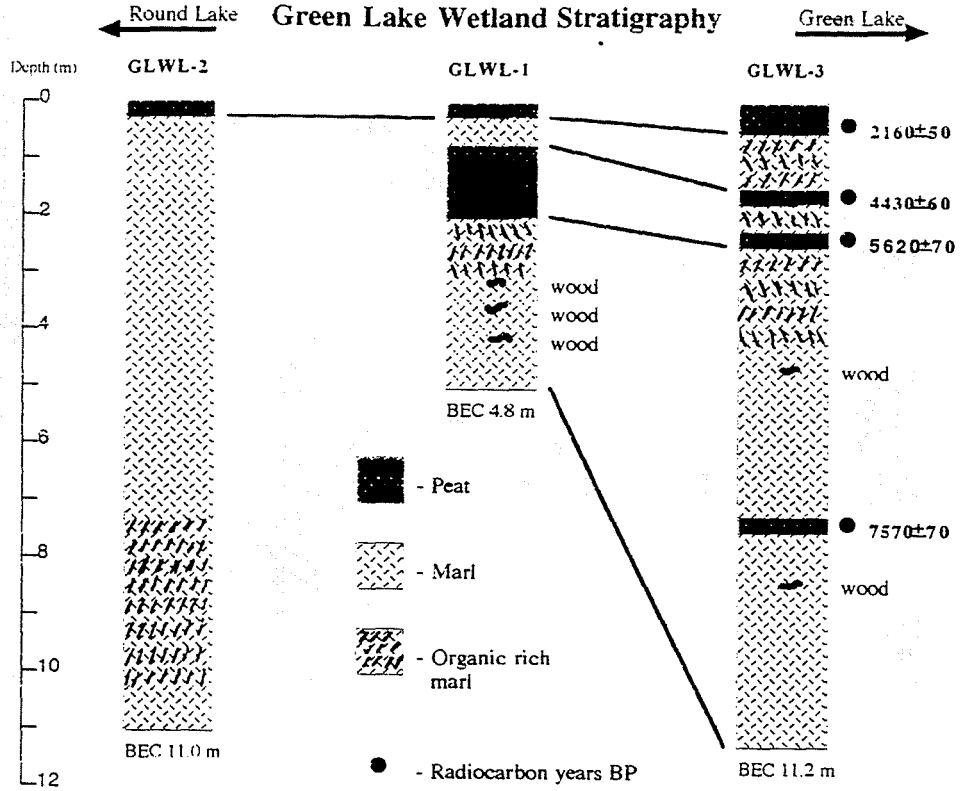

Fig. 21: Lithostratigraphy of the three wetland cores (see Fig. 20) and radiocarbon results. Note abundance of open-lacustrine marl (calcium carbonate rich deposits) with intervening peat (wetland) layers. BEC= bottom entire core.

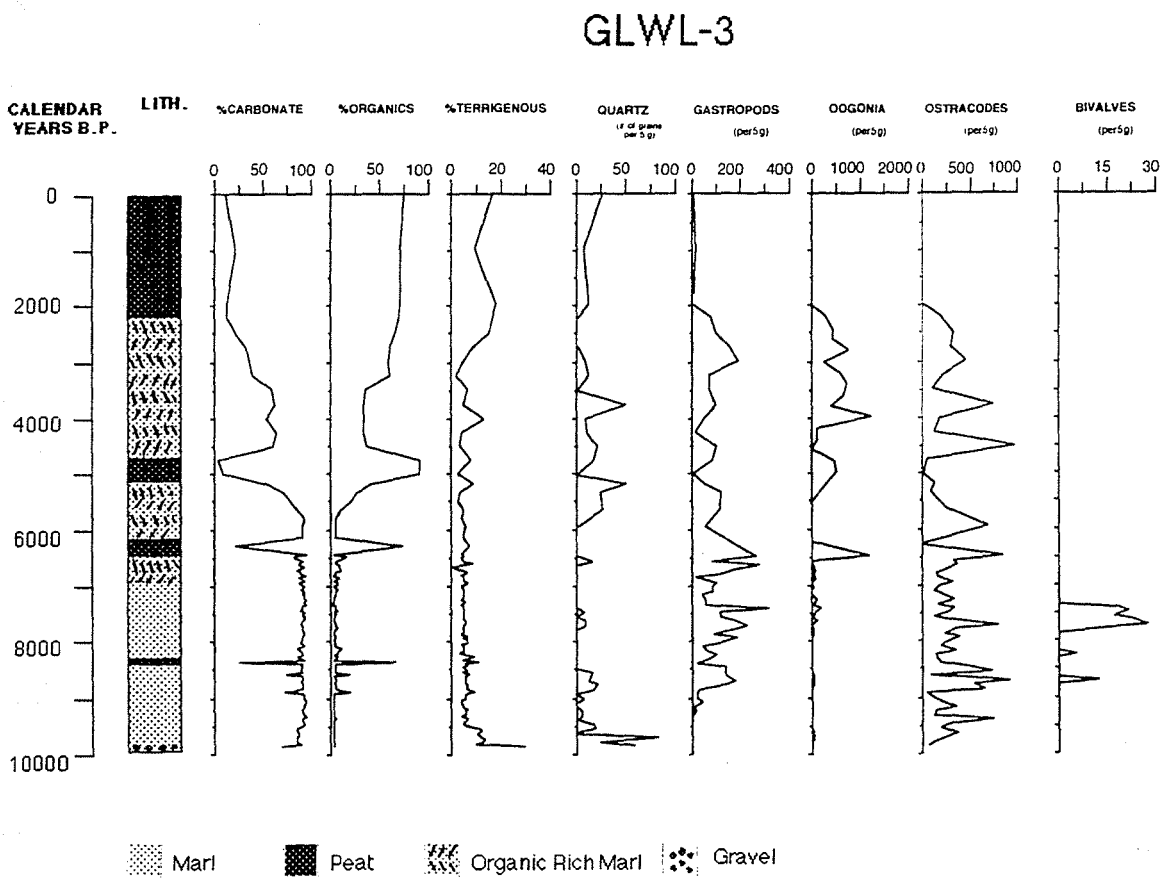

Fig. 22: Loss-on-ignition data versus depth for Green Lake wetland (GLWL) core 3. TOM= total organic matter. Note high percentage of calcium carbonate in marl layers (~90%) and high TOM values (up to 90%) for peats. Also note relatively high percentage of terrigenous material (~30%) at base of core where shale chips were also recovered, suggesting that core bottomed on bedrock.

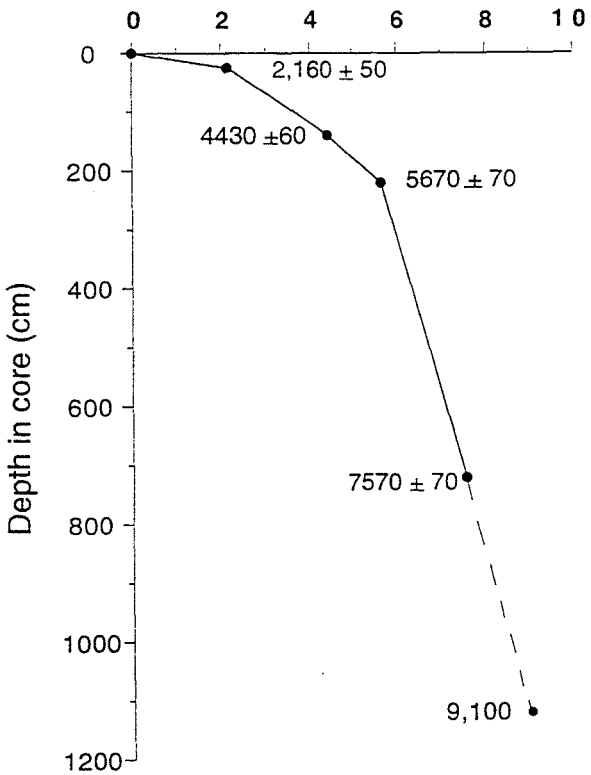

Fig. 23: Age versus depth curve for Green Lake wetland (GLWL) core 3 based on radiocarbon results. Note relatively rapid sediment accumulation between ~9.1 ka and 5.6 ka ^{14}C followed by a gradual decline, suggesting the rapid infill of a bedrock depression.

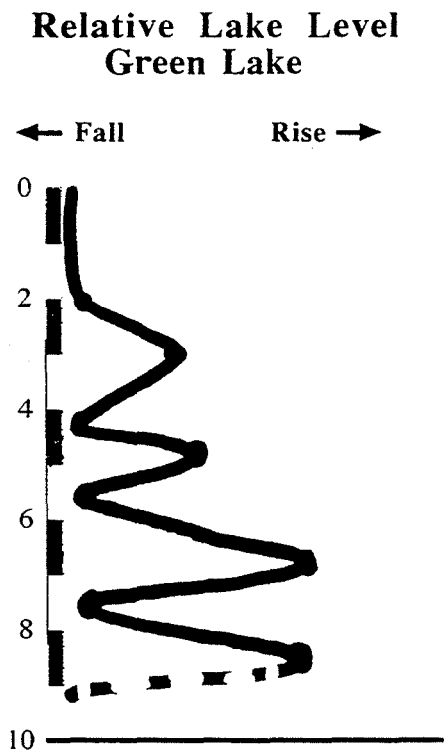

Fig. 24: Relative lake-level curve for Green Lake based on radiocarbon dates on peat layers contained in GLWL-3. Note relative lake lowstands at ~7.6 ka, 5.6 ka, 4.4 ka, and 2.2 ka ^{14}C.

end of the mid-Holocene Hypsithermal (~9-4 ka ^{14}C) in central New York State, which was mostly relatively warm and wet (Dwyer et al., 1996).

Why relative lake level fluctuations in Green Lakes should occur every ~2000 years is open to speculation. Perhaps they are related to regional climate changes caused by changes in the production of North Atlantic Deep Water (and thus heat transport) which presumably caused the Younger Dryas climate reversal (Broecker et al., 1989); or, perhaps they are related to shifts in the mean position of the jet stream and atmospheric pressure systems (Dwyer et al., 1996). However, there may also be an intriguing relationship between lake level fluctuations at Green Lake and natural variations in solar irradiance caused by sunspot activity. Wigley and Kelly (1990) have developed a proxy for prehistorical solar variation based on the difference between tree-ring counts and ^{14}C age, which they as well as Karlen and Kuylenstierna (1996), have used to explain Holocene climate changes. The peats dated from the Green Lake wetland match-up well with relatively high amounts of solar irradiance at ~8 ka, 6 ka, 4 ka and 2 ka ^{14}C (Fig. 25). Greater amounts of solar energy at these times may have led to increased rates of evaporation and thus, relative lake-level lowerings. Although this potential linkage between solar variability and lake levels is speculative, it is certainly deserving of further thought and investigation.

Stop #5: Environmental Changes During The Past 2,500 Years: Short Cores From The Deep Lake

From our previous vantage point of the wetland between Green and Round Lakes we will continue to proceed clockwise around Round Lake. During the course of this part of the fieldtrip keep a sharp eye out for littoral zone bioherms similar to (but smaller than) those at Deadman's Point as well as marl benches indicative of a previous high stand(s) of lake level. At the southwest end of Round Lake we will also be able to observe the inlet to the lake as well as the ~100 ft. (30.5 m) high cliff over which a late glacial waterfall presumably flowed to carve out this plunge-pool basin. We will then walk, uninterrupted, around all of Round Lake, past the north-side of the wetland, and back to Green Lake before our next stop. Our final stop (#5) will be along the path on the northwest side of Green Lake (across from Deadman's Point) which will afford us an open view of the circular, deep water basin of Green Lake (Figs. 2 and 3).

Because of the seasonal precipitation of calcium carbonate (whitings) coupled with the anoxic nature of waters below the chemocline, sediments in the deep main basin (and part of the "neck") of Green Lake are characterized by distinct annual laminations or varves (Fig. 26). Using sediment trap data Brunskill (1969) was able to document the summer accumulation of a light tan calcite laminae and the winter accumulation of a dark homogenous laminae of more organic-rich sediment; thus, proving the annual nature of these laminations (i.e.-varves). Ludlam (1969) further documented that the light colored laminae contain an average of ~82% calcium carbonate whereas dark laminae contain only ~55%. Average thickness of the more recent varves is on the order of ~0.7 mm.

Ludlam (1969) also noted that not all sediments below the chemocline are varved; there is also an abundance of massive or "unlaminated" sediment. Because some of these massive layers (mm to cm scale) are graded, have erosional bases and contain coarse littoral zone grains, they have been interpreted as turbidites (Fig. 26; Ludlam, 1969, 1974). We have also recovered deep lake sediments from Green Lake which contain coarse gastropod shells and other material which has obviously been derived and transported from much shallower depths. There is also very good photographic evidence (Fig. 27) for the deformation of varves via subaqueous slumping (Ludlam, 1974; Dean and Fouch, 1983). Thus, there is little question that mass wasting and sediment gravity flows are processes that operate in Green Lake.

However, Ludlam (1969, 1974) has interpreted all massive layers (even those ~1 mm thick) as turbidites and estimated that 40-65 % of basinal sediments in Green Lake were deposited as gravity flows. We do not agree with this assessment which evolved largely in the late 1960's and early 1970's when turbidity current theory was being developed and widely applied. Many of the massive layers we have examined display no objective evidence for deposition by turbidity currents; they are not graded, do not contain displaced grains, and do not have erosional bases. In fact our core 6 form the central basin of Green Lake contains relatively few unequivocal turbidites (Fig. 28). Although this does not mean that all the massive layers are not turbidites, it does highlight a need for additional hypotheses. An alternative interpretation is that these massive layers (particularly the thin 1-2 mm thick ones) are simply thicker than normal winter layers of annual couplets (varves). In fact, Ludlam (1981) stated that "...thin turbidites... can not be separated from the annual layers" (p. 85). At the time of this writing, we are

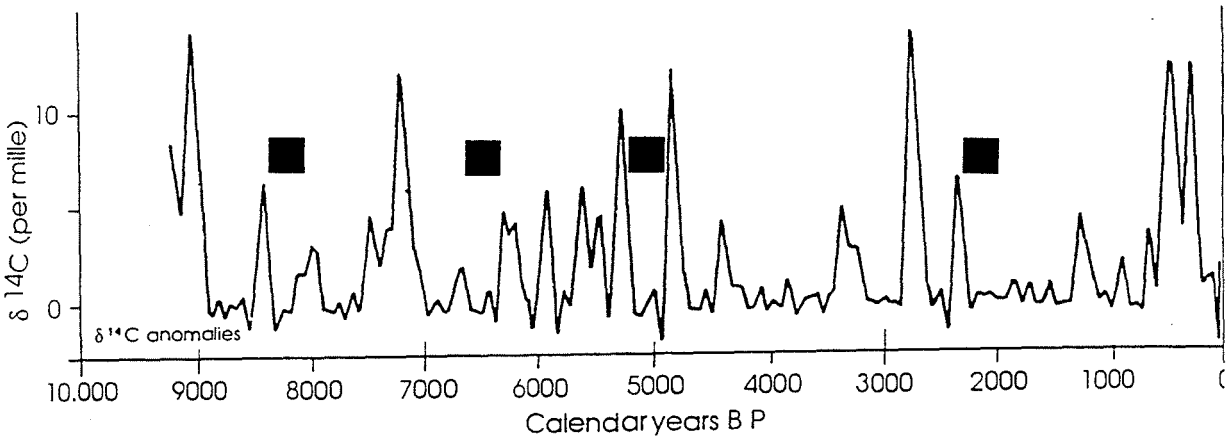

Fig. 25: Solar irradiance curve for the Holocene based on $\delta^{14}C$ anomalies. High $\delta^{14}C$ values indicate relatively low solar irradiance due to a low sunspot activity. Black squares denote ages of peat layers from core GLWL-3. Note correlation of ages of Green Lake peat layers calibrated to calendar years with low $\delta^{14}C$ (i.e.- relatively high solar irradiance) suggesting possible evaporative drawdown for lake-level lowerings. Solar irradiance curve based on Wigley and Kelley (1990): taken from Karlan and Kuylenstierna (1996).

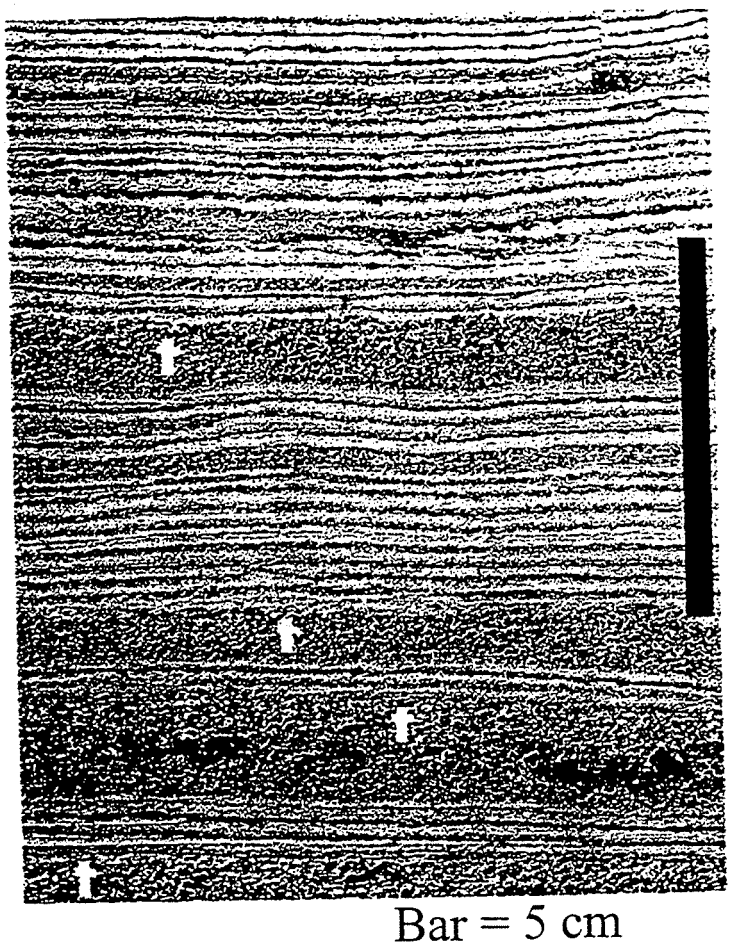

Fig. 26: Photograph of dried Green Lake sediment core recovered from below the chemocline. Note mm-scale light/dark couplets which are true annual varves as well as coarser-grained massive layers interpreted as turbidites (from Dean and Fouch, 1983).

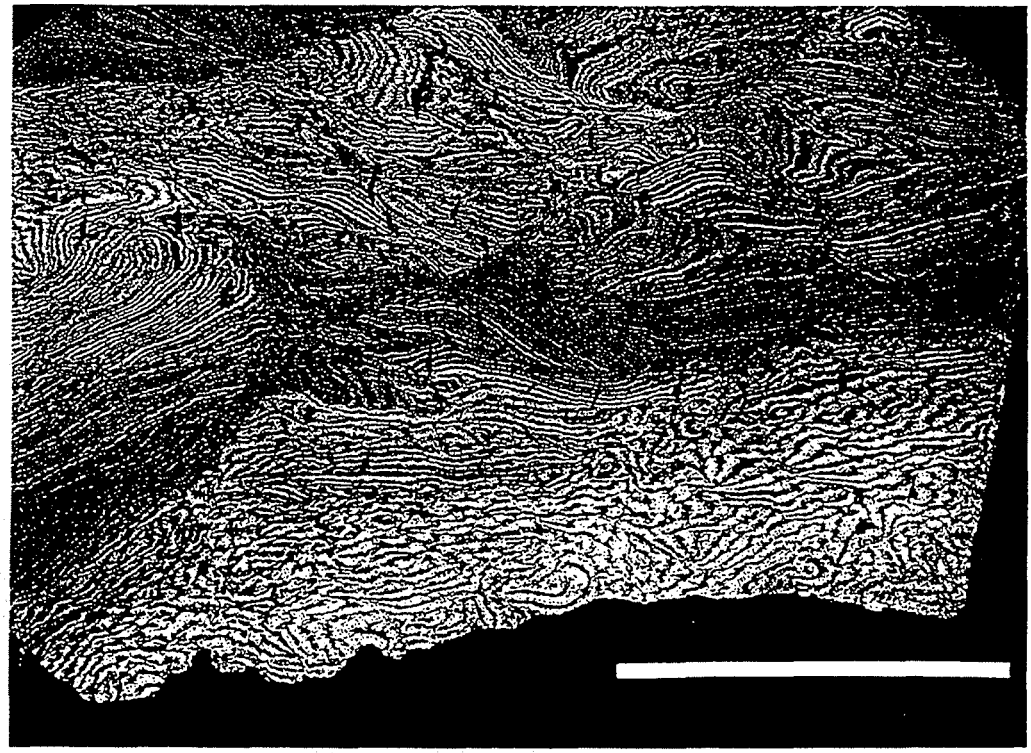

Fig. 27: Photograph of dried slab of Green Lake sediment collected from below the chemocline, illustrating contorted varves interpreted as a slump sequence. Bar scale = 5cm; from Dean and Fouch (1983).

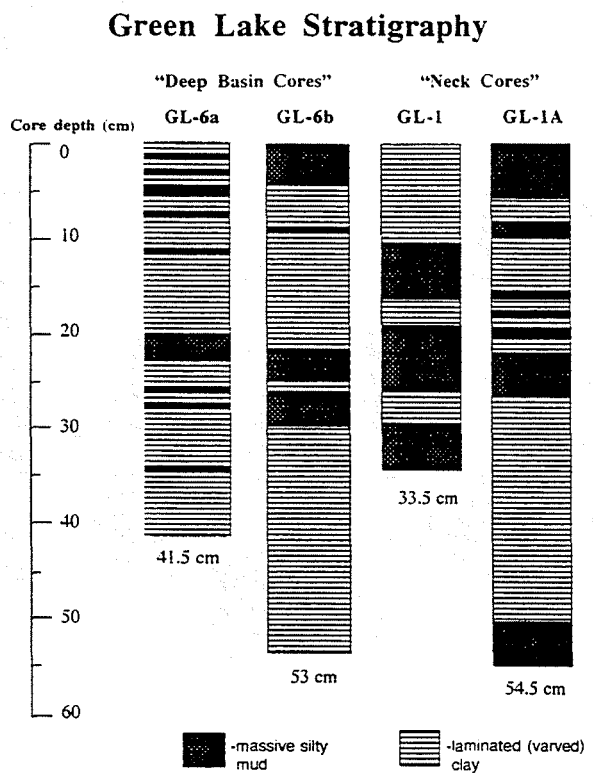

Fig. 28: Lithostratigraphy of short cores recovered from below the chemocline in Green Lake, illustrating the relative abundance of annual laminations (varves) and massive layers (turbidites). Note relative paucity of massive layers in core GL-6 from the central basin of Green Lake.

conducting compositional analyses and detailed varve versus radiocarbon chronologies in an attempt to develop objective criteria for the origin of many of these "massive layers" in Green Lake.

The accumulation rate of profundal sediment in Green Lake has also been found to be variable, both temporally and spatially. Ludlam (1981) noted a 48% increase in sedimentation rates between the late 1800's and the 1970's. Ludlam (1984) also discovered that sedimentation rates in the "neck" of Green Lake are ~27% higher than they are in the main basin, perhaps due to the reworking and focusing of sediment from shallow water.

During the summer of 1996 we collected short (<50 cm) gravity cores at seven sites in Green Lake (Fig. 20) with the objective of using the annual deposits (varves) as high-resolution recorders of relatively recent environmental change. We have focused on a pair of cores recovered at site 6 from the floor of the central basin because they contain the lowest ratio of varved sediments to gravity flow deposits (i.e.-turbidites). Because massive zones are interpreted as instantaneous events, they were subsequently subtracted from the final varved sediment record, thus yielding a total varved section of 32.5 cm. Dating of the core is based on four approaches: (1) varve counts; (2) a radiocarbon date on terrestrial organic matter; (3) geochemical correlation with a core dated by ^{210}Pb techniques (Whalen and Lewis, 1980); and, (4) recognition of a pink varve deposited in 1963 (Ludlam, 1969; Ludlam, 1984). The base of the varved section is ~2500 years B.P. (504 B.C.; Fig. 29) and is thus a record of both natural and anthropogenic processes. Sediment accumulation rates between 2500 years B.P. and 167 years B.P. (1830 A.D.) averaged ~10 cm/1000 years versus ~70 cm/1000 years over the past 167 years.

Loss-on-ignition results for total calcium carbonate content in core 6 display a marked decrease at the same depth (18.5 cm) where accumulation rates increase by nearly an order of magnitude (Fig. 30). Average total carbonate values drop from ~80% prior to 1830 A.D. to ~60-65% after 1830 A.D. (Fig. 30). In contrast, average total organic matter contents in core 6 remain relatively constant at ~10% both prior to, and after, 1830 A.D. These data indicate that starting in ~1830 A.D., the flux of terrigenous material to Green Lake increased significantly resulting in increased rates of sediment accumulation (Fig. 30). This is supported by mineralogical data (determined by X-ray diffraction) which show an abrupt increase in the relative abundance of detrital quartz and dolomite at ~1830 A.D. (Fig. 31). Prior to 1830 A.D. dolomite is generally absent from core 6 and quartz is only a minor component. Trace element data (determined by direct current plasma emission spectrometry) of the carbonate fraction in core 6 also display a marked change at ~18.5 cm depth. Concentrations of Pb, Mg, Mn, Cu, and Fe all increase above this depth, whereas Ca and Sr decrease. Lead (a common anthropogenic element) is of particular interest (Fig. 32). Prior to 1830 A.D. lead concentrations range from 5 to 55 ppm with an average ~25 ppm; whereas, after 1830 A.D. Pb concentrations range from 35 to 105 ppm with an average of ~70 ppm (Fig. 32).

Collectively, these results argue for a significant anthropogenic influence on sedimentation in Green Lake since ~1830 A.D. Whalen and Lewis (1980) have previously proposed that deforestation of the region in the early to middle 1800's increased surficial runoff and the flux of terrigenous material into Green Lake. Our results are consistent with their suggestion. Pollution of surface waters by heavy metals at this time might also explain the observed increases of Pb, Cu and Fe since 1830 A.D., although these metals may have also entered the Green Lake basin via the atmosphere as a by-product of coal burning starting with the industrial revolution.

We have also sampled (N=48) varves from core 6 for stable isotope analysis in order to evaluate both natural and potential anthropogenically-influenced climate changes over the past 2500 years. These new data represent the first stratigraphic stable isotope results for Green Lake since a brief mention of results by Stuiver (1968, 1970). $\delta^{18}O$ (a measure of the $^{18}O/^{16}O$ ratio) values vary by as much as ~2 ‰ over the length of the core (Fig. 33) which is 1 ‰ greater than the variability indicated by Stuiver (1968). $\delta^{18}O$ values also display a gradual depletion from -10.2 ‰ to -10.7 ‰ between 500 B.C. and 200 A.D. If this entire depletion (-0.5 ‰) is due solely to temperature change (0.34 ‰/1°C; Rozanski et al., 1993; Anderson et al., 1997) it would imply regional spring/summer cooling of up to 1.5 °C.[2] However, some or all of this isotopic change could also be due to shifts in atmospheric moisture sources. In this case more depleted $\delta^{18}O$ values would imply an increase of moisture from Pacific, Canadian or North Atlantic air masses, which all tend to be cooler than the warm, isotopically heavy air masses which advect into central New York State from the Gulf of Mexico (Rozanski et al., 1993).

---

[2] In terrestrial records, such as ice cores or lake sediments, $\delta^{18}O$ depletions imply relative coolings due to latitudinal fractionation of ^{18}O. This general relationship is opposite that for marine records.

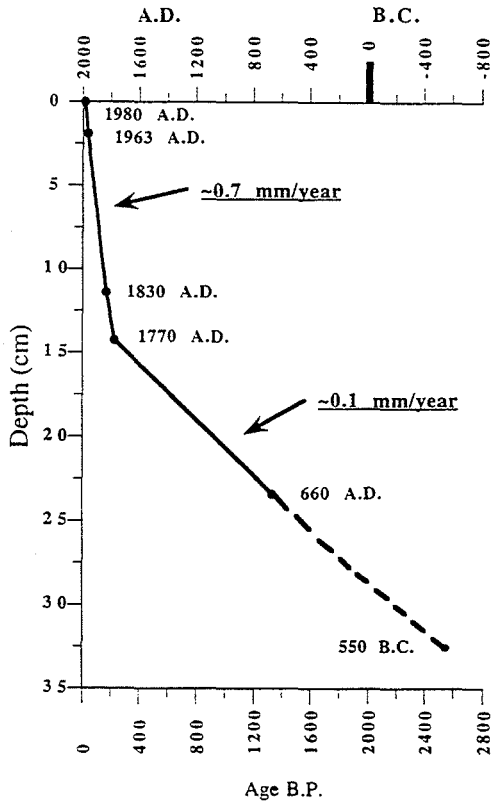

Fig. 29: Age versus depth curve for Green Lake core GL-6. Surface age of 1980 A.D. based on the recogntion of a distinctly colored 1963 varve (Ludlam, 1969, 1984) as well as replicate varve counts. Date of 1830 A.D. based on geochemical correlation with a ^{210}Pb-dated core and the 660 A.D. date is based on AMS radiocarbon results of a cedar leaf fragment calibrated to calendar years. Basal age of ~2500 years B.P. (504 B.C.) is based on linear extrapolation. Note large increase in sediment accumulation rates within the past 150-200 years.

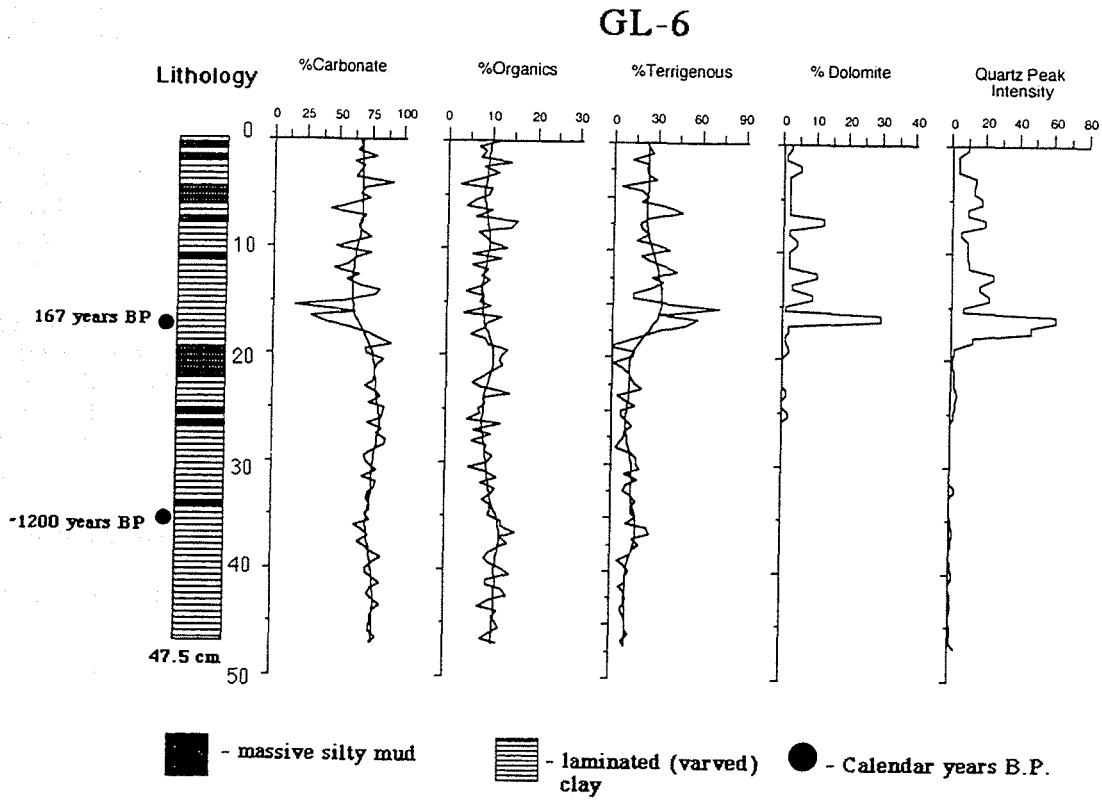

Fig. 30: Loss-on-ignition data from Green Lake core GL-6. Note high calcium carbonate contents (~60-90%) and relatively low total organic matter (TOM) values (~10%). Also note decrease in total carbonate content at 18-19 cm (~167 years B.P.; 1830 A.D.).

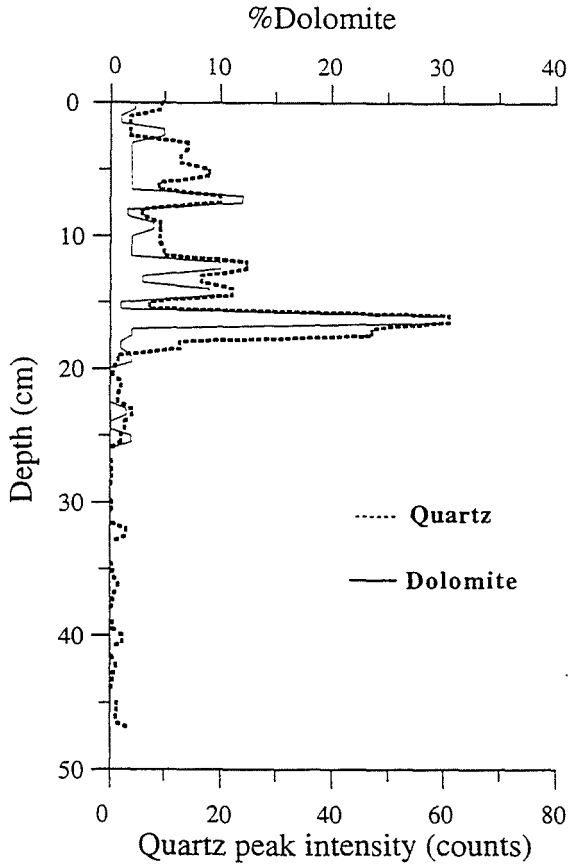

Fig. 31: Relative quartz peak intensity (based on XRD results) and percent dolomite (in the carbonate fraction) versus depth in Green Lake core GL-6. Note abrupt increase of both detrital quartz and dolomite at 18-19 cm (~1830 A.D.) coincident with increase in sediment accumulation rate.

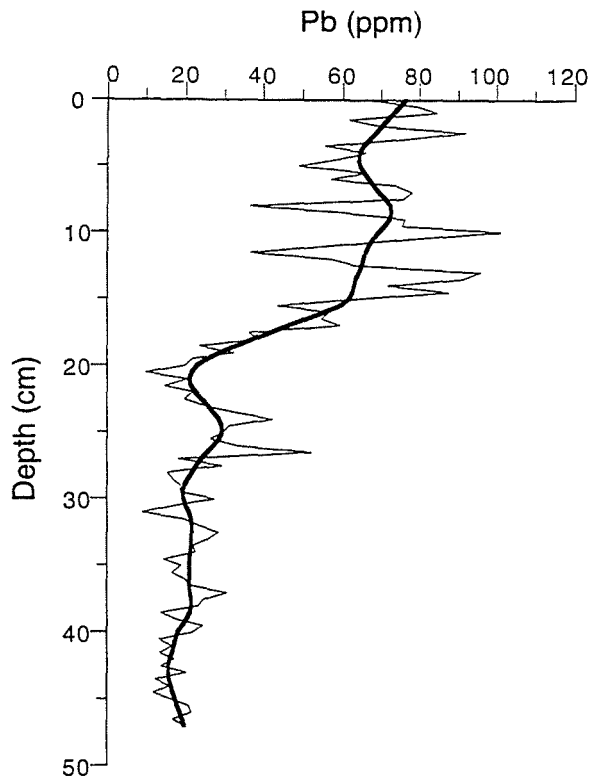

Fig. 32: Concentration of lead in the calcium carbonate fraction of Green Lake core GL-6. Note abrupt increase of Pb at 18-19 cm (~1830 A.D.) coincident with increase in sediment accumulation rates.

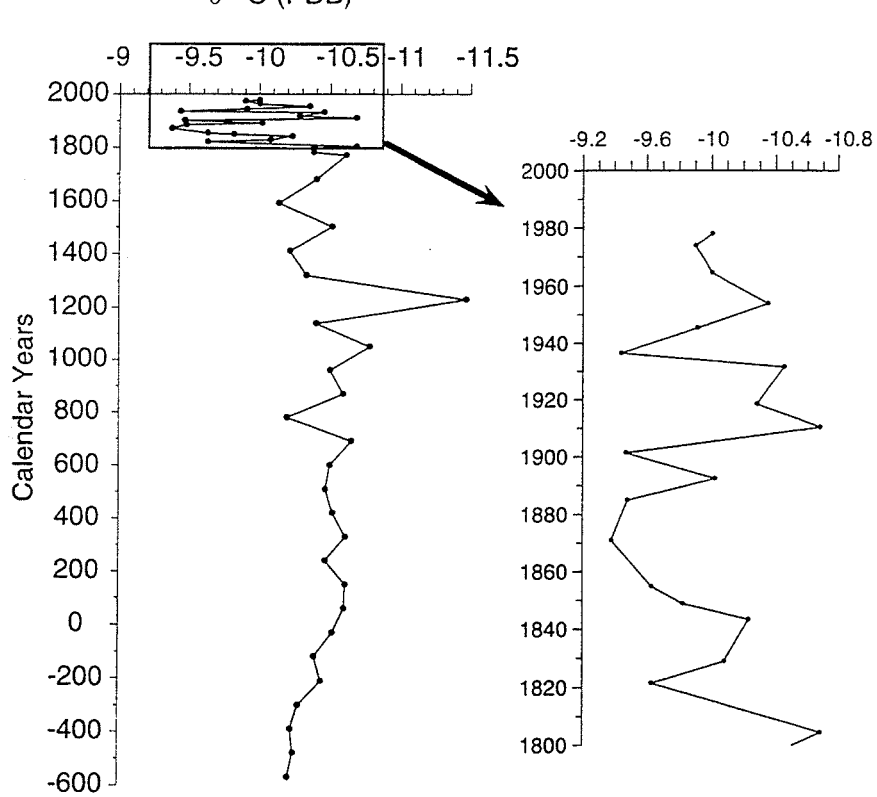

Fig. 33: Distribution of $\delta^{18}O$ values of fine-grained calcite (< μ) from Green Lake core GL-6. See text for additional discussion.

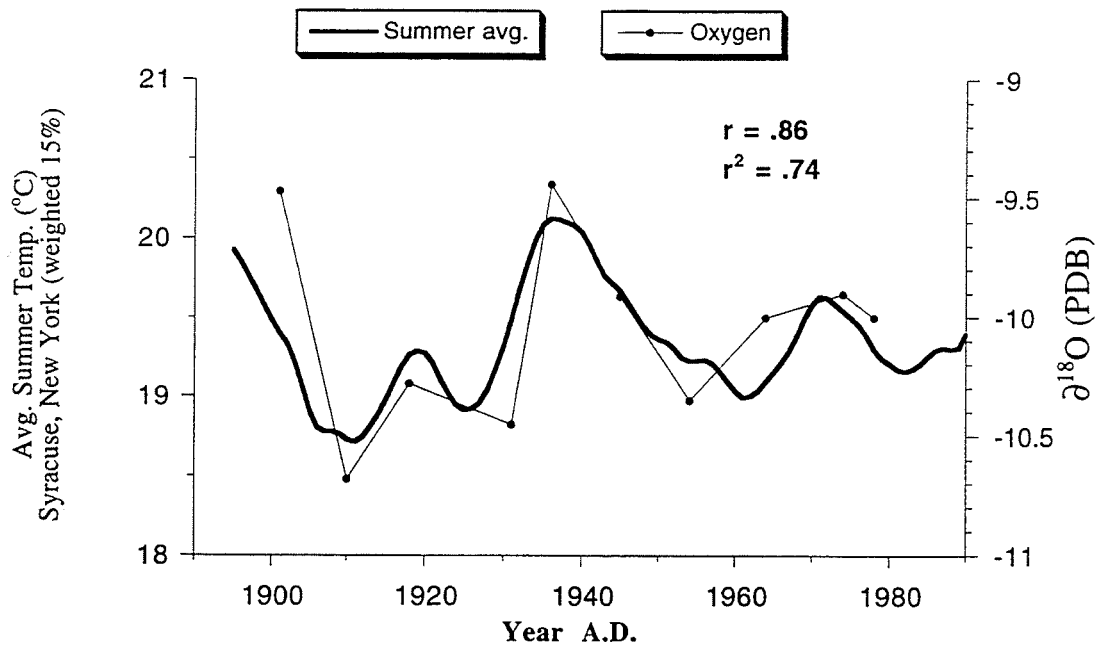

Fig. 34: Correlation of Green Lake core GL-6 $\delta^{18}C$ values over the last century with yearly average summer temperatures for Syracuse, N.Y. (smoothed 15%). The strong correlation between decadel trends in temperature and $\delta^{18}O$ (r^2=.74) is thought to be a function of the type of airmass advecting into the area. See text for additional discussion.

This isotopic evidence for a modest cooling trend between 500 B.C.. and 700 A.D. is consistent with ice core data sets which indicate global cooling during the past 4-5 ka following the mid-Holocene Hypsithermal (Larsen et al., 1995; Thompson et al., 1995). Both glacier reconstructions (Nesje and Kvamme, 1991) and general circulation models (Liao et al., 1994) indicate that Hypsithermal summer temperatures were 2-3 °C warmer than pre-industrial modern values, due to precessional changes.

Following an extreme $\delta^{18}O$ depletion event (one data point) of ~1 ‰ at ~1250 A.D. $\delta^{18}O$ values remain relatively constant until the early to middle 1800's and "colder" than modern values. Since then, $\delta^{18}O$ values become enriched (heavier) by as much as 1 ‰, although there is significant variability (Fig. 33). The increased variability is due in part to a lower sampling interval afforded by the higher accumulation rates after 1830 A.D. Whereas the pre-1830 A.D. average sampling interval is 1 sample per 90 years, the interval increases to about 1 sample every 14 years after 1830 A.D. allowing resolution of decadel scale variability.

It is tempting to speculate that the enrichment (warming) of $\delta^{18}O$ values from Green Lake after the early 1800's is related to the anthropogenic rise of atmospheric carbon dioxide and global warming since the early to middle 1800's (Keeling et al., 1989). Absolute $\delta^{18}O$ values over the past ~150 years are as heavy as -9.3 ‰ which is unprecedented over the 2500 year record in core 6 (Fig. 33). However, a 1 ‰ increase in $\delta^{18}O$ would indicate an ~3 °C summer temperature rise, assuming that the entire isotopic shift is temperature dependent. Mean global surface temperatures have risen by only ~0.5 °C since the mid-1800's. However, part of this observed increase in $\delta^{18}O$ values from Green Lake over the past ~150 years could also be due to an increase of moisture from warm, isotopically heavy Gulf of Mexico air masses, and/or evaporative enrichment.

To elucidate the potential causes of enriched and depleted $\delta^{18}O$ values in Green Lake throughout the last century, a calibration using regional climate data was performed. Figure 34 shows the graphical comparison of $\delta^{18}O$ values from ~1900 to 1980 A.D. with yearly average summer temperatures for Syracuse, N.Y. When the temperature data is smoothed (a 15% running average function was utilized to remove interannual variability) decadel trends are evident that display a remarkable correlation (r= .86) with $\delta^{18}O$ values (Fig. 34). Periods of cooler temperatures (1910 to 1930 and 1950 to 1970) correlate with isotopically depleted values while warmer periods (1900's and the late 1930's to early 1940's) correlate with isotopically enriched values. However, if the $\delta^{18}O$ values were solely recording surface water temperatures in Green Lake during these periods, the exact opposite relationship would be observed (i.e. cool periods represented by isotopically enriched values). Therefore, the dominant control on the $\delta^{18}O$ carbonate signature must be a function of the water composition in Green Lake, which is largely controlled by the type of airmass bringing precipitation into the area. As stated above, enriched values could be due to an increase of moisture from warmer temperature, isotopically heavy Gulf of Mexico source air masses while depleted values may result from cooler temperature, isotopically depleted Canadian or Pacific source airmasses. Because Green Lake lies directly below the modern day position of the jet-stream, and the position of the jet-stream controls the type of airmass coming into the region, the Green Lake $\delta^{18}O$ record provides a very sensitive proxy for jet-stream fluctuations and climate change.

Final Comments

From Stop #5 on the northwest shore of Green Lake we will proceed along the path and return to our starting point at the Park's boathouse. Here we can pause for any final comments, discussion or suggestions anyone would like to make regarding the geology, limnology and paleoclimatology of Green Lakes State Park.

Overall we hope you found this field trip educational as well as enjoyable, and that you have gained a better appreciation of the value of Green Lakes State Park as a natural laboratory for the study of fundamental natural processes such as deglaciation, meromixis and whitings as well as the enormous potential of these lakes as archives of a high-resolution record of natural climate variability over the past 10,000 years. Thanks for joining us.

Acknowledgments

We would like to thank Mr. John Livingston (Park Manager) and Green Lakes State Park for permission to conduct research, and Drs. Eugene Domack and Todd Rayne of Hamilton College for inviting us to participate in the 1997 NYSGA fieldtrip program. Funding for paleoclimatological studies was provided by the New York State Geological Survey, the Geological Society of America, and the Syracuse University Graduate School. Special thanks to Dr. Bill Patterson of Syracuse University for field assistance and numerous discussions and Dr. Don Siegel for use of his direct current plasma emmision spectrometer (DCP). Stable isotope analyses were performed at Brown University and radiocarbon dates at the University of Texas as well as the University of Arizona.

References Cited

Alley, R.B., Mayewski, P.A., Sowers, T., Stuiver, M., Taylor, F.C., Clark , P.U., 1997, Holocene climate instability: A prominent, widespread even 8,200 yr ago: Geology, v. 25, p. 483-486.

Anderson, T.W., and Lewis, C.F.M., 1985, Post glacial water level history of the lake Ontario basin: Geol. Assoc. Canada Spec. Paper 30, p. 231-253.

Anderson, W.T., Mullins, H.T., and Ito, E., 1997, Stable isotope record from Seneca Lake, New York: Evidence for a cold paleoclimate following the Younger Dryas: Geology, v. 25, p. 135-138.

Bradley, W.H., 1963, Unmineralized fossil bacteria: Science, v. 141, p. 919-921.

Broecker, W.S., plus six others, 1989, Routing of meltwater from the Laurentide ice sheet during the Younder Dryas cold episode: Nature, v. 341, p. 318-321.

Brunskill, G.J., 1969, Fayetteville Green Lake, New York. II. Precipitation and sedimentation of calcite in a meromictic lake with laminated sediment: Limnol. and Oceanog., v. 14, p. 830-847.

Brunskill, G.J., and Harriss, R.C., 1969, Fayetteville Green Lake, New York. IV. Interstitial water chemistry of the sediments: Limnol. and Oceanog., v. 14, p. 858-861.

Brunskill, G.J., and Ludlam, S.D., 1967, A summary of some studies on the calcareous sediments of Fayetteville Green Lake, New York, in - Jackson, D.F., ed., Some Aspects of Meromixis: Dept. of Civil Engineering, Syracuse University, Syracuse, N.Y., p. 216-243.

Brunskill, G.J., and Ludlam, S.D., 1969, Fayetteville Green Lake, New York. I. Physical and chemical limnology: Limnol. and Oceanog., v. 14, p. 817-829.

Clark, J.V.H., 1849, Onondaga: Reminiscences of earlier and later times: Syracuse, N.Y., Stoddard and Babcock, 229 p.

Culver, D.A., and Brunskill, G.J., 1969, Fayetteville Green Lake, New York. V. Studies of primary production and zooplankton in a meromictic marl lake: Limnol. and Oceanog., v. 14, p. 862-873.

Dean, W.E., 1981, Carbonate minerals and organic matter in sediments of modern north temperate hard-water lakes: SEPM Spec. Pub. No. 31, p. 213-231.

Dean, W.E., and Eggleston, J.R., 1975, Comparative anatomy of marine and freshwater algal reefs, Bermuda and central New York: Geol. Soc. Amer. Bull., v. 86, p. 665-676.

Dean, W.E., and Fouch, T.D., 1983, Lacustrine environment: Amer. Assoc. Petrol. Geol. Mem. 33, p. 98-130.

Deevey, E.S., Nakai, N., and Stuiver, M., 1963, Fractionation of sulfur and carbon isotopes in a meromictic lake: Science, v. 139, p. 407-408.

Dwyer, T.R., Mullins, H.T., and Good, S.C., 1996, Paleoclimatic implications of Holocene lake-level fluctuations, Owasco Lake, New York: Geology, v. 24, p. 519-522.

Eggleston, J.R., and Dean, W.E., 1976, Freshwater stromatolitic bioherms in Green Lake, New York, in - Walter, M.R., ed., Stromatolites: Amsterdam, Elsevier Pub. Co., p. 479-488.

Eggleton, F.E., 1931, A limnological study of the profundal bottom fauna of certain fresh-watr lakes: Ecological Monographs, v. 1, p. 231-331.

Eggleton, F.E., 1956, Limnology of a meromictic, interglacial plunge-basin lake: Trans. Amer. Microscopical Soc., v. 75, p. 334-378.

Fairchild, H.L., 1899, Glacial waters in the Finger Lakes region of New York: Geol. Soc. Amer. Bull., v. 10, p. 57-66.

Fairchild, H.L., 1909, Glacial waters in central New York: N.Y. State Mus. Bull., 127, 66 p.

Gibson, J.N., 1925, A study of the Fayetteville-Kirkville, New York, Green Lakes area with special reference to its recreational uses as a state park: M.S. Thesis, SUNY-ESF, Syracuse, New York, 113 p.

Hand, B.M., 1978, Syracuse meltwater channels: NYSGA Fieldtrip Guidebook 50, Syracuse, N.Y., p. 286-314.

Hand, B.M., and Muller, E.H., 1972, Syracuse channels: Evidence of a catastropic flood: NYSGA Fieldtrip Guidebook 44, Hamilton, N.Y., p. I-1 to I-12.

Harman, W.N., 1970, Alterations in the molluscan fauna of a meromictic marl lake: Nautilus, v. 84, p. 21-30.

Harrison, S.P., 1989, Lake levels and climate change in eastern North America: Climate Dynamics, v. 3, p. 157-167.

Howe, M.A., 1932, The geologic importance of the lime secreting algae: U.S. Geol. Surv. Prof. Paper 170-E, p. 57-69.

Karlen, W., and Kuylenstierna, J., 1996, On solar forcing of Holocen climate: Evidence from Scandinavia: The Holocene, v. 6, p. 359-365.

Keeling, C.D., plus seven others, 1989, A three dimensional model of atmospheric CO_2 transport based on observed winds. 1. Analysis of observation data, in - Peterson, D.H., ed., Aspects of Climate Variability in the Pacific and Western Americas: Amer. Geophys. Union, Wash., D.C., p. 165-236.

Larsen, E., Sejrup, H.P., Johnsen, S.J., and Knudsen, K.L., 1995, Do Greenland ice cores reflect NW European interglacial climate variations?: Quat. Res., v. 43, p. 125-132.

Liao, X., Street-Perrott, A., and Mitchell, J.F.B., 1994, GCM experiments with different cloud parameterization: Comparison with paleoclimatic reconstructions for 6000 years B.P.: Paleoclimates, v. 1, p.99-123.

Ludlam, S.D., 1969, Fayetteville Green Lake, New York. III. The laminated sediments: Limnol. and Oceanog. v. 14, p. 848-857.

Ludlam, S.D., 1974, Fayetteville Green Lake, New York. VI. The role of turbidity currents in lake sedimentation: Limnol. and Oceanog., v. 19, p. 656-664.

Ludlam, S.D., 1981, Sedimentation rates in Fayetteville Green Lake, New York, USA: Sedimentol., v. 28, p. 85-96.

Miner, N.A., 1933, The origin and history of Green and Round Lakes in Green Lakes State Park at Fayetteville, New York: M.S. Thesis, Syracuse University, Syracuse, New York, 47 p.

Muller, E.H., 1967, Geologic setting of Green and Round Lakes near Fayetteville, New York, in - Jackson, D.F., ed., Some Aspects of Meromixis: Dept. Civil Engineering, Syracuse University, Syracuse, New York, p. 96-121.

Muller, E.H., and Prest, V.K., 1985, Glacial lakes in the Ontario basin: Geol. Assoc. Canada Spec. Paper 30, p. 213-229.

Muller, E.H., and Calkin, P.E., 1993, Timing of Pleistocene glacial events in New York State: Can. Jour. Earth Sci. , v.30, p. 1829-1845.

Mullins, H.T., in prep., Lacustrine marls of the Cayuga Lake Basin, New York: A stratigraphic record of century-to-millennial scale climate change during the past 11,000 years: Jour. Sed. Res.

Mullins, H.T., plus six others, 1996, Seismic stratigraphy of the Finger Lakes: A continental record of Heinrich event H-1 and Laurentide ice sheet instability: Geol. Soc. Amer. Spec. Paper 311, p. 1-35.

Nesje, A., and Kvamme, M., 1991, Holocene glacier and climate variations in western Norway: Evidence for early Holocene glacier demise and multiple Neoglacial events: Geology, v. 19, p. 610-612.

Rozanski, K., Araguas-Araguas, L., and Gonfiantini, R., 1993, Isotopic patterns in modern global precipitation: Amer. Geophys. Union Mon. 78, p. 1-36.

Sissons, J.B., 1960, Submarginal, marginal and other glacial drainage in the Syracuse-Oneida area, New York: Geol. Soc. Amer. Bull., v. 71, p. 1575-1588.

Stuiver, M., 1968, Oxygen-18 content of atmospheric precipitation during the last 11,000 years in the Great Lakes region: Science, v. 162 , p. 994-997.

Stuiver, M., 1970, Ocygen and caron isotope ratios of fresh-water carbonates as climatic indicators: Journal of Geophysical Research, v. 75, p. 5247-5257.

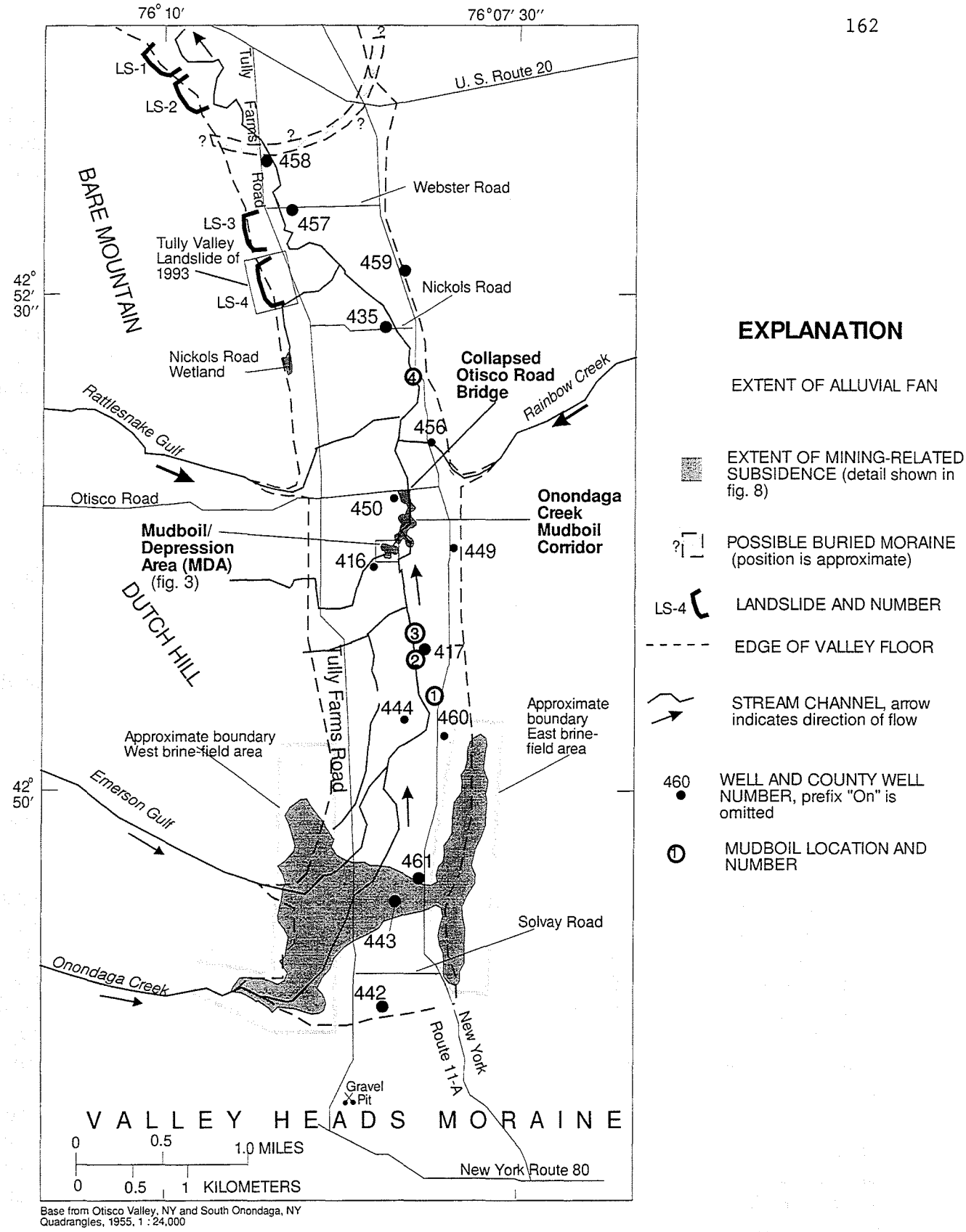

Figure 2. Principal geographic features of the Tully Valley showing wells, brinefield areas, landslides, and mudboil areas. (From Kappel and others, 1996, fig. 2.)

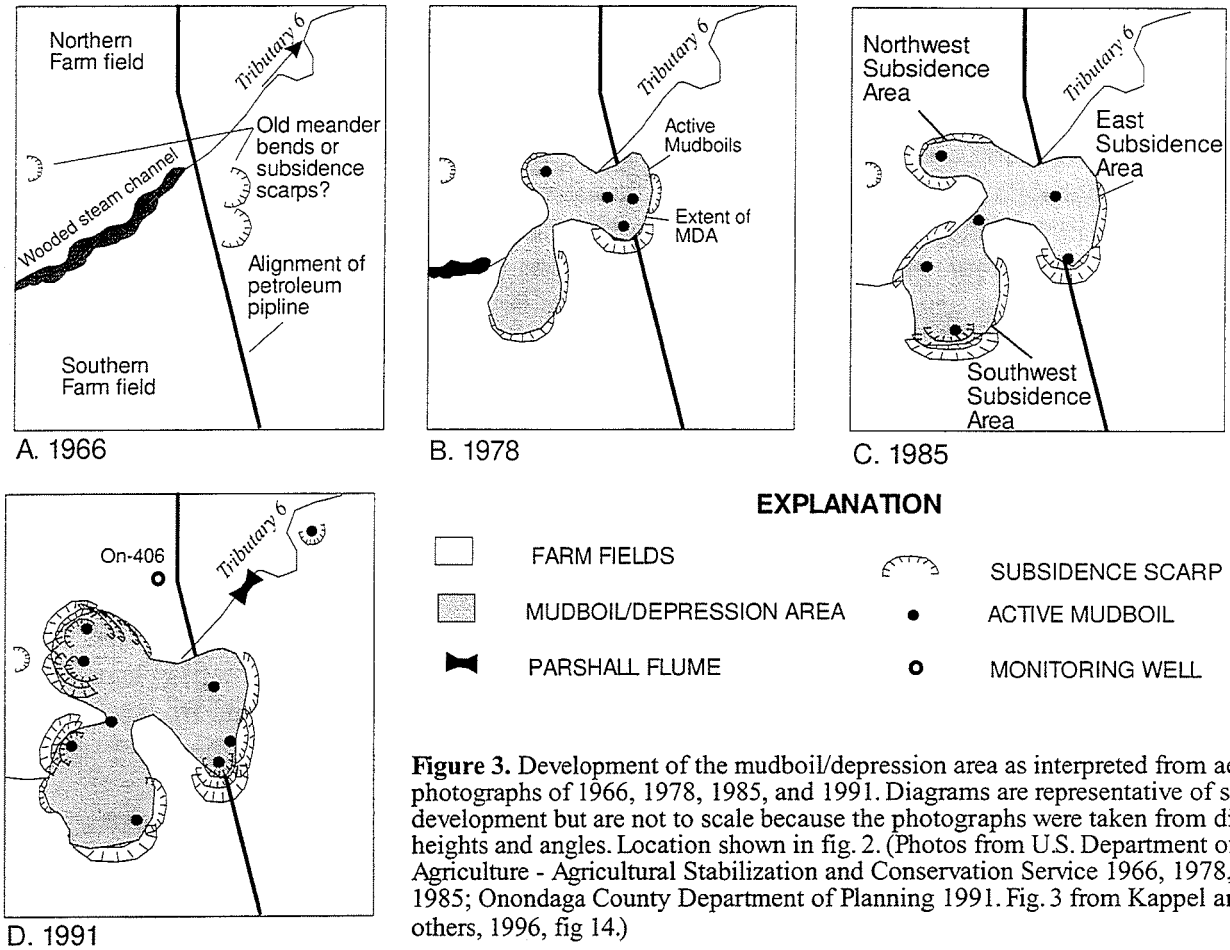

Figure 3. Development of the mudboil/depression area as interpreted from aerial photographs of 1966, 1978, 1985, and 1991. Diagrams are representative of scarp development but are not to scale because the photographs were taken from differing heights and angles. Location shown in fig. 2. (Photos from U.S. Department of Agriculture - Agricultural Stabilization and Conservation Service 1966, 1978, and 1985; Onondaga County Department of Planning 1991. Fig. 3 from Kappel and others, 1996, fig 14.)

The topographic character of the east-facing slope of the Bare Mountain hillside from Route 20 south to Otisco Road is much different from that of the other slopes in the valley. The base of the hillside is generally less steep near the valley floor, and the middle and upper slopes do not have deeply incised stream channels such as are found elsewhere in the Tully Valley. The colluvial soils and weathered bedrock on this slope allow greater water storage than do other slopes in the valley, which allow water to drain more freely to incised stream channels and flow to the valley floor. The massive Tully Limestone is found near the top of Bare Mountain, and, in several areas, is exposed as a straight wall; in one location the wall is more than 1,000 feet long and about 40 feet high (known locally as the 'Grand Canal') and these features have secondary ridges below them. The ridgetop contains fracture traces and blocklike features aligned with the Grand Canal. The flow of water from the ridgetop to the valley floor is most likely through internal (subsurface) drainage in the colluvial soils as well as through the fractured and weathered shale bedrock. A detailed discussion of the bedrock structure of the Bare Mountain hillside is given by Drs. Robert Fakundiny and Carleton Brett, in this volume.

Mudboils, or "mud volcanoes", are found on the floor of the Tully Valley near Onondaga Creek, south of the Rattlesnake and Rainbow alluvial fans. Intermittent mudboil activity has also been reported in the backscarp of the 1993 landslide area. The mudboils are small, volcanolike cones of fine sand and silt that range from several inches to several feet high, and from several inches to more than 30 feet in diameter. In some areas these mudboils can be dynamic ebb-and-flow features that erupt and form large cones of sediment within several days and cease flowing soon thereafter; others may discharge continuously for several years. Mudboils can discharge either freshwater or brackish water and together have discharged as much as 30 tons of sediment per day to Onondaga Creek. Associated with the mudboil discharge is land-surface subsidence due to the removal of fine-grained sediment at depth. More than 15 feet of land subsidence has occurred in a 5-acre area in which active mudboils have been erupting since the mid 1970's. (fig. 3). A discussion of the hydrogeology of the Tully Valley mudboils is given by this author, in this volume.

The geologic and hydrologic characteristics of the Tully Valley are typical of the Finger Lake valleys of central New York. Anomalous conditions in the central part of the valley floor and along the east-facing Bare Mountain hillside create unique hydrogeologic conditions that may have been exacerbated by man's activities. The following articles describe some noteworthy features of the valley and the research taking place.

REFERENCES CITED

Chute, N. E., 1964, Structural features in the Syracuse area, *in* New York State Geological Association Guidebook, 36th annual meeting: Syracuse, N.Y., Syracuse University, Department of Geology, p. 74-79.

Cooper, G. A., 1930, Stratigraphy of the Hamilton Group of New York, parts 1 and 2: American Journal of Science, 5th series, v. 19, p. 116-164.

DeGroff, E. R., 1950, Joint patterns in central New York: Syracuse, N.Y., Syracuse University, Department of Geology, master's thesis, 75 p.

Durham, Forrest, 1954, The geomorphology of the Tioughnioga River of central New York: Syracuse, N.Y., Syracuse University, Department of Geology, Ph.D. dissertation, 60 p.

Fickies, R.H., 1993, A large landslide in Tully Valley, Onondaga County, New York: Association of Engineering Geologists News, v. 36, no. 4, p. 22-24.

Fielding, H. K., 1956, The stratigraphy and structure of the southern half of the 7.5 minute South Onondaga quadrangle, Syracuse, N.Y., Syracuse University, Department of Geology, master's thesis, 81 p.

Faltyn, N. E., 1957, Seismic exploration of the Tully Valley overburden: Syracuse, N.Y., Syracuse University, Department of Geology, master's thesis, 145 p.

Getchell, F. A., 1983, Subsidence in the Tully Valley, New York: Syracuse, N.Y., Syracuse University, Department of Geology, master's thesis, 108 p.

Grasso, T. X., 1966, Faunal zones of the middle Devonian Hamilton Group in the Tully Valley of central New York: Ithaca, N.Y., Cornell University, master's thesis, 64 p.

_____ 1970, Proglacial lake sequence in the Tully Valley, Onondaga County, *in* New York State Geological Association Guidebook, 42nd annual meeting: Syracuse, N.Y., Syracuse University, Department of Geology, p. J1-J16.

Higgins, G.L., 1955, Saline ground water at Syracuse, New York: Syracuse, N.Y., Syracuse University, Department of Geology, master's thesis, 72 p.

Holmes, C.D., 1939, Pleistocene geology of the region south of Syracuse, New York: Syracuse, N.Y., Syracuse University, Department of Geology, doctoral thesis, 187 p.

Jäger, Stephan, and Wieczorek, G.F., 1994, Landslide susceptibility in the Tully Valley area, Finger Lakes Region, New York: U.S. Geological Survey Open-file Report 94-615, 1 pl, scale 1:50,000.

Kappel, W.M., Sherwood, D.A., and Johnston, W.H., 1996, Hydrogeology of the Tully Valley mudboils and characterization of mudboil activity, Onondaga County, New York: U.S. Geological Survey Water-Resources Investigations Report 96-4043, 71 p.

Koch, G.H., 1932, The hydrology of the Onondaga drainage basin: Syracuse, N.Y., Syracuse University, Department of Geology, master's thesis, 61 p.

Larkin, J. W., 1950, Tully brine well data and brief history: Solvay, N. Y., The Solvay Process Division - Allied Chemical and Dye Corporation, Memo dated March 21, 1950, 18 p.

Leutz, Willard P., 1959, Stratigraphy and paleontology of the Salina Group in central New York: Columbus Oh., Ohio State University, Department of Geology, Ph.D. dissertation, 463 p.

Mosley, J. D., 1983, A reconnaissance of the water resources of the Tully Moraine and the adjacent unconsolidated glacial deposits: Syracuse, N.Y., State University of New York, - College of Environmental Science and Forestry, master's thesis, 277 p.

Mullins, H. T., Wellner, R. W., Petruccione, J. L., Hinchey, E. J., and Wanzer, Steven, 1991, Subsurface geology of the Finger Lakes region, 63rd annual meeting: *in* New York State Geological Association Guidebook, Oneonta, N.Y., State University of New York at Oneonta, p. 1-54.

Phillips, J. S., 1955, Origin and significance of subsidence structures in carbonate rock overlying evaporites in Onondaga County, central New York: Syracuse, N.Y., Syracuse University, Department of Geology, master's thesis, 143 p.

Von Engeln, O. D., 1921, The Tully glacial series, *in* Sixteenth Report of the Director of the State Museum and Science Department: New York State Museum Bulletin, Albany, N.Y., nos. 227 & 228, p. 39-62.

_____, 1961, The Finger Lakes region, its origin and nature: Cornell University Press, Ithaca, N.Y., 156 p.

Walker, S. E., and Mahoney, R. J., 1993, Interpreting and projecting long-term environmental conditions in a shallow brine field: Woodstock, Il., Solution Mining Research Institute, 1993 Solution Mining Research Institute Spring Meeting, Syracuse, N.Y., 27 p.

Winkley, S. J., 1989, The hydrogeology of Onondaga County: Syracuse, N.Y., Syracuse University, Department of Geology, master's thesis, 171 p.

Yanosky, T. M. and Kappel, W. M., 1997, Effects of solution mining of salt on wetland hydrology as inferred from tree rings: Water Resources Research, v. 33, no. 3, p. 457-470.

Glacial Lithostratigraphy of the Tully Valley Onondaga County, New York

Donald L. Pair
Department of Geology, University of Dayton
Dayton, OH, 45469-2364
pair@neelix.udayton.edu

Introduction

The glacial history of the Tully Valley and the surrounding region (Figure 1) has received the attention of the New York State Geological Association through field trips spanning almost the last 35 years. The area's spectacular glacial topography has been featured on NYSGA trips led by Muller (1964), Grasso (1970), Kirkland (1970), Hand and Muller (1972), Andrews and Jordan (1978), Hand (1978, 1992), and Mullins et al. (1991). The 1997 NYSGA trip to the Tully Valley will continue to rely heavily upon the ideas and interpretations found in those guidebooks for a regional picture of the area's glacial heritage. However, mudboils, landslides, subsidence, and other phenomena in the Tully Valley (see Kappel et al. (1996), and this guidebook) have necessitated a shift from an emphasis on the landforms (or morphostratigraphy) to one that focuses more on the nature and origin of the sediments (or lithostratigraphy). This effort has already been greatly advanced by the publication of Kappel et al. (1996). In addition, recent surficial mapping at a 1:24,000 scale accompanied by sedimentologic studies of new exposures and compilation of available subsurface data from the area north of the Tully Moraine (Pair, 1995; Pair and Gomes, 1997) has hopefully clarified specific parts of the glacial history. What follows is a summary of the lithostratigraphic framework developed for use in understanding the nature, distribution, and potential hazards associated with sediments found in the Tully Valley.

Pleistocene Deposits

Glacial Till

Glacial till in the Tully Valley is comprised of a mixture of unsorted to poorly sorted clay, silt, sand, to boulder sized diamict. It may be highly compacted and is clay-rich in the floor of the valley. Till can be 2-20 meters thick in the uplands and on the sides of valleys, and greater than 30 meters thick in the floor of the valley. The surface of this unit is drumlinized in the uplands northwest of the Tully Valley.

Ice Contact Sand and Gravel

A unit of coarse to fine sand and gravel, poorly to well stratified and/or sorted, was deposited adjacent to the ice margin. The thickness of these sediments is variable (2-20 meters) and they are commonly associated with kame and kettle topography like that found on the surface of the Tully Moraine (Figure 2). Similar materials are also found at several other locations to the north on valley slopes and adjacent uplands where the ice margin stabilized temporarily and built ice-marginal landforms.

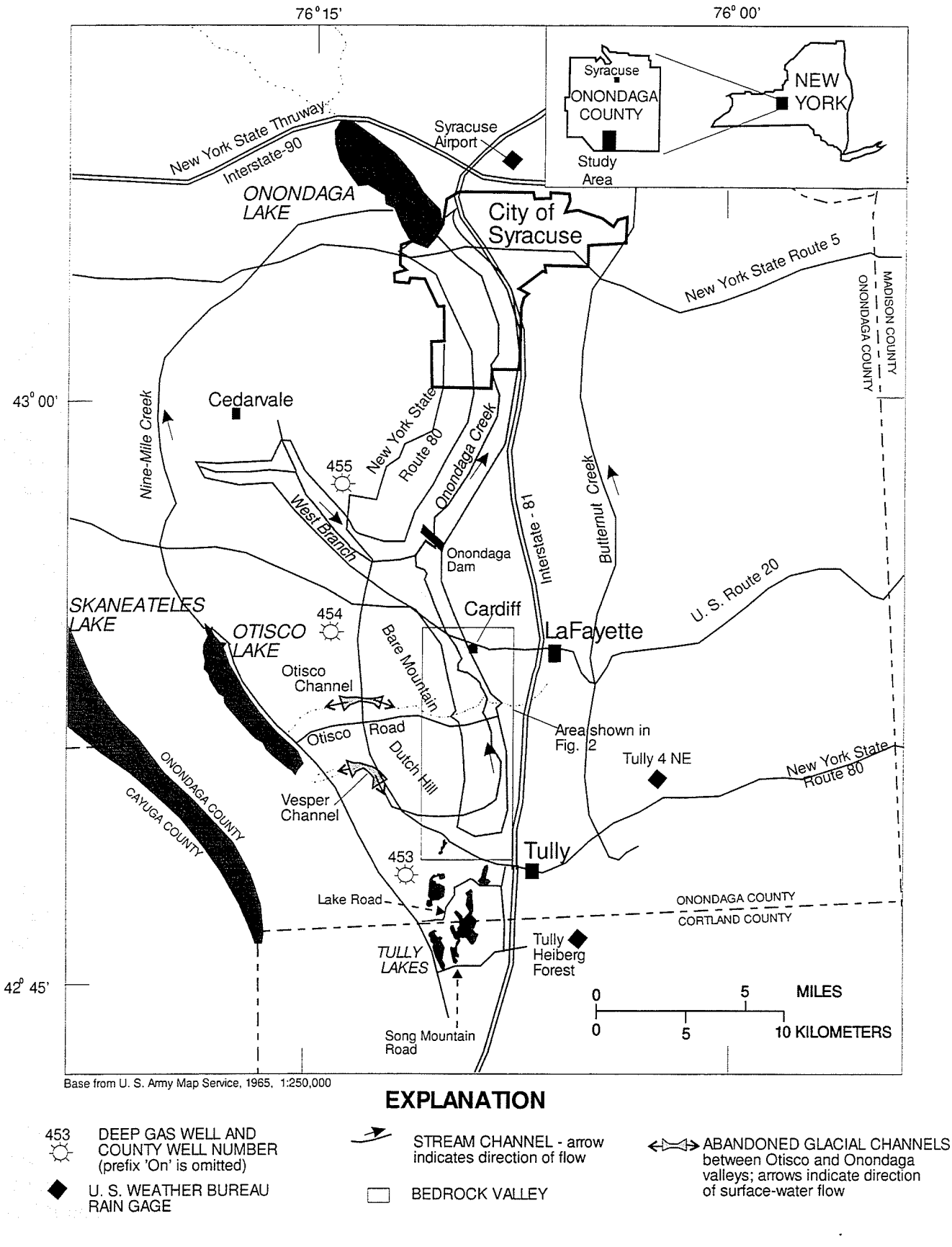

Figure 1. Location and pertinent geographic features of the Tully Valley, in southen Onondaga County, N.Y. (From Kappel and others, 1996, fig. 1.)

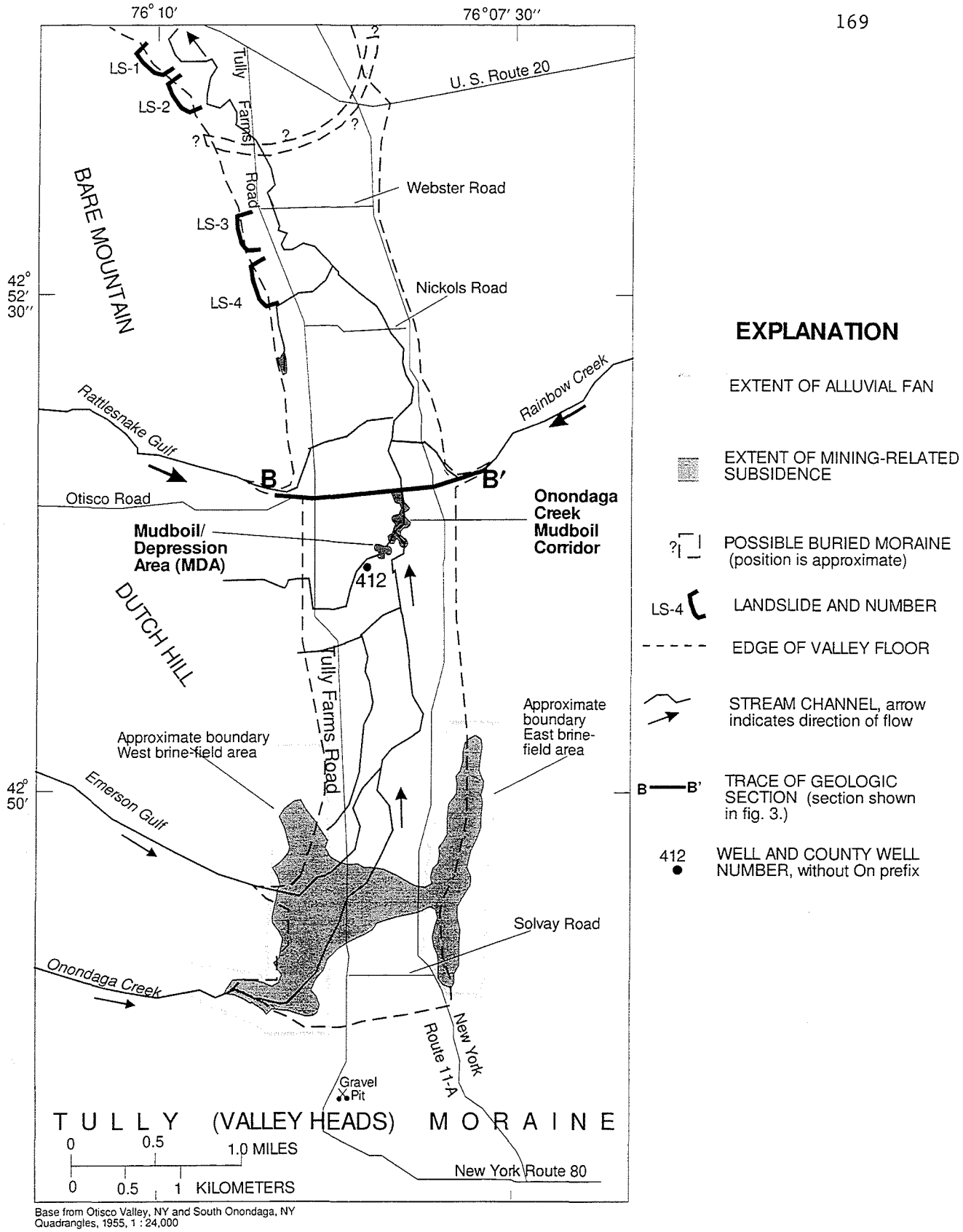

Figure 2. Principal geographic features of the Tully Valley showing glacial stratigraphic well On-412, brinefield areas, landslides, mudboil areas, and geologic section B-B′ (Geologic section shown in fig. 3. From Kappel and others, 1996, fig. 2)

Glaciolacustrine Silt and Clay

Laminated silt and clays found in the Tully Valley were deposited in proglacial lakes formed by the impoundment of meltwater between the Tully Moraine and the receding ice margin. Their thickness ranges from 3-100 meters depending on location in the valley. The clay fractions of these sediments are characteristically red in color and can include both isolated lenses of sand and gravel as well as pebbly, weakly graded diamictons interpreted as underflow (turbidites, debris flows etc.) deposits that emanated from the adjacent ice margin, moraine slopes, or valley walls. Well logs suggest that these fine-grained sediments may be ubiquitous beneath much of the valley floor.

The sequence of events associated with the deposition of these glaciolacustrine sediments remains unclear. Subsurface data and studies of new exposures indicate that the ice margin oscillated and readvanced southward towards the Tully Moraine and overrode previously deposited lake sediments. Kappel et al. (1996) logged a 3-m thick layer of dense clay till 51 m below the land surface from an exploratory hole along Otisco Road (Figure 3) which they interpreted to be the result of the compaction of lacustrine sediments by a readvance. Gomes and Pair (1997) noted the presence of tilted and glaciotectonically deformed glaciolacustrine units at a number of new exposures just north of the Tully Moraine and Gomes (1996) inferred from consolidation tests that the clays had been overridden. Based on these observations, it seems likely that glaciolacustrine deposition in the Tully Valley may have been punctuated by a number of ice marginal fluctuations.

Alluvium Overlying Lacustrine Silt and Clay

This lithostratigraphic unit includes fluvial deposits, composed of poorly stratified silt, sand, and clay, underlain by laminated silt and clay (thickness 3-30 meters). It constitutes a very important surficial unit as it is found in subsurface records and in scarp exposures at the site of the 1993 landslide. This unit indicates areas where lacustrine sediments deposited in a glacial lake have been mantled by younger alluvium or are found intercalated with alluvium. The alluvium is a remnant of earlier higher fluvial surfaces initiated as the water level of proglacial lakes in the Tully Valley dropped.

Well logs and available exposures suggest that portions of the unit near valley walls may be comprised of coalescing alluvial fans formed during periods of high discharge following deglaciation. It should also be noted that the same glacial-postglacial processes responsible for the deposition of this unit also existed in other nearby valleys and that these materials may be present at the base of other slopes in the region.

Fluvial Silt, Sand, and Gravel

A unit 20-60 meters thick of coarse to fine silt, sand, gravel, and cobbles represent a complex of outwash, outwash delta, and fluvio-deltaic sediments. These materials are found at the north end of the valley near Syracuse and were deposited during deglaciation and concomitant ice-marginal drainage from the Cedarvale Channel (Figure 1) to the west into proglacial lakes occupying the Tully Valley. The elevation of the upper surface of these deposits is graded to the

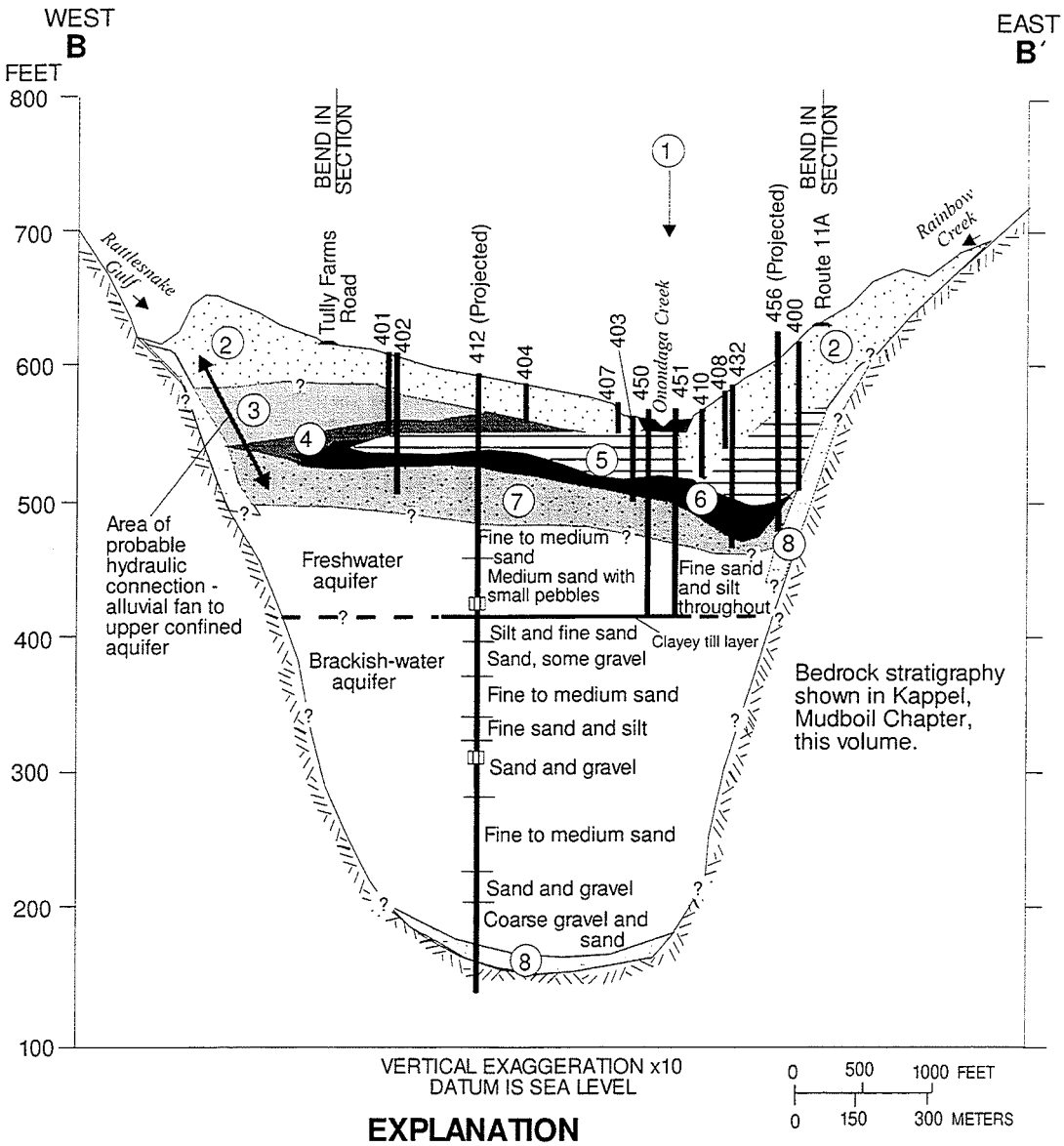

EXPLANATION

ALLUVIAL DEPOSITS

(1) FLOODPLAIN AND MUDBOIL DEPOSITS - Silt, sand and gravel deposited by Onondaga Creek and upstream mudboils.

(2) FANS - Sand and gravel deposited by Rattlesnake Gulf and Rainbow Creek.

LACUSTRINE DEPOSITS

(3) LAMINATED SAND AND SOME SILT/CLAY - Mostly fine to medium sand interbedded with minor amounts of silt and clay deposited by Rattlesnake Gulf as it flowed into a proglacial lake.

(4) LAMINATED SAND AND SILTY CLAY - Approximately equal parts of very fine sand interbedded with silty-clay that settled-out farther in the proglacial lake.

(5) LAMINATED SILTY CLAY WITH SAND - Mostly silty clay interbedded with occasional layers of medium-to-fine sand that settled out farthest in the proglacial lake. Coarser sand is found along Otisco Road; finer sand-to-silt wisps are found farther north and south of Otisco Road. Forms the top of confining unit over the liquifiable sand and silt unit in the mudboil areas.

LACUSTRINE DEPOSITS (cont'd)

(6) CLAY AND SILT - Massive unit that generally covers most of the valley floor north and south of mudboil areas. Forms confining unit over upper aquifer and grades from clay at surface to silt at depth.

(7) SILT AND SAND - Massive, grading from silt and very fine sand at the top to medium to coarse sand and fine gravel with silt at the bottom. Unit is under artesian pressure and forms upper confined aquifer.

OTHER GLACIAL DEPOSITS

(8) TILL - A dense unit of sand, gravel,and boulders embedded in a clay matrix. This unit may underlie entire glacial sequence in the valley.

BEDROCK

410 WELL AND NUMBER, without "On" prefix

MONITORING ZONE, steel casing perforated after hydraulic testing of deeper bedrock zones and grouting of the bedrock section of deep well On-416.

Figure 3. Geologic section B-B′ showing upper unconsolidated deposits along Otisco Road and deeper unconsolidated deposits projected from well On-412, southwest of the mudboil/depression area. (Location of section shown in fig. 2.. From Kappel and and others, 1996, Figure 6.)

water level of glacial lakes occupying the valley. The water levels of these lakes were controlled by the opening of progressively lower spillways as the ice margin retreated northward.

Holocene and Recent Deposits

Alluvium and Alluvial Fans

Floodplain deposits, composed of poorly stratified silt, sand, and clay were deposited along the banks of Onondaga Creek and associated tributaries. The distribution of these deposits on the valley floor indicate the lateral migration of the channel of Onondaga Creek. A unit of poorly sorted and stratified silt, sand, and gravel deposited as fans at the base of steep slopes has also been identified where a discernible fan landform can also be identified. Materials comprising these fans are fluvially reworked from glacial materials derived from the uplands and valley walls. Well developed fans are particularly evident along valley walls where tributaries drain the adjacent uplands. These fans may have been formed in postglacial time by high discharge during wet periods (cf. Wellner and Dwyer, 1996).

Colluvium

A mixture of unsorted fine clay to coarse boulder material deposited by mass wasting is found on the slopes of the Tully Valley in several locations. Interestingly, this unit is particularly extensive on the east slope of Bare Mountain above the 1993 and older landslide locations.

Acknowledgments

Surficial geological mapping was supported through USGS Statemap Program and the New York State Geological Survey. Additional support for Dr. Don Pair and undergraduate field assistants was provided by University of Dayton.

References

Andrews, D.E., and Jordan, R., 1978, Late Pleistocene history of south-central Onondaga County, in Merriam, D.F. ed., New York State Geological Association guidebook for the 50th annual meeting: Syracuse, New York, Syracuse University, p. 315-331.

Gomes, F.J. 1996. Lithostratigraphy and geotechnical properties of Late Wisconsin sediments associated with the Valley Heads moraine complex. Bachelor of Science Thesis, University of Dayton, Dayton, Ohio, 60 p.

Gomes, F.J., and Pair, D.L. 1997. Lithostratigraphy and geotechnical properties of Late Wisconsin sediments associated with the Valley Heads moraine complex, Tully, NY. Geological Society of America, Abstracts with Program, v. 29, p.49.

Grasso, T.X., 1970, Proglacial lake sequence in the Tully Valley, Onondaga County, in Heaslip, W.G., ed., New York State Geological Association guidebook for the 42nd annual meeting: Syracuse, New York, Syracuse University, p. J1-J23.

Hand, B.M., 1978, Syracuse meltwater channels, in Merriam, D.F. ed., New York State Geological Association guidebook for the 50th annual meeting: Syracuse, New York, Syracuse University, p. 286-314.

Hand, B.M., 1992, Late Pleistocene meltwater drainage through central New York, *in,* April, R. H., ed., New York State Geological Association guidebook for the 64th annual meeting: Hamilton, New York, Colgate University, p. 216-233.

Hand, B.M and Muller, E.H., 1972, Syracuse channels: evidence of a catastrophic flood, *in,* McLelland, J. ed., New York State Geological Association guidebook for the 44th annual meeting: Hamilton, New York, Colgate University, p. I1-I12.

Kappel, W.M., Sherwood, D.A., and Johnston, W.H., 1996. Hydrogeology of the Tully Valley and characterization of mudboil activity, Onondaga County, New York, United States Geological Survey Water-Resources Investigations Report 96-4043. 71 p.

Kirkland, J.T., 1970. Deglaciation of the eastern Finger Lakes region, in Heaslip, W.G., ed., New York State Geological Association guidebook for the 42nd annual meeting: Syracuse, New York, Syracuse University, p. F1-F17.

Muller, E.H., 1964. Surficial Geology of the Syracuse field area, *in,* Prucha, J.J., ed., New York State Geological Association guidebook for the 36th annual meeting: Syracuse, New York, Syracuse University, p. 25-35.

Mullins, H.T., Wellner, R.W., Petruccione, J.L., Hinchey, E.J., and Wanzer, S., 1991, Subsurface geology of the Finger Lakes region, *in,* Ebert, J. R., ed., New York State Geological Association guidebook for the 63rd annual meeting: Oneonta, New York, SUNY Oneonta, p.1-54.

Pair, D.L., 1995, The Surficial Geology of the South Onondaga, NY (7.5-minute) Quadrangle. United States Geological Survey - New York State Geological Survey Map no. 2G639, scale 1: 24,000.

Wellner, R.W., and Dwyer, T.R., 1996, Late Pleistocene-Holocene lake-level fluctuations and paleoclimates at Canandaigua Lake, New York, in Mullins, H.T., and Eyles, N., eds., Subsurface geologic investigations of New York Finger Lakes: Implications for Late Quaternary deglaciation and environmental change: Boulder, Colorado, Geological Society of America Special Paper 311, p. 65-76.

Investigation of the 1993 Tully Valley Landslide

D. Negussey, P.A. Burgmeier, C.A. Curran and M. Kawa
Department of Civil and Environmental Engineering,
Syracuse University, Syracuse, NY, USA 13244

Introduction

On April 27, 1993; a large landslide occurred in Tully Valley, in the town of Lafayette, NY (Photo 1). From the base of the east facing slope of Bare Mountain, the slide extended some 0.8 km into the center of Tully Valley. The landslide back scarp is about 400 m long and runs parallel to the north-south aligned valley centerline. Large portions of farm land slumped and displaced. A spread of reddish mud flow covered wide areas of the slide front. A 340 m section of Tully Farms Road was covered by up to 5 m of debris. The volume of displaced soil is in the order of 0.5 million cubic meters. The earth movement lasted about 30 minutes and the slide is believed to be the largest to have occurred in New York State in over 75 years. While there was no loss of life, the property damage included the loss of three homes and about 10 hectares of farm land (Fickies, 1993; Kappel et al, 1996). Following the landslide, several springs developed in the back area of the slide basin. The slide debris over Tully Farms Road was later removed. The near vertical back slope face has now re-graded with subsequent sloughing and talus accumulation. An account of an investigation to identify the nature and possible causes for the 1993 Tully Valley Landslide is given in this paper.

Tully Valley

Tully Valley is located at the foot of the northern edge of the Appalachian Uplands within Onondaga County in Central New York, approximately 20 km south of Syracuse, Fig. 1. Tully Valley is at the southern end of the Onondaga Trough which begins from the Valley Heads Moraine near the town of Tully to the south and extends north toward Onondaga Lake and Syracuse. The U shaped valley floor is about 1.5 km wide. Onondaga Creek flows north along the center of the valley and drains into Onondaga Lake. Tully Valley is sparsely populated and the land use is primarily residential and semi agricultural.

There is suggestive evidence of previous landslide activity in Tully Valley. Three locations of past sliding along the same west side of the valley but to the north of the recent slide are shown in Figure 1. The closest of these earlier slides is only 70 m north of the 1993 slide, and is estimated to have occurred more than 150 years ago (Kappel et al, 1996). Judging by their location and shape, these three previous slides and the recent 1993 slide may have been caused by a similar mechanism. Segments of undisturbed topography that may be susceptible to slide hazard presently exist between these previous slide sites. Other much older slide features have been identified in and around the general vicinity of Tully Valley. These latter prehistoric slides are believed to have been a result of rapid lowering of Pliestocene lakes (Jäeger and Wieczorek, 1994).

From 1889 to 1988, there was intensive salt solution-mining at the south end of Tully Valley about 5 km south of the 1993 Landslide. Deep wells were drilled into salt beds within the Syracuse Formation at depths below 300 m. Fresh water from the nearby Tully Lakes was injected into the deep wells to return as brine through recovery wells. An estimated 90 million metric tons of salt was removed by solution mining (Walker and Mahoney, 1993). The mining process resulted in large scale dissolution and subsidence of up to 15 m over an area of about 2 square kilometers (Kappel et al, 1996). Soon after operation of the brine fields ended in 1988, a groundwater level rise in excess of 20 m was noted at an observation well located more than a kilometer from the extraction site. In subsequent years, the seasonal variation of groundwater levels at this observation well was less than 5 m. Solution mining operations in Tully Valley have altered the groundwater levels and quality within the valley (Getchell, 1983, Rubin et al, 1991, Perkins and Romanowicz, 1996, Kappel et al, 1996). The extent of groundwater level and quality change that may have occurred at the 1993 slide site following the secession of brine mining operations in Tully Valley is not well known.

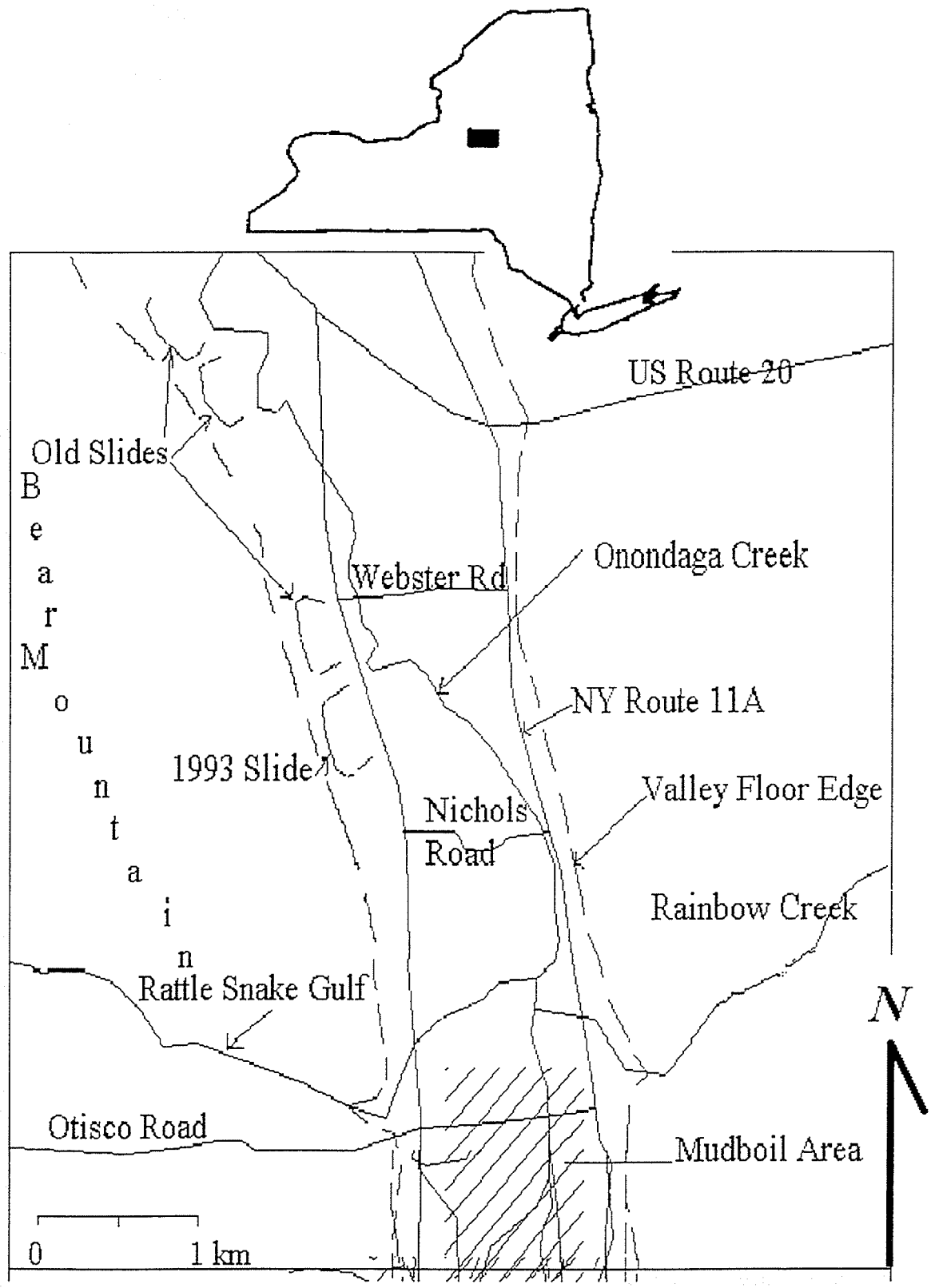

Figure 1 - Tully Valley location and features.

Mudboils were first noted in Tully Valley in 1899, ten years after the start of brine mining operations. Mudboils are volcano-like structures of up to 10 m in diameter that discharge water and fine-grained sediments. The ground surface around a mudboil subsides as sediment is removed from depth. At present, mudboil activity continues at the center of Tully Valley some 2 km south of the 1993 landslide (Figure 1) and resulted in the collapse of the Otisco Road bridge in 1991. Water quality associated with the mudboils range between turbid to clear and fresh to brackish and discharge levels tend to vary seasonally both in quality and quantity (Kappel et al, 1996). Mudboils have developed to a much lesser extent elsewhere and in the 1993 landslide basin.

Geology

The predominant bedrock sequence in Tully Valley consists of shales and limestones that range from late Silurian to middle Devonian age (Getchell, 1983, Kappel et al, 1996). At the slide site (Figure 2), Hamilton Group Shales form the lower part of Bare Mountain and extend below land surface. The Hamilton Group Shales are followed by Onondaga Limestone over Oriskany Sandstone. Below the Oriskany Sandstone lie the Helderberg Group of limestone and dolostone sequence over the Salina Group shale, dolostone and salt beds. Glacial scour at the center of the valley probably extends close to the base of the Helderberg Group and cuts through distinct water bearing bedrock zones including the Oriskany Sandstone and the Onondaga Limestone contacts. The general dip of the bedrock units is to the south at 8 to 16 m per km (Kappel et al, 1996). There are also two major joint sets that have strikes of N8°W and N80°E and dip of 87°W and 88°S, respectively (DeGroff, 1950, Getchell and Muller, 1992). A major fracture set runs through the upper east slope of Bare Mountain at an approximately parallel alignment to the joint strike of N8°W (Kappel et al, 1996). Both the fracture and joint are in line with and may extend to pass through the abandoned brine field at the southern end of the valley.

The thickness of surficial deposits in the valley have been estimated at 120 to 150 m (Faltyn, 1957, Kantrowitz, 1970) and are largely the result of Wisconsin glaciation (Muller, 1964). Glacial activity within the valley resulted in surficial deposits that range from lodgment till along the valley sides and base, fluvial outwash deposits of stratified sand and gravel sequences, and massive thick lacustrine silt and clay units deposited within proglacial lakes. The most prominent post-glacial feature in the valley is the Tully Moraine, a large deposit of mixed drift which seals off the southern end of the Onondaga Trough. The Tully Moraine is part of the Valley Heads Moraine and marks the furthest advance of the Wisconsin ice sheet (Muller, 1964). The massive red lacustrine silty clay unit exists throughout the northern Fingerlakes region of Central New York and is believed to be a proglacial sediment derived from the Vernon Shale of the Salina Group (Blagborough, 1951).

The sand and gravel, mixed drift soil acquifers of Tully Valley are separated by till, glaciolacustrine clay and silt deposits (Getchell and Muller, 1992). As is the case with surface water in Tully Valley, groundwater flows to the north at intermediate and regional scales. Regional scale flow originates from recharge areas in the Appalachian Upland and moves primarily through bedrock aquifers. The Tully Moraine is a source of intermediate scale flow which moves at or near the bedrock-soil interface. Local groundwater flow originates from the valley sides and flows toward the center of the valley recharging the valley surface deposits that act as unconfined aquifers.

Field Investigation

A field investigation program was started in 1995 to define the soil and ground water conditions and identify the probable factors responsible for the 1993 landslide. The landslide area together with locations of boreholes drilled during the field investigation and of natural springs sampled for laboratory testing are shown in Figure 3. Soil samples were recovered from boreholes for laboratory testing and detailed classification. Insitu vane shear strength tests were performed at various depths within the clay soil strata. X-ray diffraction analyses were conducted on clay samples to determine the clay mineral composition. Consolidated undrained triaxial, strain rate controlled consolidation, lab vane shear and Atterberg limit tests were performed on clay samples. Standard penetration testing and split spoon sampling was carried out in the coarse soil formations. Where bedrock was encountered, core samples were obtained for classification and assessment of rock quality. Piezometers and slope indicator casings

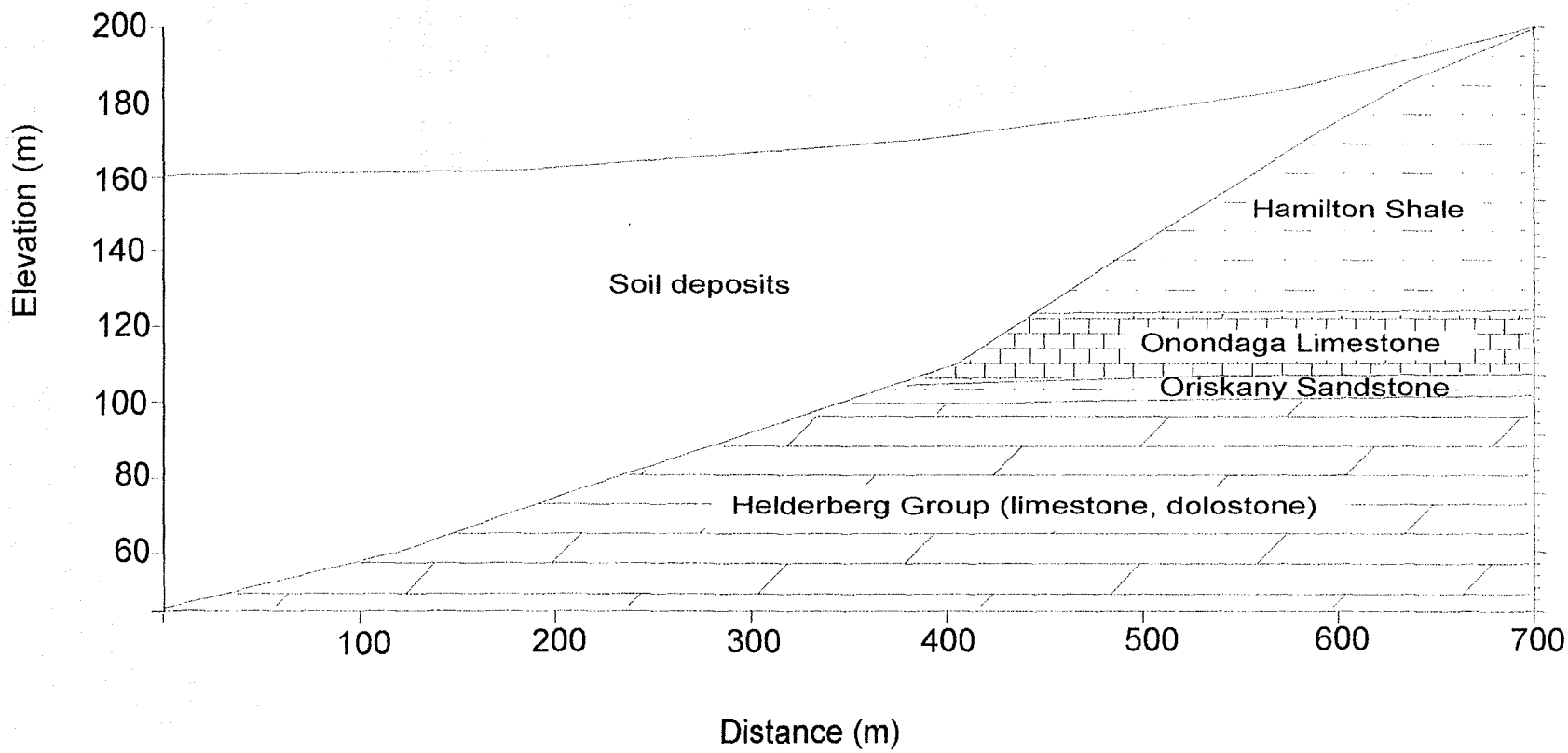

Figure 2 - Bedrock strata at the 1993 Tully Valley Slide

were installed in boreholes for long term monitoring of groundwater pressures and slope movement. Information on depths, elevations and sensors installed in boreholes is summarized in Table 1. A tipping bucket rain gage and ambient temperature sensors have also been installed to record site specific meteorological data. Water samples were collected between January and May 1996 from springs within the slide basin, boreholes and a water well for assessment of temporal and spatial variation of water quality. Temperature and dissolved oxygen measurements were made in the field. Specific conductivity, pH and ion concentrations were determined in the laboratory. More detailed accounts of the geotechnical and water quality investigations will be reported elsewhere (Burgmeier, 1997, Curran, 1997).

Pre-Slide Stratigraphy

A reconstructed cross section of the pre-slide soil stratigraphy is shown in Figure 4. The section was developed from pre-slide topographic contours and borehole records along the north and south edges of the slide as well as within the slide and from the stratigraphy exposed at the back scarp in 1993. The slope of the gently inclined ground surface is about 8°. The red silty clay thins out towards the valley wall. A wedge of sand and gravel resting on the inclined bedrock surface interfingers into the clay layer. The sand and gravel wedge is connected to a varved clay sequence that underlies the massive red clay unit. The varved clay overlies an inclined bed of till like silty sand and gravel. Brown-gray silty clay over fine sand underlies the varved clay and rests on the bedrock floor. In borehole 7, black non-calcareous shale was encountered at elevation 178 m and a depth of 6.3 m below surface. The shale sample is likely a Cardiff Member. Within the slide basin and in borehole 6, dark gray calcareous shale was encountered at elevation 127 m and depth of 39 m below surface. This shale sample is likely a Union Springs member. Both the Cardiff and Union Springs belong to the Marcellous Formation of the Hamilton Group (Grasso, 1966). The top 2 to 5 m depth of both shale units is fractured.

Precipitation and Groundwater Pressure

The long term average seasonal snowfall for the Syracuse area is 2,800 mm. A record total of 4,880 mm of snow fell in the Syracuse area in the 1992-93 season. The snowfall of 561 mm on March 13, 1993 and the total for the month of 1381 mm are also records. There was also additional snowfall of 309 mm in April. The long term precipitation data for the general area is based on weather observations at Syracuse Airport. There was an unusual depth and duration of snow cover in March and April of 1993. However, the water equivalent precipitation for the year (1110 mm) as well as for March (95 mm) and April (166 mm), were above average but have been exceeded in previous years, as in 1976. Selected piezometric observations, Figure 5, indicate seasonal groundwater level changes in the red silty clay are small but more marked changes occur within the coarse strata and in fractured bedrock zones located close to ground surface. Generally, groundwater pressures are lowest in late Summer to early Fall and highest in late winter to early Spring.

Slide Basin Water Quality

The water quality of springs, the locations of which is shown in Figure 3, in the slide basin has been variable. Specific conductance and chemical concentrations varied over a large range throughout the slide area. Springs nearest the face of the landslide scarp and at upper elevations had low total dissolved solids (TDS), with conductivities around 400 mmhos/cm. Springs farther away from the scarp face, toward the center of the slide area, had much higher TDS with specific conductivity values approaching 50,000 mmhos/cm. Water from boreholes varied in TDS according to depth and location, but all borehole samples had TDS ranging from 200 to 1,000 ppm. Brackish and slightly brackish water samples had a strong hydrogen sulfide odor. In general, brackish springs decreased in TDS and specific conductance from April to May. During the winter months, the diluting effect of precipitation and local recharge on the water chemistry was minimal. Piper plots for brackish spring water in the landslide basin, Salina brine as well as brackish mudboil water and bedrock water samples from Deep Well On-416 in the mudboil area are shown in Figure 6. The data for the mudboil sources is scattered. The other three sources show very similar composition. However, the concentrations are highest for the Salina brine followed by the deep

Table 1: Borehole installation summary

BH #	Depth (m)	Elevation (m)	Installation(s)	Completion Date	Comments
1a	4.9	165.8	SP @4.6m	10/29/95	adjacent to BH #1b
1b	30.8	165.8	SI to 30.8m	10/28/95	bentonite plugs; cement backfill; adjacent to BH #1a
2	29.6	177.7	SP @4.6m SP @15.7m PP @16.2m PP @21.9m	10/25/95	VWP and datalogger installed June 21,1996 rainfall gauge location
3	17.2	192.6	SP @7.6m PP @14.0m	10/26/95	bentonite plug above PP; hole terminates in till
4	15.7	193.2	SP @7.5m SP @15.5m	11/8/95	VWP and datalogger installed May 30,1996 hole is located above headscarp
5	16.5	194.5	SI to 16.5m	11/9/95	hole is located above headscarp ; cement backfill
6	39.3	166.1	VWP @7.8m VWP @14.1m VWP @38.3m	10/10/96	hole in center of slide basin VWP and datalogger equipped bedrock @38.3m
7	7.6	184.1	SP @7.0m	10/16/95	VWP and datalogger installed October 19, 1996 ; bedrock @6.1m
8a	29.3	171.9	PP @29.3m	10/11/95	backfilled with bentonite plug and clay cuttings; adjacent to BH #8c
8b	19.8	174.7	SI to 19.4m	10/17/95	cement backfill
8c	11.6	171.9	SP @3.7m PP @11.6m	10/12/95	no sampling; adjacent to BH #8a backfilled with bentonite plug and sand
9a	14.6	164.9	PP @14.6m	10/12/95	no sampling; adjacent to BH #9 ; backfilled with clay cuttings
9b	16.9	164.9	PP @10.7m	10/10/95	adjacent to BH #9; backfilled with clay cuttings

PP - pneumatic piezometer

SP - stand pipe

SI - slope indicator casing

VWP - vibrating wire piezometer

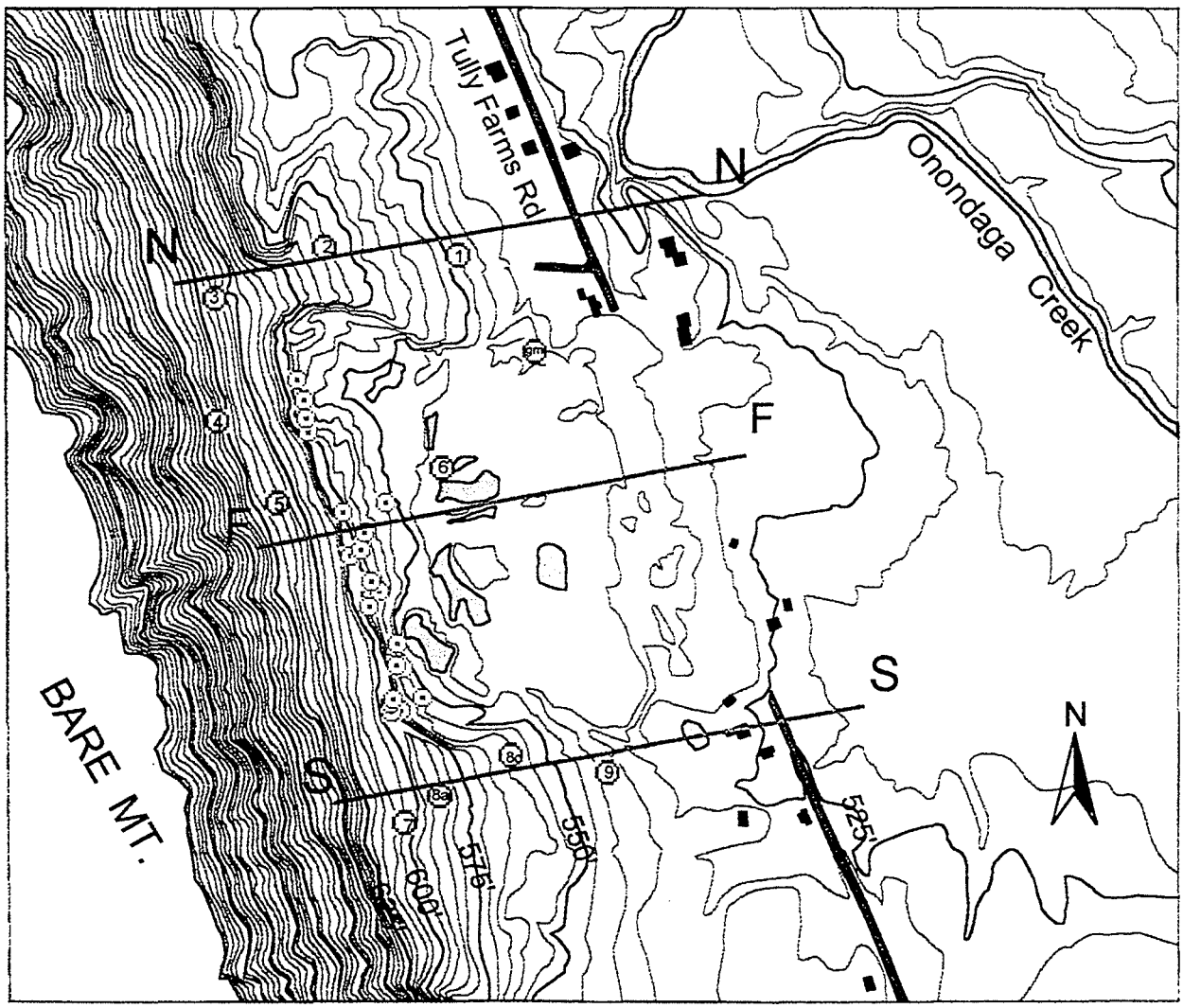

Figure 3 - The 1993 Tully Valley Slide area and locations of boreholes and springs.

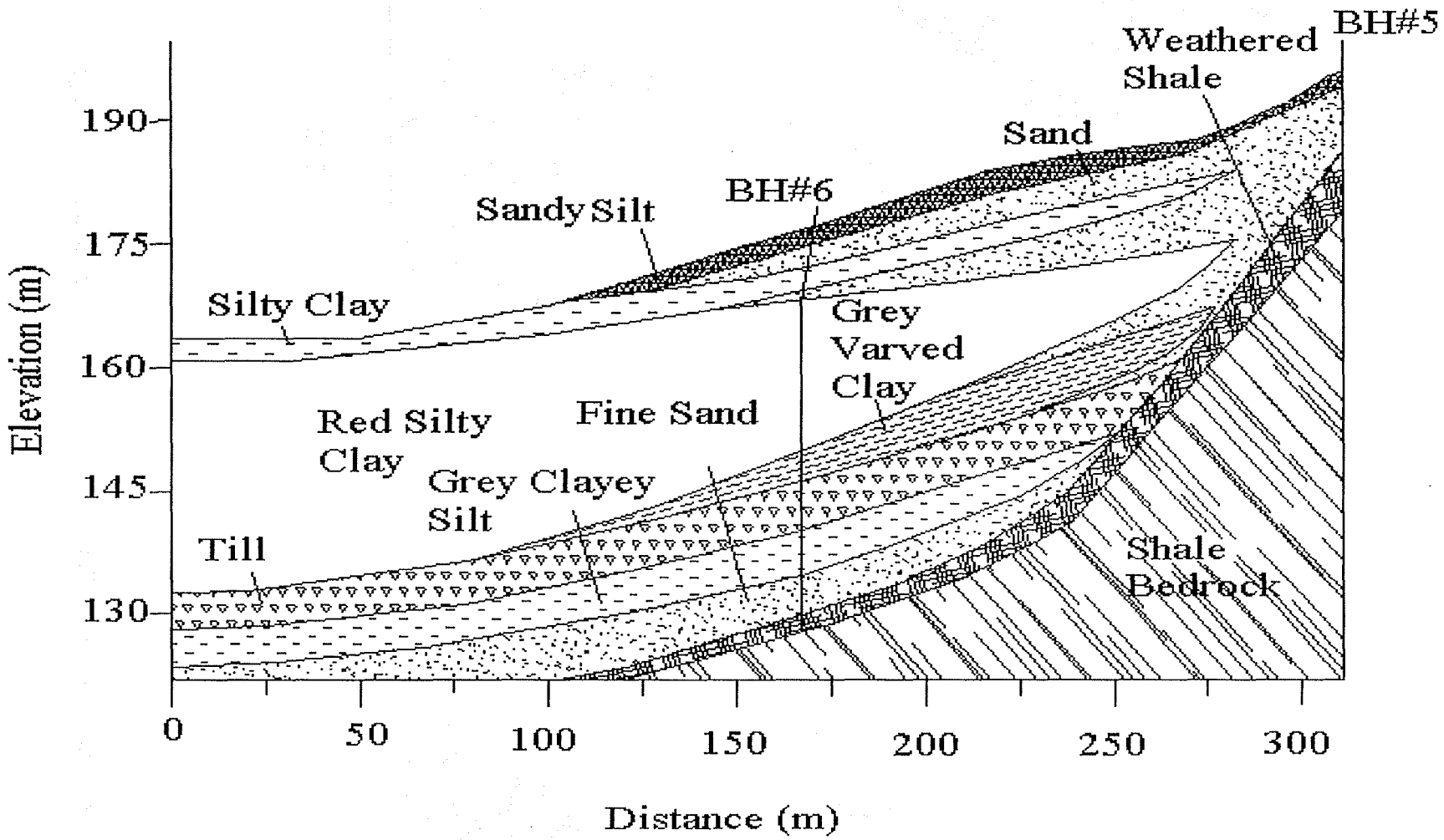

Figure 4 - A reconstructed pre-failure section of the 1993 Tully Valley Slide.

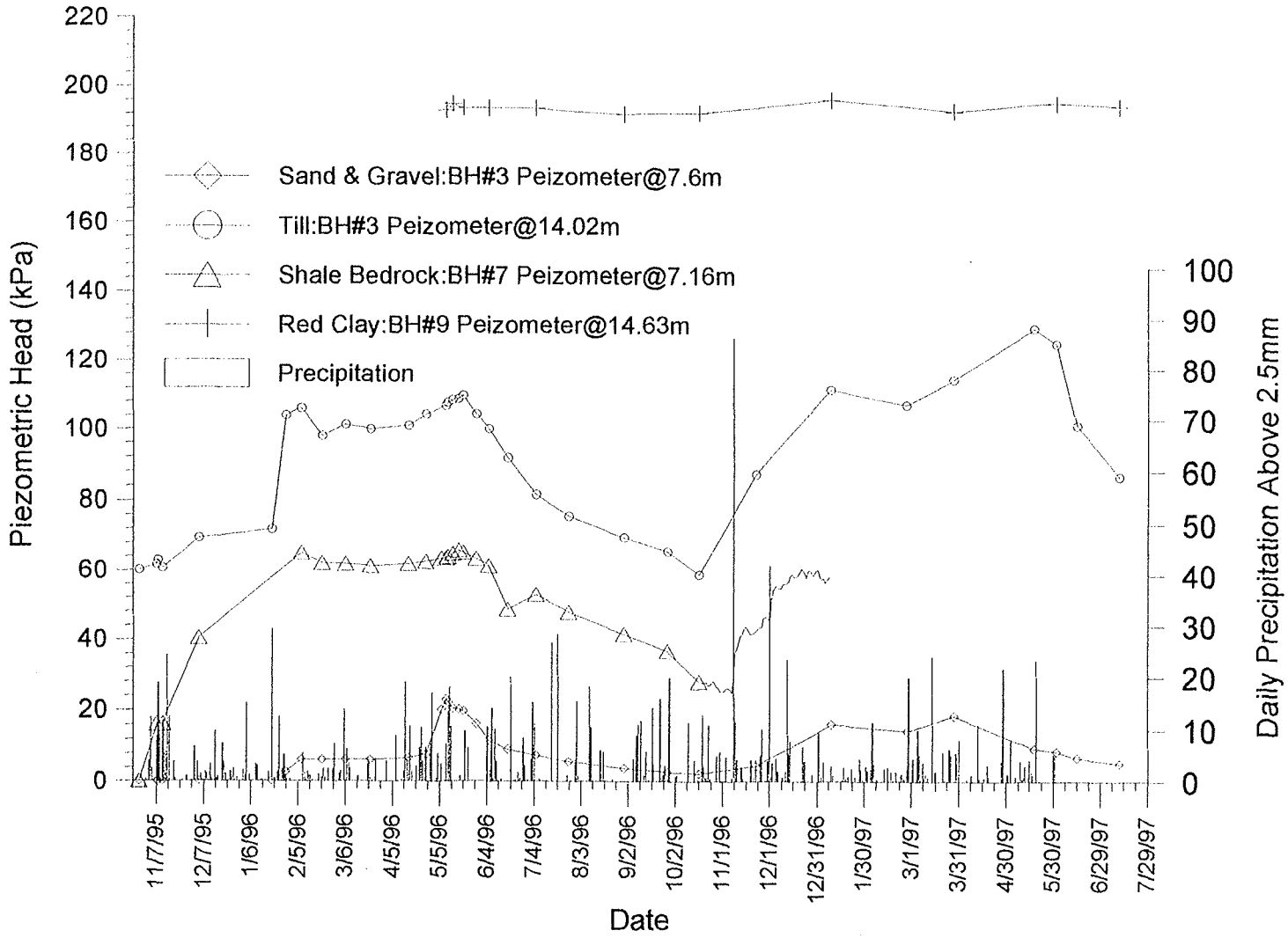

Figure 5 - Changes in groundwater pressure with time in different strata and daily precipitation record for the Syracuse area.

Figure 6a: Brackish Springs

No.	TDS	Source
1	14,600	spring 5
2	22,100	spring 6
3	9,700	spring 7
4	19,100	spring 13
5	38,800	spring 14
6	22,900	spring 15
7	13,500	spring 16

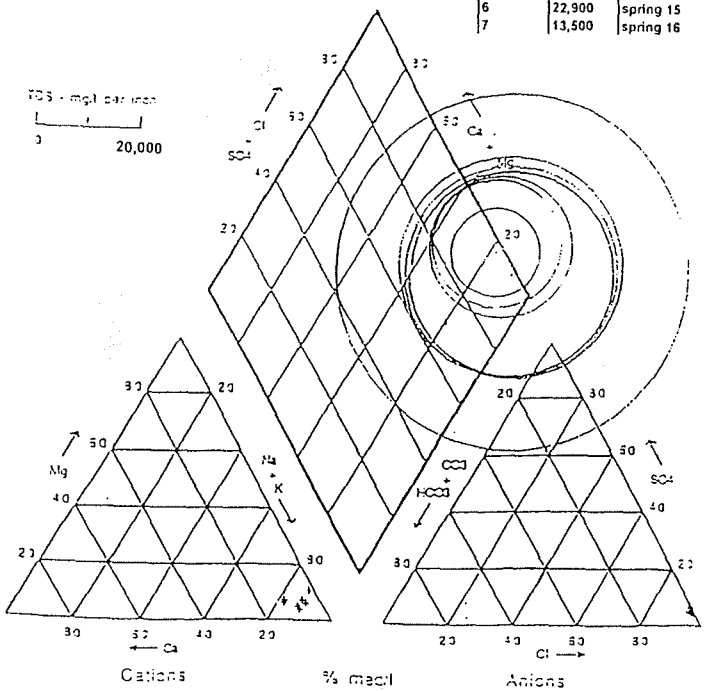

Figure 6b: Salina Salt Unit (Nobel, 1993)

No	TDS	Well Name
1	251345	USGS-1
2	81020	5306(MV-1
3	96967	G174(MV-1
4	299379	G175(RX-4
5	83733	C234(MV-1
6	1238	5303(H-7)
7	1390	C233(H-7)
8	5945	6673(RX-3
9	14324	6672(N-11

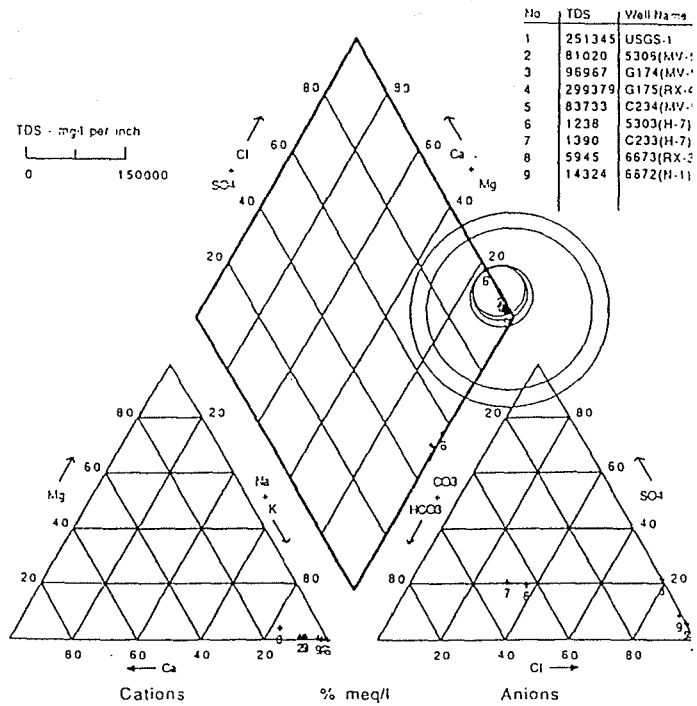

Figure 6c: Mudboils (Kappel, et al 1996)

No.	TDS	Source
1	284	MB1
2	6,760	MB2
3	12,800	MB3
4	290	MB4
5	2,800	MB5
6	686	MB6
7	370	MB7

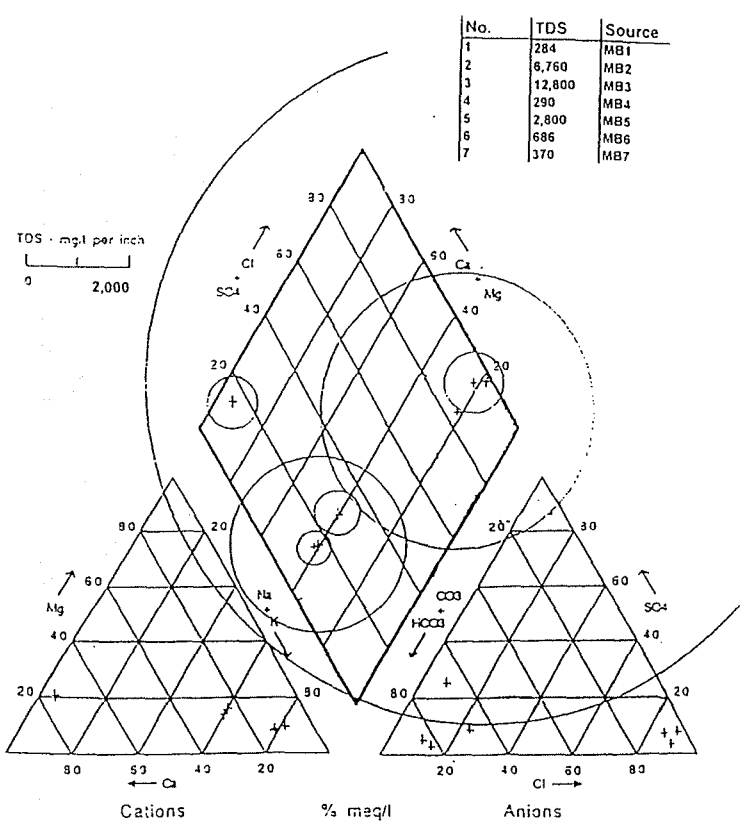

Figure 6d: Deep Well, On-416 (Kappel, et al 1996)

No.	TDS	Source
1	10,800	298' unconsolidated
2	57,500	462' Bedrock
3	27,700	517' Bedrock
4	98,400	608' Bedrock
5	170,000	633' Bedrock

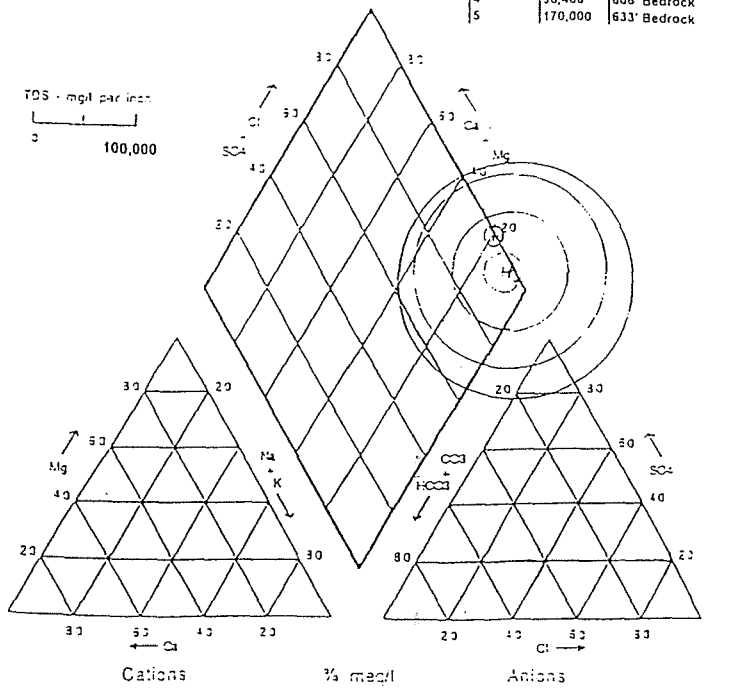

well, slide area and mudboil sources. This suggests some of the slide area springs encounter much less dilution as compared to water samples in the mudboil depression. Bivariate plots for sulfate and chloride concentrations in the slide area brackish water samples show two distinct mixing lines, Figure 7. The Salina evaporites are the probable sole sources for the chlorides and the separation of the mixing lines may therefore be due to different sulfate sources. Gypsum in the Salina evaporites is one source while the second likely source is the Chittenango shale. Of the four shale units in the Marcellus Formation of the Hamilton Group, the Chittenango is the only unit that contains abundant pyrites (Grasso, 1966). Thus in passing through fractures in the Chittenango shale, water emanating from some of the brackish springs may be picking up additional sulfates. Comparatively, sulfate concentrations are an order of magnitude less than chloride concentrations. If the two sulfate source hypotheses holds, it appears the contributions from the two sources are comparable. These observations do not resolve the question as to whether the salt source is local or linked to the brine fields. The effect of noted changes in groundwater quality on the red clay behavior have not been explored. However, previous findings suggest the infusion of dissolved solids in the clay structure by cation exchange would tend to improve the strength behavior (Di Maio, 1996).

Red Silty Clay

Index properties of the red silty clay were determined based on samples obtained from the slide exposure and debris on 4/29/93 as well as on samples recovered from boreholes during the field investigation in 1995 (Tables 2). The results indicate the natural water content of the red silty clay was in the range of 17 to 43, with the lower value being due to drying. The average liquid and plastic limits for borehole samples were 36 and 20, respectively. Liquid and plastic limits for samples recovered from exposures and debris in 1993 are higher than values for borehole samples. Samples recovered from the north side of the slide had generally lower natural water content and Atterberg limits than those obtained from the south side. The average liquidity index for all samples was about 0.8. However, a few liquidity index values that were greater than 1 were obtained. A liquidity index of 1 means the soil natural water content is at the liquid limit. When sheared and remolded, soils with a high liquidity index develop low shear strengths.

X-ray diffraction results for an air dried sample (Figure 8) of the red silty clay shows the predominant clay minerals present are illite and chlorite. Peaks for heated and glycol saturated samples are similar to those for air dried samples indicating a relative absence of active clay minerals. This finding is further confirmed by Gleason (1997). The clay fraction (<2μ) from hydrometer analyses is about 62 percent and the activity of the red silty clay is about 0.26. Atterberg limits for the red silty clay plot slightly above and along the A line in a plasticity chart. The clay minerals identified, the activity value and position of the clay in a plasticity chart suggest the red silty clay is inactive. As effective stresses reduce with rising groundwater pressure, the extent of swelling and water content increase for inactive clays would be much less as compared to clays that can be classified as active.

Results of field and laboratory vane shear tests (Table 3) indicate average strengths of 19 kPa peak and 9 kPa residual and average ratio of peak vane strength, Su, to effective overburden stress of 0.22. This ratio is the same as that reported by Larrson (1980) for inorganic clays. The average sensitivity of the red silty clay is about 2. Except for a single value of 5.3, the sensitivity of the red silty clay was below 3.6 for all vane tests. The results suggest that the red silty clay unit in Tully Valley is of low sensitivity. Consolidation results indicated the red silty clay is at near normal consolidation. Although the sensitivity of the red silty clay is relatively compared to sensitive clays, the strength difference between peak and residual is nevertheless not negligible. Where and when peak strength is not mobilized uniformly, the average shear strength over a failure surface would be much less than the peak strength.

A series of isotropically consolidated undrained (CU) triaxial tests were performed on tube samples of the red silty clay. All test samples were of nominal 71 mm diameter with height to diameter ratio of about 2. Each sample was initially consolidated for 24 hours under back pressure to at least twice the present effective stress and maximum past pressure to minimize sample disturbance effects (Ladd and Foott, 1974). At the end of consolidation, the drainage lines were closed to allow arrest of secondary consolidation and pore pressure equalization. The samples were then loaded in compression at a strain rate appropriate for 95 percent pore pressure equalization at failure. The failure envelope for the red silty clay, shown in Figure 9, can be represented by $\phi' = 28.1°$ and $c' = 0$. The average ratio of peak strength to effective consolidation stress for the undrained triaxial compression test results is about 0.30. This

Figure 7: Chloride vs Sulfate (brackish springs)

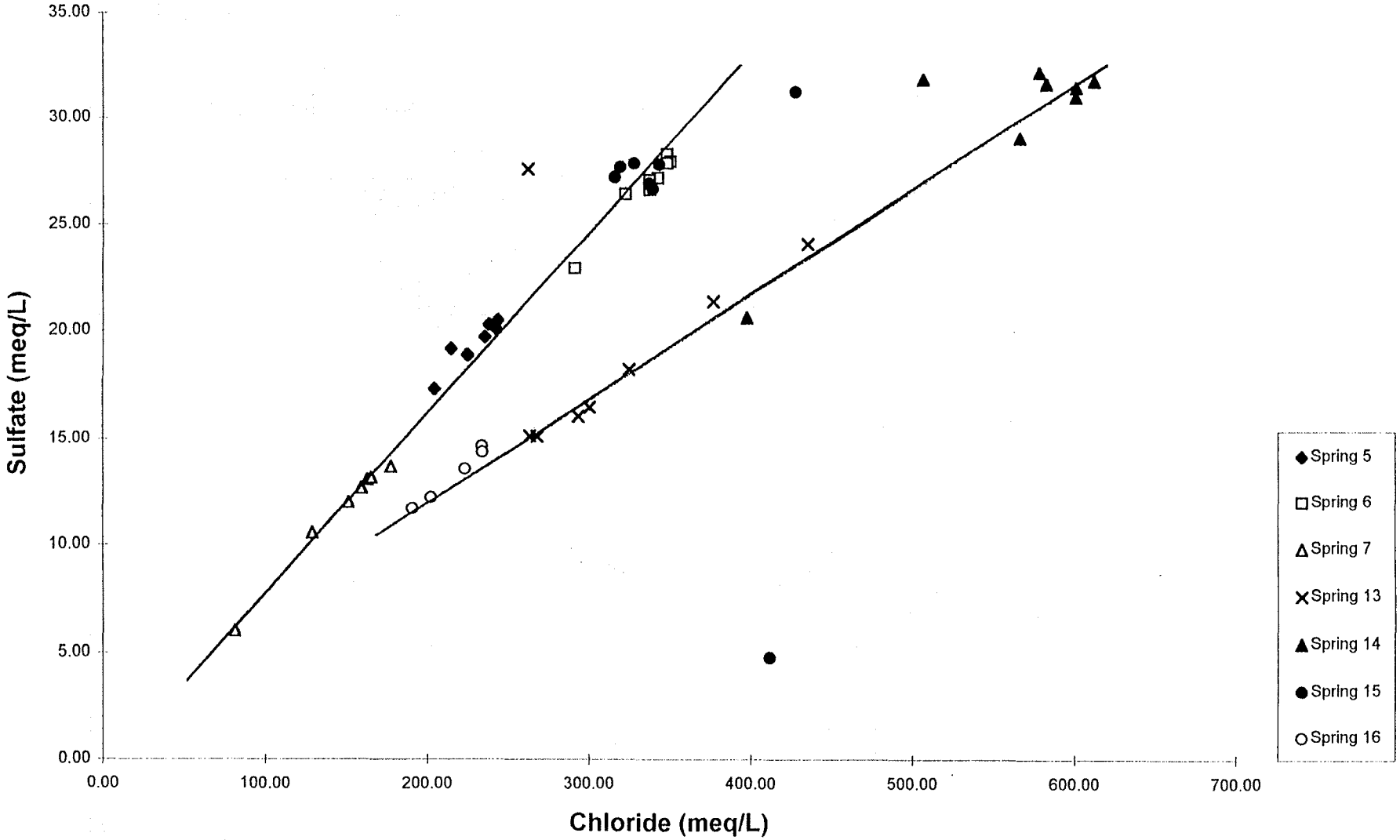

Table 2a- Water content & Atterberg limits (exposures 4/29/93)										
SAMPLE	MC	LL	PL	SL	PSS	RSS	PI	LI	SENSITIVITY	
	(%)	(%)	(%)	(%)	(kPa)	(kPa)	(%)			
UPPER CLAY										
REMOLDED SAMPLE FROM SLIDE DEBRIS										
4	25.9	52.7	30.6	21.7			22.1	-0.2		
4	27.0	55.0	26.9				28.1	0.0		
UNDISTURBED SAMPLES FROM EXPOSURE AT SLIDE BACK SCARP										
7	34.1	55.2	34.2	24.4			21.0	0.0		
7	32.1	55.4	25.9				29.5	0.2		
8	26.1	51.9	30.6	21.9			21.3	-0.2		
8	29.2	52.8	30.4				22.4	-0.1		
12	17.2	43.6	25.0	18.8	57.5	24.0	18.6	-0.4	2.4	
12	29.4	46.5	35.1				11.4	-0.5		
LOWER CLAY										
REMOLDED SAMPLES FROM SLIDE DEBRIS										
1	37.9	32.0	23.4	20.2			8.6	1.7		
1	38.0	34.3	23.3				11.0	1.3		
3	39.6	39.7	28.3	23.4			11.4	1.0		
3	44.0	44.0	27.9				16.1	1.0		
6	36.9	33.2	23.5	20.0			9.7	1.4		
6	38.0	33.3	26.9				6.4	1.7		
EXTRUDED PARTIALLY DRIED SAMPLE FROM SLIDE DEBRIS										
5	24.9	43.5	26.7	20.4			16.8	-0.1		
5	33.0	44.0	28.5				15.5	0.3		
UNDISTURBED SAMPLES FROM EXPOSURE AT SLIDE BACK SCARP										
9	31.9	38.5	23.0	18.0	33.5	12.5	15.5	0.6	2.7	
9	35.0	39.0	23.7				15.3	0.7		
11	31.5	32.4	23.4	20.1	30.7	14.4	9.0	0.9	2.1	
11	26.0	35.0	21.6				13.4	0.3		
13	38.0	40.5	25.0	19.5	29.7	13.4	15.5	0.8	2.2	
13	43.4	41.2	24.6				16.6	1.1		
UNDISTURBED SAMPLE FROM A DISPLACED BLOCK										
10	35.1	36.7	26.6	22.4	24.9	14.4	10.1	0.8	1.7	
10	36.0	37.5	17.5				20.0	0.9		

Table 2b - Natural water content & Atterberg limits (borehole samples)

Bore Hole	Depth (m)	Elevation (m)	Sample Type	Soil Type	Atterberg Limits				
					NMC	PL	LL	PI	LI
1a	5.2	164.2	SS	silty c	26.8	16.7	29.0	12.3	0.82
1a	6.1	164.0	ST	silty c	24.0	17.0	28.0	11.0	0.64
1a	12.2	162.1	ST	silty c	36.0	21.0	40.0	19.0	0.79
1a	20.4	159.6	SS	silty c	30.6	19.9	33.0	13.1	0.82
1a	24.4	158.4	ST	silty c	31.0	22.0	35.0	13.0	0.69
1a	26.5	157.7	SS	silty c	29.4	20.9	33.8	12.9	0.66
1a	30.5	156.5	ST	silty c	29.0	18.0	30.0	12.0	0.92
2	6.1	175.8	SS	silty c	40.5	25.7	47.1	21.4	0.69
2	7.0	175.6	ST	silty c	30.0	20.0	32.0	12.0	0.83
2	7.6	175.4	SS	silty c	42.5	25.7	48.3	22.6	0.74
2	9.1	174.9	ST	silty c	37.0	22.0	42.0	20.0	0.75
2	10.4	174.5	SS	silty c	38.2	23.8	41.0	17.2	0.84
2	12.2	174.0	ST	silty c	28.0	18.0	29.0	11.0	0.91
2	13.7	173.5	SS	silty c	29.4	19.4	30.8	11.4	0.88
2	16.8	172.6	SS	varved	30.2	14.5	28.1	13.6	1.15
2	27.4	169.3	SS	varved	18.2	15.1	24.7	9.6	0.32
8a	4.3	170.6	ST	sandy	19.0	22.0	30.0	8.0	-0.38
8a	5.8	170.1	ST	red sil	35.0	26.0	45.0	19.0	0.47
8a	7.9	169.5	SS	silty c	39.7	25.0	46.7	21.7	0.68
8a	9.4	169.0	SS	silty c	34.3	22.2	38.9	16.7	0.72
8a	11.0	168.6	ST	silty c	38.0	18.0	39.0	21.0	0.95
8a	12.5	168.1	SS	silty c	28.4	18.5	35.5	17.0	0.58
8a	14.0	167.6	SS	silty c	35.2	19.5	37.9	18.4	0.85
8a	15.5	167.2	SS	silty c	38.3	21.2	34.6	13.4	1.28
8a	17.1	166.7	SS	silty c	17.9	12.0	25.8	13.8	0.43
8b	8.2	172.1	SS	silty c	31.0	21.5	39.7	18.2	0.52
8b	8.5	172.0	ST	silty c	37.0	21.0	37.0	16.0	1.00
9b	9.4	162.0	SS	silty c	33.2	19.2	34.3	15.1	0.93
9b	11.0	161.6	SS	silty c	27.1	17.1	32.0	14.9	0.67
9b	14.0	160.6	SS	silty c	36.9	21.8	34.5	12.7	1.19
9b	15.5	160.2	SS	silty c	30.4	19.5	32.6	13.1	0.83

SS - split spoon ST - shelby tube

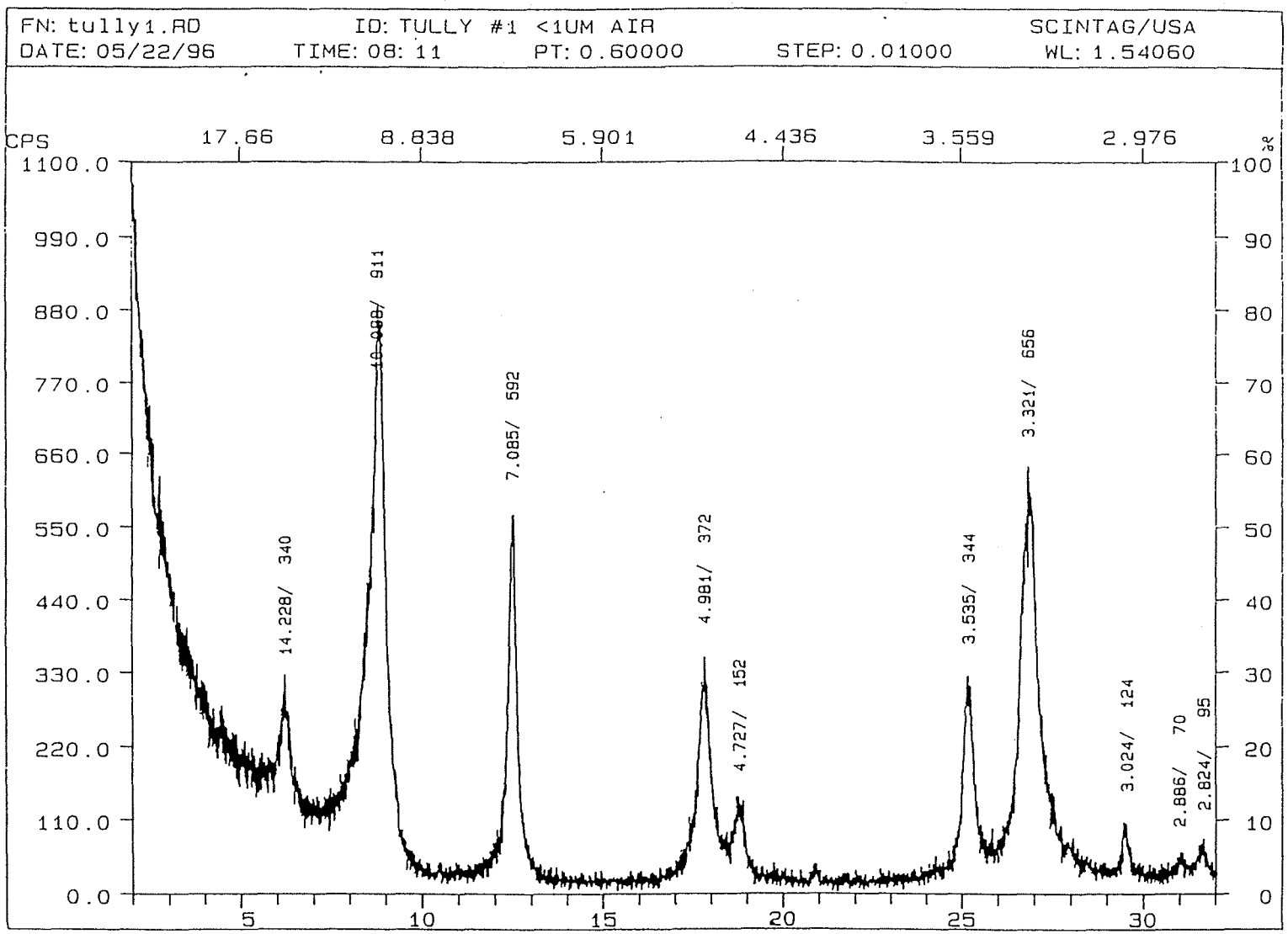

Figure 8 - X-ray diffraction for an air dry red silty clay sample.

TABLE 3 - Vane and CIU shear strengths for the red silty clay

Bore Hole	Depth (m)	Elevation (m)	Test	Soil Type	Su (kPa)	Residual Strength (kPa)	Sensi-tivity	LI	p'(est.) (kPa)	Cu* (kPa)	Su* (kPa)
1a	*3.7*	*164.7*	*field vane*	*brown-grey silty clay*	*37.8*	*15.7*	*2.4*		*54.0*	*n/a*	*n/a*
1a	6.1	164.0	mini. vane	red silty clay	21.7	11.0	2.0	0.6	59.9	0.9	0.8
1a	*7.0*	*163.7*	*field vane*	*red silty clay*	*11.3*	*6.3*	*1.8*		*67.9*	*1.0*	*0.9*
1a	12.2	162.1	mini. vane	red silty clay	14.9	4.1	3.6	0.8	52.4	0.7	0.7
1a	*12.8*	*161.9*	*field vane*	*red silty clay*	*15.7*	*6.3*	*2.5*		*55.2*	*0.8*	*0.7*
1a	*18.9*	*160.1*	*field vane*	*red silty clay*	*22.0*	*12.6*	*1.7*		*102.1*	*1.5*	*1.3*
1a	24.4	158.4	mini. vane	red silty clay	20.7	6.3	3.3	0.7	95.6	1.4	1.2
1a	*25.0*	*158.2*	*field vane*	*red silty clay*	*26.4*	*22.0*	*1.2*		*94.2*	*1.3*	*1.2*
1a	30.5	156.5	mini. vane	red silty clay	25.1	8.2	3.1	0.9	87.1	1.2	1.1
1a	*31.1*	*156.3*	*field vane*	*red silty clay*	*28.3*	*18.9*	1.5		89.4	1.3	1.2
2	7.0	175.6	mini. vane	red silty clay	23.4	4.4	5.3	0.8	91.1	1.3	0.8
2	*7.6*	*175.4*	*field vane*	*red silty clay*	*22.0*	*15.7*	*1.4*	*0.7*	*99.9*	*1.4*	*0.9*
2	9.1	174.9	mini. vane	red silty clay	8.1	5.0	1.6	0.8	104.2	1.5	0.9
2	*9.8*	*174.7*	*field vane*	*red silty clay*	*18.9*	*12.6*	*1.5*		*100.9*	*1.4*	*0.9*
2	12.2	174.0	mini. vane	red silty clay	10.7	4.0	2.7	0.9	105.6	1.5	0.9
2	*12.8*	*173.8*	*field vane*	*red silty clay*	*15.7*	*11.3*	*1.4*		*111.0*	*1.6*	*1.0*
6	*9.8*	*163.1*	*field vane*	*red silty clay*	*12.6*	*6.3*	*2.0*		*85.8*	*1.2*	*0.6*
6	*15.5*	*161.4*	*field vane*	*grey varved clay*	*18.9*	*15.1*	*1.3*		*67.9*	*n/a*	*n/a*
8a	4.3	170.6	mini. vane	stiff silt	121.7	28.8	4.2		46.8	n/a	n/a
8a	*4.9*	*170.4*	*field vane*	*brown-red silty clay*	*34.6*	*6.3*	*5.5*		*49.8*	*n/a*	*n/a*
8a	5.8	170.1	mini. vane	brown-red silty clay	63.6	18.5	3.4		60.1	n/a	n/a
8a	11.0	168.6	mini. vane	red silty clay	15.4	6.1	2.5	1.0	67.1	1.0	0.7
8b	8.5	172.0	mini. vane	red silty clay	36.7	-	-	1.0	57.0	0.8	n/a
8b	*9.1*	*171.9*	*field vane*	*red silty clay*	*15.7*	*12.6*	*1.2*		*67.1*	*1.0*	*0.7*
8b	*12.8*	*170.7*	*field vane*	*red silty clay*	*15.7*	*11.3*	*1.4*		*70.4*	*1.0*	*0.8*
9b	*16.8*	*159.8*	*field vane*	*red silty clay*	*15.7*	*12.6*	*1.4*		*92.1*	*1.3*	*0.8*

Cu* - based on Cu/p'=0.296 +- 0.047 (applies only to red silty clay)

Su/p'=0.220 +-0.074, neglecting vane tests at bh#2@30' and bh#8b@28' (applies only to red silty clay)

Su* - based on average Su/p', neglecting vane tests at bh#2@30' and bh#8b@28' (applies only to red silty clay)

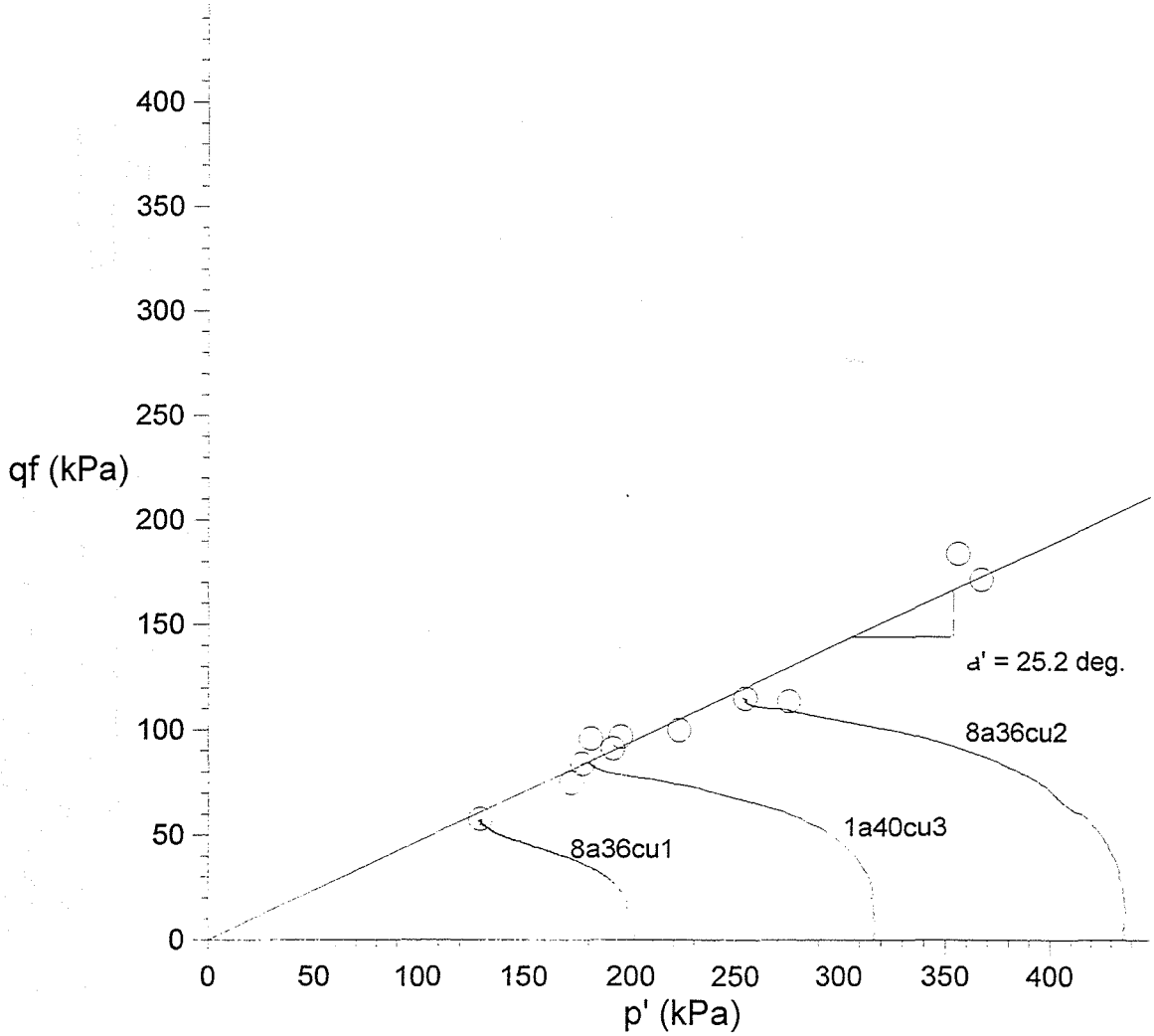

Figure 9 - Typical undrained stress paths and strength envelope for the red silty clay.

ratio is in close agreement with previous results reported for inorganic clays of 0.31 by Larrson (1980) and 0.32 by Ladd (1991). The results reported by Larrson are for isotropically consolidated specimens while those by Ladd are for anisotropically consolidated. Ladd (1991) further reports significantly lower ratios for samples tested in extension and direct simple shear modes. Different modes of failure apply for different segments of a slide surface. Thus the average strength ratio for a failure surface would be less than 0.3.

Stability Analyses

Limit equilibrium stability analyses were performed on three cross sections. Figure 10, represents a fence diagram for the reconstructed stratigraphy through the 1993 slide. Table 4 presents soil properties, other than for the red silty clay, and phreatic surfaces for the analyses. The two other sections analyzed represent existing profiles outside of the slide area along the north and south sides. High groundwater conditions measured in May, 1996 were used. The phreatic surface for the upper sand and varved clay units was later raised to simulate conditions in 1993. The stability analysis program is based on the simplified Bishop method. For a prescribed profile, strength and phreatic conditions, the program identifies the most critical failure surface. Strength parameters for the red silty clay vary depending on the type of stability analysis and depth. Three types of stability analyses; TSA (total stress analysis), ESA (effective stress analysis), and UESA (undrained effective stress analysis) were performed. These approaches to stability analyses are described by Ladd, 1991. Shear strengths used the red silty clay and safety factors obtained by the different types of analyses are given in Table 5.

The TSA analyses considered an undrained failure using shear strength values obtained from field and laboratory vane tests. A condition of $\phi = 0$ was assumed and the undrained shear strength, S_u, estimates correspond to average peak vane strengths. Different average strength values were used for the upper and lower portions of the red silty clay. The boundary separating the red silty clay into two zones is shown in the fence diagram, Figure 10. Factors of safety determined by TSA analyses were low compared to the other types of analyses and well below 1.0 for the failed section. These results are consistent with low safety factor values of 0.60 to 0.85 reported by Bishop and Bjerrum (1960) from TSA analyses for three natural slope failures in normally consolidated clay.

The ESA analyses assumes a drained failure condition using strength parameters of $c'=0$ and $\phi' = 28.1°$. These strength parameters represented the strength envelope determined from the CIU test results. The factor of safety obtained by ESA analyses was 1.35 for the failed section and 2.2 and 2.3 for the north and south sections, respectively. Phreatic surface adjustments to reflect higher estimates for 1993 did not result in values lower than 1 for the failed section. The actual slide event was of short duration and essentially no drainage could have occurred in the red silty clay within the failure time frame. TSA and ESA analyses resulted in too low and too high safety factors, respectively, and were not used in further analyses.

In the UESA analyses, the insitu effective overburden stress, σ', constituted a consolidation stress. Undrained shear strength was prescribed as either $S_u/\sigma' = 0.22$ (based on average vane strengths) or $c_u/\sigma' = 0.3$ (when based on undrained strengths from CIU test results). Failure in UESA analyses was assumed to have occurred under undrained conditions. Safety factors obtained from the UESA analyses were higher than those obtained from the TSA analysis but lower than for ESA. For the failed section, the safety factors obtained from UESA analyses were 1.05 for strengths based on vane shear and 1.31 for strength based on CIU results. The corresponding safety factors for the north and south sections were between 1.31 and 1.98.

All three types of stability analyses were based on ground water levels observed in May 1996. The accumulated precipitation record for Spring 1993 (following a record seasonal snowfall) was higher than the record for 1996. Ground water levels were therefore likely to have been higher at the time of the slide than in May 1996. The phreatic surface for the sand and varved clay interfingers in the back scarp area was raised by a modest 1 m to reflect this condition. UESA analysis with an average undrained shear strength to effective stress ratio of 0.205 resulted in a factor of safety of 0.99 for the failed section. Thus the phreatic surface rise may have been higher and/or the average shear strength to effective stress ratio mobilized over the failure surface was lower.

Table 4 - Soil properties for section F-F

Ref. #	Soil Type	N	Dr* (%)	e*	Density* kN/m3	Sat. Density kN/m3	Su kPa	ϕ deg	Piezometric Surface
1	stiff sandy silt	14	62	0.63	16.2	19.9	-	34	a
2	sand & gravel	-	61	0.4	20.3	21.6	0	36.5	a
3	brown - grey silty clay	-	-	-	-	18.1	57	-	b
4	red silty clay	-	-	-	-	18.5	**	**	b
5	red silty clay	w.r.	-	-	-	18.5	**	**	c
6	grey varved clay	w.h.	-	-	-	18.1	**	-	c
7	till material	50	-	-	-	21.2	81	42	c
8	brown-grey silty clay	56	-	-	-	18.8	167	-	d
9	fine sand	28	78	0.34	19.6	22.1	-	38.8	d
10	weathered shale	76	-	-	22.8	23.1	0	49	d
11	shale	-	-	-	23.6	23.6	240	49	d

* after "Design and Construction of Levees" figure 3-5 (assumes Gs=2.68)
w.h. = weight of hammer w.r. = weight of rod
** see Table 9 (same strength for varved and red clay assumed)

Table 5 - Undrained shear strength and FS

Section	Method	Red silty clay Undrained shear strength	FS
N-N	TSA	ϕ=0, c=Su*=19, 24 kPa	1.09
N-N	ESA	ϕ'=28.1 , c'=0	2.20
N-N	UESA(Su)	Su/p'=0.22, ϕsu=12.4 deg	1.55
N-N	UESA(Cu)	Cu/p'=0.30, ϕcu=16.5 deg	1.98
S-S	TSA	ϕ=0, c=Su*=15,16 kPa	1.15
S-S	ESA	ϕ'=28.1 , c'=0	2.30
S-S	UESA(Su)	Su/p'=0.22, ϕsu=12.4 deg	1.31
S-S	UESA(Cu)	Cu/p'=0.30, ϕcu=16.5 deg	1.56
F-F	TSA	ϕ=0, c=Su*=21,22 kPa	0.86
F-F	ESA	ϕ'=28.1 , c'=0	1.35
F-F	UESA(Su)	Su/p'=0.22, ϕsu=12.4 deg	1.05
F-F	UESA(Cu)	Cu/p'=0.30, ϕcu=16.5 deg	1.31

The deep critical failure surface, shown in Figure 10. is a composite of segments involving different modes of failure. An active mode at the back, direct simple shear at the mid section and extension mode at the front or down slope segment. Failure strengths derived from vane or CIU tests do not represent the full range of failure modes. Peak strengths would also not be mobilized simultaneously over the entire failure surface. Limit equilibrium stability analyses are not convenient for applying different strengths depending on mode of failure and mobilized strain level. Average peak strengths based on CIU compression tests would tend to be over estimates as strengths for direct simple shear and extension modes would be lower. The average strength ratio for the red silty clay suggested by the back analyses was closer to $S_u/\sigma' = 0.22$ obtained from the vane tests.

Remarks

The dramatic Tully Valley Landslide of 1993 occurred in a gentle terrain of about 8° slope. The land area affected by the slide is large and the event was sudden. By common measures of experience there was little to suggest a slide of such magnitude and speed. The stability analyses indicate the portion of slope that had the lowest factor of safety was at the back of the slide basin. Slumping of the upper portions of the slope probably resulted in more loading and subsequent failure through the red silty clay stratum below lower segments of the slope. In the aftermath of the slide, continuous longitudinal cracks normal to the direction of the slide were evident. Fresh and remolded very soft red silty clay was squeezed out through the longitudinal openings. The red silty clay deposit over Tully Farms Road and at the slide front had a high water content and was essentially a mud flow.

The base of the critical failure surface identified by the stability analyses follows a path through the underlying varved clay. Both the varved clay and the overlying sand and gravel interfinger into the red silty clay stratum. These interfingers have much higher hydraulic conductivity and penetrate more than 100 m into the red silty clay. Thus the red silty clay at the interface of the interfingers was exposed to seasonal groundwater fluctuations. Rapid recharge through the interfingers could also have fed more water to the clay, both at the interface and within the varved zone, to enable remolding at above natural water content. The coarse and varved interfinger penetrations into the soft red silty clay and sustained high groundwater levels in March through April of 1993 appear to have been detrimental. The observed difference between peak and residual strength may also have facilitated progressive failure. There is no compelling evidence to date from slope indicator monitoring of significant creep movements along either the north or south sections of undisturbed ground. However, future failure of large sections of undisturbed ground located between the previous slides can not be ruled out without additional investigation.

There is evidence to suggest that secession of the brine mining operation since 1988 has led to a general rise of groundwater levels in lower Tully Valley. How much of this rise has reached the slide site and if such rise constitutes a net increase above pre-mining groundwater levels is not known. The three slides to the north of the 1993 failure are believed to have occurred before the beginning of brine mining in Tully Valley. The recent slide may also have occurred under the record weather conditions experienced in 1993 and without the influence of post brine mining related groundwater rise. What can be said, however, is that a sustained rise in groundwater level would have been unfavorable for stability. The stability analyses confirm the overburden stratigraphy, soil strengths and prevailing piezometric pressures in the back area of the slide were in a condition to initiate a deep seated failure extending through the varved interfinger.

Conclusions

The thick red silty clay stratum is generally soft, inactive and of low sensitivity. A series of sand and varved clay interfingers penetrate into the red silty clay deposit. Piezometric pressures fluctuate seasonally within the interfingers but not significantly in the red silty clay stratum. The 1992-93 Winter produced a record snowfall in Tully Valley. Unusually high groundwater conditions appear to have been sustained throughout March and April of 1993. Portions of the red silty clay at the interface with the sand and varved clay interfingers became exposed to the high groundwater pressures. More water became readily available to permit remolding at a high water content in the failure zone at the interfinger interfaces. The observed difference between peak and residual strengths is significant. The failure probably developed slowly and progressively until the final stage of rapid sliding. These conditions

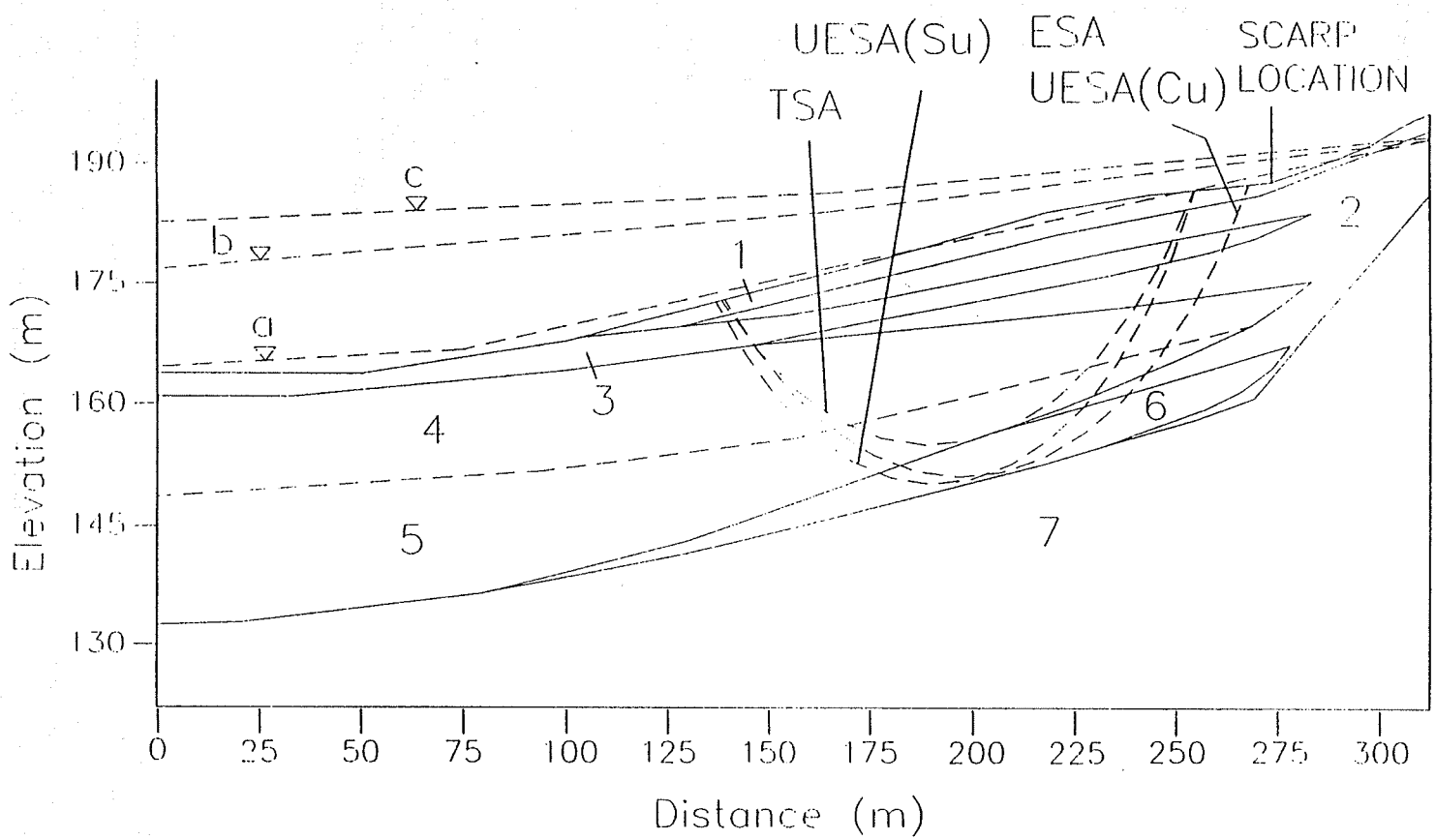

Figure 10 - Fence diagram for stability analyses and critical failure circles.

appear to have combined to cause the landslide. Prospects for future slide hazard at other locations to the north of the 1993 slide need to be observed and examined.

Acknowledgment

Financial support for this investigation provided by the National Science Foundation is gratefully acknowledged.

REFERENCES

Bishop, A.W. and Bjerrum, L. (1960). The relevance of the triaxial test to the solution of stability problems. Proceedings of the Research Conference on Shear Strength of Cohesive Soils. Soil Mechanics and Foundation Division, ASCE. Boulder, CO, 437 - 501.

Blagborough, J.W. (1951). The red clay deposits of Otisco Valley. M.S. Thesis, Syracuse University, Syracuse, NY.

Burgmeier, P.A. (1997, expected). M.S. Thesis, Syracuse University, Syracuse, NY.

Curran, C.A. (1997, expected). M.S. Thesis, Syracuse University, Syracuse, NY.

DeGroff, E.R. (1950). Joint patterns in Central New York: Syracuse, NY. M.S. Thesis, Syracuse University, Syracuse, NY.

Di Maio, C. (1996). The influence of pore fluid composition on the residual shear strength of some natural clayey slopes. Proceedings of the 7th International Symposium on Landslides. Trondheim, Norway, 1189 - 1194.

Faltyn, N.E. (1957). Seismic exploration of the Tully Valley Overburden. M.S. Thesis, Syracuse University, Syracuse, NY.

Fickies, R.H. (1993). A large landslide in Tully Valley, Onondaga County, NY. Association of Engineering Geologists, 36 (4), 22-24.

Getchell, F.J. and Muller, E.H. (1992). Subsidence and Related Features in the Tully Valley, Central New York. Proceedings of the Conference on Eastern Regional Groundwater Issues, Groundwater Management Book No. 13, National Groundwater Association, 829-843.

Getchell, F.J. (1983). Subsidence in the Tully Valley, New York. M.S. Thesis, Syracuse University, Syracuse, New York.

Gleason, A. (1997). Mineralogical and chemical analysis of the Tully Landslide red lacustrine clays and surrounding environment. Department of Geology, Colgate University, Hamilton, NY.

Grasso, T.X. (1966). Faunal Zones of the Middle Devonian Hamilton Group in the Tully Valley Central New York. M.S. Thesis, Syracuse University, Syracuse, NY.

Jäeger, S. and Wieczorek, G.F. (1994). Landslide susceptibility in the Tully Valley area, Finger Lakes region, NY: US Geological Survey, Open-file Report 94-615.

Kantrowitz, I.H., (1970). Groundwater resources in the Eastern Oswego River Basin, NY. State of New York Conservation Department, Water Resources Commission, Basin Planning Report ORB-2.

Kappel, W.M., Sherwood, D.A. and Johnston, W.H. (1996). Hydrogeology of the Tully Valley and characterization of mudboil activity, Onondaga County, NY. USGS Water Resources Investigations Report 96-4043.

Ladd, C.C. (1991). Stability evaluation during staged construction. Journal of the Geotechnical Engineering, ASCE, 117 (4), 540-615.

Ladd, C.M., Foott, R., 1974. New design procedure for stability of soft clays. Journal of the Geotechnical Engineering Division, ASCE, 100 (7), 763 - 786.

Larrson, R. (1980). Undrained shear strength in stability calculation of embankments and foundations on soft clays. Canadian Geotechnical Journal, 17 ((4), 591 - 602.

Muller, E.H. (1964). Surficial geology of the Syracuse field area, Guidebook, New York State Geological Association, 36th Annual Meeting.

Rubin, P.A., Ayers, J.C. and Grady, K.A. (1991). Solution mining and resultant evaporite karst development in Tully Valley, NY, Proceedings of the 3rd annual conference on hydrology, ecology, monitoring, and management of groundwater in karst terraines. Quinlan, J.F. and Stanley, A. editors, National Groundwater Association, Dublin, OH.

Perkins, M.G. and Romanowicz, E.A. (1996). Chapter 2 - Hydrologic Setting, Limnolgical and engineering analysis of a polluted urban lake, Prelude to environmental management of Onondaga Lake, NY, Edited by Effler, S., Springer-Verlag, publisher.

Walker, R.M. and Mahoney, R.J. (1993). Interpreting and projecting long-term environmental conditions in a shallow brine field: Woodstock, II., Solution Mining Research Institute Spring Meeting, Syracuse, NY.

Hydrology, Geology, and Remediation of Tully Valley Mudboils, Onondaga County, New York

William M. Kappel
U.S. Geological Survey - Water Resources Division
903 Hanshaw Road, Ithaca, NY 14850-1573
wkappel@usgs.gov

Introduction

The history of mudboil activity in the Tully Valley (fig. 1) can be traced back nearly 100 years. A detailed description of one mudboil is given in an article in the Syracuse, N.Y. Post Standard, dated October 20, 1899:

> "Few people are aware of the existence of a volcano in this town. It is a small one, to be sure, but very interesting. In the 20-rod gorge where the crossroad leads to and by the Tully Valley grist mill the hard highway bed has been rising foot after foot till the apex of a cone which has been booming has broken open and quicksand and water flow down the miniature mountain sides. It is an ever increasing cone obliterating wagon tracks as soon as crossed. The nearby bluff is slowly sinking. Probably the highway must sometime be changed on account of the sand and water volcano, unless it ceases its eruption."

The above account accurately describes the Tully Valley mudboils and presages the collapse of the Otisco Road bridge over Onondaga Creek (fig. 2) 92 years later, in 1991.

In the early 1900's the U.S. Geological Survey (USGS) performed a "postmaster" survey of the water resources of Onondaga County, in which local postmasters were asked to respond to a one-page questionnaire concerning springs, artesian wells, and other ground-water features. The only reference in the survey to possible mudboil activity was found on an undated map, annotated by USGS personnel, indicating a location for "sand springs" near the Otisco Road bridge. Other reports of mudboil activity in the valley have been gathered from anecdotal conversations with local residents and from various State and local governments by the New York State Department of Environmental Conservation (Snell, 1992). The bulk of the reports began after 1950 but were preceded by sparse recollections from local residents, although a a 90-year old individual in 1993 reported a vivid recollection of her brother falling into, and being rescued from a mudboil in the early 1900's.

In 1951 the New York State Health Department (Snell, 1992) reported high turbidity and stated that suspended sediment "enters the stream south of Cardiff, N.Y. from springs and potholes." Reports from the Onondaga Nation (about 2 miles north of the Tully Valley) indicated that Onondaga Creek became turbid year-round in the early 1950's. Another New York State Health Department report in 1955 indicated that the turbidity in the creek came from "quicksand pits" near Onondaga Creek tributary T-21, south of Otisco Road (Snell, 1992). A full summary of these reports is given in Kappel and others (1996).

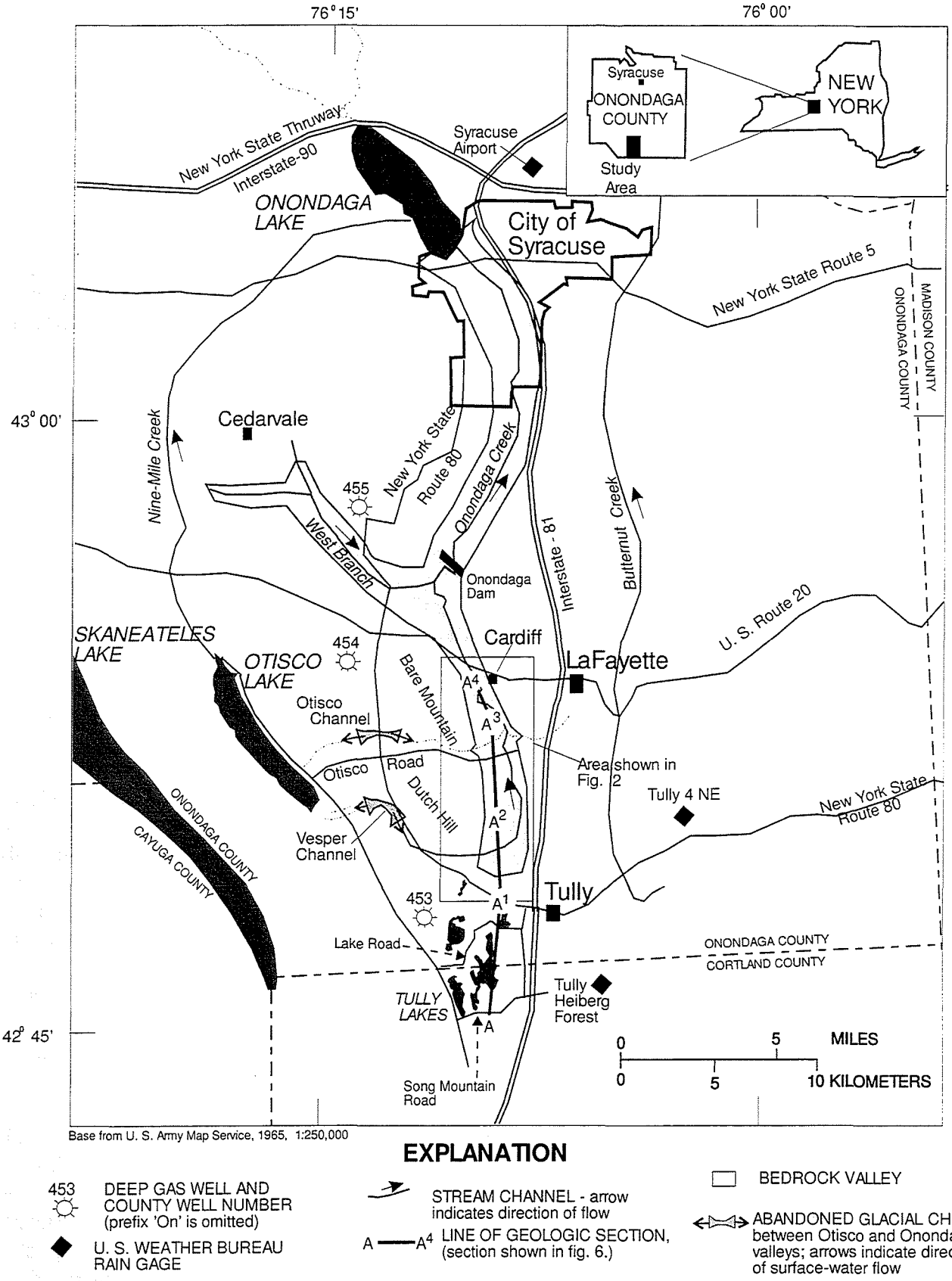

Figure 1. Location and pertinent geographic features of the Tully Valley, and location of geologic section A - A^4 in southern Onondaga County, N.Y. (Geologic section shown in fig. 6. From Kappel and others, 1996, fig. 1.)

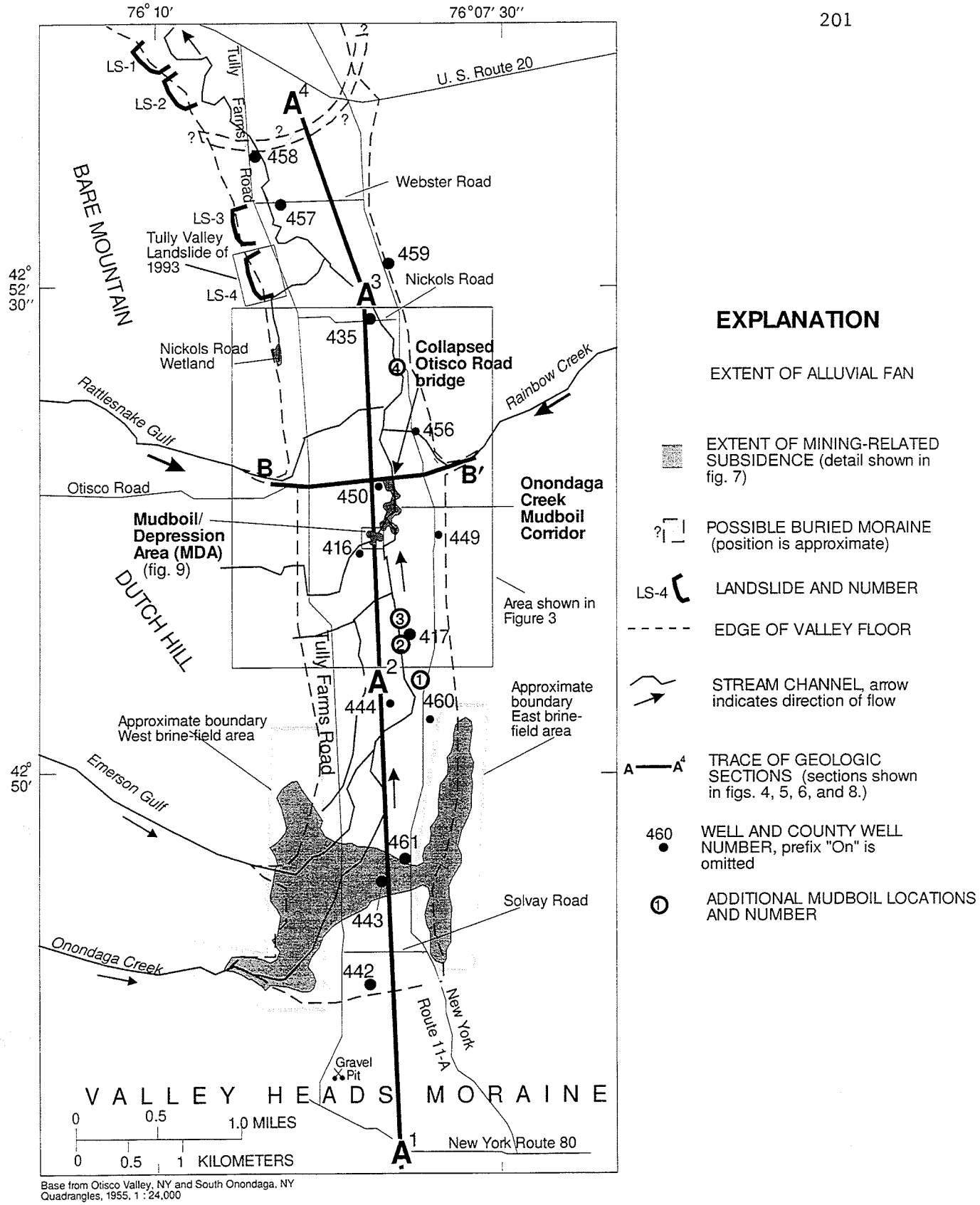

Figure 2. Principal geographic features of the Tully Valley showing wells, brinefield areas, landslides, mudboils, and geologic sections A-A^4 and B-B′ (Geologic sections shown in figs. 4, 5, 6, and 8. From Kappel and others, 1996, fig. 2)

Waller (1977) reported that water discharging from the main mudboil/depression area (MDA) in the mid-1970's was fresh, but his later fieldnotes indicate that, by 1979, some mudboils were discharging brackish water (R.M.Waller, USGS, written commun., 1993). These fieldnotes are the only source of water-quality information on the mudboils from the 1970's through the 1980's.

In 1991, the USGS, in cooperation with the Onondaga Lake Management Conference (OLMC) and the U.S. Environmental Protection Agency (USEPA), began a 4-year study to identify the extent and mechanism of mudboil development in the Tully Valley. An extensive test-well-drilling program was implemented to document the glacial stratigraphy and aquifer conditions near the mudboil area, and a deep test well was installed that penetrated the salt beds from 950 feet to about 1,100 feet below land surface. Streamflow entering and leaving the MDA, and chemical and physical quality of water upstream and downstream of the MDA, were monitored to characterize mudboil water quality and quantity within the MDA. Results are summarized below:

Mudboil Flow System

Some mudboils are found within a 300-foot-wide by 1,500-foot-long corridor along Onondaga Creek, just upstream from the two side-valley alluvial fans, and within a 5-acre subsided area (the MDA) along a tributary of Onondaga Creek, near the south end of the mudboil corridor (fig. 3). Mudboil discharge is driven by artesian pressure in two unconsolidated aquifers. The upper (freshwater) aquifer is confined by a 60-foot layer of reddish-gray silt and red clay; the lower (brackish-water) aquifer is confined by a layer of red, dense, clay till about 10 feet thick (fig. 4). Artesian pressure in these aquifers causes hydrostatic heads to be 20 to 30 feet above land surface over most of the valley floor and exceeding 30 feet along Onondaga Creek in the vicinity of the Rattlesnake and Rainbow Creek alluvial fans. The source of the artesian pressure that drives mudboil activity is recharge from the Valley Heads Moraine at the southern end of the valley, the alluvial fans of Rattlesnake Gulf and Rainbow Creek, and minor recharge from the valley walls.

Sediment Concentrations and Loading to Onondaga Creek

Suspended-sediment concentrations at the outlet of the MDA ranged from 31,200 mg/L (milligrams per liter) in October 1991 to 17 mg/L after some remediation efforts were implemented in the summer of 1993. Yearly average suspended-sediment loads to Onondaga Creek from the MDA for water years 1992-96 were 29.8, 9.75, 1.41, 1.80, and 2.80 tons per day, respectively. Sediment discharged from the MDA was initially 30 to 60 percent clay and 80 to 100 percent silt-sized or smaller particles; the sand-size fraction never exceeded 20 percent. After remediation projects were implemented, 50 to 80 percent of the discharged sediment was clay, and nearly all sediment was silt-sized or smaller. The medium sand fractions immediately settle out as a mudboil "cone" and remain within the depression area.

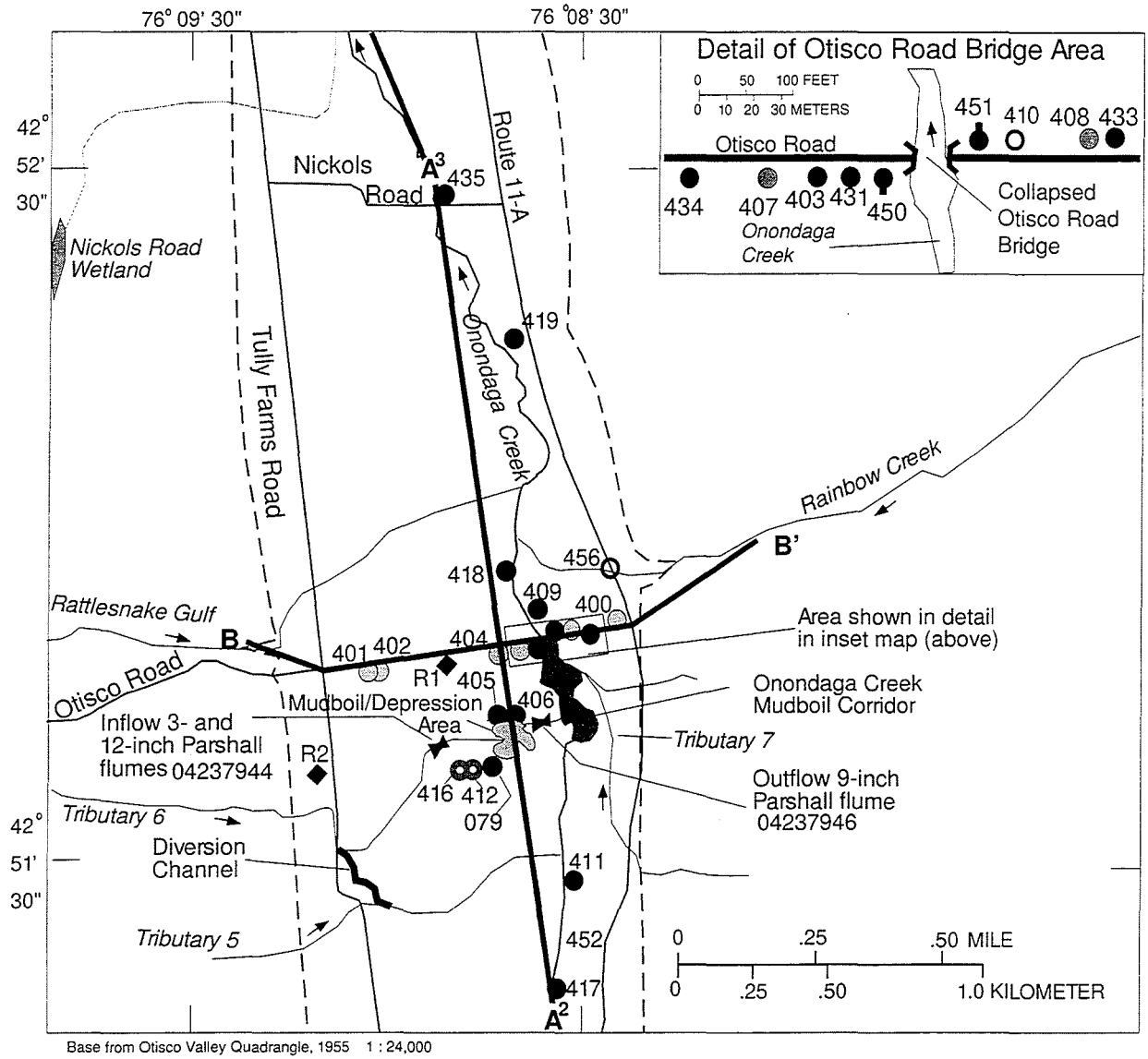

EXPLANATION

TULLY VALLEY UPLANDS

STREAM, arrow indicates direction of flow

EDGE OF VALLEY FLOOR

B — B' TRACE OF GEOLOGIC SECTION (Section shown in figs. 4, 6, and 9)

04237946 PARSHALL FLUME, AND STREAM GAGE NUMBER

R2 RAIN GAGE AND NUMBER

WELLS

[Well number prefix "On" for Onondaga County omitted]

411 WELL COMPLETED IN CONFINED FRESHWATER AQUIFER

401 WELL COMPLETED IN ALLUVIAL AQUIFER

416 WELL COMPLETED IN BEDROCK

450 DEPRESSURIZING WELL

410 SOIL BORING

Figure 3. Location of wells, Parshall flumes, raingages, and geologic sections A^2- A^3 and B-B'. (Location is shown in fig. 2. Geologic sections shown in figs. 4, 6, and 8. From Kappel and others, 1996, fig. 5.)

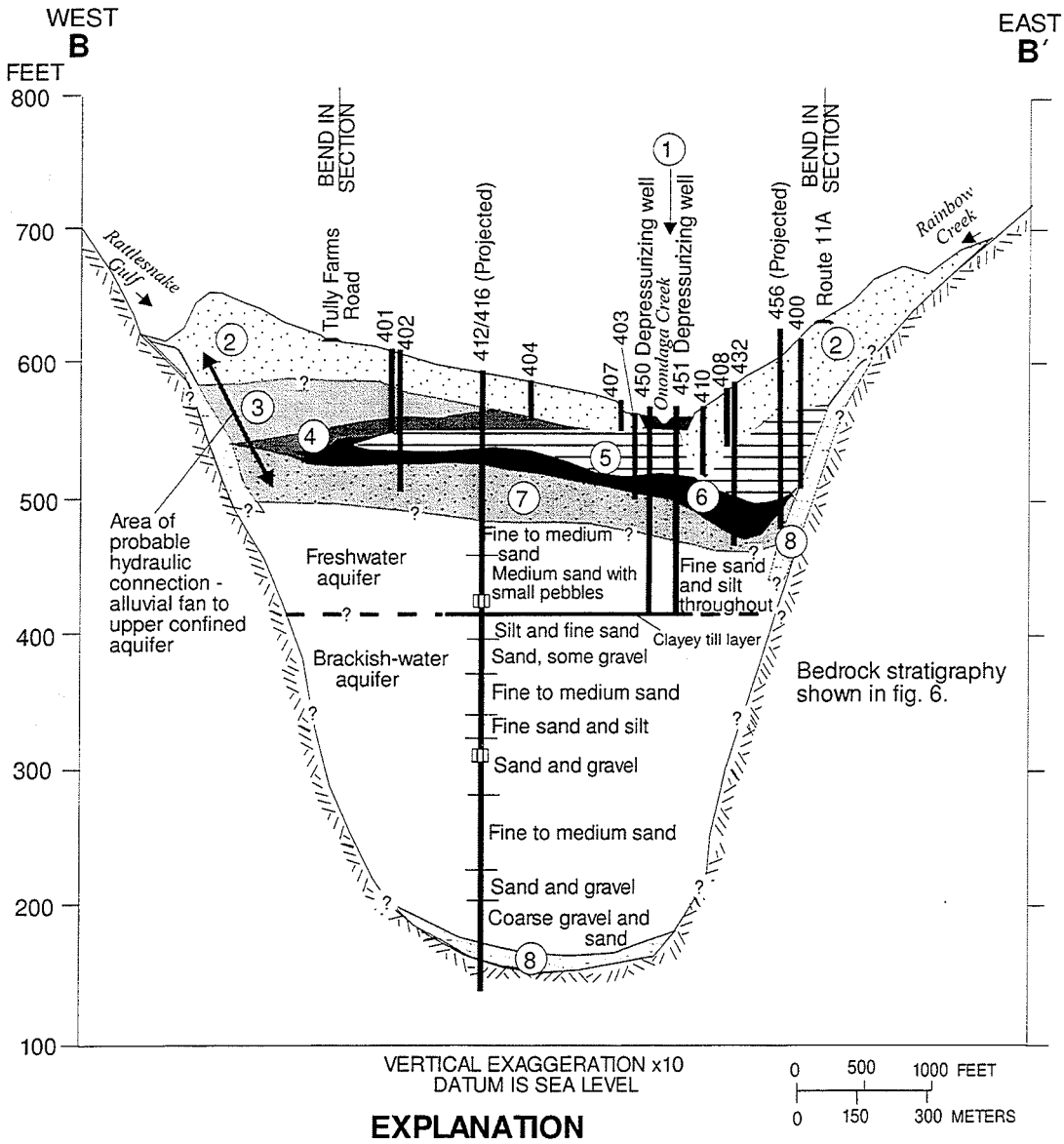

EXPLANATION

ALLUVIAL DEPOSITS

(1) FLOODPLAIN AND MUDBOIL DEPOSITS - Silt, sand and gravel deposited by Onondaga Creek and upstream mudboils.

(2) FANS - Sand and gravel deposited by Rattlesnake Gulf and Rainbow Creek.

LACUSTRINE DEPOSITS

(3) LAMINATED SAND AND SOME SILT/CLAY - Mostly fine to medium sand interbedded with minor amounts of silt and clay deposited by Rattlesnake Gulf as it flowed into a proglacial lake.

(4) LAMINATED SAND AND SILTY CLAY - Approximately equal parts of very fine sand interbedded with silty-clay that settled-out farther in the proglacial lake.

(5) LAMINATED SILTY CLAY WITH SAND - Mostly silty clay interbedded with occasional layers of medium-to-fine sand that settled out farthest in the proglacial lake. Coarser sand is found along Otisco Road; finer sand-to-silt wisps are found farther north and south of Otisco Road. Forms the top of confining unit over the liquifiable sand and silt unit in the mudboil areas.

LACUSTRINE DEPOSITS (cont'd)

(6) CLAY AND SILT - Massive unit that generally covers most of the valley floor north and south of mudboil areas. Forms confining unit over upper aquifer and grades from clay at surface to silt at depth.

(7) SILT AND SAND - Massive, grading from silt and very fine sand at the top to medium to coarse sand and fine gravel with silt at the bottom. Unit is under artesian pressure and forms upper confined aquifer.

OTHER GLACIAL DEPOSITS

(8) TILL - A dense unit of sand, gravel,and boulders embedded in a clay matrix. This unit may underlie entire glacial sequence in the valley.

BEDROCK

410 WELL AND NUMBER, without "On" prefix

MONITORING ZONE, steel casing perforated after hydraulic testing of deeper bedrock zones and grouting of the bedrock section of deep well On-416.

Figure 4. Geologic section B-B′ showing upper unconsolidated deposits along Otisco Road and deeper unconsolidated deposits projected from well On-412, southwest of the mudboil/depression area. (Location of section shown in figs. 2 and 3.)

Chemical Quality of Water from Confined Aquifers

Specific conductance of water from the confined upper (freshwater) aquifer ranges from about 400 μS/cm (microsiemens per centimeter at 25° Celsius) to almost 900 μS/cm. Dissolved-chloride concentrations range from 37 to 430 mg/L, and dissolved-solids concentrations range from 215 to 463 mg/L. Specific conductance of water from the confined lower (brackish-water) aquifer ranges from 17,000 to 28,000 μS/cm. Chloride concentrations range from 2,000 to 7,100 mg/L, and dissolved solids concentrations range from 4,200 to 12,800 mg/L. Trend analysis indicates that the specific conductance of water leaving the MDA has increased by about 200 μS/cm per year since 1992, and the chloride content in the upper (freshwater) aquifer appears to be increasing.

Bedrock Geology

Stratigraphy

The Tully Valley lies within and above bedrock units of Middle Devonian through upper Silurian ages. The bedrock ridges, 1,000 to 1,200 feet above the Tully Valley floor, are shale, limestone, and siltstone of Middle Devonian age (Rickard, 1975). The Tully Limestone is found near the top of Bare Mountain, and the valley wall consists of the Hamilton Group Shales to a depth of 300 feet below the valley floor (fig. 5). The Hamilton Group is underlain by the Onondaga Limestone Formation, the Oriskany Sandstone, and the Helderberg Group of limestones and dolomites. The Onondaga Limestone acted as an erosion-resistant ramp for glaciers in most of the other Finger Lake valleys (Mullins et. al., 1991), but the deep drillhole at the MDA (fig. 5) indicates that glacial action in the Tully Valley eroded down to the middle of the Helderberg Group, within the Manlius or Rondout formations (Brayton Foster, private consultant, written commun., 1993).

Below the Helderberg Group lies the Upper Silurian Salina Group and the Syracuse Formation which contains the evaporite deposits that were solution mined in the southern part of the valley (fig. 6). Gas-well logs west of the Tully Valley, and logs from the brine-field wells, indicate that the evaporite beds are about 150 feet thick and gradually thin and pinch out as they rise to the north. The northern end of the Tully Valley apparently is near the edge of the Salina salt basin, as indicated by Rickard (1975).

Strike and Dip

Bedrock strike and dip sets above and below the Syracuse Formation were computed from brine-field and gas wells logs in and near the Tully Valley. Four strike and dip sets are present: (1) in the valley, above the Syracuse Formation, the strike is N. 48° E., with a dip of 71 feet per mile to the southeast; (2) west of the valley, logs of gas wells indicate a strike of N. 75° W., and a dip of 83 feet per mile to the southwest; (3) data below the Syracuse Formation are limited, but the in-valley strike for the top of the F2 saltbed (fig. 5) is N. 27° E., with a dip of 89 feet per mile to the southeast; (4) the strike of the top of the Vernon Shale is N. 48° W., with a dip of 58 feet per mile to the southwest. The differences in strike and dip among these beds could be related to

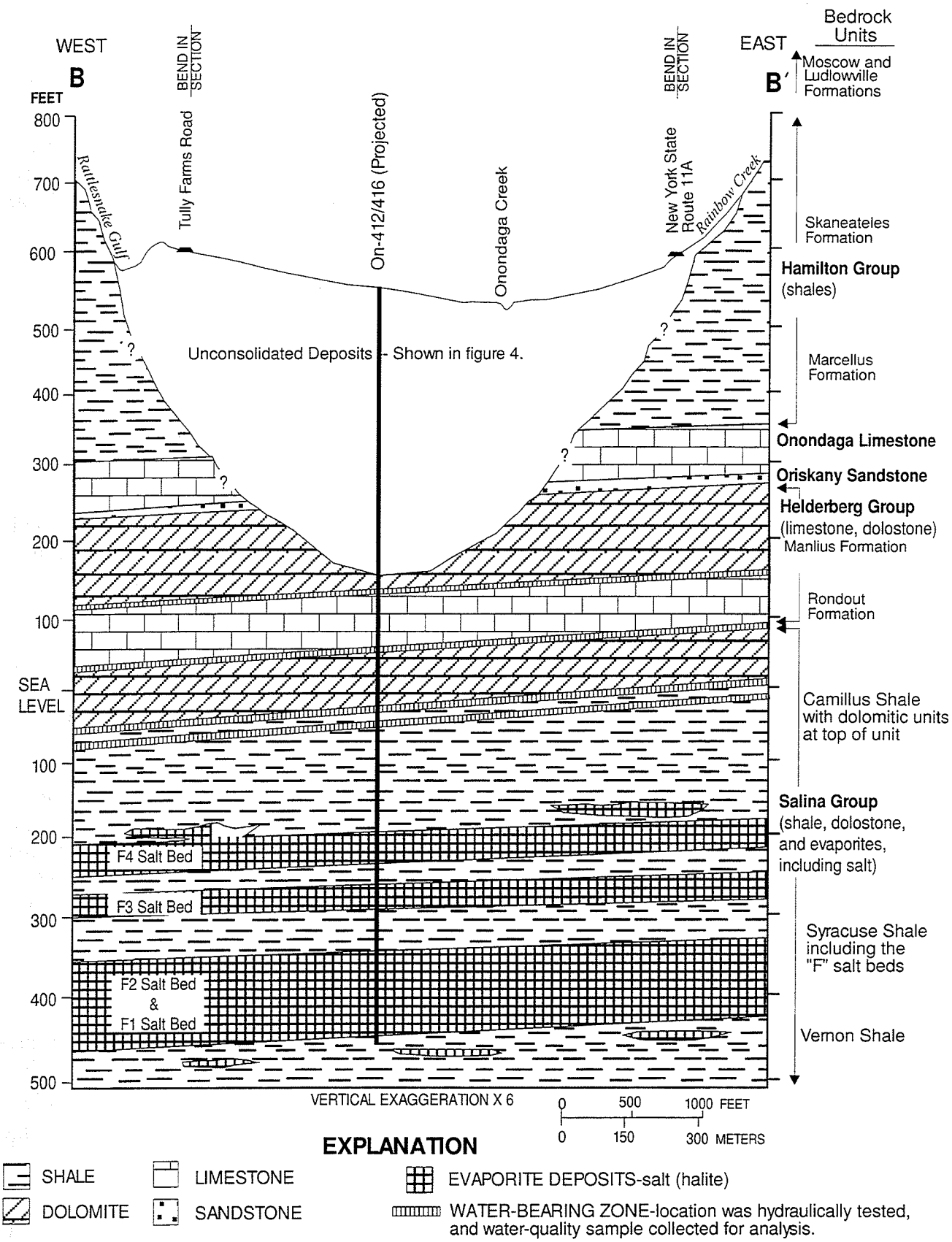

Figure 5. Geologic section B-B′ showing major bedrock units below Rattlesnake Gulf and Rainbow Creek from lower valley walls to top of Vernon Shale. (Modified from Getchell,1982, plate 1. Location of section shown in figs. 2 and 3.)

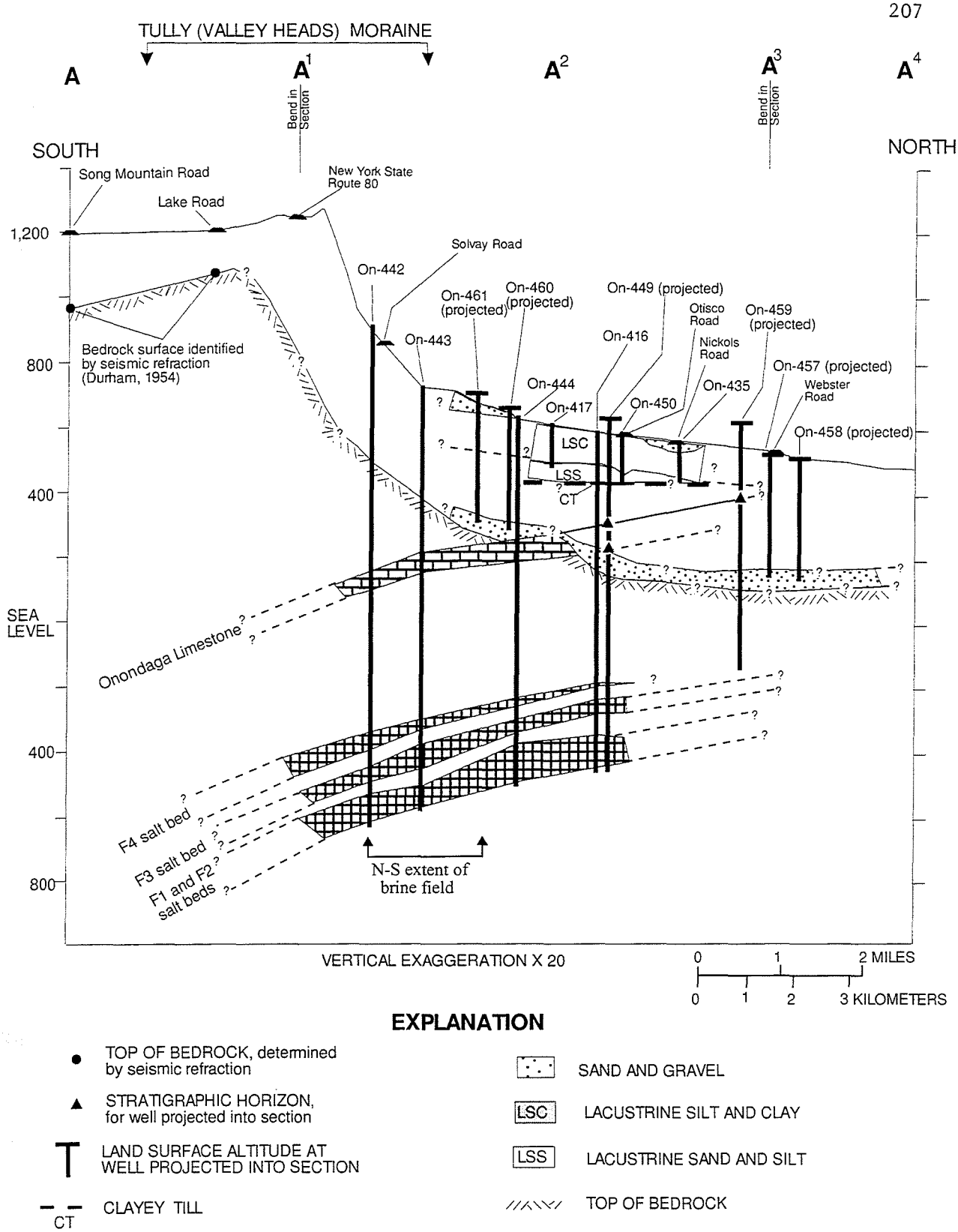

Figure 6. Geologic section A-A^4 from the Tully Lakes through middle part of the Tully Valley showing position of the Salina "F" salt beds, Onondaga Limestone, bedrock floor and generalized unconsolidated units in the mudboil area near Otisco Road (Location shown in figs. 1 and 2. From Kappel and others, 1996, fig. 5.)

localized folding above and below the décollemont surface within the saltbeds, localized upwarping (Matheson and Thomson, 1973; and Molinda and others, 1992) from the removal of 1,200 ft of bedrock by glaciation, and(or) recent rebound from glacial unloading.

Vertical fracture patterns as determined by Getchell (1983) and DeGroff (1950) are roughly north-south with a nearly orthogonal east-west set. These coincide with those on a map of photo-linear features in this area by Isachsen and McKendree (1977). Haley and Aldrich of New York (1991) describe a fault surface within the brine field striking N. 74° W. and another possible structure striking roughly north-south, in or near the east brine-field area. These north-south structures may coincide with several north-trending bedrock features on the east-facing, upper slope of Bare Mountain that strike N. 7° W. and extend hundreds of feet in the Tully Limestone and in several sections of the upper Hamilton Shales. In the brinefield area, these strike and dip features and other bedrock fractures may have been enhanced or distorted by 100 years of salt-solution mining (fig. 7).

Glacial Geology

Tully Valley Sequence

Two sequences of upward-fining deposits were indicated by analysis of split-spoon samples taken every 10 feet from the deep drillhole (On-416) near the MDA (fig. 4). The lowermost unconsolidated unit consists of a dense bed of clayey sand, gravel, and boulders (till) overlain by beds of coarse sandy and bouldery gravel with interbeds of silt. A finer grained unit above grades from coarse sand to silt and clay. A readvance of the ice front compacted the fine-grained unit and, as the glacier again receded to the north, it laid down another coarse to fine-grained sequence that was capped by the 60-foot thick silt and clay layer that forms the present valley floor.

Rattlesnake Gulf - Rainbow Creek Sequence

As the ice front was discharging fine materials into the glacial lake (Grasso, 1970), coarse to fine-grained materials were being discharged into the main valley from the two major side valleys (Rattlesnake Gulf and Rainbow Creek), and fine-grained particles (sand, silt, and clay) were settling in the central part of the lake. Stratigraphic logs from wells drilled along Otisco Road and Onondaga Creek indicate a bowl-shaped deposit of laminated clayey silt with interbeds of fine to medium sand. The deepest part of the laminated sequence appears to be at the intersection of Otisco Road with Onondaga Creek (fig. 8). This laminated sequence was laid down contemporaneously with the Tully Valley upper fine-grained valley-floor deposit.

Remediation Activities

Three remediation projects, described below, were implemented by the Onondaga Lake Management Conference on the basis of the above-mentioned research to reduce sediment discharge to Onondaga Creek and to slow or stop mudboil activity.

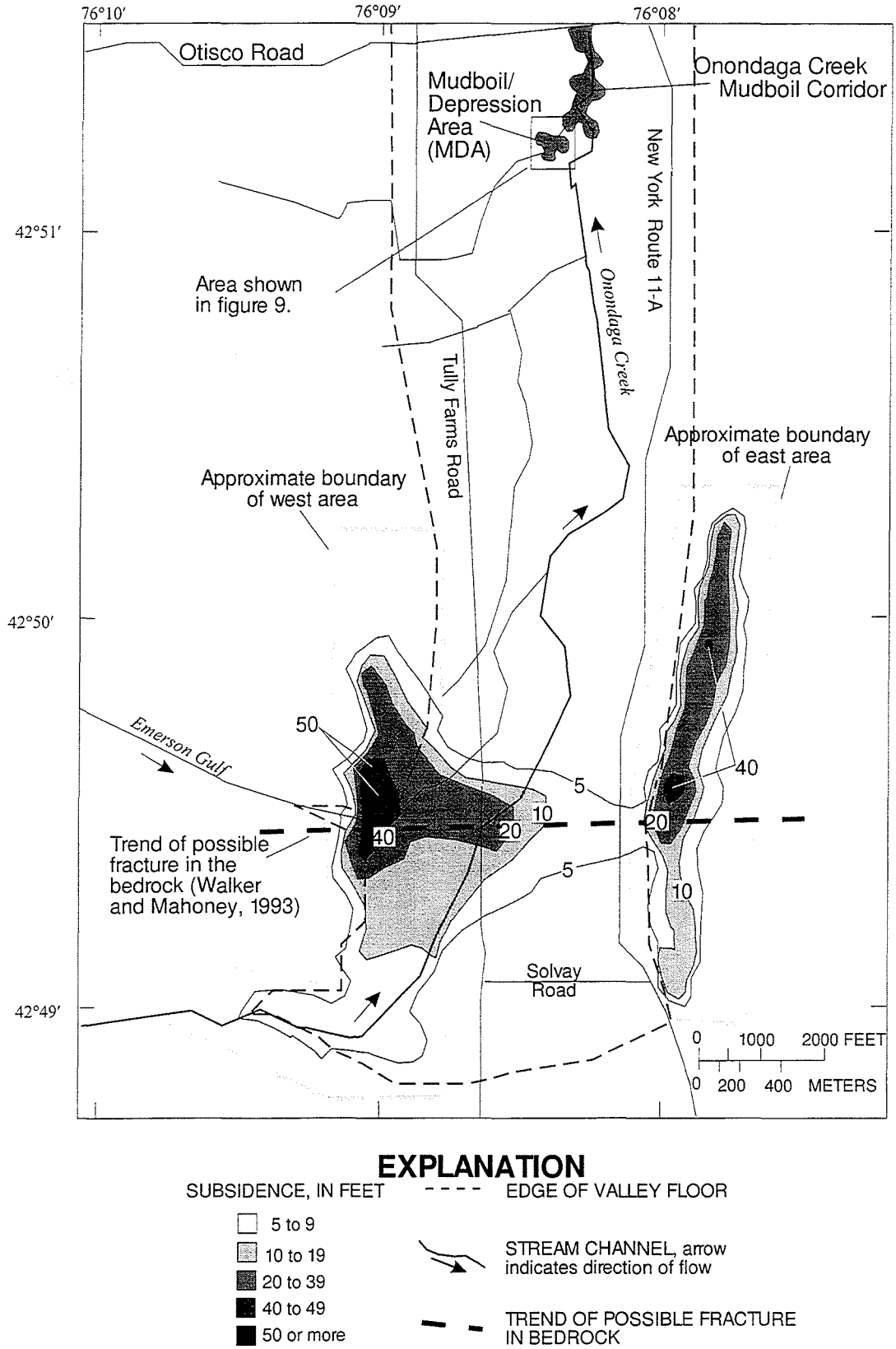

Figure 7. Extent and depth of brine-field subsidence (1957-93) in east and west areas and along a possible bedrock fracture in the southern part of Tully Valley (Modified from Walker and Mahoney, 1993, figure 7. Location shown in fig. 2.)

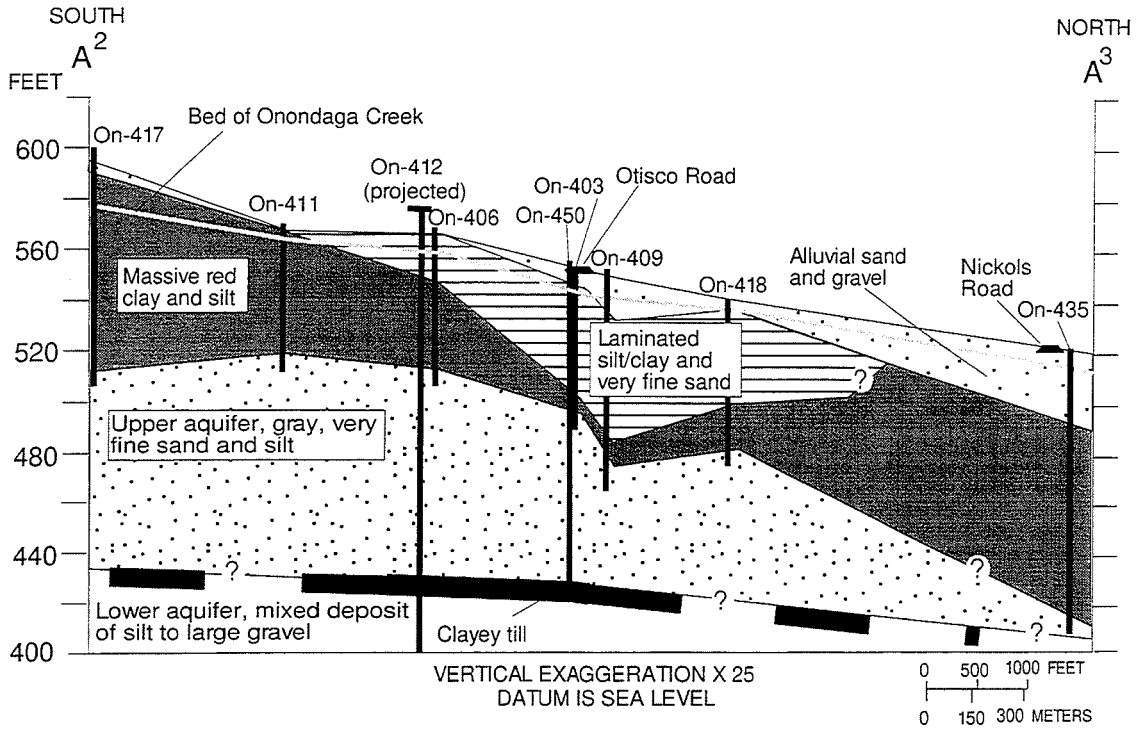

Figure 8. Geologic section A^2-A^3 showing unconsolidated deposits in the central part of the Tully Valley and the projected thickness of the confined freshwater aquifer between wells On-417 and On-435. (Location of section shown in figs. 2 and 3. From Kappel and others, 1996, fig. 5.)

Stream Diversion

Flow from the 0.7 square mile watershed above the MDA was diverted away from the MDA area to another tributary just to the south in June, 1992 (fig. 3). This diversion reduced the amount of water entering the MDA by about one-third and reduced the amount of sediment discharging to Onondaga Creek by about 30 percent of the load measured before the diversion.

MDA Impoundment

A temporary dam was constructed at the outlet of the MDA to: (1) impound flow and thereby retain sediment discharged from the mudboils, and (2) to increase the hydrostatic and lithostatic loads over mudboils within the MDA and thereby reduce discharges of water and sediment from the mudboils. The dam caused water to inundate mudboils in the eastern and central part of the MDA and was initially successful in reducing the sediment discharge to Onondaga Creek to less than 0.5 tons per day. The impounded area soon filled with sediment, however, and the loading of clay and fine silt particles to the Creek increased. A new, permanent dam that can impound up to 5 feet of water behind it was constructed in October 1996 at the outlet of the MDA. Water levels will be raised incrementally, as the pond fills with sediment, in conjunction with operation of depressurizing wells around the MDA.

Depressurizing Wells

Two depressurizing wells were installed near the Otisco Road bridge in December 1993 to lower the artesian pressure and thereby reduce mudboil activity near the bridge. A properly constructed well will keep mudboil sediments in place while discharging ground water faster than a mudboil. Each well consists of a 12-inch surface casing driven into the upper 40 feet of the upper silt and clay unit, with an interior 6-inch casing driven through the silt and clay unit into the upper freshwater aquifer. The interior casing was driven to the top of the clayey till unit, about 130 feet below land surface, and then cleaned out. The types of sediment removed from the casing were logged to identify the most permeable unit between the clayey till and the surficial silt and clay sediments. A screen was lowered to a position opposite the most permeable unit, and the casing was pulled up to expose the screen. The permeable unit outside the screen was then developed to produce a flow of sediment-free water.

Flow from the well on the west side of the bridge averaged about 23 gal/min (gallons per minute), and the well on the east side averaged about 3 gal/min. The coarsest unit observed in the well on the east side of the bridge was a fine sand; the west-side well had a medium sand. The wells reduced the artesian pressure within a radius of at least 200 feet by about 2.5 feet, as determined by monitoring wells installed previously. Mudboil activity, which caused the collapse of the bridge in 1992, has not resumed. The wells were not necessarily the sole reason for the decline in mudboil activity because the onset and cessation of flow from any given mudboil are poorly understood.

The success of the two depressurizing wells at the Otisco Road bridge prompted the installation of eight additional wells along Onondaga Creek and around the MDA in the fall of 1996, in conjunction with the reconstruction of the MDA-outlet dam. These wells were needed to reduce any increase in artesian pressure resulting from the additional water and sediment load over the

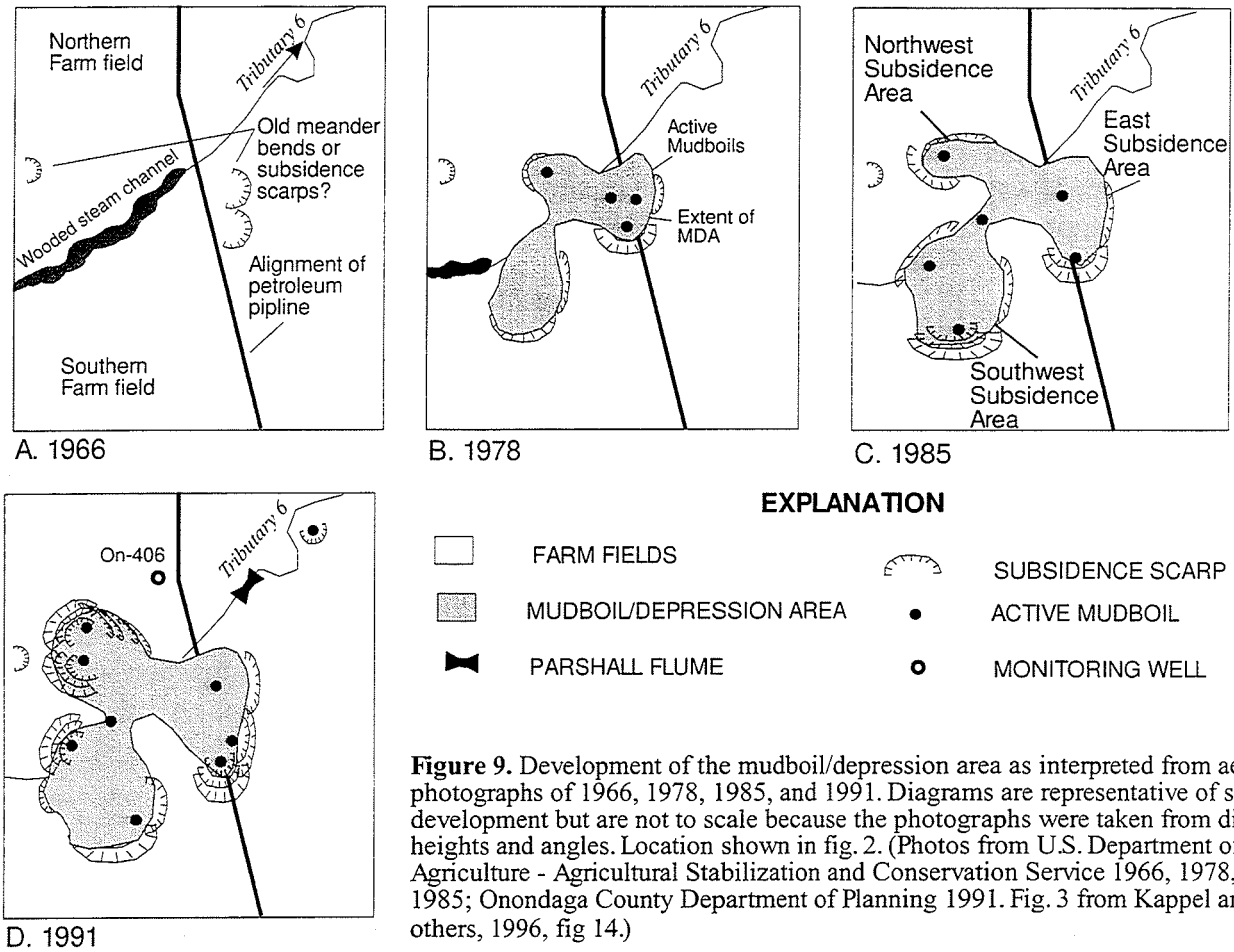

Figure 9. Development of the mudboil/depression area as interpreted from aerial photographs of 1966, 1978, 1985, and 1991. Diagrams are representative of scarp development but are not to scale because the photographs were taken from differing heights and angles. Location shown in fig. 2. (Photos from U.S. Department of Agriculture - Agricultural Stabilization and Conservation Service 1966, 1978, and 1985; Onondaga County Department of Planning 1991. Fig. 3 from Kappel and others, 1996, fig 14.)

mudboils within the MDA. The discharge from these wells ranged from more than 130 gal/min to less than 5 gal/min. Water from the MDA and Onondaga Creek wells range from fresh (<500 μS/cm) to very brackish (>19,000 μS/cm). Brackish water was encountered in some wells in which the clayey till layer was not found during drilling. In other wells, only fine-grained materials were found, and well yields were correspondingly low.

Coarse gravel was penetrated in one well on the northwest side of the MDA at a depth of about 170 feet. Flow from the well exceeded 300 gal/min initially but soon slowed to less than 50 gal/min as sand and gravel were forced up into the casing. Water from this well was extremely brackish; therefore, the decision was made to seal this well and drill another nearby. Within minutes, however, small mudboils appeared about 25 feet from the site, and the water discharged from these mudboils was also extremely brackish. This area was suspected to have been the edge of a old mudboil area (fig. 9D), and the sudden, rapid development of the mudboils discharging brackish water confirmed this. A grouting company was hired to seal the base of the well and the hydraulic connection to the surface, but this procedure failed. Within days, a large, consolidated mudboil vent developed that discharged about 100 gal/min of extremely brackish water and sediment to the upper end of the MDA. Soon thereafter the land began to subside, but within 3 months, the subsidence slowed, as did the rate of flow from the mudboil. At present (August 1997) the area is fairly stable but will probably coalesce with the MDA eventually.

Future Considerations

The mudboil area is dynamic and difficult to remediate. The wells around the MDA at present discharge about 350 gal/min, which drains to Onondaga Creek. Water leaving the MDA impoundment is almost clear and lacks coarse-grained silt and sand. The results of these remediation activities will be evaluated over the next several years to determine their effectiveness in reducing the artesian pressure, slowing mudboil activity and land subsidence, and reducing the loading of sediment to the creek. Increasing chloride concentrations discharged to the creek from the mudboils (and mudslide areas) will also need to be monitored to assess the effect of remediation on Onondaga Creek.

Acknowledgments

The Onondaga Lake Management Conference and the U.S. Environmental Protection Agency-Region 2 provided funds for the study of the Tully Valley Mudboils (1992-1997) through Interagency Agreement DW14941626-01. The author would also like to acknowledge the assistance and patience of the residents of the Tully Valley and the Allied-Signal Corporation for allowing access to their respective properties in order to conduct these investigations.

REFERENCES CITED

DeGroff, E. R., 1950, Joint patterns in central New York: Syracuse, N.Y., Syracuse University, Department of Geology, unpublished master's thesis, 75 p.

Getchell, F. A., 1983, Subsidence in the Tully Valley, New York: Syracuse, N.Y., Syracuse University, Department of Geology, unpublished master's thesis, 108 p.

Grasso, T. X., 1970, Proglacial lake sequence in the Tully Valley, Onondaga County, *in* New York State Geological Association Guidebook, 42nd annual meeting: Syracuse, N.Y., Syracuse University, Department of Geology, p. J1-J16.

Haley and Aldrich of New York, 1991, Report on mudboil occurrence in the Tully Valley, Onondaga County, New York: Rochester, N. Y., prepared for Allied Signal Corporation, 28 p.

Isachsen, Y. W., and McKendree, W. G., 1977, Preliminary brittle structures map of New York: New York State Museum Map and Chart Series, no. 31E, 1 pl., scale 1:250,000.

Kappel, W.M., Sherwood, D.A., and Johnston, W.H., 1996, Hydrogeology of the Tully Valley mudboils and characterization of mudboil activity, Onondaga County, New York: U.S. Geological Survey Water-Resources Investigations Report 96-4043, 71 p.

Matheson, D. S., and Thomson, S., 1973, Geological implications of valley rebound: Canadian Journal of Earth Science, v. 10, p. 961-978.

Molinda, G.M., Keasley, K.A., Oyler, D.C., and Jones, J. R., 1992, Effects of horizontal stress related to stream valleys on the stability of coal mine openings: U.S. Bureau of Mines, Report of Investigations 9413, 25p.

Mullins, H.T., Wellner, R.W., Petruccione, J.L., Hinchey, E.J., and Wanzer, S., 1991, Subsurface geology of the Finger Lakes region, *in,* Ebert, J. R., ed., New York State Geological Association guidebook for the 63rd annual meeting: Oneonta, New York, SUNY Oneonta, p.1-54.

Post Standard, 1899, Tully Valley -A miniature volcano: Syracuse, N.Y., Syracuse Post Standard, October 20, 1899, p. 14.

Rickard, L.V., 1975, Correlation of the Silurian and Devonian rocks in New York state: New York State Museum and Science Service, Map and Chart Series no. 245, 16 p., 2 charts.

Snell, Laura, 1992, Comments on mudboil working group management plan: Albany, N.Y., New York State Department of Environmental Conservation, Division of Mineral Resources, letter of February 19, 1992, 12 p.

Walker, S. E., and Mahoney, R. J., 1993, Interpreting and projecting long-term environmental conditions in a shallow brine field: Woodstock, Il., Solution Mining Research Institute, 1993 Solution Mining Research Institute Spring Meeting, Syracuse, N.Y., 27 p.

Waller, R.M., 1977, Subsidence in New York related to ground-water discharge, *in* Geological Survey Research 1977: U.S. Geological Survey Professional Paper 1050, p. 258.

Rock-Block Slide on Bare Mountain, Southern Onondaga County, New York

Robert H. Fakundiny
New York State Geological Survey/State Museum
3140 Cultural Education Center
Albany, NY 12230, rfakundi@museum.nysed.gov

Carlton E. Brett
Department of Earth and Environmental Sciences
227 Hutchinson Hall
Rochester, NY 14627
cebh@dbl.cc.rochester.edu

Introduction

Special Type of Landslide?

A two-mile long series of contour-parallel notches mark slivers of Devonian bedrock that are separated with 30 to 100 ft of relative-vertical displacement from their *in situ* stratigraphic equivalents high on the east side of Bare Mountain, in southern Onondaga County, NY (Fig. 1); yet downslope exposures show no chaotic or disruptive features, nor do geomorphic forms hint of a landslide foot or toe (Fakundiny, 1997.) Either the displacements took place on a series of (1) closely spaced, shallow-dipping, listric faults that have their bottoms in deep bedrock or (2) slide planes that separate long, thin, mostly intact, sliver-like blocks with toes buried in valley fill. No glacial deposits or ice-scour features have been found in the back-head notch, on top of or on the valley-side slope of the blocks. Lack of glacial deposits high on the mountain side suggests that block movement occurred during the last stages of retreat of the Laurentian ice sheet or later. If hypothesis 1 is correct, listric faults in the Finger Lakes District of central New York may indicate latent seismic hazard, whereas, hypothesis 2 may indicate possible landslide hazards at the base of Bare Mountain. With only its top exposed the feature lying on the side of Bare Mountain is difficult to characterize. Structural interpretation of faults is usually made from limited exposures at their tops and geophysical or drilling data from their buried parts. Landslides, conversely, are usually totally exposed. The feature on Bare Mountain, however, is mostly buried by colluvial, alluvial and postglacial lacustrine deposits, thus, obscuring the geomorphology of its lower parts. We are not aware of any descriptions in the literature of a rock-block slide with a buried foot and toe, although Jane Gilotti and Joseph Hull (oral communication, 1997) have observed one in Greenland. Our studies to date favor rock-block sliding over Holocene faulting. Thus, the landslide hypothesis will bias the following discussion.

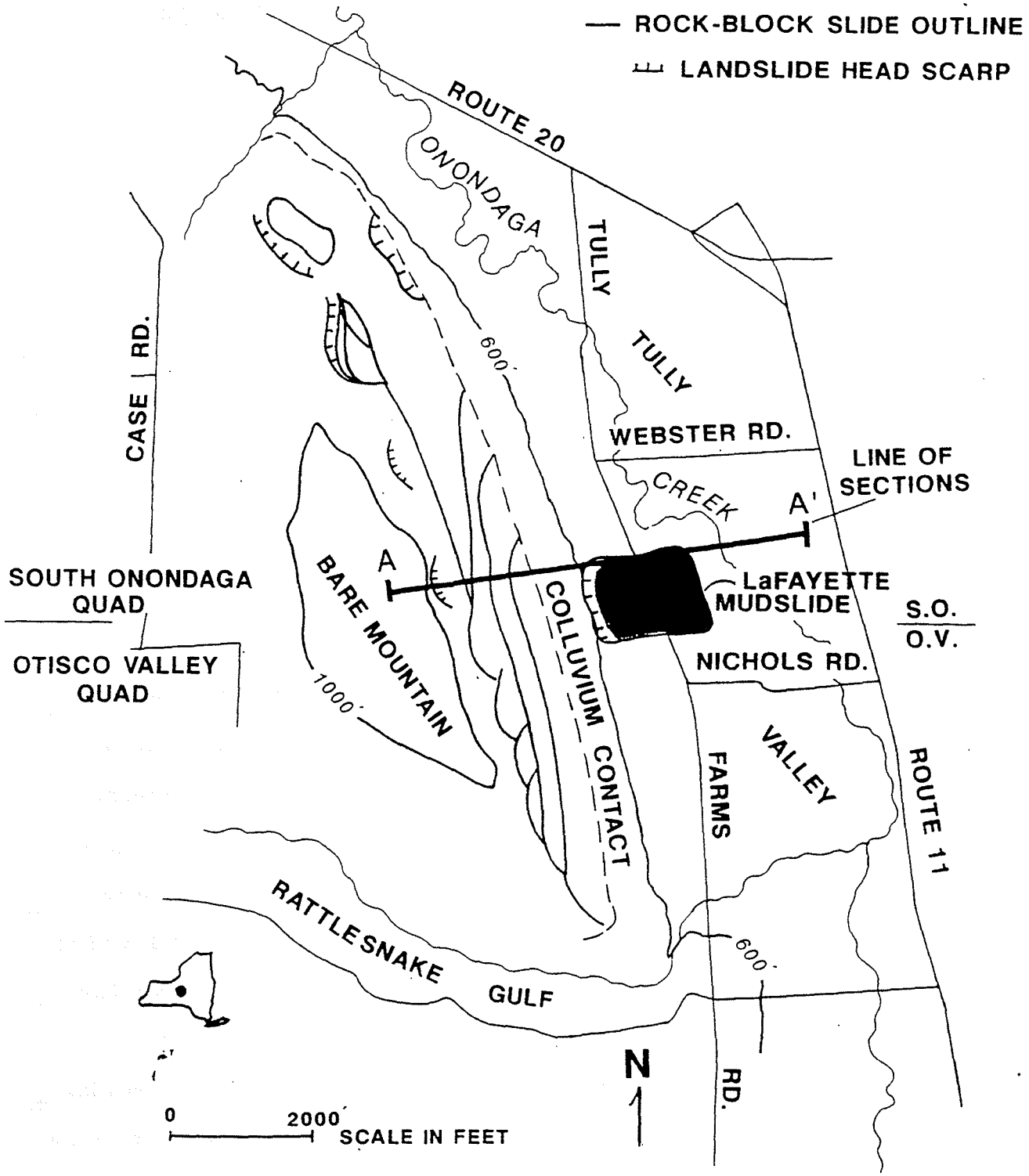

Figure 1. Location map of Bare Mountain rock-block slide in southern Onondaga County, NY. Section A-A[1] is location of Figures 4 and 5. S.O./O.V. is the South Onondaga-Otisco Valley quadrangle boundary.

Purpose and Scope

The purpose of the field trip and this essay is to show and describe what might be the first-recognized, large, rock-block landslide with a foot and toe that are presumably buried by proglacial lacustrine and postglacial alluvial and colluvial sediments. We say this on the bases of the limited literatuare search that we have been able to make. The relations between the geomorphology of the hillside where the landslide is parked and local glacial features places its time of movement from about 12000 to 15000 B.P.

The scope of this investigation was confined to only aerial photograph interpretation and cursory geologic mapping of marker beds within the Devonian bedrock sequence of central New York, as defined by Brett and others (1995) and Ver Straeten (1995.) Other types of studies could add information, such as: (1) drilling, which may soon be done in the search for potable groundwater; (2) refraction seismic profiling, which is not currently acceptable to the landowners; and (3) coring sediment-filled sags for pollin, which has yet to be undertaken. These types of studies await new resources for their undertaking.

Location

The east side of Bare Mountain faces the Tully Valley approximately 5.5 miles south of Syracuse, NY, in southern Onondaga County, central New York (Fig. 1) and lies across the border between the South Onondaga 7.5-minute topographic quadrangle to the north and the Otisco Valley 7.5-minute topographic quadrangle to the south. Bare Mountain is approximately 3 miles in length along a N25°W axis and 1.25 miles wide at its middle. The mountain rises approximately 1000 ft above the Tully Valley floor on the east and 280' above the saddle between it and Manus Hill on the west. Bare Mountain is bounded on the north by the Valley of the West Branch of Onondaga Creek and on the south by Rattlesnake Gulf, which carries an east-flowing tributary to the East Branch of Onondaga Creek in the Tully Valley. The political boundary between the towns of Otisco, to the west, and LaFayette, to the east, transects the mountain from north to south. The Village of Cardiff, which lies at the intersection of US Route 20 and State Route 11A, lies at the north end of Tully Valley across from the north end of Bare Mountain. All land is private, and access is restricted. Trespassing requires permission of the owners.

Problem

The features on the eastside of Bare Mountain have all of the characteristics of a rock-block slide (Cruden and Varnes, 1996), except that bedrock bedding does not dip into the valley. The problem with a landslide interpretation is that the

block slivers are long (up to 2 miles), thin (~250 feet thick), intact, relatively unrotated, and have no exposed foot or toe--characteristics that we have not found described in the literature. Is this a new type of rock-block slide?

Bare Mountain has a plateau top with a cliff that stands 900 ft above the Tully Valley floor. The valley floor itself is the top of a deep fill of Pleistocene and Holocene till and lacustrine units interfingered with sidewall alluvial fans and colluvium (Kappel and others, 1996; Pair, 1995, and in prep.) The intact nature of these long, thin slivers along their length is unusual for rock-block slides. Few rock-block slides have been described in the literature, as shown by the lack of references to them in Turner and Schuster (1996.) Lack of disintegration suggests that movement was steady and slow and that blocks were gently eased into their current positions without severe disruption (Fig. 2.) Advancing glacial ice may have eroded and oversteepened the preglacially sculptured bedrock wall at the mountain's base, thus destabilizing the slope above. Unlike rock-block slides that have been described from other parts of the northern Appalachian Basin (Schultz and Southworth, 1989) that have slipped along valley-dipping weak beds, the Bare Mountain slide most likely moved along a valley-dipping joint system. Slip may have been gradual, possibly the blocks accommodated by being let down against wasting ice in the valley. Concomitant infilling of lacustrine deposits around the ice and over any remaining parts of the foot of the slide could have buttressed these blocks and secured them to the side of the mountain in a metastable or dormant state. Mudslides at the foot of the valley wall, such as the LaFayette mudslide (Fickies, 1993; Fickies and Brabb, 1989; Negussey and others, this volume) (Fig. 1), could relieve that restraining load and reinitiate downslope movement of the rock-block slide. If these features are, indeed, a rock-block slide, they form (volumetrically) one of the largest landslides recognized in New York State (>$2x10^8 yd^3$), possibly in the entire northern Appalachian Basin (see Schultz and Southworth, 1989.) The morphology of the slip surfaces and their role in collecting and distributing upland surfacewater and groundwater may help interpret the artesian hydrologic systems of Tully Valley, in which mudboils abound (Kappel and others, 1996; Kappel, this volume).

Fault?

Other workers in the area have suggested the possibility that the block movement may have been along a tectonic fault or large gravity-induced fault system (William Kappel, oral communication, 1996.) Although faults have been mapped locally (References reported in Kappel and others, 1996), factors weigh against this interpretation, including: (1) no extensions have been mapped along strike in either direction from the exposed breaks; (2) interpretation of geomorphic features (discussed below) strongly suggests that the timing of fault movement would have to be latest Wisconsinan;

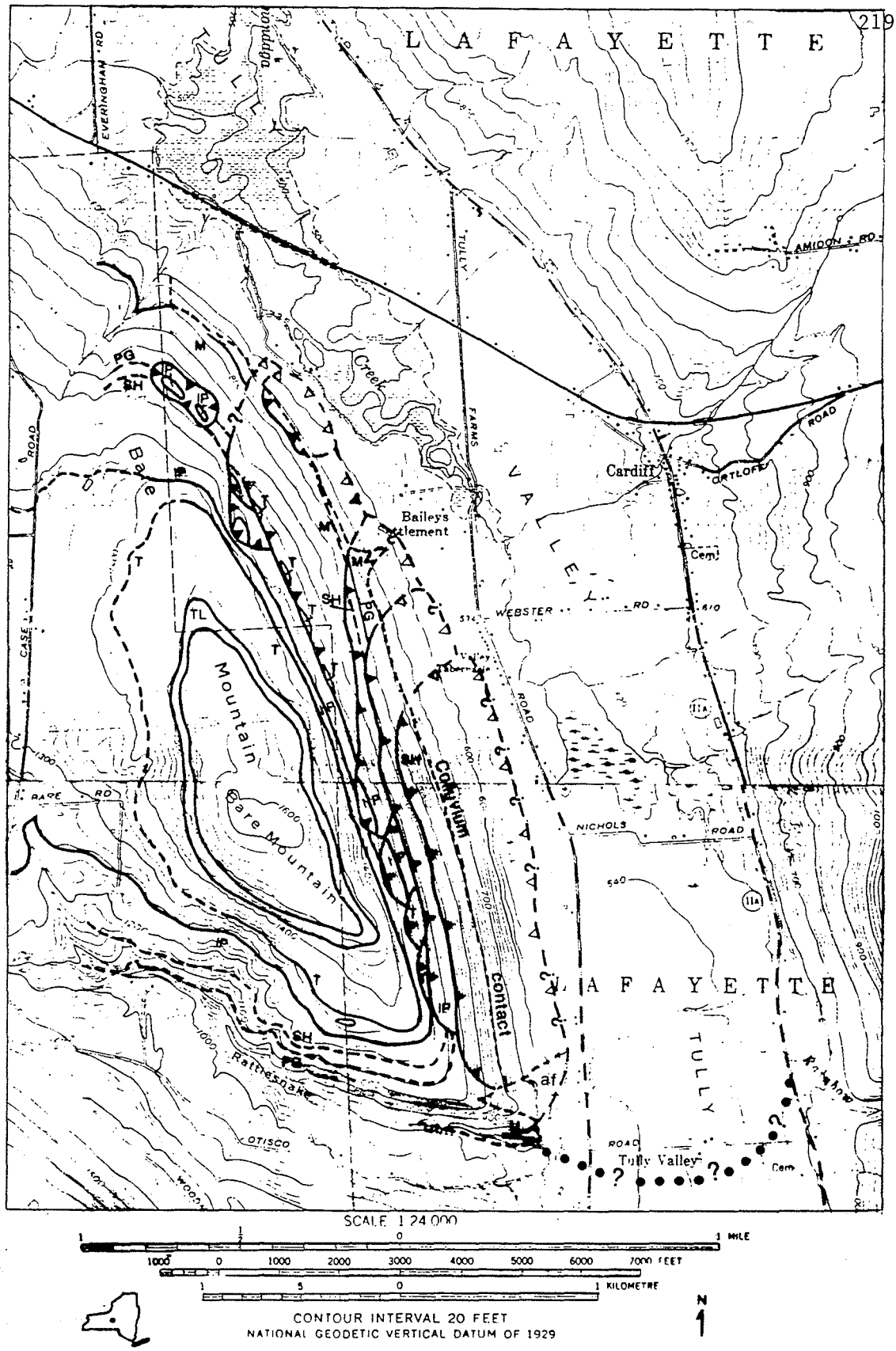

Figure 2. Geologic map of Bare Mountain showing landslide blocks outlines, colluvium contact, and several bedrock marker beds. TL=Tully Limestone; T=Tichenor Beds; IP=Top of Ivy Point Member; SH=Staghorn Coral Bed; PG=Peppermill Gulf Member; M=Mottville Member; at=diseccted alluvial fan. Solid lines with filled barbs are sliver ridge caps; dashed lines with open barbs are outlines of buried sliver toes. Dotted line with question marks is possible location of Onondaga Fm. subcrop below valley fill.

consequently, the movement took place in the modern stress field, which is compressive, with the maximum stress oriented ENE perpendicular to the strike of displacement planes and, thus, unable to promote either normal or strike-slip sheer movement; and (3) the map pattern (Fig. 2) is not typical of tectonically induced, regional fault systems in the Appalachian Basin (see Discussion below.) We, therefore, interpret the feature to be local and most likely the result of late Wisconsinan erosion and deposition upon failing bedrock strata, rather than tectonically induced faulting.

Bare Mountain structure

A block-rock slide interpretation for the Bare Mountain structure presents problems of interpretation also including: (1) its large size and intact shape, (2) the small amount of slip, (3) lack of an exposed foot and toe, and (4) timing. Note that this discussion will use the English system of measurements, consistent with the 7.5-minute topographic quadrangle scale and contour interval. The size and shape, >10,000 ft long, ≥250 ft thick, and ≥2500 ft along the 25° slope from head to toe makes the Bare Mountain feature larger than the rock-block slides in the Appalachian Valley and Ridge province of eastern North America (Schultz and Southworth, 1989). For terms used in this paper please see Appendix.

The vertical-slip component of movement, as measured by displaced, bedrock marker beds, ranges from 35 to 100 ft. The horizontal strike-slip component is not known, but is probably negligible. The unusual feature of the slide is the intact condition of the block components along strike (Fig. 2.) We would expect that $2x10^9 yd^3$ of rock crashing down a 25° slope for 100 ft would disaggregate and slump into a jumble of disoriented, rotated, jumbled blocks with no continuous mappable stratigraphy. At least 4 mappable slivers of the slide have internally coherent, traceable marker beds, that have little to no rotation of the bedding, except at the head ridges where small (<200 yd^3) rotational rock slumps locally occur. These commonly dip back into the head scar or gently to the south or southwest.

The foot and toe of the slide presumably is buried by proglacial, lacustrine and postglacial fluvial and alluvial units that were deposited in a lake in front of the receding ice lobe or on the postglacial valley floor (Kappel and others, 1996.) Burial and stabilization of the slide foot and toe took place before or during dewatering of the proglacial lake, presumably as the receding ice tongue uncovered lateral, melt-water channels across valley walls to the north (Hand, 1978; Gomes and Pair, 1997.) Timing of the movement can be roughly determined by geomorphology and relation to proglacial lacustrine and postglacial alluvial and colluvial sediments. Several colleague glacial geologists have visited the head of the slide and have expressed their opinions that none of the geomorphic features were produced by overriding ice or ice-contact, fluvial erosion that may have been associated with the Laurention ice retreat (Donald

Cadwell, G. Gordon Connally, Barbara Hill, George Kelley, Donald Pair, oral communication, 1996.) The interpretation that the morphology of these slivers at their heads is formed by post-glacial or pariglacial surface-water erosion, frost heave, and precipitation is consistent with the interpretation of Pair (in prep.) Thus, the most logical time for movement would be during ice retreat from the walls of the valley to allow for slumping, and at the time that high standing proglacial meltwater lakes drained along cross-channel fluvial systems (Hand, 1978, Jager and Wieczorek, 1994.) The latest stage of the Wisconsian would provide a unique time when: (1) some ice may have remained and foundered to buttress the slide and ease the slivers down the valley wall; (2) a proglacial lake still existed to form the sink for lacustrine deposits to cover the foot of the slide; and (3) pore-water pressure in the bedrock was still high from the pre-existing high-standing proglacial lake--all circumstance that could have aided the initiation of slide movement and eased the slivers into their current position. The age of movement would, therefore, be at the time of recession of the ice sheet from the Valley Heads moraine and when a slight readvance placed the ice tongue adjacent to the side of Bare Mountain (Gomes and Pair, 1997.) A dissected, hanging, alluvial fan that sits high on the southernmost part of the east face of Bare Mountain covers the southern end of the rock-block slivers and may help to determine the age of last movement (Fig. 2.)

Bedrock Geology

Mapping

The bedrock geologic map for the southern part of the South Onondaga and northern part of the Otisco Valley 7.5-minute topographic quadrangles was recently made by Brett and others (1996) and Ver Straeten and others (in prep) as part of the New York State Geological Survey-U.S. Geological Survey cooperative STATEMAP Program. Brett and colleagues are now mapping the Marcellus Quadrangle to the west and the Jamesville Quadrangle to the east.

Stratigraphy

Detailed stratigraphy for both quadrangles near Bare Mountain (Fig. 3) was determined by Carl Brett, Gordon Baird, and Charles Ver Straeten (Brett and others, 1996; Ver Straeten, 1995.) The bedrock section that may be incorporated in the slide possibly extends from below the Helderberg and Tristates Groups, up through the Onondaga Formation, and the Hamilton Group. The Tully Formation limestones and the section above may have been involved, but are now eroded from the top of the block sliver. Within Bare Mountain the bottom of the exposed section is in the Cardiff Member of the Oatka Creek Formation (Marcellus Formation of previous authors), and the top exposes Geneseo

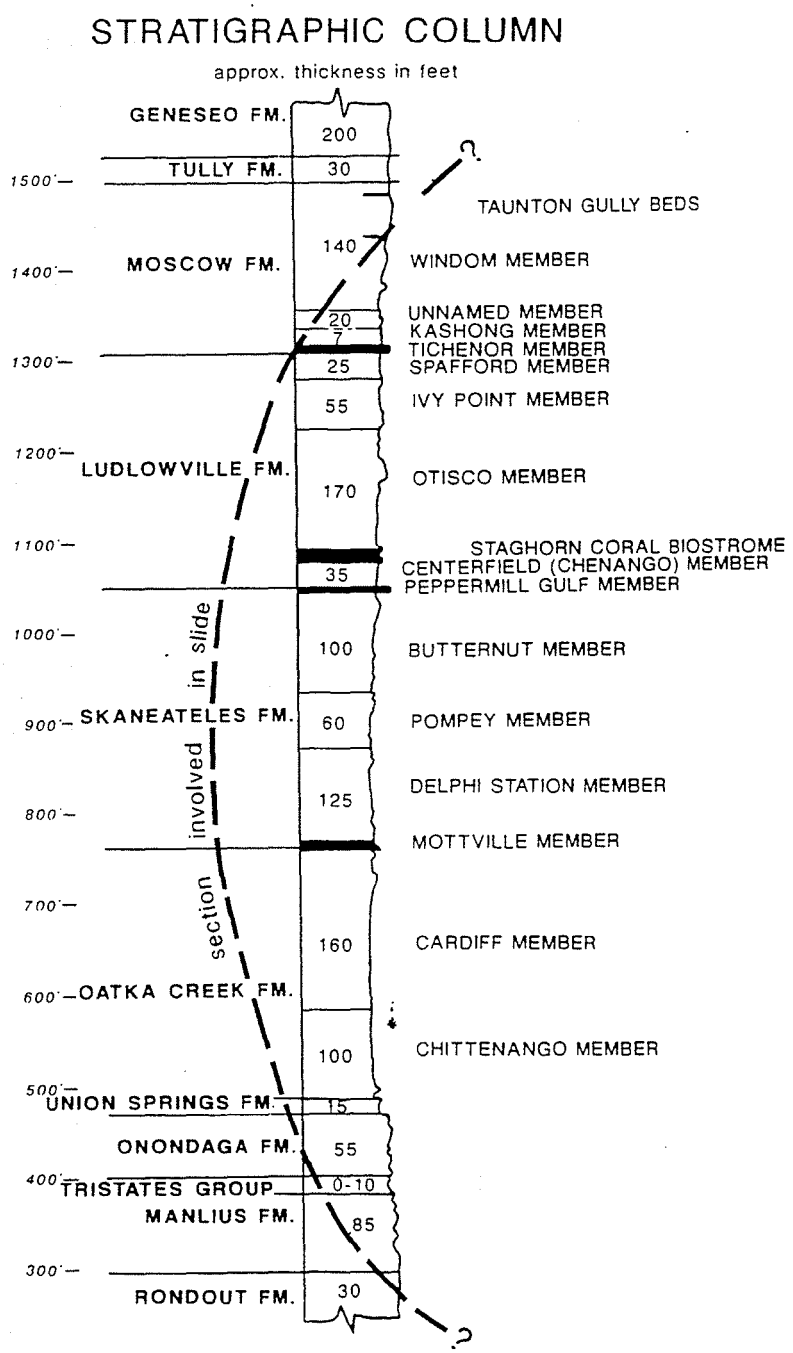

Figure 3. Stratigraphic column of Upper Silurian and Lower and Middle Devonian bedrock in the South Onondaga and northern Otisco Valley 7.5-minute quadrangles, showing formations, members, and marker beds. Also shown is section that was breached by the rock-block slide. Elevations are on Bare Mountain. Section from the top of the Manlius Formation downward to the top of the Rondout Fm. is the Helderberg Group. Section from the bottom of the Oatka Creek Formation to the top of the Moscow Formation is the Hamilton Group. Geneseo Formation is the bottom of the Genesee Group.

Formation shale. Of note are the marker beds that were used to map the slide, which include: Union Springs (in drill hole), Mottville and Peppermill Gulf bed of the Centerfield Member, the Staghorn coral biostrome, the tops of two siltstone tongues of the Ivy Point Member of the Ludlowville Formation, and the Tichenor Member of the Moscow Formation.

Regional Folds and Faults

Within the South Onondaga and Otisco Valley quadrangles the bedrock generally dips <5° to the southwest with generally a N70W (160°) strike. Local, open WNW-tending folds, NW-to N-trending monoclines, and a rare E-W-trending rupture of rock at Nedrow (ramp thrust from a deep decollement?) prevail. A north-trending monocline or fault lies west of Bare Mountain and lowers the bottom of the Tully Formation from an elevation of 1560 ft on Manus Hill to 1520 ft on Bare Mountain, against the grain of the regional dip. Another buried monocline (or fault) trending ≈N35W (325°) lies under Tully Valley and lowers the base of the Ludlowville from 1100' on the north end of Bare Mountain, with a projected elevation of about 1160' down to 1100' 1.5 miles up dip on the eastern wall of Tully Valley.

Joints

Joints control the form and attitude of the intact headwall-line scarp of eastern Bare Mountain above and behind the rock-block slide. In the scarp below the Tully Formation, joints can only be recorded from the Taunton Gully Beds (upper Windom Member) and the Tichenor Member of the Moscow Formation. In the slide blocks, joints can be measured in any exposed unit from the Ivy Point Member of the Ludlowville Formation downward. Not enough rock is exposed to allow for a statistical study of joints on the hillside, but studies elsewhere in central New York (Engelder, 1985; and Engelder and others, 1997, and references therein) show that most vertical joint sets that have been mapped in central New York State are part of a systematic regional manifestation, or genetically related to those regional systems. The vertical joints were presumably generated by regional, fluid-hydraulic pressure that resulted from tectonic loading, or from local overpressured hydraulic systems. Dipping joints are different from the vertical sets by being systematically related to local topography and are interpreted as late (post-Pleistocene?) unloading joints (Engelder, oral communication, 1997.) These "unloading" joints mostly dip toward the valley at angles less than or equal to the valley-wall slope. We propose that sets of the valley-ward dipping joints, like the ones exposed high on the east side of Bare Mountain, control the orientation and geometry of the slip surfaces beneath the slide blocks. At several headwall-line exposures a few conjugate pairs to valley-dipping joint sets dip into the hillside at comparable angles.

Vertical joints recorded from the headwall are: N-S (000/90), N25E (025/90), N60E (060/90), N80E (080/90), N30W (120/90), and N10W (170/90). Dipping joints in the headwall-line scarp are: N30E35SE (030/35), N30W55SW (150/55), N55W40NE (205/40), N30W75NE (330/75), N30W45NE (330/45), and N20W45NE (340/45). Near-vertical joints in the slide blocks are: N30E (030/90), N65E (065/90), N60W86SW (120/86), N30W (150/90), N25W (155/90.) The only dipping joint recorded in a slide block was N70W65SW (110/65.) Just south of Bare Mountain in the Unadilla 15-minute quadrangle, Parker (1942) recorded the N-S, N25E, N60E (Set III), and N60W sets and interprets them to be regionally distributed.

Groundwater

The Middle Devonian shale sequence between the limestones of the Onondaga and Tully formations generally has low permeability and low groundwater yields. Water flows mostly along joints and disaggregated bedding. The Tully Formation has high yields (Fickies in Brett and others, 1995.) The Geneseo Formation, capping Bare Mountain, has geomorphic features that are reminiscent of land surfaces over internal drainage; that is, on aerial photographs the plateau at the mountain top shows only hummocky ground without any recognizable stream courses. The Onondaga Formation and carbonate units immediately below have the highest yields of groundwater, and confine the flow to joints and solution cavities. The groundwater flow and quality in the Salina Group shales and evaporates are influenced by the dissolution of salt units and the perforation of units by brine production wells. (See Kappel, this volume and Kappel and others, 1996.)

Engineering Geology

Bedrock engineering characteristics are given by Robert Fickies (in Brett and others, 1996.) Here Fickies noted the poor to fair cut-slope stability of all of the shale sequences in the strata on Bare Mountain. These are all abundantly jointed. Fickies also notes the fair to good cut-slope stability of the Tully and Onondaga formations and underlying limestones and dolostones of the Manlius and Rondout Formations. These characteristics allow for failure in the shales, especially where interbedded strong carbonate units are breached and undercut.

Surficial Geology

Mapping

The surficial geology of both the South Onondaga and Otisco Valley Quadrangles was mapped most recently by Pair (1995, in prep., and this volume) as part of the New York State Geological Survey-U.S. Geological Survey cooperative

STATEMAP Program. Pair mapped these and the Tully quadrangles in 1995-1997 and is now continuing in the Marcellus Quadrangle to the west of the South Onondaga Quadrangle and the Jamesville Quadrangle to the east.

Stratigraphy

Pair (in prep., and this volume) has mapped seven Pleistocene units for the two quadrangles: glacial till; ice-stratified drift; fluvial silt, sand, and gravel; glaciolacustrine silt and sand; alluvium overlying lacustrine silt and clay; ice-contact sand and gravel and glacio-lacustrine silt and clay; and 5 Holocene units: alluvial fans; alluvium; colluvium; organic deposits; and artificial fill. The Pleistocene glaciolacustrine silt and clay; their overlying alluvium, and Holocene colluvium and alluvial fans are of interest to the history of sliding. A cross section of valley fill and bedrock (Kappel, 1996), shows the interfingering nature of alluvial and deltaic glaciolacustrine deposits along a line extending east from Rattlesnake Gulf. One coincidence that should be noted is that, in the Tully Valley, colluvium is only mapped at the lower parts of the rock-block slide. Colluvium, alluvium, and possibly glaciolacustrine silts and clays, bury the foot and toe of the rock-block slide. Also note that the alluvial fan at the south end of Bare Mountain (Fig. 2), which is dissected at Rattlesnake Gulf, overlies the southernmost extent of the rock-block slide.

Groundwater

Groundwater flow has greatly influenced the production of geologic hazards within the surficial deposits of the Tully Valley (see Kappel, this volume, and Negussey, this volume.) The following is summarized from Robert Fickies (in Pair, 1995.) Under relatively common circumstances, coarse-grained, non-cohesive, stratified sand and gravel deposits have groundwater yields that very widely from fair to very good and have widely varying quality. Fine-grained, cohesive, stratified clays and silts have very poor to poor groundwater yields and may be high in dissolved salts. Till deposits have low groundwater yields, some of which fluctuate seasonally.

Engineering Geology

The engineering characteristics of surficial deposits are described by Fickies (in Pair, 1995) and are subdivided into upland deposits and valley-fill deposits. The relevant units to consider at the rock-block slide are upland deposits and the glaciolacustrine sediments of the valley-fill deposits catagory.

Till covers part of the plateau on top of Bare Mountain and, contrary to what Fickies presents as general characteristics, locally accepts precipitation rather than developing a prominent overland fluvial runoff system. Depth to

bedrock varies, but is shallow. Colluvium covers the lower, eastern flank of Bare Mountain with an upper contact against rock and rock-block soil at the 800-900 ft contour interval. The lower part of the colluvial apron overlies alluvium and glaciolacustrine silts and clays down to about the 600 foot contour. Precipitation that falls on the bedrock and soil above the contact sinks directly into the slide blocks and joins the groundwater system. The resulting small drainage area developed on the colluvium does not provide enough overland flow to erode deep gullies, but rather the small amount of runoff has produced open, downslope swales.

Glaciolacustrine sediments lying above the projected, buried toe of the rock-block slide include silt, sands, and clays. Fickies (in Pair, 1995) reported that the silts and clays have low plasticity, may be varved, and may be poorly drained. The water table may be at or near the surface during and after rains (Dawit Negussey, oral communication, 1997.) These deposits may have engineering properties at or above the liquid limit below the water table and can behave as a viscous liquid. Slopes on these deposits may be marginally unstable and susceptible to landslides where greater than 10°. We believe that saline groundwater may have exacerbated the condition by reducing the attractive forces between clay particles.

Geomorphology

Topographic and Geologic Traverse along Cross Section

The topographic map (Fig. 2) does not have the precision to show the back-head depression (notches) and composite, head-ridge morphology. Although 20-foot contour intervals should reveal the notches and ridges, the aerial photographs that were used to make the topographic map must have been taken during summer when full foliage obscured the detailed morphology. Before the rock-block slide can be adequately described a precise and accurate topographic map, preferably at a 5' contour interval, must be constructed. In the meantime, the map presented in Figure 2 will have to suffice. A west-to-east traverse from the top of Bare Mountain to the break in slope at the valley bottom across the midpoint of Bare Mountain illustrates the complexity of the slide and the difficulty in determining the mechanistic cause and timing (see Fig. 4.) The traverse starts at the top of Bare Mountain (elevation >1600') in Geneseo Formation shales that are vegetated with grasing crops and sparse woods. A small cliff of exposed Tully Formation (limestones) rings the top of the Mountain at about 1580-1540'. Below the cliff is a bench or secondary plateau cut on the top of the Taunton Gully Beds of the Windom Member of the Moscow Formation. The Taunton Gully Beds are jointed and form a vertical cliff, in places more than 100' high, with talus below. This is not a head scarp, but a post-sliding, back-wasted cliff that

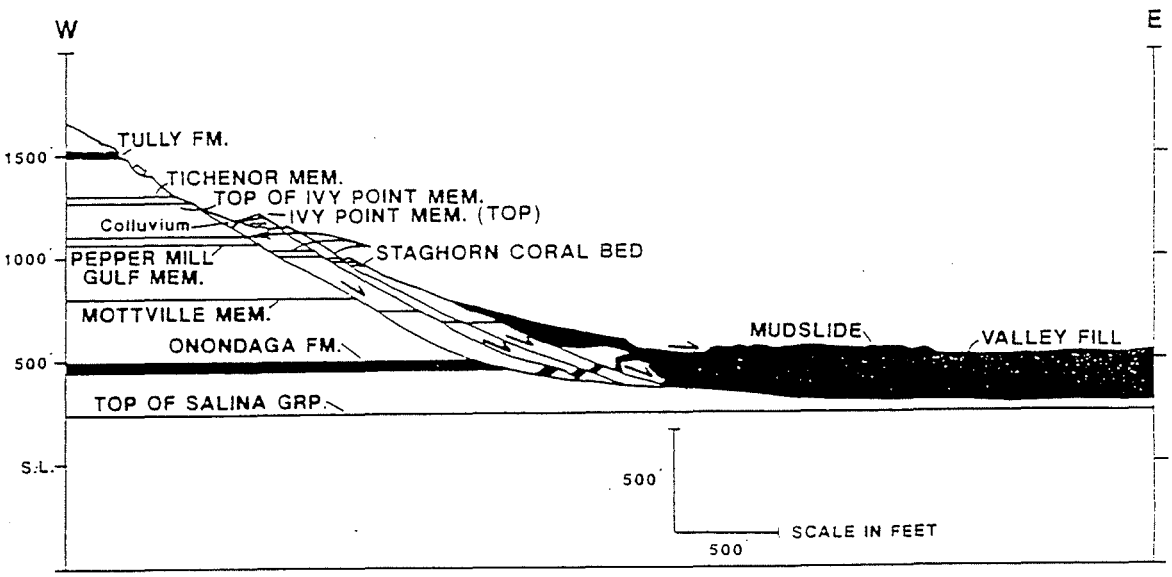

Figure 4. Cross section showing preferred interpretation of structure on the east side of Bare Mountain.

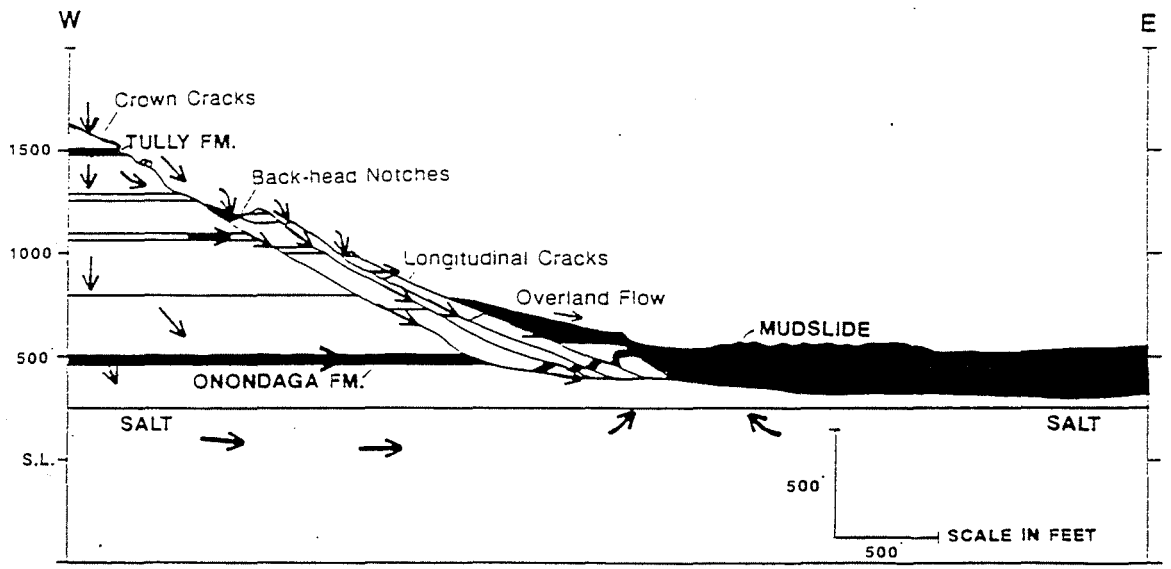

Figure 5. Cross section showing possible groundwater migration routes.

has retreated from the head-scarp position and is controlled by prominent vertical and valley-dipping joints. We are informally calling this a headwall-line scarp in the fashion of a "fault-line scarp" that is used for back-eroded fault scarps. Small, modern, rotational rock slumps and rock slides in the cliff and talus reveal other marker beds within the Moscow Formation, such is the basal Tichenor Beds, in sparsely distributed localities at about 1300'. Talus from the shale of the Windom Member (Moscow Formation) fills much of the linear depression behind the first head ridge. To the south, large blocks of Tully Formation (limestone) have toppled or have been let down without much rotation onto talus from the Moscow Formation. The in-filling talus along the back-head notch has internal drainage and local sag holes, some of which are plugged with clay. One such sag south of the traverse has a small pond. This filled sag would be a favorable locality for pollin studies. Talus covers the Otisco, Ivy Point, and Spafford members of the upper Ludlowville Formation and extends to the foot of the back slope of the head ridge of the uppermost block slivers. The head ridges stand 15 to 40 feet above the back-head linear depression (notch) and are themselves covered by talus below their tops. The top of the head ridge is held up by either the Tichenor Member of the Moscow Formation or the top of the upper cycle of the Ivy Point Member of the Ludlowville Formation. Thus, the head ridge can have a cap that varies 30' in stratigraphic position, consistent with the variation in elevation of the cap. If one leaves the traverse at this point and ventures north along the top of the head ridge, one can travel .6 mi and not leave this 30 ft interval of the stratigraphic section nor vary in elevation more than about 50 ft. Returning to the traverse, locally the head ridge is segmented and small blocks from the cap of the ridge have sloughed off either outward or inward such that the rotated blocks have large dips of bedding that trend outward toward the valley or inward toward the main scarp. Many head-ridge segments will have slight dips of bedding to the north or south, possibly reflecting the small rotation of the slide slivers along their length. On the head ridge and the valley-side slope, the vegetational stress during spring and fall is evident from the apparent poor health of the trees, probably a symptom of lack of water. Farther down the valley-side slope the other ridge crests have similar stressed vegetation. Species of trees appear to vary also in correspondence with the location of back-head notches, where surface water sinks. At least two other notches and ridges are encountered while traversing down the slope. The most prominent notch is between 900' and 1000' and is capped by the Staghorn Coral Biostrome of the Otisco Member of the Ludlowville Formation. Below the Staghorn Coral, easily recognizable markers that are exposed on the slope where colluvium has been eroded through include the limestones of the Peppermill Gulf Bed and the Mottville Member at the top and bottom, respectively, of the Skaneateles Formation. Generally below about 800' elevation the slope is covered by colluvium, and bedrock is obscured, except in a gully near

Bailey's Settlement where the Skaneateles and Oatka Creek formations are exposed and provide a stratigraphically lower opportunity to determine total movement of the slivers. Evidence of transverse ridges or cracks, radial cracks, or toes is not apparent on the valley-side slope from the top of the lowest slide sliver to the valley floor.

The unnamed gully north of Case Road at the north end of Bare Mountain (Fig. 2) has a relatively complete, in-place, exposed section, from the Cardiff Member of the Oatka Creek Formation up to the Joshua coral bed within the Otisco Member of the Ludlowville Formation. This section and exposures in Rattlesnake Gulf provide the intact, undisturbed stratigraphic sequence used for reference to the displaced stratigraphy in the block slivers.

Discussion

Problems of Timing and Mechanism

Bedrock on the east side of Bare Mountain has slipped into the Tully Valley with apparent vertical displacement from 35 to >100' along 4 or more slivers of relatively intact rock. Dipping and vertical joint sets have influenced the location of the slip planes and the present morphology of the slope. Yet the amount of mass that has been transported should have left a morphological expression of the displaced foot and toe. The only place for the zone of accumulation material to reside is within or under valley fill and colluvium, a situation that makes this rock-block slide unusual and questions the mechanisms, history of movement, and the current state of stability, especially for those slices immediately above the LaFayette mudslide where some restraining valley-fill cover of the foot and toe has been removed.

Timing

If we assume that most of the major motion of the rock-block slide occurred in a single episode and that a single mechanism was involved, then we can closely pinpoint the time of slip. Lack of evidence of glacial scouring or ice modification high on the slope or at the ridge caps of the slivers and lack of ice-contact glaciofluvial erosion in the back-head depressions places the timing of the event after the uncovering of the slope by the Laurentian ice sheet. At the valley floor, the foot of the slide is covered by glaciolucustrine sediments with no morphological evidence that the toe shoved or warped the lacustrine bedding. This would place the event before or during the dewatering of the proglacial lake. Thus, the ice sheet would have backed away from the slope, but not far enough to have uncovered the lowest up-ice, cross-ridge dewatering cross channel. Pair (oral communication) places this time at 12000-15000 b.p.

Mechanisms

Mechanisms for movement must consider the processes for destabilizing the lower slopes by either undercutting or increasing the slope's angle. Loading the top of the slope (by ice?) is possible, but improbable. Kappel (oral communication, 1996) indicated that the cross-valley subcrop of the Onondaga Formation below the valley fill is located somewhere near Rattlesnake Gulf (See Fig. 2.) Consequently, the Onondaga Formation has been removed by glacial ice or preglacial fluvial erosion at the base of the east side of Bare Mountain. The mechanism that is finally chosen should incorporate the removal of the Onondaga Formation bench, and must also explain how the long, thin, slivers of rock could have moved vertically downward over 100' without any substantial disruption, breakage, or block rotation.

Several mechanisms can be speculated for triggering the slide, once the slope is destablized. Among them are earthquakes and dewatering sequences (see Cruden and Varnes, 1996.) Speculation about earthquake occurrences 1200 years ago is beyone the scope of this paper, except that the following scenarios may have happened in conjunction with seismicity, either regionally distributed tectonic earthquakes or hydraulically induced, high, local, proglacial lake-induced, hydrostatic pressures.

One possible mechanism for slow block movement considers contact with stagnent, wasting ice. In this speculative scenario, huge blocks of ice become detached and remain in front of the retreating ice sheet while bracing the block slivers against the intact part of the mountainside. Gradual wasting reduces the confining weight on the toe and gently lets the slivers descend. Meanwhile proglacial lacustrine deposits build up and replace the ice as the confining and bracing mass. This hypothesis requires a delicate balance between the mass of the grounded ice and lake levels. It might be expected that the ice block would float off of the toe before the lake sediments could be deposited to a necessary confining depth.

Gomes and Pair (1997, and oral communication, 1997) have postulated a readvance of the ice lobe in Tully Valley on the basis of geomorphic features of the valley sides and a buried moraine (Kappel and others, 1996,) presumably with a proglacial lake waxing and waning in front of it. The first advance might have undercut the slope at the Onondaga Formation bench and produced the sub-ice conditions that would prepare the slope for failure. The retreat would remove the confining pressure on the toe and allow for slip. Proglacial lacustrine sediments then begin to cover the toe. The readvance could compact the glaciolacustrine sediments and remove any morphological irregularities on the lower slopes and the top of the lake-bottom sediments. Glaciolacustrine sediments would continue to build until

the slide is stabilized. The slide would then be placed in a metastable condition as the ice retreats and the lake drains.

A third scenario involves proglacial lake conditions without ice. Jager and Wieczorek (1994) and Grasso (1970) discuss the formation and drainage of proglacial lakes in the Tully Valley. Jager and Wieczorek (1994) also discuss the mechanisms for slope failure during the drainage of lakes and dewatering of the adjacent valley-wall groundwater system. The rise of Lake Otisco/Cardiff to an approximate elevation of 1253-1292 ft would pump up the pore pressure of the groundwater system in the bedrock of the lake walls. Sudden dewatering to lower stages such as Lake Heath Grove at 1023-1059 ft elevation could initiate the failure and produce incipient movement. The process involves removing the hydrostatic head of the lake while slow-draining materials, such as the Devonian shales of the hillside, still retain high pore-water pressure. Further dewatering to the first Lake Marietta stage (919-955 ft) could then allow the high pore-water pressure of the bedrock slope to destablize the slope and detach the slide. The drop from Lake Otisco/Cardiff to Lake Heath may have triggered the rotational block slumps that lie at the cap of parts of the highest ridge crests.

Another sliding mechanism, which will not be discussed here in detail, involves the gentle stopping of block slide movement by its plowing into uncompacted glaciolacustrine sediments with gradual enough deceleration to allow the slivers to remain intact. Later, lake-bottom water currents and gravity would have smoothed and flattened the lake bottom surface and removed evidence of disruption. This hypothesis could be tested by determining whether a significant section of early, varved clays is disrupted.

The final possible circumstance involves the downslope movement of frozen ground with a basal surface parallel to the mountain's slope. The frozen surface layer that would lie parallel to the mountain slope, with some given thickness, could dam groundwater behind and raise the pore pressure to failure levels (see Cruden and Varnes, 1996, for discussion).

Faulting

A fault interpretation would require a sloping, graben-like structure, which would have to die at both ends of the Mountain. Yet, the greatest displacements lie at the ends and are contrary to most accounts of faulting, where the greatest amount of displacement occurs near the fault's center. Whatever the fault geometry that is suggested, it must account for greatest displacements at the ends of the graben. A fault interpretation also implies Late Pleistocene-Early Holocene seismic activity in the central part of New York State great enough to generate >100' of displacement at the

Paleozoic bedrock surface. Such a large, post-glacial, seismically active, tectonic feature has not been described anywhere else in the eastern United States. This interpretation would demand an immediate, intensive, and comprehensive study. The available evidence is not compelling enough to initiate such a required study.

Groundwater Flow

The groundwater regime of the Tully Valley maintains artesian springs in the valley floor with saline water (Kappel, this volume). Springs also sit at the break in slope at the base of Bare Mountain. The logical source of the artesian head would be precipitation on the mountain. Contributors to the groundwater system include water: (1) from internal drainage that is located on the top of the mountain where crown cracks may receive local precipitation, (2) in the back-head notches, and (3) in any longitudinal cracks that may exist on the upper slopes of the slivers above the upper contact of the colluvium apron. Local capture depletes the overland flow, which thirsts the vegetation and fails to erode the slope at normal regional rates.

Groundwater flow is presumed to move along joints and bedding planes, especially in limestones and dolostones (Fig. 5.) Such a system could provide the current artesian head and saline concentrations in the valley floor.

Geologic Hazards

Bare Mountain and its presumed groundwater system provide several geologic hazards, which include: rock-block slides, rock slides, and other slope failure types on the bedrock surfaces; mudflows on the lower slopes; artesian water systems in the valley; and parched surface conditions on the upper slopes. One speculation combines these conditions and suggests that each contributes to the others: the initial drainage caused by the geometry of the rock-block slide feeds the saline artesian system that possibly triggered the LaFayette mudslide, which, in turn, has lessened the load over the buried foot and toe of the rock-block slide. The unloading may have placed the slide into a metastable condition that could allow the slivers to be reactivated, especially if another wet winter and spring occurs.

Acknowledgments

Geologic mapping was supported by a grant to the New York State Geological Survey from the U.S. Geological Survey through the STATEMAP Program. Bedrock and surficial geology mappers other than the authors are Gordon Baird, Charles Ver Straeten, Stephen Davala, Donald Pair, Francisco Gomes, Robert H. Fickies, John B. Skiba, and Erin Fallis. Other colleagues who have visited the slide and given advice and opinions include Donald Cadwell, Gordon Connally, Barbara Hill, George Kelley, Ed Landing, and Dawit Negussey. We thank Clay Smith, LaFayette Town Supervisor, for

his cooperation and aid. We are also indebted to the Onondaga Nation for allowing us access to their lands for the guidance of Peter J. Edwards who escorted us in our investigation of their rock. We also thank the private landowners for their gracious permission to work on their property.

References

Brett, Carton E., Baird, Gordon C., and Fakundiny, Robert H., 1995. Draft Bedrock Geologic Map of the South Onondaga 7½' Quadrangle, Onondaga County, New York: New York State Geological Survey Open File No. 1g1104, map with Engineering geology and groundwater characteristics interpretations by R.H. Fickies.

Cruden, David M. and Varnes, David J., 1996. Landslide types and processes in Landslides: Investigation and mitigation, A. Keith Turner and Robert L. Schuster (eds.): Transportation Research Board, Special Report 247, p. 36-75.

Engelder, T., 1985. Loading paths to joint propagation during a tectonic cycle: An example from the Appalachian Plateau, U.S.A.: Journal of Structural Geology, v.7, p. 459-476.

Engelder, Terry, Loewy, Staci, McConaughy, David, and Younes, Amgad, 1997. The Catskill Delta Complex: Analog for modern continental shelf & delta sequences containing overpressured sections: Seal Evaluation Consortium and Appalachian Tectonics Studies Group Field Guide, Department of Geosciences, The Pennsylvania State University, 100p.

Fakundiny, Robert H., 1997. Bare Mountain displacement: huge rock-block slide with buried toe, or post-glacial fault in central New York? (abs.): Northeastern Section Geological Society of America Abstracts with Programs, v. 29, no. 1, p. 44.

Fickies, Robert H., 1993. A large landslide in Tully Valley, Onondaga County, New York: Association of Engineering Geologists News, v. 36, no. 4., p. 22-24.

Fickies, Robert H. and Brabb, Earl E., 1989. Landslide Inventory of New York: New York State Museum Circular 52, map.

Gomes, Francisco J. and Pair, Donald L., 1997. Lithostratigraphy and geotechnical properties of late Wisconsinan sediments associated with the Valley Heads Moraine Complex, Tully, NY (abs.): Northeastern Section Geological Society of America Abstracts with Programs, v. 29, no. 1, p. 49.

Grasso, T.X., 1970. Proglacial Lake Sequence in the Tully Valley, Onondaga County: Field Trip Guide Book, New York State Geological Association, 42nd Annual Meeting, p. J1-J16.

Jager, Stefan and Wieczorek, Gerald, 1994. Landslide susceptibility in the Tully Valley Area , Finger Lakes Region, New York: U.S. Geological Survey, Open File Report 94-615, map.

Hand, B.M., 1978. Syracuse meltwater channels: Guidebook, New York State Geological Association, 50th Annual Meeting, p. 286-314.

Kappel, William M., Sherwood, Donald A., and Johnston, William H., 1996. Hydrogeology of the Tully Valley and characterization of mudboil activity, Onondaga County, New York: U.S. Geological Survey, Water Resources Investigations Report 96-4043, 71p.

Pair, Donald L., 1995. Draft surficial geologic map of the South Onondaga 7½' Quadrangle, Onondaga County, New York: New York State Geological Survey Open File No. 2g639, map with Engineering geology and groundwater interpretations by R.H. Fickies.

Pair, Donald L., (in prep.). Draft Surficial geologic map of the Otisco Valley and Tully 7½' Quadrangle, Onondaga County, NY: New York State Geological Survey Open File.

Schultz, Arthur P. and Southworth, C. Scott, 1989. Large bedrock landslides of the Appalachian Valley and Ridge Province of eastern North America in Landslide processes of the eastern United States and Puerto Rico, Arthur P. Schultz and Randall W. Jibson (eds.): Geological Society of America Special Paper 236, p. 57-74.

Parker, J.M., 1942. Regional systematic jointing in slightly deformed sedimentary rocks: Geological Society of America Bulletin, v. 53, p. 381-408.

Turner, A. Keith and Schuster, Robert L. (eds.), 1996. Landslides: Investigation and Mitigation, Transportation Research Board, Special Report 247, 675p.

Varnes, D.J., 1978. Slope movement types and processes, in Schuster, R.L. and Krizek, R.J. (eds.), Landslide Analysis and Control: Transportation Research Board Special Report 176, p. 11-33.

Ver Straeten, C.A., 1995. Stratigraphic synthesis and tectonic and sequence stratigraphic framework, upper Lower and Middle Devonian, northern and central Appalachian basin. Unpublished Ph.D. dissertation, University of Rochester, 779p.

Ver Straeten, Charles, Brett, Carlton E., and Fakundiny, Robert H., (in prep.). Draft bedrock geologic maps of the Otisco Valley and Tully 7½' Quadrangles, Onondaga County, New York: New York State Geological Survey Open File.

Wieczorek, Gerald F., 1996. Landslide Triggering Mechanisms in Landslides: Investigations and Mitigation, A. Keith Turner and Robert L. Schuster (eds.): Transportation Research Board Special Report 247, p. 76-90.

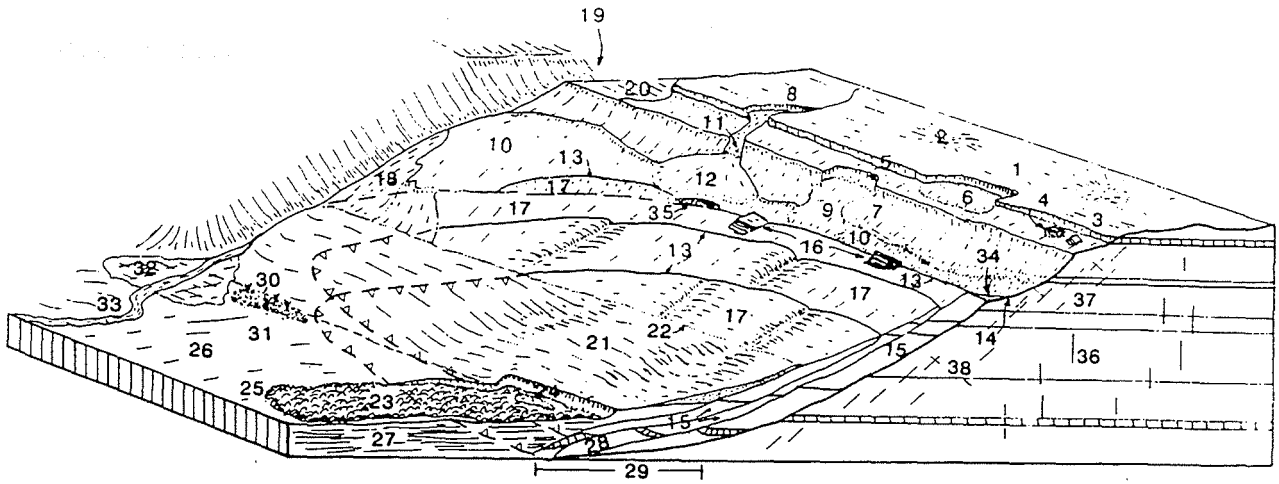

Appendix. Hypothetical block diagram showing nomenclature used in this paper. 1=plateau crown; 2=depression; 3=crown cracks; 4=topple block; 5=plateau cliff (Tully Limestone); 6=cliff slump; 7=headwall-line scarp; 8=stream-dissected crown; 9=headwall-line slump; 10=headwall colluvium; 11=headwall waterfall; 12=headwall alluvial fan; 13=block (sliver) ridge crest; 14=back-head notch; 15=rock-block sliver; 16=rotated ridge-crest slump block; 17=front or valley-side slope; 18=hanging alluvial fan (delta?); 19=gulf; 20=secondary plateau; 21=colluvial apron; 22=colluvium contact; 23=mudslide; 24=mudslide headwall; 25=mudslide toe; 26=valley floor (flood plain); 27=lacustrine deposits; 28=rock-block slide toe; 29=rock-block slide foot; 30=spring; 31=wetland; 32=alluvial fan; 33=stream; 34=back-ridge colluvium; 35=sag and sink hole; 36=vertical joints; 37=valley-dipping joints; 38=joints conjugate to valley-dipping joints. Dashed, barbed lines show presumed toe of slivers where buried. (Partly taken from Varnes, 1978, and Cruden and Varnes, 1996.)

Stratigraphic Incompleteness: Milankovitch in the Manlius at the Margin

Peter W. Goodwin and E. J. Anderson
Temple University
Philadelphia, PA 19122

Introduction

As a result of lower subsidence rates, stratigraphic sections at basin margins are less complete than those in shelfal and basinal positions. Determining degree of incompleteness and its specific stratigraphic location or locations have been difficult tasks dependent on the accuracy of detailed chronologic correlations from complete basinal sections to less complete marginal sections. In the Helderberg Group (Fig. 1), large-scale models of gradual stratigraphic accumulation (e.g. Rickard, 1962: Laporte, 1969) were able to recognize major group-bounding unconformities, but did not identify internal smaller-scale unconformities. Using a model of small-scale episodic accumulation of time-stratigraphic allocycles, Goodwin and Anderson (1986, 1988) recognized cryptic unconformities internal to the Helderberg Group, surfaces at which detailed correlation of cycles revealed missing cycles (Figs. 2 and 3).

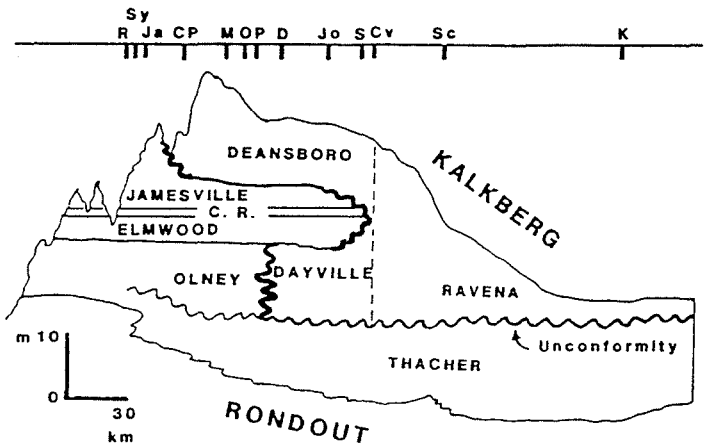

Figure 1. Schematic cross-section, Helderberg Group (from Goodwin and Anderson, 1988).

One such unconformity, traced from the Hudson Valley westward to the Syracuse area (Figs. 2 and 4), was interpreted as a sequence-bounding unconformity separating tectonically distinct portions of the Helderberg Group (Goodwin and Anderson, 1988). That third-order unconformity is the Manlius-Coeymans contact in the Hudson Valley and the Thacher-Olney contact in western sections (Fig. 1). Lesser unconformities, with fewer missing cycles, were recognized in the Manlius, but not fully explained (Fig. 2). It is the purpose of this trip to examine stratigraphic discontinuities of all scales within the Manlius Formation at four localities on the western margin of the Helderberg Basin, and to explain these unconformities in the context of the hierarchic model of orbital forcing.

The Milankovitch Hierarchy

Recent allostratigraphic studies (e.g. deBoer and Smith, 1994) have documented an orbital forcing mechanism for the origin of a stratigraphic record increasingly recognized as both hierarchic and allostratigraphic. The most frequently recognized orbital-forcing mechanisms are precession (approx. 20 ky period) and eccentrcity (periods of 100 ky and 400 ky). Obliquity is rarely recognized as a cycle-producing mechanism; studies supposedly documenting obliquity may well be describing highly incomplete sections of precessional cycles or sections

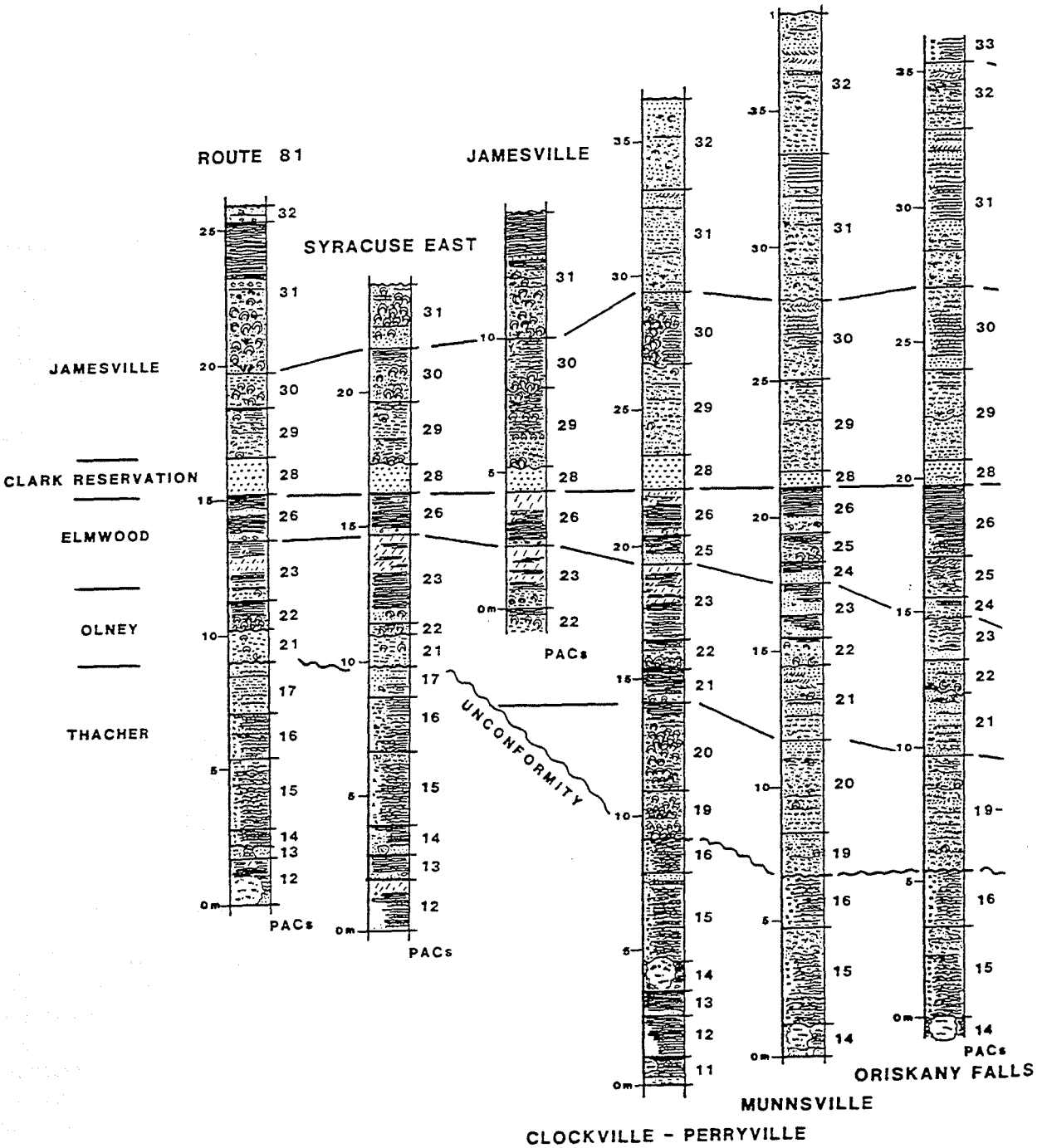

Figure 2. Correlated columnar sections, Helderberg Group, central New York (from Goodwin and Anderson, 1988).

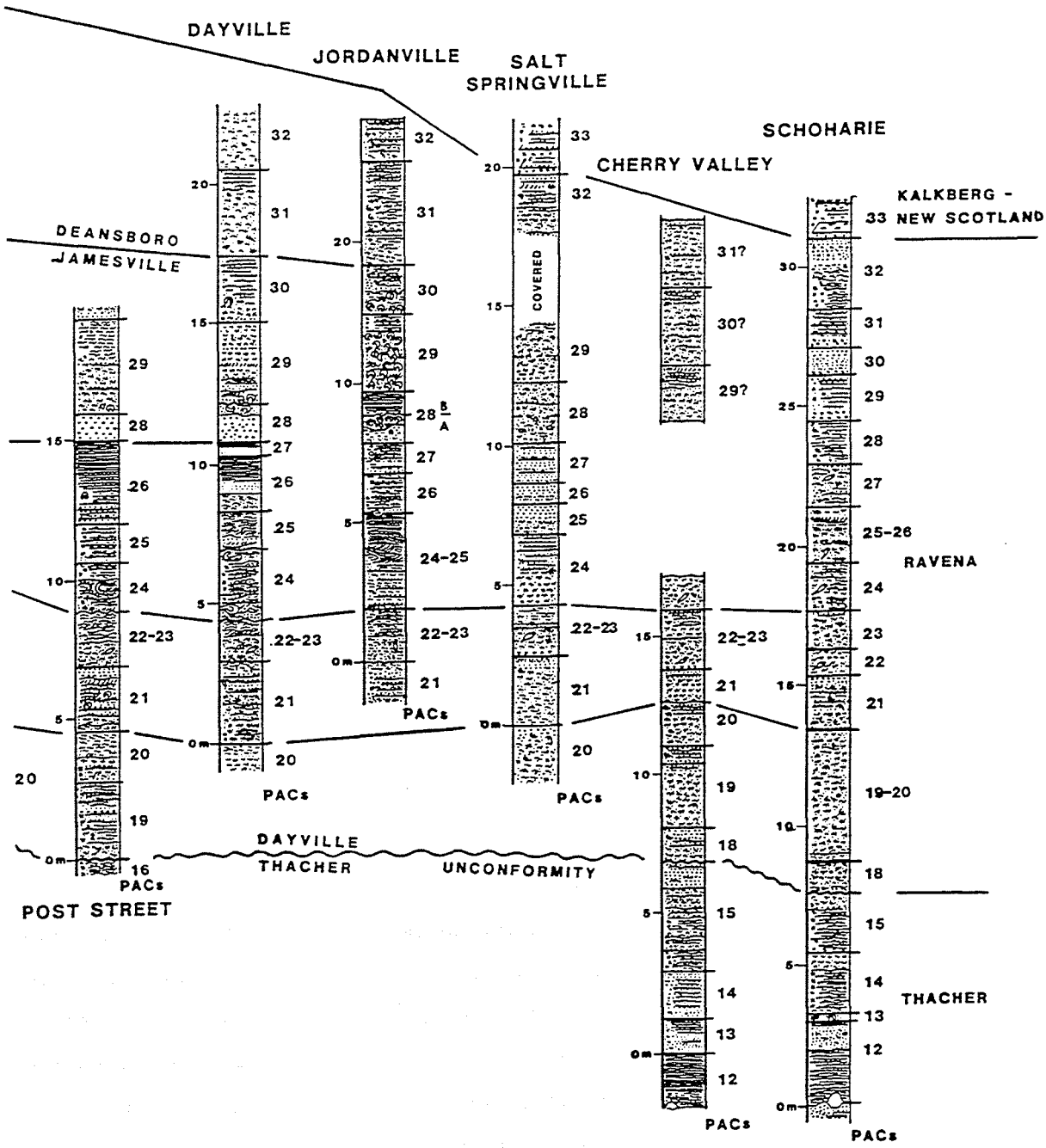
DAYVILLE
JORDANVILLE
SALT SPRINGVILLE
SCHOHARIE
CHERRY VALLEY
KALKBERG - NEW SCOTLAND
DEANSBORO
JAMESVILLE
COVERED
RAVENA
THACHER
DAYVILLE
THACHER
UNCONFORMITY
PACs
POST STREET

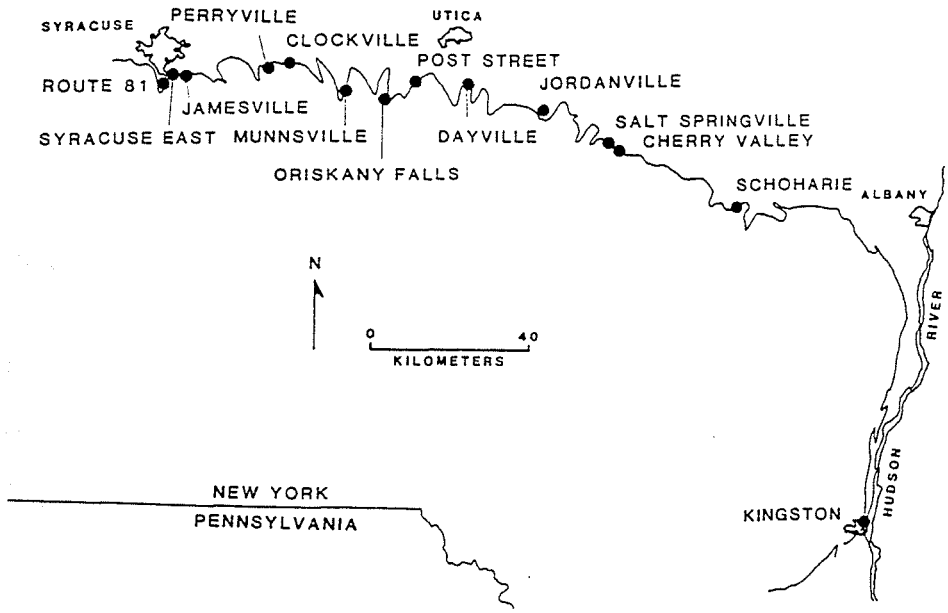

Figure 3. Helderberg outcrop belt, New York State. Localities for this trip are Munnsville, Clockville, Perryville, Jamesville and Route 81.

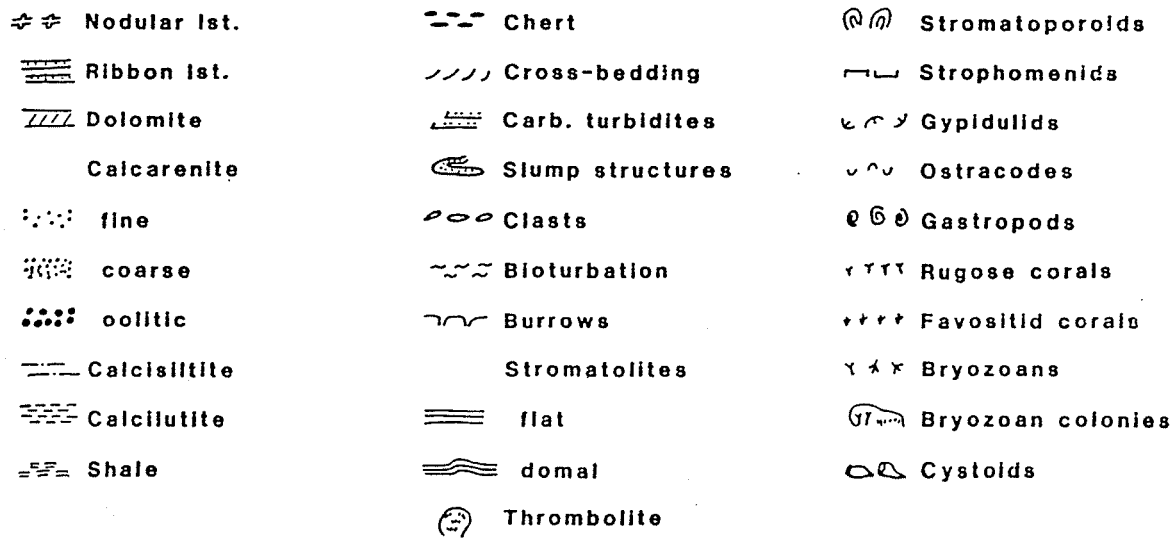

Figure 4. Symbols used in all columns.

consisting of poorly discriminated precessional and eccentricity-modulated cycles. Therefore, the hierarchic model used in this study is one which does not include obliquity (Table 1).

Rank	Period	Mechanism
2nd Order (Supersequence)	10 million years	Tectono-Eustasy
3rd Order (Sequence)	2 million years	Eccentricity ?
4th Order	400,000 years	Long Eccentricity
5th Order	100,000 years	Short Eccentricity
6th Order (PAC)	20,000 years	Precession

Table 1. Genetic Hierarchy of Allocycles

In this model (Table 1), the fundamental cycle-producing mechanism is precession (Fig. 5); eccentricity functions as a modulator of the precessional signal by enhancing or dampening its effect (Fig. 6). Precession produces a sharply bounded, shallowing-upward cycle (PAC) defined by disjunct facies relationships at its boundaries (Fig. 5). The sharp bounding surfaces are formed during times of non-deposition when sea level is rising at its maximum rate (i.e. the inflection point on the sea-level-rise curve). Modulation of the precessional signal by eccentricity produces fifth-order bundles of sixth-order precessional cycles (Fig. 6); these bundles are defined by major facies change (enhanced sea-level rises) at their boundaries. Internally, fifth-order sequences generally contain their deepest facies in the second PAC and exhibit a shallowing trend in successive PACs (Fig. 7).

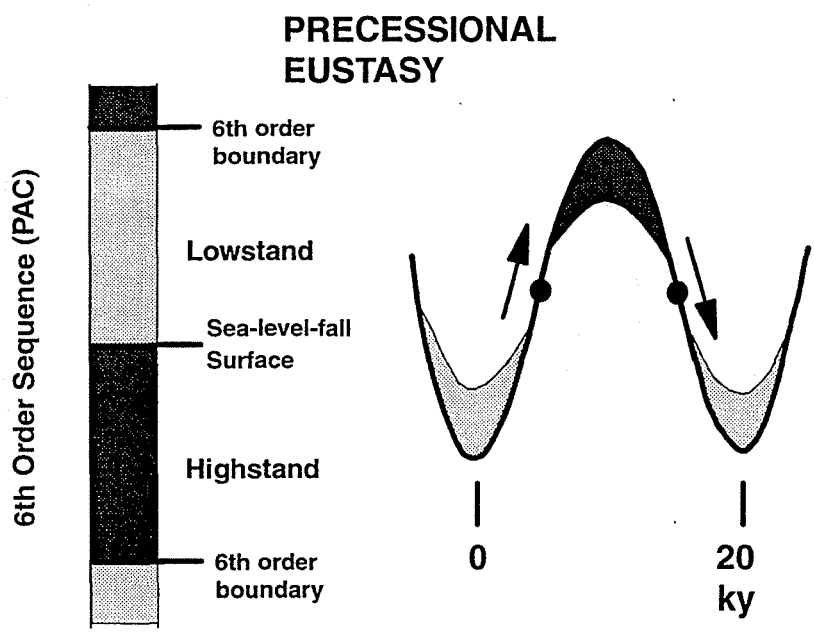

Figure 5. Relationship between precessional eustasy and sixth-order sequences. Sixth-order boundaries are produced at times of non-deposition associated with the maximum rate of sea-level rise (near the inflection point of the rising curve). Sea-level-fall surfaces, when present, are produced in a similar manner at times of rapid sea-level fall.

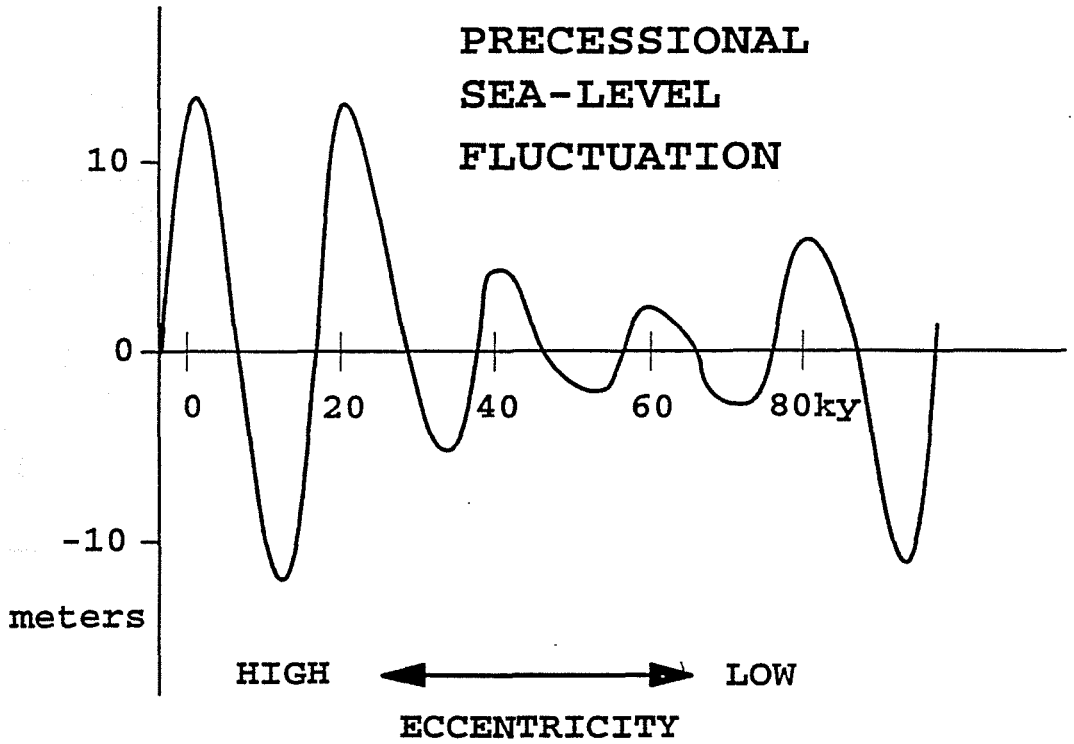

Figure 6. Eccentricity modulation of the precessional sea-level curve. At times of high eccentricity, precessional rises and falls are enhanced; at times of low eccentricity precessional rises and falls are dampened. Modulation by eccentricity produces asymmetric bundles of sixth-order sequences (Fig. 7).

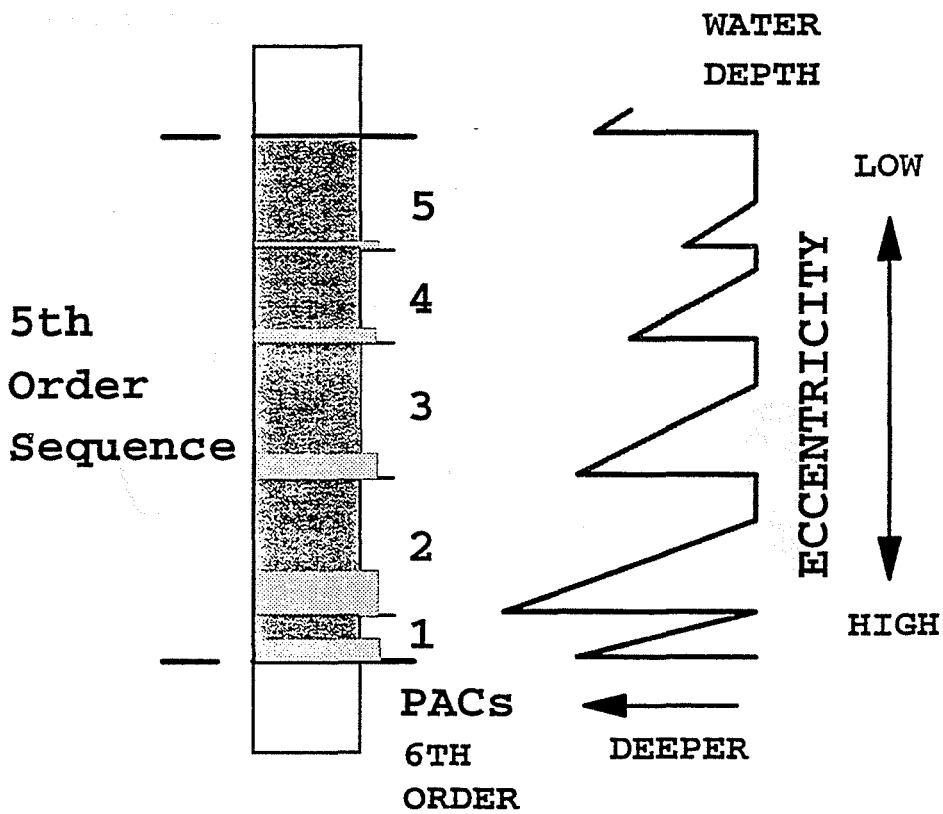

Figure 7. Asymmetric fifth-order bundle of sixth-order sequences. Enhanced precessional rises produce major facies changes at bundle boundaries; dampened rises produce a generally shallowing-upward upper portion of the fifth-order sequence. Deepest facies commonly occur at the base of the second PAC.

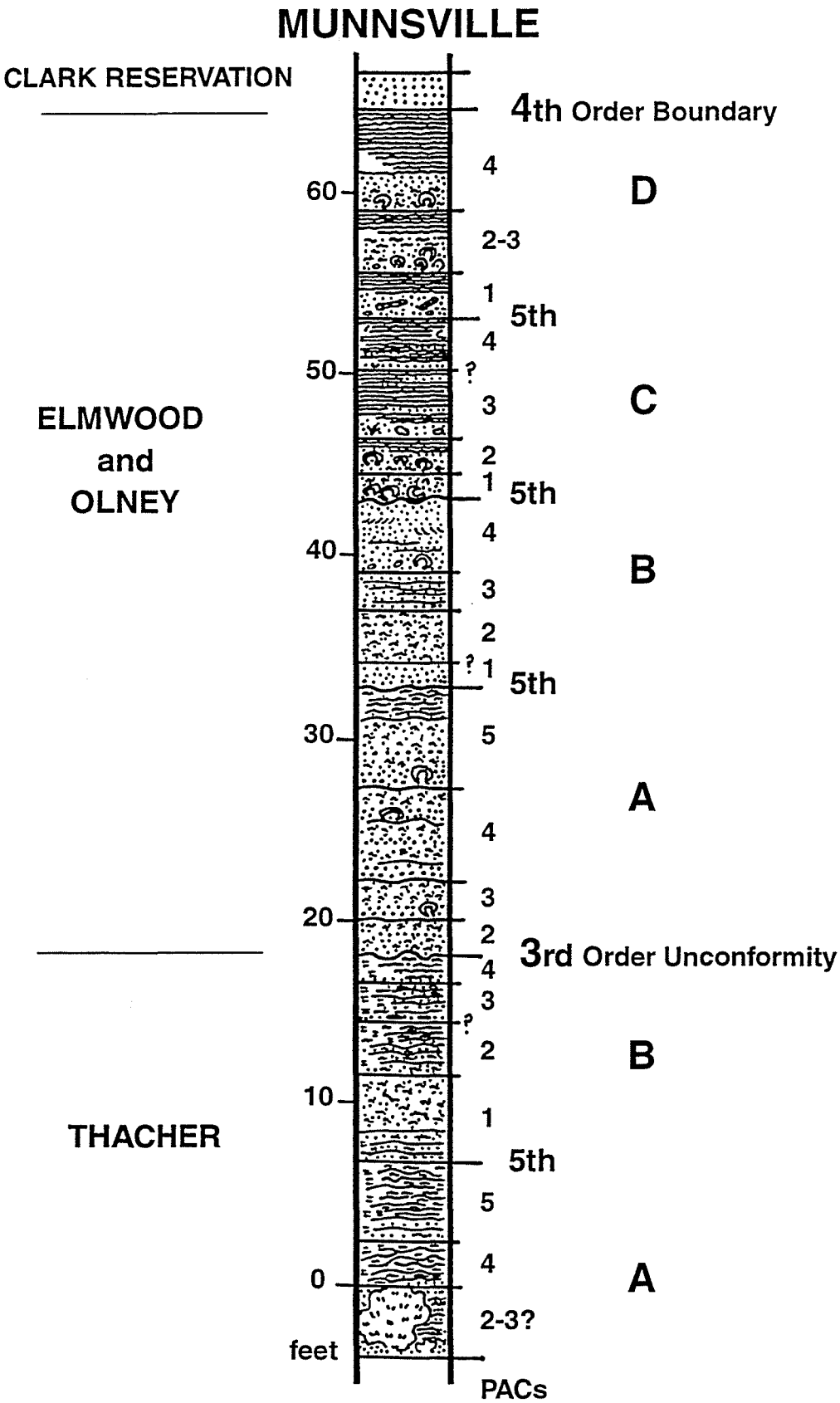

Figure 8. Columnar section, Munnsville Quarry, Munnsville, New York

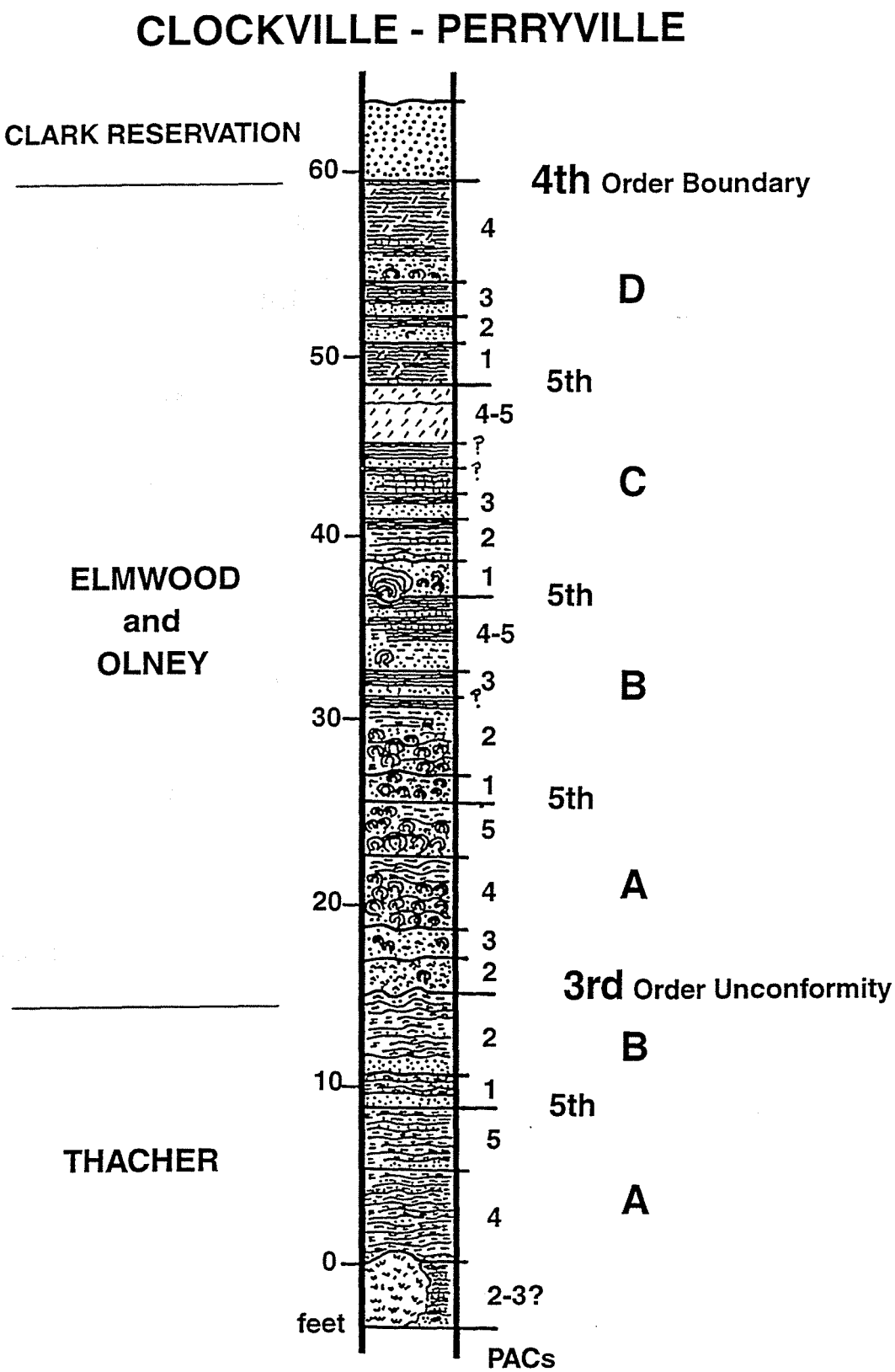

Figure 9. Columnar section, Clockville - Perryville, New York

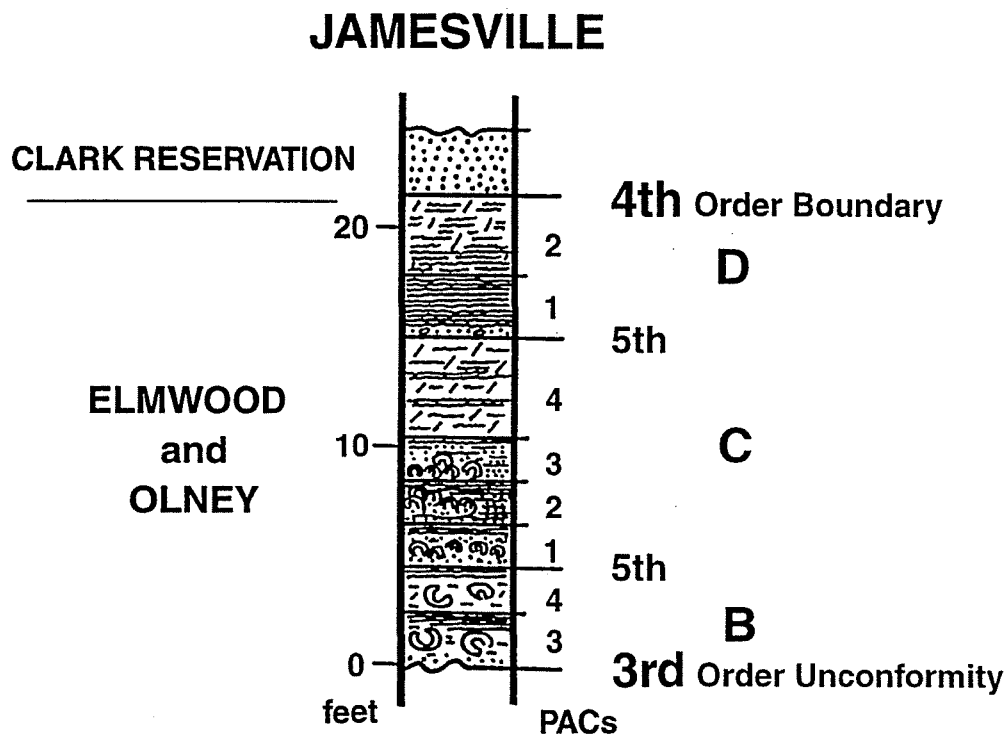

Figure 10. Columnar section, Onondaga County Quarry, Jamesville, New York

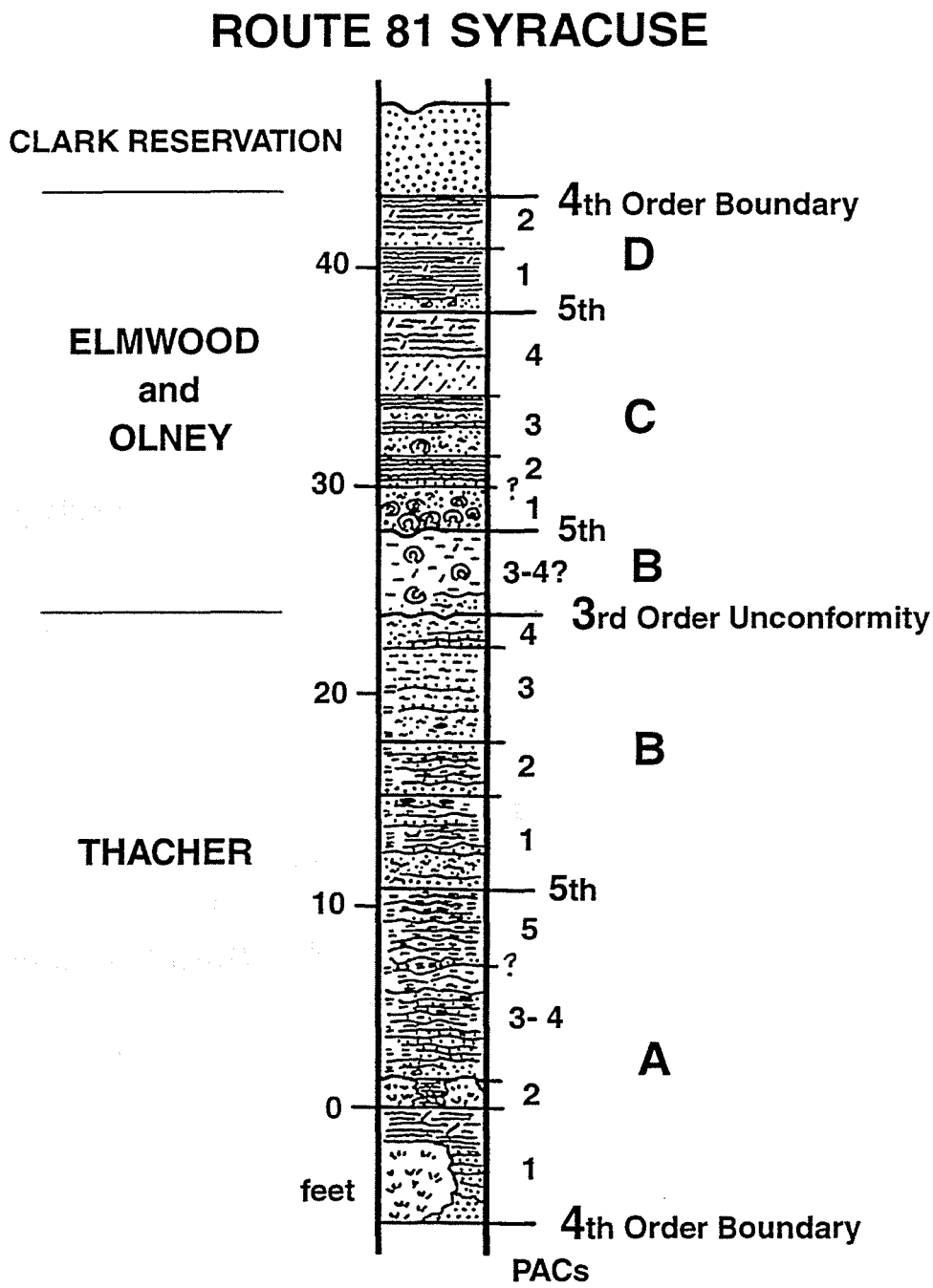

Figure 11. Columnar section, Interstate 81 northbound lanes south of Syracuse, New York

Stratigraphic Incompleteness in the Manlius Formation

In the Mohawk Valley, Olney-Elmwood sections to the East are more complete (thicker and containing more cycles) than those to the West. In contrast, Upper Thacher sections reveal the opposite trend, thickening by the westward addition of more cycles beneath the Thacher-Olney unconformity. At four localities from Munnsville to Syracuse (Fig. 4), this trip will document these trends, focussing on the Manlius interval between the third-order unconformity at the Thacher-Olney contact and the major facies change at the fourth-order boundary between the Elmwood and Clark Reservation Members. Application of the hierarchic orbital forcing model reveals that stratigraphic incompleteness (missing cycles) is a function of vacuity (erosion) and hiatus (non-deposition) at third-, fourth- and fifth-order boundaries, not simply at major unconformities. Incompleteness at fourth- and fifth-order boundaries is largely a function of eccentricity-modulated eustasy, whereas third-order incompleteness has a significant tectonic component.

The interval covered on this trip includes three fourth-order boundaries, one of which is also a third-order unconformity (Figs. 8-11). Principal focus is on the fourth-order sequence between the third-order Thacher-Olney unconformity and the fourth-order boundary at the Elmwood-Clark Reservation contact. This fourth-order sequence is nearly complete at Munnsville (Fig. 8), where it consists of the requisite four fifth-order sequences, each containing four or five sixth-order sequences (PACs). Westward, this fourth-order sequence is less complete, consisting of just three fifth-order sequences at Jamesville (Fig. 10) and at Route 81 (Fig. 11). Furthermore, at these western localities the basal fifith-order sequence consists of only two or three sixth-order PACs, suggesting significant hiatus at the third-order unconformity. Similarly, the uppermost fifth-order sequence consists of fewer PACs to the West, probably as a function of erosion or non-deposition at the fourth-order boundary and/or hiatus at the lower fifth-order boundary. Thus, westward thinning of this fourth-order sequence is a function of:

1. longer hiatus at the third-order unconformity;
2. fourth-order erosion or hiatus at the Elmwood-Clark Reservation contact; and
3. fifth-order hiatus and/or erosion within the fourth-order sequence.

In contrast, the highly incomplete fourth-order sequence beneath the third-order unconformity (Thacher-Olney contact) exhibits a different East-West trend (Figs. 8-11). Westward from the Hudson Valley (Goodwin et al., 1986), this interval thickens because additional cycles are preserved beneath the unconformity, indicating that uplift to the East caused deeper erosion (vacuity) at the eastern localities. Thus, the origin of the third-order unconformity has a tectonic component: first greater uplift to the East and then greater subsidence at those same localities. In other words, vacuity is greater at eastern localities and hiatus is greater at western localities.

In summary, stratigraphic incompleteness of the Manlius Formation is a function of a hierarchy of eustatic sea-level fluctuations superimposed on a tectonic component. Differential uplift and subsidence produced a third-order sequence-bounding unconformity, at which fifth- and sixth-order cycles are missing by vacuity and hiatus. At smaller scales, sixth-order cycles are missing in some fifth-order sequences to the West as a result of erosion and/or non-deposition at fifth-order boundaries at the low-subsidence basin margin. Assuming that the detailed correlations of this hierarchic allostratigraphic fabric are accurate, this approach facilitates the determination of the exact location of missing section as well as the amount of time (number of 20,000 year cycles) encompassed by those missing cycles.

References

Anderson, E. J. and Goodwin, P. W., 1990, The significance of metre-scale allocycles in the quest for a fundamental stratigraphic unit: Journal of the Geological Society, London, v. 147, p. 507-18.

Anderson, E. J., Goodwin, P. W. and Sobieski, T. H., 1984, Episodic accumulation and the origin of formation boundaries in the Helderberg Group of New York State: Geology, v. 12, p. 120-123.

deBoer, P. L. and Smith, D. G., 1994, eds. Orbital forcing and cyclic sequences: Spec. Pub. No. 19, International Association of Sedimentologists, London, Blackwell Scientific Publications, 559 p.

Goodwin, P. W. and Anderson, E. J., 1988, Episodic development of Helderbergian paleogeography, New York State, Appalachian Basin: *in* McMillan, N. J., Embry, A. F. and Glass, D. J. eds. Devonian of the world: Second International

Symposium on the Devonian System, Canadian Society of Petroleum Geologists, v. 2, p. 553-568.
Goodwin, P. W., Anderson, E. J., Goodman, W. M. and Saraka, L. J., 1986, Punctuated aggradational cycles: Implications for stratigraphic analysis: in Arthur, M. A. and Garrison, R. E. eds. Milankovitch cycles through time: Paleoceanography v. 1, p. 417-429.
Laporte, L. F., 1969, Recognition of a transgressive carbonate sequence within an epeiric sea: Helderberg Group (Lower Devonian) of New York State: in Friedman, G. M. ed. Depositional environments in carbonate rocks: Special Publication of the Society of Economic Paleontologists and Mineralogists, no. 14, p. 98-119.
Rickard, L. V., 1962, Late Cayugan (Upper Silurian) and Helderbergian (Lower Devonian) stratigraphy in New York: New York State Museum and Science Billetin, 386, 157 p.

Road Log

Cumulative Mileage	Miles From Last Point	Route Description
0.0	0.0	Road log starts at Hamilton College entrance on Route 412
4.8	4.8	From Hamilton College, go west on Route 412 to Vernon Center
9.3	4.5	Turn south (left) on Route 26 to Knoxboro Rd
13.3	4.0	Turn west (right) on Knoxboro Rd, through Knoxboro to Cook Rd.
14.7	1.4	South on Cook Rd. to Munnsville and intersection with Route 46
15.7	1.0	South on Route 46 to Quarry Rd.
16.2	0.5	Left on Quarry Rd. to Munnsville Quarry entrance (STOP 1)

STOP 1. Manlius Formation at Munnsville Quarry (Rickard Loc. 137)

The Munnsville Quarry Manlius section begins in the Thacher Member at the quarry entrance and continues into the Olney Mbr. on the north wall of the quarry. The upper Olney, Elmwood , Clark Reservation and Jamesville members are exposed in the west wall of the quarry.

At this locality, a third-order unconformity forms the Thacher-Olney contact (Fig. 8); extended eastward this unconformity becomes the Thacher-Ravena contact at Schoharie and in the Hudson Valley (Figs. 1 and 2). Between this unconformity and the fourth-order boundary at the base of the Clark Reservation Mbr. the Olney-Elmwood interval (46.5 ft thick) consists of four relatively complete fifth-order sequences (A, B, C and D). Each of these fifth-order sequences consists of four or five sixth-order sequences (PACs). The fourth-order sequence below the unconformity consists of portions of two fifth-order sequences (A and B), the upper two missing by vacuity (erosion) at the unconformity.

16.7	0.5	Return to Route 46 on Quarry Rd.
17.7	1.0	North on Rte. 46 into Munnsville to intersection with Williams Rd.
22.1	4.4	West (left) on Williams Rd. to intersection with Peterboro Rd.
23.2	1.1	West (left) on Peterboro Rd., through Peterboro to Old Country Rd.
23.3	0.2	North (right) on Old Country Rd. to Oxbow Rd.
28.8	5.5	Left on Oxbow Rd. to picnic/parking area across from Stop 2.

STOP 2. Clockville Roadcut (Thacher-Olney Interval, Manlius Fm., Rickard Loc 142)

At this locality, the Thacher Mbr. and the lower Olney Mbr. are exposed. The described section (Fig. 9) begins near the top of the thick-bedded Thacher of Rickard (1962). The third-order unconformity (Thacher-Olney contact) is exposed near the top of the outcrop. The Olney-Elmwood portion of the columnar section was described at Perryville, 3.5 miles to the West.

As at Munnsville (Fig. 8), the fourth-order sequence below the unconformity consists of two incomplete fifth-order sequences (A and B). The smaller number of sixth-order cycles in fifth-order sequence B at Clockville relative to Munnsville suggests slightly deeper erosion at the third-order unconformity at this locality.

29.3	0.5	South on Oxbow Rd. to Ingalls Corners Rd.
32.5	3.2	West (right) on Ingalls Corners Rd. to Quarry Rd.
33.3	0.8	North (right) on Quarry Rd. to entrance to Madison Products Quarry (Stop 3)

STOP 3. Madison Highway Products Quarry, Perryville (Rickard Loc. 144)

At this locality, the upper Thacher, Olney, Elmwood and Clark Reservation Members are exposed in the north wall of the old pit behind the maintenance shed and scale house. The base of the section begins six feet below the Thacher-Olney third-order unconformity (Fig. 9). The Thacher portion of the column was described at Stop 3.

As at Munnsville, the Olney-Elmwood fourth-order sequence consists of four nearly complete fifth-order sequences (A, B, C and D). The slight difference in thickness (less at Perryville) and the generally more restricted facies at Perryville suggest that this locality is onshore of Munnsville. However, the similar stratigraphic structure of the two sections indicates very little topographic relief between the two localities.

36.1	2.8	From quarry entrance north (left) on Quarry Rd. to Route 5
39.3	3.2	West (left) on Rte. 5 to intersection with Rte. 173 in Chittenango
50.7	11.4	West on Rte. 173, through Manlius to intersection with Rte 91
51.2	0.5	South (left) on Rte. 91 to the County Quarry on left (Stop 4)

STOP 4. Onondaga County Quarry, Jamesville (Rickard Loc. 151)

At the Jamesville locality, the section (Fig. 10) begins in the Elmwood Mbr. on the road north of the quarry entrance. The upper Elmwood, Clark Reservation and Jamesville Mbrs. are exposed in the east wall of the quarry.

At Jamesville (Fig. 10), the Olney-Elmwood fourth-order sequence is less complete than at Perryville (Fig.9), consisting of portions of three fifth-order sequences (B, C and D). Sequence A was not deposited because this area remained positive until flooding during the deposition of sequence B. As yet, we have not determined which two sixth-order flooding events in sequence B are recorded at this locality. Similarly, fifth-order sequence D is less complete at Jamesville than at localities to the East. Whether this difference is the result of hiatus at the base of the sequence or erosion at its top has not been determined.

51.7	0.5	North on Rte. 91 to Rte. 173
55.6	3.9	West (left) on Rte. 173, under I 81 to Rte. 11
58.6	3.0	South (left) on Rte. 11 to intersection with I 81
61.5	2.9	North on I 81 to Manlius roadcut on right, beyond guardrail (Stop 5)

STOP 5. Interstate 81 Roadcut (Olney, Elmwood, Clark Reservation, Jamesville Mbrs.)

This roadcut south of Syracuse exposes the upper Thacher, Olney, Elmwood, Clark Reservation and lower Jamesville Mbrs. of the Manlius Fm. The Thacher Member is completely exposed in the roadcut of the southbound lanes of Interstate 81, a locality not visited on this trip.

At this locality (Fig. 11), the Olney-Elmwood fourth-order sequence is even less complete than at Jamesville, approximately 4 miles to the East. As at Jamesville (Fig. 10), the sequence cosists of three fifth-order sequences (B, C and D), but sequence B consists of just one sixth-order cycle (PAC). Beneath the third-order unconformity (Thacher-Olney contact), the Thacher fourth-order sequence contains more sixth-order cycles than at locaities to the East, indicating that erosion did not cut as deeply (vacuity is less). Still, this fourth-order sequence is far from complete, consisting of just two fifth-order sequences.

Herkimer Diamond Mine Field Trip

Hugh Humpreys
Tibbits Road, New Hartford, NY 13413

Herkimer "diamonds" are doubly-terminated quartz crystals found near Herkimer, New York. The clarity and perfection of these crystals make them one of central New York's most collectable minerals. The crystals are found in muddy pockets, or vugs, up to a meter in diameter in the Late Cambrian Little Falls formation near Middleville, Little Falls and Herkimer, New York. As many as 1000 crystals have been found in a single pocket (Moore, 1989).

This trip will visit the Herkimer Diamond Mine, owned by the Herkimer Diamond Development Co. near Middleville, New York. The trip will be led by Hugh Humphreys. Hugh has been an avid miner and collector of Herkimer diamonds for 15 years. After a visit to the museum at the mine, he will discuss the occurrence of the crystals and will demonstrate different mining techniques. Ample time will be provided for participants to explore the mining area and search for "diamonds." Although this trip is scheduled for a half-day, you may stay as long as the mine is open. The following description is taken from information displayed with Herkimer diamonds in the mineral collection at Hamilton College, Clinton, New York.

> *The exact origin of the pockets and the quartz crystals is unknown; several related theories exist. One theory is that in Late Cambrian time, quartz sand grains and minor amounts of clay were deposited in a predominantly carbonate environment where there was significant algal growth. The sand, clay, and algae were incorporated into limestone, which was dolomitized by circulating waters. The formation is a rather normal dolostone or dolomitic sandstone.*
>
> *After burial, entrapped sea water or water from some other source dissolved some of the sand grains, dolomite, and algae to form the pockets. Many pockets today contain a black carbonaceous material called anthraxolite, which may represent an insoluble residue from the algae. Thus, the algae may have served as sites for solution and pocket formation.*
>
> *As the pH of the water in the pockets decreased, quartz crystals started to grow. The source of the silica was the dissolved sand and clay or the remains of silica-secreting animals such as radiolaria. Some quartz crystals started their growth on the pocket wall and grew into the pocket. Many crystals, however, grew freely in the pocket water or in the mud that was the insoluble residue from pocket formation, allowing the doubly-terminated crystals to form. Most of the crystals are short hexagonal prisms terminated by rhombohedrons.*

Some crystals show solid or fluid inclusions. Solid inclusions are usually specks of anthraxolite. Fluid inclusions are mostly salt water with bubbles of CO_2 or water vapor. Based on a homogenization temperature of 51°C, the crystals formed at a depth of approximately 3500 feet (Dunn and Fisher, 1954).

References

Dunn, J.R. and Fisher, D.W., 1954, Occurrence, properties, and paragenesis of anthraxolite in the Mohawk Valley [New York]. American Journal of Science, v. 252, n. 8, p. 489-501

Moore, B.S., 1989, *Herkimer Diamonds*, Herkimer Diamond Development Company, Herkimer, NY, 63 p.

Eurypterids and Associated Fauna at Litchfield, A Classic Locality in Herkimer County

Victor P. Tollerton, Jr.
23 Shepherd Place
Utica, New York 13502-5417, mltolrton@borg.com

Introduction

The Upper Silurian Bertie Formation (Group of D.W. Fisher, 1960; Ciurca, 1973) of New York State and Ontario, Canada, is world renowned for its spectacular eurypterids. One of these, *Eurypterus remipes* Dekay, 1825, holds the distinction of being the first eurypterid in the world to be described. This species is also the state fossil of New York, as signed into law by Mario Cuomo on 27 June 1984. Another species, the second one in the world to be described, *Eurypterus lacustris* Harlan, 1834, has been figured on a postage stamp of Canada (as *Eurypterus remipes*).

Central New York is fortunate to boast of four localities where eurypterids can still be collected from the Bertie (Forge Hollow, Litchfield, Lang's Quarry, and Passage Gulf). Two others mentioned in the literature (Jerusalem Hill and Crane's Corners) are not currently accessible. The Litchfield, Herkimer County locality is a classic outcrop that displays both vertical and horizontal sections amenable for paleoecological study.

The main purpose of this trip is to examine the paleoecology of eurypterids. Too often, matters of their habit and habitat are studied without regard for both the stratigraphic and sedimentologic context, as well as ignoring evidence from associated fauna.

History

The Bertie Formation was named by Chapman (1864, p. 190-191) for a 50 foot thick section of "...thin-bedded grayish dolomites, interstratified towards the base with a few brownish shales, and with a brecciated bed composed chiefly of dolomite fragments" that were exposed near the Township of Bertie, Welland County, Ontario, Canada. The name was first used in New York State by Schuchert (1903) in his study of the Manlius Formation. A more complete historical perspective is found in Rickard, (1953, 1962). The unit was raised to the rank of group by D.W. Fisher (1960). The New York State Geological Survey currently uses the term formation (Rickard, 1975). Others use the term group (Ciurca, 1973, 1978, 1982, 1990; Hamell, 1981; Hamell and Ciurca, 1986; and Ciurca and Hamell, 1994).

In this paper, I prefer to use the term formation for the entire Bertie on the basis that the subunits are too thin to map as formations on a scale of 1:24,000 (the standard 7.5 minute topographic quadrangle). However, as shown by Hamell (1981), Hamell and Ciurca (1986), and Ciurca and Hamell (1994), the subunits are of utility for finer-scale interpretations of paleoenvironments within the entire unit.

The outcrop across from the Litchfield Town Hall is a classic locality for eurypterids and associated fauna. Specimens of eurypterids and other invertebrate fossils from this location have been cited in the works of Clarke and Ruedemann (1912), Ruedemann (1916; 1925), and Kjellesvig-Waering (1958).

In July and August 1992, this roadcut was cut back by the New York State Department of Transportation for road improvements. Although no blasting was done, an estimated 30,000 cubic feet of rock was removed and used for road fill. At present, 9.5 feet of section are exposed. Prior to the road work, only 5.5 feet of section was exposed (Leutze, 1959).

Age

Historically, the age of the Bertie formation has been considered to be Pridoli (Late Silurian). Rickard (cited in Berry and Boucot, 1970, p. 122) found the conodont *Spathognathodus*, perhaps *S. steinhornensis remscheidensis* from the basal part of the Bertie in the Syracuse, New York area. Recently, Johannessen, et al. (1997) reported a sparse and fragmentary fauna of ozarkodinid conodonts from the Fiddlers Green Member at Litchfield. Their identifications suggested to them a Ludlow age (Late Silurian) for the Bertie Formation. Considering the long temporal range of the species encountered and the fragmentary nature of the conodont elements, it might be prudent to take a more conservative view and consider the Bertie as Late Silurian (Ludlow-Pridoli). More study on the conodont faunas of the entire Bertie from the entire geographic range is definitely required. How the conodont faunas correlate with the inferred unconformaties within the Bertie (Ciurca and Hamell, 1994) is unknown.

Eurypterids

Eurypterids are extinct aquatic chelicerate arthropods. Growth, as in all arthropods, was accomplished after the hard exoskeleton was moulted. It is generally accepted that most specimens represent cast-off exoskeletons (Clarke and Ruedemann, 1912; Størmer, 1934; Selden, 1984). The exact number of instars (periods between moults) is unknown. Statistical analyses of measurements of prosomas (heads) reveals nearly isometric growth (Kaneshiro, 1962; Andrews, et al., 1974). Examination of bivariate graphs of various measurements show no discrete clusters (Tollerton, 1993) indicative of instar groups. However, work by Sekiguchi, et al. (1988) on horseshoe crabs suggests that the instar groupings identified by Andrews, et al. (1974) for *E. remipes* may be correct.

As of May 1997, there are 59 genera and 236 named species within the Order Eurypterida. Another 108 specimens remain in open nomenclature. The most recent classification of the Order is by Tollerton (1989). Eurypterids are sexually dimorphic, with the two sexes denoted as either Type A or Type B. Which type is which sex has yet to be unequivocally determined. Depending on the species and sexual type, there are on average 110 parts to a complete eurypterid.

The temporal range of the Order is from the lower Upper Ordovician (Harnagian Stage, Caradoc Series; approximately 460 mya (absolute ages from Harland, et al., 1990)) to the upper Lower Permian (Artinskian Stage, Rotliegendes Series; approximately 265 mya). The range is therefore about 195 million years, or a little more than half of the Paleozoic. The oldest and youngest eurypterids known so far (from the stages given above) are, respectively, *Brachyopterus stubblefieldi* Størmer, 1950, from Wales, and *Adelophthalmus sellardsi* (Dunbar), 1924, from Kansas. The acme of the Order is the Silurian.

Eurypterids are found on every continent except Antartica. They occur in most sedimentary lithologies except conglomerates and coarse sandstones. Only two groups of invertebrates never occur with eurypterids; crinoids and sponges. Five groups of invertebrates rarely occur with eurypterids; barnacles, bryozoans, scaphopods, corals, and trilobites. Table 1 lists the invertebrate groups known to occur with eurypterids. Various plants are known to occur with eurypterids, especially from the Late Silurian to the Early Permian. The record of vertebrate associations, besides conodonts, is not reliable and needs further study.

TABLE 1. Invertebrate groups known to occur with eurypterids.

Nautilid cephalopods	Pelecypods	Gastropods	Conularids
Tentaculities	Ostracods	Worms	Insects
Inarticulate Brachiopods	Articulate Brachiopods	Graptolites	Scorpions
Phyllocarids			

Paleoecology

The literature on the paleoecology of eurypterids is varied and sparse. Two different approaches have been followed. One is based on evidence from external factors of occurrences (lithology, trace fossils, associated fauna, etc.). The comprehensive summaries of all the then known eurypterid occurrences by O'Connell (1916), and the identification of ecological phases for Silurian eurypterids by Kjellesvig-Waering (1961) are examples of this approach.

The second, more common approach is based on evidence from functional morphology. These studies have inferred (among other things) the mechanics of swimming (Selden, 1981; Plotnick, 1985; Knight, 1996), walking (Hanken and Størmer, 1975; Waterston, 1979), and feeding (Kjellesvig-Waering, 1964; Selden, 1984); and respiration (Selden, 1985; Manning and Dunlop, 1995); and the biomechanics of the cuticle (Dalingwater, 1985).

I prefer the first approach because I feel it is subject to closer scrutiny, and relies on fewer ambiguous assumptions. However, both approaches are necessary, as is some reliance on what Plotnick (1983, p. 218) calls the *Limulus* paradigm (the interpretation of eurypterid paleoecology based in large part on the ecology of horseshoe crabs). Some of the more pertinent aspects of this paradigm follow.

Limulus polyphemus (linneaus), 1758, is generaly considered the closest (phylogenetically) living marine relative of eurypterids. Most of the literature on the ecology of *Limulus* cannot be applied to eurypterids because the soft parts (muscles, nerves, etc.) are not preserved, and many behaviors or responses to stimuli cannot be observed in the fossils. However, the following ecological aspects of *Limulus* are probably applicable to eurypterids.

Limulus comes ashore to sandy beaches to mate, with the male attached to the back of the female. The female burrows into the sand and deposits her eggs, but not all in one nest (Sekiguchi and Nakamura, 1979). The male then fertilizes the eggs. Fertilization is external. When the eggs hatch, the larvae are morphologically very similar to the adults.

During the course of its life cycle from hatching to mature adult, *Limulus* inhabits progressively deeper water settings (Rudloe, 1979; Shuster, 1979). Hatchlings are found in the supralittoral setting where the nests were dug by the mature female. Larvae and small juveniles occur in the intertidal snad and mud flats. Larger juveniles are found in subtidal settings. Small adults occur in deeper water (up to about 30 meters (Rudloe, 1979), while the mature adults occur on the continental shelf (Shuster, 1979).

According to Shuster (1979, p. 13), the usual mode of locomotion of large juveniles and adults is an ambling stiff-legged gait along the bottom. Aspects of swimming and burrowing have been described in several papers (Vosatka, 1970; Eldrege, 1970; D.C. Fisher, 1975). Moulting in *Limulus* has been described by Laverock (1927) and Jegla (1982). Of particular interest is the similarity of movements in both burrowing and moulting, the only significant difference being the position of the animal; when burrowing, it's oriented dorsal up and when moulting, ventral up.

Limulus is normally a nocturnal animal, spending most of its time buried just below the surface (Lochhead, 1950; Eldredge, 1970). The diet of the young animals is polychaete worms, while bivalves and polychaetes constitute the diet of larger individuals (D.C. Fisher, 1984). According to Reynolds and Casterlin (1979), *Limulus* is tolerant of a wide range of temperatures (less than 0 C to 40 C) and salinities (5% to fully marine), under both artificial and natural conditions.

Taphonomy

The taphonomy of eurypterids is virtually an open topic for study. With one exception (O'Connell, 1916), none of the papers that deal specifically with the paleoecology of eurypterids consider aspects of taphonomy except in a cursory fashion. Minor comments and observations have been made, but without reference to context of in situ occurrences. Here, information that may be of value for the study of eurypterids has been gleaned from the more abundant literature on trilobites, and on arthropod fossils in general (e.g., Mikulic, 1990).

As noted by Brett and Baird (1986), the position of the fossil in the sediment and the arrangement of the skeletal elements are important in determing the condition of the animal at the timeof its burial. In this way, the fossil is treated as a primary sedimentary structure, and its preservation (or lack of it) can provide clues to infer depositional environments.

The multi-element skeletons of arthropods can only be preserved intact if individuals are buried rapidly (Brett and Baird, 1986), because the decay process occurs very rapidly (Plotnick, 1986). However, the decay rate in carbonate environments is slower than in fine-grained clastic environments (Plotnick, et al., 1988).

According to Størmer (1934), Henningsmoen (1975) and Mikulic (1990) moulted exoskeletons are much less attractive to scavengers than are dead individuals. Moulted exoskeletons are also lighter than corpses and are more likely to float, and be moved by currents (Mikulic, 1990).

A number of studies have emphasized the instability of concave-up orientations of various skeletal parts (e.g., Seilacher, 1973), in even weak (<10 cm/sec) currents (Brett and Baird, 1986, p. 209). Furthermore, concave-down or concave-up orientations suggest current action or lack of, respectively, prior to or during burial (Brett and Baird, 1986).

Application

It is generally agreed that the Phelps beds of the Fiddlers Green Member reflects a low energy intertidal setting of an epeiric sea (Hamell, 1981; Tollerton and Muskatt, 1984; Hamell and Ciurca, 1986; Ciurca and Hamell, 1994). More detailed analyses have not, as yet, appeared.

Earlier this year (February, March and May 1997) I collected five specimens of eurypterids in situ from two different layers of the Phelps beds at the Litchfield locality. Jim Pospichal collected a sixth specimen in situ. The top/bottom orientations of all six specimens were recorded. Three specimens are from the lowest layer of the Phelps beds and the other three are from the uppermost layer. Approximately 18 inches separate these two layers. The different orientations, and contrasts in preservation and taphonomy between the specimens from the two layers are remarkable and suggest differences in micro-depositional histories, with different causes for the orientations of the eurypterids.

The three specimens (to date) from the lowest layer are unusual in that all are oriented ventral up (dorsal down). Two are incomplete specimens, being prosomas articulated with 2 and 7 body segments. They are oriented at nearly right angles to each other. The carapace and posterior segments of *Ceratiocaris aculeatus* Hall, 1859, also occurs on the slab. The third specimen on another slab is an incomplete Type A individual with legs V and VI preserved. This specimen is unusual in that it is a 3-dimensional specimen removable from the matrix. It is, however, much flattened. All three specimens are undoubtedly moulted exoskeletons.

There are no indications of predation or scavenging on these specimens, even though they are poorly preserved. The poor preservation suggests decayed exoskeletons, although it may also be due to extreme weathering along the bedding plane. There are no signs of bioturbation. Sedimentary features of tidal action (flaser and lenticular bedding) are located 1cm above the plane of the eurypterids, while massive bedding is seen below the plane of the eurypterids.

The three specimens (to date) from the uppermost layer are unusual, relative to those from the lowest layer, in that two are oriented dorsal up while the third is oriented ventral up. Two are prosomas articulated with the first body segment, and it is one of these that is ventral up. The third specimen is an incomplete individual, missing the telson, and all the legs. The telson is missing only because the pretelson (12th body segment) abuts a joint plane. The rest of the bed (with the telson) was missing when the specimen was collected.

These specimens from the uppermost layer are preserved better than those from the lowest layer. The uppermost layer shows flaser and lenticular bedding, which are absent about 1cm above the plane of the eurypterids. These three specimens were separated from each other by about 9 inches. The gross orientations of the prosomas to each other was almost parallel, but in opposite directions.

To use the line from Yul Brenner in the movie The King and I, the contrast in orientations of the eurypterids between the two layers is a puzzlement. I believe that the specimens from the lowest layer represent one of two situations. First is that they represent re-settling of moulted exoskeletons after a storm. The consistent ventral up orientation would be expected because the convex dorsal surface is more hydrodynamically stable in this position (Seilacher, 1973; Brett and Baird, 1986; Mikulic, 1990). The articulated nature of the exoskeletons is in partial agreement with the results of Allison (1986, p. 981) whereby the state of preservation (including degree of articulation) is not an indicator of distance of transport or duration of agitation.

The second explanation is that after moulting (where eurypterids may have turned on their backs to moult, like *Limulus*), the partly anchored, cast-off exoskeletons were undisturbed by tides, currents, or scavengers. They probably remained in this position until buried by precipitated carbonate sediment.

The three specimens from the uppermost layer may represent moulted exoskeletons that were turned over by low velocity currents or by tidal action. The good preservation indicates fairly rapid burial, in contrast to those specimens from the lowest layer. Furthermore, the near parallel orientation also suggests some current or tidal activity.

Unfortunately, the associated fauna known to occur with eurypterids in the Phelps beds (Table 2) only indicate near shore, shallow marine intertidal conditions (see Tollerton and Muskatt, 1984, for a fuller discussion of the paleoecology of the associated fauna). However, more detailed analyses of the associated fauna are possible, if the orientations are recorded when they are found.

Table 2 is also a revision of the associated fauna listed in Tollerton and Muskatt (1984), and provides both a stratigraphic and geographic overview. Several forms previously listed are omitted here (e.g., the pelecypods, and the cephalopod *Mitroceral gebhardi*) becuase they occur in the stratigraphically lower Syracuse Formation or stratigraphically higher Cobleskill Formation, respectively. Both of these units are lithologically similar to parts of the Bertie Formation.

As it is, many forms whose life position is normal to bedding are observed oriented parallel to bedding (e.g., the lingulid brachiopods, and the conularids). These observed orientations are another indication of some sort of disturbance of the sediment. Predation can be ruled out by the absence of damage caused by predators.

In summary, the study of the paleoecology of eurypterids collected is situ and based on external factors of the environment (lithology, taphonomy, and associated fauna) is wide open for study.

Apology

I intended to include a measured section, but I've had problems with collectors (?) Who have continually removed the numbers I have placed on the beds.

Acknowledgment

I express my deepest and most sincere thanks to my wife, Mary, for her support, and for her help with the computer.

Table 2. Geographic and stratigraphic occurrences of associated fauna.

		Quarries in Ontario, Canada	Buffalo, NY area	Black Creek, Morganville, NY	East Victor, NY	Phelps, NY	Jamesville, NY area	Forge Hollow, NY	Jerusalem Hill Herkimer County	Litchfield Herkimer County	Lang's Quarry Herkimer County	Passage Gulf Herkimer County
Conularid	*Metaconularia perglabra*		w 5 3									p13
Articulate brachiopods	*Eccentricosta jerseyensis*	wb 9	w 9		w 9							
	Morinorhynchus? interstriatus		1								v 13	
	Protathyris sulcata (=Whitfieldella in) many papers)	ECB 9			v 12	v 6		v 13		v 13		p 13 v 9
Inarticulate brachiopods	*Lingula semina*		3						5	2 v 13		v 13
	L. subtrigonia											
	L. sp.	w 9	w 8 ? 3		w 6		w 7					P 7 v 7
	Orbiculoidea cf. numulus		3									
	O. sp.						w 7					
Gastropods	high-spired		3							4 v 13		P 13 v 13
	low spired		3							v 13		v 13
	undifferentiated	w 9	w 8		w 6							v 7
Cephalopods	*Pristeroceras timidum*		3		?p? 5			p 13		p 13		p 13
	orthocone nautiloids	w 9 ECB 9	3			p 7	w 7			v 13		p 13
Worm	*Ruedemannella obesa*		3									
Conodonts	*Spathognathodus remscheidensis*					v 8						
	unidentified		w 13							14		
Scorpions	*Archaeophonus eurypteroides*										p 13	p 7
	Proscorpius osborni							1			p 13	p 7
Phyllocarids	*Ceratiocaris acuminata*		3									

Table 2. (Continued).

		Quarries in Ontario, Canada	Buffalo, NY area	Black Creek, Morganville, NY	East Victor, NY	Phelps, NY	Jamesville, NY area	Forge Hollow, NY	Jerusalem Hill Herkimer County	Litchfield Herkimer County	Lang's Quarry Herkimer County	Passage Gulf Herkimer County
	C. aculeata							3		p 13		
	C. maccoyana		3									
	C. minuta		3									
	unidentified	w 9	w 8		w 6		w 7					p 8
Xiphosurans	*Bunaia woodwardi*		3									
	Hemiaspis eriensis		3									
	Pseudoniscus clarkei		wd 11							3		
Ostracodes	*Eukloadenella umbilicata*		w 4							v 13		
	Herrmannia alta		3							?v 13		?v 13
	Leperditia scalaris		1							v 13		p 13 v 13
	Zygobeyrichia regina		w 4							v 13		
	unidentified	9	w9 ECB 9 v9		v 12	p 7	p 7		5			v 7
Plants	*Cooksonia sp.*	w 12										p 7
	Medusaegraptis gramminiformis		3				w 7					p 13
	stromatolites	12						p 13		p 13	p 13	p 13

Notes for Tables 2 and 3.

1. Geographic occurrences are arranged from west (left) to east (right).
2. Stratigraphic units: w = Williamsville beds
   ECB = Ellicott Creek Breccia
   P = Phelps beds
   V = Victor beds
   FG = Fiddlers Green Member
3. Taxonomy of species as in Leutze (1959) and Tollerton and Muskatt (1984).
4. References: 1= Clarke and Ruedemann, 1912
   2=Ruedemann, 1916
   3=Ruedemann, 1925
   4=Monahan, 1931
   5=Leutze, 1959
   6=Ciurca, 1973
   7=Ciurca, 1978
   8=Hamell, 1981
   9=Ciurca, 1982
   10=Hamell and Ciurca, 1986
   11=Ciurca, 1990
   12=Ciurca and Hamell, 1994
   13=Personal observation and/or collection
   14=Johannessen, et al., 1997

Table 3. Geographic and stratigraphic occurrences of the eurypterids.

Eurypterids	Quarries in Ontario, Canada	Buffalo, NY area	Black Creek, Morganville, NY	East Victor, NY	Phelps, NY	Jamesville, NY area	Forge Hollow, NY	Jerusalem Hill Herkimer County	Litchfield Herkimer County	Lang's Quarry Herkimer County	Passage Gulf Herkimer County
Acutiramus cummingsi	w 9	1 w 8				w 7					
A. macrophthalmus							1	1	1 P 13	P 13	P 13 V 7
A. sp. (=Pterygotus in many papers)	ECB 9			w 7	P7						V 7
Buffalopterus pustulosus		1									
Dolichopterus herkimerensis								1			
D. jewetti							1	1	P 13		P 13
D. macrocheirus	w 9	1 w 8									
D. siluriceps		1								P 13	
D. testudineus	ECB 9							1			
D. sp.	ECB 9	w 9		w 9	P7						P 8
Erettoptorus grandis		1								P 13	
Eurypterus dekayi	w 9	1					P13		P 13	P 13	P 13
E. laculatus	ECB 12		V 6								
E. lacustris	1 w 9	1 w 9		w 7							
E. remipes	ECB 9	1 ECB9 FG 6			P6	P6	1 P13 V13	1	P 13 V 13	P 13	P 6 V 7
E. sp.											V 7
Paracarcinosoma scorpionis	w 9	1 w 8				w7					
Pterygotus cobbi		1								P 13	
unidentified fragments	V 9		V 10	V 12					V 13		V10

References

Allison, P.A., 1986, Soft-bodied animals in the fossil record: The role of decay in fragmentation during transport: Geology, v. 14, p. 979-981.

Andrews, H.E., Brower, J.C., Gould, S.J., and Reyment, R.A., 1974, Growth and variation in *Eurypterus remipes* DeKay: Bulletin of the Geological Institutions of the University of Uppsala, New Series, v. 4, p. 81-114.

Berry, W.B.N., and Boucot, A.J., 1970, Correlation of the North American Silurian rocks: Geological Society of America Special Paper 102, 289p.

Brett, C.E., and Baird, G.C., 1986, Comparative taphonomy: A key to paleoenvionmental interpretation based on fossil preservation: Palaios, v. 1, p. 207-227.

Chapman, E.J., 1864, A popular and practical exposition of the minerals and geology of Canada: Toronto, 236p.

Ciurca, S.J., Jr., 1973, Eurypterid horizons and the stratigraphy of the Upper Silurian and ?Lower Devonian of Western New York State: New York State Geological Association, 45th Annual Meeting and Guidebook, p. D1-D14.

_____, 1978, Eurypterid horizons and the stratigraphy of Upper Silurian-Lower Devonian rocks of Central-Eastern New York State: New York State Geological Association, 50th Annual Meeting and Guidebook, p.225-249.

_____, 1982, Eurypterids, stratigraphy, Late Silurian-Early Devonian of Western New York State and Ontario, Canada: New York State Geological Association, 54th Annual Meeting and Guidebook, p. 99-120.

_____, 1990, Eurypterid biofacies of the Silurian-Devonian evaporite sequence; Niagara Peninsula, Ontario, Canada, and New York: New York State Geological Association, 62nd Annual Meeting and Guidebook, p. D1-D30.

_____, and Hamell, R.D., 1994, Late Silurian sedimentation, sedimentary structures and paleoenvironmental settings within an eurypterid-bearing sequence (Salina and Bertie Groups), Western New York State and Southwestern Ontario, Canada: New York State Geological Association, 66th Annual Meeting and Guidebook, p. 457-488.

Clarke, J.M., and Ruedemann, R., 1912, The Eurypterida of New York: New York State Museum Memior 14, Albany, 628p.

Dalingwater, J.E., 1985, Biomechanical approaches to eurypterid cuticles and chelicerate exoskeletons: Transactions of the Royal Society of Edinburgh, v. 76, p. 359-364.

Eldredge, N., 1970, Observations on burrowing behavior in *Limulus polyphemus* (Chelicerata, Merostomata), with implications on the functional anatomy of trilobites: American Museum Novitates 2436, 17p.

Fisher, D.C., 1975, Swimming and burrowing in *Limulus* and *Mesolimulus*: Fossils and Strata, v. 4, p. 281-290.

_____, 1984, The Xiphosurida: Archetypes of bradytely?, *in* Eldredge, N., and Stanley, S.M., eds., Living fossils. New York, Springer-Verlag, p. 196-213.

Fisher, D.W., 1960, Correlation of the Silurian rocks in New York State: New York State Museum Map and Chart Series 1.

Hamell, R.D., 1981, Stratigraphy, petrology, and paleoenvironmental interpretation of the Bertie Group (Late Cayugan) in New York State: Unpublished Master's thesis, University of Rochester, 89p.

_____, and Ciurca, S.J., Jr., 1986, Paleoenvironmental analysis of the Fiddlers Green Formation (Late Silurian) in New York State: New York State Geological Association, 58th Annual Meeting and Guidebook, p. 199-218.

Hanken, N.-M., and Størmer, L., 1975, The trail of a large Silurian eurypterid. Fossils and Strata, v. 4, p. 255-270.

Harland, W.B., Armstrong, R.L., Cox, A.V., Craig, L.E., Smith, A.G., and Smith, D.G., 1990, A geologic time scale 1989: Cambridge, England, Cambridge University Press, 263p.

Henningsmoen, G., 1975, Moulting in trilobites: Fossila and Strata, V. 4, p. 179-200.

Jegla, T., 1982, A review of the molting physiology of the trilobite larva of *Limulus*, *in* Bonaventura, J., Bonaventura, C., and Tesh, S., eds., Physiology and biology of horseshoe crabs. New York, Alan R. Liss, p. 83-101.

Johannessen, K.M., Natel E.M., and Ebert, J.R., 1997, An Upper Silurian conodont-rich facies from the Rondout Formation of Central New York: Approximating the Ludlovian-Pridoli Boundary and a note on possible diagenetic influences on conodont color alteration indices (CAI): Geological Society of America Abstracts with Programs, Northeastern Section, v. 29, p. 55.

Kaneshiro, E.S., 1962, Growth patterns in *Eurypterus remipes remipes* Dekay 1825. Unpublished Master's thesis, Syracuse University, 37p.

Kjellesvig-Waering, E.N., 1958, The genera, species and subspecies of the Family Eurypteridae, Burmeister, 1845: Journal of Paleontology, v. 32, p. 1107-1148.

_____, 1961, the Silurian Eurypterida of the Welsh Borderland: Journal of Paleontology, v. 35, p. 789-835.

_____, 1964, A symopsis of the Family Pterygotidae Clarke and Ruedemann, 1912 (Eurypterida): Journal of Paleontology, v. 38, p. 331-361.

Knight, G.J., 1996, Making rocks swim, *in* Repetski, J.E., ed., Sixth North American Paleontological Convention Abstracts of Papers: The Paleontological Society Special Publication 8, p. 214.

Laverock, W., 1927, On the casting of the shell in *Limulus*. Proceedings and Transactions of the Liverpool Biological Society, v. 41, p. 13-16.

Leutze, W.P., 1959, Stratigraphy and paleontology of the Salina Group in Central New York: Unpublished Ph.D. dissertation, The Ohio State University, 463p.

Lochhead, J.H., 1950, *Xiphosura polyphemus*, *in* Brown, F.A., ed., Selected invertebrate types. New York, Wiley, p. 360-381

Manning, P.L., and Dunlop, J.A., 1995, The respiratory organs of eurypterids: Palaeontology, v. 38, p. 287-297.
Mikulic, D.G., 1990, The arthropod fossil record: Biologic and taphonomic controls on its composition, *in* Mikulic, D.G., convenor, Arthropod paleobiology, Short Courses in Paleontology 3, p. 1-23.
Monahan, J.W., 1931, Studies of the fauna of the Bertie Formation: The American Midland Naturalist, V.12, p. 377-400.
O'Connell, M., 1916, The habitat of the Eurypterida: Bulletin of the Buffalo Society of Natural Sciences, v. 11, 278p.
Plotnick, R.E., 1983, Patterns in the evolution of the eurypterids: Unpublished Ph.D. dissertation, University of Chicago, 411p.
_____, 1985, Lift based mechanisms for swimming in eurypterids and portunid crabs: Transactions of the Royal Society of Edinburgh, v. 76, p. 325-337.
_____, 1986, Taphonomy of a modern shrimp: Implications for the arthropod fossil record: Palaios, v. 1, p. 286-293.
_____, Baumiller, T., and Wetmore, K.L., 1988, Fossilization potential of the mudcrab *Panopeus* (Brachyura: Xanthidae) and temporal variability in crustacean taphonomy: Palaeogeography, Palaeoclimatology, Palaeoecology, v. 63, p. 27-43.
Reynolds, W.W., and Casterlin, M.E., 1979, Thermoregulatory behavior and diel activity of *Limulus polyphemus*, *in* Cohen E., ed., Biomedical applications of the horseshoe crab (Limulidae). New York, Alan R. Liss, p. 47-59.
Rickard, L.V., 1953, Stratigraphy of the Upper Silurian Cobleskill, Bertie, and Brayman Formations of New York State: Unpublished Master's thesis, University of Rochester, 178p.
_____, 1962, Late Cayugan (Upper Silurian) and Helderbergian (Lower Devonian) Stratigraphy in New York State: New York State Museum Bulletin 386, 157p.
_____, 1975, Correlation of the Silurian and Devonian rocks of New York State: New York State Museum and Science Service Map and Chart Series 24, 16p.
Rudloe, A., 1979, *Limulus polyphemus*: A review of the ecologically significant literature, *in* Cohen, E., ed., Biomedical applications of the horseshoe crab (Limulidae). New York, Alan R. Liss, p. 27-35.
Ruedemann, R., 1916, Account of some new or little-known species of fossils: New York State Museum Bulletin 189, p. 7-97.
_____, 1925, Some Silurian(Ontarian) faunas of New York: New York State Museum Bulletin 265, 134p.
Schuchert, C., 1903, On the Manlius Formation of New York: The American Geologist, v. 31, p. 160-178.
Seilacher, A., 1973, Biostratinomy: The sedimentology of biologically standardized particles, *in* Ginsburg, R.N., ed., Evolving concepts in sedimentology: Johns hopkins University Press, p. 159-177.
Sekiguchi, K., and Nakamura, K., 1979, Ecology of the extant horseshoe crab, *in* Cohen, E., ed., Biomedical applications of the horseshoe crab (Limulidae). New York, Alan R. Liss, p. 37-45.
_____, Seshimo, H., and Sugita, H., 1988, Post-embryonic development of the horseshoe crab: Biological Bulletin, v. 174, p. 337-345.
Selden, P.A., 1981, Functional morphology of the prosoma of *Baltoeurypterus tetragonophthalmus* (Fischer) (Chelicerata: Eurypterida): Transactions of the Royal Society of Edinburgh, v. 72, p. 9-48.
_____, 1984, Autecology of Silurian eurypterids, *in* Bassett M.G., and Lawson, J.D., eds., Autecology of Silurian organisms: Special papers in Paleontology 32, p. 39-54.
_____, 1985, Eurypterid respiration: Philosophical Transactions of the Royal Society, B, v. 309, p. 219-225.
Shuster, C.N., Jr., 1979, Distribution of the American horseshoe "crab", *Limulus polyphemus* (L.), *in* Cohen, E., ed., Biomedical applications of the horseshoe crab (Limulidae). New York, Alan R. Liss, p. 3-26.
Størmer, L., 1934, Merostomata from the Downtonian Sandstone of Ringerike, Norway: Skrifter utgitt av Det Norske Videnskaps Akademi I Oslo I. Matematiisk-naturvidskapelig, Klasse 1933 No. 10, 125p.
Tollerton, V.P., Jr., 1989, Morphology, taxonomy, and classification of the Order Eurypterida, Burmeister, 1843: Journal of Paleontology, v. 63, p. 642-657.
_____, 1993, Comparative ontogeny of *Eurypterus remipes* Dekay, 1825, and *Eurypterus lacustris* Harlan, 1834: Unpublished Master's thesis, SUNY at Buffalo, 123p.
_____, and Muskatt, H.S., 1984, Sedimentary structures and paleoenvironmental analysis of the Bertie Formation (Upper Silurian, Cayugan Series) of Central New York State: New York State Geological Association, 56th Annual Meeting and Guidebook, p. 117-155.
Vosatka, E.D., 1970, Observations on the swimming, righting, and burrowing movements of young horseshoe crabs, *Limulus polyphemus*: The Ohio Journal of Science, v. 70, p. 276-283.
Waterston, C.D., 1979, Problems of functional morphology and classification in stylonurid eurypterids (Chelicerata, Merostomata), with observations on the Scottish Silurian Stylonuroidea: Transactions of the Royal Society of Edinburgh, v. 70, p. 251-322.

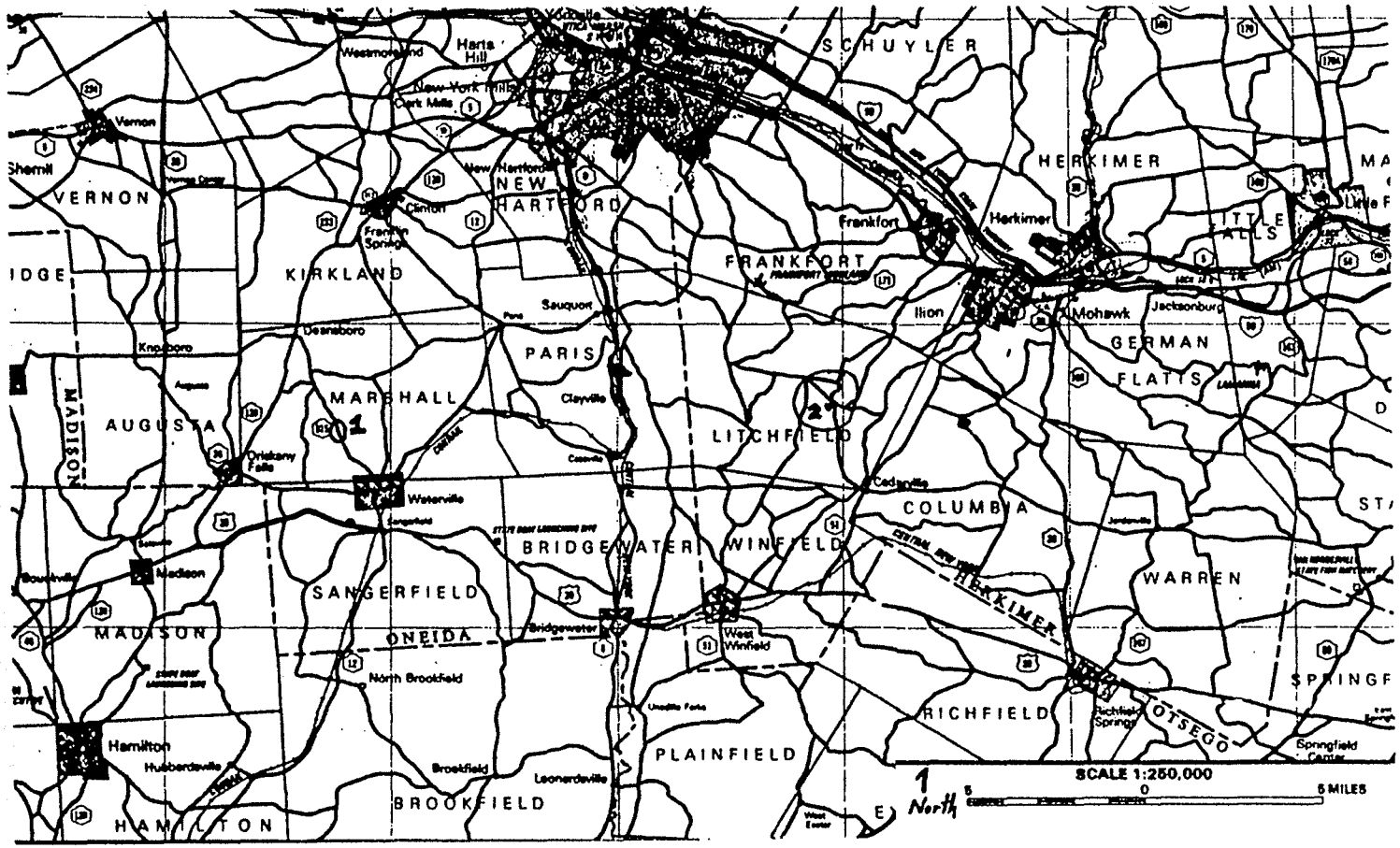
SCHUYLER
HERKIMER
VERNON
NEW HARTFORD
KIRKLAND
FRANKFORT
PARIS
MARSHALL
AUGUSTA
LITCHFIELD
COLUMBIA
BRIDGEWATER
WINFIELD
WARREN
SANGERFIELD
MADISON
ONEIDA
RICHFIELD
OTSEGO
PLAINFIELD
BROOKFIELD
HAMILTON
GERMAN FLATTS
Utica
Rome
Herkimer
Frankfort
Ilion
Mohawk
Jacksonburg
Little Falls
Waterville
Madison
Hamilton
Oriskany Falls
Bridgewater
West Winfield
North Brookfield
Brookfield
Leonardsville
Cedarville
Clayville
Sauquoit
Deansboro
Knoxboro
Vernon
Clinton
Westmoreland
Harts Hill
New York Mills
Cork Mills
Franklin Springs
Richfield Springs
Springfield Center
1
2
North
SCALE 1:250,000
5 0 5 MILES

Figure 1

Road Log

Cumulative Mileage	Miles From Last Point	Route Description
0.0	0.0	Start at the flashing traffic light at the bottom of Hamilton College road. This is the intersection of Routes 233 and 412. After coming down the hill, turn right onto Route 233.
1.2	1.2	End of Route 233. "T" intersection with Route 12B. Turn right onto Route 12B (south).
3.8	2.6	Village of Deansboro highway sign.
4.2	0.4	Intersection of Route 315 and 12B. Turn left onto Route 315 (south).
7.1	2.9	STOP 1. Park on the right. Outcrop on the right. BE CAREFUL...blind curves at both ends of the outcrop.

STOP #1. Forge Hollow, Oneida County, New York.

This locality is the type locality for the eurypterid *Eurypterus remipes* Dekay, 1825, and the scorpion *Proscorpius osborni* (Whitfield), 1885. It is also the type locality for a new genus and species of eurypterid being described.

This outcrop exposes the following units (in ascending order): Camillus Shale; the Morganville, Victor, and Phelps beds of the Fiddlers Green Member, Bertie Formation; Scajaquada Member (= Rickard's 1962 Forge Hollow Member), Bertie Formation; Williamsville Member, Bertie Formation; Cobleskill Formation; and Manlius Formation.

Continue south on Route 315.

7.2	0.1	Bogan Road on the right, at the extreme southern edge of the outcrop. Road cuts on the right of this road expose the higher units. Continue south on Route 315.
9.0	1.8	Village of Waterville highway sign
9.55	0.55	End of Route 315. Flashing traffic light and stop sign. Intersection of Routes 315 and 12 (south). Turn right onto Route 12 (south).
9.65	0.1	Route 12 (south) curves left. Stay on Route 12 (south).
9.7	0.05	Route 12 (south) curves left. Stay on Route 12 (south).
10.6	0.9	Township of Sangerfield highway sign.
10.9	0.3	Intersection of Routes 12 and 20. Turn left onto Route 20 (east).
17.0	6.1	Village of Bridgewater highway sign.
17.35	0.35	First of two traffic lights. Continue straight on Route 20 (east).
17.45	0.1	Second traffic light. Intersection of Routes 8 and 20. Continue straight on Route 20 (east).
20.2	2.75	Village of West Winfield highway sign.
20.6	0.4	Intersection of Routes 20 and 51 (south). Continue straight on Route 20 (east).
22.65	2.05	Village of East Winfield highway sign.
23.5	0.85	Intersection of Routes 20 and 51 (north). Turn left onto Route 51 (north).
26.5	3.0	Village of Cedarville highway sign.
26.7	0.2	Village of Cedarville. Turn left onto Route 51 (north).
26.85	0.15	Intersection of Jerusalem Hill Road and Route 51 (north). Continue straight on Jerusalem Hill Road.
29.6	2.75	STOP 2. Park in the small parking lot on the right, in front of the Litchfield Town garage. Outcrop on the left.

STOP # 2. Litchfield eurypterid locality.

End of trip.